UNIVERSIDAD DE CÓRDOBA

FACULTAD DE CIENCIAS

Departamento de Química Inorgánica e Ingeniería Química

Programa de Doctorado en Biociencias y Ciencias Agroalimentarias

"Cuantificación de la emisión, impacto y control odorífero derivado del tratamiento de aguas residuales municipales"

"Quantification of the emission, impact and control of odour derived from urban wastewater treatment"

Tesis Doctoral presentada por

Pedro Márquez García

Directores:

María de los Ángeles Martín Santos

José Ángel Siles López

Córdoba, enero de 2023

TITULO: *Cuantificación de la emisión, impacto y control odorífero derivado del tratamiento de aguas residuales municipales*

AUTOR: *Pedro Márquez García*

© Edita: UCOPress. 2023
Campus de Rabanales
Ctra. Nacional IV, Km. 396 A
14071 Córdoba

https://www.uco.es/ucopress/index.php/es/
ucopress@uco.es

Cuantificación de la emisión, impacto y control odorífero derivado del tratamiento de aguas residuales municipales

LOS DIRECTORES,

MARTIN SANTOS MARIA ANGELES - 30797589Z
Firmado digitalmente por MARTIN SANTOS MARIA ANGELES - 30797589Z
Fecha: 2023.01.26 10:17:53 +01'00'

Fdo.: Dra. María de los Ángeles Martín Santos

Catedrática de Universidad.
Departamento de Química Inorgánica e Ingeniería Química, Área de Ingeniería Química, de la Universidad de Córdoba.

SILES LOPEZ JOSE ANGEL - 30964419W
Firmado digitalmente por SILES LOPEZ JOSE ANGEL - 30964419W
Fecha: 2023.01.26 09:22:37 +01'00'

Fdo.: Dr. José Ángel Siles López

Profesor Titular de Universidad.
Departamento de Química Inorgánica e Ingeniería Química, Área de Ingeniería Química, de la Universidad de Córdoba.

Trabajo presentado para aspirar al grado de Doctor por la Universidad de Córdoba.

EL DOCTORANDO,

MARQUEZ GARCIA PEDRO - 80167070H
Firmado digitalmente por MARQUEZ GARCIA PEDRO - 80167070H
Fecha: 2023.01.26 15:28:34 +01'00'

Fdo.: Pedro Márquez García

Graduado en Ciencias Ambientales por la Universidad de Córdoba

UNIVERSIDAD DE CÓRDOBA

FACULTAD DE CIENCIAS

Departamento de Química Inorgánica e Ingeniería Química

Los Doctores: María de los Ángeles Martín Santos, Catedrática de Universidad, y José Ángel Siles López, Profesor Titular de Universidad,

CERTIFICAN:

Que la Tesis Doctoral: "*Cuantificación de la emisión, impacto y control odorífero derivado del tratamiento de aguas residuales municipales*", se ha realizado bajo nuestra dirección en los laboratorios de este Departamento por el Graduado D. Pedro Márquez García y reúne los requisitos vigentes, por lo que autorizamos su presentación y posterior defensa pública.

Córdoba, 26 de enero de 2023

MARTIN SANTOS MARIA ANGELES - 30797589Z
Firmado digitalmente por MARTIN SANTOS MARIA ANGELES - 30797589Z
Fecha: 2023.01.26 10:18:15 +01'00'

Fdo.: Prof. Dra. Mª Ángeles Martín Santos

SILES LOPEZ JOSE ANGEL - 30964419W
Firmado digitalmente por SILES LOPEZ JOSE ANGEL - 30964419W
Fecha: 2023.01.26 09:23:03 +01'00'

Fdo.: Prof. Dr. José Ángel Siles López

UNIVERSIDAD DE CÓRDOBA

FACULTAD DE CIENCIAS

Departamento de Química Inorgánica e Ingeniería Química

Dr. Luis Sánchez Granados, Director del Departamento de Química Inorgánica e Ingeniería Química, de la Universidad de Córdoba,

CERTIFICA:

Que la Tesis Doctoral: "*Cuantificación de la emisión, impacto y control odorífero derivado del tratamiento de aguas residuales municipales*", se ha realizado en el Departamento de Química Inorgánica e Ingeniería Química de la Universidad de Córdoba por el Graduado D. Pedro Márquez García y reúne los requisitos vigentes, por lo que autorizo su presentación y posterior defensa pública.

Córdoba, 26 de enero de 2023

SANCHEZ GRANADOS LUIS RAFAEL - 30524375V

Firmado digitalmente por SANCHEZ GRANADOS LUIS RAFAEL - 30524375V
DN: C=ES, SERIALNUMBER=IDCES-30524375V, G=LUIS RAFAEL, SN=SANCHEZ GRANADOS, CN=SANCHEZ GRANADOS LUIS RAFAEL - 30524375V
Razón: Soy el autor de este documento
Ubicación:
Fecha: 2023.01.26 10:24:42+01'00'
Foxit PDF Reader Versión: 12.0.2

Fdo.: Prof. Dr. Luis Sánchez Granados

TÍTULO DE LA TESIS: Cuantificación de la emisión, impacto y control odorífero derivado del tratamiento de aguas residuales municipales

DOCTORANDO: Pedro Márquez García

INFORME RAZONADO DE LOS DIRECTORES DE LA TESIS

El doctorando Pedro Márquez García, viene participando desde el curso 2016-2017, desarrollando una beca de Iniciación a la Investigación, con gran interés y dedicación en las tareas propias del grupo de investigación RNM-271, tras cursar los estudios que dieron acceso al Programa oficial de Doctorado: Grado en Ciencias Ambientales (Universidad de Córdoba) y Máster Universitario en Ingeniería Ambiental (Universidad de Sevilla). Durante este periodo ha desarrollado muy buenas cualidades de investigación y laborales, tanto de forma individual como con el equipo de trabajo, con el que ha compartido éxitos y sin sabores de la investigación. Adicionalmente, ha mostrado muy buenas cualidades en tareas docentes, habiendo desarrollado su actividad en asignaturas de diferentes Grados Académicos de la Universidad de Córdoba (Ciencias Ambientales, Ciencia y Tecnología de los Alimentos y Relaciones Laborales y Recursos Humanos). Desde su comienzo, abordó las etapas de recopilación de información bibliográfica, desarrollo de experimentación y toma de datos de laboratorio, discusión de los resultados y redacción de los informes correspondientes, de forma muy exitosa.

Los diversos artículos científicos incluidos en su Tesis Doctoral tienen un eje común, que es la evaluación, el control y el seguimiento de las emisiones odoríferas asociadas al tratamiento de las aguas residuales. Para ello, como punto de partida, se ha realizado la cuantificación de la emisión odorífera de diferentes EDAR a escala industrial. En términos experimentales, la investigación se ha centrado no solo en evaluar las emisiones odoríferas (cuantificación por olfatometría dinámica, análisis cromatográfico de los compuestos presentes en tales emisiones y modelado de la dispersión odorífera), sino también en el estudio de dos tecnologías de control empleadas habitualmente en las EDAR: la adsorción mediante carbón activado granular y la biofiltración. Como novedad, aparte del seguimiento de estos sistemas en términos odoríferos, se ha perseguido la valorización del carbón activado una vez agotada su vida útil, bien para constituir nuevos lechos adsorbentes de olores, o bien para formar parte del soporte carbonoso del cátodo en las prometedoras baterías de litio-azufre. Adicionalmente, también se ha llevado a cabo la identificación y el seguimiento de las comunidades bacterianas implicadas en los diferentes experimentos de biofiltración implementados a escala piloto, correlacionándolas con la evolución de los parámetros fisicoquímicos de los lechos. La calidad de los **artículos derivados** de los estudios bibliográficos y experimentales desarrollados está contrastada con los indicios de

calidad – índice de impacto, posición de la revista dentro de las diferentes categorías – situándose dentro del primer cuartil en las revistas del JCR. A continuación, se detallan las publicaciones derivadas del desarrollo de la Tesis Doctoral:

- Márquez, P., Muñoz-Serrano, E., Gutiérrez, M.C., Siles, J.A., Martín, M.A. **Odor impact simulation of a large urban wastewater treatment plant through the numerical solution of an Eulerian model**. J. Environ. Manage. (JCR Impact factor 2021: **8.910**; Rank (Environmental Sciences): 34/279; Quartile: Q1) (*Under Review*).
- Márquez, P., Benítez, A., Chica, A.F., Martín, M.A., Caballero, A., 2022. **Evaluating the thermal regeneration process of massively generated granular activated carbons for their reuse in wastewater treatments plants**. J. Clean. Prod. 366, 132685 (JCR Impact factor 2021: **11.072**; Rank (Environmental Sciences): 24/279; Quartile: Q1).
- Márquez, P., Gutiérrez, M.C., Toledo, M., Alhama, J., Michán, C., Martín, M.A., 2022. **Activated sludge process versus rotating biological contactors in WWTPs: Evaluating the influence of operation and sludge bacterial content on their odor impact**. Process Saf. Environ. Prot. 160, 775–785 (JCR Impact factor 2021: **7.926**; Rank (Engineering, Chemical): 21/142; Quartile: Q1).
- Márquez, P., Siles, J.A., Gutiérrez, M.C., Alhama, J., Michán, C., Martín, M.A., 2022. **A comparative study between the biofiltration for air contaminated with limonene or butyric acid using a combination of olfactometric, physico-chemical and genomic approaches**. Process Saf. Environ. Prot. 160, 362–375 (JCR Impact factor 2021: **7.926**; Rank (Engineering, Chemical): 21/142; Quartile: Q1).
- Márquez, P., Herruzo-Ruiz, A.M., Siles, J.A., Alhama, J., Michán, C., Martín, M.A., 2021. **Influence of packing material on the biofiltration of butyric acid: A comparative study from a physico-chemical, olfactometric and microbiological perspective**. J. Environ. Manage. 294, 113044 (JCR Impact factor 2021: **8.910**; Rank (Environmental Sciences): 34/279; Quartile: Q1).
- Benítez, A., Márquez, P., Martín, M.Á., Caballero, A., 2021. **Simple and sustainable preparation of cathodes for Li−S batteries: Regeneration of granular activated carbon from the odor control system of a wastewater treatment plant**. ChemSusChem. 14, 3915–3925 (JCR Impact factor 2021: **9.140**; Rank (Chemistry, Multidisciplinary): 30/180; Quartile: Q1).
- Márquez, P., Benítez, A., Hidalgo-Carrillo, J., Urbano, F.J., Caballero, A., Siles, J.A., Martín, M.A., 2021. **Simple and eco-friendly thermal regeneration of granular activated carbon from the odour control system of a full-scale WWTP: Study of the process in oxidizing atmosphere**. Sep. Purif. Technol. 255, 117782 (JCR Impact factor 2021: **9.136**; Rank (Engineering, Chemical): 14/142; Quartile: Q1).
- Márquez, P., Benítez, A., Caballero, A., Siles, J.A., Martín, M.A., 2021. **Integral evaluation of granular activated carbon at four stages of a full-scale WWTP deodorization system**. Sci. Total Environ. 754, 142237 (JCR Impact factor 2021: **10.753**; Rank (Environmental Sciences): 26/279; Quartile: Q1).

Dichos trabajos han podido realizarse gracias a la financiación recibida por parte del Ministerio de Educación Cultura y Deporte (beca FPU16/07214), así como del Ministerio de Ciencia e Innovación y la Agencia Española de Investigación, a través de

los proyectos de Investigación CTQ2014-60050-R, CTM2017-88723-R y PID2020-117438RBI00, además de los proyectos UCO-FEDER-1262384-R (AT21_00189) y PYC20_RE-048 (Junta de Andalucía y FEDER).

Es destacable que el doctorando, durante el disfrute de una beca FPU, ha realizado una **estancia de investigación** de tres meses de duración en el Laboratorio de Bioingeniería y de Servicios Químicos y Ambientales, Facultad de Ingeniería, Universidad Nacional del Centro de la Provincia de Buenos Aires (Argentina), con el objetivo de optar a la Mención Internacional en el título de Doctor de la Universidad de Córdoba. Adicionalmente, el desarrollo de los distintos estadios de los que ha estado compuesta la investigación predoctoral, ha estado acompañado de diversas **comunicaciones a congresos** (8 orales y 8 pósteres), en congresos nacionales e internacionales relacionados directamente con el trabajo de la Tesis o con la gestión de residuos sólidos y líquidos. En este contexto, destaca la participación oral del doctorando en la 9ª Conferencia de la IWA (*International Water Association*) sobre Olores y COVs/Emisiones al Aire (26 y 27 de octubre de 2021, Bilbao), una de las conferencias sobre olor más importantes del mundo.

En conclusión, dada la trayectoria del doctorando y la originalidad de las investigaciones desarrolladas, los directores informamos favorablemente la labor realizada y autorizamos la presentación y defensa de esta Tesis Doctoral.

Córdoba, a 26 de enero de 2023.

MARTIN SANTOS MARIA ANGELES - 30797589Z
Firmado digitalmente por MARTIN SANTOS MARIA ANGELES - 30797589Z
Fecha: 2023.01.26 19:01:23 +01'00'

Fdo.: Dra. Mª Ángeles Martín Santos

SILES LOPEZ JOSE ANGEL - 30964419W
Firmado digitalmente por SILES LOPEZ JOSE ANGEL - 30964419W
Fecha: 2023.01.26 19:05:19 +01'00'

Fdo.: Dr. José Ángel Siles López

Mediante la defensa de esta Memoria, se pretende optar a la obtención del Doctorado Internacional, habida cuenta que el Doctorando reúne los requisitos exigidos para tal mención:

1. Se cuenta con los informes favorables de dos Doctores pertenecientes a instituciones de reconocido prestigio, de países diferentes al país en el que se ha realizado la estancia.

2. En el Tribunal que ha de evaluar la Tesis Doctoral existe un miembro de un Centro de Enseñanza Superior o de Investigación de otro país.

3. Parte de la defensa de la Tesis Doctoral se realizará en la lengua oficial de otro país.

4. El doctorando ha realizado una estancia de investigación de tres meses de duración en el Laboratorio de Bioingeniería y de Servicios Químicos y Ambientales, Facultad de Ingeniería, Universidad Nacional del Centro de la Provincia de Buenos Aires (Argentina), gracias a la concesión de una ayuda para la realización de estancias para la obtención de la Mención Internacional en el título de Doctor de la Universidad de Córdoba.

5. La Tesis consta de siete artículos aceptados definitivamente en revistas internacionales de reconocido prestigio y con índice de impacto.

Agradecimientos / Acknowledgements

De la misma manera que un olor es la sensación única que se recibe a través del olfato humano y que a menudo se genera por una mezcla compleja de compuestos odoríferos, la presente Tesis Doctoral constituye un documento único que se ha conformado gracias a la ayuda de multitud de personas, a las que me gustaría expresar mi más sincero agradecimiento.

A mis directores

María de los Ángeles Martín Santos y José Ángel Siles López, por vuestra inestimable ayuda profesional desde que comencé a ser alumno colaborador del Departamento de Química Inorgánica e Ingeniería Química, allá por el curso académico 2013/2014. Gracias por guiarme de una manera sin igual desde aquel momento, con todo vuestro esfuerzo, constancia y dedicación. A ti Mª Ángeles, por las innumerables horas de aprendizaje científico, enseñándome a valorar y valorizar cada dato obtenido y nunca bajar los brazos ante cualquier problema. A ti José Ángel, por empujarme siempre a dar un pasito más en favor de la calidad, transmitiéndome tu buen hacer y aconsejándome cuando lo he necesitado.

A mis compañeros del Área de Ingeniería Química

A los "jinetes" de laboratorio por excelencia: Inma, Marisa, Manu y Aída. Gracias Inma por ser la madre de ese lugar cargado de vivencias de todo tipo, por enseñarme a trabajar con alegría, orden, eficiencia y un sinfín de adjetivos positivos desde que era un alumno de carrera y por tus consejos, tanto profesionales como personales. A ti Marisa, por mostrarte siempre predispuesta a ayudarme y por narrar historias científicas y no tan científicas con las pausas y el humor que a cada una de ellas hay que darle. Gracias Manu por guiarme desde el primer segundo, tanto a nivel de "despachillo" (artículos, congresos, software, etc.), como práctico (equipos de laboratorio, muestreos olfatométricos, etc.), con numerosas experiencias de por medio, incluso hasta en Portugal. Y a ti Aída, por tus consejos docentes, investigadores, de amigo invisible, festivos y de un largo etcétera. Mención especial también requieren los "Javieres": Javier Hungría, por ser compañero de casi todo (trabajo, piso, estancia, running, ...) y Javier Reyes, por ayudarme a dar mis

primeros pasos en el mundo de la biofiltración y por aparecer siempre cuando la vista se nublaba. No olvido tampoco a las personas que llegaron un poco más tarde: María del Carmen (gracias por compartir tus conocimientos odoríferos y por alentarme desde tu llegada) y Alberto (gracias por tus soluciones al instante, unas más satisfactorias que otras).

También me gustaría agradecer a todos los compañeros que se han incorporado recientemente al grupo de investigación por su interés en mis avances, así como a otros que también han tenido la oportunidad de colaborar en él. A todos los "becarios papeleros", especialmente a aquéllos con los que he tenido el placer de compartir más tiempo y experiencias, profesionales y de ocio: Isa, Mónica, Esther, Edu y Juan. De igual forma a Sixto, por enseñarme, entre otras muchas cosas, que en el polígono de Las Quemadas está todo cuanto necesitas para una Tesis. Y también al resto de profesores y compañeros del Área de Ingeniería Química.

A mis excelentes colaboradores

A Almudena Benítez y Álvaro Caballero por vuestra magnífica colaboración carbonosa, gracias a la cual empecé a ver la luz al final del túnel. A Carmen Michán, José Alhama y Ana María Herruzo, por "estrujar" el mundo microscópico para obtener grandes resultados. A Jesús Hidalgo, por tu predisposición a colaborar enérgicamente, independientemente de la naturaleza del artículo a desarrollar. Y a Encarni Muñoz y María de los Baños García-Moreno por compartir durante multitud de horas vuestros conocimientos físicos y estadísticos, respectivamente.

A todas las personas involucradas en mi estancia doctoral

A Verónica Córdoba por darme la posibilidad de trabajar contigo en la Facultad de Ingeniería (FIO) de la Universidad del Centro de la Provincia de Buenos Aires (Argentina). Muchas gracias por depositar en mí tu confianza cuando mi andadura doctoral estaba recién empezada. A Estela Santalla por tu bondad, amabilidad e inestimable ayuda durante toda la estancia. A Luisina, por siempre tender tu mano ante los diferentes problemas e integrarme con tu familia y amigos. A la "bostera" Mica, por compartir tus conocimientos sobre cromatografía de gases en lo que fue mi primer

contacto con esta técnica. Y al resto de personas de la FIO y del pueblo de Olavarría que hicieron que me sintiera como en casa aún estando a miles de kilómetros.

A toda mi familia

En especial a mis padres, la base de la pirámide, por ser el mejor ejemplo en cuanto a esfuerzo y sacrificio, por preocuparse en todo momento y a los que debo todo lo que soy. También a mi hermano, por interesarte regularmente en mis avances y facilitar la aventura argentina con aquel viaje a Buenos Aires. Y por supuesto a Soledad, mi gran compañera de viaje, por tu incondicional apoyo, cariño y comprensión durante esta etapa.

Finalmente, a todas las personas que han pasado por el laboratorio olfatométrico

De no ser por su ayuda desinteresada, yo no estaría escribiendo estos renglones.

"Caminante, no hay camino, se hace camino al investigar"

(Adaptación de Antonio Machado)

"Las preguntan son eternas, son las respuestas las que van cambiando"

(Anónimo)

ÍNDICE

INDEX

Página / Page

RESUMEN

SUMMARY

En la sociedad actual, especialmente en los países más desarrollados, no se concibe una urbe donde no se realice un adecuado tratamiento de las aguas residuales, previamente canalizadas hasta una estación depuradora (EDAR). Sin embargo, el impacto odorífero de este tipo de instalaciones es fuente de frecuentes quejas y protestas en las áreas residenciales cercanas a las mismas, debido a que la contaminación por olores puede causar importantes efectos negativos sobre la salud humana y el medio ambiente. Dicha contaminación suele derivar de la presencia de compuestos orgánicos volátiles (COV) y otros nitrogenados o sulfurados en las emisiones gaseosas de las EDAR, algunos de los cuales presentan umbrales olfativos muy bajos (ppb o ppt).

En el marco de la economía circular, abordar las prioridades sociales con un enfoque múltiple es una de las directrices marcadas por todas las instituciones gubernamentales. Siguiendo esa dinámica, este trabajo de investigación se ha centrado en dos retos sociales marcados por la Unión Europea: "Acción por el clima, eficiencia de recursos y materias primas" y "Energía segura, limpia y eficiente". El tratamiento integral del agua residual en las EDAR, y todos los factores asociados a él, forman parte del primer reto, lo que incluye, por tanto, la correcta gestión de las emisiones odoríferas contaminantes. En este sentido, en la presente Tesis Doctoral se ha abordado el origen, cuantificación y modelado de la dispersión de dichas emisiones, así como su control a través de dos tecnologías de desodorización: la adsorción mediante carbón activo granular (CAG) y la biofiltración.

En el primer bloque de este trabajo, se ha realizado una comparación entre dos EDAR urbanas de pequeño-mediano tamaño con diferentes tecnologías biológicas y ampliamente implantadas en el tratamiento secundario de las aguas residuales (fangos activos de aireación prolongada y biodiscos), demostrando que el modo de operación y el consecuente contenido bacteriano de los lodos generados tienen gran influencia en el impacto odorífero resultante. Por otra parte, también se ha estudiado la emisión odorífera de una EDAR urbana de gran tamaño (950.000 habitantes equivalentes) que dispone de desodorización mediante CAG. Así, se ha cuantificado la emisión de sus principales puntos críticos de olor, con el añadido de estimar el impacto odorífero que en su conjunto produce la EDAR en zonas colindantes. Dicho objetivo se ha alcanzado a través del desarrollo de un modelo de dispersión Euleriano, demostrándose de forma satisfactoria cómo varía de forma cuantitativa dicho impacto en función de las diferentes estaciones del año.

En un segundo bloque, gracias al estudio del CAG contaminado (procedente de distintos emplazamientos en la desodorización de la EDAR urbana mencionada con anterioridad), desde diferentes perspectivas como la olfatométrica, fisicoquímica y textural, así como al análisis cuantitativo de los compuestos volátiles retenidos, se ha profundizado en la comprensión del proceso de eliminación de olores en EDAR mediante la tecnología de adsorción. Sin embargo, una vez cubierta su función, el citado material adsorbente es catalogado como residuo peligroso y generalmente termina siendo depositado en vertedero sin tratamiento ni valorización alguna. Entre las alternativas de valorización, la regeneración térmica del CAG en atmósfera inerte es la más utilizada a escala industrial, pero las complejas condiciones en las que es necesario realizarla hacen que actualmente su depósito en vertedero siga resultando la opción más económica, puesto que, aunque el producto resultante sea de valor añadido, el coste de implantación de un proceso supone la inversión en la nueva instalación, sumado a los costes de operación para mantener las condiciones inertes y el aporte energético, dado que se requieren altas temperaturas de operación. Todo ello, hacen poco atractiva la inversión en este sistema de valorización. Además, transportar el CAG contaminado a otras localizaciones geográficas alejadas incrementa aún más el coste de regeneración haciendo poco escogida esta opción. En este contexto, este trabajo ha permitido demostrar que la regeneración térmica oxidativa del CAG procedente de la desodorización, a bajas temperaturas comprendidas entre 250 y 350ºC, constituye una alternativa más simple y económica que la citada anteriormente, al objeto de obtener carbones regenerados cuyas propiedades texturales y estructurales hacen que sean susceptibles de ser reutilizados como rellenos adsorbentes de olores en EDAR.

Desde una perspectiva también circular, y dando respuesta al reto "Energía segura, limpia y eficiente", en este segundo bloque se ha enlazado el problema de la generación de residuos en forma de carbón activado contaminado de las EDAR con la necesidad de materiales carbonosos para la nueva generación de baterías de litio-azufre (Li-S), las cuales han ido adquiriendo gran importancia, hasta el punto de convertirse en un sistema de almacenamiento de energía muy efectivo. Con esta investigación, se ha conseguido demostrar el notable rendimiento electroquímico obtenido en baterías Li-S usando electrodos preparados a partir de carbones procedentes de la regeneración oxidativa de carbones activados procedentes del control de emisiones olorosas de EDAR. De esta manera, se ha demostrado que, tras un proceso sencillo y económico de regeneración en

atmósfera oxidativa (aire), también es posible obtener carbones con excelentes propiedades para permitir una segunda aplicación de los mismos en el desarrollo de baterías Li-S sostenibles.

Finalmente, en el tercer y último bloque, se ha abordado la eliminación mediante biofiltración de dos compuestos gaseosos presentes de forma habitual en las emisiones odoríferas de EDAR: ácido butírico y D-limoneno. Para ello, se han realizado experimentos de biofiltración a escala piloto con diferentes rellenos (virutas de madera de forma exclusiva o mezcladas con compost estabilizado de lodos de EDAR), estudiando la influencia que tienen tanto el material de relleno como la naturaleza del compuesto a eliminar mediante biofiltración en las eficacias de eliminación de olor de los diferentes biofiltros seleccionados. Todo ello acompañado de análisis microbiológicos que han permitido cuantificar los microorganismos aerobios que sobreviven durante la experimentación, así como la identificación taxonómica de las comunidades bacterianas presentes en los rellenos de los biofiltros, con el objetivo de evaluar la evolución de estas comunidades microbianas cuando se exponen a corrientes gaseosas independientes de ácido butírico y D-limoneno.

Gracias a la presente Tesis Doctoral, se aporta nueva y relevante información, así como conocimiento científico que puede servir de apoyo para una correcta implantación y gestión de EDAR, sobre todo en la línea de olor, línea menos estudiada frente a las líneas de aguas y lodos. Además, este trabajo tiene una repercusión muy favorable sobre el medio ambiente, en tanto que contribuye a profundizar en el conocimiento sobre las emisiones odoríferas generadas en las EDAR y su minimización, así como en la búsqueda de alternativas de valorización de los residuos que se generan en el tratamiento de tales emisiones contaminantes.

Wastewater treatment is essential for the development of cities in today's society, especially in the most developed countries. Nevertheless, the odour impact of wastewater treatment plants (WWTPs) is the source of many complaints and protests in nearby residential areas, since odour pollution can cause significant negative effects on human health and the environment. This is due to the large number of volatile organic compounds (VOCs) and other nitrogenous or sulphur compounds contained in the gaseous emissions derived from such facilities, some of which have very low odour threshold values in terms of ppb_v or ppt_v.

In the context of the circular economy, addressing social priorities with a multiple approach is one of the guidelines set by all government institutions. In this regard, this research work focuses on two societal challenges set by the European Union: "Climate action, environment, resource efficiency and raw materials" and "Secure, clean and efficient energy". The integral wastewater treatment carried out in WWTPs, and all the factors associated with it, are part of the first challenge, which therefore includes the adequate management of odour pollution. In this sense, this Doctoral Thesis has addressed the origin, quantification and modelling of the dispersion of odour emissions, as well as their control through two deodorisation technologies: adsorption by means of granular activated carbon (GAC) and biofiltration.

In the first section of this research study, two small-medium sized municipal WWTPs, based on activated sludge process (extended aeration) and rotating biological contactors as biological treatments, were comparatively evaluated, demonstrating that the biological wastewater treatment technology and the consequent bacterial content in the sludge generated have a marked influence on the odour impact of such facilities. On the other hand, the odour emission from a large urban WWTP (950,000 equivalent inhabitants), with deodorisation thorough GAC, has also been studied. Thus, the emission from the most critical odour sources has been quantified, also estimating the odour impact that this WWTP has in neighbouring areas. This objective has been achieved through the development of an Eulerian dispersion model, successfully demonstrating how such impact varies quantitatively depending on the different seasons of the year.

In the second section, physicochemical, olfactometric and textural characterizations of the GAC used by the above mentioned facility as odour treatment system at four different stages, as well as the chromatographic quantification of the retained odoriferous compounds, have been carried out in order to better understand the odour removal process

by GAC adsorption. However, when the lifespan of GAC used in deodorisation is completed, it becomes hazardous industrial waste, which is mostly discarded in landfills. Among the recovery technologies of such waste, thermal regeneration in inert atmosphere is the most widely used one at industrial scale, but the complex conditions in which it is necessary to carry it out entail that landfilling continues to be the most economical alternative nowadays, although the resulting product has added value. This is due to the fact that implementing a process involves investing in the new installation, added to the operational costs to maintain the inert conditions and the energy input, since high operating temperatures are required. For those reasons, such recovery technology is not an attractive alternative for facilities that use CAG routinely. In this context, this study has proven that the oxidative thermal regeneration of GAC derived from deodorisation, at low temperatures between 250 and 350 ºC, constitutes a simpler and cheaper alternative than its counterpart in an inert atmosphere to obtain regenerated carbons whose textural and structural properties make them susceptible to being reused as odour adsorbents in WWTPs.

Furthermore, from a circular perspective as well and responding to the challenge "Secure, clean and efficient energy", the problem of the generation of waste in terms of contaminated activated carbon from WWTPs has been linked to the need for carbonaceous materials for the sustainable development of emerging energy storage systems, such as lithium-sulphur (Li-S) batteries. In this sense, this PhD Thesis demonstrates the remarkable electrochemical performance of Li-S batteries using electrodes prepared from carbon from the oxidative thermal regeneration of activated carbons used in WWTP deodorisation. In this way, it has been shown that, after a simple and economical process of regeneration in air atmosphere, it is also possible to obtain carbon with excellent properties for contributing to the development of sustainable Li-S batteries.

Finally, in the third and last section, the removal through biofiltration of two gaseous compounds commonly present in odour emissions derived from WWTPs, butyric acid and D-limonene, has been evaluated. For this purpose, several biofiltration experiments have been carried out on a pilot scale with different packed beds (wood chips exclusively or mixed with sewage sludge compost), studying the influence of the biofiltered compound as well as the filter bed on the odour removal performance. The study has been successfully complemented with microbiological monitoring to quantify

the aerobic microorganisms that survived during the experimentation, as well as the taxonomic identification of the bacterial communities present in the above mentioned packing materials, with the aim of evaluating the evolution of such communities when they are subjected to separate gaseous streams of butyric acid and D-limonene.

As a result of this Doctoral Thesis, new and relevant results are provided, as well as scientific knowledge that might serve as support for an adequate implementation and management of WWTPs, especially in the odour line, which is a less studied field compared to the wastewater line and sludge line. In addition, this research study has a significant favourable impact on the environment, since it contributes to deepen the knowledge on odour emissions derived from WWTPs and their minimization, as well as on the search for alternatives to recover waste generated in the treatment of such polluting emissions.

INTRODUCCIÓN

INTRODUCTION

1. Necesidad de depuración de las aguas residuales

El agua es un recurso fundamental para la vida, pero la disponibilidad de agua dulce de calidad en el planeta es limitada. Del volumen total de agua existente, el 97,5% es salada, el 2,24% corresponde a agua dulce congelada en los casquetes polares y aguas subterráneas profundas, mientras que sólo el 0,26% restante es agua dulce disponible para el consumo. Sin embargo, este pequeño porcentaje no siempre es aprovechable para ciertos usos por su grado de contaminación (Organización de las Naciones Unidas para la Educación, la Ciencia y la Cultura [UNESCO], 2003; World Health Organization, 2018).

La contaminación del medio hídrico es un problema del que existen referencias históricas, que se ha visto agravado por el crecimiento exponencial de la población y el gran desarrollo industrial experimentado desde la década de los 50. De hecho, hasta hace relativamente poco tiempo, los vertidos producidos por los asentamientos poblacionales y la escasa industria existente eran asimilados por los cauces receptores mediante los procesos de dilución y autodepuración natural de las aguas, volviendo éstas a adquirir unas características aceptables para poder ser reutilizadas por otros usuarios del cauce. Actualmente, los vertidos producidos son de tal magnitud e importancia que en la mayoría de los casos la capacidad de autodepuración del cauce resulta insuficiente, deteriorándose gravemente su calidad e imposibilitando la reutilización posterior del agua (González et al., 2014; Nugraha et al., 2020; Sainz, 2005).

Las **aguas residuales urbanas** contemplan siempre las **aguas residuales domésticas** (procedentes de zonas de vivienda y de servicios, generadas principalmente por el metabolismo humano y las diferentes actividades domésticas), pero también puede haber, dependiendo del grado de industrialización de la aglomeración urbana, **aguas industriales** resultantes de actividades de este tipo, que descargan sus efluentes a la red de alcantarillado municipal, así como **aguas de escorrentía pluvial**, si la red de saneamiento es unitaria. Las aguas residuales presentan diferentes tipos de contaminantes (**Tabla 1.1**) y su vertido incontrolado puede causar graves efectos negativos sobre el medio ambiente y la salud humana, entre los que destacan (Confederación Hidrográfica del Duero [CHD], 2012):

- **Aparición de fangos y flotantes**, lo que puede provocar **malos olores**, impacto visual y degradación de los lechos de los ríos.

- **Disminución del contenido de oxígeno de las aguas** por degradación de la materia orgánica, perjudicando a la flora y la fauna propia de los ecosistemas acuáticos.
- **Aporte excesivo de nutrientes**, principalmente nitrógeno y fósforo, que provocan crecimiento excesivo de algas y otras plantas (eutrofización).
- **Fomento de la propagación de organismos patógenos**, que pueden causar daños a la salud al transmitir enfermedades.
- **Dificultad para la posterior aplicación del agua en otros usos** (reutilización), comprometiendo el uso racional y sostenible de un recurso limitado.

Tabla 1.1. Tipos de contaminantes en las aguas residuales (CHD, 2012).

Tipos de contaminantes	Ejemplos
Materiales flotantes	Aceites y grasas, plásticos, material celulósico y colillas.
Materia coloidal y disuelta	Orina y heces disueltas, aceites y grasas en emulsión, tensioactivos y detergentes, sustancias nitrogenadas (proteínas, urea, etc.), hidratos de carbono (azúcares, celulosa, etc.), sales (sulfatos, fosfatos, silicatos, perboratos, etc.) y microorganismos patógenos.
Materiales sedimentables	Restos de alimentos, arenas y cabello.

Todo ello justifica la necesidad de depurar las aguas residuales, lo que resulta imprescindible para garantizar la protección del medio ambiente, la salud de las personas y el uso racional y sostenible de los recursos hídricos.

1.1. Situación actual del saneamiento y la depuración en España

La **Directiva 91/271/CEE** del Consejo, de 21 de mayo de 1991, permitió establecer una serie de obligaciones para los Estados miembros de la Unión Europea en lo que se refiere a recogida, tratamiento y vertido de las aguas residuales urbanas y las aguas procedentes de determinados sectores industriales. La norma europea se refiere esencialmente a aglomeraciones urbanas cuyo vertido total supera una carga mayor de 2.000 habitantes equivalentes (hab-eq). Para dichas aglomeraciones, la citada Directiva fijó medidas concretas de recogida y tratamiento de sus aguas residuales, en plazos determinados, mientras que para los vertidos con carga inferior a 2.000 hab-eq se limitó

a señalar que se debe contar con un tratamiento adecuado. Sin embargo, el plazo máximo de cumplimiento de las obligaciones fijadas por la Directiva 91/271/CEE expiró el 31 de diciembre de 2005 y España aún está lejos de tratar apropiadamente todas sus aguas residuales y, en consecuencia, de cumplir con las obligaciones establecidas por la norma comunitaria.

Tras la entrada en vigor de la Directiva 91/271/CEE y su transposición al ordenamiento jurídico español mediante el **Real Decreto-ley 11/1995**, desarrollado a su vez por otros Reales Decretos posteriores, los distintos Gobiernos consideraron necesaria y estratégica la inversión en las actuaciones de saneamiento y depuración. Para ello, se impulsaron dos planes nacionales específicos: el Plan Nacional de Saneamiento y Depuración 1995-2005 (PNSD) y el Plan Nacional de Calidad de las Aguas: Saneamiento y Depuración 2007-2015 (PNCA). Estos planes catalogaron las actuaciones a acometer, las distribuyeron entre los correspondientes responsables y conformaron el principal impulso dado hasta ahora en materia de aguas residuales a nivel nacional.

Actualmente, se encuentra vigente el **Plan Nacional de Depuración, Saneamiento, Eficiencia, Ahorro y Reutilización (Plan DSEAR)**, de reciente aprobación por la Orden TED/801/2021, de 14 de julio. El Plan DSEAR indica que "*buena parte de las infraestructuras levantadas en el marco del primer Plan Nacional están concluyendo su vida útil, por lo que en los próximos años debe afrontarse un notable esfuerzo inversor para la construcción de una nueva generación de estaciones depuradoras de aguas residuales (EDAR) con tecnologías avanzadas y sujetas a crecientes exigencias de calidad y eficiencia.*", a la vez que hace alusión a la contaminación odorífera derivada de las aguas residuales: "*… en el corto y medio plazo será necesario no sólo la construcción de nuevas instalaciones sino también la renovación de ciertas plantas ya construidas que, además de cumplir la nueva regulación,* ***han de incorporar las más modernas tecnologías capaces de reducir el impacto por olor de las infraestructuras hidráulicas***".

En España se depuran alrededor de **5.000 hm^3/año de aguas residuales** y, como consecuencia de su tratamiento, se genera un volumen de lodos de algo más de un millón de toneladas de materia seca/año (Instituto Nacional de Estadística [INE], 2018). En la **Figura 1.1.1**, se observa que el volumen de aguas residuales tratadas se ha incrementado en los últimos años, pasando de 2.830 hm^3 en el año 2000, a 4.995 hm^3 en el año 2018. Por su parte, la carga total de aguas residuales urbanas vertidas en España se encuentra

en torno a **75 millones de hab-eq**. Según el último informe bienal de notificación de la Directiva 91/271/CEE (denominado Q-2019), trasladado por el Ministerio para la Transición Ecológica y el Reto Demográfico (MITECO) a la Comisión Europea, la carga de aguas residuales en aglomeraciones urbanas mayores de 2.000 hab-eq asciende a 64,5 millones. Dicha carga procede de 2.059 aglomeraciones urbanas de las que 516 no cumplen con todas las condiciones de recogida y tratamiento exigidas por la norma europea, lo que ha provocado que en la actualidad existan cinco procedimientos de infracción abiertos contra España por la incorrecta implementación de la Directiva 91/271/CEE, dos de ellos ya con sentencia firme condenatoria.

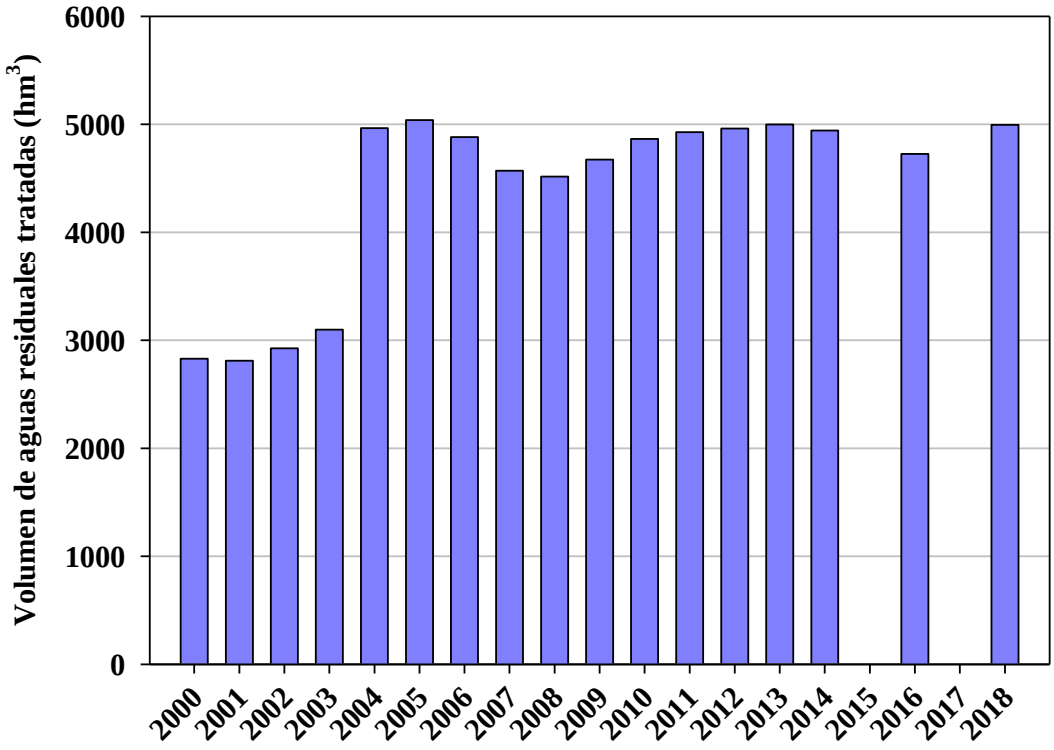

Figura 1.1.1. Evolución temporal del volumen de aguas residuales tratadas en España (INE, 2018).

1.2. Tratamiento de las aguas residuales

Después de su uso, el agua residual es recogida por las redes urbanas de saneamiento, concentrada en colectores emisarios y conducida a las EDAR, donde es tratada para su posterior vertido a cauce público, cumpliendo las garantías medioambientales exigibles. La composición de un agua residual urbana tipo es la que se muestra en la **Tabla 1.2.1**.

Tabla 1.2.1. Composición de un agua residual tipo (Ministerio de Medio Ambiente y Medio Rural y Marino [MARM], 2010).

Parámetro	Concentración (mg/L)
Sólidos en suspensión (SS)	250
Demanda bioquímica de oxígeno (DBO_5)	300
Demanda química de oxígeno (DQO)	600
Nitrógeno amoniacal ($N\text{-}NH_4^+$)	30
Nitrógeno total (N_{total})	50
Fósforo total (P_{total})	10
Coliformes fecales (UFC/100mL)	10^7

El tratamiento de las aguas residuales urbanas incluye **varias etapas fisicoquímicas y biológicas** para la eliminación de la materia orgánica e inorgánica en suspensión y la materia orgánica disuelta biodegradable (**Figura 1.2.1**). En el pretratamiento y tratamiento primario, la manipulación de la corriente de aguas residuales conduce a la separación de sólidos sedimentables y flotantes, generando lodos primarios. El posterior tratamiento secundario (biológico) tiene por objeto la eliminación de la materia orgánica biodegradable disuelta o en forma coloidal, generando lodos secundarios. Finalmente, el tratamiento terciario, en caso de que tenga lugar, persigue la eliminación de nutrientes (principalmente nitrógeno y fósforo) y patógenos, lo que permitiría obtener efluentes de mayor calidad para ser vertidos en zonas con requisitos más exigentes (zonas sensibles). Aparte de los compuestos odoríferos presentes en el agua residual de entrada, otros se originan como consecuencia de las operaciones unitarias mencionadas anteriormente, tanto en la línea de aguas como la de fangos. La mayoría de los compuestos que causan **olores** en EDAR se generan en aguas o fangos en condiciones anaerobias o sépticas (muy baja concentración de oxígeno y nitratos). Tales condiciones se desarrollan con gran rapidez debido a la baja solubilidad del O_2 en el agua residual y a las altas tasas de consumo microbiano del mismo por microorganismos en suspensión y en *biofilms* adheridos a las paredes de las diferentes unidades implicadas en el proceso de depuración. Todo ello viene acompañado de un descenso en el potencial redox en el agua residual (Lebrero y Estrada, 2010). En este contexto, las bacterias sulfato-reductoras adquieren gran importancia, utilizando sulfato (u otros compuestos oxidados de azufre) como aceptor final de electrones para la producción de altos niveles de **sulfuro de**

hidrógeno, gas altamente maloliente que se transfiere al aire ambiente en zonas donde predomina el tratamiento de agua residual bruta o sedimentada, como el pretratamiento y los decantadores primarios (Jiang et al., 2017). Además de los compuestos azufrados, también es importante la emisión de **compuestos olorosos nitrogenados** (como el amoníaco), siendo ésta mayor en condiciones aerobias (como las que tienen lugar en el desarenado-desengrasado del agua residual), debido a las reacciones de amonificación y nitrificación que realizan las bacterias amonificantes y nitrificantes, respectivamente (Nguyen et al., 2019). En las primeras etapas del tratamiento integral del agua residual, el impacto odorífero de los productos de fermentación que se generan es relativamente bajo en comparación con el impacto del sulfuro de hidrógeno. Sin embargo, dichos productos de fermentación son, a menudo, la principal fuente de malos olores en las operaciones de la línea de fangos, como el espesamiento, la deshidratación o el almacenamiento de los mismos. Durante estas etapas, se generan concentraciones significativas de ácidos orgánicos volátiles (AOV) y otros productos de fermentación, lo que resulta en un aumento de olores nauseabundos bajo tiempos de retención crecientes y condiciones anaerobias. La producción de AOV tiene como resultado una reducción de los valores de pH, favoreciendo, por tanto, unas condiciones ácidas. Bajo tales condiciones (ácidas y anaeróbicas), se produce la liberación de compuestos orgánicos volátiles (**COV**) malolientes, así como de H_2S, que contribuyen significativamente al elevado impacto odorífero característico de las mencionadas operaciones de la línea de fangos (Karageorgos et al., 2010).

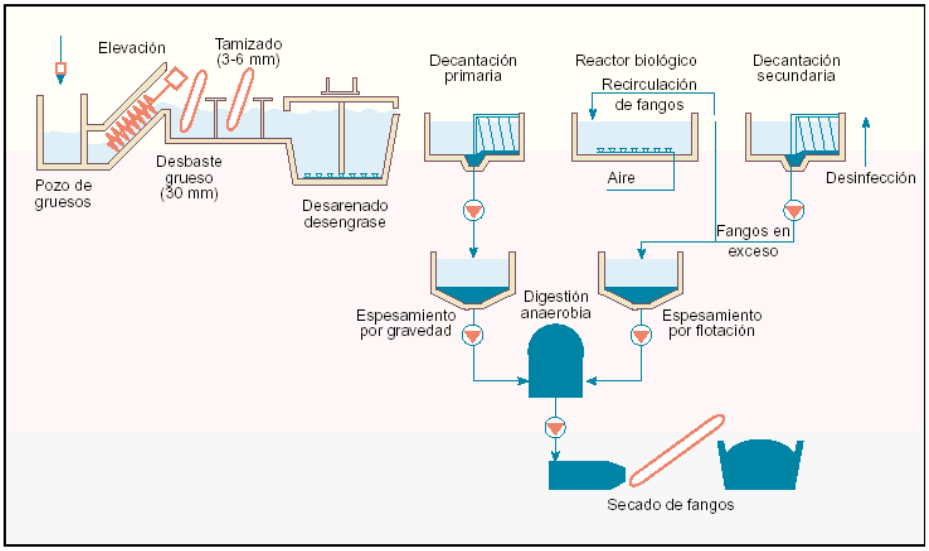

Figura 1.2.1. Esquema sinóptico de una EDAR urbana convencional (Doménech, 2003).

Respecto al tratamiento secundario, es importante mencionar que el proceso de **fangos activos** es el más utilizado para el tratamiento biológico aerobio de las aguas residuales, siendo comúnmente una de las operaciones unitarias con menor emisión de olor en las EDAR. En dicho proceso, de carácter intensivo y ampliamente implementado en las instalaciones de gran tamaño, una población de microorganismos, constituida fundamentalmente por bacterias, convierte los constituyentes orgánicos biodegradables de las aguas residuales, y ciertas fracciones inorgánicas, en nueva biomasa y subproductos (agua, dióxido de carbono o sales minerales como nitratos y sulfatos), que posteriormente son eliminados fundamentalmente en la sedimentación secundaria o por otros medios físicos (Sikosana et al., 2019; Van den Broeck et al., 2009).

En las EDAR de pequeño y mediano tamaño, y en función de la superficie disponible, pueden implementarse tanto tratamientos secundarios extensivos como intensivos. Entre los primeros destacan los humedales artificiales, el lagunaje y los filtros de turba, mientras que los segundos se dividen a su vez en (MARM, 2010):

- **Sistemas de cultivo en suspensión**: fangos activos de aireación prolongada y reactores secuenciales.
- **Sistemas de biopelícula**: lechos bacterianos, contactores biológicos rotativos (CBR) o biodiscos y sistemas de biopelícula sobre lecho móvil (*moving bed biofilm reactor, MBBR*).

De acuerdo con el Plan DSEAR, de las 2.300 EDAR existentes en España, sólo 128 instalaciones poseen una capacidad de diseño superior a 100.000 hab-eq, lo que representa un 5,5% del total. Además, es importante destacar que aproximadamente el 58% de las EDAR tiene menos de 10.000 hab-eq. En base a estas cifras, se puede decir que a nivel nacional existe un **importante predominio de las EDAR de pequeño-mediano tamaño**. En el caso concreto de la provincia de Córdoba, la Empresa Provincial de Aguas de Córdoba, S.A. (EMPROACSA) gestiona actualmente 38 EDAR de pequeño-mediano tamaño, tratando el agua residual de 34 núcleos principales de población, 3 aldeas y 5 polígonos industriales y dando servicio a una población total cercana a los 155.000 habitantes (EMPROACSA, 2021). En este contexto, la **Figura 1.2.2** muestra la distribución de las diferentes tecnologías de tratamiento secundario de aguas residuales en la provincia de Córdoba: aireación prolongada 35,85%; biodiscos 16,98%; lagunaje

1,89%; lechos bacterianos 1,89%; pendiente de licitación 35,85%; en construcción 7,55%.

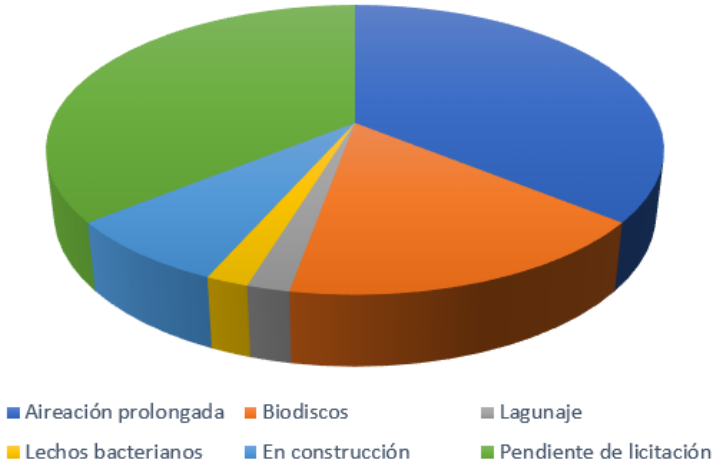

Figura 1.2.2. Tecnologías de las EDAR de la provincia de Córdoba (EMPROACSA, 2021).

Por tanto, las tecnologías predominantes en las EDAR de la provincia de Córdoba son la **aireación prolongada** y los **biodiscos** o CBR, que se corresponden con sistemas intensivos de tratamiento biológico aerobio y cuyas principales características se abordarán en las siguientes secciones.

1.2.1. Fangos activos de aireación prolongada

La aireación prolongada es una variante del proceso de fangos activos, donde se intensifica la aireación fundamentalmente incrementando el tiempo de retención hidráulico (TRH) en el reactor biológico, en comparación con los procesos de fangos activos de elevada carga o convencionales. En las EDAR que disponen de dicha tecnología, el agua residual, tras un pretratamiento eficaz, se introduce en una cuba de aireación o reactor biológico aerobio (**Figura 1.2.1.1**), el cual alberga un **cultivo bacteriano en suspensión**, formado por una gran comunidad de microorganismos individuales o agrupados en flóculos y que recibe el nombre de "**licor de mezcla**". Las condiciones aerobias en dicho reactor se consiguen mediante el uso de aireadores mecánicos (turbinas o eyectores) o aireadores por difusión (principalmente difusores de membrana). El sistema de aireación, además de cumplir la función de oxigenación, permite la homogeneización del licor de mezcla, evitando que los flóculos sedimenten. Tras un prolongado tiempo de permanencia en el reactor, el mencionado licor de mezcla pasa a un decantador o clarificador, que puede ser independiente de la cuba de aireación

o formar parte del mismo módulo si el sistema de separación de fango se realiza mediante membranas de microfiltración en lugar de decantación, y cuyo objetivo es separar el efluente depurado de los fangos. A su vez, parte de estos se recirculan de nuevo a la cuba de aireación, lo que permite mantener en ella una concentración determinada de microorganismos, y el resto (fangos en exceso) se purgan periódicamente.

Figura 1.2.1.1. Reactor de aireación prolongada de la EDAR de Espiel (Córdoba).

Adicionalmente, la edad del fango y la carga másica son dos parámetros fundamentales para el diseño de este tipo de procesos. La edad del fango hace referencia al tiempo de retención de los microorganismos en el sistema, se mide en días y es inversamente proporcional a la velocidad específica de crecimiento celular. Por su parte, la carga másica se define como la relación entre la materia orgánica que entra al reactor biológico por unidad de tiempo y la cantidad de microorganismos existentes en el mismo, expresándose en kg DBO_5/kg SS·d (MARM, 2010).

La aireación prolongada opera con altas edades del fango (y, como consecuencia, con cargas másicas muy bajas) y altos TRH, prescindiendo de la decantación primaria en la mayoría de las plantas por ser de pequeño y mediano tamaño con un pretratamiento más compacto, y generando unos fangos ya estabilizados como consecuencia del alto tiempo de permanencia de los microorganismos en el sistema. Como en estos sistemas las edades del fango son superiores a las necesarias para que tenga lugar el proceso de nitrificación, ello puede derivar en fenómenos de desnitrificación incontrolada en la decantación secundaria, con posibles escapes de fangos ascendentes. Por este motivo, es aconsejable someter al licor de mezcla a una etapa anóxica previa a la decantación, que

puede ser temporal en reactores con aireación intermitente, o espacial en reactores que alternan zonas anóxicas y aerobias. De esta manera, se favorece la desnitrificación biológica de los nitratos formados, lo que redunda tanto en una mejor clarificación como en un ahorro considerable de energía de aireación empleada en nitrificación (hasta del 25%). Este ahorro energético se debe a que una parte importante de la DBO_5 se oxida empleando el oxígeno contenido en los nitratos, de tal manera que dicho oxígeno no tendría que aportarse mediante el sistema de aireación empleado y se produce desnitrificación. A pesar de ello, el oxígeno utilizado en la oxidación de la materia orgánica del elevado metabolismo endógeno incluso puede llegar a superar el ahorro por eliminación de nitrógeno (Gandiglio et al., 2017; Siatou et al., 2020). En la **Tabla 1.2.1.1** se recogen los valores de algunos **parámetros de diseño** que habitualmente se emplean en reactores de aireación prolongada.

Tabla 1.2.1.1. Parámetros de diseño habituales en la aireación prolongada (MARM, 2010).

Parámetro	Rango habitual
Edad del fango (d)	20-25
Carga másica (kg DBO_5/kg SS·d)	0,03-0,07
Tiempo de retención hidráulico (h)	18-36
Sólidos en suspensión en la cuba (kg/m^3)	3,0-5,0
Relación recirculación externa (Q_r/Q) (%)	100-150
Necesidades de oxígeno en la aireación (kg O_2/kg DBO_5 eliminada)	2,0-3,0
Concentración de oxígeno disuelto en el reactor (mg/L)	2,0*
Porcentaje de la zona anóxica (%)	30-40

*En caso de desnitrificación simultánea el valor es 0,5 mg/L.

Considerando los parámetros de diseño anteriores y operando en régimen de nitrificación de las formas amoniacales, la **Tabla 1.2.1.2** muestra los **rendimientos medios** habituales de una EDAR con aireación prolongada, a la vez que se presentan las características del efluente final cuando se trata un agua residual tipo.

Tabla 1.2.1.2. Rendimientos medios de una EDAR de aireación prolongada con nitrificación y características del efluente final (MARM, 2010).

Parámetro	% Reducción	Efluente final (mg/L)
SS	85-95	15-35
DBO_5	85-95	15-25
DQO	80-90	60-120
$N\text{-}NH_4^+$	90-95	2-5
N_{total}	30-40	30-35
P_{total}	20-30	7-8

Sin embargo, cuando se opera en régimen de nitrificación-desnitrificación, se pueden alcanzar eficacias de eliminación de nitrógeno total de 80-85%, a la vez que se incrementaría el resto de rendimientos del proceso al mejorarse el comportamiento de la etapa de decantación secundaria o clarificación. Por otra parte, la eliminación de fósforo puede abordarse por vía química, añadiendo sales de hierro o aluminio, o alternado la vía biológica con la química, de tal manera que se alcanzarían rendimientos de eliminación del 80-90% y concentraciones de salida inferiores a la establecida por la legislación vigente (< 2 mg P_{total}/L).

Además, los **fangos biológicos** generados en instalaciones con aireación prolongada suelen encontrarse ya parcialmente **estabilizados**, presentando una concentración de sólidos volátiles en el rango de 55-65%. Debido a esto y a la ausencia de fangos primarios, cabe esperar que el **nivel de olor** generado sea **bajo** en las EDAR con aireación prolongada. En concreto, para este tipo de tecnología, se estima una producción de fangos en exceso del tratamiento biológico de 0,8-1,0 kg materia seca/kg DBO_5 eliminada, la cual variará en función de la relación SS/DBO_5 del agua bruta, así como de la edad del fango en el reactor biológico (MARM, 2010).

1.2.2. Contactores biológicos rotativos

Los CBR o biodiscos son **sistemas de biopelícula** en los que los microorganismos se encuentran adheridos a un material que actúa como soporte y que gira semisumergido (aproximadamente el 40% de su superficie) en el agua residual a depurar. El soporte, al girar lentamente (1-2 rpm), expone su superficie al agua y al aire de manera alternativa. Sobre el mencionado soporte se desarrolla, de forma natural y gradualmente, una **película de biomasa bacteriana**, la cual emplea como sustrato la materia orgánica soluble

presente en el agua residual. En cuanto al oxígeno necesario para su respiración, ésta lo tomará del aire atmosférico durante la fase en que el soporte se encuentra fuera del agua. Durante la fase de emersión del soporte, la cantidad de aire captado debe ser suficiente para cubrir el consumo por parte de los microorganismos durante la fase de inmersión y para mantener las condiciones aerobias en el recinto que alberga al rotor. En este tipo de sistemas, se estima que el 90% de la biomasa activa se encuentra adherida al soporte, siendo la que ejerce la contribución mayoritaria a los rendimientos de depuración (Scholz, 2006).

El crecimiento de la biopelícula continúa hasta llegar a un cierto espesor (unos 5 mm), momento en el cual se ve muy dificultada la difusión de oxígeno y nutrientes hasta las capas bacterianas más profundas y cercanas al soporte, produciéndose en estas zonas fermentaciones y burbujeo gaseoso. En tales condiciones, el esfuerzo cortante, producido por la rotación del soporte en el seno del líquido, es suficiente para provocar su desprendimiento. En el mismo lugar donde ocurre el desprendimiento de la porción de película bacteriana comienza a crecer nueva biomasa, repitiéndose el proceso indefinidamente y regulándose, de esta forma, el espesor de la biopelícula. Posteriormente, la biomasa desprendida se separa del efluente depurado gracias a la etapa de decantación (Elenter et al., 2007; Melo, 2003).

Dentro de los CBR, los **biodiscos** constituyen el sistema más utilizado. En ellos, el soporte para la fijación de la biopelícula está constituido por un conjunto de discos de material plástico de 1 a 5 m de diámetro, encontrándose paralelos y a corta distancia entre ellos (2-3 cm), gracias a un eje central que pasa a través de sus centros. La distancia entre los discos depende de la carga orgánica con la que se opere, de tal manera que los discos de la primera etapa pueden encontrarse más separados entre sí, pues son los que reciben una mayor carga. Generalmente, los CBR constan de 2 a 4 etapas, colocadas en confinamientos separados entre sí, lo que se conoce como disposición en cascada (**Figura 1.2.2.1-A**). Dicha configuración permite operar en cada confinamiento con cargas diferentes, presentando los discos distintos espesores de biopelícula en cada uno de ellos (MARM, 2010). Como se puede observar en la **Figura 1.2.2.1-B**, los biodiscos operan bajo cubierta con el objetivo de evitar posibles daños sobre la biomasa adherida a los rotores por acción de los agentes atmosféricos (elevada irradiancia, lluvias, heladas, etc.), y para preservarla en caso de averías electromecánicas que detengan el giro del rotor.

Figura 1.2.2.1. (A) Disposición en cascada de los CBR y (B) sistema de biodiscos de la EDAR de Villaviciosa de Córdoba (Córdoba).

En la tecnología de biodiscos, los **parámetros de diseño** son diferentes a los de la aireación prolongada, siendo los más representativos los que se recogen en la **Tabla 1.2.2.1**.

Tabla 1.2.2.1. Parámetros de diseño de los biodiscos (MARM, 2010).

Parámetro	Valor
Carga orgánica en la primera etapa	< 40 g $DBO_5/m^2 \cdot d$
Carga hidráulica:	
• Eliminación DBO_5	≤ 0,15 $m^3/m^2 \cdot d$
• Nitrificación	≤ 0,07 $m^3/m^2 \cdot d$

Superficie específica del biodisco:	
• Eliminación DBO_5	110 m^2/m^3
• Nitrificación	200 m^2/m^3
Solo eliminación de DBO_5 (sin nitrificación)	
Carga orgánica total:	
• 2 etapas	$\leq$ 8 g $DBO_5/m^2 \cdot d$
• 3-4 etapas	$\leq$ 10 g $DBO_5/m^2 \cdot d$
Número mínimo de etapas:	
• Para DBO_5 en efluente entre 15 y 25 mg/L	2 etapas
• Para DBO_5 en efluente entre 10 y 15 mg/L	3 etapas
Para eliminación de DBO_5 y nitrificación	
Carga orgánica total:	
• 3 etapas	$\leq$ 8 g $DBO_5/m^2 \cdot d$ $\leq$ 1,6 g $NTK/m^2 \cdot d$
• 4 etapas	$\leq$ 10 g $DBO_5/m^2 \cdot d$ $\leq$ 2 g $NTK/m^2 \cdot d$

Teniendo en cuenta los parámetros de diseño anteriores, los **rendimientos medios** habituales que se consiguen mediante el empleo del sistema de biodiscos son los que se presentan en la **Tabla 1.2.2.2**, cuya última columna muestra también las características del efluente final cuando se trata un agua residual tipo.

Tabla 1.2.2.2. Rendimientos medios de una EDAR con sistema de biodiscos y características del efluente final (MARM, 2010).

Parámetro	% Reducción	Efluente final (mg/L)
SS	85-95	25-50
DBO_5	85-95	15-25
DQO	80-90	60-120
N-NH_4^+ (sin nitrificación)	20-30	20-25
N_{total}	20-35	30-40
P_{total}	10-35	6-9

Si los rendimientos de eliminación de nutrientes necesitaran ser incrementados, se podría operar con biodiscos que nitrifiquen las formas amoniacales y que desnitrifiquen en reactores anóxicos integrados en la propia unidad de depuración (Mirbagheri et al., 2016; Teixeira and Oliveira, 2001). Si además se deseara aumentar el rendimiento de eliminación de fósforo, lo habitual es proceder a un tratamiento fisicoquímico, mediante la adición de sales de hierro o aluminio, que provocarían la precipitación de los fosfatos, extrayéndose posteriormente junto con los fangos en exceso.

En lo que se refiere al impacto odorífero, si las cargas orgánicas aplicadas a los biodiscos son las recomendadas y los recintos que los albergan se mantienen bien ventilados, la **generación de olores** en dicha zona debería ser **mínima**. Sin embargo, los fangos del decantador secundario, que se generan a razón de aproximadamente 0,8 kg de materia seca/kg DBO_5 eliminada, no se encontrarán estabilizados, a diferencia de los que se obtienen con la tecnología de aireación prolongada (MARM, 2010). Por tanto, este hecho podría acarrear el incremento de los niveles de olor en las subsecuentes operaciones de manejo y tratamiento del lodo.

2. Cambio de paradigma en la depuración del agua: Economía circular

En las últimas décadas, el tratamiento de las aguas residuales está sufriendo un profundo cambio por la necesidad de integrar las EDAR dentro del concepto de **economía circular**, fomentándose de esta forma la recuperación y valorización de todos los recursos presentes en las aguas residuales (Ferrer y Seco, 2021). En este contexto, el Plan DSEAR menciona entre sus conclusiones lo siguiente: "*El gran volumen de recursos movilizados en los procesos de depuración, saneamiento y reutilización de las aguas residuales en España y la consecuente generación de lodos como resultado de los procesos de tratamiento aconsejan promover medidas que mejoren la eficiencia energética de las plantas y la valorización de los subproductos que se acumulan, contribuyendo de este modo a los objetivos perseguidos por la* ***Estrategia Española de Economía Circular 2030: España Circular 2030***". Dicha Estrategia se configura como elemento clave para avanzar hacia la consecución de varios Objetivos de Desarrollo Sostenible (ODS) de la Agenda 2030 en España, entre los que cabe destacar el objetivo n.º 12, que tiene por objeto garantizar modalidades sostenibles de consumo y producción, y el objetivo n.º 6, que persigue garantizar la disponibilidad de agua, su gestión sostenible y el saneamiento

para todos, y que se relaciona, a su vez, con el objetivo n.º 2, "Hambre cero" (MITECO, 2020).

En línea con lo establecido por el Plan DSEAR, se puede decir que un cambio de paradigma está teniendo lugar en la depuración del agua, pasando de "un modelo lineal de depuradoras" a "**un modelo circular de biofactorías**" (**Figura 2.1**). En el modelo lineal, una EDAR se configura como una instalación consumidora de energía para depurar el agua residual, a la vez que genera residuos (arenas, fangos, grasas, etc.) y devuelve el agua limpia al medio ambiente, mientras que en el modelo circular, una biofactoría depura el agua residual al mismo tiempo que permite, entre otros, la generación de biocombustibles, energía térmica y energía eléctrica renovable, la valorización de fangos, grasas, la reutilización de agua para diferentes usos y la valorización de arenas para la construcción.

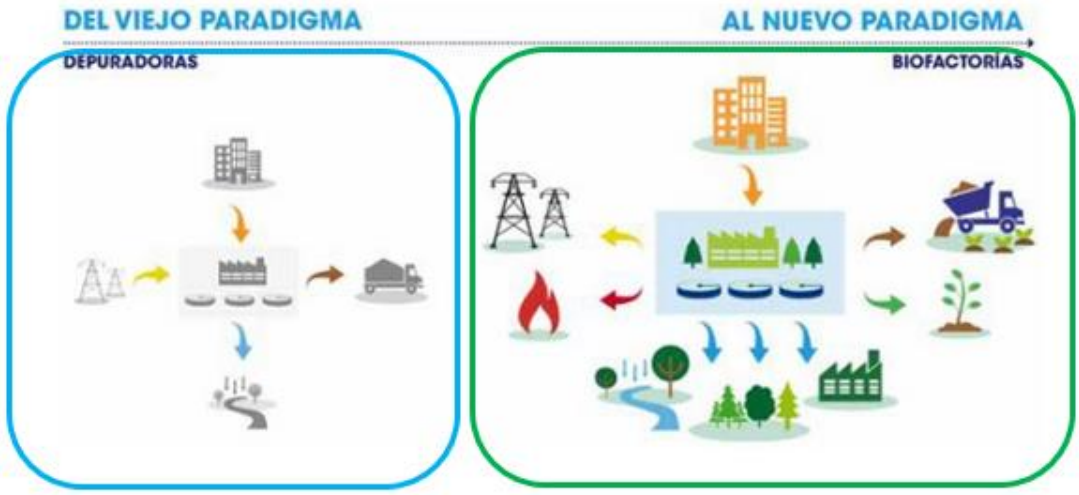

Figura 2.1. Cambio de paradigma en la depuración del agua (Empresa Municipal de Abastecimiento y Saneamiento de Granada, S.A., 2021).

Tal y como se indica en el reciente Informe Mundial de las Naciones Unidas sobre el Desarrollo de los Recursos Hídricos (UNESCO, 2021), las aguas residuales depuradas están cobrando un creciente interés como **fuente de agua** para la agricultura, sobre todo en regiones que sufren estrés hídrico. Según dicho informe, se estima una producción anual mundial de 380 km^3 de aguas residuales que equivaldrían al 15% del agua que se utiliza de forma global en agricultura. Por otra parte, se señala la importancia de las aguas residuales como **fuente de nutrientes**, de tal manera que la completa recuperación de los mismos (nitrógeno, fósforo y potasio) presentes en las aguas residuales compensaría más del 13% de la demanda mundial de nutrientes en agricultura. Con respecto al **potencial**

energético de las aguas residuales, también se destaca que el agua residual contiene más energía que la necesaria para su depuración, acorde a los estándares actuales de vertido. Por tanto, más allá de la autosuficiencia energética, las EDAR actuales presentan un amplio margen de mejora como potenciales productores de energía.

Sin embargo, a pesar del gran potencial de las aguas residuales como fuente de recursos, existen todavía importantes pasos a seguir, tanto a nivel de desarrollo tecnológico como normativos, para hacer realidad la transformación de EDAR a biofactorías. En relación con la parte tecnológica, durante los últimos años se ha llevado a cabo un **importante desarrollo de tecnologías para la valorización de recursos** (combinación de tecnologías y métodos para valorizar los recursos del agua residual en distintos puntos de las instalaciones, procesos y métodos para maximizar la valorización energética de la materia orgánica en los digestores anaerobios existentes, utilización del digestado, etc.). Estas tecnologías presentan grados de madurez más o menos elevados, por lo que los esfuerzos deben dirigirse ahora hacia su implementación a escala industrial, permitiendo validar su viabilidad tecnológica económica y ambiental. Finalmente, y al objeto de hacer realidad la circularidad en el campo del tratamiento de las aguas residuales, también resultaría conveniente **eliminar** las importantes **barreras legislativas** que en muchos casos no permiten el uso de los distintos subproductos obtenidos a partir de las aguas residuales, incentivando, a su vez, toda acción dirigida a la aceptación de los recursos recuperados en las EDAR por todos los actores implicados (Ferrer y Seco, 2021).

El cambio de paradigma en la depuración del agua posee, por tanto, un gran potencial desde el punto de vista de la economía circular, existiendo numerosos proyectos en esta línea, que fomentan la recuperación y reutilización de los recursos, como (Centro Tecnológico del Agua, 2020):

- **Recuperación de energía**: A partir del biogás procedente de la digestión anaerobia de los lodos de depuradora se puede generar biometano. Así, por ejemplo, en el proyecto LIFE Nimbus se trabaja en la revalorización de los lodos procedentes de la EDAR del Baix Llobregat (Barcelona) para producir combustible gas apto para el uso en el transporte y, de esta forma, fomentar el consumo de energía procedente de fuentes renovables.
- **Reutilización del agua**: El uso de agua regenerada se convierte en una gran alternativa sostenible para hacer frente a la escasez hídrica. En este contexto, el

proyecto B-Water Smart constituye una iniciativa innovadora para demostrar el potencial de la reutilización de agua mediante la implementación de espacios de innovación en los que desarrollar tecnologías y soluciones digitales para hacer frente a la escasez de agua. En concreto, la EDAR de Rincón de León (Alicante) está permitiendo testar un conjunto de tecnologías para potenciar el modelo de biofactoría e identificar oportunidades circulares en la región de Alicante.

- **Recuperación de nutrientes**: A partir de los fangos generados durante el proceso de depuración también se pueden recuperar nutrientes con un gran valor agronómico para ser utilizados como fertilizantes. En proyectos como LIFE Enrich y DigesTake se ha desarrollado un tren de tratamiento innovador que permite recuperar nitrógeno y fósforo de las aguas residuales.
- **Recuperación de productos de alto valor añadido**: Proyectos como Cigat-Biofactoría y Ecoval permiten la obtención de ácidos grasos volátiles a partir de fangos producidos en la EDAR de Ourense y de efluentes líquidos de una industria conservera. Estos productos con base de carbono se utilizan como materia prima para diferentes industrias como la plástica, petroquímica y de lubricantes, entre otras.
- **Recuperación de metales**: En este apartado destaca el proyecto europeo LIFE Remine Water, que, mediante la combinación de tecnologías electroquímicas y *Zero Liquid Discharge* (ZLD), busca recuperar recursos como el cobre y el zinc en los vertidos generados por la industria minera.

3. Generación de olores en la gestión de las aguas residuales

3.1. El olor: conceptos generales

El olor se define como la sensación resultante de la recepción de un estímulo por el sistema sensorial olfativo. Dicho de otra forma, el olor es la sensación que se percibe cuando uno o varios odorantes se introducen en la nariz humana, definiéndose odorante como un compuesto químico que posee un olor detectable por el olfato humano (Asociación Medioambiental Internacional de Gestores del Olor [AMIGO], 2019). La manera en que se evalúa la respuesta humana a un olor va a depender de la propiedad sensorial particular que se esté midiendo, siendo la **concentración**, **intensidad**, **carácter** y **tono hedónico** las cuatro propiedades fundamentales de los olores. El efecto combinado

de dichas propiedades se relaciona con el grado de molestia (o placer) que pueden causar los olores, realizándose a continuación una breve descripción de tales propiedades fundamentales (AMIGO, 2019; Olores.org, 2008).

Concentración de olor

El término de concentración de olor se establece en la Norma Europea EN 13725 (2003) de olfatometría dinámica, definiéndose como "***el número de unidades de olor europeas (ou_E) por metro cúbico en condiciones normales***", y expresándose, por tanto, como $\mathbf{ou_E/m^3}$. En general, la concentración de olor es un parámetro que se calcula a partir del número de veces que hay que diluir un determinado gas para que pueda ser detectado por un grupo de personas seleccionadas que constituyen un panel. Esto constituye una aproximación básica, pues lo que se calcula realmente es la media geométrica de los umbrales de olor individuales de cada persona o panelista, entendiéndose por umbral de olor de cualquier odorante la concentración de éste a partir de la cual una persona es capaz de olerlo.

Intensidad

La intensidad de un olor hace referencia a la **fuerza** con la que se percibe la sensación de olor. La siguiente ecuación, desarrollada por Stevens (1957), es la más utilizada actualmente para definir la relación entre intensidad de olor (*I*) y concentración de olor (*C*):

$$I_{percibida} = k \cdot C^n$$

donde *k* es una constante que depende del tipo de sustancia olorosa y *n* es el exponente, que para olores puede variar entre aproximadamente 0,2 y 0,8, dependiendo del compuesto oloroso.

Cuando los olores se detectan en campo, la intensidad de los mismos se determina mediante las denominadas inspecciones de campo. La determinación se realiza bajo las mismas condiciones que para la determinación del umbral de olor. Este tipo de técnica se describe en las guías alemanas VDI 3881 (hojas 1-4) y VDI 3882 (hoja 1). En este contexto, la **Tabla 3.1.1** muestra los distintos niveles de intensidad de olor para inspecciones de campo.

Tabla 3.1.1. Escala de intensidad del olor según la norma VDI 3882 – parte 1 (1992).

Olor	Nivel de intensidad
No perceptible	0
Muy débilmente perceptible	1
Débilmente perceptible	2
Distinguible	3
Fuerte	4
Muy fuerte	5
Extremadamente fuerte	6

Carácter

El carácter o calidad de un olor es aquella propiedad que lo **identifica** y lo **diferencia de otros** olores con la misma intensidad. Esta propiedad es caracterizada mediante un método conocido como perfilado o escalado multidimensional. Mediante esta metodología, el olor es definido por el grado de similitud a un conjunto de olores de referencia o el grado por el que se corresponde con una escala de varios términos descriptivos (**Figura 3.1.1**). El resultado de estos tests permite obtener lo que se denomina como "perfil del olor".

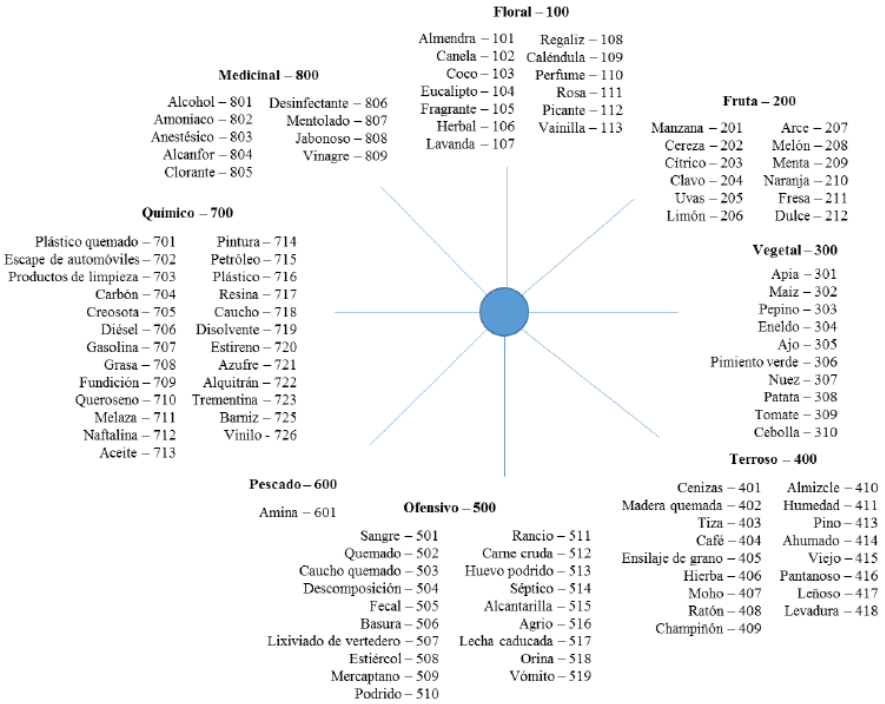

Figura 3.1.1. Típicos descriptores de olor (St. Croix Sensory, 2003).

Tono hedónico

El tono hedónico es la propiedad de un olor relativa a su **agrado o desagrado**, es decir, es un juicio de categoría del placer o no-placer relativo del olor (**Tabla 3.1.2**). Se trata, por tanto, de una de las propiedades más subjetivas del olor, ya que el grado de agrado o desagrado en este caso es determinado siempre dependiendo de las experiencias personales y asociaciones emocionales de cada persona.

Tabla 3.1.2. Escala del tono hedónico según la norma VDI 3882 – parte 2 (1994).

Descripción del olor	Tono hedónico
Extremadamente desagradable	-4
Moderadamente desagradable	-3
Desagradable	-2
Ligeramente desagradable	-1
Neutro / sin olor	0
Ligeramente agradable	+1
Agradable	+2
Moderadamente agradable	+3
Extremadamente agradable	+4

3.2. Olores derivados del saneamiento y depuración de las aguas residuales

Las aguas residuales contienen en disolución gran variedad de compuestos orgánicos e inorgánicos, muchos de los cuales se pueden volatilizar bajo determinadas condiciones, migrando del medio líquido al aire ambiente en forma de gases que pueden ser tóxicos o causantes de olores desagradables. Son **muchos** los **factores** que intervienen para que los compuestos presentes en el agua residual se volatilicen durante su recorrido y/o su tratamiento integral en las EDAR, entre los que destacan los siguientes (AMIGO, 2019): temperatura, pH, presión de vapor de cada compuesto, concentración de materia orgánica, área de los colectores, tiempo de residencia, velocidad del flujo, fricción por cambios de sentido o pendientes, agitación por saltos de agua y aireaciones, y enriquecimiento del ion sulfato por intrusión marina en zonas costeras. Este último factor constituye, a su vez, una de las principales causas por las que suele existir una mayor incidencia de problemas relacionados con malos olores en las zonas de litoral. En base a

lo anterior, se pueden liberar compuestos odoríferos en unas zonas más que otras y en algunos puntos del trazado con más probabilidad que en otros, destacándose particularmente la emisión de olores en los pozos de bombeo, las tapas de registro de colectores con poca pendiente y en los puntos de descarga final en las EDAR. Ya en el interior de dichas instalaciones, también se van combinando diferentes circunstancias que facilitan la emisión de gases malolientes en las diferentes fases u operaciones unitarias del proceso de depuración.

De todos los gases tóxicos derivados de las aguas residuales, hay dos que destacan por ser especialmente característicos y predominantes en los procesos de saneamiento y depuración: el **sulfuro de hidrógeno** (H_2S), originado por la actividad bacteriana a partir de los sulfatos presentes en el agua (actividad sulfato reductora), y el **amoniaco** (NH_3), procedente de los compuestos nitrogenados (Jiang et al., 2017; Talaiekhozani et al., 2016). Además de estos compuestos característicos, también se emiten un elevado número de sustancias odoríferas como (Lebrero y Estrada, 2010):

- **Compuestos orgánicos e inorgánicos derivados del azufre** como mercaptano de metilo, sulfuro de dimetilo, disulfuro de metilo, etc.
- **Compuestos orgánicos derivados del nitrógeno** como aminas.
- **Ácidos orgánicos volátiles** como ácido acético, butírico, etc.
- **Hidrocarburos aromáticos y alifáticos** como tolueno, benceno, hexano, etc.
- **Aldehídos** como acetaldehído, propionaldehído, etc.
- **Cetonas** como butanona, acetona, etc.
- **Terpenos** como limoneno, alfa-pineno, etc.

En última instancia, lo que recibe el olfato es una mezcla de compuestos, algunos con mayor o menor concentración que otros, que interaccionan entre ellos provocando sinergias, interferencias, inhibiciones o enmascaramientos (Iglesias, 2008). Además, es muy importante destacar el **bajo umbral de detección** de gran parte de los compuestos odoríferos provenientes de las instalaciones de saneamiento y depuración. De hecho, existen algunos odorantes, como muchos compuestos derivados del azufre, que tienen umbrales de detección de olor del orden de ppb (partes por billón) o ppt (partes por trillón), siendo por tanto los que más **molestias** generan en materia de contaminación por malos olores (Muñoz, 2010a). Una exposición continuada a emisiones odoríferas intensas puede afectar negativamente a la **salud** de la población vecinal de las instalaciones (sobre

todo a personas con alta sensibilidad odorífera), causando dolores de cabeza, náuseas, pérdida de apetito, insomnio, problemas respiratorios, etc. (Byliński et al., 2019; Jehlickova et al., 2008; Sucker et al., 2009). Además, no hay que olvidar que tales emisiones odoríferas también pueden conllevar un alto riesgo ocupacional en recintos, generalmente poco ventilados de las EDAR, como pueden ser las instalaciones de cabecera de planta o las de la línea de tratamiento de lodos, ya que en algunas ocasiones el sulfuro de hidrógeno puede llegar a alcanzar concentraciones letales de hasta 300 ppm (Stuetz y Frechen, 2001).

En España, el porcentaje de viviendas afectadas por **olores derivados del saneamiento de las aguas residuales** se situó en 2008 alrededor del 12% (sobre el total de viviendas cuyos residentes han sufrido problemas de malos olores en su entorno), convirtiéndose en la **principal causa de contaminación por malos olores**, por delante de otras causas como las explotaciones agrarias, los contenedores de residuos y las industrias (INE, 2008). En otros países, como es el caso de los Países Bajos, el porcentaje de población afectada por olores derivados del saneamiento de las aguas aumentó del 6% en 1993 al 13% en 2003, constituyendo también la principal causa de contaminación odorífera (Muñoz, 2010a). Esto ha llevado a un aumento considerable del número de quejas y protestas por problemas de olores en los últimos años (Easter et al., 2008; Hayes et al., 2017). Las quejas por molestias repetidas que no son atendidas de forma adecuada suelen acabar en **denuncias** por malos olores, lo que hace perder la confianza en las empresas gestoras de aguas residuales, empeorándose las relaciones con ellas. Además, es importante destacar que las mencionadas molestias también afectan a la pérdida del valor patrimonial o turístico de la zona (Van Broeck et al., 2008). Y por último, y no menos importante, las emisiones gaseosas derivadas de la gestión de las aguas residuales provocan también la **corrosión** de los materiales y equipos empleados, constituyendo este deterioro uno de los principales costes de operación y mantenimiento en los sistemas de saneamiento y depuración (Talaiekhozani et al., 2016).

Por todos los motivos anteriormente expuestos, resulta imprescindible un **adecuado control y gestión global de los olores**, interviniendo en todas las etapas posibles que constituyen el tratamiento de las aguas residuales, desde los colectores hasta las últimas operaciones unitarias de la depuración, y desde el diseño de las instalaciones hasta las medidas correctoras que se tengan que implementar para corregir posibles desviaciones.

3.3. Sistemas de evaluación y seguimiento del olor

En los sistemas de saneamiento y depuración resulta habitual el seguimiento de los gases generadores de olor. Generalmente, el compuesto al que se le realiza un seguimiento más exhaustivo es el sulfuro de hidrógeno, lo que se debe a su prevalencia, peligrosidad e impacto odorífero. Debido a ello, es frecuente encontrar **sensores electroquímicos fijos de H_2S** en las salas de las estaciones de bombeo, salas de pretratamiento, zona de deshidratación y sótanos con equipos de bombeo. El rango habitual de los citados sensores se encuentra entre 0 y 100 ppm, siendo cada vez más habitual la medición de H_2S a bajas concentraciones (ppb), y suelen estar conectados a una central de alarmas con el objetivo de automatizar señales luminosas y acústicas de alarma, así como conectar de forma automática los posibles sistemas de desodorización de las zonas de emisión (AMIGO, 2019).

Otra práctica común en las instalaciones es disponer de **equipos portátiles multigases** para tomar medidas puntuales de la concentración química de los compuestos odoríferos habitualmente implicados en la generación de olor: H_2S, NH_3, COV, mercaptanos (R-SH) y aminas (R-NH_2). Otros sistemas que se suelen utilizar para medir la concentración de un determinado compuesto químico gaseoso son los **dosímetros pasivos** y/o los **tubos colorimétricos**. Los dosímetros proporcionan la concentración media de un contaminante en un periodo de tiempo determinado, mientras que los tubos colorimétricos permiten medir de manera sencilla la concentración puntual de un gas. Así, a partir de las medidas puntuales en diferentes puntos de una EDAR se pueden elaborar "mapas de gases", que se deben asociar a las condiciones de operación y ambientales registradas en el momento de las mediciones (AMIGO, 2019). En el marco de la caracterización química, también se puede recurrir a la determinación de compuestos volátiles a partir de su adsorción activa en tubos multilecho, analizándolos posteriormente por desorción térmica acoplada a **cromatografía de gases** y detección por **espectrometría de masas** (TD-GC-MS), o bien mediante técnicas de cromatografía de gases que emplean distintos detectores (FID, PID, FPD, etc.). Aunque la caracterización analítica de las emisiones odoríferas no aporta información sobre el potencial de molestia que éstas generan, ayuda a identificar las fuentes del problema, constituyendo una información clave en la gestión de olores en EDAR (Muñoz, 2010a).

En este contexto, cada vez es más habitual evaluar la concentración de olor, sobre todo cuando se producen quejas vecinales. En este sentido, lo más común es realizar

estudios basados en **olfatometría dinámica** (EN 13725, 2003) al objeto de cuantificar la concentración de olor (ou_E/m^3) en los puntos críticos, las tasas de emisión (ou_E/s) y los rendimientos de los sistemas de desodorización (%). Las mediciones olfatométricas se llevan a cabo en olfatómetros, siendo determinaciones laboriosas, costosas (entre 200 y 400€ por muestra) y de alta incertidumbre, pero necesarias por constituir la base de las regulaciones de olor en Europa y en gran parte del resto del mundo (Muñoz, 2010a). Además, los resultados olfatométricos suelen complementarse con el modelado de la dispersión del olor, permitiendo evaluar el impacto odorífero (inmisión) en los alrededores de las instalaciones.

En los últimos años, se han desarrollado dispositivos que permiten medir concentración de olor (ou/m^3) in situ en la propia instalación. El **olfatómetro de campo** es un dispositivo que permite realizar medidas puntuales de la concentración de olor, pero dichas medidas deben ser realizadas por panelistas previamente "calibrados" para ello. Por otro lado, las **narices electrónicas** (*e-noses*) y los sistemas de vigilancia instrumental del olor (*instrumental odour monitoring systems*, ***IOMS***, **Figura 3.3.1**) son dispositivos que han entrado recientemente en el sector, permitiendo medir en continuo la concentración de olor. Sin embargo, hasta la fecha, los sistemas mencionados anteriormente no pueden utilizarse para evaluar la concentración de olor a menos que se hayan calibrado antes con un olor de referencia con las mismas propiedades químicas (AMIGO, 2019).

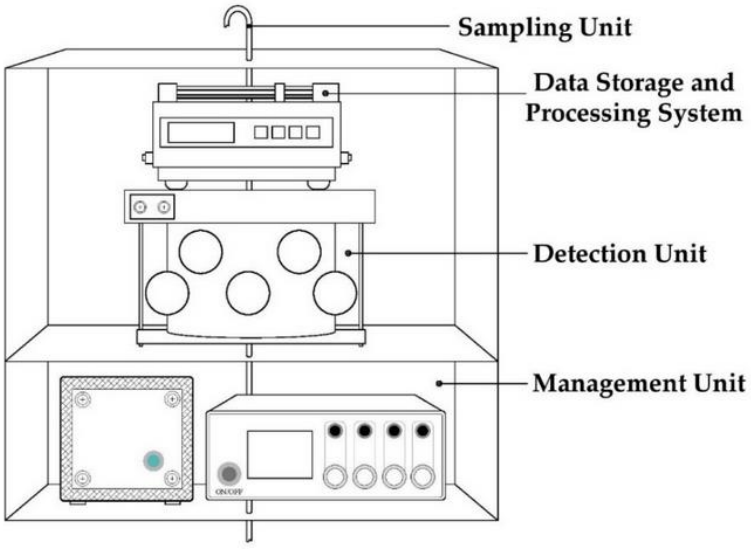

Figura 3.3.1. Unidades funcionales principales de los IOMS (Zarra et al., 2021).

Existe también un uso creciente de herramientas en las EDAR que permiten predecir el comportamiento de los gases y de los procesos generadores de olor, así como evaluar el impacto en las áreas circundantes. Algunas de ellas son: cañones de humo, software de simulación en redes de saneamiento, sistemas pronóstico del impacto por olor y cálculo de retrotrayectorias, herramientas de mecánica de fluidos computacional (*computational fluid dynamics, CFD*) y herramientas para el mapeo de molestias (AMIGO, 2019).

4. Normativa aplicable en materia de olores

4.1. Normas técnicas relacionadas con la medición del olor

A nivel internacional, existen numerosas normas técnicas que se relacionan con la medición de olores, sea olor ambiente, la determinación de su intensidad, la determinación de umbrales de olor, paneles en campo, olfatometría dinámica y el entrenamiento de panelistas, entre otros. En la **Tabla 4.1.1** se enumeran algunas de las más relevantes.

Tabla 4.1.1. Normas técnicas internacionales y campos de aplicación (ECOTEC, 2013).

Campo de aplicación	ASTM*	ISO*/EN*	VDI*	Otras
Determinación del umbral de olor	ASTM E679		VDI 3881	
Determinación de la intensidad de olor	ASTM E544		VDI 3882-1	
Selección y entrenamiento de panelistas		ISO 5496 ISO 8586 EN 13725	VDI 3940	NCh* 3190
Muestreo			VDI 3880	
Olfatometría dinámica	ASTM E679	EN 13725		NVN* 2820 AS/NZS* 4323.3 NCh* 3190
Paneles de terreno		prEN 264086	VDI 3940	
Encuestas			VDI 3883	

*ASTM: American Society for Testing and Materials; ISO: International Organization for Standardization; EN: European Standard; VDI: Verein Deutscher Ingenieure; NVN: Netherlands Normalization Institute; AS/NZS: Standards Australia and Standards New Zealand; NCh: Normas Chilenas del Instituto Nacional de Normalización.

4.1.1. Olfatometría dinámica (EN 13725)

El paso más significativo hacia la estandarización de la olfatometría en Europa fue la introducción, en 2003, de la **Norma Europea EN 13725** "*Calidad del aire: determinación de la concentración de olor por olfatometría dinámica*", que se ocupa de varios aspectos de la medición, como los procedimientos y materiales de muestreo, la presentación de muestras a los evaluadores, el registro de datos, el cálculo y la presentación de informes y los requisitos de calidad de la ejecución. Es importante destacar que en 2022 la citada norma ha sido actualizada ("*Emisiones de fuentes estacionarias. Determinación de la concentración de olor por olfatometría dinámica y tasa de emisión de olor*"), con algunos cambios técnicos significativos que se recogen en su Anexo N. Sin embargo, la versión de 2003 es la que se ha tomado como referencia en la realización de la presente Tesis Doctoral.

Según el apartado 5.1 del Estándar Europeo EN 13725 (2003), "*el requisito más importante se refiere a los criterios de calidad para el funcionamiento completo del método de medida sensorial. Estos requisitos se enfocan a la evaluación de la calidad dentro del laboratorio, usando un material de referencia*". Los criterios de calidad que un laboratorio debe tener para cumplir la citada norma se definen en base a parámetros que describen la exactitud y la precisión. En el caso que nos ocupa, los requisitos de calidad son los siguientes:

- **Requisitos de calidad en el análisis sensorial**. Para asegurar la calidad de la medida de la concentración de olor, se deben calibrar los dos elementos más importantes que intervienen en la medición: las diluciones que realiza el olfatómetro y la sensibilidad olfativa de los panelistas.
- **Calibración de panelistas**. Dado que el umbral de olor puede llegar a ser muy diferente entre distintas personas, la norma, en su apartado 6.7.2 y anexo E, define rigurosamente un protocolo de selección de individuos utilizando un gas de referencia, el **n-butanol** en nitrógeno (con una incertidumbre expandida inferior al 5%). En este contexto, el laboratorio olfatométrico debe determinar el umbral para el n-butanol de los evaluadores potenciales a través de al menos diez ensayos recogidos en tres días no consecutivos entre sesiones. Para convertirse en un panelista, la persona debe cumplir con los siguientes requisitos:

  - La **media geométrica de las estimaciones de umbral individual**, expresada en unidades de concentración de masas del gas de referencia, debe estar en un intervalo entre los **20-80 ppb**.
  - El **antilogaritmo de la desviación estándar**, calculada a partir de los logaritmos de las estimaciones de umbral individual, debe ser **inferior a 2,3**.

- **Calibración del olfatómetro**. La calibración del olfatómetro (apartado 6.5.5 y anexo C de la norma) debe realizarse regularmente (al menos una vez al año), usando un material trazador adecuado, por ejemplo, monóxido de carbono, y una incertidumbre inferior al 3%, así como un método de análisis fisicoquímico, por ejemplo, un medidor de infrarrojos en continuo. Para cada una de las diluciones que ofrece el equipo se determina la exactitud, precisión e inestabilidad.
- **Ambiente de la sala de olfatometría**. Según se indica en el apartado 6.6.1 de la norma, "*el ambiente de trabajo para los panelistas debe ser agradable e inodoro. Debe evitarse cualquier emisión de olor del equipo, muebles y materiales instalados (pinturas, recubrimientos del suelo, etc.) en el interior de la sala, así como cualquier liberación de los componentes olorosos a medir*". Además, "*las fluctuaciones de temperatura durante el proceso de medida deben ser inferiores a ± 3ºC, y la temperatura máxima en la habitación no debe superar los 25ºC*". Asimismo, "*debe evitarse la exposición directa de los panelistas a la luz solar y la habitación debe estar exenta de cualquier fuente de ruido y luz, que podrían afectar negativamente las medidas*". Según se indica en el apartado 6.6.2, "*la sala de mediciones de olor debe estar ventilada para mantener un ambiente inodoro y proporcionar aire fresco a los miembros del panel. Para mantener un ambiente de trabajo confortable la fracción en volumen de CO_2 debe ser inferior a 0,15%. El aire de la habitación debe estar ventilado y pasado a través de un filtro de carbón activo antes de entrar en la habitación*".
- **Código de comportamiento de los miembros del panel y calibración diaria**. Los panelistas, de acuerdo con en el apartado 6.7.1 de la norma, deben tener al menos 16 años y cumplir un código de comportamiento: motivación en su trabajo, no fumar ni comer ni beber (excepto agua) media hora antes de la prueba, no usar cosméticos ni perfumes, no tomar parte en la prueba si se sufre un resfriado o cualquier enfermedad que afecte a su percepción de olor y no comentar la marcha de la prueba con otros panelistas. Adicionalmente, y conforme se especifica en los

apartados 6.7 y 9.2, en cada sesión de trabajo, y antes del análisis de las muestras, cada panelista debe ser calibrado con n-butanol con objeto de evaluar su idoneidad. Si por cualquier motivo (resfriado, rinitis, etc.) un panelista no cumple con esta calibración diaria, se debe reemplazar por otro panelista. Por último, para cada una de las muestras analizadas y con los resultados de los panelistas que han superado la calibración previa, se hace el estudio de las "Z-score" (denominado "estudio retrospectivo" en la norma), con objeto de descartar resultados con desviaciones elevadas frente al valor medio. En este sentido, la concentración de olor resultante de una muestra debe ser la media geométrica de la concentración de olor determinada por cuatro panelistas diferentes (que hayan superado la calibración y el estudio retrospectivo).

4.2. Legislación internacional sobre contaminación por olores

A nivel internacional, existen diferentes estrategias a la hora de regular la contaminación ambiental por olores, las cuales se pueden resumir en el siguiente decálogo (Bokowa et al., 2021):

1. Establecimiento de un marco legal basado en leyes que eviten molestias o de protección de la "calidad de vida".
2. Establecimiento de valores límite de concentración y emisión para compuestos químicos (H_2S, NH_3, ácidos orgánicos, hidrocarburos aromáticos, etc.).
3. Establecimiento de valores límite de concentración de olor en inmisión utilizando la olfatometría dinámica.
4. Establecimiento de frecuencia y duración de los episodios problemáticos.
5. Establecimiento de distancias mínimas de separación.
6. Establecimiento de una escala de graduación de olor.
7. Establecimiento del índice de olor.
8. Establecimiento del registro de quejas (umbral de quejas).
9. Establecimiento de criterios cuantitativos de emisión (olor o compuestos químicos).
10. Establecimiento de criterios de utilización de tecnología innovadora (desodorización y manual de buenas prácticas).

En los países de la Unión Europea, el olor es regulado a través de la **Directiva 2010/75/UE** del Parlamento Europeo y del Consejo, de 24 de noviembre de 2010, sobre

las emisiones industriales. Esta Directiva establece un marco general para determinar los límites, incluidos los de olor, para muchas actividades/procesos industriales, al objeto de controlar, entre otros, las emisiones odoríferas. De esta manera, se cubren sectores como las industrias energéticas, la producción y transformación de metales, las industrias minerales, la industria química, la gestión de residuos y otros que se detallan específicamente en su Anexo I.

Dicha norma comunitaria establece que las instalaciones deben operar solo si tienen un permiso por escrito o, en ciertos casos, si están registradas. Las condiciones del permiso están definidas para lograr un alto nivel de protección para el medio ambiente y comúnmente se basan en el concepto de la mejor técnica disponible (**MTD**). Para determinar las MTD y limitar los desequilibrios en los países de la Unión Europea con respecto al nivel de emisiones de las actividades industriales, se elaboran documentos de referencia para las MTD, denominados **BREF**. Hasta la fecha, se han publicado más de 30 documentos BREF relacionados con diferentes sectores. Ahora, los nuevos BREF también incluyen niveles de emisión asociados a la mejor técnica disponible (**NEA-MTD**), definiéndose un rango de límites de emisión para cualquier instalación que solicite un permiso (Bokowa et al., 2021). Actualmente, el único BREF europeo que establece un límite de olor es el recientemente publicado **BREF de Tratamiento de Residuos** (*Waste Treatment BREF*), que establece un rango de **200 a 1.000 ou_E/Nm^3** (media a lo largo del periodo de muestreo) para algunas MTD relacionadas con el tratamiento biológico de residuos (Decisión de ejecución (UE) 2018/1147 de la Comisión, de 10 de agosto de 2018). Es importante destacar que los BREF no son prescriptivos ni exhaustivos. Los BREF no tienen en cuenta las condiciones locales, por lo que su aplicación no exime a las autoridades de los países miembros de la Unión Europea de la obligación de emitir juicios específicos del lugar. Esto significa que, durante el procedimiento de autorización de una determinada actividad, la autoridad responsable no sólo debe tener en cuenta toda la información proporcionada por el BREF, sino también las condiciones locales para establecer un límite de olor.

Otros documentos y directrices legalmente vinculantes relacionados con los olores se encuentran disponibles en algunos países europeos. Estas regulaciones sobre olores se utilizan cuando no se establecen criterios específicos en un BREF, o cuando la Directiva 2010/75/UE no cubre la actividad generadora de olores.

A diferencia de España (donde sólo existen algunas ordenanzas municipales), en diversos países como Alemania, Australia, Bélgica, Canadá, Chile, China, Colombia, Estados Unidos, Francia, Italia, Japón, Nueva Zelanda o Países Bajos, ya existe una regulación sólida en materia de contaminación odorífera. En este sentido, la **Tabla 4.2.1** muestra una breve revisión relativa a cómo se aplican las regulaciones de olores en los diferentes países mencionados anteriormente. Para una información más detallada de la situación en estos y otros países, la publicación de Bokowa et al. (2021) realiza una amplia revisión relativa a normas, políticas y/o guías específicas que se aplican a la hora de evaluar la contaminación ambiental por olores en los diferentes países.

Tabla 4.2.1. Breve resumen sobre la regulación de la contaminación odorífera a nivel internacional (Izquierdo et al., 2021).

País	Legislación sobre olores existente	¿En qué se basa?	¿A qué actividades generadoras de olor afecta?
Alemania	Nacional	Olfatometría dinámica + modelado	Todas. Especial atención a las actividades ganaderas y el tratamiento biológico de residuos
Australia	Regional	Olfatometría dinámica + modelado o sensibilidades poblacionales	Todas
Bélgica	Nacional y regional	Olfatometría dinámica + modelado o inspecciones de campo	Plantas de compostaje y granjas en Valonia. Mataderos y EDAR en Flandes
Canadá	Regional	Olfatometría dinámica + modelado	Todo tipo de negocios. Instalaciones de fritura de alimentos o plantas de tostado de café para la región de Quebec

Chile	Nacional	Olfatometría dinámica + modelado	Granjas porcinas
China	Nacional	Olfatometría dinámica	Todas. Normas específicas para la cría de ganado y aves de corral
Colombia	Nacional	Olfatometría dinámica + modelado	Todas
España	Local	Olfatometría dinámica + modelado; otros	Depende de las ordenanzas locales
Estados Unidos	Regional y local	Olfatometría de campo (D/T); quejas ciudadanas	Todo tipo de actividades. Especial atención a la agricultura
Francia	Nacional	Olfatometría dinámica + modelado u olfatometría dinámica	Plantas de procesamiento de subproductos animales, plantas de compostaje e industria de procesamiento de alimentos y bebidas
Italia	Regional	Olfatometría dinámica + modelado	Todas
Japón	Nacional	Olfatometría dinámica	Todas
Nueva Zelanda	Nacional	Olfatometría dinámica + modelado o sensibilidades poblacionales	Todas
Países Bajos	Nacional y regional	Olfatometría dinámica + modelado	Actividades ganaderas

4.3. Legislación nacional sobre contaminación por olores

España, como país miembro de la Unión Europea, tiene una regulación general de olores basada en la Directiva 2010/75/UE para cualquier actividad incluida en esta norma. La **Ley 5/2013** y el **Real Decreto 815/2013** realizaron la transposición de la mencionada Directiva al ordenamiento jurídico español. A nivel nacional, las competencias de la Directiva 2010/75/UE residen en las Comunidades Autónomas. En este contexto, **Andalucía**, por ejemplo, cuenta con el **Decreto 239/2011**, que en su artículo n.º 19 hace referencia al procedimiento a seguir en el caso de actividades que produzcan olores. De forma general, el procedimiento consiste en establecer límites de olor del aire ambiente para actividades industriales, teniendo en cuenta las siguientes consideraciones (Bokowa et al., 2021):

- La instalación / actividad (nueva o existente) solicita la obtención de un permiso.
- La administración ambiental competente evalúa si existe preocupación por malos olores y, si es necesario, se solicita una evaluación del olor.
- No existe una guía para la toma de decisiones sobre los resultados de las evaluaciones de olores. El resultado depende completamente del funcionario ambiental asignado al caso.
- Una vez completada la evaluación de olores (en caso de realizarse), el funcionario ambiental establece los criterios de impacto por olor, que generalmente se basan en los resultados de la evaluación.

En junio de 2005, Cataluña presentó el **Borrador del Anteproyecto de Ley contra la contaminación odorífera**. Este documento estaba inspirado en la guía horizontal de olores del Reino Unido *H4 Odour Management* y su propósito era regular y controlar la contaminación por olores mediante el establecimiento de normas técnicas para la realización de estudios de impacto ambiental, niveles límite, régimen sancionador, etc. Este Borrador de Anteproyecto nunca fue aprobado, pero fue tomado como referencia por muchos consultores de olor en España. Para los **sistemas de saneamiento de aguas residuales**, el Anteproyecto fijaba un valor objetivo de **inmisión** (percentil 98 de las medias horarias durante un año) de **5 ou_E/m^3**.

En febrero de 2019, la Comunidad Autónoma de Canarias sometió a los trámites de información pública y audiencia el **Proyecto de Decreto de protección de la atmósfera de Canarias**. Sin embargo, los cambios políticos en el gobierno impidieron la publicación

de esta regulación, que también fijaba valores objetivo de inmisión de olor por categorías para las actividades generadoras de olor. En este caso, el "**tratamiento de aguas residuales e instalaciones accesorias**" formaba parte de la categoría 1 (nivel de molestia alto), estableciéndose un valor objetivo de **inmisión** de olor de **3 ou_E/m^3** para esta categoría.

Por otro lado, es importante destacar que los **ayuntamientos** tienen también competencias plenas para regular problemas de contaminación acústica y por olores. Sin embargo, los municipios que cuentan con **ordenanzas específicas** para regular la contaminación odorífera no superan la decena a nivel nacional. Con mayor o menor acierto, en tales ordenanzas se han establecido métodos de diagnóstico del problema, niveles de cumplimiento, régimen sancionador, etc. (AMIGO, 2019). Cabe destacar el caso de Las Palmas de Gran Canaria (Ordenanza Municipal de protección de la atmósfera frente a la contaminación por formas de la materia de 1999), que de igual manera a San Vicente del Raspeig (Ordenanza de protección de la atmósfera de 1994), ha desarrollado un **índice de percepción de olor** (IP), quedando prohibida la emisión de sustancias olorosas en cantidades tales que supongan, en el límite de la propiedad, un índice de percepción superior a 0,04. Según las citadas Ordenanzas Municipales, el IP se calcula mediante la siguiente ecuación:

$$IP = log_{10}(C) \cdot FC \cdot FD \cdot FI \cdot FP \cdot FV$$

donde *C* es la concentración de olor, *FC* es el factor de calidad de olor, *FD* es el factor de duración de emisión, *FI* es el factor de intermitencia, *FP* es el factor de periodo de emisión y *FV* es el factor de dirección del viento. La definición y evaluación de los factores indicados se expresa en el Anexo V de la Ordenanza Municipal de San Vicente del Raspeig y en el Anexo VI en el caso homólogo de Las Palmas de Gran Canaria.

Todo lo expuesto anteriormente permite concluir que en España todavía **no existe una legislación estatal específica** que unifique, regule o limite las emisiones de olor, aunque existen propuestas que han abordado la problemática a nivel local o autonómico. Actualmente, la mayoría de los conflictos pasan por un tratamiento mediático carente de rigor científico que en ocasiones acaba en los tribunales, los cuales tampoco disponen de herramientas suficientes en las que basar sus juicios. De esta forma, se generan litigios prolongados que son perjudiciales tanto para los ciudadanos como para los gestores de las instalaciones causantes de malos olores (Iglesias, 2014). En todo caso, para los gases

considerados como predominantes en los procesos de saneamiento y depuración (**H_2S y NH_3**), se dispone de **límites de seguridad** establecidos por el **Instituto Nacional de Seguridad y Salud en el Trabajo** (INSST), los cuales se deben tomar como referencia en la gestión de olores (**Tabla 4.3.1**).

Tabla 4.3.1. Límites de seguridad ocupacional para H_2S y NH_3 (INSST, 2021).

Gas	VLA-ED[1]		VLA-EC[2]	
	(ppm)	(mg/m^3)	(ppm)	(mg/m^3)
H_2S	5	7	10	14
NH_3	20	14	50	36

[1]VLA-ED: Valor Límite Ambiental - Exposición Diaria. La mayoría de los trabajadores pueden estar expuestos 8 horas diarias y 40 horas semanales durante toda su vida laboral, sin sufrir efectos adversos para su salud.

[2]VLA-EC: Valor Límite Ambiental - Exposición de Corta Duración. La concentración media del agente químico en la zona de respiración del trabajador, medida o calculada para cualquier período de 15 minutos a lo largo de la jornada laboral.

5. Estrategias para el control del olor

El control de olores derivados del saneamiento y depuración de las aguas residuales engloba la prevención de la formación y emisión de malos olores, la minimización del impacto y las tecnologías de tratamiento de final de línea. Entre las citadas estrategias para el control de olor, la prevención de la formación y emisión de olores debe considerarse prioritaria al tratamiento o la minimización del impacto, ya que a menudo la prevención constituye una alternativa más simple y económica en comparación con las últimas (Capodaglio et al., 2002; Estrada et al., 2015; Talaiekhozani et al., 2016; Tchobanoglous et al., 2003).

5.1. Prevención de la formación y emisión de olores

La prevención de olores incluye una combinación de diseño y prácticas de operación eficientes, así como la contención de olores mediante la instalación de cubiertas de proceso. En este contexto, la **prevención de la formación de olores en las redes de alcantarillado** resulta de gran importancia, ya que la mayoría de los compuestos odoríferos que se emiten desde las EDAR tienen su origen en las condiciones de septicidad (ausencia de O_2 y NO_3^-) que se dan en las redes de saneamiento de aguas residuales. De hecho, generalmente resulta difícil prevenir la formación de emisiones

odoríferas en los sistemas de alcantarillado, como es el caso particular de los sulfuros, que se generan como resultado de los diseños ya existentes y la elevada concentración de materia orgánica presente en las aguas residuales. En este sentido, es importante destacar que los cambios físicos en la red de saneamiento para reducir este tipo de emisiones requieren de una elevada inversión económica (Lebrero et al., 2011). Por tanto, los esfuerzos deben dirigirse al diseño adecuado de las redes de alcantarillado en lugar de a su costosa modificación posterior. Si no se puede actuar sobre el diseño de la red, otra opción consiste en minimizar la formación y emisión de malos olores, bien previniendo la producción de sulfuros mediante la adición de NO_3^-, O_2, ozono, etc., o bien evitando su emisión a través de su precipitación química mediante la adición de sales de hierro, como el cloruro férrico (Lebrero et al., 2011; WEF, 2017).

En las EDAR, la prevención de la formación de olores implica principalmente **buenas prácticas de operación**, como la limpieza periódica de rejas y canales, la minimización del tiempo de retención del fango en espesadores o unidades de deshidratación y el aseguramiento de una correcta aireación y un mezclado adecuado del licor de mezcla, entre otras. La reducción de las emisiones odoríferas también puede lograrse mediante un diseño correcto de la instalación (evitando o reduciendo saltos de agua que favorezcan la liberación de los compuestos volátiles desde el agua residual) y la instalación de cubiertas. El **empleo de cubiertas** (de bajo y alto nivel) evita la emisión en el caso de las fuentes pasivas, al reducir de forma notable el movimiento natural del aire sobre la fuente, y en el caso de las fuentes activas permite concentrar y conducir la emisión odorífera hasta el sistema de tratamiento de final de línea (AMIGO, 2019). Sin embargo, a pesar de la amplia gama de medidas disponibles para minimizar las emisiones odoríferas, no siempre es posible una reducción completa de la formación y liberación de olores (Lebrero et al., 2011).

5.2. Minimización del impacto

La implementación de **zonas buffer** o de amortiguamiento (separación entre la fuente de olor y la población potencialmente afectada), **estructuras inductoras de turbulencia** (como árboles o barreras de alto nivel) o **chimeneas** pueden conseguir una disminución de la emisión odorífera y reducir la concentración de olor, con la consiguiente reducción del impacto oloroso (Tchobanoglous et al., 2003). Por otra parte, el uso de **agentes enmascarantes**, **inhibidores** o **neutralizadores** también puede contribuir a mitigar las molestias por malos olores en las áreas circundantes a las EDAR.

Estos agentes, constituidos principalmente por terpenos, aldehídos alifáticos y aromáticos, y alcoholes, se aplican mediante pulverización con aire, mezcla o aplicación directa en superficie y tienen por objeto enmascarar, inhibir o neutralizar el tono hedónico desagradable inherente a la emisión. En este contexto, es importante destacar que esta opción sólo constituye una alternativa temporal para el control de olores en escenarios en los que la implementación de una técnica de tratamiento es compleja, como emisiones difusas o fuentes con tasas de emisión de olor muy variables (Bruchet et al., 2008; Decottignies et al., 2007).

5.3. Tratamiento de final de línea

Cuando la prevención de la formación y emisión de olores o la minimización del impacto odorífero no son suficientes para evitar molestias o cumplir con los límites de las regulaciones existentes, resulta necesaria la aplicación de tecnologías de tratamiento de final de línea al objeto de reducir la concentración de los compuestos odoríferos a niveles aceptables para su descarga. La selección de la tecnología más rentable para cada caso específico de contaminación por olores está determinada por la naturaleza y concentración de los odorantes, el caudal de aire a tratar, el nivel de eficacia requerido o el tipo de fuentes (activas o pasivas), entre otros (Lebrero et al., 2011). En este sentido, la **Figura 5.3.1** muestra un ejemplo de las diferentes tecnologías que podrían seleccionarse en función de la concentración de compuestos y el flujo de aire a tratar.

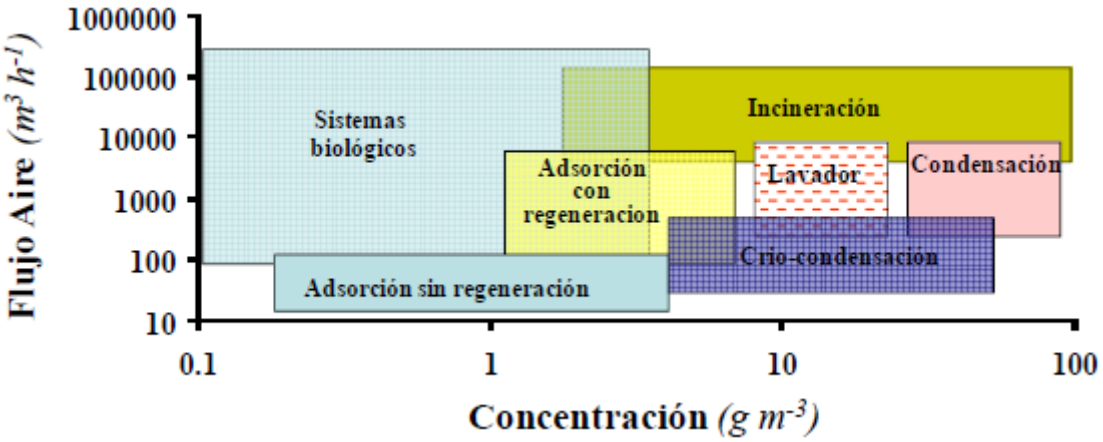

Figura 5.3.1. Rangos de aplicación de tecnologías de eliminación de contaminantes gaseosos (Muñoz, 2010b).

Entre las tecnologías de tratamiento de emisiones odoríferas, se distinguen dos tipos principales dependiendo del mecanismo empleado para la eliminación de los

contaminantes: **fisicoquímico** o **biológico** (AMIGO, 2019; Ren et al., 2019; Senatore et al., 2021). En base a esta clasificación, se realiza a continuación una revisión de los sistemas más comunes de tratamiento que se pueden implementar en las EDAR.

5.3.1. Sistemas de tratamiento fisicoquímico

Entre las diferentes tecnologías de tratamiento fisicoquímico, los sistemas de lavado químico (*scrubber*) y los sistemas de adsorción son los más extendidos en las EDAR (Lebrero et al., 2011).

Sistemas de lavado químico

Los lavadores químicos se encuentran entre las tecnologías de eliminación más comúnmente empleadas para la eliminación de olores en EDAR, debido a la amplia experiencia en su diseño y operación, los bajos tiempos de residencia del gas (1,0-2,5 s) y su alta robustez cuando se operan de forma correcta (Card, 2001; Gabriel y Deshusses, 2004). En estos sistemas, **los contaminantes odoríferos son transferidos desde la corriente gaseosa a una fase líquida** (a menudo ácido sulfúrico o hidróxido de sodio, dependiendo de los compuestos a eliminar), donde son posteriormente destruidos por reacción química. La velocidad de transferencia se encuentra determinada por la concentración del odorante en la fase gas y en la fase líquida, por el coeficiente de partición aire/agua del compuesto odorífero (ley de Henry) y por la resistencia al transporte de materia del sistema (Revah y Morgan-Sagastume, 2005).

La absorción química puede llevarse a cabo en torres de absorción o lavadores químicos (**Figura 5.3.1.1**), ya sea en configuraciones de contracorriente o flujo cruzado, o en cámaras de neblina (opción menos frecuente), utilizando hipoclorito de sodio, hidróxido de sodio, permanganato potásico o peróxido de hidrógeno como oxidantes, dependiendo del compuesto mayoritario. Las **torres de absorción o lavadores** son columnas verticales donde el flujo de aire contaminado se pone en contacto con un flujo descendente de solución acuosa, que es bombeada desde un depósito situado en la parte inferior de la torre. Por su parte, las **cámaras de neblina** presentan una configuración de flujo cruzado, donde la solución oxidante es atomizada sobre la corriente gaseosa maloliente, que atraviesa horizontalmente la cámara (AMIGO, 2019).

La **eficacia de eliminación** de los sistemas de lavado químico depende fundamentalmente de la solubilidad de los compuestos a eliminar, siendo de

aproximadamente el 98% para sulfuro de hidrógeno y amoniaco, 95 y 90% para dióxido de azufre y mercaptanos, respectivamente, y entre 70 y 90% para otros compuestos oxidables como los COV (Sanchez et al., 2006; Tchobanoglous et al., 2003).

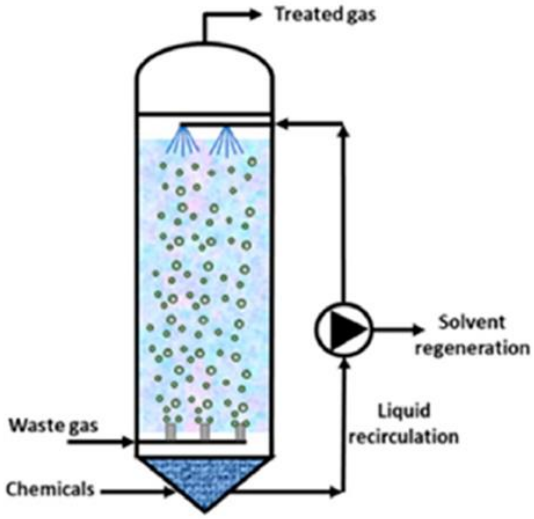

Figura 5.3.1.1. Esquema de funcionamiento de un lavador químico (Senatore et al., 2021).

Sistemas de adsorción

Desde el punto de vista de la composición química, los adsorbentes pueden clasificarse en materiales carbonosos (fundamentalmente carbones activados) y materiales inorgánicos. Sin embargo, la capacidad de eliminación para H_2S de materiales inorgánicos tales como alúmina, zeolitas, sílice o varios óxidos inorgánicos se encuentra bastante alejada de los valores obtenidos mediante carbones activados. Además, los citados materiales inorgánicos presentan bajas eficacias de eliminación de COV a los bajos niveles de concentración que caracterizan las emisiones odoríferas. Por estas razones, en el tratamiento de los olores es frecuente asociar la adsorción a la utilización de **carbones activados** (Martin et al., 2010; Ren et al., 2019).

El término carbón activado hace referencia a un gran número de materiales carbonosos, los cuales se caracterizan por presentar **elevadas áreas específicas** (hasta 2.000 m^2/g) y **altas porosidades** (hasta 1 mL/g), con poros cuyo diámetro va desde unos pocos hasta varios cientos de Angstroms (AMIGO, 2019). Casi todos los materiales con un alto contenido en carbón pueden servir como materia prima para la fabricación de

carbón activado, aunque de forma mayoritaria se producen a partir de distintos grados de carbón mineral, cáscara de coco o madera. Dependiendo de las características del material de partida y de las propiedades finales deseadas, el desarrollo de la porosidad se puede conseguir mediante dos métodos diferentes (Martin et al., 2010):

- **Activación química**: Consiste en mezclar una sustancia deshidratante (generalmente ácido fosfórico) con la materia prima, sometiendo la mezcla a un tratamiento térmico (con temperaturas inferiores a 700°C), seguido de un proceso de lavado con el fin de eliminar el agente activante residual.
- **Activación física**: Consta de dos etapas: carbonización del precursor carbonoso y posterior activación mediante un proceso de gasificación parcial a altas temperaturas (800-1.000ºC), en presencia de un agente activante como dióxido de carbono, vapor de agua, oxígeno o bien una combinación de ellos.

La activación conduce al desarrollo de la estructura porosa característica de los carbones activados, así como a la formación de funcionalidades químicas en los bordes de los planos grafíticos. La tipología y cantidad de grupos funcionales superficiales va a depender de la materia prima de partida y del tratamiento de activación. Debido al carácter general apolar de la superficie, los carbones activados adsorben compuestos orgánicos y algunos inorgánicos (con preferencia al vapor de agua), de tal manera que la cantidad adsorbida depende parcialmente de las características físicas y químicas del compuesto. En general, COV de elevado peso molecular y altos puntos de ebullición se adsorberán más fácilmente (Le-Minh et al., 2018). La **capacidad de adsorción** de un carbón activado puede alcanzar entre 5-40% del peso del adsorbente, dependiendo de los siguientes **factores** (Le-Minh et al., 2018; Martin et al., 2010):

- Concentración del adsorbato en la proximidad de la superficie del carbón activado.
- Características fisicoquímicas de la sustancia a eliminar (polaridad, peso molecular, punto de ebullición, estructura o tamaño).
- Presencia de otros compuestos y humedad relativa de la corriente gaseosa a tratar.
- Superficie total y volumen de poro disponible del adsorbente.
- Polaridad del carbón activado.
- Temperatura.
- Tiempo de contacto.

En términos generales, la capacidad de adsorción se ve favorecida por una elevada concentración del adsorbato, ausencia de sustancias competitivas, baja temperatura y humedad relativa, y elevados valores de áreas superficiales y volúmenes de poro del adsorbente.

Con el objetivo de mejorar las eficacias de eliminación (de compuestos inorgánicos sobre todo), los carbones, una vez activados, pueden ser impregnados con algún reactivo o con algún catalizador (metales pesados) para incrementar la selectividad de la eliminación y/o acelerar las reacciones deseadas (AMIGO, 2019). En los sistemas de adsorción que se implementan en las EDAR, es frecuente el empleo de **carbones activados impregnados con NaOH o KOH**, formando por reacción con el CO_2 atmosférico, los correspondientes carbonatos. Tales componentes básicos facilitan la transferencia del sulfuro de hidrógeno hacia la fase sólida, a la vez que favorecen los procesos de oxidación a azufre elemental como subproducto mayoritario y, en menor medida, a sulfatos y dióxido de azufre (Ren et al., 2019). Con la impregnación alcalina, las capacidades de eliminación para sulfuro de hidrógeno y metil mercaptano se sitúan en porcentajes del 25 al 27% en peso, frente a valores del 3-5% en peso en el caso de los carbones vírgenes (Martin et al., 2010).

Los sistemas de adsorción para el control de olores en EDAR consisten generalmente en **lechos estáticos de carbón activado granular** (CAG), contenidos en columnas cilíndricas verticales (**Figura 5.3.1.2**). Dichos lechos suelen emplear hasta un máximo de 10.000 kg de CAG (Turk y Bandosz, 2001), siendo algunos valores típicos de diseño y operación los siguientes (U.S. Environmental Protection Agency [US EPA], 1985): alturas de lecho de hasta un metro, velocidades lineales de 15-25 m/min y tiempos de contacto de 0,25-2,00 s. La adsorción con carbón activado es un sistema no selectivo, altamente versátil, por lo que se puede utilizar como única etapa de tratamiento (lo que es habitual en EDAR de pequeño tamaño), o bien como etapa final de afinado en sistemas de eliminación de olores más complejos que incluyan operaciones biológicas o de lavado químico (Martin et al., 2010; Ren et al., 2019; Senatore et al., 2021). En este contexto, es importante destacar que los sistemas de adsorción con CAG presentan elevadas **eficacias de eliminación** de olor y compuestos hidrofóbicos, entre 90 y 99% (AMIGO, 2019). Sin embargo, a pesar de la extendida aplicación del carbón activado para la reducción del impacto odorífero, no siempre se obtienen las eficacias previstas, lo que resulta en problemas prematuros de operación que acaban provocando impactos por olor en los

receptores cercanos (Shammay et al., 2016a, 2016b; Wang et al., 2014). Dado que el rendimiento de estos sistemas se establece principalmente en la etapa de diseño y las prácticas de diseño se basan fundamentalmente en relaciones empíricas y pruebas piloto, se requieren conocimientos fundamentales adicionales para evitar este tipo de problemas, atendiendo en gran medida a todos los factores que afectan a la capacidad de adsorción de los carbones activados y que se han mencionado con anterioridad (Le-Minh et al., 2018; Shammay et al., 2016a).

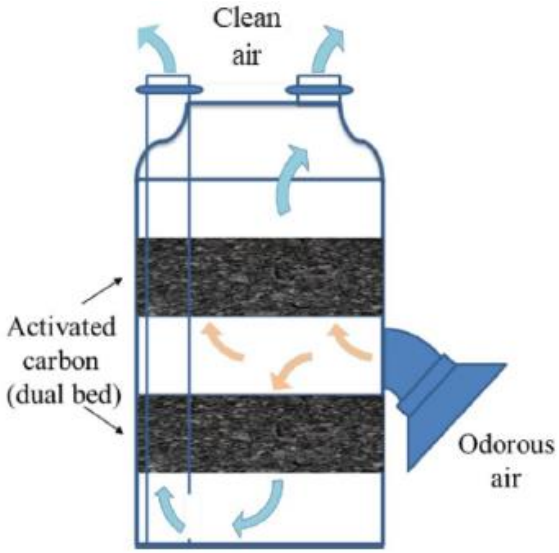

Figura 5.3.1.2. Esquema de funcionamiento de una torre de CAG (Ren et al., 2019).

La **selección del CAG idóneo** para el tratamiento de olores en EDAR suele basarse en su eficacia para el control del sulfuro de hidrógeno, siendo este gas utilizado como medida subrogada, de fácil medición, de la problemática de olores. Por otra parte, el reemplazo de los lechos de CAG suele basarse en la experiencia, ya que los fabricantes de CAG no suelen garantizar la vida útil de este adsorbente en las aplicaciones de desodorización en EDAR (Estrada et al., 2011; Martin et al., 2010; Ren et al., 2019). En este contexto, tanto la eficacia de eliminación de olores como el **reemplazo de los lechos** a menudo se basan también en la **eliminación de H_2S**. Sin embargo, la desodorización de efluentes gaseosos de las EDAR requiere la eliminación de una mezcla compleja de compuestos con una amplia gama de pesos moleculares, volatilidades y funcionalidades químicas. En estas condiciones, el potencial de olor puede verse afectado por efectos antagónicos o inhibitorios, de modo que no resulta sencillo establecer una correlación entre la concentración medida analítica o instrumentalmente y la percepción sensorial.

Por tanto, se deben combinar mediciones analíticas y sensoriales para el diseño óptimo de las operaciones de adsorción con CAG (Martin et al., 2010).

El principal inconveniente de la desodorización basada en la adsorción con CAG es que este sistema presenta altos requerimientos anuales de material adsorbente, lo que se debe a su **corta vida útil**, que generalmente oscila entre seis y nueve meses (AMIGO, 2019; Estrada et al., 2011). Cuando se utilizan tecnologías híbridas, por ejemplo un biolavador seguido de un sistema de adsorción con carbón activado, se genera un menor impacto ambiental en comparación con la filtración convencional con CAG, como resultado del reemplazo bianual del material adsorbente (Estrada et al., 2011). El CAG, una vez concluida su vida útil, se convierte en un **residuo industrial peligroso** con código LER *06 13 02** (Comunicación de la Comisión — Orientaciones técnicas sobre la clasificación de los residuos, 2018/C 124/01), lo que obliga a su **depósito en vertedero** a través de gestores autorizados, operación que conlleva un coste económico y ambiental destacable. Así, tanto los elevados requerimientos de carbón activado como la necesidad de procedimientos específicos para su deposición como residuo peligroso provoca que los sistemas de adsorción mediante CAG presenten **costes de operación bastante elevados** (10-200 €/m^3·h) en comparación con los lavadores químicos (5-6 €/m^3·h) y con otras tecnologías habituales de tratamiento biológico en EDAR, como los biofiltros (2-4 €/m^3·h), los biofiltros percoladores (3-6 €/m^3·h) y los biolavadores (3-5 €/m^3·h) (Senatore et al., 2021). Por tanto, aunque se han realizado importantes esfuerzos dirigidos al desarrollo de diferentes adsorbentes para el tratamiento de olores en EDAR, los altos costes de operación siguen representando un gran inconveniente para una más amplia aplicación ingenieril de los sistemas de adsorción mediante CAG (Ren et al., 2019).

Por los motivos anteriormente descritos, la desodorización mediante CAG constituye **una de las alternativas menos sostenibles** para el tratamiento de emisiones odoríferas (Estrada et al., 2011; Senatore et al., 2021). De este modo, con el objetivo de mejorar la sostenibilidad de los sistemas de adsorción y, por ende, de las EDAR, se hace necesario un cambio en la legislación unido al desarrollo de tecnologías simples y de bajo coste dirigidas a la **regeneración** del CAG, más aun teniendo en cuenta que el tratamiento de las aguas residuales, que incluye la desodorización de las emisiones gaseosas, es un sector sin ánimo de lucro.

5.3.2. Sistemas de tratamiento biológico

Los sistemas de tratamiento biológico para la eliminación de olores se basan en la **oxidación enzimática** de los contaminantes olorosos una vez que estos han sido transferidos desde la corriente gaseosa a una fase acuosa donde se encuentran los **microorganismos** responsables de su biodegradación. En este tipo de sistemas, dichos contaminantes (en su mayoría COV, sulfurados y nitrogenados) son oxidados a compuestos más simples y con menor impacto odorífero, como agua, dióxido de carbono y sales minerales (sulfatos, nitratos, etc.). Como subproductos de esta biodegradación, también se genera nueva biomasa y energía disipada en forma de calor (Barbusinski et al., 2017; Mudliar et al., 2010; Muñoz, 2010b; Revah and Morgan-Sagastume, 2005).

En comparación con las alternativas fisicoquímicas para el tratamiento de olores, las tecnologías con procesos biológicos suelen ser más **respetuosas con el medio ambiente**, pues no requieren el uso de productos químicos nocivos y pueden llevarse a cabo a presión y temperatura ambiente (10-40ºC). Además, los bajos consumos de reactivos químicos (principalmente asociados al control de pH) y de energía, en comparación con los sistemas de lavado químico, filtros de carbón activado, etc., hacen que los sistemas biológicos presenten **menores costes de operación** en comparación con sus homólogos fisicoquímicos (Delhoménie and Heitz, 2005; Prado et al., 2009; Senatore et al., 2021). También es importante destacar la **alta robustez** de los sistemas biológicos de eliminación de olores en EDAR frente a fluctuaciones de carga y temperatura, y fallos de operación como averías en el sistema de irrigación, en el de regulación de pH o paradas de planta, entre otros (Kraakman et al., 2012). Este hecho, unido a las ventajas anteriormente mencionadas, hace que se esté incrementando el uso de los tratamientos biológicos en detrimento de las tecnologías fisicoquímicas convencionales o como parte de tecnologías híbridas (Ren et al., 2019; Senatore et al., 2021). No obstante, como desventaja, los sistemas biológicos presentan unos **mayores requerimientos de terreno** debido a que generalmente operan a tiempos de residencia mayores (2-120 s) que los sistemas fisicoquímicos (1-5 s) (AMIGO, 2019; Stuetz and Frechen, 2001).

La biodegradación de los contaminantes odoríferos (**Figura 5.3.2.1**) se fundamenta en el uso de los mismos como fuente de carbono y/o energía por parte de los microorganismos presentes en el biorreactor a utilizar (Revah y Morgan-Sagastume, 2005). Por un lado, los COV de la corriente gaseosa son utilizados como fuente de carbono para la síntesis de nuevo material celular y como fuente de energía (mediante su

oxidación a H_2O y CO_2, usando como aceptor de electrones el oxígeno que difunde desde la emisión). Por otro lado, odorantes como H_2S y NH_3 son empleados por las comunidades microbianas como fuente de energía (mediante su oxidación a sulfato y nitrato, respectivamente) para sostener un mantenimiento y/o crecimiento celular basado en la asimilación de carbono inorgánico del medio. Para todo ello, es necesario tanto la existencia de un **medio acuoso** que sustente todas las reacciones metabólicas, así como la presencia de **macronutrientes** (nitrógeno, fósforo, potasio, azufre, etc.) y **micronutrientes**, generalmente metales pesados, para la síntesis de enzimas (Barbusinski et al., 2017; Mudliar et al., 2010; Muñoz, 2010b).

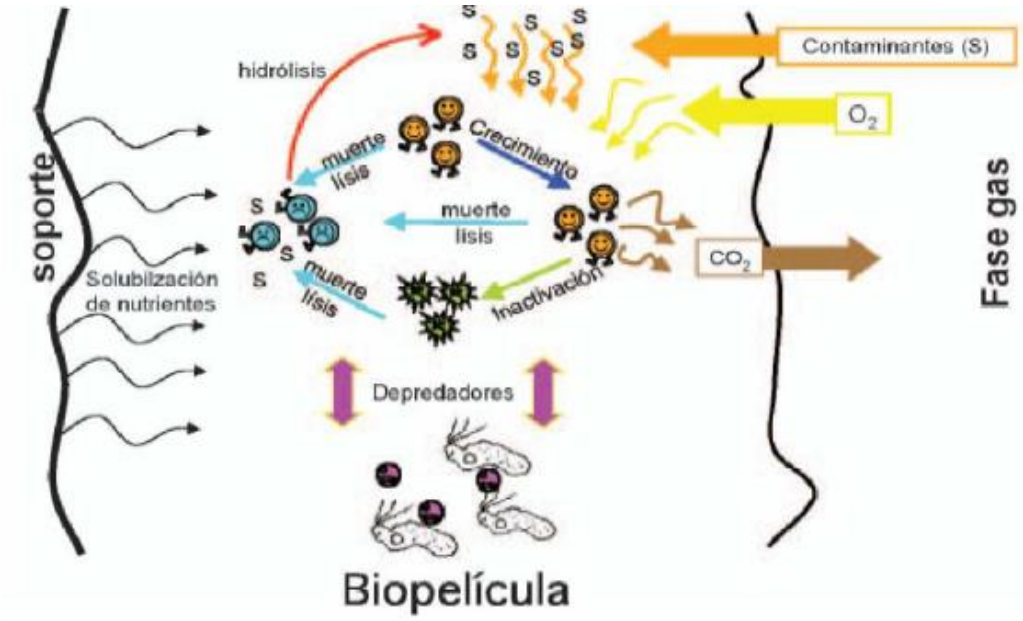

Figura 5.3.2.1. Esquema simplificado del proceso de biodegradación de compuestos odoríferos en los biorreactores de biopelícula (Muñoz, 2010b).

Es destacable que, en la mayoría de los sistemas biológicos de desodorización, las bacterias y también los hongos (en menor medida) constituyen los principales grupos de microorganismos responsables de la eliminación de olores. Las **bacterias** presentan altas tasas de crecimiento y biodegradación y un amplio espectro de compuestos gaseosos a degradar, junto con una alta resistencia a la toxicidad. Sin embargo, su rango de pH óptimo se encuentra en torno a la neutralidad y requieren elevados valores de humedad para un correcto metabolismo celular. En concreto, las bacterias del género *Pseudomonas* se encuentran entre los géneros más comúnmente descritos en biofiltros que eliminan COV. Por su parte, los **hongos** presentan un menor espectro de contaminantes gaseosos a degradar, pero son capaces de soportar condiciones adversas, como bajos valores de pH

(2-5), baja humedad y limitación de nutrientes. Una vez transferidos tales contaminantes desde la corriente gaseosa a la fase acuosa donde residen los microorganismos, estos difunden a través de las paredes y/o membranas celulares hasta el interior de las células, donde tiene lugar su transformación. La **eliminación de los contaminantes** se lleva a cabo mediante reacciones catabólicas en serie, denominadas globalmente **rutas metabólicas**, que tienen como resultado la descomposición de los compuestos odoríferos en metabolitos que pueden entrar en las rutas centrales del metabolismo microbiano. Las mencionadas rutas van a depender tanto del tipo de contaminante a degradar como del tipo de microorganismo, siendo común la existencia de varias rutas metabólicas dentro de una misma especie de bacterias (Barbusinski et al., 2017; Muñoz, 2010b). Por tanto, el conocimiento de la comunidad bacteriana en los sistemas de tratamiento biológico y su dinámica es fundamental para comprender los procesos que tienen lugar en ellos (Allievi et al., 2018). En este contexto, dado que la gran mayoría de los microbios presentes en entornos naturales no son cultivables, la **secuenciación del ARNr 16S** ha demostrado ser un método eficaz para revelar la composición, estructura y/o diversidad de las comunidades bacterianas (Delgado-Baquerizo et al., 2018). Además, la predicción funcional se puede inferir de la microbiota identificada, aumentando la comprensión de su potencial de biodegradación (Lin et al., 2021). Sin embargo, hasta la fecha, se desconocen en gran medida los efectos de los compuestos odoríferos en la estructura de la comunidad microbiana de los sistemas biológicos de tratamiento de olores.

En dicho contexto, los sistemas de tratamiento biológico más implementados en EDAR se pueden clasificar en función del estado de la biomasa y de la fase acuosa (Muñoz, 2010b). Así, si la **biomasa** se encuentra en forma de **biopelícula** (*biofilm*), se puede distinguir entre biofiltros (fase acuosa fija) y biofiltros percoladores (fase acuosa en recirculación), mientras que si la biomasa se encuentra **en suspensión**, es posible distinguir entre biolavadores y sistemas de difusión en lodos activos. Al tratarse de sistemas biológicos, todos ellos son eficaces para tratar elevados caudales de aire contaminado con bajas concentraciones de compuestos olorosos (Mudliar et al., 2010; Muñoz, 2010b).

Biofiltros

En los biofiltros, la circulación del aire contaminado es forzada a través de un **lecho fijo** (o empacado), que contiene la comunidad microbiana responsable de la mineralización de los contaminantes odoríferos (**Figura 5.3.2.2**). El mencionado lecho

sirve de soporte (y en algunos casos de fuente de nutrientes) para la adhesión de una **biopelícula** de naturaleza acuosa, que es realmente la responsable de la biodegradación de los contaminantes olorosos que difunden desde la corriente gaseosa (AMIGO, 2019; Muñoz, 2010b).

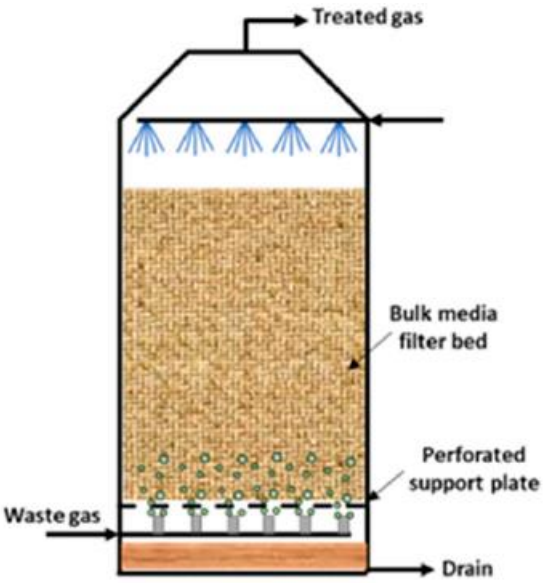

Figura 5.3.2.2. Esquema de funcionamiento de un biofiltro (Senatore et al., 2021).

El **material de relleno** del biofiltro suele constituir el **parámetro clave** que determina la eficacia de eliminación, la caída de presión y, por tanto, los costes de operación, así como el tiempo de vida del lecho. En este contexto, un material adecuado debe presentar las siguientes **características principales** (Elias et al., 2002; Muñoz, 2010b): (i) alta porosidad, (ii) capacidad adecuada de retención de agua, (iii) alta capacidad tampón, (iv) una población microbiana diversa y adaptable, (v) alto contenido de nutrientes disponibles, (vi) larga vida útil y (vii) bajo coste. El compost, la turba, los suelos porosos y las astillas de madera son ejemplos de materiales que cumplen la mayoría de estos criterios, pudiéndose utilizar de manera aislada o formando mezclas (Mudliar et al., 2010). En este sentido, el compost de diversos materiales orgánicos (lodos de depuradora, fracción orgánica de residuos sólidos urbanos, etc.) se utiliza con frecuencia como material de relleno y a menudo se mezcla con astillas de madera para evitar la compactación del lecho fijo (Barbusinski et al., 2017; López et al., 2011).

En la **Tabla 5.3.2.1** se muestran algunos de los **parámetros de diseño y operación** empleados habitualmente en biofiltración. El tiempo de contacto entre la corriente gaseosa y el lecho del biofiltro, comúnmente denominado **tiempo de residencia en lecho**

vacío (*empty bed residence time, EBRT*), es también considerado como una variable operacional con impacto significativo en las eficacias de biofiltración, especialmente cuando se trata de COV hidrofóbicos (Elmrini et al., 2004; Lebrero et al., 2011). Según Delhoménie y Heitz (2005), con el objetivo de mejorar los rendimientos de biofiltración, el tiempo de residencia en lecho vacío debe ser siempre superior al tiempo requerido para los procesos de difusión de los contaminantes a la biopelícula. Por el contrario, cuando el tiempo de residencia es demasiado corto, los tiempos de contacto entre los microorganismos y los compuestos gaseosos a eliminar no son suficientes para completar las reacciones de biodegradación, lo que se traduce en un descenso de las eficacias de biofiltración. A este respecto, es importante destacar que los tiempos de residencia suelen variar de 15 segundos a 2 minutos en la mayoría de los sistemas de biofiltración (AMIGO, 2019; Delhoménie and Heitz, 2005).

Tabla 5.3.2.1. Valores recomendados para el diseño y operación de biofiltros (Iranpour et al., 2005).

Parámetro	Rango habitual
Temperatura (ºC)	25-35
pH	6-8
Contenido de humedad (%)	40-60
Porosidad (%)	40-80
Contenido en materia orgánica (% en peso)	35-55
Pérdida de carga (cm H_2O)	<10
Tamaño de las partículas del lecho (mm)	>4 mm (al menos el 60% de ellas)

La principal **limitación** de los biofiltros es la **elevada superficie requerida** para su instalación, ya que los tiempos de residencia del gas son elevados y la altura de lecho no suele exceder de 1,5 m con el objetivo de limitar la pérdida de carga del sistema. Otra de sus limitaciones es la **falta de control sobre las condiciones de crecimiento de los microorganismos** como pH, temperatura, humedad (que se consigue mediante irrigación intermitente), aporte de nutrientes o acumulación de metabolitos de degradación (Muñoz, 2010b). Por ejemplo, la acidificación del ecosistema microbiano por compuestos ácidos (como el sulfuro de hidrógeno), cuando estos se encuentran en altas concentraciones

(> 50 ppm de H_2S), constituye una situación irreparable en los sistemas de biofiltración, ya que el reemplazo del lecho suele ser la única forma de controlar el pH (Lebrero et al., 2011). Sin embargo, en comparación con el resto de sistemas de tratamiento biológico, la biofiltración requiere **poco mantenimiento**, es **fácil de operar** y conlleva los **menores costes de inversión y operación**, lo que hace que los biofiltros sean la **tecnología biológica más utilizada** para el tratamiento de malos olores (Barbusinski et al., 2017; Muñoz, 2010b). A esto hay que sumar que la biofiltración de emisiones gaseosas en EDAR permite conseguir elevadas **eficacias de eliminación** de sulfuro de hidrógeno (90-100%) y olores (80-100%), aunque las eficacias de eliminación de COV pueden ser inferiores (20-95% en función de su solubilidad y biodegradabilidad) (AMIGO, 2019; Lebrero et al., 2011). En este contexto, los COV de naturaleza hidrofílica se eliminan más fácilmente de la corriente gaseosa debido a su relativa alta solubilidad en agua y biodisponibilidad. En este caso, la capacidad de eliminación del biofiltro estará limitada por la velocidad de las reacciones de biodegradación. Sin embargo, cuando se desean eliminar COV hidrofóbicos, la etapa limitante del proceso es la difusión de tales contaminantes desde la fase gaseosa a la biopelícula acuosa (Rybarczyk et al., 2020). Por tanto, las eficiencias de eliminación de los compuestos hidrófobos son generalmente más bajas que las de los compuestos hidrófilos (Cheng et al., 2016; Yang et al., 2018).

Biofiltros percoladores

En los biofiltros percoladores (*biotrickling filters*), las emisiones gaseosas pasan a través de un **lecho empacado con material estructural inerte** (rellenos plásticos, resinas, materiales cerámicos, roca volcánica, etc.) en el que se encuentran inmovilizados los microorganismos, siendo irrigado continuamente por una **solución de nutrientes** (**Figura 5.3.2.3**). Los contaminantes odoríferos son inicialmente absorbidos en la solución de nutrientes recirculada y degradados posteriormente en la biopelícula (AMIGO, 2019; Lebrero et al., 2011).

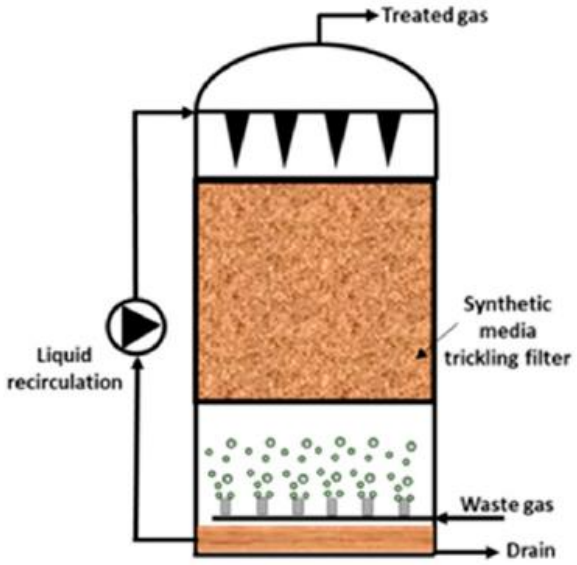

Figura 5.3.2.3. Esquema de funcionamiento de un biofiltro percolador (Senatore et al., 2021).

A diferencia de los biofiltros convencionales, estos sistemas ofrecen un **buen control de las condiciones de operación** (pH, humedad, aporte de nutrientes, temperatura, etc.). Además, la elevada superficie de contacto gas-líquido proporcionada por el lecho empacado permite operar a tiempos de residencia en lecho vacío entre 1 y 10 s, con eficacias de eliminación de sulfuro de hidrógeno superiores al 99% (AMIGO, 2019; Muñoz, 2010b). El **bajo volumen de biorreactor** resultante de estos cortos tiempos de residencia ofrece una ventaja competitiva para su implementación en EDAR con limitaciones de espacio (Lebrero et al., 2011). Sin embargo, la presencia de una fase acuosa continua limita la eficacia de los biofiltros percoladores para el tratamiento de compuestos odoríferos de naturaleza hidrofóbica (Gabriel y Deshusses, 2003; Revah y Morgan-Sagastume, 2005).

Biolavadores

Los biolavadores (*biocrubbers*) están compuestos por una **torre de absorción** (a menudo empacada para aumentar el contacto gas-líquido) donde tiene lugar la transferencia de los compuestos gaseosos a una solución acuosa recirculante, que se transfiere constantemente a un segundo **reactor de cultivo en suspensión** en el que se produce la biodegradación de los contaminantes odoríferos (**Figura 5.3.2.4**). Parte del cultivo bacteriano presente en el mencionado reactor se purga periódicamente con el

objetivo de mantener una concentración de sales por debajo de niveles inhibitorios (2% en peso) y aportar los nutrientes necesarios para el crecimiento de los microorganismos (Muñoz, 2010b).

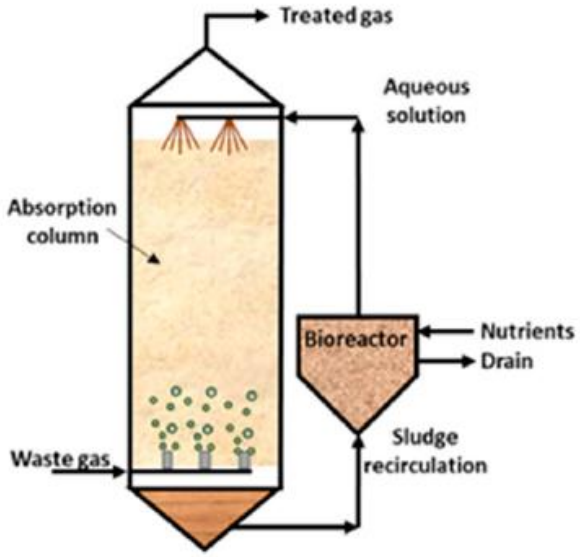

Figura 5.3.2.4. Esquema de funcionamiento de un biolavador (Senatore et al., 2021).

Las principales ventajas de los lavadores biológicos son el **excelente control** de pH, humedad, temperatura y acumulación de metabolitos, la **baja caída de presión** generada y los **bajos costes de operación**. Además, permiten obtener excelentes **eficacias de eliminación** de sulfuro de hidrógeno (≈ 99%) y de COV altamente solubles (AMIGO, 2019). Sin embargo, los biolavadores presentan **altos costes de construcción** y bajas eficacias de eliminación de COV hidrofóbicos (Estrada et al., 2011).

Sistemas de difusión en lodos activos

En los sistemas de difusión en lodos activos, **las emisiones gaseosas son introducidas en el tanque de aireación junto con el aire necesario para satisfacer la DBO** del agua residual (**Figura 5.3.2.5**). De esta manera, los compuestos odoríferos difunden en el medio de cultivo junto con el oxígeno, siendo degradados posteriormente por los microrganismos presentes en el reactor de lodos activos. Estos sistemas de tratamiento biológico **reúnen todas las ventajas** propias del resto de las tecnologías biológicas (bajos costes de operación y respeto por el medio ambiente, principalmente), al tiempo que permiten **superar** la mayoría de sus **limitaciones** (secado, canalizaciones y problemas estructurales en el lecho, control de pH y acumulación de metabolitos tóxicos

en biofiltros, altos costes de inversión en biolavadores, etc.). Además, el uso de los tanques de aireación existentes en EDAR como sistema de tratamiento de malos olores presenta una ventaja competitiva desde el punto de vista económico en instalaciones con limitaciones de espacio y sistemas de aireación por difusión ya implantados (Lebrero et al., 2011; Muñoz, 2010b).

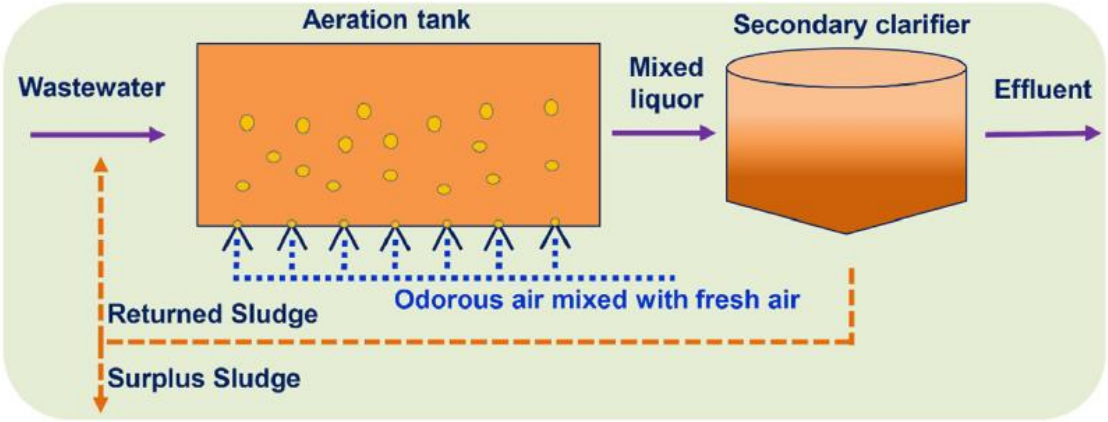

Figura 5.3.2.5. Esquema de funcionamiento de un sistema de difusión en lodos activos (Fan et al., 2020).

Los sistemas de difusión en lodos activos permiten alcanzar elevadas **eficacias de desodorización** (> 99%), incluso con elevadas concentraciones de sulfuro de hidrógeno (120 ppm), lo que demuestra el **alto potencial de eliminación de olores** de esta tecnología de carácter biológico (Bowker, 2000; Fan et al., 2020; Muñoz, 2010b). Sin embargo, hay que tener en cuenta los problemas de operación derivados de la corrosión por H_2S en tuberías, compresores o filtros, los cuales pueden minimizarse mediante el uso de materiales resistentes a la corrosión (acero inoxidable, PVC o fibra de vidrio) o trampas de humedad (Stuetz and Frechen, 2001).

6. Evaluación del impacto de la contaminación odorífera

La contaminación por olores es un tipo de estresor ambiental que con frecuencia no se ha tenido en cuenta en el contexto de la contaminación atmosférica y en el establecimiento de las correspondientes regulaciones. En este sentido, para que exista **contaminación ambiental por olores** han de darse tres factores (AMIGO, 2019): **emisión** de compuestos odoríferos, **dispersión** de estos y la existencia de una **población receptora** a la cual pueda causar molestias (**Figura 6.1**).

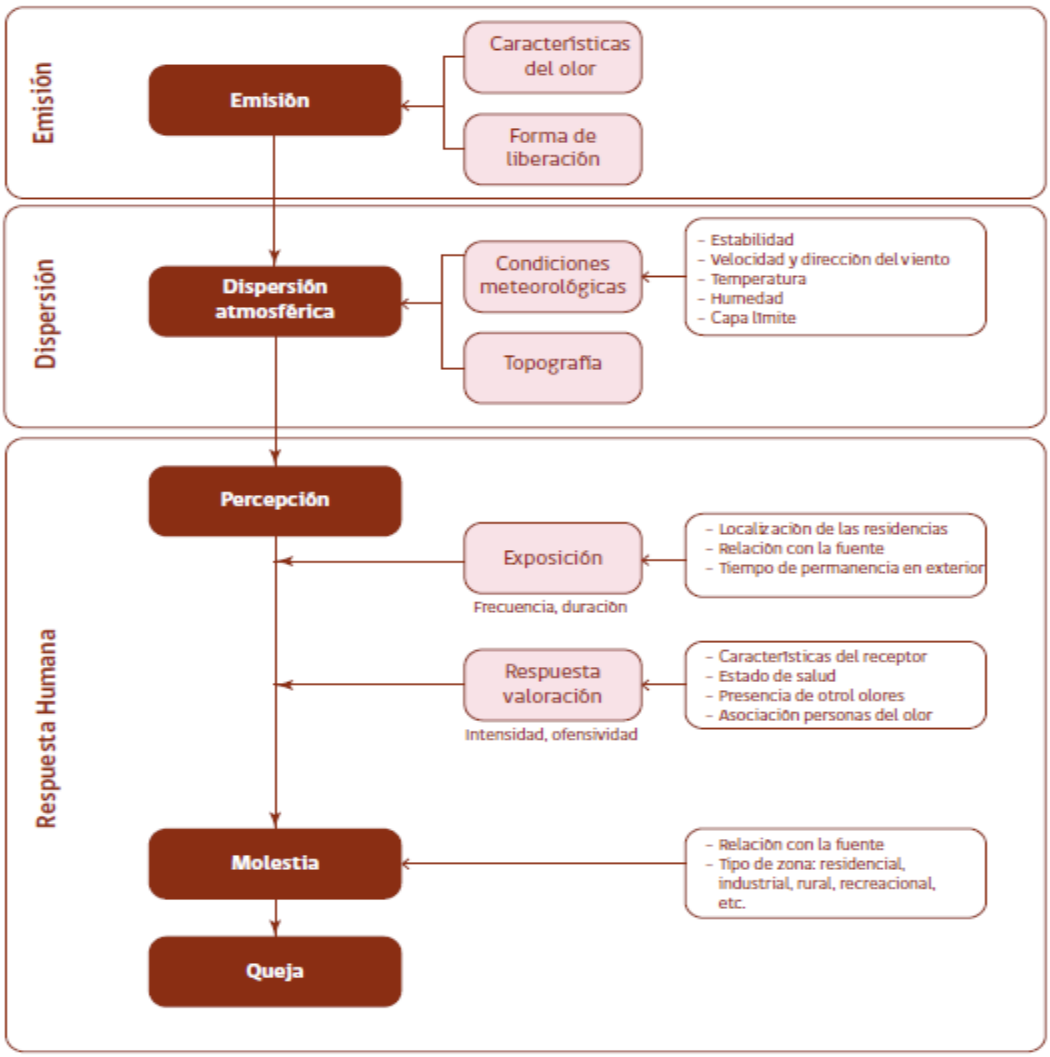

Figura 6.1. Proceso de emisión, dispersión y respuesta humana al olor (Servicio de Evaluación Ambiental [SEA], 2017).

En las siguientes secciones se analizarán los diferentes factores que contribuyen al impacto por olor, así como la evaluación de dicho impacto, que se puede medir o evaluar mediante planes de seguimiento en los receptores o bien mediante modelos de dispersión a partir de las fuentes de olor.

6.1. Factores que contribuyen al impacto odorífero

El impacto odorífero depende de varios factores, no existiendo un método único para medir o evaluar de manera confiable tal impacto. En este contexto, el acrónimo **FIDOL** es un recordatorio útil de los principales factores que muchas legislaciones internacionales tienen en cuenta a la hora de establecer límites en la contaminación por olor: Frecuencia, Intensidad, Duración, Ofensividad y Localización. A continuación, se procede a realizar un breve análisis de los mismos (AMIGO, 2019; Naddeo et al., 2012).

Frecuencia

La frecuencia es una medida que proporciona información sobre **cada cuánto tiempo un individuo se expone a un olor** en el medio ambiente. La frecuencia está influenciada por las características de la fuente emisora de olores y su ubicación con respecto a los receptores, las condiciones climáticas y la topografía de la región. La frecuencia de exposición al olor es generalmente mayor en las áreas que se encuentran a sotavento de la fuente, especialmente en condiciones de estabilidad atmosférica con bajas velocidades del viento (siempre que el olor no se emita a una altura significativa sobre el suelo).

Numerosas jurisdicciones han puesto **límites a la frecuencia** con la que se pueden experimentar episodios de malos olores fuera de la propiedad que los emite. En este sentido, los criterios más comunes se basan en que una instalación generadora de olores debe cumplir con los límites de concentración (en inmisión), con una frecuencia que puede ser del 98,0, 99,0, 99,5 ó 99,9%, lo que quiere decir que sólo se pueden superar los límites fijados entre un 0,1 y un 2,0% del periodo considerado (generalmente un año).

Intensidad

La respuesta individual a un estrés olfativo está directamente relacionada con la intensidad (fuerza) con la que se percibe. Sin embargo, teniendo en cuenta su mejor reproducibilidad, casi siempre se prefiere la olfatometría dinámica, de tal manera que cuando se hace referencia a la intensidad dentro de los factores FIDOL, en realidad todas las legislaciones se refieren en este factor a la **concentración de olor límite en el receptor**. La relación entre intensidad de olor y concentración de olor se ha abordado en la Sección 3.1.

Duración

La duración se refiere al **periodo de tiempo en el que se está detectando un olor**. Al igual que la frecuencia, la duración de la exposición al olor está relacionada con el tipo de fuente de olor, la posición de los receptores con respecto a ella y la meteorología local. El olor puede detectarse durante periodos cortos e intermitentes o periodos largos y continuos. En general, cabe esperar que cuanto mayor sea la duración, mayor será el impacto. Sin embargo, no existe un estudio completo sobre el impacto de la duración de un episodio olfativo. Además, es importante destacar que el factor duración no se puede

separar de los parámetros de frecuencia ni de intensidad. Por ejemplo, un olor percibido durante muchos periodos cortos puede tener un impacto diferente al olor percibido en periodos largos y continuos, incluso si la cantidad total de horas fuese la misma. Asimismo, es probable que una exposición de alta intensidad, pero por periodos cortos, tampoco tenga el mismo impacto que exposiciones largas de baja intensidad. En cualquier caso, no existen ejemplos de límites legales que impongan una duración máxima de un solo evento.

Ofensividad

La ofensividad o tono hedónico es la **evaluación subjetiva** de lo **agradable** o **desagradable** que puede resultar un olor. Existen varias formas de evaluar el tono hedónico, siendo la más común aquélla en la que el panel utiliza una escala bipolar que va de -4 a +4 (ver Sección 3.1). En ella, las sensaciones desagradables se marcan con el signo (-), las positivas con el signo (+), mientras que el 0 se utiliza para identificar olores neutros.

La ofensividad se utiliza en algunas legislaciones para **regular de manera diferente a distintos grupos de actividades**. Generalmente, se toleran mayores concentraciones de olor de actividades menos ofensivas (por ejemplo, las industrias panaderas), mientras que se establecen valores más restrictivos para las actividades cuyas emisiones odoríferas tienen un tono hedónico más desagradable (por ejemplo, las EDAR).

Localización

La ubicación o **lugar donde se percibe un olor** es un factor importante a tener en cuenta cuando se evalúa la probabilidad de que ocurra una respuesta negativa, debido al tipo o cantidad de receptores que se pueden encontrar en un lugar determinado. El parámetro localización debe tener en cuenta el tipo de actividad que se realiza en esa zona, la sensibilidad de los posibles receptores, así como la posible presencia de olores de fondo. De forma general, el grado de impacto de un olor está directamente relacionado con las expectativas de las personas que viven, trabajan, visitan o pasan por una zona determinada. Por ejemplo, olores asociados con la ganadería o la agricultura es más probable que sean tolerados en áreas donde se espera que este tipo de actividades se lleven a cabo, como pueden ser áreas rurales alejadas de las ciudades.

En lo que respecta a la legislación, existe una tendencia general a establecer **límites de concentración de olor más bajos en zonas residenciales**, siendo algo más altos en zonas donde el uso del terreno se destina principalmente a actividades industriales o agrícolas o terreno catalogado como no urbanizable.

6.2. Evaluación del impacto odorífero a partir de la exposición

La evaluación del impacto odorífero a partir de la medición de la exposición únicamente puede llevarse a cabo cuando las **actividades generadoras de olor existen físicamente** y **causan efectos adversos** en términos de olor. Al evaluar las actividades existentes que pueden estar causando tales efectos, es importante determinar el tipo de efecto adverso que es más probable que ocurra, distinguiendo entre efectos de olor crónicos o agudos, debidos a emisiones regulares o incontroladas, respectivamente. La correcta identificación de estos efectos ayudará a seleccionar la técnica o las técnicas de evaluación de olores más adecuadas. En este contexto, las principales herramientas para la evaluación del impacto odorífero a partir de la exposición son (Naddeo et al., 2012): (i) **inspecciones olfatométricas de campo** (aportan información sobre intensidad y ofensividad) como el método de la rejilla o malla (VDI 3940 Part 1, 2006) y el de la pluma o penacho (VDI 3940 Part 2, 2006), (ii) **registros de quejas** por malos olores, (iii) **encuestas de molestia** por olores y (iv) **seguimiento continuo del olor** mediante el uso de narices electrónicas o *IOMS*. Lo habitual es utilizar varias técnicas de forma combinada. En cualquier caso, se deben tener en cuenta las siguientes consideraciones en cuanto al uso de las herramientas mencionadas anteriormente (Naddeo et al., 2012):

- Resulta difícil presenciar incidentes de olor que son eventuales y de corta duración.
- Las emisiones odoríferas se diluyen en gran medida desde su punto de emisión y, a menudo, registran valores de concentración de olor por debajo de los límites de detección de los instrumentos, pero las personas aún pueden detectarlas.
- Los picos de exposición pueden deberse a cambios en las condiciones de dispersión (dirección del viento, turbulencia) o a emisiones variables (puertas abiertas).
- Las emisiones de chimeneas elevadas pueden llegar al suelo más allá del punto de seguimiento del olor.

- Puede resultar difícil determinar de dónde proviene una emisión o distinguirla de otras fuentes.

6.3. Evaluación del impacto por olores a partir de sus fuentes

El impacto por olores también puede evaluarse a partir de las fuentes emisoras mediante modelos de dispersión. A diferencia del enfoque anterior, éste constituye la única vía para evaluar la posible contaminación odorífera de **nuevas instalaciones** potencialmente emisoras de olor, aunque también se utiliza a menudo para las **ya existentes**. En el caso de nuevos proyectos, la evaluación a partir de las fuentes puede resultar bastante difícil de realizar, pues en este caso no hay historial de quejas, ni rendimientos de la instalación a partir de los cuales determinar los posibles episodios de olor, de tal manera que el equipo evaluador debe depender en gran medida de la experiencia con actividades similares y de los resultados del modelo de dispersión. La evaluación puede resultar complicada si existe poca información sobre la cual seleccionar las tasas de emisión de olor, por lo que a menudo se requerirá un enfoque conservador para este tipo de evaluación. En este enfoque, la evaluación del impacto odorífero consta de las siguientes **etapas** (Lebrero et al., 2010; Naddeo et al., 2012): (i) **identificación y caracterización de las fuentes** de olor, (ii) estimación o medición de la **tasa de emisión** de olores, (iii) caracterización de las **condiciones atmosféricas** y de la **topografía** de la posible zona expuesta (iv) **modelización de la dispersión** y (v) **evaluación del impacto odorífero** mediante los niveles de exposición (inmisión).

Las **utilidades principales** de la evaluación del impacto odorífero a partir de sus fuentes son las que se detallan a continuación (Naddeo et al., 2012):

- Predecir el impacto de una nueva instalación.
- Investigar la/s causa/s de las quejas por olores de las instalaciones existentes y la influencia de las condiciones climáticas en la dispersión de olores.
- Establecer límites de emisión para las emisiones de fuentes puntuales, ya sea en mg/m^3 para una sola sustancia olorosa o en ou_E/m^3 para mezclas de sustancias.
- Ayudar a decidir las mejoras que se necesitan o la envergadura de los sistemas de eliminación de olor.
- Calcular la altura adecuada de una chimenea para proporcionar una exposición aceptable en los receptores.

Etapa I: Identificación y caracterización de las fuentes de olor

La identificación y caracterización de las fuentes de olor constituye la **primera etapa** de esta evaluación y puede llevarse a cabo mediante un enfoque comparativo de actividades similares, en el caso de un nuevo proyecto, o mediante un estudio preciso, en el caso de actividades ya existentes. En este contexto, es importante destacar que existen diferentes tipos de fuentes de emisión de olor (Vergara y Zorich, 2013):

- **Fuentes puntuales**: Corresponden a fuentes estacionarias de emisión canalizadas al ambiente. Se trata principalmente de chimeneas, ductos, etc. Las emisiones de este tipo de fuentes presentan un amplio rango de temperaturas (20-750ºC), y humedades relativas que pueden oscilar entre 0 y 100%.
- **Fuentes difusas**: Corresponden también a fuentes estacionarias que cuentan con una superficie de emisión en contacto directo con el ambiente. Este tipo de fuentes corresponden principalmente a lagunas, balsas, biofiltros de lecho abierto, etc. Además, es posible distinguir entre fuentes difusas **pasivas** (sin aireación o ventilación natural) y fuentes difusas **activas** (con aireación o ventilación forzada).
- **Fuentes fugitivas**: Corresponden a fuentes que no cuentan con un único punto o superficie de emisión. Se trata de emisiones no controladas al ambiente, siendo difíciles de identificar, y dadas en general por emisiones accidentales de equipos presurizados y/o emisiones irregulares de gases de proceso.
- **Fuentes móviles**: Corresponden a fuentes en constante movimiento o en tránsito. Si bien en su mayoría pueden ser puntuales o difusas, no obedecen a un patrón estacionario de emisión.

Esta primera etapa no debe centrarse únicamente en fuentes que sean fáciles de identificar y/o medir, como las puntuales y las difusas. En este sentido, es igualmente importante la búsqueda de emisiones fugitivas, siendo este un proceso complejo que requiere un conocimiento detallado de las válvulas, respiraderos, etc., así como de los procesos que están teniendo lugar. Para cada fuente de emisión, la caracterización debe incluir, entre otros aspectos, el tipo de gases olorosos emitidos, la altura de liberación de los mismos y la frecuencia con la cual se lleva a cabo una determinada operación emisora de olores. Tales aspectos pueden influir en la tasa de emisión, así como en la dispersión de los contaminantes odoríferos.

En el campo del tratamiento de las aguas residuales, numerosos estudios han descrito que el **pretratamiento**, la **sedimentación primaria** y las **operaciones unitarias de la línea de fangos**, como el espesamiento y la deshidratación, constituyen las **principales fuentes de olor en EDAR** convencionales (Capelli et al., 2009; Frechen, 2004; Gebicki et al., 2016; Lebrero et al., 2011; Stuetz y Frechen, 2001). Este hecho se ilustra en la **Figura 6.3.1**.

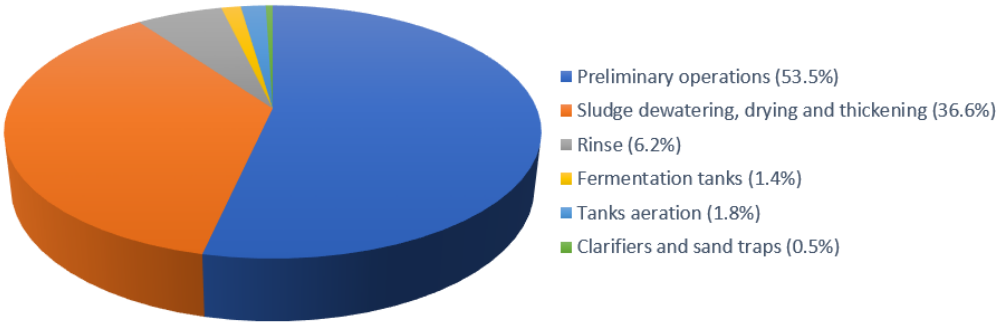

Figura 6.3.1. Distribución porcentual de las fuentes de olor en una EDAR urbana (Gebicki et al., 2016).

Etapa II: Estimación o medición de la tasa de emisión de olores

Una vez llevada a cabo la identificación y caracterización cualitativa de las fuentes de emisión de olor, es necesario proceder a su **caracterización cuantitativa**, tomando generalmente como referencia la **Norma Europea EN 13725** (2003) de olfatometría dinámica. La caracterización cuantitativa requiere, a su vez, de tres etapas: (i) **toma de muestras** en aquellas fuentes que se han seleccionado previamente mediante un plan de muestreo, (ii) **análisis sensorial** para determinar la concentración de olor (ou_E/m^3) y (iii) determinación de la **tasa de emisión de olor** de cada una de las fuentes implicadas en el estudio, expresándose como el número de unidades de olor europeas emitidas por unidad de tiempo (ou_E/s), en condiciones normales para olfatometría (20ºC y 101,3 kPa en base húmeda).

En el campo de los olores, la medición de las tasas de emisión y la predicción posterior de los niveles de inmisión utilizando modelos de dispersión resulta una tarea más compleja que para muchos otros contaminantes atmosféricos (Burlingame et al., 2004). El seguimiento de los focos olorosos comúnmente deriva en **tasas de emisión marcadamente variables**. Por ejemplo, una balsa olorosa puede generar tasas de emisión que varíen significativamente en la superficie de una temporada a otra y en diferentes

momentos del día. En este sentido, las tasas de emisión pueden ser varios órdenes de magnitud más altas durante eventos perturbadores que durante un funcionamiento normal. Además, para escenarios simples de modelado de la dispersión, con sólo una o dos fuentes, se suele utilizar la tasa de emisión máxima para los cálculos de dispersión. Sin embargo, debido a la **naturaleza intermitente de los olores**, el uso de las tasas de emisión más desfavorables que se supone que se generan continuamente puede derivar en resultados demasiado conservadores y poco realistas. Aun así, garantizan la cuantificación de los picos de percepción de olor, comúnmente fuente de quejas vecinales.

Etapa III: Caracterización de las condiciones atmosféricas y la topografía

La dispersión de olores depende en gran medida de la **topografía** existente alrededor de la fuente emisora y de las **condiciones atmosféricas locales**. Para los nuevos proyectos, así como para las actividades existentes, la **evaluación de la micrometeorología local**, en términos tanto cualitativos como cuantitativos, constituye un **aspecto esencial** que habitualmente se subestima. La aparición de episodios inesperados de olores de actividades recién establecidas a menudo se debe a que la micrometeorología local está caracterizada de forma demasiado simplista o errónea. Así, para representar las condiciones de un "año medio", se deben utilizar **datos meteorológicos horarios** de al menos **tres años** (preferiblemente cinco años), que deben obtenerse de una o varias **estaciones meteorológicas representativas**.

Generalmente, los **principales parámetros** utilizados para describir las condiciones atmosféricas son la temperatura ambiente, la capa de mezcla, la clase de estabilidad atmosférica, velocidad y dirección de viento, humedad relativa y radiación solar. En el caso concreto del impacto por olores de fuentes que emiten a nivel del suelo (como es el caso de las EDAR), la dispersión se suele producir a pocos metros del nivel del suelo y lentamente. Por tanto, la altura de capa de mezcla no suele ser un factor muy influyente en la dispersión para este tipo de casos, mientras que sí lo es para emisiones desde focos puntuales a gran altura (Díaz et al., 2014).

Etapa IV: Modelización de la dispersión

Aunque la olfatometría dinámica es una técnica generalizada para la cuantificación de las emisiones odoríferas, ésta no resulta suficiente para dar cuenta del **impacto efectivo de los olores sobre la población receptora**. Por este motivo, es necesario disponer de herramientas que ayuden a entender el comportamiento de las emisiones

odoríferas en un área de estudio determinada. En este contexto, los **modelos matemáticos de dispersión de contaminantes atmosféricos** permiten simular cómo se dispersa el olor en la atmósfera. Así, una vez que se incorpora a tales modelos la información de variables meteorológicas, topográficas y características propias de la fuente emisora (tasas de emisión, superficie emisora, etc.), es posible predecir los niveles de concentración de olor en el espacio modelado y sus variaciones a lo largo del tiempo (AMIGO, 2019; Capelli et al., 2013).

Existen distintos modelos de dispersión de contaminantes atmosféricos, que pueden clasificarse en función del alcance espacial, la escala temporal, el tipo de campo de vientos utilizado, la forma del cálculo del campo de vientos y según como se trata la ecuación de la dispersión desde una perspectiva determinista (Sánchez et al., 2008). Desde un punto de vista conceptual, los **tipos de modelos** más importantes son los siguientes (SEA, 2012):

- **Modelos Gaussianos**: En un modelo Gaussiano se supone una fuente que emite continuamente y que está ubicada en un ambiente con una velocidad del viento (*u)* que sopla en forma paralela al eje x. También se asume que la pluma, que tiene origen en la fuente emisora, se desplaza paralela a la dirección de viento y que dentro de la pluma la distribución de los contaminantes tiene una forma Gaussiana (**Figura 6.3.2**). Además, se supone que los gases salen con un cierto empuje de la chimenea (debido a su velocidad y temperatura); en consecuencia, los modelos Gaussianos calculan la dispersión a partir de una altura efectiva (H_e) de la chimenea, que justamente tiene en cuenta este empuje (H_e siempre es mayor que la altura real de la chimenea, H_c). En este tipo de modelos, lo que determina la amplitud y el ancho de esa distribución son la velocidad del viento y la estabilidad atmosférica. Mientras que la velocidad del viento se puede medir directamente, no ocurre lo mismo para la estabilidad atmosférica, por lo que su estimación se basa fundamentalmente en algunas relaciones empíricas, usando observaciones de temperatura, viento y cobertura nubosa.

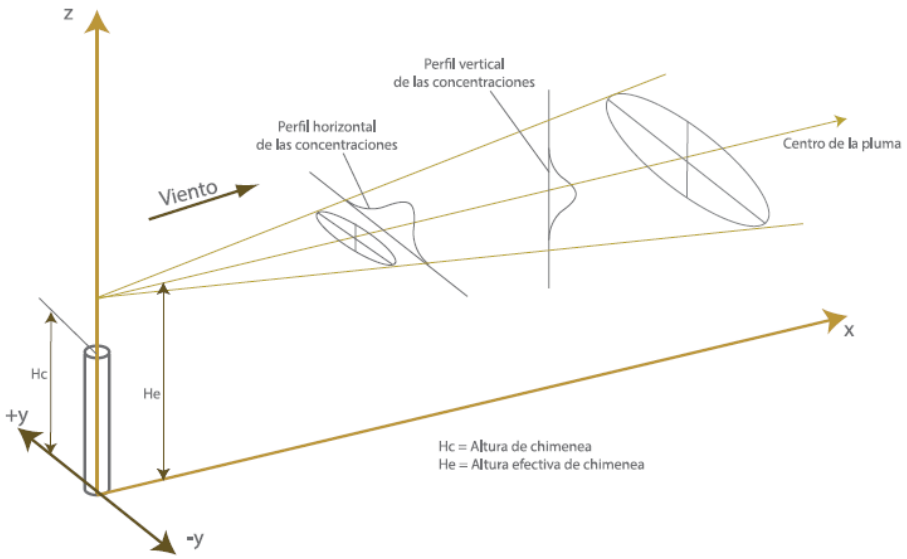

Figura 6.3.2. Concepto de un modelo Gaussiano (SEA, 2012).

Los modelos Gaussianos pueden exhibir distintos grados de complejidad. Así, por ejemplo, pueden incluir procesos como deposición y sedimentación o también efectos de topografía. No obstante, en términos generales, todos tienen el mismo fundamento matemático. Además, todos se basan en las mismas suposiciones y aproximaciones, entre las que destacan:

- Las **emisiones** son **constantes** en el periodo de la evaluación. Se asume un estado estacionario, cuyo tiempo característico depende de la escala espacial del problema y de la magnitud del viento.
- Las **condiciones meteorológicas** son **constantes** durante el periodo de la evaluación.
- **Vientos homogéneos en la horizontal**, es decir, que el viento en la fuente sea representativo para todo el dominio de evaluación. Esta suposición hace muy limitado el uso de estos modelos en un terreno complejo con un campo de viento muy heterogéneo, así como con velocidades muy bajas del viento (calmas).

La gran ventaja de los modelos Gaussianos es su uso fácil y rápido y que no requieren demasiados recursos computacionales. Sin embargo, son las suposiciones anteriormente mencionadas las que hacen que su uso sea muy limitado. Un ejemplo de modelo Gaussiano es el **AERMOD**, que es el modelo recomendado por la *US EPA* para estimar la calidad del aire a nivel local (hasta 50 km). Por tanto, es el modelo recomendado para la mayoría de los estudios de emisiones de actividades industriales (Díaz et al., 2014).

- **Modelos Eulerianos**: Los modelos Eulerianos tienden a tratar todos los procesos atmosféricos relacionados con la dispersión de contaminantes y su transformación química. Con este objetivo, estos modelos incorporan ecuaciones matemáticas (basadas en leyes físicas y químicas) que son, en su gran mayoría, de tipo diferencial. Otra característica de estos modelos es que **discretizan el espacio** en forma de una **grilla** (o malla) **tridimensional** definida por puntos con un determinado espaciamiento horizontal y vertical, lo que se denomina resolución espacial de la grilla. El modelo integra las ecuaciones matemáticas en el tiempo en cada uno de los puntos de la grilla, generándose la información de la evolución temporal de las concentraciones en las tres dimensiones de la grilla. Existen distintos grados de complejidad en los modelos Eulerianos en términos de la representación de procesos, desde modelos que consideran solo la dispersión, hasta modelos que incluyen todos los procesos fotoquímicos y de aerosoles. Ejemplos de modelos Eulerianos son: **WRF-Chem**, **CAMx** y **CMAQ**.
- **Modelos Lagrangianos**: Estos modelos se basan en el concepto de seguir matemáticamente el movimiento de una parcela de aire o de una partícula en la atmósfera. Es decir, si en la posición inicial de una partícula se conoce tanto la velocidad como la dirección del viento, fácilmente se puede calcular a dónde se dirige esa partícula en un intervalo de tiempo finito (integración en el tiempo). Después de esta integración, la partícula tiene una nueva posición en el espacio, donde el viento puede ser distinto al de la posición inicial. Considerando esto, nuevamente se puede integrar y así sucesivamente. El camino que se describe a través de esta integración se llama trayectoria. Con el fin de obtener una estimación de las concentraciones en un **modelo de trayectorias**, se requiere el cálculo de muchas trayectorias, del orden de un millón para la dispersión de un contaminante desde una fuente. Además de los procesos de transporte por advección (transporte por la acción del viento), también se pueden incorporar los **procesos turbulentos** de la atmósfera. Los modelos Lagrangianos tienen una capacidad más limitada que los modelos Eulerianos para incorporar procesos químicos.

  A nivel internacional, los modelos Lagrangianos se usan en muy pocos países con fines regulatorios. Uno de los más conocidos es el modelo **AUSTAL2000**, desarrollado para la Agencia de Medio Ambiente de Alemania y usado como referencia en este país (Díaz et al., 2014).

- **Modelos tipo "puff"**: Son una **combinación** entre los modelos Gaussianos y los Lagrangianos. Estos modelos se basan esencialmente en calcular la dispersión de una emisión puntual (puntual en el tiempo), llamada "puff", a lo largo de una trayectoria. Su aproximación matemática consiste en **estimar la dispersión en forma Gaussiana en cada punto de una trayectoria**. A diferencia de los modelos Lagrangianos, que necesitan el cálculo de un gran número de trayectorias para una fuente, en el caso de los modelos tipo "puff" sólo se requiere una trayectoria por "puff", lo que hace que su cálculo sea mucho más rápido. En el caso de emisiones continuas, se simulan las trayectorias y la dispersión Gaussiana de muchos "puffs". Además, estos modelos son capaces de simular muchas fuentes (y de distinto tipo) al mismo tiempo. Generalmente, son muy rápidos en su uso sin gran exigencia computacional. Sin embargo, sus limitaciones se basan en que no simulan procesos, sino que la dispersión depende fuertemente de los principios de la aproximación Gaussiana.

  Un ejemplo de modelo tipo "puff" es **CALPUFF**. Hasta 2018, este modelo se encontraba entre los recomendados por la *US EPA* para evaluar la calidad del aire en el caso de fenómenos de transporte a grandes distancias y en aquellos casos donde el modelo AERMOD no podía usarse (Olores.org, 2018).

Una vez descritos los principales tipos de modelos de dispersión, es importante destacar que el **coste** de estos se incrementa conforme aumenta la **complejidad** y los **recursos computacionales** necesarios, de la siguiente manera: modelos Gaussianos < modelos Lagrangianos < modelos Eulerianos. Además, existe cierta tendencia a etiquetar la bondad de los modelos según su complejidad, lo que puede provocar errores en la elección del modelo de dispersión, pues dicha elección debe basarse en la adecuación del modelo al caso de estudio en cuestión. Por tanto, resulta de gran importancia armonizar los criterios de elección, así como validar los métodos y los resultados obtenidos (Díaz et al., 2014).

Etapa V: Evaluación del impacto odorífero

Finalmente, la evaluación del impacto odorífero se basa en los resultados de la modelización de la dispersión, que se expresan con frecuencia en forma de **líneas de contorno de olores** (isopletas o isodoras, **Figura 6.3.3**), las cuales conectan puntos con la misma frecuencia de ocurrencia para concentraciones de olor medias horarias a un

determinado percentil, utilizándose a menudo el **percentil 98** (P98). Por ejemplo, si una isodora es de 5 ou/m^3 (P98), la concentración promedio horaria no superará las 5 unidades de olor por metro cúbico durante 175 horas al año (un 2% de las horas anuales). Es importante reiterar que la información mencionada se refiere a **concentraciones horarias promedio**. Por tanto, la concentración puntual en el área dentro de la isolínea de 5 ou/m^3 (P98) puede alcanzar valores máximos de, por ejemplo, 20 ou/m^3, alejado en cualquier caso de la concentración horaria promedio (Díaz et al., 2014).

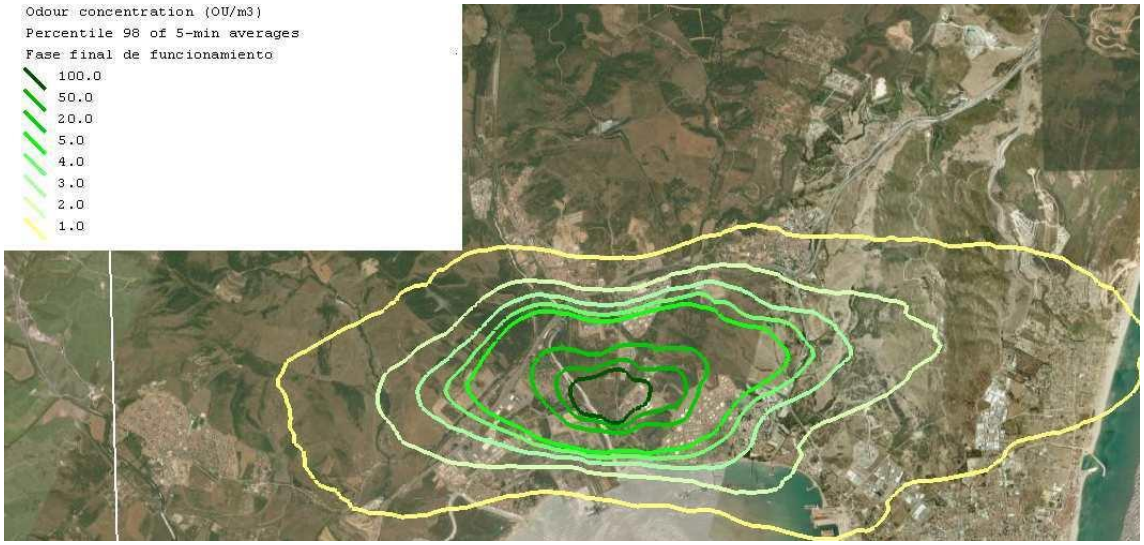

Figura 6.3.3. Mapa de isodoras que refleja el impacto odorífero de una EDAR en Santiago de Chile (Díaz et al., 2014).

En este contexto, no hay que olvidar que la **percepción de los olores** suele ocurrir en un intervalo que va desde unos segundos a algunos minutos, es decir, en **tiempos de exposición cortos**. Por tanto, en el caso de los olores, sería recomendable trabajar con datos meteorológicos subhorarios, o incluso, subminutales. Sin embargo, esto obligaría a **replantear** los **valores límite de concentración de olor establecidos en base a percentiles horarios**, lo que es habitual en las legislaciones que regulan el impacto odorífero (Díaz et al., 2014).

Aunque el olor es una percepción con parte de componente subjetivo, a fecha de hoy, la nariz humana es la más indicada para la cuantificación del mismo. No obstante, la heterogeneidad entre individuos, los distintos niveles de sensibilidad y la repercusión que sobre la salud puede tener la inhalación continuada de determinados compuestos causantes de olor, están promoviendo que sean cada vez más numerosos los estudios en este campo, ya sea en su emisión o impacto posterior. De ahí la gran cantidad de

herramientas disponibles para su medición y/o estimación una vez que se ha generado y se emite al medio ambiente (Bax et al., 2020; Byliński et al., 2019; Capelli et al., 2013; Gebicki et al., 2016; Hawko et al., 2021; Nakamoto, 2005).

7. Bibliografía

Allievi, M.J., Silveira, D.D., Cantão, M.E., Filho, P.B., 2018. Bacterial community diversity in a full scale biofilter treating wastewater odor. Water Sci. Technol. 77, 2014–2022. https://doi.org/10.2166/WST.2018.114

Asociación Medioambiental Internacional de Gestores del Olor, 2019. Guía Básica de Gestión del Olor.

Barbusinski, K., Kalemba, K., Kasperczyk, D., Urbaniec, K., Kozik, V., 2017. Biological methods for odor treatment – A review. J. Clean. Prod. https://doi.org/10.1016/j.jclepro.2017.03.093

Bax, C., Sironi, S., Capelli, L., 2020. How Can Odors Be Measured? An Overview of Methods and Their Applications. Atmosphere (Basel). 11, 92. https://doi.org/10.3390/ATMOS11010092

Bokowa, A., Diaz, C., Koziel, J.A., McGinley, M., Barclay, J., Schauberger, G., Guillot, J.M., Sneath, R., Capelli, L., Zorich, V., Izquierdo, C., Bilsen, I., Romain, A.C., Del Carmen Cabeza, M., Liu, D., Both, R., Van Belois, H., Higuchi, T., Wahe, L., 2021. Summary and overview of the odour regulations worldwide. Atmosphere (Basel). 12, 1–53. https://doi.org/10.3390/atmos12020206

Borrador del Anteproyecto de Ley contra la contaminación odorífera, 2005. Departamento de Medio Ambiente y Vivienda. Generalitat de Cataluña.

Bowker, R.P.G., 2000. Biological odour control by diffusion into activated sludge basins. Water Sci. Technol. 41, 127–132. https://doi.org/10.2166/WST.2000.0101

Bruchet, A., Decottignies, V., Filippi, G., 2008. Efficiency of masking agents: outcome of a 3 year study at pilot and full scales. Paper presented at the 3rd IWA International Conference on Odour and VOCs, Barcelona, Spain.

Burlingame, G.A., Suffet, I.H., Khiari, D., Bruchet, A.L., 2004. Development of an odor wheel classification scheme for wastewater. Water Sci. Technol. 49, 201–209. https://doi.org/10.2166/WST.2004.0571

Byliński, H., Gębicki, J., Namieśnik, J., 2019. Evaluation of health hazard due to emission of volatile organic compounds from various processing units of wastewater treatment plant. Int. J. Environ. Res. Public Health 16. https://doi.org/10.3390/ijerph16101712

Capelli, L., Sironi, S., Del Rosso, R., Céntola, P., 2009. Predicting odour emissions from wastewater treatment plants by means of odour emission factors. Water Res. 43, 1977–1985. https://doi.org/10.1016/j.watres.2009.01.022

Capelli, L., Sironi, S., Del Rosso, R., Guillot, J.M., 2013. Measuring odours in the environment vs. dispersion modelling: A review. Atmos. Environ. 79, 731–743. https://doi.org/10.1016/J.ATMOSENV.2013.07.029

Capodaglio, A.G., Conti, F., Fortina, L., Pelosi, G., Urbini, G., 2002. Assessing the environmental impact of WWTP expansion: odour nuisance and its minimization. Water Sci. Technol. 46, 339–346. https://doi.org/10.2166/wst.2002.0620

Card, T., 2001. Chemical odour scrubbing systems, in: Stuetz, R., Frechen, F.B. (Eds.), Odours in Wastewater Treatment: Measurement, Modelling and Control. IWA, London, England.

Centro Tecnológico del Agua, 2020. Biofactorías, la solución al saneamiento sostenible y cambio climático [WWW Document]. URL https://www.cetaqua.com/actualidad/-/asset_publisher/gHLnSnNh62TN/content/noticia-biofactorias-la-solucion-al-saneamiento-sostenible-y-cambio-climatico (accessed 1.11.22).

Cheng, Y., He, H., Yang, C., Zeng, G., Li, X., Chen, H., Yu, G., 2016. Challenges and solutions for biofiltration of hydrophobic volatile organic compounds. Biotechnol. Adv. https://doi.org/10.1016/j.biotechadv.2016.06.007

Comunicación de la Comisión — Orientaciones técnicas sobre la clasificación de los residuos (2018/C 124/01). Diario Oficial de la Unión Europea C 124, 9 de abril de 2018, pp. 1–134.

Confederación Hidrográfica del Duero, 2012. Guía práctica para la depuración de aguas residuales en pequeñas poblaciones. Ministerio de Agricultura, Alimentación y Medio Ambiente, Gobierno de España.

Decisión de Ejecución (UE) 2018/1147 de la Comisión, de 10 de agosto de 2018, por la que se establecen las conclusiones sobre las mejores técnicas disponibles (MTD) en el tratamiento de residuos, de conformidad con la Directiva 2010/75/UE del Parlamento Europeo y del Consejo. Diario Oficial de la Unión Europea L 208, 17 de agosto de 2018, pp. 38–90.

Decottignies, V., Filippi, G., Bruchet, A., 2007. Characterisation of odour masking agents often used in the solid waste industry for odour abatement. Water Sci. Technol. 55, 359–364. https://doi.org/10.2166/wst.2007.198

Decreto 239/2011, de 12 de julio, por el que se regula la calidad del medio ambiente atmosférico y se crea el Registro de Sistemas de Evaluación de la Calidad del Aire en Andalucía. Boletín Oficial de la Junta de Andalucía, núm. 152, 4 de agosto de 2011.

Delgado-Baquerizo, M., Oliverio, A.M., Brewer, T.E., Benavent-González, A., Eldridge, D.J., Bardgett, R.D., Maestre, F.T., Singh, B.K., Fierer, N., 2018. A global atlas of the dominant bacteria found in soil. Science (80-.). 359, 320–325. https://doi.org/10.1126/SCIENCE.AAP9516

Delhoménie, M.C., Heitz, M., 2005. Biofiltration of air: A review. Crit. Rev. Biotechnol. https://doi.org/10.1080/07388550590935814

Díaz, C., Cartelle, D., Barclay, J., 2014. Revision of Regulatory Dispersion Models, an Important Key in Environmental Odour Management. Ist International Seminar of Odours in the Environment, Santiago, Chile.

Directiva 2010/75/UE del Parlamento Europeo y del Consejo, de 24 de noviembre de 2010, sobre las emisiones industriales (prevención y control integrados de la contaminación). Diario Oficial de la Unión Europea L 334, 17 de diciembre de 2010, pp. 17–119.

Directiva 91/271/CEE del Consejo, de 21 de mayo de 1991, sobre el tratamiento de las aguas residuales urbanas. Diario Oficial de la Unión Europea L 135, 30 de mayo de 1991, pp. 40–52.

Doménech, J., 2003. Depuración y potabilización del agua. Offarm 22, 110–116.

Easter, C., Witherspoon, J., Voigt, R., Cesca, J., 2008. An odor control master planning approach to public outreach programs. Pap. Present. 3rd IWA Int. Conf. Odour VOCs, Barcelona, Spain.

ECOTEC, 2013. Antecedentes para la Regulación de Olores en Chile. Informe desarrollado a solicitud de la Subsecretaria del Medio Ambiente.

Elenter, D., Milferstedt, K., Zhang, W., Hausner, M., Morgenroth, E., 2007. Influence of detachment on substrate removal and microbial ecology in a heterotrophic/autotrophic biofilm. Water Res. 41, 4657–4671. https://doi.org/10.1016/J.WATRES.2007.06.050

Elias, A., Barona, A., Arreguy, A., Rios, J., Aranguiz, I., Peñas, J., 2002. Evaluation of a packing material for the biodegradation of H2S and product analysis. Process Biochem. 37, 813–820. https://doi.org/10.1016/S0032-9592(01)00287-4

Elmrini, H., Bredin, N., Shareefdeen, Z., Heitz, M., 2004. Biofiltration of xylene emissions: bioreactor response to variations in the pollutant inlet concentration and gas flow rate. Chem. Eng. J. 100, 149–158. https://doi.org/10.1016/J.CEJ.2004.01.030

Empresa Municipal de Abastecimiento y Saneamiento de Granada S.A., 2021. Depuración [WWW Document]. URL https://www.emasagra.es/depuracion (accessed 12.1.21).

Empresa Provincial de Aguas de Córdoba S.A., 2021. Depuración de Aguas Residuales [WWW Document]. URL http://www.aguasdecordoba.es/servicios/depuracion-de-aguas-residuales (accessed 12.1.21).

EN 13725, 2003. Air Quality - Determination of Odour Concentration by Dynamic Olfactometry. European Committee for Standardization, Brussels.

Environment Agency UK, 2011. H4 Odour Management. How to comply with your environmental permit.

Estrada, J.M., Kraakman, N.J.R., Lebrero, R., Muñoz, R., 2015. Integral approaches to wastewater treatment plant upgrading for odor prevention: Activated Sludge and Oxidized Ammonium Recycling. Bioresour. Technol. https://doi.org/10.1016/j.biortech.2015.08.044

Estrada, J.M., Kraakman, N.J.R.B., Muñoz, R., Lebrero, R., 2011. A comparative analysis of odour treatment technologies in wastewater treatment plants. Environ. Sci. Technol. 45, 1100–1106. https://doi.org/10.1021/es103478j

Fan, F., Xu, R., Wang, D., Meng, F., 2020. Application of activated sludge for odor control in wastewater treatment plants: Approaches, advances and outlooks. Water Res. 181, 115915. https://doi.org/10.1016/J.WATRES.2020.115915

Ferrer, J., Seco, A., 2021. Economía circular de las aguas residuales. RETEMA 231, 18–19.

Frechen, F.B., 2004. Odour emission inventory of German wastewater treatment plants - Odour flow rates and odour emission capacity. Water Sci. Technol. 50, 139–146. https://doi.org/10.2166/WST.2004.0244

Gabriel, D., Deshusses, M.A., 2004. Technical and economical analysis of the conversion of a full-scale scrubber to a biotrickling filter for odor control. Water Sci. Technol. 50, 309–318. https://doi.org/10.2166/WST.2004.0292

Gandiglio, M., Lanzini, A., Soto, A., Leone, P., Santarelli, M., 2017. Enhancing the energy efficiency of wastewater treatment plants through co-digestion and fuel cell systems. Front. Environ. Sci. 5, 70. https://doi.org/10.3389/FENVS.2017.00070/BIBTEX

Gebicki, J., Byliński, H., Namieśnik, J., 2016. Measurement techniques for assessing the olfactory impact of municipal sewage treatment plants. Environ. Monit. Assess. 188, 1–15. https://doi.org/10.1007/s10661-015-5024-2

González, S.O., Almeida, C.A., Calderón, M., Mallea, M.A., González, P., 2014. Assessment of the water self-purification capacity on a river affected by organic pollution: application of chemometrics in spatial and temporal variations. Environ. Sci. Pollut. Res. 21, 10583–10593. https://doi.org/10.1007/S11356-014-3098-Y/TABLES/7

Hawko, C., Verriele, M., Hucher, N., Crunaire, S., Leger, C., Locoge, N., Savary, G., 2021. A review of environmental odor quantification and qualification methods: The question of objectivity in sensory analysis. Sci. Total Environ. 795, 148862. https://doi.org/10.1016/J.SCITOTENV.2021.148862

Hayes, J.E., Stevenson, R.J., Stuetz, R.M., 2017. Survey of the effect of odour impact on communities. J. Environ. Manage. 204, 349–354. https://doi.org/10.1016/j.jenvman.2017.09.016

Iglesias, A.R., 2014. Contaminación odorífera. CONAMA 2014, Madrid, España.

Iglesias, A.R., 2008. Contaminación atmosférica por olores: unas técnicas de medida avanzadas y una legislación específica inexistente. CONAMA 2008, Madrid, España.

Informe bienal de notificación (Q-2019), de la Directiva 91/271/CEE [WWW Document] URL https://cdr.eionet.europa.eu/es/eu/uwwt17/envx2y1uq/ (accessed 12.1.21).

Instituto Nacional de Estadística, 2018. Estadística sobre el suministro y saneamiento del agua. Serie 2000-2018 [WWW Document]. URL https://www.ine.es/jaxi/Tabla.htm?path=/t26/p067/p01/serie/l0/&file=01005.px&L=0 (accessed 12.1.21).

Instituto Nacional de Estadística, 2008. Encuesta de Hogares y Medio Ambiente 2008. VIVIENDAS: Clasificación por características de la vivienda [WWW Document]. URL https://www.ine.es/jaxi/Tabla.htm?path=/t25/p500/2008/p01/l0/&file=01031.px&L=0 (accessed 12.1.21).

Instituto Nacional de Seguridad y Salud en el Trabajo, 2021. Límites de exposición profesional para agentes químicos en España.

Iranpour, R., Cox, H.H.J., Deshusses, M.A., Schroeder, E.D., 2005. Literature review of air pollution control biofilters and biotrickling filters for odor and volatile organic compound removal. Environ. Prog. 24, 254–267. https://doi.org/10.1002/ep.10077

Izquierdo, C., Diaz, C., Anton, A., Kavanagh, R., Capelli, L., Arias, R., Salas Seoane, N., Burbano, J., Francis, L., 2021. Analysis of existing regulations in odour pollution, odour impact criteria 2, D-NOSES, H2020-SwafS-23-2017-789315.

Jehlickova, B., Longhurst, P.J., Drew, G.H., 2008. Assessing effects of odour: A critical review of assessing annoyance and impact on amenity. Paper presented at the 3rd IWA International Conference on Odour and VOCs, Barcelona, Spain.

Jiang, G., Melder, D., Keller, J., Yuan, Z., 2017. Odor emissions from domestic wastewater: A review. Crit. Rev. Environ. Sci. Technol. 47, 1581–1611. https://doi.org/10.1080/10643389.2017.1386952

Karageorgos, P., Latos, M., Kotsifaki, C., Lazaridis, M., Kalogerakis, N., 2010. Treatment of unpleasant odors in municipal wastewater treatment plants. Water Sci. Technol. 61, 2635–2644. https://doi.org/10.2166/wst.2010.211

Kraakman, B., Estrada, J., Lebrero, R., Cesca, J., Munoz, R., 2012. Sustainability and Robustness Assessment of Odor Control Technology at Water Treatment Plants. Proc. Water Environ. Fed. 2012, 108–122. https://doi.org/10.2175/193864712811700480

Le-Minh, N., Sivret, E.C., Shammay, A., Stuetz, R.M., 2018. Factors affecting the adsorption of gaseous environmental odors by activated carbon: A critical review. Crit. Rev. Environ. Sci. Technol. 48, 341–375. https://doi.org/10.1080/10643389.2018.1460984

Lebrero, R., Bouchy, L., Stuetz, R., Muñoz, R., 2011. Odor Assessment and Management in Wastewater Treatment Plants: A Review. Crit. Rev. Environ. Sci. Technol. 41, 915–950. https://doi.org/10.1080/10643380903300000

Lebrero, R., Estrada, J.M., 2010. Fuentes de olores, in: Muñoz, R., Lebrero, R., Estrada, J.M. (Eds.), Caracterización Y Gestión de Olores En Estaciones Depuradoras de Aguas Residuales. Gráficas Germinal S.C.L., Valladolid, España, pp. 13–28.

Lebrero, R., Estrada, J.M., Escorial Briso-Montiano, G., 2010. Legislación y Evaluación de Impacto, in: Muñoz, R., Lebrero, R., Estrada, J.M. (Eds.), Caracterización Y Gestión de Olores En Estaciones Depuradoras de Aguas Residuales. Gráficas Germinal S.C.L., Valladolid, España, pp. 71–80.

Ley 5/2013, de 11 de junio, por la que se modifican la Ley 16/2002, de 1 de julio, de prevención y control integrados de la contaminación y la Ley 22/2011, de 28 de julio, de residuos y suelos contaminados. Boletín Oficial del Estado, núm. 140, 12 de junio de 2013, pp. 44257–44288.

Lin, G., Lu, J., Sun, Z., Xie, J., Huang, J., Su, M., Wu, N., 2021. Characterization of tissue-associated bacterial community of two Bathymodiolus species from the adjacent cold seep and hydrothermal vent environments. Sci. Total Environ. 796, 149046. https://doi.org/10.1016/J.SCITOTENV.2021.149046

López, R., Cabeza, I.O., Giráldez, I., Díaz, M.J., 2011. Biofiltration of composting gases using different municipal solid waste-pruning residue composts: Monitoring by using an electronic nose. Bioresour. Technol. 102, 7984–7993. https://doi.org/10.1016/j.biortech.2011.05.085

Martin, M.J., Anfruns, A., Lebrero, R., Estrada, J.M., Canals, C., Vega, E., 2010. Procesos de adsorción, in: Muñoz, R., Lebrero, R., Estrada, J.M. (Eds.), Caracterización Y Gestión de Olores En Estaciones Depuradoras de Aguas Residuales. Gráficas Germinal S.C.L., Valladolid, España, pp. 115–126.

Melo, L.F., 2003. Biofilm formation and its role in fixed film processes, in: Handbook of Water and Wastewater Microbiology. Academic Press, pp. 337–349. https://doi.org/10.1016/B978-012470100-7/50021-2

Ministerio de Medio Ambiente y Medio Rural y Marino, 2010. Manual para la implantación de sistemas de depuración en pequeñas poblaciones. Centro de Publicaciones del Ministerio de Medio Ambiente y Medio Rural y Marino, Madrid.

Ministerio para la Transición Ecológica y el Reto Demográfico, 2020. Estrategia Española de Economía Circular. España Circular 2030.

Mirbagheri, S.A., Ahmadi, S., Biglari-Joo, N., 2016. Denitrification of nitrate-contaminated groundwater in an anoxic rotating biological contactor: a case study. Desalin. Water Treat. 57, 4694–4700. https://doi.org/10.1080/19443994.2014.994106

Mudliar, S., Giri, B., Padoley, K., Satpute, D., Dixit, R., Bhatt, P., Pandey, R., Juwarkar, A., Vaidya, A., 2010. Bioreactors for treatment of VOCs and odours - A review. J. Environ. Manage. https://doi.org/10.1016/j.jenvman.2010.01.006

Muñoz, R., 2010a. Percepción y caracterización de olores, in: Muñoz, R., Lebrero, R., Estrada, J.M. (Eds.), Caracterización Y Gestión de Olores En Estaciones Depuradoras de Aguas Residuales. Gráficas Germinal S.C.L., Valladolid, España, pp. 1–12.

Muñoz, R., 2010b. Oxidación Biológica, in: Muñoz, R., Lebrero, R., Estrada, J.M. (Eds.), Caracterización Y Gestión de Olores En Estaciones Depuradoras de Aguas Residuales. Gráficas Germinal S.C.L., Valladolid, España, pp. 127–140.

Naddeo, V., Belgiorno, V., Zarra, T., 2012. Procedures for Odour Impact Assessment, in: Belgiorno, V., Naddeo, V., Zarra, T. (Eds.), Odour Impact Assessment Handbook. John Wiley & Sons, Ltd, pp. 187–203. https://doi.org/10.1002/9781118481264.CH7

Nakamoto, T., 2005. Odor recorder. Sens. Lett. 3, 136–150. https://doi.org/10.1166/SL.2005.018

Nguyen, T.K.L., Ngo, H.H., Guo, W., Chang, S.W., Nguyen, D.D., Nghiem, L.D., Liu, Y., Ni, B., Hai, F.I., 2019. Insight into greenhouse gases emissions from the two popular treatment technologies in municipal wastewater treatment processes. Sci. Total Environ. 671, 1302–1313. https://doi.org/10.1016/j.scitotenv.2019.03.386

Nugraha, W.D., Sarminingsih, A., Alfisya, B., 2020. The Study of Self Purification Capacity Based on Biological Oxygen Demand (BOD) and Dissolved Oxygen (DO) Parameters. IOP Conf. Ser. Earth Environ. Sci. 448, 12105. https://doi.org/10.1088/1755-1315/448/1/012105

Olores.org, 2018. CALPUFF ha dejado de ser un modelo regulatorio por la EPA de EEUU [WWW Document]. URL https://www.olores.org/index.php?option=com_content&view=article&id=816:calpuff-ha-dejado-de-ser-un-modelo-regulatorio-para-la-epa-de-eeuu&catid=86&lang=es&Itemid=307 (accessed 12.1.21).

Olores.org, 2008. Olores [WWW Document]. URL https://www.olores.org/website/index.php?option=com_content&view=article&id=1&Itemid=3&lang=es (accessed 11.10.21).

Ordenanza de protección de la atmósfera, 1994. Ayuntamiento de San Vicente del Raspeig. Boletín Oficial de la Provincia, 17 de febrero de 1994.

Ordenanza Municipal de protección de la atmósfera frente a la contaminación por formas de la materia, 1999. Concejalía de Medio Ambiente. Ayuntamiento de Las Palmas de Gran Canaria. Boletín Oficial de la Provincia, 25 de junio de 1999.

Organización de las Naciones Unidas para la Educación, la Ciencia y la Cultura, 2003. Informe de las Naciones Unidas sobre el Desarrollo de los Recursos Hídricos en el Mundo: Agua para todos, agua para la vida.

Organización de las Naciones Unidas para la Educación, la Ciencia y la Cultura, 2021. Informe Mundial de las Naciones Unidas sobre el Desarrollo de los Recursos Hídricos 2021: El valor del agua.

Plan Nacional de Calidad de las Aguas: Saneamiento y Depuración 2007-2015 (PNCA). Acuerdo del Consejo de Ministros de 8 de julio de 2007.

Plan Nacional de Depuración, Saneamiento, Eficiencia, Ahorro y Reutilización (Plan DSEAR). Orden TED/801/2021, de 14 de julio. Boletín Oficial del Estado, núm. 178, 27 de julio de 2021, pp. 90608–90615.

Plan Nacional de Saneamiento y Depuración 1995-2005 (PNSD). Resolución de 28 de abril de 1995, de la Secretaría de Estado de Medio Ambiente y Vivienda, por la que se dispone la publicación del Acuerdo del Consejo de Ministros de 17 de febrero de 1995. Boletín Oficial del Estado, núm. 113, 12 de mayo de 1995, pp. 13808–13824.

Prado, Ó.J., Gabriel, D., Lafuente, J., 2009. Economical assessment of the design, construction and operation of open-bed biofilters for waste gas treatment. J. Environ. Manage. 90, 2515–2523. https://doi.org/10.1016/J.JENVMAN.2009.01.022

Proyecto de Decreto de protección de la atmósfera de Canarias, 2019. Consejería de Política Territorial, Sostenibilidad y Seguridad. Gobierno de Canarias.

Real Decreto-ley 11/1995, de 28 de diciembre, por el que se establecen las normas aplicables al tratamiento de las aguas residuales urbanas. Boletín Oficial del Estado, núm. 312, 30 de diciembre de 1995, pp. 37517–37519.

Real Decreto 815/2013, de 18 de octubre, por el que se aprueba el Reglamento de emisiones industriales y de desarrollo de la Ley 16/2002, de 1 de julio, de prevención y control integrados de la contaminación. Boletín Oficial del Estado, núm. 251, 19 de octubre de 2013, pp. 85173–85276.

Ren, B., Zhao, Y., Lyczko, N., Nzihou, A., 2019. Current Status and Outlook of Odor Removal Technologies in Wastewater Treatment Plant. Waste Biomass Valorization 10, 1443–1458. https://doi.org/10.1007/s12649-018-0384-9

Revah, S., Morgan-Sagastume, J.M., 2005. Methods of odor and VOC control, in: Biotechnology for Odor and Air Pollution Control. Springer Berlin Heidelberg, pp. 29–63. https://doi.org/10.1007/3-540-27007-8_3

Rybarczyk, P., Szulczyński, B., Gospodarek, M., Gębicki, J., 2020. Effects of n-butanol presence, inlet loading, empty bed residence time and starvation periods on the performance of a biotrickling filter removing cyclohexane vapors from air. Chem. Pap. 74, 1039–1047. https://doi.org/10.1007/s11696-019-00943-2

Sainz, J.A., 2005. Tecnologías para la sostenibilidad: procesos y operaciones unitarias en depuración de aguas residuales. Fundación Escuela de Organización Industrial, Madrid, España.

Sanchez, C., Couvert, A., Laplanche, A., Renner, C., 2006. New compact scrubber for odour removal in wastewater treatment plants. Water Sci. Technol. 54, 45–52. https://doi.org/10.2166/WST.2006.862

Sánchez, J.I., Amo, A., Martínez, J.V., Valor, I., 2008. Contaminación ambiental por olores (I). Fundamentos básicos. Contraste Publicaciones, S.L., Murcia, España.

Scholz, M., 2006. Rotating biological contactors, in: Wetland Systems to Control Urban Runoff. Elsevier, pp. 111–113. https://doi.org/10.1016/B978-044452734-9/50020-7

Senatore, V., Zarra, T., Galang, M.G., Oliva, G., Buonerba, A., Li, C.-W., Belgiorno, V., Naddeo, V., 2021. Full-Scale Odor Abatement Technologies in Wastewater Treatment Plants (WWTPs): A Review. Water 13. https://doi.org/10.3390/w13243503

Servicio de Evaluación Ambiental, 2017. Guía para la Predicción y Evaluación de Impactos por Olor en el SEIA. Ministerio del Medio Ambiente. Gobierno de Chile.

Servicio de Evaluación Ambiental, 2012. Guía para el Uso de Modelos de Calidad del Aire en el SEIA. Ministerio del Medio Ambiente. Gobierno de Chile.

Shammay, A., Sivret, E.C., Le-Minh, N., Lebrero Fernandez, R., Evanson, I., Stuetz, R.M., 2016a. Review of odour abatement in sewer networks. J. Environ. Chem. Eng. 4, 3866–3881. https://doi.org/10.1016/J.JECE.2016.08.016

Shammay, A., Sivret, E.C., Wang, B., Evanson, I., Stuetz, R.M., 2016b. Performance of Field Based Activated Carbon Systems for Odour Control. Chem. Eng. Trans. 54, 277–282. https://doi.org/10.3303/CET1654047

Siatou, A., Manali, A., Gikas, P., 2020. Energy Consumption and Internal Distribution in Activated Sludge Wastewater Treatment Plants of Greece. Water 12, 1204. https://doi.org/10.3390/W12041204

Sikosana, M.L., Sikhwivhilu, K., Moutloali, R., Madyira, D.M., 2019. Municipal wastewater treatment technologies: A review. Procedia Manuf. 35, 1018–1024. https://doi.org/10.1016/j.promfg.2019.06.051

St. Croix Sensory, 2003. A Detailed Assessment of The Science and Technology of Odor Measurement [WWW Document]. URL https://www.pca.state.mn.us/sites/default/files/p-gen2-01.pdf (accessed 11.20.21).

Stuetz, R., Frechen, F.B., 2001. Odours in Wastewater Treatment - Measurement, Modelling and Control. IWA, London, England. https://doi.org/10.2166/9781780402932

Sucker, K., Both, R., Winneke, G., 2009. Review of adverse health effects of odours in field studies. Water Sci. Technol. 59, 1281–1289. https://doi.org/10.2166/WST.2009.113

Talaiekhozani, A., Bagheri, M., Goli, A., Talaei Khoozani, M.R., 2016. An overview of principles of odor production, emission, and control methods in wastewater collection and treatment systems. J. Environ. Manage. 170, 186–206. https://doi.org/10.1016/j.jenvman.2016.01.021

Tchobanoglous, G., Burton, F.L., Stensel, H.D., 2003. Wastewater Engineering: Treatment and Reuse. McGraw Hill, New York, NY.

Teixeira, P., Oliveira, R., 2001. Denitrification in a closed rotating biological contactor: effect of disk submergence. Process Biochem. 37, 345–349. https://doi.org/10.1016/S0032-9592(01)00216-3

Turk, A., Bandosz, T.J., 2001. Adsorption systems for odour treatment, in: Stuetz, R., Frechen, F.B. (Eds.), Odours in Wastewater Treatment: Measurement, Modelling and Control. IWA, London, England.

U.S. Environmental Protection Agency, 1985. Design manual: Odor and corrosion control in sanitary sewerage systems and treatment plants. Washington, DC, EPA/625/1-85/018.

Van Broeck, G., Bogaert, S., De Meyer, L., 2008. Monetary valuation of odour nuisance as a tool to evaluate cost effeciveness of possible odour reduction techniques. Paper presented at the 3rd IWA International Conference on Odour and VOCs, Barcelona, Spain.

Van den Broeck, R.M.R., Van Impe, J.F.M., Smets, I.Y.M., 2009. Assessment of activated sludge stability in lab-scale experiments. J. Biotechnol. 141, 147–154. https://doi.org/10.1016/J.JBIOTEC.2009.02.019

VDI 3882 part 1, 1992. Olfactometry – Determination of odour intensity. Verein Deutscher Ingenieure, Germany.

VDI 3882 part 2, 1994. Olfactometry – Determination of hedonic odour tone. Verein Deutscher Ingenieure, Germany.

VDI 3940 Part 1, 2006. Measurement of Odour Impact by Field Inspection - Measurement of the Impact Frequency of Recognizable Odours Grid Measurement. VDI-Verlag GmbH, Germany.

VDI 3940 Part 2, 2006. Measurement of Odour Impact by Field Inspection - Measurement of the Impact Frequency of Recognizable Odours Plume Measurement. VDI-Verlag GmbH, Germany.

Vergara, H., Zorich, V., 2013. Experiencias en la aplicación de la Normativa Alemana VDI 3880:2011, en muestreos de olores en Chile [WWW Document]. URL https://www.olores.org/index.php?option=com_content&view=article&id=276&lang=es (accessed 12.1.21).

Wang, B., Sivret, E.C., Parcsi, G., Wang, X., Le, N.M., Kenny, S., Bustamante, H., Stuetz, R.M., 2014. Is H2S a suitable process indicator for odour abatement performance of sewer odours? Water Sci. Technol. 69, 92–98. https://doi.org/10.2166/WST.2013.559

Water Environment Federation, 2017. Liquid Stream Fundamentals: Odor Management and Control [Fact Sheet] [WWW Document]. URL https://www.wef.org/globalassets/assets-wef/direct-download-library/public/03---resources/wsec-2017-fs-028-liquid-stream-fundamentals--odor-control_final.pdf (accessed 3.11.20).

World Health Organization, 2018. WHO Water, Sanitation and Hygiene strategy 2018-2025. Geneva: World Health Organization; 2018 (WHO/CED/PHE/WSH/18.03). Licence: CC BY-NC-SA 3.0 IGO.

Yang, C., Qian, H., Li, X., Cheng, Y., He, H., Zeng, G., Xi, J., 2018. Simultaneous Removal of Multicomponent VOCs in Biofilters. Trends Biotechnol. https://doi.org/10.1016/j.tibtech.2018.02.004

Zarra, T., Galang, M.G.K., Belgiorno, V., Naddeo, V., 2021. Environmental Odour Quantification by IOMS: Parametric vs. Non-Parametric Prediction Techniques. Chemosens. 2021, Vol. 9, Page 183 9, 183. https://doi.org/10.3390/CHEMOSENSORS9070183

OBJETIVOS

OBJECTIVES

Los objetivos globales de la presente Tesis Doctoral se centran en evaluar la emisión odorífera derivada del tratamiento de aguas residuales municipales, así como su seguimiento y control, para poder así actuar sobre dichos procesos con el fin de minimizar su impacto odorífero y proponer alternativas sostenibles para la valorización de los materiales que se emplean en el control de la mencionada emisión.

Estos objetivos generales se desglosan en los siguientes objetivos específicos:

- Comparar las emisiones odoríferas de dos EDAR urbanas de pequeño-mediano tamaño con tecnologías de tratamiento biológico diferentes y habituales (fangos activos de aireación prolongada y biodiscos), desde el punto de vista de su operación y el contenido bacteriano de los lodos generados en cada instalación (*Márquez y col. 2022. Activated sludge process versus rotating biological contactors in WWTPs: Evaluating the influence of operation and sludge bacterial content on their odor impact. Process Saf. Environ. Prot. 160, 775–785*).
- Cuantificar la emisión odorífera de los puntos críticos de una EDAR urbana de gran tamaño que opera con tecnología de fangos activos en la línea de aguas y, en la línea de fangos, con codigestión anaerobia de lodo y otros residuos y/o subproductos orgánicos biodegradables agroalimentarios e industriales. A continuación, simular cuantitativamente y de manera estacional la dispersión del olor emitido por los mismos, con el objetivo de evaluar su posible impacto en las poblaciones cercanas. Para ello, se ha desarrollado un modelo de dispersión Euleriano, considerando la orografía del terreno y las condiciones meteorológicas y atmosféricas más desfavorables en cada estación del año (*Márquez y col. Odor impact simulation of a large urban wastewater treatment plant through the numerical solution of an Eulerian model. J. Environ. Manage. Under review*).
- Caracterización integral de la emisión odorífera de la citada EDAR urbana de gran tamaño, tanto a través de la cuantificación cromatográfica de los compuestos volátiles retenidos en el CAG empleado en su desodorización, como del análisis fisicoquímico, olfatométrico y textural de dicho material adsorbente (*Márquez y col. 2021. Integral evaluation of granular activated carbon at four stages of a full-scale WWTP deodorization system. Sci. Total Environ. 754, 142237*).

- Evaluar la viabilidad de la regeneración térmica oxidativa del CAG contaminado para la posterior reutilización del carbón regenerado como adsorbente de malos olores en EDAR, todo ello en base al estudio de sus propiedades fisicoquímicas, texturales y estructurales (*Márquez y col. 2021. Simple and eco-friendly thermal regeneration of granular activated carbon from the odour control system of a full-scale WWTP: Study of the process in oxidizing atmosphere. Sep. Purif. Technol. 255, 117782*).
- Comparar la regeneración térmica del carbón activado en atmósfera de aire con su homóloga en atmósfera inerte de nitrógeno, no sólo atendiendo al análisis fisicoquímico, textural y estructural del material adsorbente sino también al coste económico operacional de cada uno de los procesos regenerativos mencionados, bien para una posible valorización de los carbones como nuevos adsorbentes de olores o bien para otras aplicaciones de alto valor añadido (*Márquez y col. 2022. Evaluating the thermal regeneration process of massively generated granular activated carbons for their reuse in wastewater treatments plants. J. Clean. Prod. 366, 132685*).
- Analizar el comportamiento electroquímico de baterías sostenibles de litio-azufre (Li-S) desarrolladas a escala de laboratorio mediante el empleo del carbón activado regenerado (en atmósfera oxidante), como matriz para alojar azufre en el cátodo carbonoso de las mencionadas baterías (*Benítez y col. 2021. Simple and Sustainable Preparation of Cathodes for Li−S Batteries: Regeneration of Granular Activated Carbon from the Odor Control System of a Wastewater Treatment Plant. ChemSusChem. 14, 3915–3925*).
- Evaluar la influencia de diferentes rellenos filtrantes (virutas de madera exclusivamente o en mezcla con compost estabilizado de lodos de EDAR) en el rendimiento de eliminación de olores de biofiltros alimentados con corrientes gaseosas contaminadas con ácido butírico, abordando, de forma conjunta, el seguimiento de las eficacias de eliminación de olor mediante olfatometría dinámica, los cambios en los parámetros fisicoquímicos de los lechos empleados y la evolución de las comunidades microbianas presentes en ellos (*Márquez y col. 2021. Influence of packing material on the biofiltration of butyric acid: A comparative study from a physico-chemical, olfactometric and microbiological perspective. J. Environ. Manage. 294, 113044*).

- Comparar, desde las perspectivas antes mencionadas, la biofiltración de corrientes gaseosas independientes con concentraciones de ácido butírico y D-limoneno, analizando cómo influyen tanto la naturaleza química de cada compuesto como el material de relleno (virutas de madera exclusivamente o en mezcla con compost estabilizado de lodos de EDAR) en los rendimientos de eliminación de olor (*Márquez y col. 2022. A comparative study between the biofiltration for air contaminated with limonene or butyric acid using a combination of olfactometric, physico-chemical and genomic approaches. Process Saf. Environ. Prot. 160, 362–375*).

The main purposes of this Doctoral Thesis focus on evaluating the odour emission derived from municipal wastewater treatment, as well as its monitoring and control, to proceed on the basis of such processes to mitigate the odorous impact, and propose sustainable alternatives in order to valorise the materials used to control odour emissions from the WWTPs.

Such general purposes can be segregated in the following specific objectives:

- To compare the odour emissions from two small-medium sized urban WWTPs with different and common biological treatment technologies (activated sludge process based on extended aeration, and rotating biological contactors), considering their operation and the bacterial content of the sewage sludge generated in each facility (*Márquez et al. (2022). Activated sludge process versus rotating biological contactors in WWTPs: Evaluating the influence of operation and sludge bacterial content on their odor impact. Process Saf. Environ. Prot. 160, 775–785*).
- To quantify the odour emission from the critical odour sources of a large urban WWTP which operates with activated sludge process in the wastewater line, and with anaerobic co-digestion of sludge and other organic biodegradable agri-food and industrial waste in the sludge line. Then, to quantitatively simulate the dispersion of the odour emitted by such sources in each season of the year, with the aim of evaluating their possible impact on nearby populations. For this purpose, an Eulerian dispersion model has been developed, considering the orography and the most unfavourable meteorological and atmospheric conditions in each season of the year (*Márquez et al. Odor impact simulation of a large urban wastewater treatment plant through the numerical solution of an Eulerian model. J. Environ. Manage. Under review*).
- To carry out the physico-chemical, olfactometric and textural characterisation of GAC used by the above mentioned large urban WWTP as a deodorisation system, as well as the chromatographic quantification of the retained odoriferous compounds (*Márquez et al. (2021). Integral evaluation of granular activated carbon at four stages of a full-scale WWTP deodorization system. Sci. Total Environ. 754, 142237*).

- To evaluate the feasibility of the oxidative thermal regeneration process of contaminated GAC for subsequent reuse as odour adsorbent in WWTPs, based on its physico-chemical, textural and structural properties (*Márquez et al. (2021). Simple and eco-friendly thermal regeneration of granular activated carbon from the odour control system of a full-scale WWTP: Study of the process in oxidizing atmosphere. Sep. Purif. Technol. 255, 117782*).
- To compare the thermal regeneration of GAC in air atmosphere with its counterpart in inert nitrogen atmosphere, considering both the physico-chemical, textural and structural analysis of the adsorbent material and the operational economic cost of each regenerative processes, either for a possible valorisation of activated carbon as new odour adsorbent or for other applications with high added value (*Márquez et al. (2022). Evaluating the thermal regeneration process of massively generated granular activated carbons for their reuse in wastewater treatments plants. J. Clean. Prod. 366, 132685*).
- To analyse the electrochemical behaviour of sustainable lithium-sulphur (Li-S) batteries developed on a laboratory scale by using regenerated activated carbon (in oxidizing atmosphere) as a matrix to accommodate sulphur in the carbonaceous cathode of such batteries (*Benítez et al. (2021). Simple and sustainable preparation of cathodes for Li−S batteries: Regeneration of granular activated carbon from the odor control system of a wastewater treatment plant. ChemSusChem. 14, 3915–3925*).
- To evaluate the influence of different packed beds (wood chips exclusively or mixed with sewage sludge compost) on the odour removal performance of non-inoculated biofilters fed with gaseous streams contaminated with butyric acid. Monitoring odour removal efficiencies by dynamic olfactometry, the changes in the physico-chemical parameters of the beds and the evolution of the microbial communities present in them (*Márquez et al. (2021). Influence of packing material on the biofiltration of butyric acid: A comparative study from a physico-chemical, olfactometric and microbiological perspective. J. Environ. Manage. 294, 113044*).

- To compare, from the approaches mentioned above, the biofiltration of independent gaseous streams containing butyric acid and D-limonene, assessing the influence of the biofiltered compound and the filter bed material (wood chips exclusively or mixed with sewage sludge compost) on the odour removal performance by biofiltration (*Márquez et al. (2022). A comparative study between the biofiltration for air contaminated with limonene or butyric acid using a combination of olfactometric, physico-chemical and genomic approaches. Process Saf. Environ. Prot. 160, 362–375*).

MATERIALES Y MÉTODOS

MATERIALS AND METHODS

1. Consideraciones generales

Aunque la metodología y los materiales empleados en la presente Tesis Doctoral se desarrollarán minuciosamente en cada uno de los artículos científicos que la componen, en este apartado se ofrece una visión general, a la vez que sintética, de los diferentes materiales y métodos que se han utilizado en su desarrollo. En este sentido, se ha realizado una recopilación de los mismos en función de si se han caracterizado muestras sólidas, líquidas o gaseosas.

2. Caracterización de muestras sólidas

Las muestras sólidas analizadas han sido de muy diversa índole. A continuación, se describen las diferentes caracterizaciones a las que han sido sometidas, detallándose en cada una de ellas las muestras sólidas que han sido objeto de tal caracterización. En concreto, se abordan tres grandes grupos: por un lado, la caracterización fisicoquímica, textural, estructural y morfológica, por otro el análisis respirométrico y, finalmente, la caracterización microbiológica.

2.1. Caracterización fisicoquímica, textural, estructural y morfológica

2.1.1. Caracterización fisicoquímica

La determinación de los parámetros fisicoquímicos que se detallan a continuación se ha llevado a cabo (por triplicado) de acuerdo con la **metodología** propuesta por **The US Department of Agriculture and the US Composting Council (2002)**:

- Humedad, sólidos minerales, sólidos volátiles, nitrógeno total Kjeldahl, nitrógeno amoniacal y fósforo se han analizado en la fracción sólida de cada muestra.
- Conductividad, pH, nitrógeno total soluble, carbono total soluble, carbono inorgánico soluble y carbono orgánico total soluble se han determinado en extracto acuoso (1:25).

Muestras analizadas: lodos de EDAR, CAG y materiales de relleno de los sistemas de biofiltración.

Por otra parte, la determinación de la concentración de grupos superficiales ácidos y básicos del carbón activado se ha basado en el **método de Boehm** (Boehm, 1994),

mediante titulaciones ácido-base, cuyo fundamento es la reacción de neutralización entre ácidos y bases. El hidróxido de sodio (NaOH) es el reactivo que se ha empleado como base, permitiendo la neutralización de todos los grupos ácidos (incluyendo fenoles, grupos lactónicos y ácidos carboxílicos), mientras que el ácido clorhídrico (HCl) es el que ha permitido la neutralización de los grupos básicos (grupos tipo cromeno, pirona y quinona).

Muestras analizadas: muestras de CAG contaminadas, regeneradas y prístina.

2.1.2. Análisis elemental: Fluorescencia de rayos X (XRF)

La fluorescencia de rayos X es una técnica de espectrometría atómica basada en la detección de la radiación X emitida por átomos excitados. Los fotones fluorescentes son característicos de cada elemento en cuestión y su intensidad determina la concentración del mismo. La mencionada técnica se ha utilizado para analizar la composición elemental de las muestras de CAG, tanto contaminadas y regeneradas, como la muestra prístina, utilizando para ello un espectrómetro de fluorescencia de rayos X dispersivos, de longitud de onda secuencial (WDXRF), marca Rigaku, modelo ZSX Primus IV (**Figura 2.1.2.1**). En concreto, se ha determinado el porcentaje en peso de los siguientes elementos: Al, C, Ca, Cl, Fe, K, Mg, Na, P, S, Si y Sr.

Figura 2.1.2.1. Espectrómetro de fluorescencia de rayos X Rigaku ZSX Primus IV.

2.1.3. Análisis termogravimétrico (TGA)

El análisis termogravimétrico es una técnica basada en el control de la masa de una muestra sólida en función del tiempo, o de la temperatura, mientras es sometida a un programa de temperatura controlado en una atmósfera determinada. El programa de temperatura puede consistir en mantener la temperatura constante (isotermo), calentar a

velocidad constante, enfriar o cualquier combinación de ellos. La atmósfera puede ser estática o dinámica, con un caudal determinado (también se emplean condiciones de presión reducida) y los gases más utilizados son N_2, aire, O_2, Ar y CO_2 (los dos primeros son los que se han utilizado para los diferentes análisis termogravimétricos de las muestras de CAG). Una característica fundamental de este tipo de análisis es que sólo permite detectar procesos en los que se produce una variación de masa (por ejemplo, descomposición, sublimación, reducción o absorción).

Para llevar a cabo el análisis termogravimétrico es necesario colocar la muestra en el interior de una electrobalanza de alta sensibilidad, que está cerrada al ambiente. Una vez cerrada, se hace pasar un determinado flujo de gas a través de la muestra y se empieza a calentar mediante una rampa diseñada de temperatura. El instrumento puede constar de un ordenador que registra en continuo la temperatura, la pérdida de peso y el flujo de calor. Conforme ocurre algún proceso de tipo térmico que modifique el peso de la muestra sólida se observará una variación en la curva y un máximo o un mínimo en el flujo de calor (según lo desprenda o lo absorba en dicho proceso).

Figura 2.1.3.1. Analizador termogravimétrico TGA/DSC 1 Star System Mettler Toledo.

Actualmente, los instrumentos comerciales empleados en termogravimetría constan de cuatro partes: una balanza analítica de alta precisión, un horno, un sistema de gas de purga para proporcionar una atmósfera inerte y un microprocesador para el control del instrumento y la adquisición y visualización de datos. El sistema de purga permite, además, cambiar el gas de purga. Los análisis termogravimétricos se han llevado a cabo en un analizador TGA/DSC 1 Star System Mettler Toledo (**Figura 2.1.3.1)**, perteneciente al grupo FQM-175 del Departamento de Química Inorgánica e Ingeniería Química de la Universidad de Córdoba. Las condiciones empleadas en las medidas han dependido de la muestra de CAG a analizar y del tipo de información que se ha pretendido obtener.

2.1.4. Isotermas de adsorción-desorción de nitrógeno

La técnica de fisisorción de gases es la más habitual en la determinación de áreas superficiales y distribución de tamaño de poros de materiales. La fisisorción tiene lugar cuando un gas se pone en contacto con un sólido desgasificado, originándose fuerzas de Van der Waals. El adsorbato más empleado es el nitrógeno, pero también se puede utilizar argón y otros gases inertes e hidrocarburos. Esta técnica se utiliza habitualmente para estudiar las características texturales de la superficie externa e interna de los materiales. En la presente Tesis Doctoral, dicha técnica se ha empleado para caracterizar la estructura porosa de las muestras de CAG (prístina, contaminadas y regeneradas), atendiendo a los siguientes parámetros: superficie específica (S_{BET}, m^2/g), superficie de microporos (S_{micro}, m^2/g), volumen total de poros (V_t, cm^3/g), volumen de microporos (V_{micro}, cm^3/g), diámetro medio de poro (D_{pore}, nm) y distribución de tamaño de poro.

La interacción del gas con la superficie de una muestra sólida produce un equilibrio entre las moléculas adsorbidas y las moléculas en fase gaseosa, que depende de la presión del gas y de la temperatura. La relación entre las moléculas de gas adsorbidas (moles por gramo de adsorbente) y la presión relativa p/p_0 en el intervalo $0< p/p_0 <1$ (donde, p = presión de vapor de equilibrio del adsorbato, p_0 = presión de vapor del adsorbato líquido puro), a temperatura constante, se puede recoger en una isoterma de adsorción. Las isotermas de adsorción-desorción de nitrógeno constan de un proceso de adsorción y un proceso de desorción. Cuando el camino de desorción no coincide con el de adsorción se produce un ciclo de histéresis debido a una interacción del adsorbato dentro de los poros del material.

Figura 2.1.4.1. Sortómetro Micromeritics ASAP 2020.

La forma de la isoterma obtenida para cada material puede proporcionar información acerca de su porosidad. Además, se han desarrollado numerosos métodos con el objetivo de estimar algunas de las propiedades relacionadas con este parámetro, algunos de los cuales se indican más adelante. Las isotermas de adsorción-desorción de nitrógeno se han determinado a la temperatura constante del nitrógeno líquido (77 K), utilizando un analizador automático de adsorción-desorción de gases Micromeritics ASAP 2020 (**Figura 2.1.4.1**), perteneciente al grupo FQM-175 del Departamento de Química Inorgánica e Ingeniería Química de la Universidad de Córdoba. De forma previa a las medidas, todas las muestras se han desgasificado a 0,1 Pa y a una temperatura determinada, en función del tipo de muestra. Las isotermas de adsorción obtenidas permiten mostrar la cantidad de N_2 adsorbido en función de la presión relativa (p/p_0).

Para el cálculo de la superficie específica se ha empleado el método Brunauer-Emmet-Teller (BET). Para la distribución del tamaño de poro, se ha empleado el método DFT (density functional theory), asumiendo un modelo de poro cilíndrico y utilizando la rama de adsorción de la isoterma. Además, se ha empleado el método t-plot para estimar el área de microporos, mientras que el volumen de los mismos se ha calculado de acuerdo con la ecuación de Dubinin-Radushkevich (Nguyen and Do, 2001).

2.1.5. Porosimetría de intrusión de mercurio

La porosimetría de intrusión de mercurio es una técnica que, mediante la aplicación de presión, fuerza la entrada de mercurio en los poros del sólido a analizar. El valor del volumen de mercurio intruido permite calcular el área, distribución de tamaños de poro y el porcentaje de porosidad del material, entre otros parámetros. Esta técnica se emplea fundamentalmente cuando el material objeto de estudio presenta macro y mesoporos, como es el caso de los materiales de relleno que se han empleado en los biofiltros objeto de estudio (virutas de madera y compost estabilizado de lodos de EDAR). El equipamiento utilizado para analizar las propiedades texturales de los materiales anteriormente mencionados ha consistido en un porosímetro de intrusión de mercurio Micromeritics AutoPore IV 9500 (**Figura 2.1.5.1**).

Figura 2.1.5.1. Porosímetro Micromeritics AutoPore IV 9500.

2.1.6. Difracción de rayos X (XRD)

La técnica de difracción de rayos X se basa en la incidencia de un haz de rayos X, de una determinada longitud de onda y con un determinado ángulo, sobre la superficie plana de un sólido cristalino. Esta interacción produce una dispersión de parte del mencionado haz en todas las direcciones, producto de los electrones que integran los átomos e iones, mientras que el resto del haz de rayos X puede dispersarse elásticamente en ciertas direcciones mediante interferencia constructiva, dando lugar al fenómeno físico de difracción. El fundamento de esta técnica se caracteriza principalmente por la disposición ordenada de los átomos en la estructura cristalina del material (Linden and Reddy, 2002).

Al objeto de caracterizar estructuralmente las diferentes muestras de CAG (prístina, contaminadas y regeneradas), los difractogramas de rayos X han sido obtenidos gracias a un difractómetro Bruker D8 Discover A25 (**Figura 2.1.6.1**) perteneciente al Instituto Químico para la Energía y el Medioambiente (IQUEMA) de la Universidad de Córdoba.

Figura 2.1.6.1. Difractómetro Bruker D8 Discover A25.

2.1.7. Espectroscopía Raman

El análisis mediante espectroscopia Raman se fundamenta en la incidencia de un haz de luz monocromática de frecuencia (ν_0) sobre una muestra cuyas características moleculares se pretenden determinar, y examinar la luz dispersada por dicha muestra. La mayor parte de la luz dispersada presenta la misma frecuencia que la luz incidente pero una fracción muy pequeña experimenta un cambio frecuencial, resultado de la interacción de la luz con la materia. La luz que mantiene la misma frecuencia (ν_0) que la luz incidente se conoce como dispersión Rayleigh y no aporta ninguna información relevante acerca del material. La luz dispersada que presenta frecuencias distintas a la de la radiación incidente, sí proporciona información sobre la composición estructural de la muestra analizada y es la que se conoce como dispersión Raman (Warner et al., 2013). Esta técnica proporciona información química y estructural del material mediante el conocimiento de los modos vibracionales presentes en cada una de las muestras. De esta forma, proporciona un análisis cualitativo de los componentes orgánicos o inorgánicos de una muestra, así como posibles estructuras que se presenten.

En el caso de carbones, la espectroscopía Raman puede aportar información referente a la estructura e incluso a sus propiedades electrónicas. Es por ello por lo que esta técnica se ha utilizado para analizar las muestras de CAG, tanto la prístina como las contaminadas y las regeneradas, al objeto de establecer comparaciones de carácter estructural entre ellas. Se presentan pocas señales vibracionales importantes en el intervalo de 1000–2000 cm^{-1}: los modos vibracionales más importantes son el G y el 2D,

correspondientes a las señales observadas a 1580 cm^{-1} y a 2700 cm^{-1}, respectivamente. Otros dos picos pueden aparecer ocasionalmente, uno asignado a la vibración D (1350 cm^{-1}) y el otro a la vibración G* (2450 cm^{-1}). El modo vibracional G corresponde al estiramiento de todos los pares de enlaces de átomos sp^2, tanto en los anillos como en las cadenas, mientras que el modo vibracional D surge como resultado del modo de relajación de los átomos sp^2 en los anillos. Otro parámetro a tener en cuenta, derivado del espectro Raman, es la relación de intensidades de los picos D y G (I_D/I_G), puesto que aporta información acerca del desorden estructural y la presencia de defectos en el carbón.

Figura 2.1.7.1. Espectrómetro Raman Renishaw (inVia Raman Microscope).

Los espectros Raman de las muestras anteriormente mencionadas han sido registrados en un espectrómetro Raman Renishaw (inVia Raman Microscope) equipado con un microscopio Leica con varias lentes, monocromadores, filtros, un detector de carga acoplada (en inglés *charge-coupled device*, conocido también como *CCD*) y dos videocámaras (**Figura 2.1.7.1**). El equipamiento citado anteriormente pertenece al grupo FQM-162 del Departamento de Química Orgánica de la Universidad de Córdoba.

2.1.8. Microscopía electrónica de barrido (SEM)

La microscopía electrónica de barrido (SEM) se emplea, principalmente, en la evaluación de la topología de materiales y de la morfología de partículas. Esta técnica se fundamenta en el bombardeo de un haz de electrones que, manejado a través de lentes electromagnéticas, se proyecta sobre una muestra muy delgada situada en una columna de alto vacío (Akhtar et al., 2018).

La interacción de los electrones incidentes con la materia genera una serie de emisiones (electrones secundarios, rayos X característicos, fotones de distintas energías, etc.) que son detectadas, convertidas en señales electrónicas y amplificadas convenientemente, proporcionando información de gran relevancia para la caracterización de la muestra. Cuando el haz primario de electrones entra en contacto con

la superficie de la muestra, una parte de ellos es reflejada de la superficie, pero el resto penetra algunas capas atómicas, siguiendo una trayectoria muy diferente de una recta, antes de volver a emerger a la superficie. Modulando la acción de estos electrones es posible obtener la imagen deseada de las partículas que conforman el material.

Figura 2.1.8.1. Microscopio electrónico de barrido JEOL JSM 7800F.

En esta técnica, la imagen se forma a partir de los electrones secundarios de baja energía (< 50 eV) emitidos desde la superficie de la muestra. La variación de intensidad sobre la pantalla genera una sensación de relieve correspondiente a la topografía de la superficie analizada. La gran profundidad de campo y alta resolución permiten obtener información sobre tamaño de partículas, poros, etc. Mediante SEM se han analizado las cenizas derivadas de la calcinación de dos muestras de CAG contaminadas, procedentes de distintos puntos de la desodorización de una EDAR urbana, y los composites catódicos carbón (regenerado)-azufre. Para ello, las muestras se han colocado en un portamuestras de bronce sobre un adhesivo conductor de doble cara. Las muestras se han introducido en el equipo y se ha aplicado vacío para evitar interferencias entre los electrones generados y la humedad o el aire. El equipamiento utilizado para obtener las microfotografías ha sido un microscopio JEOL JSM 7800F (**Figura 2.1.8.1**), perteneciente al Servicio Central de Apoyo a la Investigación (SCAI) de la Universidad de Córdoba.

2.1.9. Microanálisis de energía dispersiva de rayos X (EDAX)

La técnica de energía dispersiva de rayos X (EDAX) se basa en la emisión de rayos X característicos de los elementos presentes en una muestra, cuando ésta es excitada con un haz de electrones energéticos. Así, al incidir este haz sobre la superficie de un sólido,

dichos fotones sufren procesos de dispersión inelástica, cediendo energía a electrones de átomos de la muestra y, por tanto, excitándolos hasta niveles superiores de energía. Estos niveles vacantes que se originan son ocupados por electrones de niveles superiores emitiéndose fotones de rayos X con una energía idéntica al salto energético entre ambos niveles (excitado y fundamental). Esta energía o longitud de onda del fotón es característica del átomo emisor y se determina según la posición de los picos correspondientes a los rayos X (Smith and McCartney, 2005). Mediante EDAX es posible obtener la composición cualitativa de la muestra (elementos presentes), y por integración y tratamiento adecuado, la composición semicuantitativa de la misma. Esta técnica es considerada superficial (sensible a la composición en superficie), pero se puede controlar de una forma aproximada la profundidad del análisis, variando el potencial de aceleración aplicado al haz de electrones. De esta manera, cuanto mayor sea el potencial, más grueso es el volumen de muestra analizado (desde la superficie), con lo que se podrá decir que más detallado y preciso es el análisis.

Es importante destacar que esta técnica se ha utilizado en combinación con la anterior (SEM), para analizar las mismas muestras citadas en el apartado anterior. Para el caso del EDAX, el programa utilizado ha sido Aztec 3.0 SP2, con un voltaje de aceleración de 15 kV y una altura del detector de 10.1 mm, obteniéndose tanto determinación de elementos como imágenes de distribución espacial (mapeado) de los mismos.

2.2. Caracterización respirométrica

La realización de test respirométricos se ha llevado a cabo con el propósito de evaluar la actividad microbiológica aerobia de los lodos de diferentes EDAR y de los rellenos biológicos de los sistemas de biofiltración estudiados. Concretamente, las variables respirométricas analizadas han sido la velocidad específica de consumo de oxígeno (VECO, mg O_2/g SV·h) y el consumo acumulado de oxígeno a las 20 horas de experimento (CAO_{20}, mg O_2/g SV). Para ello, se ha utilizado un respirómetro estático en fase líquida, patentado por el Grupo RNM-271 del Departamento de Química Inorgánica e Ingeniería Química de la Universidad de Córdoba (España, publicación Nº ES2283171 A1 del 16 de octubre de 2007) y desarrollado por Chica et al. (2003) (**Figura 2.2.1**).

El mencionado respirómetro consiste en un baño termostático en el que se introducen dos matraces Erlenmeyer (con un volumen útil de 1 L cada uno), los cuales

constituyen los dos reactores biológicos del experimento respirométrico. En dichos matraces, se introduce una cantidad de muestra determinada que, en función de su concentración en materia orgánica y materia mineral, suele variar de 1 a 10 g en el caso de las muestras sólidas. Además, con el objetivo de favorecer la actividad microbiológica, también se introducen los siguientes micronutrientes en cada uno de los matraces:

- 10 mL de cloruro de calcio ($CaCl_2$; 27,50 g/L).
- 10 mL de cloruro de hierro ($FeCl_3$; 0,25 g/L).
- 10 mL de sulfato de magnesio ($MgSO_4$; 22,50 g/L).

Además, a cada matraz se añaden 30 mL de una disolución de tampón fosfato (K_2HPO_4 (8,50 g/L), $Na_2HPO_4 \cdot 7H_2O$ (33,40 g/L) y NH_4Cl (1,70 g/L)) que permite tamponar el medio a un pH de 7,2, así como 1 g de tiourea al objeto de inhibir el proceso de nitrificación. Este compuesto permite bloquear el consumo de oxígeno por parte de las bacterias nitrificantes, de manera que es posible atribuir todo el consumo de oxígeno a la oxidación del carbono (Wang et al., 2017).

Figura 2.2.1. Respirómetro estático en fase líquida**.**

Una vez que los matraces contienen el medio nutritivo, el tampón fosfato, la tiourea y la muestra, estos se enrasan con agua destilada hasta alcanzar el litro. También es importante destacar que para homogeneizar el contenido de los matraces y favorecer la transferencia de oxígeno en el medio, estos recipientes se mantienen en constante agitación a 300 r.p.m., utilizando agitadores magnéticos (marca Selecta, modelo Agimatic-S). Además, dado que la actividad microbiana depende la temperatura, el baño

en el cual se introducen los matraces dispone de un termostato que permite que la temperatura se mantenga constante (30ºC).

La concentración de oxígeno disuelto se mide con un electrodo Mettler Toledo, modelo IMPRO-6000, conectado a un oxímetro Mettler Toledo, modelo 4200. Además, el respirómetro dispone de difusores de aire que permiten mantener un feedback de oxígeno determinado, estableciéndose en este caso la concentración oxígeno disuelto entre 6,8 y 7,0 mg O_2/L. Dado que el oxígeno del medio se consume por la respiración microbiana, resulta necesario aportarlo al mismo. Por este motivo, ambos reactores biológicos constan de una entrada en su parte superior por la que se introduce aire en función de la demanda respiratoria de los microorganismos. La entrada de aire está regulada por las necesidades existentes, de modo que se accionan unas electroválvulas que permiten, o no, el flujo de aire. Cuando tiene lugar la inyección de aire en el matraz Erlenmeyer, el líquido que ocupa todo el volumen del recipiente y el gas sobrante rebosan por el orificio superior y son conducidos a través de un tubo a un depósito situado en la parte superior del matraz. Cuando la aireación se detiene, caen de nuevo al matraz por acción de la gravedad hasta su llenado, permitiendo así que el sistema pueda considerarse prácticamente hermético.

2.3. Caracterización microbiológica

2.3.1. Recuento de microorganismos aerobios mesófilos

Este análisis se ha llevado a cabo con el objetivo de determinar el total de microrganismos aerobios mesófilos (UFC/g) presentes a distintos tiempos en los diferentes experimentos de biofiltración realizados. Se ha llevado a cabo de acuerdo con la norma ISO4833-1 (2013) y ha sido realizado por el Laboratorio Agroalimentario de Córdoba (LABAGCO). El mencionado estándar internacional describe un método horizontal para la determinación del número de microorganismos capaces de crecer y formar colonias en un medio sólido tras una incubación aerobia a 30ºC.

2.3.2. Análisis genómico

El análisis genómico se ha realizado tanto para las muestras de lodos de EDAR como para las muestras de los rellenos de biofiltración, al objeto de conocer la composición, estructura y/o diversidad de las comunidades bacterianas implicadas en la depuración de las aguas residuales en función del tipo de tratamiento biológico

implementado o en la biofiltración de compuestos gaseosos en función del tipo de relleno biológico empleado y/o el compuesto oloroso contaminante. El análisis genómico se ha realizado en colaboración con el Departamento de Bioquímica y Biología Molecular (BIO-187) de la Universidad de Córdoba.

2.3.2.1. Extracción de ADN

De forma previa a la extracción del ADN de las comunidades microbianas, todas las muestras citadas anteriormente se congelaron a -20ºC. El método empleado para la extracción del ADN ha sido diferente en función del tipo de muestra (lodo de EDAR o relleno de biofiltración) y se ha detallado específicamente en cada uno de los estudios en los que se ha recurrido al análisis genómico. No obstante, independientemente del tipo de muestra, la cantidad de ADN aislado se ha cuantificado espectrofotométricamente y su integridad se ha comprobado mediante visualización en un gel de agarosa al 1%.

2.3.2.2. Secuenciación, predicción de genes y asignación de taxonomía

La amplificación y secuenciación del ARNr 16S han sido realizadas por la Unidad de Genómica del SCAI de la Universidad de Córdoba. Esta metodología se ha realizado en un secuenciador Ion Torrent (PGM), utilizando su kit específico de metagenómica Ion 16S™ y siguiendo las instrucciones del fabricante. Para identificar los microorganismos, las secuencias obtenidas se han analizado con el software de análisis Ion Reporter™ 5.0 para Ion 16S™ Metagenomics. Los cebadores V3 siempre proporcionaron el número máximo de identificaciones y, por tanto, son los que se utilizaron para estimar la comunidad bacteriana de las diferentes muestras.

3. Caracterización de muestras líquidas

Las muestras líquidas analizadas en la presente Tesis Doctoral han consistido, exclusivamente, en las aguas residuales influentes y efluentes de las EDAR de Villaviciosa de Córdoba y Espiel, ambas localidades pertenecientes a la provincia de Córdoba. En tales muestras, solamente se ha analizado DQO, DBO_5 y SS, siendo todas ellas variables de control establecidas por la Directiva 91/271/CEE en el tratamiento de aguas residuales en zonas no sensibles (tal es el caso de las localidades antes mencionadas). Para ello, se han seguido los métodos estándar para el examen de agua y aguas residuales propuestos por APHA (2017).

4. Caracterización de muestras gaseosas

Las muestras gaseosas se han tomado a diferentes escalas: **laboratorio** (muestras gaseosas que contienen compuestos volátiles anteriormente retenidos en las muestras contaminadas de CAG), **piloto** (muestras gaseosas tomadas a la entrada y salida de los biofiltros) e **industrial** (muestras gaseosas tomadas en diferentes EDAR a escala real). Aunque la metodología de toma de muestras gaseosas se define específicamente en cada uno de los artículos que componen esta Tesis Doctoral, resulta de especial interés dedicar un apartado a la toma muestras a escala industrial, considerando los diferentes dispositivos específicos de muestreo que se emplean.

4.1. Toma de muestras gaseosas a escala industrial

Para la toma de muestras gaseosas a escala industrial se ha utilizado una campana de muestreo ventilada (*ventilated sampling hood*) y un sistema de toma de muestras denominado *CSD30 odour sampling device*. Ambos dispositivos han sido desarrollados por la empresa alemana Olfasense GmbH y cumplen con el estándar EN 13725 (2003) y la directriz VDI 3880 (2011).

La **campana de muestreo ventilada** (**Figura 4.1.1**) se utiliza principalmente para focos de emisión pasivos (no ventilados), siendo adecuada para el muestreo de superficies sólidas y líquidas. Para estas últimas, como es el caso que ocurre en las EDAR, es posible acoplar unos flotadores a los lados de la campana. Este dispositivo está fabricado en acero inoxidable y permite cubrir 1 m^2 de superficie. La campana es ventilada automáticamente por dos ventiladores radiales con un flujo volumétrico constante. El ventilador de entrada aspira aire exterior a través de un orificio intercambiable y transporta el aire desde la parte superior a una esquina de la campana a través de un filtro de carbón activo. Desde allí, el aire se distribuye por toda la superficie de la campana, absorbiendo los olores emitidos. A continuación, el aire cargado de olor es extraído hacia la esquina opuesta por el segundo ventilador radial, a través de otro orificio intercambiable con el mismo caudal volumétrico. La muestra para el posterior análisis olfatométrico se toma de las boquillas de aspiración gracias al sistema de toma de muestras CSD30. Es importante destacar que se proporciona el mismo flujo volumétrico en el lado de entrada y en el lado de succión.

Figura 4.1.1. Campana de muestreo ventilada con flotadores acoplados.

Como se ha mencionado anteriormente, para llevar a cabo el proceso de toma de muestra en focos pasivos, la campana de muestreo ventilada ha de conectarse al dispositivo ***CSD30 odour sampling device*** (**Figura 4.1.2**) a través de las boquillas de succión, haciendo uso de un tubo plástico de muestreo. El CSD30 consiste en un contenedor de vacío construido con politetrafluoroetileno (PTFE) y acero inoxidable, que aspira el aire mediante una bomba de vacío durante un tiempo de muestreo de olor predeterminado de 30 minutos. Alternativamente, es posible seleccionar una duración de muestreo más corta, utilizando para ello un temporizador de cuenta regresiva localizado en la cabeza del mencionado dispositivo. El flujo de muestra se regula mediante una boquilla calibrada que está integrada en el dispositivo CSD30 y se cierra automáticamente una vez que la bolsa de muestreo de gas está llena. La velocidad de muestreo de olores es independiente de las condiciones de presión estática en el punto de muestreo si la diferencia de presión es inferior a 150 mbar. Además, el CSD30 funciona con una batería de Ni-Cd recargable integrada, no requiriéndose una conexión de alimentación de corriente alterna. En el caso del muestreo en focos de olor puntuales (como por ejemplo pueden ser las torres de desodorización de CAG de una EDAR), solamente se ha utilizado el dispositivo CSD30, siendo necesario introducir la sonda (tubo plástico de muestreo) en el interior del conducto por donde circula el aire que se pretende muestrear.

Figura 4.1.2. CSD30 odour sampling device.

4.2. Análisis olfatométrico

Al objeto de conocer la concentración de olor de las muestras gaseosas (recogidas en bolsas de muestreo de Nalophan®), todas ellas se han analizado mediante la técnica de **olfatometría dinámica**, en base a la **Norma Europea EN 13725** "*Calidad del aire: determinación de la concentración de olor por olfatometría dinámica*". La olfatometría dinámica utiliza un panel humano de expertos (panelistas) como "elemento sensor" y un equipo denominado olfatómetro que permite realizar diluciones precisas y eficientes. Mediante el olfatómetro, el panel humano es expuesto a diferentes diluciones de la muestra problema con gas neutro (aire limpio), yendo siempre de mayor a menor dilución.

El olfatómetro utilizado en la presente Tesis Doctoral ha sido un olfatómetro TO8 (**Figura 4.2.1**), desarrollado también por Olfasense GmbH. Este equipo se basa en el método "Sí / No", lo que significa que los panelistas deben pulsar un botón para indicar que "Sí" han detectado el olor de la muestra gaseosa. Las muestras odoríferas han sido caracterizadas por cuatro panelistas, previamente calibrados con el gas de referencia, que es el n-butanol (60 ppm). El momento en el cual un panelista pulsa el botón de manera acertada en dos series consecutivas es conocido como ITE (individual threshold estimate), es decir, el límite (umbral) de detección individual. La concentración de olor, expresada en unidades de olor europeas por metro cúbico (ou_E/m^3), es calculada de acuerdo con la media geométrica de los umbrales de olor de cada panelista, multiplicada por el valor resultante de la raíz cuadrada del factor de paso de dilución del olfatómetro (para el olfatómetro TO8 es 2). La mencionada concentración de olor es calculada de forma automática por el software del olfatómetro que, a su vez, permite calcular la concentración detectada por cada uno de los panelistas y crear una base de datos con los resultados obtenidos en cada medida.

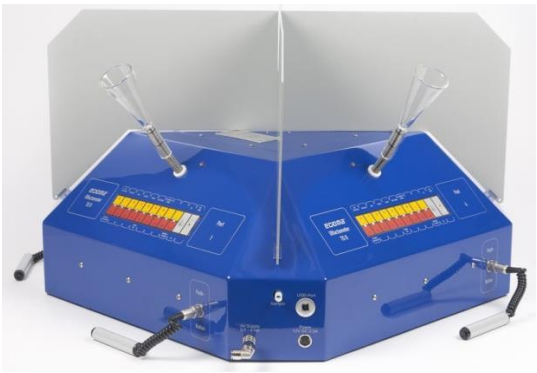

Figura 4.2.1. Olfatómetro TO8.

El olfatómetro se conecta a un compresor (Silent DE-204, **Figura 4.2.2.A**) que le suministra el aire necesario para la dilución de las muestras de olor, debiendo operar entre 4 y 5 bares de presión. También es importante mencionar que el aire procedente del compresor se hace pasar por un filtro (**Figura 4.2.2.B**) que permite eliminar humedad, compuestos orgánicos y partículas del aire antes de llegar al olfatómetro.

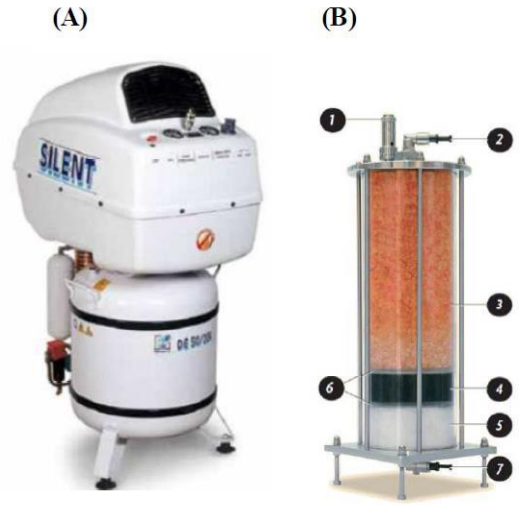

Figura 4.2.2. (A) Compresor de aire; (B) Filtro de aire: (1) Válvula de limitación de presión, (2) Orificio de entrada de aire, (3) gel de sílice, (4) carbón activo, (5) fibra de algodón, (6) filtro extra-fino y (7) salida de aire hacia el olfatómetro.

Todos los análisis olfatométricos se han llevado a cabo en el laboratorio de olfatometría del grupo RNM-271 de la Universidad de Córdoba, a una temperatura de 25ºC y a 1 atm de presión. Además, todas las muestras odoríferas se han analizado dentro de las 30 horas posteriores a la toma de muestra, según establece la norma EN 13725 (2003).

Para determinar la emisión de olor de un foco no es suficiente con cuantificar el valor de la concentración de olor (ou_E/m^3), sino que es necesario determinar su tasa de emisión de olor (*odour emission rate*, OER), la cual se expresa en ou_E/s. Para un foco puntual, la tasa de emisión se calcula multiplicando la concentración de olor (ou_E/m^3) por el flujo de aire (m^3/s), normalizado a 20ºC, que es la temperatura de referencia según la norma EN 13725 (2003). Cuando la emisión proviene de un área determinada (ejemplo: un decantador de una EDAR) en lugar de un foco puntual, se requiere el cálculo de la tasa de emisión específica (*specific odour emission rate*, SOER), la cual se expresa en $ou_E/s \cdot m^2$. Esta tasa se calcula como el producto de la concentración de olor (ou_E/m^3) y el

flujo de aire neutro introducido en el muestreador (m^3/s) y dividido entre el área del muestreador (m^2). Finalmente, para este tipo de focos, la tasa de emisión de olor (OER) se obtiene del producto de la tasa de emisión específica (SOER) por la superficie del área de emisión (m^2) (Sironi et al., 2006).

Con la finalidad de determinar el impacto de las emisiones odoríferas sobre poblaciones colindantes, las tasas de emisión de olor previamente calculadas son utilizadas para simular procesos de dispersión de olor y estimar las inmisiones que afectan a dichas zonas. Entre otras variables, dichas tasas de emisión se han utilizado en esta Tesis Doctoral como parámetros de entrada de un modelo de dispersión Euleriano que ha permitido estimar el impacto odorífero de una EDAR urbana de gran tamaño en diferentes estaciones del año.

4.3. Cuantificación de compuestos volátiles

La cuantificación de compuestos volátiles se ha realizado en los estudios relacionados con el CAG y los sistemas de biofiltración. Para la cuantificación de los compuestos volátiles retenidos en el citado material adsorbente (tras una desorción previa a 40 ºC) se ha utilizado la técnica de cromatografía de gases acoplada a la espectrometría de masas (**GC-MS**). La cromatografía de gases permite la separación de los compuestos de una mezcla gaseosa compleja. Una vez realizada tal separación, el cromatógrafo ofrece información de los tiempos de retención de cada compuesto expresada mediante picos cromatográficos. Para poder llevar a cabo la identificación de los compuestos es necesario acoplar la cromatografía de gases a una técnica como la espectrometría de masas, que permite identificar sustancias puras de manera individual. De esta manera, los COV desorbidos de las diferentes muestras de CAG se volvieron a adsorber en tubos multilecho (TenaxTA/Carbograph5, Markes International, UK), los cuales se insertaron posteriormente en un equipamiento constituido por una unidad de desorción térmica (Unity2-xr Markes International, UK), un cromatógrafo de gases (TRACE 1310, Thermo Fisher Scientific) y un espectrómetro de masas (ISQ 7000, Thermo Fisher Scientific). Los picos cromatográficos de los diferentes compuestos gaseosos se han cuantificado comparando su área bajo la curva con el área de pico obtenida de una cantidad conocida de una sustancia de referencia (tolueno-d_8), que se ha adsorbido (mediante inyección directa con una jeringa) en un tubo limpio adicional. El pico producido por el compuesto de referencia se ha utilizado como pico de referencia para cuantificar los picos obtenidos en el análisis de la muestra gaseosa. Este método basado en el tolueno-d_8 constituye un

método de cuantificación semicuantitativo. Para la cuantificación de otros compuestos volátiles de interés retenidos en las muestras de CAG (y que no pudieron analizarse mediante el equipamiento anteriormente mencionado), como el sulfuro de hidrógeno y el dióxido de azufre, se ha utilizado un cromatógrafo de gases (Chroma S) acoplado a un detector fotométrico de llama (**GC-FPD**) desarrollado por Chromatotec. Chroma S es un cromatógrafo de gases isotérmico completamente automatizado, adecuado para el análisis de compuestos de azufre. Esta técnica permite un análisis individual sensible (ppb_v) de compuestos específicos de azufre. Por ejemplo, para H_2S y SO_2 presenta un límite de detección de hasta 7 ppb_v.

Finalmente, las muestras gaseosas con los COV (ácido butírico y D-limoneno) que se han utilizado como contaminantes gaseosos a degradar en los diferentes experimentos de biofiltración, se han analizado mediante cromatografía de gases con un detector de ionización de llama (**GC-FID**) en un cromatógrafo de gases Agilent Technologies 7890A (Agilent, Santa Clara, CA, EE. UU.), utilizando 1 mL de gas de las bolsas de muestreo llenadas a la entrada y salida de los distintos biofiltros. Es importante destacar que todas las condiciones específicas para la determinación de los compuestos volátiles citados en este apartado se han descrito específicamente en cada uno de los estudios en los que se ha recurrido al análisis cromatográfico.

5. Bibliografía

Akhtar, K., Khan, S.A., Khan, S.B., Asiri, A.M., 2018. Scanning Electron Microscopy: Principle and applications in nanomaterials characterization, in: Handbook of Materials Characterization. Springer, Cham, pp. 113–145. https://doi.org/10.1007/978-3-319-92955-2_4

APHA, 2017. Standard methods for the examination of water and wastewater, 23rd ed. American Public Health Association, Washington DC.

Boehm, H.P., 1994. Some aspects of the surface chemistry of carbon blacks and other carbons. Carbon N. Y. https://doi.org/10.1016/0008-6223(94)90031-0

Chica, A., Mohedo, J.J., Martín, M.A., Martín, A., 2003. Determination of the stability of MSW compost using a respirometric technique. Compost Sci. Util. 11, 169–175. https://doi.org/10.1080/1065657X.2003.10702122

Directiva 91/271/CEE del Consejo, de 21 de mayo de 1991, sobre el tratamiento de las aguas residuales urbanas, n.d.

EN 13725, 2003. Air Quality - Determination of Odour Concentration by Dynamic Olfactometry. European Committee for Standardization, Brussels.

ISO4833-1, 2013. Microbiology of the food chain–Horizontal method for the enumeration of microorganisms–Part 1: Colony count at 30 degrees C by the pour plate technique.

Linden, D., Reddy, T., 2002. Handbook of batteries, Third. ed. McGraw Hill, New York.

Nguyen, C., Do, D.D., 2001. The Dubinin-Radushkevich equation and the underlying microscopic adsorption description. Carbon N. Y. 39, 1327–1336. https://doi.org/10.1016/S0008-6223(00)00265-7

Sironi, S., Capelli, L., Céntola, P., Del Rosso, R., Il Grande, M., 2006. Odour emission factors for the prediction of odour emissions from plants for the mechanical and biological treatment of MSW. Atmos. Environ. 40, 7632–7643. https://doi.org/10.1016/j.atmosenv.2006.06.052

Smith, D.J., McCartney, M.R., 2005. Microscopy Applications | Semiconductors. Encycl. Anal. Sci. Second Ed. 84–91. https://doi.org/10.1016/B0-12-369397-7/00394-0

US Department of Agriculture and the US Composting Council, 2002. Test Methods for the Examination of Composting and Compost (TMECC). Edaphos International, Houston (TX).

VDI 3880, 2011. Olfactometry – Static Sampling. Beuth Verlag GmbH, Berlin, pp. 10772.

Wang, Y., Jin, X., He, L., Zhang, W., 2017. Inhibitory effect of thiourea on biological nitrification process and its eliminating method. Water Sci. Technol. 75, 2900–2907. https://doi.org/10.2166/WST.2017.177

Warner, J.H., Schaffel, F., Bachmatiuk, A., Rummeli, M.H., 2013. Graphene: Fundamentals and emergent applications. Elsevier Ltd, Oxford.

RESULTADOS Y DISCUSIÓN

RESULTS AND DISCUSSION

BLOQUE I. EMISIONES ODORÍFERAS EN EDAR: ORIGEN, CUANTIFICACIÓN Y MODELADO DE SU DISPERSIÓN

SECTION I. ODOR EMISSIONS DERIVED FROM WWTPs: ORIGIN, QUANTIFICATION AND MODELING OF DISPERSION

I. Resumen del Bloque: "*Emisiones odoríferas en EDAR: Origen, cuantificación y modelado de su dispersión*"

El impacto odorífero de las EDAR es fuente de frecuentes quejas y protestas en las áreas residenciales cercanas a estas instalaciones, debido a que la contaminación por olores puede causar importantes efectos negativos sobre la salud humana y el medio ambiente. La mencionada contaminación suele derivar de la presencia de COV y otros nitrogenados o sulfurados en las emisiones gaseosas de las EDAR, algunos de los cuales presentan umbrales olfativos muy bajos (ppb o ppt).

Este primer bloque trata de dar luz a diversos aspectos relativos al seguimiento de las actividades en instalaciones de tratamiento de aguas residuales, potencialmente generadoras de contaminación ambiental por olores, a escala industrial. En este sentido, se han evaluado tres EDAR urbanas, cuantificándose en todas ellas la emisión odorífera de los principales focos generadores de malos olores. De forma más específica, en el primer artículo del presente bloque, se han comparado dos EDAR de pequeño-mediano tamaño (< 2.000 habitantes equivalentes) con diferentes tecnologías biológicas y ampliamente implantadas en el tratamiento secundario de las aguas residuales (fangos activos de aireación prolongada y biodiscos), permitiendo evaluar cómo influye su operación y el contenido bacteriano de los lodos generados en su impacto odorífero. Las EDAR de pequeño y mediano tamaño, si bien contribuyen individualmente en menor medida a la contaminación atmosférica por compuestos olorosos, es conveniente resaltar el gran número de ellas, ubicadas inicialmente en terrenos rurales en su mayoría, cerca de los municipios por necesidades orográficas y de conducción de las aguas hasta ellas y que se han ido integrando en terreno industrial (polígonos fundamentalmente). De ahí que estudios como los planteados contribuyan al conocimiento de la actual situación y posibilidades de mejora en el contexto de estudio.

Por otra parte, en el segundo estudio del bloque que nos ocupa, se ha evaluado la emisión odorífera de una EDAR de gran tamaño, con capacidad de diseño para una población total de 950.000 habitantes equivalentes y que trata actualmente más de 250.000 m^3/d, operando con fangos activos y digestión anaerobia de lodos. Para ello, se han determinado las tasas de emisión de olor para los diferentes puntos críticos considerados (algunos de los cuales disponían de lechos desodorizantes basados en la adsorción mediante carbón activado granular) y su contribución relativa a la problemática emisión global de olor. También es importante destacar que el impacto odorífero no sólo

se ha cuantificado en los puntos de emisión, sino que además se han estimado los valores de concentración de olor en términos de inmisión, donde intervienen las distintas condiciones climatológicas, estabilidad atmosférica y orografía del lugar en el que se encuentra la citada instalación. Para ello, se han establecido mapas de concentración de inmisión mediante la aplicación de un modelo Euleriano, considerándose las diferentes estaciones del año y las condiciones meteorológicas más desfavorables en cada ocasión.

Investigaciones como las de este bloque permiten evaluar los puntos críticos de olor de diferentes EDAR con distintas operaciones unitarias implantadas y, por tanto, mejorar la gestión de los mismos. Dicha gestión puede ir desde la selección de la tecnología de tratamiento biológico más adecuada, ya que ésta condiciona las características de los lodos (y, en definitiva, la emisión odorífera de las instalaciones), como desde el reforzamiento o rediseño de las estrategias de control de olores en tanto en cuanto el impacto odorífero pueda afectar a la seguridad ocupacional de los trabajadores de la propia EDAR o a la situación de bienestar de los núcleos de población colindantes. En este contexto, la cobertura de instalaciones, conducción de corrientes gaseosas e implantación de sistemas de control de olor son las alternativas tecnológicas existentes, aunque el cambio en el modo de operación de las EDAR, aunque no es frecuente, también se considera como una solución posible.

I.1. Breve descripción del artículo: "*Activated sludge process versus rotating biological contactors in WWTPs: Evaluating the influence of operation and sludge bacterial content on their odour impact*"

I.1. Breve descripción del artículo: "*Activated sludge process versus rotating biological contactors in WWTPs: Evaluating the influence of operation and sludge bacterial content on their odour impact*"

En este estudio se han comparado dos estaciones depuradoras de aguas residuales con diferentes tratamientos biológicos, fangos activos de aireación prolongada (ASP) y biodiscos (RBC), en cuanto a sus condiciones de operación, características fisicoquímicas de sus lodos y contenido bacteriano de los mismos, con el objetivo de determinar su influencia en el impacto odorífero de tales instalaciones. Los valores medios de caudal de agua residual entrante, DQO de entrada y eficacia de eliminación de DQO fueron los siguientes (ASP-WWTP *vs.* RBC-WWTP): 447 *vs.* 689 m^3/d, 300 *vs.* 423 mg/L y 88,28 *vs.* 83,17%, respectivamente. En lo referente a la emisión global de olor, ambas EDAR tuvieron una tasa de emisión de olores similar (11.177 ou_E/s para ASP-WWTP y 12.784 ou_E/s en el caso de RBC-WWTP), siendo el espesamiento de lodos y su deshidratación las principales fuentes de olor en ambas instalaciones.

Proteobacteria, Bacteroidetes y Firmicutes fueron los tres filos predominantes en las EDAR evaluadas, representando el 83% en el lodo de la planta con aireación prolongada (ASP-SL) y el 97% en el lodo correspondiente a la instalación con biodiscos (RBC-SL). Este último mostró una biodiversidad bacteriana más baja que el lodo derivado de la EDAR con aireación prolongada.

En la EDAR con biodiscos, las operaciones de la línea de fangos emitieron una mayor concentración de olor, lo que se relacionó con los incrementos significativos en la abundancia de las familias Porphyromonadaceae, Clostridiales, Lachnospiraceae (todos ellos anaerobios obligados) y Moraxellaceae (aerobios) en comparación con la planta de aireación prolongada. Sin embargo, cuando se evaluaron las emisiones de olor por habitante equivalente (EI), se obtuvo un mayor valor para la EDAR de aireación prolongada (16,22 ou_E/s·EI) en comparación con la instalación de biodiscos (6,84 ou_E/s·EI). Este hecho se relacionó con la diferente actividad respirométrica de los lodos generados. En este sentido, la velocidad específica de consumo de oxígeno (mg O_2/g VS·h) fue 2,41 veces mayor en ASP-SL con respecto a RBC-SL.

Process Safety and Environmental Protection 160 (2022) 775–785

Contents lists available at ScienceDirect

Process Safety and Environmental Protection

journal homepage: www.elsevier.com/locate/psep

Activated sludge process *versus* rotating biological contactors in WWTPs: Evaluating the influence of operation and sludge bacterial content on their odor impact

Márquez P. [a], Gutiérrez M.C. [a], Toledo M. [a], Alhama J. [b], Michán C. [b], Martín, M.A. [a,*]

[a] Department of Inorganic Chemistry and Chemical Engineering, Area of Chemical Engineering. Institute of Nanochemistry (IUNAN). Universidad de Córdoba, Campus de Excelencia Internacional Agroalimentario ceiA3, Campus Universitario de Rabanales, Carretera N-IV, km 396, Edificio Marie Curie, 14071 Córdoba, Spain

[b] Department of Biochemistry and Molecular Biology, Universidad de Córdoba, Campus de Excelencia Internacional Agroalimentario CeiA3, Edificio Severo Ochoa, 14071 Córdoba, Spain

* Corresponding author: iq2masam@uco.es

Received 8 December 2021; Received in revised form 2 February 2022; Accepted 27 February 2022; Available online 2 March 2022

Abbreviations: ASP, activated sludge process; BOD_5, biochemical oxygen demand at 5 days; C/N, carbon/nitrogen ratio expressed as VS/N-TKN; COD, chemical oxygen demand; DO, dissolved oxygen; EI, equivalent inhabitant; F/M, food-to-microorganism ratio; FS, fixed solids; HRT, hydraulic retention time; IC, soluble inorganic carbon; MLTSS, mixed liquor total suspended solids; MLVSS, mixed liquor volatile suspended solids; $N\text{-}NH_4^+$, ammoniacal nitrogen; N-TKN, total Kjeldahl nitrogen; $N\text{-}TN_s$, soluble total nitrogen; OC, odor concentration; OD_{20}, cumulative oxygen demand at 20 h; OER, odor emission rate; ou_E, European odor units; $P\text{-}P_2O_5$, phosphorus content expressed as P_2O_5; Q_e, effluent waterflow; Q_i, influent waterflow; RBC, rotating biological contactors; SBR, sequencing batch reactor; SL, sludge; SOER, specific odor emission rate; $SOUR_{max}$, maximum specific oxygen uptake rate; SRT, solids retention time; TC, soluble total carbon; TOC, soluble total organic carbon; TSS, total suspended solids; VOCs, volatile organic compounds; VS, volatile solids; VSCs, volatile sulfur compounds; WWTP, wastewater treatment plant.

Graphical abstract

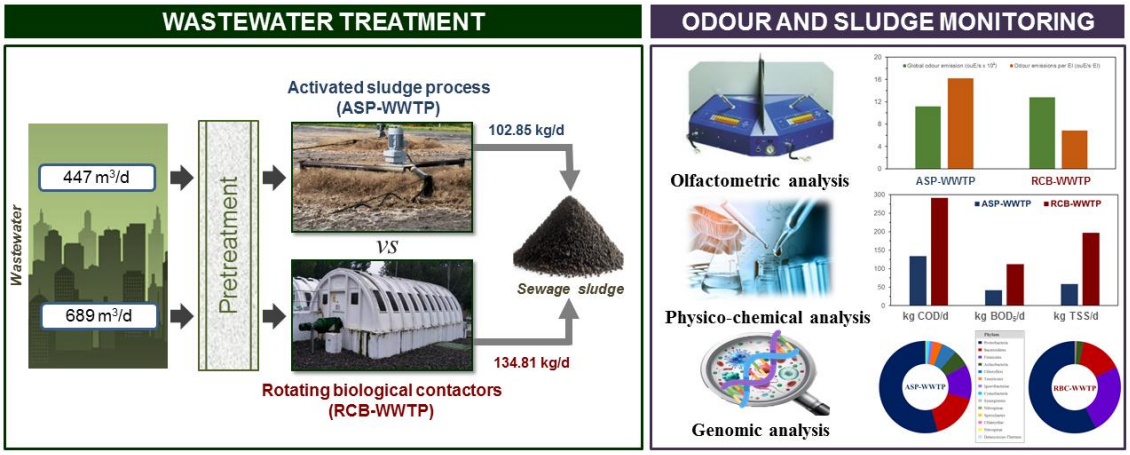

Abstract

Two municipal wastewater treatment plants (WWTPs), based on activated sludge process (ASP) and rotating biological contactors (RBC) as biological treatments, were comparatively evaluated in terms of their operational conditions, bacterial content and physicochemical characteristics of their derived sludge (SL) to determine their influence on odor impact. The average values of influent wastewater flow, inlet chemical oxygen demand (COD) and COD removal efficiency were (ASP-WWTP *vs.* RBC-WWTP): 447 *vs.* 689 m^3/d, 300 *vs.* 423 mg/L and 88.28 *vs.* 83.17%, respectively. Regarding the global odor emissions, ASP-WWTP and RBC-WWTP had a similar odor emission rate (11,177 ou_E/s and 12,784 ou_E/s, respectively), with sludge thickening and dewatering being the major sources of odor in both facilities. Proteobacteria, Bacteroidetes and Firmicutes were the three predominant phyla in both WWTPs, representing the 83% in ASP-SL and the 97% in RBC-SL. RBC-SL showed lower bacterial biodiversity than ASP-SL. The higher odor concentration from the sludge handling activities in RBC-WWTP were linked to the significative increments in the abundance of Porphyromonadaceae, Clostridiales, Lachnospiraceae (obligate anaerobe) and Moraxellaceae (aerobic) families compared to ASP-WWTP. However, when odor emissions were evaluated per equivalent inhabitant (EI), a higher value was obtained for ASP-WWTP (16.22 ou_E/s·EI) compared to RBC-WWTP (6.84 ou_E/s·EI).

Keywords: activated sludge process; genomic analysis; odor emissions; rotating biological contactors; sewage sludge.

1. Introduction

The generation of wastewater is an inevitable consequence of human and industrial activities due to urbanization, industrialization and population growth. In contemporary society, protecting the environment, reducing energy consumption, preserving raw materials and minimizing waste generation are becoming increasingly important. For this reason, the implementation and development of wastewater treatment technologies are required to enhance their efficiency, so that they not only comply with necessary standards and a low energy footprint but also boost economic feasibility and environmental sustainability (Sikosana et al., 2019). Wastewater treatment is a key operation based on physical, chemical and biological processes that allow several pollution parameters to be reduced (Kalbar et al., 2012). Whether to comply with environmental regulations or to avoid negative impacts on nearby bodies of water, it is convenient to know the basics of the wastewater treatment (*i.e.*, multiple factors including technical, economic, regulatory, microbiological and operational behavior as well as limitations) and the advantages and disadvantages of existing technologies to achieve the required treatment goals in accordance with the size and the needs of the population served (Prasse et al., 2015, Ullah et al., 2020).

The design of a wastewater treatment plant (WWTP) mainly depends on the pollutant load to be treated in terms of biochemical oxygen demand (BOD_5) or chemical oxygen demand (COD) (Dominguez and Gujer, 2006). One of the main concerns in the treatment of wastewater is selecting the most appropriate technology, which depends on various factors such as pollutant load, energy efficiency, governmental and regulatory factors, and environmental impact, including the emission of volatile organic compounds (VOCs) and nuisance odors (Ullah et al., 2020). In this context, a technology's appropriateness is not limited to its physical properties (referred to as 'hard aspects'), but also includes knowledge about transfer mechanisms, microbiological aspects and waste generation, among other factors.

Among the various operations of a WWTP, biological treatment is considered the most complex and influential process in the elimination of soluble pollutants in the integral wastewater treatment (Liu et al., 2019). It has the purpose of digesting and transforming biodegradable organic material into cells or cellular tissue and other harmless by-products, such as carbon dioxide and water or even mineral salts (*e.g.*, nitrates and sulfates) (Chahal et al., 2016, Saeed et al., 2021). Compared to chemical

treatments, biological treatments have proved to be more efficient in resource consumption, having lower chemical and energy requirements, which can be translated into economic savings and environmentally friendly methods for municipal wastewater treatment (Oh et al., 2010, Wei et al., 2018).

More specifically, activated sludge process (ASP) and rotating biological contactors (RBC) are conventional biological treatments commonly implemented in medium-sized municipal WWTPs (Sikosana et al., 2019, Wee Seow et al., 2016, Zhang et al., 2020). The main microorganisms involved in these treatments are protozoa, fungi, algae, filamentous organisms and bacteria, the latter making up 90–95% of the process (Aonofriesei and Petrosanu, 2007). For ASP, biological oxidation takes place in an aerated biological reactor or aeration tank, where the biological culture (mixed liquor) is in contact with the wastewater with the purpose of transforming soluble organic matter through oxidation reactions (Waqas et al., 2020). The above-mentioned biological culture is formed by a large number of microorganisms grouped into flocs, the most abundant being the bacterial population, in the sequence Proteobacteria, Actinobacteria, Bacteroidetes and Firmicutes (Yu and Zhang, 2012). On the other hand, for RBC, the microorganisms are attached onto a rigid surface (disks) to form a biofilm, which is responsible for the degradation of organic pollutants (Rana et al., 2018). In the latter case, bacteria constitute about 98% of the total community (Ziembińska-Buczyńska et al., 2019). Moreover, a high biomass concentration (about 200 g dry weight/m^2) is maintained on the disc surface, having a metabolic effect similar to that produced by a concentration of 4000–6000 mg MLTSS/L in ASP (MLTSS stands for mixed liquor total suspended solids) (Jácome et al., 2015). Regarding the two technologies' technical aspects, it is important to highlight that ASP has a higher removal efficiency of organic pollutant load than processes based on a biofilm culture on a solid support. In turn, the energy consumption of RBC is about 60% lower than in ASP (*i.e.*, lower electricity consumption to remove the same amount of organic matter). However, the maintenance costs of systems equipped with RBC are approximately 35% higher than with ASP (Ferrer et al., 2008).

Given that biological treatment is very efficient in removing biodegradable soluble organic pollutants (except for emerging pollutants such as antibiotics, drugs, endocrine disruptors, industrial additives, *etc.*), and much of the removed matter is transformed into biological sludge, large amounts of sludge are generated (García et al., 2021). Sewage

sludge is an inevitable by-product produced in the wastewater treatment process, in which numerous nutrients and organic materials are retained (*i.e.*, 24–34% of total NPK); recycling them as fertilizer can promote sustainability and a circular economy (Kominko et al., 2019). Sludge production in WWTPs varies widely, from 31 to 85 g of dry solids per equivalent inhabitant (EI) and per day (g TS/EI·d), related to the amount of settleable solids in raw wastewater and whose total suspended solids (TSS) content is in a range of 50–60 g TSS/EI·d or 110–170 g TSS/m^3 of treated wastewater (Tchobanoglous et al., 2003). In ASP, organic matter is oxidized by heterotrophic microorganisms, whereby the biodegradable particulate fraction is subjected to hydrolysis to generate new cellular biomass (cryptic growth), while the endogenous fraction (8–20%) remains and accumulates in the sludge. This endogenous fraction has many cellular capsules that sediment poorly, increasing the settling volume and the odor-producing compounds caused by sludge storage, such as volatile organic sulfur compounds, VOCs, volatile fatty acids, H_2S, NH_3, *etc.* (Bhatla, 1975, Carrera-Chapela et al., 2014, Karageorgos et al., 2010). In the case of RBC, the low concentration of sloughed-off biofilm improves sludge settlement quickly and freely, minimizing the odoriferous emission surface, *i.e.*, with a lower sludge volume and a shorter hydraulic retention time (HRT), allowing the efficient separation and management of the sludge (Cortez et al., 2008, Hassard et al., 2015, Jácome et al., 2015, Waqas and Bilad, 2019). In this respect, odor emissions are inherently associated with wastewater management, being volatile sulfur compounds (VSCs) primarily responsible for unpleasant odors. Certainly, previous studies have reported that VSCs can account for up to 80–90% of malodorous compounds in WWTPs (Li et al., 2021, Omri et al., 2011). Unpleasant odors (VSCs and VOCs) are closely associated with the generation, treatment and management of solid waste (such as biological sludge) as well as with the different types of treatment to which wastewater is subjected. However, most of the literature available deals with the odor emissions derived from biological treatment technologies individually, such as sequencing batch reactors (SBR) (Li et al., 2021), ASP (Dinçer et al., 2020, Kim et al., 2014, Varela-Bruce and Antileo, 2021, Zwain et al., 2020) or RBC (Cortez et al., 2008), rather than evaluating them comparatively. The presence of odor-causing compounds reduces the quality of ambient air and can result in the discomfort of the WWTP's workers as well as the residents of neighboring areas. It is well known that long-term exposure to odorants can cause psychological stress and symptoms such as headaches, nausea, insomnia, respiratory affections and even cancer (Byliński et al., 2019).

Therefore, considering the importance of identifying and controlling the odor emissions related to wastewater management, two municipal WWTPs with different and widespread biological treatments (ASP and RBC) were jointly evaluated in this study with the aim of: (i) comparing the physicochemical and respirometric characteristics of the sewage sludge derived from both types of plants; (ii) taxonomically identifying the bacteria responsible for the degradation processes to compare the most predominant families in the sludge generated in both types of plants and connecting them to their operational conditions; and finally (iii) performing a comparative evaluation of the odor emissions derived from both types of WWTPs, analysing the odor contributions of the different treatment stages. To the best of our knowledge, this integral approach to improve understanding of the characteristics of odor emissions depending on the biological treatment implemented has not been previously reported in the literature. This information may help wastewater managers to select the most appropriate wastewater treatment technology for minimizing the impact of odors when building new WWTPs close to population centers or to make decisions regarding odor abatement in existing ones, with the consequent social and environmental benefits.

2. Material and methods

2.1. Location, characteristics and treatment capacity of the WWTPs

In this study, which was carried out in 2019, two municipal WWTPs were selected according to the most predominant biological technologies implemented in the province of Cordoba (Spain): ASP and RBC. The sampled facilities (satellite images are shown in **Fig. S1**, Supplementary material) were the following:

- **ASP-WWTP**: This facility operates with ASP as biological treatment (based specifically on extended aeration) and is located in Espiel (Cordoba). It has a design treatment capacity of 2424 EI. The average urban wastewater flow treated in 2019 was approximately 447 m^3/d (**Table 1**).
- **RBC-WWTP**: This facility has a biological treatment based on RBC and a design capacity of 6000 EI. It is situated in Villaviciosa de Córdoba (Cordoba) and treated around 689 m^3/d of urban wastewater in 2019 (**Table 1**).

Table 1. Wastewater treated flow and operational variables of both WWTPs.

	ASP-WWTP		RBC-WWTP	
	Influent (i)	Effluent (e)	Influent (i)	Effluent (e)
Q (m^3/d)	447 ± 331	394 ± 262	689 ± 186	677 ± 169
COD (mg/L)	300 ± 44	40 ± 9	423 ± 62	72 ± 15
BOD_5 (mg/L)	93 ± 22	5 ± 3	163 ± 39	12 ± 3
TSS (mg/L)	131 ± 32	6 ± 2	286 ± 67	19 ± 4

ASP-WWTP, wastewater treatment plant with activated sludge process; BOD_5, biochemical oxygen demand at 5 days; COD, chemical oxygen demand; Q, waterflow; RBC-WWTP, wastewater treatment plant with rotating biological contactors; TSS, total suspended solids.

As can be observed in **Scheme 1**, both WWTPs have the same unit operations, except for the type of biological treatment conducted. Moreover, ASP-WWTP has an anoxic reactor to perform wastewater denitrification, with internal and external recirculation between this reactor and the extended aeration tank. The HRT for the biological treatment of ASP-WWTP is approximately 20 h (about 14 h for the aerobic reactor and 6 h for the anoxic reactor), while the value of this parameter is considerably lower in the case of RBC-WWTP (≈ 4 h). More operational conditions such as energy consumption, dissolved oxygen (DO) and sludge concentration in the reactor, food-to-microorganism ratio (F/M), and solids retention time (SRT) can be observed in **Table S1** (Supplementary material). Sludge thickening and mechanical sludge dewatering by centrifugation are common to both WWTPs.

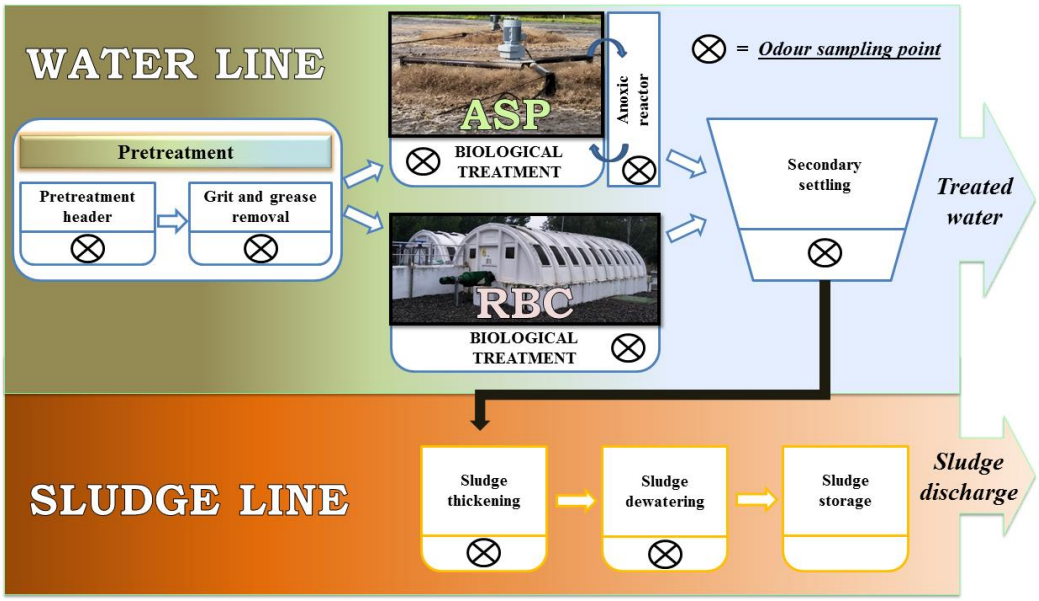

Scheme 1. General flow diagram of the WWTPs evaluated (ASP-WWTP and RBC-WWTP).

Table 1 shows the mean values of the operational variables considered in the sampled WWTPs in 2019, which are COD (mg/L), BOD_5 (mg/L) and TSS (mg/L). These are variables of relevant interest established by Directive 91/271/CEE (EU Council, 1991) in non-sensitive areas (such is the case of Espiel and Villaviciosa de Córdoba) and were determined in accordance with the Standard Methods of the APHA (2017). This information as well as the above-mentioned annual mean values and operational conditions were provided by EMPROACSA, which is the wastewater manager in the province of Cordoba.

The treatment capacity of both plants in 2019 was also calculated in term of EI. To do so, Directive 91/271/CEE (EU Council, 1991) establishes that 1 EI has a biodegradable organic load with a BOD_5 equivalent to 60 g O_2/day. Therefore, the number of EIs depends on the influent waterflow to be treated (Q_i) and the inlet's average BOD_5, calculated according to Eq. (1):

$$EI = \frac{Q_i(^L/_d)\cdot BOD_5(^{gO_2}/_L)}{60\ gO_2/d} \quad (1)$$

where *EI* is the number of equivalent inhabitants, Q_i is the average influent waterflow and BOD_5 is the average biochemical oxygen demand at the facilities' inlets.

In accordance with the information provided about the two WWTPs (**Table 1**), the received pollutant load in both WWTPs, expressed in terms of chemical oxygen demand (kg COD/d), biochemical oxygen demand (kg BOD_5/d) or total suspended solids (kg TSS/d), was estimated through Eq. (2):

$$\textit{Received pollutant load (kg/d)} = Q_i \cdot C_i \quad (2)$$

where Q_i is the average influent waterflow (L/d) and C_i refer to the average inlet concentrations (COD, BOD_5 or TSS, kg/L).

The COD, BOD_5 and TSS average removal efficiencies of these facilities were also calculated according to Eq. (3):

$$\textit{Average removal efficiency (\%)} = \frac{Q_i\cdot C_i - Q_e\cdot C_e}{Q_i\cdot C_i} \quad (3)$$

where Q_i is the average influent waterflow, Q_e is the average effluent waterflow and C_i and C_e refer to the average inlet and outlet concentrations (COD, BOD_5 or TSS), respectively.

2.2. Physicochemical characterization and respirometric analysis of the sludge

The sludge evaluated for both technologies was subjected to physicochemical analysis following the methodology established by the United States Department of Agriculture and the United States Composting Council (2002). The sludge was identified as ASP-SL for ASP-WWTP and RBC-SL for RBC-WWTP. Fixed solids (FS, %), volatile solids (VS, %), total Kjeldahl nitrogen (N-TKN, %), ammoniacal nitrogen ($N\text{-}NH_4^+$, %) and phosphorus content ($P\text{-}P_2O_5$, %) were analyzed in the solid fraction, while pH, conductivity (µS/cm), soluble total nitrogen ($N\text{-}TN_s$, %), soluble total carbon (TC, %), soluble inorganic carbon (IC, %), and soluble total organic carbon (TOC, %) were measured in the aqueous extract (1:25 v/v ratio). All variables were determined in triplicate, showing the mean values and standard deviation. It is important to highlight that the C/N ratio was also determined as VS/N-TKN.

In order to evaluate the microbial activity of the sludge of both facilities, the maximum specific oxygen uptake rate ($SOUR_{max}$, mg O_2/g VS·h) and cumulative oxygen demand at 20 h (OD_{20}, mg O_2/g VS) were determined under standardized conditions by using a static-liquid respirometer patented by the Department of Inorganic Chemistry and Chemical Engineering of the University of Cordoba, Spain (P2004–02908) and developed by Chica et al. (2003). The evolution of SOUR determines the reaction rate to stabilize organic matter. For its part, OD_{20} refers to the oxygen consumption per gram of VS added (measured on a dry basis) in the respirometric test, and it is a respirometric variable proportional to the biodegradability of the substrate (Martín et al., 2018). The respirometric analysis consisted of two 1-L reactors (Erlenmeyer flasks) with a discontinuous aeration system that maintained the oxygen concentration within a previously established interval (6.8—7.0 mg O_2/L). In such analysis, sludge samples were introduced into the reactors, both containing a nutritional medium with the same composition: 10 mL of $CaCl_2$ (27.50 g/L), 10 mL of $FeCl_3$ (0.25 g/L) and 10 mL of $MgSO_4$ (22.50 g/L). In addition, 30 mL of a phosphate buffer solution (K_2HPO_4 (8.50 g/L), $Na_2HPO_4.7\,H_2O$ (33.40 g/L), NH_4Cl (1.70 g/L)) were added to each reactor, providing a buffered medium at a pH of 7.2. In order that all oxygen uptake was attributed to the biological oxidation of the carbonaceous matter, thiourea was also added (1 g per

reactor). This compound has a strong ability to inactivate ammonia-oxidizing bacteria, and therefore has a long history of being used as a nitrification inhibitor (Wang et al., 2017). Once all the substances were added, the reactors were made up to 1 L with distilled water. Because the metabolic activity of microorganisms depends on the temperature, both Erlenmeyer flasks were placed in a water thermostatic bath at 30 ºC. Finally, the reactors were also kept under constant agitation (300 rpm) to homogenize the solution and facilitate the transfer of oxygen (Chica et al., 2003). Each respirometric test was carried out by using 10 g of wet sludge. Moreover, each sample was analyzed in duplicate, yielding the mean values and standard deviation.

2.3. Odor sampling and analysis

The odor sources sampled were the same in both WWTPs and can be observed in **Scheme 1**, comprising pretreatment header (roughing operations), grit and grease removal, biological treatment (ASP or RBC), secondary settling, sludge thickening and sludge dewatering. According to the guideline VDI 3880 (2011), all of them were passive odor sources. Sludge storage was not sampled in any of the WWTPs because it takes place in closed silos.

The CSD30 (manufactured by Olfasense GmbH) was the sampling device used for collecting odor samples in 10-L Nalophan® sampling bags. The ventilated sampling hood (Olfasense GmbH) was connected to the CSD30 device for sampling all passive odor sources mentioned above. Both sampling devices were fully compliant with the standard EN 13725 (2003) and the guideline VDI 3880 (2011). The main characteristics and operation of these devices can be found in Toledo et al. (2018a). The sampling time was 30 min per sample. All gaseous samples were analyzed within 6 h in order to minimize the permeation and/or adsorption of odorants through/on the sampling bag walls, as proposed by the guideline VDI 3880 (2011).

Dynamic olfactometry (EN 13725, 2003) was the method used to quantify the odor concentration (OC). The units of this variable are ou_E/m^3 (European odor units per cubic meter). According to the European standard, 1 ou_E/m^3 is defined as the amount of odorant that, when evaporated into 1 m^3 of gas air at standard conditions, causes a physiological response from a panel (detection threshold) equivalent to that of n-butanol (reference gas) evaporated into 1 m^3 of neutral gas. A TO8 olfactometer (Olfasense GmbH), based on the 'Yes/No' method, was used to determine the OC of each sample. The group of panelists

consisted of 4 people, each of whom was selected based on their sensitivity to the n-butanol reference gas as described in EN 13725 (2003). Each sample was analyzed in duplicate and the OC was calculated as the geometric mean of the odor threshold values of each panelist, multiplied by the square root of the olfactometer dilution factor. All odor concentration data were expressed in accordance with the reference conditions described in EN 13725 (2003) (*i.e.*, 20 ºC, 101.3 kPa on a wet basis).

The OC results were necessary to subsequently determine the specific odor emission rate (SOER) and the odor emission rate (OER) of the sampled odor sources. The first variable was determined by Eq. (4):

$$SOER\ (ou_E/m^2 \cdot s) = \frac{OC \cdot Q_{air}}{A_H} \quad (4)$$

where *OC* is the odor concentration (ou_E/m^3), Q_{air} is the airflow rate circulating through the sampling hood ($2.08 \cdot 10^{-3}$ m^3/s) and A_H is the covered area of the above-mentioned hood (1 m^2).

The SOER determination was the first step in estimating the OER from passive sources, which was calculated according to Eq. (5):

$$OER\ (ou_E/s) = SOER \cdot A \quad (5)$$

where the *SOER* is the specific odor emission rate ($ou_E/m^2 \cdot s$) and *A* is the odor emission surface of each odor source (m^2), which is detailed in **Table 5**.

Finally, a global odor emission rate (ou_E/s) was estimated for each of the WWTPs, calculated as the sum of the OER values of the different odor sources sampled.

2.4. DNA and genomic analysis

2.4.1. DNA isolation from WWTP sludge

The sludge of each WWTP was collected and kept at −20 °C. Samples were washed 3 times with Tris-HCl (pH 8.3) 50 mM; NaCl 200 mM; Na_2EDTA 5 mM; Triton X-100 0.05%. DNA was isolated from 700 mg of 3 independent batches using aluminum sulfate to avoid the interference of humic acids (Dong et al., 2006). Prior to the 16S analysis, DNA concentration was determined spectrophotometrically. DNA integrity was checked by running the samples on a 1% agarose gel electrophoresis. Furthermore, the removal of PCR inhibitors was checked with a PCR test using bacterial 16 S standard primers

(forward: 5′-TGGTGGAATTTCCTGTGTAGCGGTGAA-3′ and reverse 5′-GCAACGCGAAGAACCTTACCTGGCCTT-3′). Amplifications were performed in a 50 µl reaction volume, using 0.5 µM (each) primer and approximately 20 ng of template DNA. The PCR cycling protocol consisted of the following: 95 °C for 1 min, 30 cycles 95 °C for 15 s, 55 °C for 30 s, 72 °C for 30 s, and a final elongation at 72 °C for 7 min.

2.4.2. Library construction, sequencing, gene prediction and taxonomy assignment

To identify the bacteria present in both sludges, DNA was independently amplified and sequenced using the specific kit for 16S sequencing (Ion Torrent System) at the Central Service for Research Support (SCAI) of the University of Cordoba (Spain). The results were analyzed using Ion Reporter™ 5.0 software for Ion 16 S™ Metagenomics. The primers for the V3 region always provided the largest identification numbers and were thus used to estimate the bacterial community.

3. Results and discussion

3.1. Operating conditions of the two WWTPs: removal efficiencies of organic matter

The odor impact generated by a WWTP on surrounding areas is closely related to the organic load of the wastewater treated by the plant, sludge production and its subsequent treatment. In this sense, the operational variables of both WWTPs, provided by EMPROACSA, should be carefully considered. As can be observed in **Table 1**, the average influent waterflow in the case of RBC-WWTP was considerably higher than in ASP-WWTP (about 1.5-fold). This fact, together with the higher average concentration values of COD, BOD_5 and TSS of the influent wastewater in RBC-WWTP compared to ASP-WWTP (1.41, 1.75 and 2.18-fold, respectively), led to the first facility also receiving a higher pollutant load than ASP-WWTP, expressed in terms of chemical oxygen demand (291.46 *vs.* 133.99 kg COD/d), biochemical oxygen demand (112.31 *vs.* 41.54 kg BOD_5/d) or total suspended solids (197.07 *vs.* 58.51 kg TSS/d). This marked difference between the organic loads of the wastewater treated in the WWTPs also led to an important difference in the treatment capacity between both facilities (year 2019). Thus, **Table 2** shows that RBC-WWTP had a higher treatment capacity (1870 EI) compared to

ASP-WWTP (689 EI). Regarding the average removal efficiencies of organic matter, **Table 2** also shows the COD, BOD_5 and TSS average removal efficiencies (%) of the WWTPs evaluated. In this respect, the results revealed a small difference between the two WWTPs, ASP technology being the most efficient. It should be noted that the biodegradation of organic matter involves the generation of sewage sludge (in solid stage), a liquid effluent that contains non-biodegradable organic matter and malodorous gaseous emissions with the potential to affect the health and well-being of nearby population areas (Lebrero et al., 2011). The proportion of each type of effluent depends on the technology applied to develop the biological treatment. In a comparative manner, ASP is an intensive technology, which requires an elevated energy supply, generating highly mineralized sewage sludge. As can be observed in **Table 2**, sludge production (on a dry basis) using ASP was 102.85 kg/d (year 2019). On the other hand, RBC is a technology in which microorganisms are expanded on biofilms, and organic matter is biodegraded in alternating anoxic and aerobic conditions. The sludge generated by using this treatment is less mineralized than that generated by ASP. In RBC-WWTP, sludge production in 2019 reached 134.81 kg/d (on a dry basis).

Table 2. Treatment capacity, average removal efficiencies of organic matter according to the implemented biological treatment (ASP or RBC) and sludge production in each WWTP evaluated.

Treatment capacity		
	ASP-WWTP	**RBC-WWTP**
Capacity in year 2019 (EI)	689	1870
Average removal efficiency		
	ASP-WWTP	**RBC-WWTP**
COD (%)	88.28	83.17
BOD_5 (%)	95.58	92.74
TSS (%)	96.05	93.60
Sludge production (dry basis) provided by the wastewater manager		
	ASP-WWTP	**RBC-WWTP**
Sludge amount (kg/d)	102.85	134.81

ASP-WWTP, wastewater treatment plant with activated sludge process; BOD_5, biochemical oxygen demand at 5 days; COD, chemical oxygen demand; EI, equivalent inhabitant; RBC-WWTP, wastewater treatment plant with rotating biological contactors; TSS, total suspended solids.

3.2. Assessment of physicochemical and respirometric results

As previously mentioned, the characteristics of sludge are closely related to the odor emissions generated during its treatment. Therefore, the physicochemical and respirometric characterization of the sewage sludge samples for the two WWTPs is shown in **Table 3**. Among the most relevant differences, the lower organic matter content of ASP-SL in comparison with RBC-SL, expressed as VS (%) or as TOC (%) in the soluble form, can be observed. The differences associated with nitrogen content (N-TKN, N-NH_4^+ or N-TN_s) in the two sludges were marked by the presence of an anoxic reactor to perform wastewater denitrification in ASP-WWTP, yielding an ASP-SL with low nitrogen content. Due to the distinctive carbon and nitrogen contents in the sludges, the C/N ratio also differed considerably between them. Maintaining total Kjeldahl nitrogen (N-TKN, %) and phosphorus content (P-P_2O_5, %) in the sewage sludge after the biological treatment would favor its valorization through the composting process for its subsequent merchandizing as fertilizer (Cao et al., 2021). Finally, the respirometric behavior of both types of sludge was indicative of the metabolic state of the microbial communities present in them. In this context, **Table 3** depicts the microbiological activity of the sewage sludge, expressed in $SOUR_{max}$ (mg O_2/g VS·h), and its biodegradability, expressed as OD_{20} (mg O_2/ g VS). The $SOUR_{max}$ of both sewage sludges exhibited low values, although far from values that would suggest microbiological stability, that is, $SOUR_{max}$ < 1 mg O_2/g VS·h (Chica et al., 2003, Toledo et al., 2019). In a graphical manner, **Fig. 1** shows the evolution of SOUR during the analysis, with a very different behavior at the beginning. In this sense, a marked decrease in SOUR was observed for ASP-SL, going from an initial maximum value of 41 ± 2 mg O_2/g VS·h to values lower than 5 mg O_2/g VS·h after 7 h of respirometric analysis. By contrast, the SOUR of RBC-SL increased slowly from the beginning until reaching its maximum value at approximately 8 h (17 ± 1 mg O_2/g VS·h). Afterwards, the above-mentioned parameter decreased rapidly until the 11 h (≈ 9 mg O_2/g VS·h) and continued to decrease slowly until the end of the analysis (≈ 3 mg O_2/g VS·h). Therefore, **Fig. 1** shows that ASP-SL was in a more active metabolic state than RBC-SL, due to the endogenous respiration activity of microbes in the first sludge. It is well known that facilities operating with extended aeration, as a modification of the activated sludge process (such is the case of ASP-WWTP), give long HRTs to the aeration operation (≈ 14 h in ASP-WWTP). This extended aeration process is usually designed for complete-mix conditions, which means

that high solids content or a low food-to-microorganism ratio and long sludge age will exist (see values of these parameters in **Table S1**). Thus, endogenous respiration of the sludge will occur and the sludge will "burn itself up" (Englande and Krenkel, 2003, Von Sperling, 2007). Nevertheless, regarding the cumulative oxygen demand, OD_{20} values indicated the high biodegradability of both sewage sludges, the biodegradability of RBC-SL being slightly higher (**Table 3**). It is important to note that the OD_{20} (mg O_2/ g VS) corresponded to the area under the curve for SOUR (mg O_2/g VS h) *versus* time (h).

Table 3. Physico-chemical and respirometric characterization of sewage sludge from the WWTPs evaluated.

	ASP-SL	**RBC-SL**
pH	7.66 ± 0.08	7.12 ± 0.01
Conductivity (µS/cm)	122 ± 1	521 ± 4
FS (%)	38.31 ± 0.75	23.34 ± 1.38
VS (%)	61.69 ± 1.52	76.66 ± 1.49
N-TKN (%)	5.24 ± 0.03	8.29 ± 0.35
N-NH_4^+ (%)	0.79 ± 0.04	2.76 ± 0.09
N-TN_s (%)	0.43 ± 0.01	2.54 ± 0.03
C/N	11.78 ± 0.37	9.25 ± 0.58
P-P_2O_5 (%)	5.41 ± 1.72	4.93 ± 1.28
TC (%)	1.67 ± 0.01	6.13 ± 0.01
IC (%)	1.01 ± 0.01	1.69 ± 0.01
TOC (%)	0.66 ± 0.01	4.44 ± 0.01
$SOUR_{max}$ (mg O_2/g VS·h)	41 ± 2	17 ± 1
OD_{20} (mg O_2/g VS)	152 ± 3	160 ± 2

ASP-SL, sludge from the wastewater treatment plant with activated sludge process; C/N, carbon/nitrogen ratio expressed as VS/N-TKN; FS, fixed solids; IC, soluble inorganic carbon; N-NH_4^+, ammoniacal nitrogen; N-TKN, total Kjeldahl nitrogen; N-TN_s, soluble total nitrogen; OD_{20}, cumulative oxygen demand at 20 h; P-P_2O_5, phosphorus content expressed as P_2O_5; RBC-SL, sludge from the wastewater treatment plant with rotating biological contactors; $SOUR_{max}$, maximum specific oxygen uptake rate; TC, soluble total carbon; TOC, soluble total organic carbon; VS, volatile solids. Note: All variables, except pH and conductivity, are expressed on a dry basis.

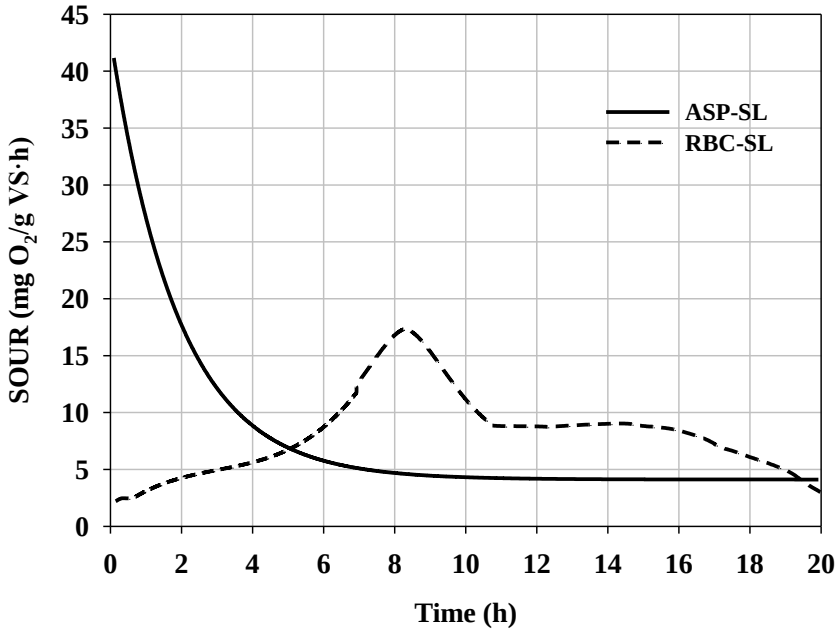

Fig. 1. Respirometric activity of sludge from ASP-WWTP and RBC-WWTP (ASP-SL and RBC-SL, respectively).

The efficiency of a biological treatment could be determined by quantifying and characterizing the sewage sludge produced. The amount of generated sewage sludge and its physicochemical characteristics have a close relationship with the odorous impact generated by the wastewater treatment process. In this context, it is noteworthy that the amounts of sewage sludge (on a dry basis) generated by ASP-WWTP and RBC-WWTP were 149.19 g/EI·d and 72.08 g/EI·d, respectively. These results show that ASP is a more efficient technology in the biological treatment of wastewater, allowing a higher amount of sewage sludge per EI to be obtained as well as increasing the quality of the treated water (**Table 2**). Regarding the characteristics of the sewage sludge evaluated, **Table 4** shows the nutrient content of both sludges generated by EI. Remarkably, ASP-SL was found to contain more organic matter (91.59 g VS/EI·d) than RBC-SL (55.26 g VS/EI·d), both expressed as VS. However, N-TKN and P-P_2O_5 showed slight variations, with ranges of similar magnitude in the two technologies. In the case of RBC-WWTP, N-TKN was maintained in the wastewater, avoiding its metabolization and emission as volatile compounds. As expected, ASP-SL was found to contain less nitrogen as ammoniacal nitrogen or in the soluble form (which are more biodegradable forms), due to the nitrification-denitrification processes of the sewage during biological treatment.

Table 4. Nutrient outlet flows (dry basis) with the sewage sludge from the WWTPs evaluated.

	ASP-SL	**RBC-SL**
C-VS (g/d·EI)	91.59	55.26
N-TKN (g/d·EI)	7.82	5.98
N-NH_4^+ (g/d·EI)	1.18	1.99
N-TN_s (g/d·EI)	0.64	1.83
P-P_2O_5 (g/d·EI)	8.07	3.55

ASP-SL, sludge from the wastewater treatment plant with activated sludge process; C-VS, organic matter expressed as volatile solids; EI, equivalent inhabitant; N-NH_4^+, ammoniacal nitrogen; N-TKN, total Kjeldahl nitrogen; N-TN_s, soluble total nitrogen; P-P_2O_5, phosphorus content expressed as P_2O_5; RBC-SL, sludge from the wastewater treatment plant with rotating biological contactors.

3.3. Odor emission assessment

Having evaluated the wastewater and sludge characteristics, it was important to establish differences between the two WWTPs in terms of odor emission. In this sense, **Table 5** shows the OCs and the odor emissions of each odor source sampled in both facilities. Regarding the preliminary treatment operations (pretreatment header and grit and grease removal), RBC-WWTP presented a higher OC in these stages, possibly due to the higher organic load received compared to ASP-WWTP. Moreover, regardless of the type of treatment technology used, the OCs associated with the first stages of the integral wastewater treatment were always found to be higher than the OCs emitted in the biological treatment of this water (Capelli et al., 2009). This important unit operation constituted a low-potential (and not unpleasant) odor source in both WWTPs, as is typical in most facilities of this type (Jiang et al., 2017). In this context, a higher OC was emitted in the biological treatment of ASP-WWTP, possibly owing to the fact that this technology favors a higher liquid-gas transfer (as a result of the extended aeration that takes place) compared to RBC technology, where biological disks rotate at very low speed, typically between 1 and 2 rpm (Cortez et al., 2008). Furthermore, ASP implies a greater transformation of organic compounds, as this technology has a higher performance in the elimination of organic pollutant load than RBC. The presence of the anoxic reactor in ASP-WWTP also contributed to increase the OC emitted at the biological treatment stage in this facility, since VSC emissions can be increased during the anoxic cycle (Kim et al., 2014). After the biological treatment, the OC emitted increased again for both WWTPs in the secondary settling step (**Table 5**), potentially related to the formation and release

of volatile organic sulfur compounds due to the anoxic environment in settled sludge (Sekyiamah et al., 2008).

On the other hand, the sludge handling activities (sludge thickening and dewatering) constituted the major sources of odor emissions regardless of the WWTP evaluated (99.46% and 99.80% in ASP-WWTP and RBC-WWTP, respectively). The high odor potential of the aforementioned activities has been widely reported in the literature, this being mainly due to the acidic and anaerobic conditions that exist at these steps, leading to the formation of H_2S and malodorous organic compounds, mainly VSCs (Karageorgos et al., 2010, Lebrero et al., 2011, Márquez et al., 2021). Nevertheless, as can be observed in **Table 5**, RBC-WWTP presented higher emitted OCs than those of ASP-WWTP at the sludge thickening and dewatering stages. This could be due to the fact that RBC-SL was less mineralized than ASP-SL, given its higher organic matter content (76.66% *vs*. 61.69% of VS, respectively). In line with the above, a positive relationship between the organic matter content of different wastes and its odor impact is widely reported in the literature (Dunlop et al., 2016, Toledo et al., 2018a).

Regarding the global odor emissions, and considering that olfactometric values have a deviation between half and double (EN 13725, 2003), it might be said that ASP-WWTP and RBC-WWTP had a similar global odor emission rate, although this parameter is slightly higher in the second facility (**Table 5**). However, when considering odor emissions per equivalent inhabitant (that is, a specific odor emission rate with units of $ou_E/s \cdot EI$), a higher value was obtained for ASP-WWTP (16.22 $ou_E/s \cdot EI$) compared to RBC-WWTP (6.84 $ou_E/s \cdot EI$). Therefore, it can be said that RBC-WWTP would generate lower odor emissions than ASP-WWTP for the same organic load to be treated. In other words, regardless of the influent organic load, lower values of specific odor emission rate ($ou_E/s \cdot EI$) indicate a lower odor impact on the environment. At this point, it is important to note that the higher odor emission per EI associated with ASP-WWTP could have been related to the lower biological stability of the sludge generated (ASP-SL), since its microbiological activity, expressed in terms of specific oxygen uptake rate (SOUR, mg O_2/g VS·h), was up to 2.41 times higher than in RBC-SL (**Table 3** and **Fig. 1**). Consistent with the above, a positive correlation was found in the literature between the emitted OC and SOUR in other biological processes, such as composting, where odor emission tends to decrease as the biological stability of the material increases (González et al., 2019, Gutiérrez et al., 2014, Toledo et al., 2018c).

Table 5. Odor emissions from the WWTPs.

	Odor source	OC (ou_E/m^3)	SOER ($ou_E/m^2 \cdot s$)	Emission surface (m^2)	OER (ou_E/s)	Global odor emission (ou_E/s)
ASP-WWTP	Pretreatment header	108	0.22	20.00	4.49	11,177
	Grit and grease removal	108	0.22	29.75	6.68	
	Biological treatment (aerobic reactor)	76	0.16	68.00	10.79	
	Biological treatment (anoxic reactor)	93	0.19	22.50	4.35	
	Secondary settling	128	0.27	127.23	33.89	
	Sludge thickening	2030	897.46	7.00	6282.20	
	Sludge dewatering	1024	452.66	10.68	4834.40	
RBC-WWTP	Pretreatment header	256	0.53	1.80	0.96	12,784
	Grit and grease removal	197	0.41	6.31	2.59	
	Biological treatment	41	0.09	21.68	1.87	
	Secondary settling	152	0.32	63.62	20.14	
	Sludge thickening	2903	1283.41	3.00	3850,22	
	Sludge dewatering	2048	905.36	9.84	8908.71	

ASP-WWTP, wastewater treatment plant with activated sludge process; OC, odor concentration; OER, odor emission rate; RBC-WWTP, wastewater treatment plant with rotating biological contactors; SOER, specific odor emission rate.

Table 6. Studies on odor emissions depending on the wastewater treatment technology.

Wastewater treatment technology	**What is evaluated?**	**How is it evaluated?**	**Reference**
ASP (extended aeration)	Odor, H_2S and NH_3 emissions	Olfactometry analysis and air quality measurements of H_2S and NH_3	Dinçer et al. (2020)
ASP (extended aeration)	H_2S emission	Estimated H_2S through TOXCHEM model (it is based on mass balance of several compounds in WWTPs for each operation unit)	Zwain et al. (2020)
ASP	VSCs emission	Real-time total reduced sulphur analyser	Kim et al. (2014)
ASP	Odor emission	OEFs calculated from measurements using dynamic olfactometry	Varela-Bruce and Antileo (2021)
RBC	H_2S emission	Appearance of H_2S emission due to organic overload	Cortez et al. (2008)
SBR	VSCs emission	Chemical analysis (GC-FPD), odor active values and emission factors	Li et al. (2021)
ASP (extended aeration) versus RBC	Odor emission	Olfactometry analysis	The present study

ASP, activated sludge process; GC-FPD, gas chromatography – flame photometric detector; OEFs, odor emission factors; RBC, rotating biological contactors; SBR, sequencing batch reactor; VSCs, volatile sulphur compounds.

Therefore, in small and medium-sized WWTPs (such is the case under study), the biological treatment technology used plays a key role in their odor impact, as it conditions sludge characteristics in subsequent sludge handling activities, which are the major sources of odor emission. Moreover, this study shows that RBC-WWTP would generate a lower odor impact than ASP-WWTP (based on extended aeration) for the treatment of the same organic load. This information might help to select the most appropriate biological wastewater treatment for minimizing the impact of odors when it is necessary to build new WWTPs, with the consequent social and environmental benefits.

By way of example, **Table 6** shows how other authors have addressed the problem of odor emission in WWTPs with different biological treatment technologies. As can be observed in this table, most of the studies have focused on WWTPs with activated sludge process in its different modifications (Dinçer et al., 2020, Kim et al., 2014, Varela-Bruce and Antileo, 2021, Zwain et al., 2020). The odor impact of the technology based on rotating biological contactors has been much less studied and based solely on the emission of H_2S (Cortez et al., 2008). On the other hand, although the implementation of sequencing batch reactors is not very widespread in full-scale sewage treatment plants, Li et al. (2021) have characterized VSC emissions from a SBR-WWTP at the water-air interface. However, the present study goes a step further because, to date, it is the only one that performs a comparative evaluation of the odor emissions derived from two full-scale WWTPs with ASP (based on extended aeration) and RBC technologies, widely implemented in facilities of small and medium-sized municipalities (Sikosana et al., 2019, Wee Seow et al., 2016).

3.4. Bacterial microbiome analysis

Globally, the 16S sequencing analysis identified over 370,000 bacteria from the two WWTP sludges and 3 biological replicates analyzed in this study. RBC-SL showed a higher number of identifications than ASP-SL, with almost 215,000 *versus* 160,000 counts, respectively. The difference in the number of identified bacteria in these sludges was in accordance with the higher VS concentration in RBC-SL than ASP-SL. The endogenous respiration of ASP-SL reduced the concentration of biodegradable organic matter and thus the number of identified bacteria in this sludge.

Eleven and 13 different phyla were identified in ASP-SL and RBC-SL, respectively (**Fig. 2**). Proteobacteria, Bacteroidetes and Firmicutes were the three predominant phyla

in both WWTPs, albeit with some differences. Proteobacteria represented the most common phylum in both, reaching a similar percentage (≈55%). Bacteroidetes also presented similar levels in both WWTPs (≈16%), although whereas they were the second-most abundant in ASP-SL, they were only the third-most abundant in RBC-SL due to the presence of a higher proportion of Firmicutes (25.6%). In ASP-SL, the three predominant phyla accounted for over 83% of all identifications, with 3 additional phyla ranging from 3.1% to 5.7% (Actinobacteria, Chloroflexi and Tenericutes), while the rest were infrequent (less than 1.2%). On the other hand, the three predominant phyla in RBC-SL collectively represented 97%, followed by Actinobacteria (2.3%), while the other 9 phyla identified were very scarce (less than 0.24%). Bacteria belonging to the Ignavibacteriae phylum were only identified in ASP-SL and those belonging to the Chlamydiae, Nitrospinae and Spirochaetes phyla were exclusive to RBC-SL (**Fig. 2**).

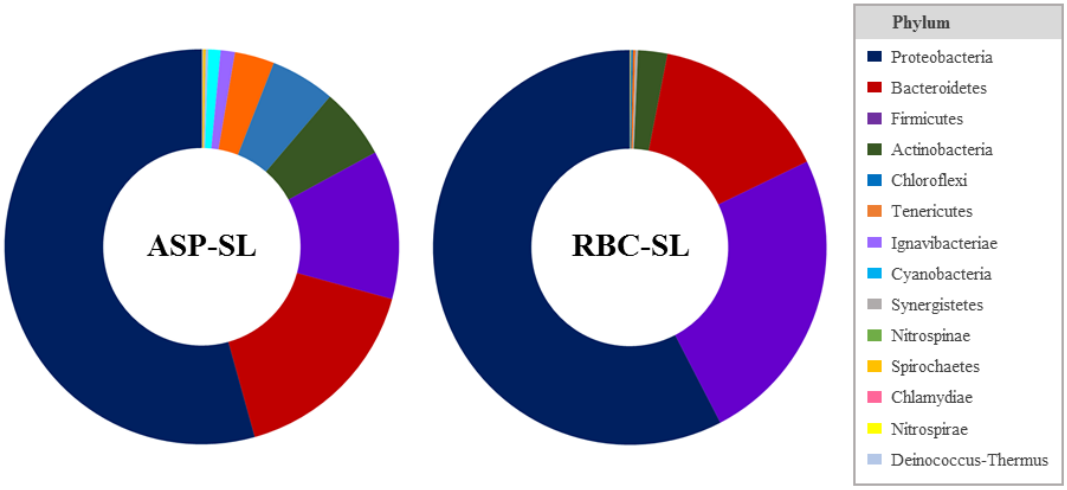

Fig. 2. Relative bacterial community composition at the phylum level, obtained after massive 16S rRNA sequencing of sludge from ASP-WWTP and RBC-WWTP (ASP-SL and RBC-SL, respectively). The mean of the 3 biological replicates per location is represented.

At the family level, the profiles of both sludges differed in accordance with the different biological processes analyzed (**Fig. 3** and **Table S2**, Supplementary material). The high degree of similarity among the biological replicate profiles in both sludges should be acknowledged. Among the 142 families identified, 90 were present in both WWTPs (63%), while 35 and 17 were only detected in ASP-SL and RBC-SL, respectively. This imbalance was also quantified using the Shannon–Wiener index (H′), which estimates microbial biodiversity in a specific environment using the abundance of

species against their relative evenness. As can be observed in **Fig. 3**, the biodiversity of the bacterial microbiota in RBC-SL was significatively lower than in ASP-SL, according to the lower number of families detected in the first sludge. These data are in line with previous reports indicating that ASP sludges present highly diverse microbial ecosystems (Wu et al., 2019). The presence of pollutants has been previously associated with biodiversity reduction and thus with more vulnerable aquatic ecosystems (Johnston and Roberts, 2009). Although nutrient enrichment can have positive effects on species richness (Johnston and Roberts, 2009), the pressure of a high organic pollutant load in RBC-WWTP contributed to its reduced bacterial diversity. The Proteobacteria Comamonadaceae was the most common family in both sludges, representing 13.2% and 25.6% in ASP-SL and RBC-SL, respectively. Fifty-two families presented significantly different counts between the two WWTP sludges (**Table S2**, Supplementary material). Although RBC-SL presented a higher global number of identifications, most of the families with significant differences (77%) had higher levels in ASP-SL, being Beijerinckiaceae up to 254 higher than in RBC-SL. Only 12 families (23%) were more abundant in RBC-SL, most notably Ruminococcacea which was 71 times more common than in ASP-SL.

Most studies of the microbiomes in WWTPs are focused on ASP-based facilities. Recently, a very comprehensive study of the bacterial composition of ASP sludges from a wide range of locations across the world proposed a core bacterial community, highlighting certain genera that were present in most samples, for instance *Dokdonella*, *Zoogloea*, *Nitrospira* and *Arcobacter* (Wu et al., 2019). On the other hand, studies on the microbial composition of RBC-based facilities remain scarce, although several operational taxonomic units (OTUs) have been identified and related to nitrification, ammonia-oxidizing and denitrification processes in these reactors, *e.g. Nitrospira* , *Nitrosomonas*, *Paracoccus*, *Rhodobacter* and *Thauera* (Peng et al., 2014, Spasov et al., 2020). All these genera were also identified in our samples, but no significant differences in their abundance were found between the ASP-SL and RBC-SL samples (data not shown).

Sludge contains a lot of anaerobic organisms, which produce odors when they consume organic matter (Holman and Wareham, 2003). Thus, odors are usually the result of the activity of microbiota, as by consuming organic matter, they produce VOCs and odorous gases such as hydrogen sulfide or ammonia. In concordance with the higher

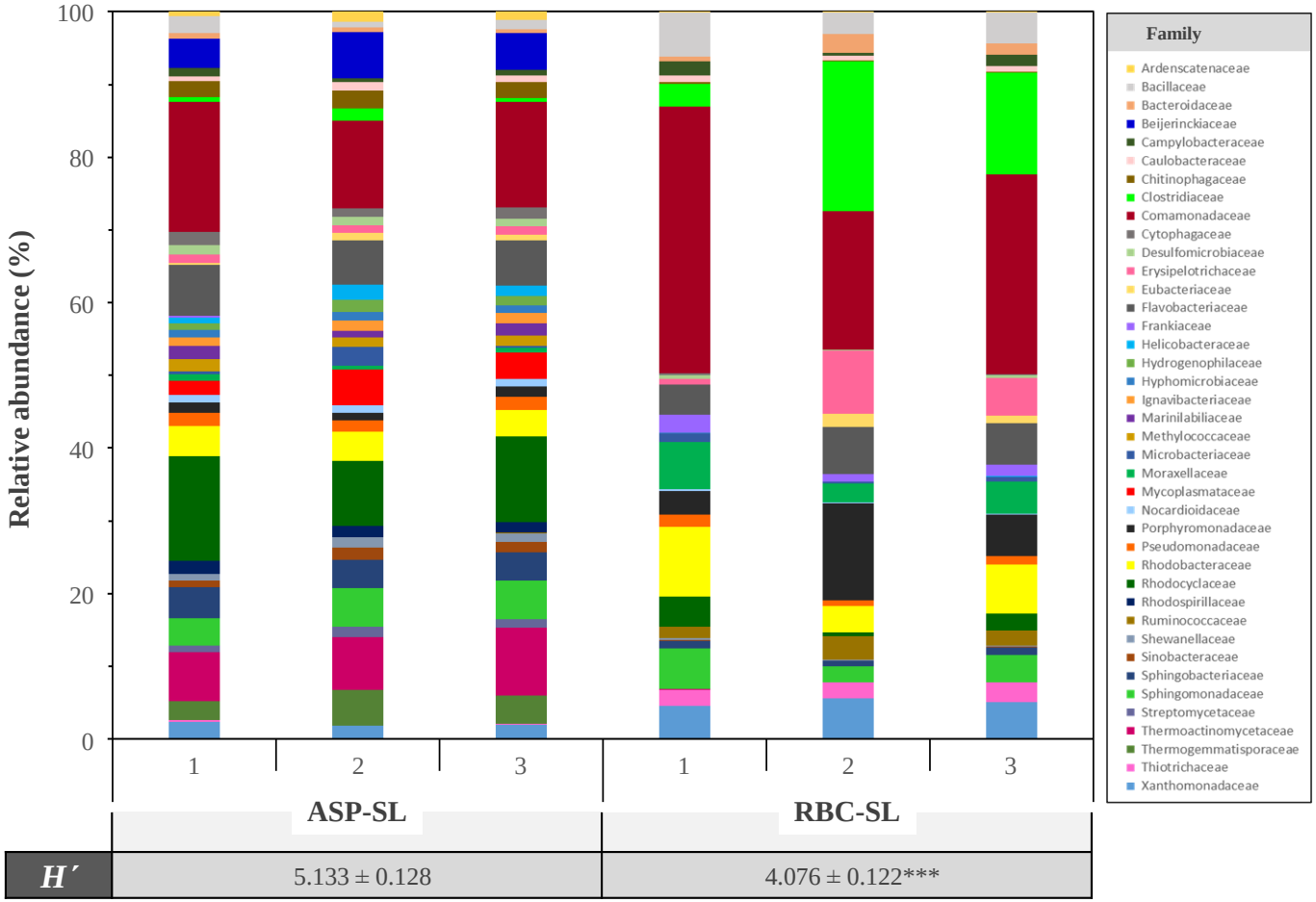

Fig. 3. Relative abundances of bacterial families and estimation of microbial biodiversity in ASP-SL and RBC-SL. The 3 biological replicates for each location are represented individually. Alpha diversity values are shown in terms of richness using the Shannon–Wiener index (H′). H´max was 7.15.

global odor emission in RBC-WWTP compared to ASP-WWTP, several microorganisms that the present study found to be significantly higher in RBC-SL have previously been linked to the production of unpleasant odors. In this sense, Porphyromonadaceae, Clostridiales, Lachnospiraceae and Moraxellaceae are some examples (see **Table S2**, Supplementary material), all members of the first three families being obligate anaerobes (Hummelen et al., 2010, Kubota et al., 2012, Kumpitsch et al., 2019, Million et al., 2020). Therefore, this fact is in line with the higher OC from the sludge handling activities (sludge thickening and dewatering) in RBC-WWTP compared to ASP-WWTP (**Table 5**). However, it is also worth noting that sulfur-oxidizing bacteria, that are able to consume some of these odor compounds and thus participate in nuisance odor removal (Fan et al., 2020, Ren et al., 2019), were found to be higher in RBC-SL than in ASP-SL, specifically Halothiobacillaceae (12.9-fold), Thiotrichaceae (32.2-fold) and Xanthomonadaceae (3.5-fold).

In WWTPs with rotating biological contactors it is difficult to minimize odor emissions due to the presence of anaerobic metabolic pathways that depend on both the influent organic load and the thickness of the biodiscs´ biofilm (Cortez et al., 2008). In this context, the use of closed systems for the sludge handling activities that are equipped with a deodorization system based on GAC beds could be the most appropriate technology for efficient odor removal in small and medium-sized WWTPs operating with RBC. However, the consumption of resources in the facility would increase notably (especially in terms of energy and adsorbent material). For its part, WWTPs with activated sludge process have a better responsiveness to increases in influent organic load (that could generate higher odor emissions) than RBC-WWTPs, due to the possibility of increasing the solids concentration in the reactor. Nevertheless, increasing the concentration of solids also has some disadvantages, because as such concentration increases the efficiency of aeration decreases. In this sense, if the oxygenation capacity is not sufficient, the organic overload could even lead to anaerobic conditions and, therefore, higher odor emissions (Von Sperling, 2007). Thus, maintaining the solids concentration at optimal levels in the reactor is critical for both wastewater treatment performance and odor management in ASP-WWTPs. However, it would be also advisable to implement a deodorization system (such as the one previously mentioned) to control the odor emissions derived from the sludge handling activities, which also constitute the major

odor emission sources in small and medium-sized ASP-WWTPs based on extended aeration.

4. Conclusions

The WWTP with activated sludge process based on extended aeration had a global odor emission very close to that of the WWTP with rotating biological contactors (11,177 and 12,784 ou_E/s, respectively), although ASP-WWTP received an organic load approximately 2.7 times lower than that of RBC-WWTP. The sludge handling activities constituted the major odor emission sources in both facilities (accounting for 99.46% and 99.80% of the global odor emission in ASP-WWTP and RBC-WWTP, respectively). The significative increments in the abundance of anaerobic microbial families such as Porphyromonadaceae, Clostridiales, Lachnospiraceae and the aerobic Moraxellaceae in RBC-SL helped to justify the higher odor concentration from the sludge handling activities in RBC-WWTP compared to ASP-WWTP. However, regardless of the influent organic load, ASP-WWTP would have a higher specific odor emission than RBC-WWTP (16.22 and 6.84 $ou_E/s \cdot EI$, respectively), which is related to the different respirometric activity of the sludge generated. In this sense, the maximum specific oxygen uptake rate (mg O_2/g VS·h) was 2.41 times higher in ASP-SL than RBC-SL.

Given the above, this study provides relevant information about the odor emission of small and medium-sized full-scale WWTPs, which may help wastewater managers to select the most appropriate biological wastewater treatment technology from an environmental and human health point of view, since it conditions sludge characteristics, and therefore, the odor impact of those facilities.

Acknowledgements

This work was supported by the Spanish Ministry of Economy, Industry and Competitiveness (MINECO), the Spanish State Research Agency (AEI) and the European Regional Development Fund (FEDER) through Projects CTM2017-88723-R & PID2020-117438RB-I00, and the Ministry of Education, Culture and Sport of Spain (Grant FPU2016). The European Regional Development Fund (Project UCO-FEDER-1262384-R) and the Chelonia Association (Mares Circulares Project) also supported this

work. Furthermore, we wish to express our gratitude to EMPROACSA (especially Miguel Ranchal and Manuel Dios) and Inmaculada Bellido for their contributions to this research and to Mercedes Cousinou and Laura Redondo (Genomic Unit, SCAI, UCO) for their technical help in the microbiome identification. Funding for open access charge: Universidad de Córdoba / CBUA.

Appendix A. Supplementary data

Fig. S1. Satellite images of ASP-WWTP (A) and RBC-WWTP (B).

Source: Google Earth.

Table S1. Comparison of operational conditions between ASP-WWTP and RBC-WWTP in 2019.

	ASP-WWTP	**RBC-WWTP**
Energy consumption (kW·h/d)	195	150
DO in the reactor (mg O_2/L)	1.20	—
MLVSS (mg/L)	1650	—
MLTSS (mg/L)	2550	—
F/M (kg BOD_5/kg MLVSS·d)	0.09	—
HRT (h)	14	4
SRT (d)	36	—

ASP-WWTP, wastewater treatment plant with activated sludge process; DO, dissolved oxygen; F/M, food-to-microorganism ratio; HRT, hydraulic retention time; MLTSS, mixed liquor total suspended solids; MLVSS, mixed liquor volatile suspended solids; RBC-WWTP, wastewater treatment plant with rotating biological contactors; SRT, solids retention time.

Table S2. Microbial families showing significant abundance differences between both WWTPs.

Phylum	Family	Counts Mean ± SD		Ratio ASP/RBC[a]
		ASP-SL	RBC-SL	
Actinobacteria	Acidimicrobiaceae	76.33 ± 22.94	9.00 ± 0.00	8.48**
	Catenulisporaceae	216.0 ± 90.0	9.00 ± 0.00	24.00*
	Dietziaceae	361.7 ± 133.7	9.00 ± 0.00	40.19*
	Frankiaceae	43.00 ± 38.63	1129.0 ± 600.7	0.038*
	Gordoniaceae	66.67 ± 12.06	9.00 ± 0.00	7.41**
	Iamiaceae	43.00 ± 20.07	9.00 ± 0.00	4.78*
	Microthrixaceae	429.3 ± 77.3	9.67 ± 1.16	44.41***
	Nocardioidaceae	514.3 ± 96.0	99.67 ± 61.61	5.16**
	Sporichthyaceae	117.7 ± 12.86	9.00 ± 0.00	13.08***
	Streptomycetaceae	571.7 ± 194.6	10.33 ± 2.31	55.34**
Bacteroidetes	Chitinophagaceae	1078.0 ± 216.6	119.0 ± 66.46	9.06**
	Cryomorphaceae	155.0 ± 14.93	9.33 ± 0.58	16.61****
	Cytophagaceae	682.3 ± 50.1	91.33 ± 65.26	7.47***
	Marinifilaceae	129.7 ± 5.1	9.00 ± 0.00	14.41****
	Marinilabiliaceae	695.3 ± 147.5	9.00 ± 0.00	77.26**
	Porphyromonadaceae	590.7 ± 60.5	4457 ± 2169	0.13*
	Prolixibacteraceae	70.00 ± 17.35	23.33 ± 11.50	3.00*
	Sphingobacteriaceae	1891 ± 161	673.7 ± 272.9	2.81**
	unclassified Bacteroidetes	42.67 ± 0.58	9.00 ± 0.00	4.74****
Chloroflexi	Ardenscatenaceae	514.0 ± 252.5	81.67 ± 23.97	6.29*
	Ardenticatenaceae	425.7 ± 77.0	18.00 ± 13.89	23.65***
	Thermogemmatisporaceae	1836 ± 782	9.00 ± 0.00	204.00*
Deinococcus-Thermus	Thermaceae	115.3 ± 38.2	9.67 ± 1.16	11.93**
Firmicutes	Bacillaceae	670.3 ± 252.4	3005 ± 1374	0.22*
	Clostridiales F XI. Incertae Sedis	58.00 ± 6.56	206.3 ± 59.5	0.28*
	Lachnospiraceae	16.00 ± 12.12	170.0 ± 60.7	0.09*
	Peptococcaceae	225.0 ± 99.1	13.67 ± 8.08	16.46*
	Peptoniphilaceae	256.0 ± 134.0	9.00 ± 0.00	28.44*
	Ruminococcaceae	20.00 ± 9.54	1467 ± 352	0.014**
	Thermoactinomycetaceae	3688 ± 849	23.67 ± 12.86	155.81**
	Veillonellaceae	15.67 ± 8.33	343.0 ± 130.8	0.046*
Ignavibacteriae	Ignavibacteriaceae	625.7 ± 147.6	9.00 ± 0.00	69.52**
Proteobacteria	Bdellovibrionaceae	9.33 ± 0.58	193.7 ± 61.8	0.048**
	Beijerinckiaceae	2457 ± 908	9.667 ± 1.155	254.2**
	Desulfomicrobiaceae	535.7 ± 49.9	211.7 ± 148.4	2.53*
	Desulfovibrionaceae	311.7 ± 60.5	19.67 ± 9.71	15.85**
	Hahellaceae	134.7 ± 15.8	9.00 ± 0.00	15.00***
	Halothiobacillaceae	9.00 ± 0.00	116.0 ± 40.9	0.078*
	Helicobacteraceae	698.3 ± 374.1	17.00 ± 11.36	41.08*
	Hydrogenophilaceae	625.0 ± 292.1	9.00 ± 0.00	69.44*
	Hyphomicrobiaceae	514.7 ± 101.6	85.00 ± 50.86	6.06**
	Methylococcaceae	650.3 ± 3.5	9.00 ± 0.00	72.26****
	Methylocystaceae	35.33 ± 12.01	9.00 ± 0.00	3.93*
	Moraxellaceae	300.3 ± 71.9	3093 ± 1628	0.097*
	OMG group	57.00 ± 20.66	9.33 ± 0.58	6.11*
	Rhodocyclaceae	5397 ± 571	1654 ± 1304	3.26*
	Rhodospirillaceae	748.3 ± 76.1	11.00 ± 3.46	68.03****
	Shewanellaceae	582.7 ± 230.6	119.3 ± 64.9	4.88*
	Sinobacteraceae	624.7 ± 248.6	17.33 ± 7.37	36.05*
	Thiotrichaceae	50.00 ± 46.16	1611 ± 614	0.031*
	Xanthomonadaceae	959.0 ± 49.9	3335 ± 800	0.29**
Tenericutes	Mycoplasmataceae	1708 ± 924.0	9.00 ± 0.00	189.78*

[a] The statistical significance is shown as: *, $p < 0.05$; **, $p < 0.01$; ***, $p < 0.001$; *****, $p < 0.0001$

References

Aonofriesei, F., Petrosanu, M., 2007. Activated sludge bulking episodes and dominant filamentous bacteria at wastewater treatment plant Constanţa Sud (Romania). Microbiology 2, 83–87.

APHA, 2017. Standard methods for the examination of water and wastewater, 23rd ed. American Public Health Association, Washington DC.

Bhatla, M.N., 1975. Control of Odors at an Activated Sludge Plant. Water Pollut. Control Fed. 47, 281–290.

Byliński, H., Gębicki, J., Namieśnik, J., 2019. Evaluation of health hazard due to emission of volatile organic compounds from various processing units of wastewater treatment plant. Int. J. Environ. Res. Public Health 16. https://doi.org/10.3390/ijerph16101712

Cao, L., Liao, L., Su, C., Mo, T., Zhu, F., Qin, R., Li, R., 2021. Metagenomic analysis revealed the microbiota and metabolic function during co-composting of food waste and residual sludge for nitrogen and phosphorus transformation. Sci. Total Environ. 773, 145561. https://doi.org/10.1016/j.scitotenv.2021.145561

Capelli, L., Sironi, S., Del Rosso, R., Céntola, P., 2009. Predicting odour emissions from wastewater treatment plants by means of odour emission factors. Water Res. 43, 1977–1985. https://doi.org/10.1016/j.watres.2009.01.022

Carrera-Chapela, F., Donoso-Bravo, A., Souto, J.A., Ruiz-Filippi, G., 2014. Modeling the odor generation in WWTP: An integrated approach review. Water. Air. Soil Pollut. 225, 1–15. https://doi.org/10.1007/S11270-014-1932-Y

Chahal, C., van den Akker, B., Young, F., Franco, C., Blackbeard, J., Monis, P., 2016. Pathogen and Particle Associations in Wastewater: Significance and Implications for Treatment and Disinfection Processes. Adv. Appl. Microbiol. 97, 63–119. https://doi.org/10.1016/BS.AAMBS.2016.08.001

Chica, A., Mohedo, J.J., Martín, M.A., Martín, A., 2003. Determination of the stability of msw compost using a respirometric technique. Compost Sci. Util. 11, 169–175. https://doi.org/10.1080/1065657X.2003.10702122

Cortez, S., Teixeira, P., Oliveira, R., Mota, M., 2008. Rotating biological contactors: a review on main factors affecting performance. Rev. Environ. Sci. Biotechnol. 7, 155–172. https://doi.org/10.1007/s11157-008-9127-x

Dinçer, F., Dinçer, F.K., Sarı, D., Ceylan, Ö., Ercan, Ö., 2020. Dispersion modeling and air quality measurements to evaluate the odor impact of a wastewater treatment plant in İzmir. Atmos. Pollut. Res. 11, 2119–2125. https://doi.org/10.1016/J.APR.2020.05.018

Dominguez, D., Gujer, W., 2006. Evolution of a wastewater treatment plant challenges traditional design concepts. Water Res. 40, 1389–1396. https://doi.org/10.1016/j.watres.2006.01.034

Dong, D., Yan, A., Liu, H., Zhang, X., Xu, Y., 2006. Removal of humic substances from soil DNA using aluminium sulfate. J. Microbiol. Methods 66, 217–222. https://doi.org/10.1016/j.mimet.2005.11.010

Dunlop, M., Blackall, P., Stuetz, R., 2016. Odour emissions from poultry litter - a review litter properties, odour formation and odorant emissions from porous materials. J. Environ. Manage. 177, 306–319. https://doi.org/10.1016/J.JENVMAN.2016.04.009

EN 13725, 2003. Air Quality - Determination of Odour Concentration by Dynamic Olfactometry. European Committee for Standardization, Brussels.

Englande, A.J., Krenkel, P.A., 2003. Waste water Treatment and Water Reclamation, in: Encyclopedia of Physical Science and Technology. Academic Press, pp. 639–670. https://doi.org/10.1016/B0-12-227410-5/00818-8

EU Council, 1991. Council Directive 91/271/EEC of 21 May 1991 concerning urban waste-water treatment.

Fan, F., Xu, R., Wang, D., Meng, F., 2020. Application of activated sludge for odor control in wastewater treatment plants: Approaches, advances and outlooks. Water Res. 181, 115915. https://doi.org/10.1016/j.watres.2020.115915

Ferrer, C., Miguel, D., Ferrer, L., Alonso, S., Sangüesa, I., Basiero, A., Bernacer, I., Morenilla, J.J., 2008. Análisis comparativo entre procesos de tratamiento de agua residual de pequeñas poblaciones de la provincia de Castellón. Tecnol. del Agua 28, 30–36.

García, L., Leyva-Díaz, J.C., Díaz, E., Ordóñez, S., 2021. A review of the adsorption-biological hybrid processes for the abatement of emerging pollutants: Removal efficiencies, physicochemical analysis, and economic evaluation. Sci. Total Environ. 780, 146554. https://doi.org/10.1016/J.SCITOTENV.2021.146554

González, D., Colón, J., Sánchez, A., Gabriel, D., 2019. A systematic study on the VOCs characterization and odour emissions in a full-scale sewage sludge composting plant. J. Hazard. Mater. 373, 733–740. https://doi.org/10.1016/J.JHAZMAT.2019.03.131

Gutiérrez, M.C., Serrano, A., Martín, M.A., Chica, A.F., 2014. Odour in composting processes at pilot scale: Monitoring and biofiltration. Environ. Technol. (United Kingdom) 35, 1676–1684. https://doi.org/10.1080/09593330.2014.880132

Hassard, F., Biddle, J., Cartmell, E., Jefferson, B., Tyrrel, S., Stephenson, T., 2015. Rotating biological contactors for wastewater treatment – a review. Process Saf. Environ. Prot. 94, 285–306. https://doi.org/10.1016/J.PSEP.2014.07.003

Holman, J.B., Wareham, D.G., 2003. Oxidation-Reduction Potential as a Monitoring Tool in a Low Dissolved Oxygen Wastewater Treatment Process. J. Environ. Eng. 129, 52–58. https://doi.org/10.1061/(ASCE)0733-9372(2003)129:1(52)

Hummelen, R., Fernandes, A.D., Macklaim, J.M., Dickson, R.J., Changalucha, J., Gloor, G.B., Reid, G., 2010. Deep sequencing of the vaginal microbiota of women with HIV. PLoS One 5. https://doi.org/10.1371/journal.pone.0012078

Jácome, A., Suárez, J., Ures, P., 2015. Rotating biological contactors (biodiscs) (FS-BIO-004) [Fact sheet] [WWW Document]. URL https://www.wateractionplan.com/documents/177327/558166/Rotating+biological+contactors.pdf (accessed 5.25.21).

Jiang, G., Melder, D., Keller, J., Yuan, Z., 2017. Odor emissions from domestic wastewater: a review. Crit. Rev. Environ. Sci. Technol. 47, 1581–1611. https://doi.org/10.1080/10643389.2017.1386952

Johnston, E.L., Roberts, D.A., 2009. Contaminants reduce the richness and evenness of marine communities: a review and meta-analysis. Environ. Pollut. 157, 1745–1752. https://doi.org/10.1016/j.envpol.2009.02.017

Kalbar, P.P., Karmakar, S., Asolekar, S.R., 2012. Technology assessment for wastewater treatment using multiple-attribute decision-making. Technol. Soc. 34, 295–302. https://doi.org/10.1016/j.techsoc.2012.10.001

Karageorgos, P., Latos, M., Kotsifaki, C., Lazaridis, M., Kalogerakis, N., 2010. Treatment of unpleasant odors in municipal wastewater treatment plants. Water Sci. Technol. 61, 2635–2644. https://doi.org/10.2166/wst.2010.211

Kim, H., Lee, H., Choi, E., Choi, I., Shin, T., Im, H., Ahn, S., 2014. Characterization of odor emission from alternating aerobic and anoxic activated sludge systems using real-time total reduced sulfur analyzer. Chemosphere 117, 394–401. https://doi.org/10.1016/j.chemosphere.2014.08.008

Kominko, H., Gorazda, K., Wzorek, Z., 2019. Potentiality of sewage sludge-based organo-mineral fertilizer production in Poland considering nutrient value, heavy metal content and phytotoxicity for rapeseed crops. J. Environ. Manage. 248, 109283. https://doi.org/10.1016/j.jenvman.2019.109283

Kubota, H., Mitani, A., Niwano, Y., Takeuchi, K., Tanaka, A., Yamaguchi, N., Kawamura, Y., Hitomi, J., 2012. Moraxella species are primarily responsible for generating malodor in laundry. Appl. Environ. Microbiol. 78, 3317–3324. https://doi.org/10.1128/AEM.07816-11

Kumpitsch, C., Koskinen, K., Schöpf, V., Moissl-Eichinger, C., 2019. The microbiome of the upper respiratory tract in health and disease. BMC Biol. 17, 1–20. https://doi.org/10.1186/s12915-019-0703-z

Lebrero, R., Bouchy, L., Stuetz, R., Muñoz, R., 2011. Odor Assessment and Management in Wastewater Treatment Plants: a review. Crit. Rev. Environ. Sci. Technol. 41, 915–950. https://doi.org/10.1080/10643380903300000

Li, R., Han, Z., Shen, H., Qi, F., Ding, M., Song, C., Sun, D., 2021. Emission characteristics of odorous volatile sulfur compound from a full-scale sequencing batch reactor wastewater treatment plant. Sci. Total Environ. 776, 145991. https://doi.org/10.1016/j.scitotenv.2021.145991

Liu, Y., Ngo, H.H., Guo, W., Peng, L., Wang, D., Ni, B., 2019. The roles of free ammonia (FA) in biological wastewater treatment processes: a review. Environ. Int 123, 10–19. https://doi.org/10.1016/j.envint.2018.11.039

Márquez, P., Benítez, A., Caballero, Á., Siles, J.A., Martín, M.A., 2021. Integral evaluation of granular activated carbon at four stages of a full-scale WWTP deodorization system. Sci. Total Environ. 754, 142237. https://doi.org/10.1016/j.scitotenv.2020.142237

Martín, M.A., Gutiérrez, M.C., Dios, M., Siles, J.A., Chica, A.F., 2018. Application of ATAD technology for digesting sewage sludge in small towns: Operation and costs. J. Environ. Manage. 215, 185–194. https://doi.org/10.1016/J.JENVMAN.2018.03.062

Million, M., Armstrong, N., Khelaifia, S., Guilhot, E., Richez, M., Lagier, J.C., Dubourg, G., Chabriere, E., Raoult, D., 2020. The Antioxidants Glutathione, Ascorbic Acid and Uric Acid Maintain Butyrate Production by Human Gut Clostridia in The Presence of Oxygen In Vitro. Sci. Rep. 10, 1–11. https://doi.org/10.1038/s41598-020-64834-3

Oh, S.T., Kim, J.R., Premier, G.C., Lee, T.H., Kim, C., Sloan, W.T., 2010. Sustainable wastewater treatment: How might microbial fuel cells contribute. Biotechnol. Adv. 28, 871–881. https://doi.org/10.1016/j.biotechadv.2010.07.008

Omri, I., Bouallagui, H., Aouidi, F., Godon, J.J., Hamdi, M., 2011. H2S gas biological removal efficiency and bacterial community diversity in biofilter treating wastewater odor. Bioresour. Technol. 102, 10202–10209. https://doi.org/10.1016/j.biortech.2011.05.094

Peng, X., Guo, F., Ju, F., Zhang, T., 2014. Shifts in the microbial community, nitrifiers and denitrifiers in the biofilm in a full-scale rotating biological contactor. Environ. Sci. Technol. 48, 8044–8052. https://doi.org/10.1021/es5017087

Prasse, C., Stalter, D., Schulte-Oehlmann, U., Oehlmann, J., Ternes, T.A., 2015. Spoilt for choice: A critical review on the chemical and biological assessment of current wastewater treatment technologies. Water Res. 87, 237–270. https://doi.org/10.1016/j.watres.2015.09.023

Rana, S., Gupta, N., Rana, R.S., 2018. Removal of Organic pollutant with the use of Rotating Biological Contactor, in: Materials Today: Proceedings. Elsevier Ltd, pp. 4218–4224. https://doi.org/10.1016/j.matpr.2017.11.685

Ren, B., Zhao, Y., Lyczko, N., Nzihou, A., 2019. Current Status and Outlook of Odor Removal Technologies in Wastewater Treatment Plant. Waste and Biomass Valorization 10, 1443–1458. https://doi.org/10.1007/s12649-018-0384-9

Saeed, M.U., Hussain, N., Sumrin, A., Shahbaz, A., Noor, S., Bilal, M., Aleya, L., Iqbal, H.M.N., 2021. Microbial bioremediation strategies with wastewater treatment potentialities – a review. Sci. Total Environ. 151754. https://doi.org/10.1016/J.SCITOTENV.2021.151754

Sekyiamah, K., Kim, H., McConnell, L.L., Torrents, A., Ramirez, M., 2008. Identification of Seasonal Variations in Volatile Sulfur Compound Formation and Release from the Secondary Treatment System at a Large Wastewater Treatment Plant. Water Environ. Res. 80, 2261–2267. https://doi.org/10.2175/106143008X304677

Sikosana, M.L., Sikhwivhilu, K., Moutloali, R., Madyira, D.M., 2019. Municipal wastewater treatment technologies: a review. Procedia Manuf. 35, 1018–1024. https://doi.org/10.1016/j.promfg.2019.06.051

Spasov, E., Tsuji, J.M., Hug, L.A., Doxey, A.C., Sauder, L.A., Parker, W.J., Neufeld, J.D., 2020. High functional diversity among Nitrospira populations that dominate rotating biological contactor microbial communities in a municipal wastewater treatment plant. ISME J. 14, 1857–1872. https://doi.org/10.1038/s41396-020-0650-2

Tchobanoglous, G., Burton, F.L., Stensel, H.D., 2003. Wastewater Engineering: Treatment and Reuse. McGraw Hill, New York, NY.

Toledo, M., Gutiérrez, M.C., Siles, J.A., García-Olmo, J., Martín, M.A., 2018a. Chemometric analysis and NIR spectroscopy to evaluate odorous impact during the composting of different raw materials. J. Clean. Prod. 167, 154–162. https://doi.org/10.1016/j.jclepro.2017.08.163

Toledo, M., Siles, J.A., Gutiérrez, M.C., Martín, M.A., 2018c. Monitoring of the composting process of different agroindustrial waste: Influence of the operational variables on the odorous impact. Waste Manag. 76, 266–274. https://doi.org/10.1016/j.wasman.2018.03.042

Toledo, M., Márquez, P., Siles, J.A., Chica, A.F., Martín, M.A., 2019. Co-composting of sewage sludge and eggplant waste at full scale: Feasibility study to valorize eggplant waste and minimize the odoriferous impact of sewage sludge. J. Environ. Manage. 247, 205–213. https://doi.org/10.1016/j.jenvman.2019.06.076

Ullah, A., Hussain, S., Wasim, A., Jahanzaib, M., 2020. Development of a decision support system for the selection of wastewater treatment technologies. Sci. Total Environ. 731, 139158. https://doi.org/10.1016/j.scitotenv.2020.139158

US Department of Agriculture and the US Composting Council, 2002. Test Methods for the Examination of Composting and Compost (TMECC). Edaphos International, Houston (TX).

Varela-Bruce, C., Antileo, C., 2021. Assessment of odour emissions by the use of a dispersion model in the context of the proposed new law in Chile. J. Environ. Manage. 295, 113208. https://doi.org/10.1016/J.JENVMAN.2021.113208

VDI guideline 3880, 2011. Olfactometry – Static Sampling. Beuth Verlag GmbH, Berlin, pp. 10772.

Von Sperling, M., 2007. Basic Principles of Wastewater Treatment. IWA Publishing. https://doi.org/10.2166/9781780402093

Wang, Y., Jin, X., He, L., Zhang, W., 2017. Inhibitory effect of thiourea on biological nitrification process and its eliminating method. Water Sci. Technol. 75, 2900–2907. https://doi.org/10.2166/WST.2017.177

Waqas, S., Bilad, M.R., 2019. A review on Rotating Biological Contactors. Indones. J. Sci. Technol. 4, 241–256. https://doi.org/10.17509/IJOST.V4I2.18181

Waqas, S., Bilad, M.R., Man, Z., Wibisono, Y., Jaafar, J., Indra Mahlia, T.M., Khan, A.L., Aslam, M., 2020. Recent progress in integrated fixed-film activated sludge process for wastewater treatment: a review. J. Environ. Manag. 268, 110718. https://doi.org/10.1016/j.jenvman.2020.110718

Wee Seow, T., Lim, C.K., Hanif, M., Nor, M., Fahmi, M., Mubarak, M., Lam, C.Y., Yahya, A., Ibrahim, Z., 2016. Review on Wastewater Treatment Technologies. Int. J. Appl. Environ. Sci. 11, 111–126.

Wei, W., Wang, Q., Zhang, L., Laloo, A., Duan, H., Batstone, D.J., Yuan, Z., 2018. Free nitrous acid pre-treatment of waste activated sludge enhances volatile solids destruction and improves sludge dewaterability in continuous anaerobic digestion. Water Res. 130, 13–19. https://doi.org/10.1016/j.watres.2017.11.050

Wu, L., Ning, D., Zhang, B., Li, Y., Zhang, P., Shan, X., Zhang, Q., Brown, M., Li, Z., Van Nostrand, J.D., Ling, F., Xiao, N., Zhang, Y., Vierheilig, J., Wells, G.F., Yang, Y., Deng, Y., Tu, Q., Wang, A., Zhang, T., He, Z., Keller, J., Nielsen, P.H., Alvarez, P.J.J., Criddle, C.S., Wagner, M., Tiedje, J.M., He, Q., Curtis, T.P., Stahl, D.A., Alvarez-Cohen, L., Rittmann, B.E., Wen, X., Zhou, J., Acevedo, D., Agullo-Barcelo, M., Andersen, G.L., de Araujo, J.C., Boehnke, K., Bond, P., Bott, C.B., Bovio, P., Brewster, R.K., Bux, F., Cabezas, A., Cabrol, L., Chen, S., Etchebehere, C., Ford, A., Frigon, D., GÃ^{3}mez, J.S., Griffin, J.S., Gu, A.Z., Habagil, M., Hale, L., Hardeman, S.D., Harmon, M., Horn, H., Hu, Z., Jauffur, S., Johnson, D.R., Keucken, A., Kumari, S., Leal, C.D., Lebrun, L.A., Lee, J., Lee, M., Lee, Z.M.P., Li, M., Li, X., Liu, Y., Luthy, R.G., MendonÃ§a-Hagler, L.C., de Menezes, F.G.R., Meyers, A.J., Mohebbi, A., Oehmen, A., Palmer, A., Parameswaran, P., Park, J., Patsch, D., Reginatto, V., de los Reyes, F.L., Noyola, A., Rossetti, S., Sidhu, J., Sloan, W.T., Smith, K., de Sousa, O.V., Stephens, K., Tian, R., Tooker, N.B., De los Cobos Vasconcelos, D., Wakelin, S., Wang, B., Weaver, J.E., West, S., Wilmes, P., Woo, S.G., Wu, J.H., Wu, L., Xi, C., Xu, M., Yan, T., Yang, M., Young, M., Yue, H., Zhang, Q., Zhang, W., Zhang, Y., Zhou, H., 2019. Global diversity and biogeography of bacterial communities in wastewater treatment plants. Nat. Microbiol. 4, 1183–1195. https://doi.org/10.1038/s41564-019-0426-5

Yu, K., Zhang, T., 2012. Metagenomic and Metatranscriptomic Analysis of Microbial Community Structure and Gene Expression of Activated Sludge. PLoS One 7, e38183. https://doi.org/10.1371/journal.pone.0038183

Zhang, H., Zheng, S., Zhang, X., Duan, S., Li, S., 2020. Optimizing the inclined plate settler for a high-rate microaerobic activated sludge process for domestic wastewater treatment: A theoretical model and experimental validation. Int. Biodeterior. Biodegrad. 154, 105060. https://doi.org/10.1016/j.ibiod.2020.105060

Ziembińska-Buczyńska, A., Ciesielski, S., Żabczyński, S., Cema, G., 2019. Bacterial community structure in rotating biological contactor treating coke wastewater in relation to medium composition. Environ. Sci. Pollut. Res. 26, 19171–19179. https://doi.org/10.1007/s11356-019-05087-0

Zwain, H.M., Nile, B.K., Faris, A.M., Vakili, M., Dahlan, I., 2020. Modelling of hydrogen sulfide fate and emissions in extended aeration sewage treatment plant using TOXCHEM simulations. Sci. Reports 2020 101 10, 1–11. https://doi.org/10.1038/s41598-020-79395-8

I.2. Breve descripción del artículo: "*Odor impact simulation of a large urban wastewater treatment plant through the numerical solution of an Eulerian model*"

I.2. Breve descripción del artículo: "*Odor impact simulation of a large urban wastewater treatment plant through the numerical solution of an Eulerian model*"

La combinación de la olfatometría dinámica con un modelo de dispersión Euleriano ha permitido tanto la cuantificación de las emisiones odoríferas de los principales focos contaminantes de una EDAR urbana de gran tamaño como la evaluación de su impacto odorífero, en áreas cercanas y en diferentes estaciones del año. La línea de aguas residuales es la que más contribuyó a la emisión global de olor de la citada EDAR, representando el 98,86% de la emisión total de la instalación, registrándose altas tasas de emisión de olor (OER) asociadas a diferentes operaciones unitarias: 62.100, 55.800, 88.400 y 11.300 ou_E/s, correspondientes a la cabecera de pretratamiento, desarenado−desengrasado, decantación primaria y tratamiento biológico, respectivamente. Se trata de valores de emisión correspondientes a verano, que es la estación en la que se registraron las mayores emisiones de olor. De los mencionados focos de olor, los dos primeros disponían de un sistema de tratamiento de olores basado en la adsorción mediante CAG, así como también el espesamiento por gravedad, el espesamiento por flotación y la deshidratación de los lodos. La operación correspondiente al espesamiento por gravedad fue la que presentó la mayor OER (1.500 ou_E/s en verano) de todas las operaciones de la línea de lodos, cuya contribución a la emisión global de la EDAR urbana fue solamente del 1,14% debido al tratamiento de los fangos mediante digestión anaerobia, el cual reduce considerablemente la manipulación del fango y la emisión de olor asociada. En las restantes estaciones del año, las tasas de emisión de olor fueron similares, aunque algo inferiores. La velocidad del viento y su dirección principal en cada estación del año, las características de los focos contaminantes y sus tasas de emisión de olor, así como los coeficientes de difusión turbulenta fueron los parámetros de entrada de un novedoso modelo Euleriano de dispersión de olor con tamaño regulable de la malla espacial en función de la proximidad a cada foco emisor. El cálculo de la concentración de inmisión de olor se realizó mediante el desarrollo de un código en el lenguaje de programación Fortran90. El mayor impacto odorífero (538 ou/m^3), que quedó dentro del perímetro de la EDAR, se pronosticó en la dirección sur en otoño, lo que correspondió a la menor velocidad del viento en la dirección principal (1,23 m/s). Sin embargo, en las poblaciones más cercanas a la instalación objeto de estudio, los valores de inmisión de olor fueron despreciables, siendo muy inferiores a 1 ou/m^3, valor que representa el umbral de percepción de olores para la población humana.

Under review

Contents lists available at ScienceDirect

Journal of Environmental Management

journal homepage: www.elsevier.com/locate/jenvman

Odour impact simulation of a large urban wastewater treatment plant through the numerical solution of an Eulerian model

Márquez, P. [a], Muñoz-Serrano, E. [b], Gutiérrez, M.C. [a], Siles, J.A. [a], Martín, M.A. [a,*]

[a] Department of Inorganic Chemistry and Chemical Engineering, Area of Chemical Engineering, Campus de Excelencia ceiA3, Instituto Químico para la Energía y el Medioambiente (IQUEMA). University of Cordoba, Campus Universitario de Rabanales, Carretera N-IV, km 396, Edificio Marie Curie, 14071 Córdoba, Spain

[b] Departamento de Física, Universidad de Córdoba, Campus Universitario de Rabanales, Edificio Albert Einstein, 14071 Córdoba, Spain

* Corresponding author: iq2masam@uco.es

Abbreviations: GAC, granular activated carbon; OC, odour concentration (ou_E/m^3); OER, odour emission rate (ou_E/s); OIC, odour immission concentration (ou/m^3); ou_E, European odour units; S1, pre-treatment header; S2, sand and fat removal; S3, primary settling; S4, biological treatment; S5.1, gravity thickening; S5.2, flotation thickening; S6, sludge dehydration; S7, sludge storage; S8, sludge discharge; SOER, specific odour emission rate ($ou_E/m^2 \cdot s$); STP, standard temperature and pressure; VOCs, volatile organic compounds; VOEF, volumetric odour emission factor ($ou_E/s \cdot m^3$ GAC); WWTP, wastewater treatment plant.

Graphical abstract

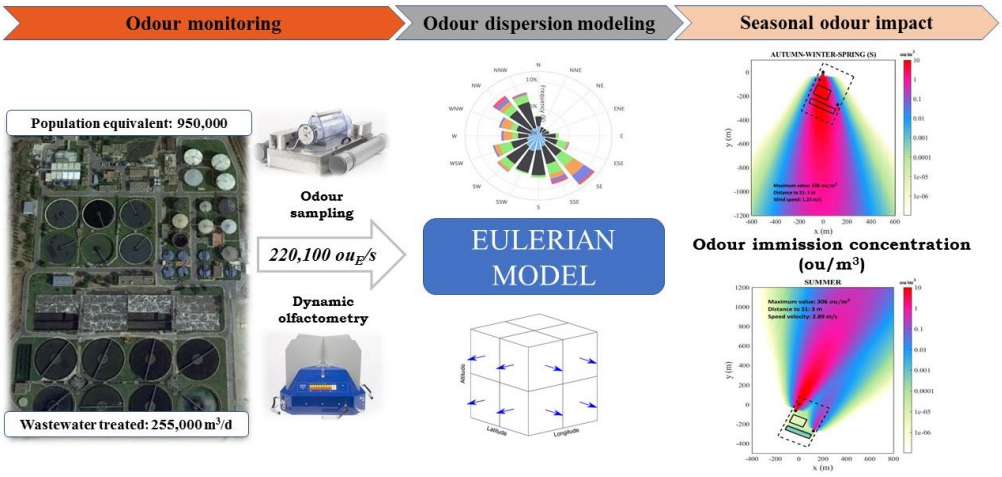

Abstract

The combination of dynamic olfactometry and Eulerian dispersion modelling allowed both the quantification of odour emissions from the main sources of a large urban wastewater treatment plant (WWTP) and the evaluation of its seasonal odour impact in nearby areas. Odour emissions from the WWTP were mainly due to the wastewater line, which contributed 98.86% of the total emission of the facility, with high odour emission rates (OERs): 62,100, 55,800, 88,400 and 11,300 ou_E/s, corresponding to pre-treatment header, sand and fat removal, primary settling and biological treatment, respectively, in summer, which is the season that registered the highest emissions. The first two odour sources had an odour treatment system based on adsorption by granular activated carbon, as well as gravity thickening, flotation thickening and sludge dehydration. Gravity thickening showed the highest OER (1500 ou_E/s) of the sludge line, which only contributed 1.14% to the total emission of the WWTP. In other seasons of the year, the OERs were similar, although somewhat lower. The wind speed and its main direction in each season of the year, the characteristics of the sources and their odour emissions, and the turbulent diffusion coefficients were considered as input parameters of an Eulerian odour dispersion model. A code in the programming language Fortran90 was developed to calculate the odour immission concentration. The highest odour impact (538 ou/m^3) was predicted in the south direction in autumn, which corresponds to the lowest wind speed in the main direction (1.23 m/s). However, in the closest populations to the WWTP, the odour immission was negligible, being much lower than 1 ou/m^3.

Keywords: Dynamic olfactometry; Granular activated carbon; Eulerian model; Odour dispersion; Odour immission; WWTP.

1. Introduction

Odour impact is inherently associated with wastewater treatment plants (WWTPs). Population growth around these facilities has led to an increase in the number of complaints and protests, which has forced public authorities to develop stricter environmental regulations to control odour emissions resulting from industrial activities and waste management (Beghi et al., 2012; Hayes et al., 2017; Sironi et al., 2012; Wroniszewska and Zwoździak, 2020). It is well known that long-term exposure to odorants harms the quality of life of local communities, leading to psychological stress and symptoms such as nausea, headache, insomnia, respiratory diseases and even cancer (Byliński et al., 2019; Naddeo et al., 2012; Sucker et al., 2009). There is a wide presence of odorants in gaseous emissions from WWTPs (**Table S1**, Supplementary Material), some of which have very low odour threshold values in terms of ppb or ppt (Nagata, 2003). According to Lebrero et al. (2011) and Senatore et al. (2021), some of the main volatile compounds present in the abovementioned emissions include hydrogen sulphide, methyl mercaptan, dimethyl sulphide, dimethyl disulphide, trimethylamine, butyric acid, butanone, toluene, benzene and skatole. The first of them is commonly considered the main odour-causing compound in WWTPs (Jiang et al., 2017; Talaiekhozani et al., 2016).

In the above-mentioned facilities, it is also important to know the different sources which contribute to odour impact to a greater or lesser extent since odour control strategies should focus especially on those with the highest odour emissions. In this sense, Gostelow et al. (2001b) propose the following classification of the emission sources from a WWTP: (i) sources, such as aerated grit separator and activated sludge treatment, which promotes mass transfer when the odoriferous compounds have already been formed and (ii) areas where new odorants are formed, such as primary/secondary sedimentation and thickening tanks. This latter case occurs to a greater extent under anaerobic conditions, where new odorants are generated as a result of anaerobic processes (Karageorgos et al., 2010). Consequently, odour emissions are different depending on the treatment units, where primary operations and sludge handling activities are widely considered the main odour sources in sewage treatment plants (Capelli et al., 2009; Fisher et al., 2018; Gebicki et al., 2016; Senatore et al., 2021).

Due to the enforcement of new environmental regulations, odour control strategies have become a priority for WWTPs. The regulation of odour through Directive

2010/75/EU of the European Parliament and of the Council of 24 November 2010 on Industrial Emissions in the European Union countries is one such example (Bokowa et al., 2021). Odour management in WWTPs includes preventive actions to avoid odorant formation, impact minimisation and end-of-pipe odour abatement systems. Prevention should be the priority strategy, combining efficient design and operation practices (Capodaglio et al., 2002; Estrada et al., 2015; Talaiekhozani et al., 2016). When prevention or impact minimisation actions are not sufficient to mitigate these emissions, odour treatment technologies must be applied. In this context, it is possible to distinguish between biological and physicochemical methods. The first methods are based on the capability of certain microorganism to break down odorous pollutants into simpler and odourless compounds (Barbusinski et al., 2017; Mudliar et al., 2010). Biofilters, bioscrubbers and biotrickling filters are the most widespread odour treatment technologies in WWTPs because of their low operating costs. However, biofilm-based biological systems are less effective at removing hydrophobic compounds (Lamprea Pineda et al., 2021; Márquez et al., 2022). Moreover, some physicochemical methods such as chemical scrubbers and adsorption on activated carbon are also commonly used for odour removal in these facilities because of the extensive experience in their design and operation, low empty bed residence times and rapid start-up, among other factors (Ren et al., 2019; Senatore et al., 2021). Activated carbon is in very widespread use since it can easily adsorb a wide range of odorants, such as volatile organic compounds (VOCs), ammonia, mercaptans and hydrogen sulphide (Lebrero et al., 2011; Márquez et al., 2021a, 2021b).

On the other hand, odour impact can be evaluated utilising a wide range of dispersion models (Conti et al., 2020; Ferrero and Oettl, 2019; Gutiérrez et al., 2015; Schiffman et al., 2005; Toledo et al., 2018). These models enable simulation of odour immissions to prevent odour problems when an industrial facility does not yet exist or the odour impacts are unknown and then implement control methods when an industrial activity is causing odour annoyance in nearby residential areas because of its operation. In this sense, olfactometric data, obtained by the unique legally valid methodology for odour concentration (OC) quantification such as dynamic olfactometry (EN 13725, 2003), are used to build odour dispersion models since odour emission rates are input data in such models. These simulations are also mainly subjected to the topography around the odour sources as well as atmospheric conditions (Botta et al., 2020; Giungato et al., 2018).

Table 1. Comparative of different odour dispersion models.

Eulerian models	**Gaussian models (as AERMOD)**	**Lagrangian models (as CALPUFF)**
Unsteady-state	Steady-state	Unsteady-state
Non-steady emission, different types (point, area, surface), geometry and localization of sources.	Multiple surface/elevates emission sources including point, area, and surface sources. Emissions are constant.	Non-steady emission rates. Need realistic emission rates, difficult to obtain.
Non-steady meteorological conditions. Require 3D fields of air temperature and vertical velocity. Valid for low wind speed.	Meteorological conditions constants and horizontally uniform (AERMET Module). Limitations in low wind speeds (calm atmospheric conditions).	Time- and space-varying meteorological conditions. Require complex meteorological sounding data.
Small spatial-time scale. Highly time resolved. More realistic dispersion transport.	Short-range simulations (up to 50 km). Uncertainty increases with distance to source.	Long-range transport (scale > 50 km). Tend to underestimate peak intensities close to the source.
More accurate spatial-temporal representation than Lagrangian and Gaussian models.	Manageable computational time and reasonable accuracy.	Less accurate than Eulerian models.
Flat and complex terrain, within urban and rural areas.	Flat and complex terrain, within urban and rural areas (AERMAP Module).	Complex terrain effects, over-water transport and simple chemical transformation.
Require more computing power.	Under-predict odour concentrations when configured as an area source. Overestimate the concentrations downwind under stable atmospheric conditions.	Need a marked number of input parameters.
	References	
Botta et al. (2020), Conti et al. (2020), Liu et al. (2019) and Seinfeld and Pandis (2016)	Busini et al. (2012), Conti et al. (2020), Dinçer et al. (2020), Dresser and Huizer (2011) and Liu et al. (2019)	Busini et al. (2012), Conti et al. (2020), Ferrero and Oettl (2019) and Wang et al. (2006)

Nevertheless, in an odour dispersion model, all the elements with an impact on air quality should be integrated. Apart from the topography and atmospheric conditions, other factors, such as the molecular weight of the gaseous compounds and their residence time in the atmosphere, the chemical reactions between odorants and so on, also influence odour dispersion. Therefore, obtaining a reliable value of odour immission concentration (OIC) is a difficult task (Díaz et al., 2014).

Currently, three large types of air dispersion models used for odour assessment are distinguished: Gaussian, Lagrangian and Eulerian. **Table 1** shows a comparison of these models. In addition, there are a variety of improvements to these models and combinations of them, such as the well-known AERMOD and CALPUFF models. The United States Environmental Protection Agency (US EPA) instructs that the dispersion model used to establish the odour impact of industrial activity is the Gaussian AERMOD model, while CALPUFF, is used only for complex cases (Díaz et al., 2014). However, the Support Center for Regulatory Atmospheric Modeling (SCRAM, 2018), which belongs to the US EPA, no longer considers CALPUFF as a recommended air quality dispersion model, alleging concerns about its ability to deal with long-range transport of pollutants. For its part, Eulerian models (grid models) numerically solve the advection–dispersion continuity equation in a wind-generated turbulent flow and calculate the average concentration of pollutants in a 3D domain subdivided into grids (Liu et al., 2019; Seinfeld and Pandis, 2016). Eulerian models allow non-homogeneous and non-stationary emissions and weather conditions, obtaining instant solutions. Different types and geometries of sources located at different heights can be simulated. Eulerian models use a non-uniform grid to obtain more accurate spatial-temporal concentrations and at a small scale than Gaussian and Lagrangian models, with high time resolution. More realistic dispersion transport is obtained but requires more computing resources. Flat or complex terrains can be included in urban or rural areas. Therefore, it might be said that odour dispersion modelling is a complex and changing field, where new approaches are required to fully understand and simulate such an important environmental issue.

This work aims to develop software that allows quantitative simulation of the dispersion of the emitted odour from the main sources located in a large urban WWTP and to evaluate its impact on surrounding areas, including nearby populations. Although this paper presents the results of the normal operation of the WWTP, which could be simulated with simpler models such as a Gaussian model, the objective is to have software

prepared to evaluate the impact of specific episodes of odour due to industrial spills or a defective punctual operation of the plant. Therefore, the odour dispersion in the atmosphere was calculated using a 3D unsteady-state numerical Eulerian dispersion model by considering the weather conditions throughout the different seasons of the year. The Eulerian model provides the advantages shown in **Table 1**, although in the present work some of them will not be revealed since (i) a stable meteorology representative of each season will be adopted, (ii) a flat terrain (given by the location of the WWTP) will be established and (iii) a stationary emission that describes the normal operation of the plant will be used as input model parameter. However, the model has the advantage of (i) high time-space resolution, (ii) being reliable for small distances from the source, (iii) in the transport of odour over long distances and (iv) for low wind speed values. The involved processes were turbulent diffusion, transport of wind by advection and emission of sources. The non-linear resulting equation was reformulated in terms of odour flows to achieve the convergence to the solution by numerical methods. An exponential control volume formulation was used to discretise the equation in the calculation domain. The evolution time led to a stationary OC spatial distribution in the atmosphere using the Gauss-Seidel method. To the best of our knowledge, the numerical strategy used to solve the dispersion model applied to the estimation of the WWTP odour impact (evaluated by both unit operations and seasons of the year) has not been previously reported in the literature. Consequently, the results presented in this study might aid wastewater managers to increase or modify odour control strategies in odour annoyance situations, with the consequent social and environmental benefits.

2. Material and methods

2.1. Description of the urban WWTP and odour sources

The large urban WWTP under study is located in the province of Seville (Spain). It can treat wastewater from a population equivalent of 950,000 and has a current treatment capacity of 255,000 m^3/d, including contributions from industrial wastewater. It operates with biological secondary treatment (active sludge) and sludge stabilisation by anaerobic digestion and dehydration. **Scheme 1** shows the schematic diagram of this WWTP. The odour sources of this facility are described below, considering the wastewater line and the sludge line.

Concerning the wastewater line, the main odour sources are as follows. *Source 1* (S1) is the pre-treatment header and includes roughing operations, water elevation using worm screws and screening. This area is covered. The air confined inside is sucked in and deodorised in an activated carbon tower (provided with two chimneys), before its emission into the atmosphere. *Source 2* (S2) is the sand and fat removal. This odour source is also covered. The indoor air is drawn and conducted homogeneously to two towers of activated carbon (with two chimneys per tower), where it is deodorised; *Source 3* (S3) is the primary settling area. This operation is carried out in not covered primary decanters; *Source 4* (S4) is the biological treatment area. In this WWTP, a conventional active sludge system is used, through eight uncovered aeration basins.

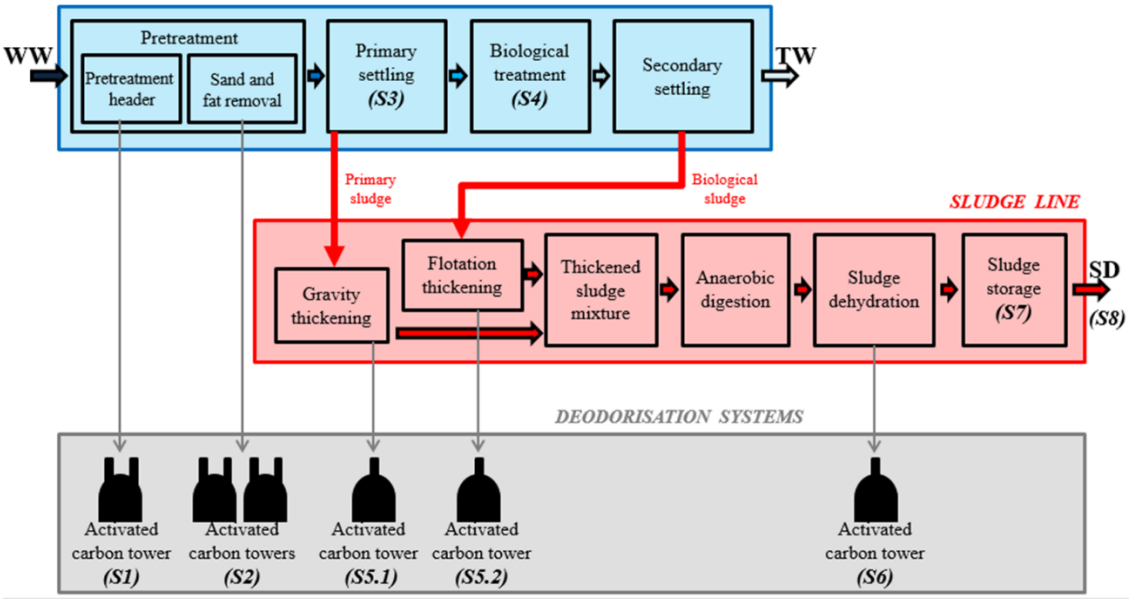

Scheme 1. General flow diagram of the urban WWTP (WW, inlet wastewater; TW, treated wastewater; SD, sludge discharge).

About the sludge line, the main odour sources are as follows. *Source 5* (S5) is the sludge thickening area. This area includes gravity thickeners and floating decanters, which receive sludge from primary and biological treatment, respectively. Both devices are covered. On the one side, the air from gravity thickeners (S5.1) is deodorised in an activated carbon tower provided with a single chimney, while the air from floating decanters (S5.2) is decontaminated in another tower of activated carbon with a single chimney. *Source 6* (S6) is the sludge dehydration area. It includes centrifuges that dehydrate sludge from anaerobic digestion. The air from the centrifuge room is deodorised in an activated carbon tower provided with a single chimney. *Source 7* (S7) is

the sludge storage area. Dehydrated sludge is stored in four conical tanks for its later discharge in trucks. The conical tanks are closed but they have a hatch at the top for venting. *Source 8* (S8) is where the discharge of sludge in trucks occurs. This area is not covered. It has been considered an average of four daily sludge discharges and the discharge time is approximately 25 minutes.

Table 2. Description of the point sources of odour.

	S1	**S2**	**S5.1**	**S5.2**	**S6**	**S7**
Number of gas outlets (chimneys)	2	4	1	1	1	4
Outlet diameter (m)	0.64	0.76	0.48	0.48	0.30	0.15
Height above ground (m)	6.0	6.0	3.5	3.5	3.5	12.0
Unit airflow rate (m^3_{STP}/h)	10,000	10,000	4000	4000	2000	Natural ventilation*
Annual operating regime (%)	33	33	100	100	67	100

S1, pre-treatment header; **S2**, sand and fat removal; **S5.1**, gravity thickening; **S5.2**, flotation thickening; **S6**, sludge dehydration; **S7**, sludge storage; **STP**, standard temperature and pressure.

* S7 does not have a deodorisation system, but it is a point source of odour.

The sources S1, S2, S5.1, S5.2, S6 and S7 were grouped into point sources of odour, whereas S3, S4 and S8 corresponded to surface sources. The main characteristics of each of these sources are shown in **Table 2** and **Table 3**, respectively. The data specified in these tables were used to calculate the odour emission of the urban WWTP and, subsequently, to estimate its odour impact through the dispersion model.

Table 3. Description of the surface sources of odour.

	S3	**S4**	**S8**
Number of units	6	8	1
Unit surface (m^2)	1452	1232	450
Height above ground (m)	1.5	-1.5	3.0
Annual operating regime (%)	67	100	7

S3, primary settling; **S4**, biological treatment; **S8**, sludge discharge.

2.2. Activated carbon towers: description and operation

In all covered sources, polluted air is sucked in by fans until it reaches the active carbon filters, where malodourous compounds are adsorbed. After that, clean air is expelled into the atmosphere through different chimneys. Granular activated carbon (GAC) used in deodorisation towers was made from coconut shell, while its manufacturer technical specifications were as follows: ash content, 4%; average particle diameter, 3.7 mm; iodine number (minimum), 1000 mg/g and BET specific surface area, 406 m^2/g. The GAC was impregnated with an alkaline solution (NaOH or KOH) to neutralise inorganic H_2S (Water Environment Federation, 2017). The use of NaOH or KOH for the GAC impregnation does not modify its adsorbing properties (Martin et al., 2010; Ren et al., 2019).

The concentration of H_2S at the system output is the most frequently used parameter in the urban WWTP to proceed with the replacement of the GAC. Then, the contaminated material is deposited in a landfill and replaced by fresh activated carbon. The total numbers of GAC beds per odour source are two in S1, four in S2, one in S5.1, one in S5.2 and one in S6. For its part, the bed capacity follows a descending order of 4.81 m^3 (S2) > 3.53 m^3 (S1) > 2.39 m^3 (S5.1 and S5.2) > 0.92 m^3 (S6).

2.3. Odour sampling and olfactometric analysis

The gaseous samples were collected at the different odour sources detailed in Section 2.1. Concerning sources with activated carbon towers (S1, S2, S5.1, S5.2 and S6), it is important to note that all GAC beds had the same operation time. The odour samples were collected in a single chimney per source. For the chimneys not evaluated (one in S1 and three in S2), the OC values obtained in the chimneys analysed were assimilated. Similarly, the four sludge storage conical tanks (S7) were not sampled, but only one of them. Also, odour emission was considered homogeneous in the primary decanters (S3) as well as in the biological aeration basins (S4). The sampling related to the discharge of sludge in trucks (S8) was carried out by taking an odour sample from a sludge pile, extracted from one of the storage conical tanks and especially enabled for its quantification.

The CSD30 (manufactured by Olfasense GmbH) was the sampling device for collecting odour samples in 10-L Nalophan® sampling bags. The ventilated sampling

hood, developed by the same manufacturer, was connected to the CSD30 device for sampling non-ventilated, odour-emitting solid (S8) or liquid area sources (S3 and S4). When sampling liquids, floats were attached to the sides of the hood. Both sampling devices are fully compliant with the standard EN 13725 (2003) and the guideline VDI 3880 (2011). The main characteristics and operation of these devices were previously reported by Toledo et al. (2018). The sampling time was 30 minutes per sample. All gaseous samples were collected in duplicate and were analysed within 6 hours to minimise the permeation and/or adsorption of odorants through/on the sampling bag walls, as proposed by the guideline VDI 3880 (2011).

Dynamic olfactometry was the method used to quantify the OC. This variable was expressed in terms of European odour units per cubic metre (ou_E/m^3). All odour concentration data were expressed following the reference conditions described in EN 13725 (i.e. 20 °C, 101.3 kPa on a wet basis). A TO8 olfactometer (also manufactured by Olfasense GmbH), based on the 'Yes/No' method, was used to determine the OC in each sample. The panellist group consisted of four people each being selected based on their sensitivity to the n-butanol reference gas as described in EN 13725 (2003). The odour concentration was calculated as the geometric mean of the odour threshold values of each panellist, multiplied by the square root of the olfactometer dilution factor. The OC results presented in this work are the geometric mean of the odour concentration of two samples from the same odour source. These results are necessary to subsequently determine the specific odour emission rate (SOER), the annual average odour emission rate (OER) and the relative odour contribution of the different odour sources (Gutiérrez et al., 2015; Toledo et al., 2018).

2.4. Determination of SOER, OER, VOEF and relative odour contribution

Each surface source has a different SOER ($ou_E/m^2 \cdot s$), which was calculated as follows:

$$SOER = \frac{OC \cdot Q_{air}}{A_H} \quad (1)$$

where *OC* is the odour concentration (ou_E/m^3), Q_{air} is the airflow rate circulating through the sampling hood ($2.08 \cdot 10^{-3}$ m^3/s), and A_H is the covered area of the above-mentioned hood (1 m^2).

SOER determination is the first step to estimate the OER from surface sources, which was calculated according to Eq. (2):

$$OER = SOER \cdot N_U \cdot US \cdot \left(\frac{OR}{100}\right) \quad (2)$$

where *OER* is the annual average odour emission rate (ou_E/s) for a surface source, *SOER* is its specific odour emission rate ($ou_E/m^2 \cdot s$), N_U is the number of units, the *US* is the unit surface (m^2), and *OR* is the annual operating regime (%). The values of N_U, US and OR are shown in **Table 3**.

In the case of point sources, the OER was calculated as follows:

$$OER = OC \cdot N_{GO} \cdot UAR \cdot \left(\frac{293}{273}\right) \cdot \left(\frac{OR}{100}\right) \quad (3)$$

where *OER* is the annual average odour emission rate (ou_E/s) for a point source, OC is the odour concentration (ou_E/m^3), N_{GO} is the number of gas outlets (or chimneys), *UAR* is the unit airflow rate (m^3_{STP}/s), and *OR* is the annual operating regime (%). The values of N_{GO}, UAR and OR are specified in **Table 2**.

To know the odour emission per cubic metre of GAC of the odour sources with deodorisation towers, the volumetric odour emission factor was calculated as follows:

$$VOEF = \frac{OER}{V_{GAC}} \quad (4)$$

where *VOEF* is the volumetric odour emission factor ($ou_E/s \cdot m^3$ GAC), *OER* is the annual odour emission rate in ou_E/s (for an odour source with GAC deodorisation), and V_{GAC} is the total volume (m^3) of GAC used to deodorise the odour source.

Finally, the relative odour contribution (%) of each odour source, regardless of its nature, was calculated according to Eq. (5):

$$Relative\ odour\ contribution\ (\%) = \frac{OER_i}{OER_G} \cdot 100 \quad (5)$$

where OER_i is the annual odour emission rate (ou_E/s) for an odour source, and OER_G is the total annual odour emission rate (ou_E/s), this being the sum of all OER_i (i.e. $OER_G = \sum OER_i$).

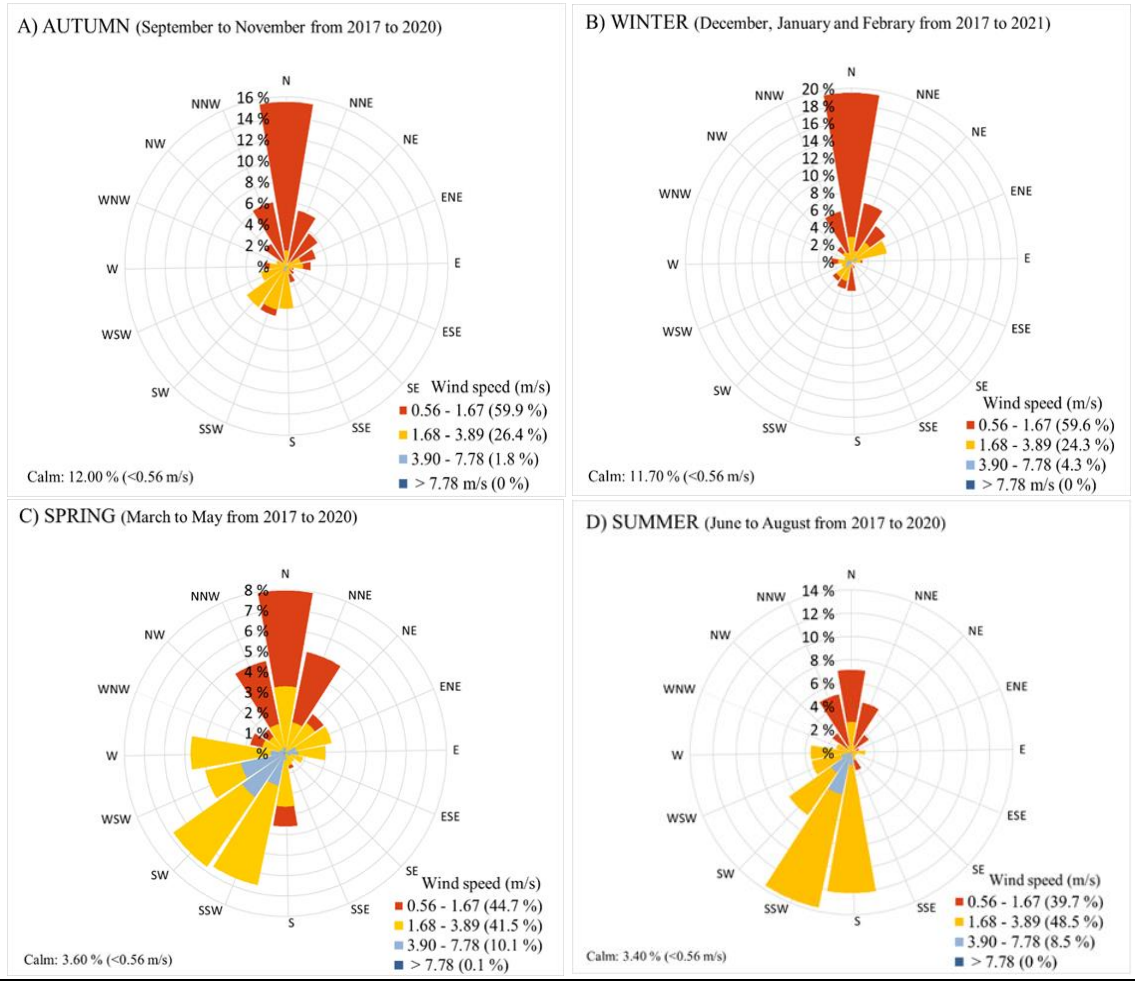

	A) Autumn	B) Winter	C) Spring	D) Summer
Average value of the wind speed in the main direction (m/s)	1.23 (S)	1.31 (S)	1.66 (S); 3.00 (NE)	2.89 (NNE)
Highest value of the average wind speeds (m/s) and direction	2.27 (ESE)	2.55 (ENE)	3.09 (ENE)	2.97 (NE)
Lowest value of the average wind speeds (m/s) and direction	1.08 (SSE)	1.20 (SSE)	1.51 (SSW)	1.26 (SSE)
Average value of the wind speed (m/s) for the period considered	1.44	1.51	2.19	2.27

Fig. 1. Wind rose in each season for the period between December 2017 and January 2021.

2.5. Dispersion model

A dispersion model was developed to predict the odour impact generated by the urban WWTP in nearby areas. The meteorological information (temperature, wind direction and wind speed) was provided by the Meteorological State Agency (AEMET, Spain). This information was obtained from the closest weather station to the WWTP under study. The station is located about 6 km (as the crow flies in a northerly direction) to the above-mentioned WWTP, at an altitude of 9 m and its geographic coordinates are 37° 21' 51" North, 6° 0' 21" West. **Figure 1** shows the wind rose in each season for the period between December 2017 and January 2021. Regarding the terrain orography, it is important to note that the WWTP under study is located in the Guadalquivir River valley and at a distance of 60 km in a straight line from the nearest coast. The terrain is an

extensive plain with very few slopes. The facility is between 2 and 10 m above sea level and the Guadalquivir River is on its west side (at approximately 2 km in a straight line), which can influence the wind direction.

The study of the WWTP odour impact was carried out by considering the sources that had the highest OER, being those: two surface sources (S3 and S4) and three point sources (S1, S2 and S5.1). **Figure 2** shows the outline of the sources considered (surface sources are considered rectangular sources and point sources are small squares). In addition, the ground clearance, collected in **Tables 2** and **3**, was considered. The height of source S4 is negative, which means that it is below ground level taken as a reference.

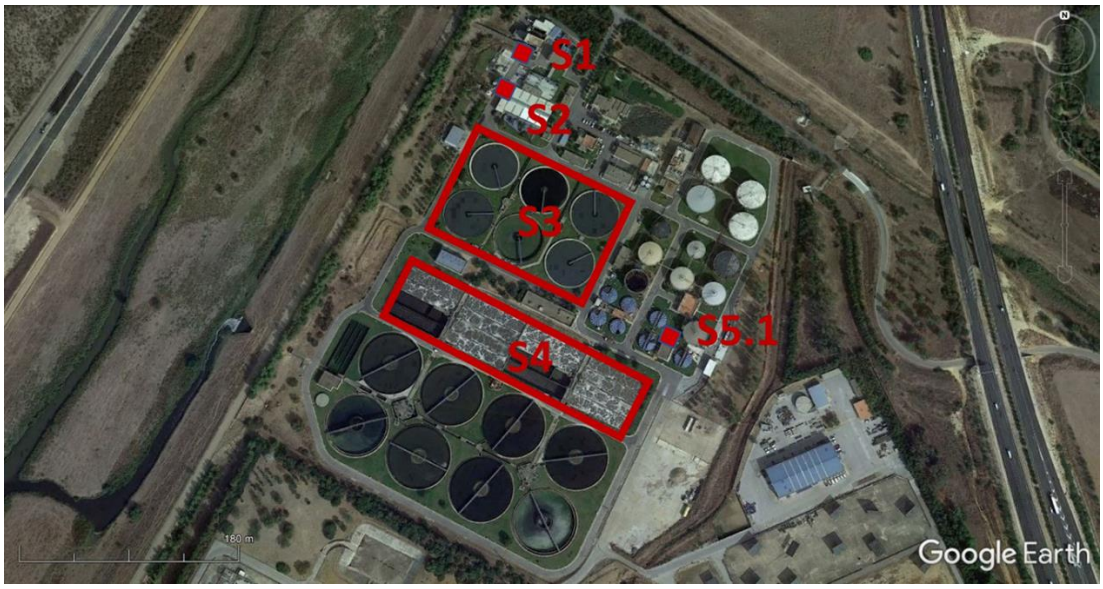

Fig. 2. Outline of the sources considered for the modelling of the odour dispersion (S1, pre-treatment header; S2, sand and fat removal; S3, primary settling; S4, biological treatment; S5.1, gravity thickening).

To study the mass transport of odour and its dispersion in the atmosphere, a 3D Cartesian coordinate system was used, whose origin was located at the emitting source and the x-axis was consistent with the direction of the wind, which was different according to the season of the year. The XY plane corresponded to the ground level since the plant is located on flat land without remarkable elevations. However, the model allows the establishment of different terrain elevations if necessary. The z-coordinate determined the ground clearance. The calculation domain, where the OIC was calculated, was the half-space $z \geqslant 0$, which corresponded to the atmosphere. The domain limits were located

several kilometres from the WWTP where the OIC was very low. In this way, a reflection on the boundary that may affect the dispersion result was avoided.

The accumulation of odour at one point in the atmosphere is the result of the odour emitted by the sources in the WWTP that are dispersed into the atmosphere by wind advection and turbulent diffusion. In a volume element of the atmosphere, the odour concentration must satisfy a balance of the amount of odour that enters and leaves the volume. This balance was expressed mathematically through the continuity equation (Eq. 6) in the advection-turbulent dispersion approach, called the Eulerian approach (Seinfeld and Pandis, 2016), using the Einstein summation convention:

$$\frac{\partial\langle c\rangle}{\partial t} + u_j \frac{\partial\langle c\rangle}{\partial x_j} = \frac{\partial}{\partial x_j}\left(K_{jj}\frac{\partial\langle c\rangle}{\partial x_j}\right) + Q(\vec{x},t) \quad (6)$$

where $\langle c\rangle$ represents the mean odor concentration at each point of the atmosphere and ground level (expressed in ou/m^3), t is time (s), u_j ($j = 1,2,3$) are the components of the wind vector (m/s), x_j ($j = 1,2,3$) are the spatial components of the vector $\vec{x}$ that describe the position of each point of the atmosphere and the ground level (m), K_{jj} ($j = 1,2,3$) are the three diagonal elements of the turbulent diffusivity tensor (m^2/s) and $Q(\vec{x},t)$ is the source odor emission rate by unit volume (ou/m^3·s). From now on we will omit the symbol mean value < > for simplicity in the notation. Eq. (6) is obtained assuming the molecular diffusion is negligible compared with turbulent diffusion and considering the atmosphere incompressible $\left(\frac{\partial u_j}{\partial x_j} = 0\right)$. The turbulent odour flux area is related to the mean odour concentration using the mixing-length model (Seinfeld and Pandis, 2016).

Using a Cartesian coordinate system and giving the X axis as the wind direction, the resulting three-dimensional continuity equation was the following (Liu et al., 2019):

$$\frac{\partial c}{\partial t} + u\frac{\partial c}{\partial x} = \frac{\partial}{\partial x}\left(K_x(x,u)\frac{\partial c}{\partial x}\right) + \frac{\partial}{\partial y}\left(K_y(x,u)\frac{\partial c}{\partial y}\right) + \frac{\partial}{\partial z}\left(K_z(x,u)\frac{\partial c}{\partial z}\right) + Q(\vec{x}) \quad (7)$$

where x, y and z are the Cartesian coordinates (m), u denotes the x component of the wind velocity (m/s), K_x and K_y are the horizontal turbulent diffusion coefficients and K_z is the vertical turbulent diffusion coefficient (m^2/s). The emitted odour represented by Q($\vec{x}$) is calculated from the sources OER in normal operation and is considered in steady conditions independent of time.

The Pasquill-Gifford-Turner (PGT) atmospheric stability classes (Turner, 1970) are used to calculate turbulent diffusion coefficients in each point of the calculation domain. The coefficients K_x, K_y and K_z were parameterised as a function of the distance x of each point from the emitting source in the wind direction and the wind speed u, according to Eq. (8) and Eq. (9):

$$K_y = K_x = 0{,}5\ \sigma_t^2\ \frac{u}{x} \tag{8}$$

$$K_z = 0{,}5\ \sigma_z^2\ \frac{u}{x} \tag{9}$$

where σ_t and σ_z are the standard horizontal and vertical diffusion coefficients, respectively. These coefficients were calculated, depending on the PGT atmospheric stability classes, using Martin´s formula (Martin, 1976).

In general, it is necessary to solve Eq. (7) coupled with the Navier-Stokes equation for wind components. However, the OC is so low relative to the air density that the presence of odour compounds does not affect the meteorology, and Eq. (7) can be solved independently of the coupled Navier-Stokes momentum equation. Therefore, the wind vector is introduced as a parameter of the model. The wind direction was obtained from the wind rose (**Fig. 1**) and the distribution of wind speed was used as a function of height relative to the ground by the Hellmann exponential model (Bañuelos-Ruedas et al., 2010), according to Eq. (10):

$$u = u_{ref}\left(\frac{z}{z_{ref}}\right)^p \tag{10}$$

where u_{ref} is the wind speed at a reference ground clearance $z_{ref} = 10\ m$. The value u_{ref} is taken from the wind rose for each season, shown in **Table 4**. The exponent *p* is obtained experimentally and depends on the PGT atmospheric stability category and the typology of the soil, whether rural or urban (EPA, 1987). Below a ground clearance of 0.5 m, a constant wind speed is considered.

Since both the sources of emission and the atmospheric conditions used are representative of the normal operation of the WWTP in the weather conditions typical of a season of the year, the solution of Eq. (7) will take us to a stationary state. Nevertheless, it is usual to find difficulties in obtaining convergence of the solution to the stationary state because of the advection term created by the wind field. Therefore, it is useful to

define, in the direction of the wind, a diffusive-advective flow $J_x = uc - K_x(x,u)\frac{\partial c}{\partial x}$, leaving Eq. (7) as Eq. (11):

$$\frac{\partial c}{\partial t} + \frac{\partial J_x}{\partial x} + \frac{\partial J_y}{\partial y} + \frac{\partial J_z}{\partial z} = Q(\vec{x}) \quad (11)$$

where $J_y = -K_y(x,u)\frac{\partial c}{\partial y}$ and $J_z = -K_z(x,u)\frac{\partial c}{\partial z}$ are diffusive flows on the y and z axes, respectively.

The problem formulation was completed establishing a constant initial OC and Neumann boundary conditions in calculation domain limits.

2.6. Numerical resolution: control volume formulation

The first step is the spatiotemporal discretisation of the model equation. Equation (11) was discretised spatially using the control volume formulation combined with the exponential scheme. A detailed description of the control volume formulation can be obtained in (Patankar, 1980). The calculation domain was divided into cells named control volume and the differential Eq. (11) was integrated over each control volume ΔV, in a time interval from t to $t + \Delta t$.

$$\int_t^{t+\Delta t}\int_V \left(\frac{\partial c}{\partial t} + \frac{\partial J_x}{\partial x} + \frac{\partial J_y}{\partial y} + \frac{\partial J_z}{\partial z}\right) dVdt = \int_t^{t+\Delta t}\int_V Q(\vec{x})\, dVdt \quad (12)$$

The control volumes were defined in Cartesian coordinates; therefore, $dV = dxdydz$. Each control volume surrounds a point *P* in the atmosphere where we want to calculate the OC. The point *P* has six neighbouring points: *E* and *W* (*E* denotes east and *W* stands for the west, located on the right and left of *P* on the X axis), *N* and *S* (north and south, on the Y axis) and *T* and *B* (top and bottom, on the Z axis). The control volume surrounds *P* midway between it and neighbouring points. The control-volume faces are located at points *e, w, n, s, t* and *b* of each axis and are perpendicular to the Cartesian axes. The surface of each face is symbolised as $S_{xe}, S_{xw}, S_{yn}, S_{ys}, S_{zt}, S_{zb}$. The points *P*, *E*, *W*, *N*, *S*, *T* and *B* are the nodes of a mesh grid in which the calculation domain is discretised.

Table 4. Characteristics of the speed vector in each season and estimated odour immission concentrations (OIC) in the nearby population centres.

			Autumn-Winter-Spring	**Spring**	**Summer**
Wind direction			S	NE	NNE
Wind speed (m/s)			1.23	3.00	2.89
Population center	**Distance (m)**	**Direction (º)**	**Odour immission concentration (ou/m^3)**		
I) Barrio Los Bermejales	3402	359	-	$1.2 \cdot 10^{-16}$	$2.5 \cdot 10^{-7}$
II) Barrio Bellavista	1607	46	-	$7.4 \cdot 10^{-2}$	$4.1 \cdot 10^{-5}$
III) Urbanización Fuente del Rey	826	77	-	$3.0 \cdot 10^{-4}$	$2.4 \cdot 10^{-9}$
IV) Base militar El Copero	1564	285	-	-	-
V) Gelves	4917	314	-	-	-
VI) Urbanización Tixe	4855	198	$1.2 \cdot 10^{-9}$	-	-
VII) Polígono industrial La Isla	1541	205	$1.5 \cdot 10^{-3}$	-	-
VIII) La Puebla del Río	8137	236	-	-	-
IX) Coria del Río	6400	248	-	-	-

The control volume formulation is an improvement on the usual discretisation methods, based on the finite-difference scheme via the Taylor-series expansion because the integration of the differential equation expresses the conservation principle in the finite control volume. The integrals of Eq. (12) are performed as follows:

$$\int_t^{t+\Delta t}\int_V \frac{\partial c}{\partial t}dVdt = (c_P^1 - c_P^0)\,\Delta V \tag{13}$$

$$\int_t^{t+\Delta t}\int_V \frac{\partial J_x}{\partial x}dx\,dy\,dz\,dt = (J_{xe}^1 S_{xe} - J_{xw}^1 S_{xw})\Delta t \tag{14}$$

$$\int_t^{t+\Delta t}\int_V \frac{\partial J_y}{\partial y}dx\,dy\,dz\,dt = \left(J_{yn}^1 S_{yn} - J_{ys}^1 S_{ys}\right)\Delta t \tag{15}$$

$$\int_t^{t+\Delta t}\int_V \frac{\partial J_z}{\partial z}dx\,dy\,dz\,dt = (J_{zt}^1 S_{zt} - J_{zb}^1 S_{zb})\Delta t \tag{16}$$

$$\int_t^{t+\Delta t}\int_V Q(\vec{x})\,dVdt = Q_P\,\Delta V\,\Delta t \tag{17}$$

where c_P is the OC at a node *P*, J_{xe} is the component x of the flow particularised to point *e* and so on. The product $Q_p \Delta V$ is the OER at node *P* if there is a source at that point (otherwise it is null). Superscript 1 indicates the new values (unknown) and 0 indicates the old values (given).

To replace the values of the components of the odour flow at points e, w, n, s, t and b, it is necessary to assume the flow profile between the neighbouring points. On the x-axis, which is where the advection of the wind occurs, an exponential scheme is assumed, based on the exponential exact solution of the steady one-dimensional diffusion-advection problem. This exponential profile is an improvement over the traditional piecewise-linear profile (known as the central-differences scheme and limited to low Reynolds numbers) avoiding divergence of the solution. Using the exponential profile, the x component of the flow at points *e* and *w* is given by:

$$J_{xe} = u_e\left[c_P + \frac{c_P - c_E}{e^{PC_e}-1}\right] \tag{18}$$

$$J_{xw} = u_w\left[c_W + \frac{c_W - c_P}{e^{PC_w}-1}\right] \tag{19}$$

where u_e, u_w, PC_e and PC_w are the wind speeds and the Peclet numbers at points *e* and *w*, respectively. The Peclet number is the ratio of the strengths of advection and turbulent diffusion and is defined as $PC_e = \frac{u_e \delta x_e}{K_{xe}}$, where δx_e is the distance between point *P* and

the east point *E* at the x-axis. A similar expression is obtained for PC_w. Diffusive flows in the Y and Z directions can be more easily discretised by the finite difference scheme, obtaining:

$$J_{yn} = K_{yn}\left[\frac{c_P - c_N}{\delta y_n}\right]; J_{ys} = K_{ys}\left[\frac{c_S - c_P}{\delta y_s}\right]; J_{zt} = K_{zt}\left[\frac{c_P - c_T}{\delta z_t}\right]; J_{zb} = K_{zb}\left[\frac{c_B - c_P}{\delta z_b}\right] \quad (20)$$

where δy_n, δy_s are the distance between the central node *P* and the north and south nodes, *N* and *S*; δz_t, δz_b are the distance between the central node *P* and the top and bottom nodes, *T* and *B*.

A fully implicit scheme was used in the time discretisation of Eqs (14–17), which ensures convergence of the method without restrictions for the time step. The main idea of this scheme is that the new value of OC prevails over the entire time step.

As a result, a discretised equation containing the OC in each point of the atmosphere at a time instant, depending on neighbouring points, was obtained.

$$a_P c_P^1 + a_W c_W^1 + a_E c_E^1 + a_N c_N^1 + a_S c_S^1 + a_T c_T^1 + a_B c_B^1 = D \quad (21)$$

where $a_E = -\frac{u_e S_{xe}}{e^{PC_e}-1}$, $a_W = -\frac{u_w\, e^{PC_w} S_{xw}}{e^{PC_w}-1}$, $a_N = -\frac{K_{yn} S_{yn}}{\delta y_n}$, $a_S = -\frac{K_{ys} S_{ys}}{\delta y_s}$, $a_T = -\frac{K_{zt} S_{zt}}{\delta z_t}$, $a_B = -\frac{K_{zb} S_{zb}}{\delta z_b}$, $a_P = \frac{\Delta V}{\Delta t} - a_E - a_W - a_N - a_S - a_T - a_B + u_e S_{xe} - u_w S_{xw}$ and $D = \frac{\Delta V}{\Delta t} c_P^0 + Q_P\, \Delta V$.

When Eq. (21) applies to each node of the mesh grid, an algebraic system of equations is obtained. This system can be expressed in matrix form:

$$[A]\{c\} = \{d\} \quad (22)$$

where [A] is the coefficient matrix, $\{c\}$ is the vector of OIC unknowns at the grid nodes and $\{d\}$ is the independent term vector. The matrix [A] is a sparse matrix with 7 diagonals non-nulls (linked to node *P* and its 6 neighbouring nodes). The rest of the elements of the matrix are null. Since this is a 3D problem, the system matrix [A] is very large, so the resolution of the problem by direct methods becomes unapproachable, making it necessary to use iterative methods. The resolution of Eq. (22) can be optimised using a modified strongly implicit (MSI) procedure for a 7-point formulation based on the decomposition of [A] into a lower and upper triangular matrix product (named LU

factorisation) involving much less computation than solving directly [A] (Zedan and Schneider, 1983). The temporal evolution was implemented using the Gauss-Seidel point-by-point method (Hoffman and Frankel, 2001). This is an iterative method where each OIC that has been calculated is refreshed in the unknown vector $\{c\}$ for the calculation of the next node. A code in Fortran90 was programmed to solve the matrix system.

Since the turbulent diffusion coefficients depend on the distance from the point to the source, Eq. (11) was independently performed for each source, placing the coordinate system origin in each emitting source so that the turbulent diffusion coefficients were calculated correctly. The x-axis was established coincident with the main wind direction provided by the wind rose in each season of the year. Next, the solutions were interpolated in a common mesh, with the coordinate origin in S1 and the y-axis coincident with the north direction. Finally, the OIC values from all sources were added together to obtain the total OIC from the WWTP.

3. Results and discussion

3.1. Odour emission assessment

In the quantification of odoriferous emissions from the treatment of organic waste, the temperature of the source has a marked influence on the volatility of compounds (Li et al., 2021). Next, the difference in temperature between the emitting source and the environment affects the elevation of the gases in the atmosphere and therefore their dispersion (Li et al., 2020). The annual average odour emission rates (ou_E/s) for each odour source were calculated in each season of the year. The OER for each odour source as well as their relative contribution (%) relative to the total odour emission of the WWTP under study are shown in **Table 5** (summer season). The OERs of the other seasons are shown in **Table 6**. As can be observed, the unit operations of the wastewater line represented the highest contribution over the total odour emission (98.86% compared to 1.14% of the sludge line). Primary decanters (S3) made the largest contribution (40.17%) to the total emission because of their extensive surface area. Deodorisation towers corresponding to S1 and S2 represented 28.21% and 25.33%, respectively, due to the high OC emitted. In this context, it is also important to note that S1 had the highest VOEF (**Table 5**), thus explaining the greater losses in surface area and micropore volume of the

GAC from S1 for the same operating time (Márquez et al., 2021a). Moreover, the VOEFs of S1 and S2 were considerably higher than those of S5.1, S5.2 and S6, which caused that in S1 and S2 the odour treatment system has recently been replaced by a hybrid system of biofilters and adsorption by GAC. This engineering modification makes the control of odoriferous emissions more sustainable, extending the lifespan of the GAC and generating, therefore, less hazardous waste in the process. For instance, the hybrid technology composed of biotrickling and GAC filtration generates one-fourth of the impact of conventional GAC filtration as a result of the biannual adsorbent replacement (Estrada et al., 2011). Biological treatment (S4), despite its large surface area, only had a relative odour contribution of 5.14%, which was due to its low SOER of 1.15 $ou_E/m^2 \cdot s$ compared to that of primary settling (15.15 $ou_E/m^2 \cdot s$).

Capelli et al. (2009) found that the highest OC values related to the wastewater line were observed in wastewater arrival, pre-treatments and primary sedimentation in a study based on the evaluation of different WWTPs located all over Italy, with a wastewater treatment capacity ranging from 1000 m^3/d to 80,000 m^3/d and treating mostly municipal wastewaters and an amount of industrial wastewater comprising 10–25%. The highest OER values corresponded to this last-mentioned unit operation in medium and large WWTPs, which is in line with the results of the present study. It is well known that in the areas mentioned above, the high organic matter content as well as the high presence of microorganisms and anaerobic conditions lead to higher emission of acidic and malodorous compounds (especially H_2S) compared to the rest of the WWTP operations (Jiang et al., 2017). Given the above, intensifying odour control in the first steps of integral wastewater treatment is essential to avoid significant deterioration in ambient air quality, with the consequent social and environmental benefits.

Concerning the sludge line, the contributions of the three deodorisation towers (S5.1, S5.2 and S6) to the total odour emission were relatively insignificant, given the low OC determined at their outlets. The highest measured OC value (37,908 ou_E/m^3) in the sludge line (and in the whole WWTP) corresponded to the sludge storage in conical tanks (S7), which is mainly due to the anaerobic conditions that predominate in these places (Karageorgos et al., 2010). However, S7 had a minimum contribution (0.13%) to the total odour emitted since it does not have a forced aeration system (it is naturally ventilated). Finally, the sludge discharge in trucks (S8) had an intense punctual contribution but it was not significant due to the low frequency of discharge (**Table 3**).

Table 5. Odour emissions from the WWTP in summer.

	Odour source	OC (ou_E/m^3)	SOER ($ou_E/m^2 \cdot s$)	OER (ou_E/s)	VOEF ($ou_E/s \cdot m^3$ GAC)	Relative odour contribution (%)	
Wastewater line	S1	31,564	–	62,107	8797	28.21	**98.86**
	S2	14,167	–	55,753	2898	25.33	
	S3	7282	15.15	88,432	–	40.17	
	S4	555	1.15	11,323	–	5.14	
Sludge line	S5.1	1285	–	1532	641	0.70	**1.14**
	S5.2	240	–	287	120	0.13	
	S6	686	–	274	298	0.12	
	S7	37,908	–	288	–	0.13	
	S8	1902	3.96	125	–	0.06	

OC, odour concentration; **SOER**, specific odour emission rate; **OER**, odour emission rate; **VOEF**, volumetric odour emission factor; **S1**, pre-treatment header; **S2**, sand and fat removal; **S3**, primary settling; **S4**, biological treatment; **S5.1**, gravity thickening; **S5.2**, flotation thickening; **S6**, sludge dehydration; **S7**, sludge storage; **S8**, sludge discharge.

Table 6. Odour emissions from the WWTP in other seasons of the year.

	Odour source	Autumn-Winter-Spring	Spring
		OER* (ou_E/s)	OER (ou_E/s)
Wastewater Line	S1	49,668	46,885
	S2	46,833	39,339
	S3	81,357	68,340
	S4	10,304	8655
Sludge Line	S5.1	1486	1248
	S5.2	275	231
	S6	249	209
	S7	271	227
	S8	118	99

*Average values; **OER**, odour emission rate; **S1**, pre-treatment header; **S2**, sand and fat removal; **S3**, primary settling; **S4**, biological treatment; **S5.1**, gravity thickening; **S5.2**, flotation thickening; **S6**, sludge dehydration; **S7**, sludge storage; **S8**, sludge discharge.

A little contribution from the sludge line to the total odour emission, as is the case here, is not common in most WWTPs. In this context, Gebicki et al. (2016) have reported that sludge thickening and dehydration, both unit operations of the sludge line, present a joint average odour contribution of 35% in a sewage treatment plant. Other authors have also highlighted that sludge handling activities are, together with the first unit operations of the integral treatment of wastewater, the main contributors to the total odour emission in WWTPs (Capelli et al., 2009; Frechen, 2004; Lebrero et al., 2011; Senatore et al., 2021; Stuetz and Frechen, 2001). Nevertheless, it is important to note that ferric chloride ($FeCl_3$) is added to the wastewater line in the WWTP under study before the sludge thickening with a two-fold aim: on the one hand, to help phosphorus precipitation and, on the other hand, to avoid the presence of H_2S in the biogas from anaerobic digestion. Ferric chloride reacts with hydrogen sulphide to form a precipitate of iron sulphide (Fe_2S_3), which settles in quiescent conditions (Water Environment Federation, 2017). Furthermore, anaerobic digestion itself produces a biostabilised residual sludge, also helping to reduce the potential emission of malodours (Orzi et al., 2015). Therefore, both the $FeCl_3$ addition and anaerobic digestion may justify the low relative odour contribution of the sludge line in the WWTP studied.

3.2. Analysis of the dispersion model parameters

The wind vector, the stability category (considered both as a function of the season of the year), the characteristics and geometry of the sources (**Fig. 2**, **Tables 2** and **3**) and their odour emissions (**Tables 4** and **5**) are the input parameters of the model. The wind roses shown in **Fig. 1** establish the main wind direction and the average wind speed representative of a season of the year. The analysis of the wind roses in **Fig. 1** shows that in autumn and winter, the main wind direction was the southerly direction (S), and the average wind speed was very similar, somewhat higher in winter (1.31 m/s) than in autumn (1.23 m/s). In spring, the winds coming from the N and SW directions show the highest percentages since it is a season with more unstable weather. In the southerly direction, the average wind speed was 1.66 m/s, and in the NE direction, it was 3.00 m/s. Finally, in summer the main wind direction was north-northeast (NNE) and the average wind speed was 2.89 m/s, very similar to spring NE and more than twice the wind speed in winter and autumn. Due to the coincidence of the south direction of the wind in different seasons, given the location of the WWTP and the similarity of the average wind speed in all of them, a single calculation will be carried out that groups these meteorological conditions, choosing as the average wind speed the smallest value (1.23 m/s). Lower wind speeds for emission with few variations lead to less dispersion and generate worse surrounding air quality (Tian et al., 2021). Even those known as calm episodes, absent from wind, represent a significant reduction in the transportation of gaseous pollutants through the atmosphere (Gadian et al., 2004). This simulation represents the autumn-winter and spring (south direction) seasons and symbolises the worst conditions for odour dispersion and, therefore, higher odour immission values will be obtained. In addition, the summer and spring (in the NNE and NE wind directions, respectively) seasons will be simulated. **Table 4** shows the main wind directions considered in the three simulations and the average wind speeds.

Besides, a category of stability B was considered the most common in the WWTP region in all the seasons of the year. **Figure 3** shows an analysis of the stability classes in the different seasons of the year, depending on the intensity of incoming solar radiation during the day. The classification of the Pasquill-Gifford-Turner stability classes, according to the range of surface wind speed (at 10 m) and the daytime incoming solar radiation, has been used as a reference to set the range of wind speeds that correspond to a stability category. For strong solar radiation (>700 W/m^2): stability category A ranges

from 0.56 to 2.5 m/s wind speed, stability category B ranges from 2.6 to 5.0 m/s, and stability category C ranges for wind speeds above 5.0 m/s. For moderate solar radiation (350–700 W/m^2): stability category A ranges from 0.56 to 1.0 m/s wind speed, stability category B ranges from 1.1 to 4 m/s, and stability category C ranges from 4.1 to 5.5 m/s. Finally, for slight solar radiation (<350 W/m^2): stability category B ranges from 0.56 to 2.0 m/s wind speed, and stability category C ranges from 2.1 to 5 m/s (Gavira et al., 2022).

In autumn and winter (**Fig. 3a**), the incoming solar radiation can be considered to be moderate. In these cases, the predominant stability category in all directions is B. The calculations for light solar radiation have also been carried out (although these figures have not been added so as not to overload) and it has been found that the category of stability B is again the predominant one in direction S, obtaining a figure very similar to that shown for moderate solar radiation. In summer (**Fig. 3b**), both moderate and intense incoming solar radiation has been considered. Given the location of the plant, light solar radiation is very unlikely. In both cases, in the main wind direction (NNE), the predominant category is B. Spring (**Fig. 3c**) is the most unstable season, and we can observe that the stability category can be presented from A to C, for light, moderate and strong incoming solar radiation. In the NE wind direction, the predominant category is B for strong and moderate solar radiation and C for light solar radiation. In the S direction, the predominant category is B for moderate and light solar radiation and A for strong. As in the rest of the cases, it will choose as the predominant category B, which corresponds to the most common conditions of moderate radiation. Preliminary results showed that the results are very similar if stability category A or C is considered instead of B, as the wind speed is relatively low. On the other hand, the exponent *p* in Eq. (10) for stability category B is 0.15, valid in rural or urban soil.

It was verified that the final solution for the stationary OC that was reached was not influenced by the initial OC used for the iterative numerical method. The null flow (no mass transport) condition was used as a boundary condition at the ground level to simulate a reflecting surface at z = 0. This boundary condition is usually used by many authors as in Liu et al. (2019) and is equivalent to adding the OC resulting from a hypothetical image source located symmetrically relative to the ground in the region $z \leq 0$, as explained in Seinfeld and Pandis (2016) or the classical textbook of De Nevers (1998). At borders far from sources, an open boundary condition (OBC) was used (Hesthaven and Gottlieb,

2012), which simulated a very distant boundary that did not alter the solution of the problem, without the need to employ a large calculation domain.

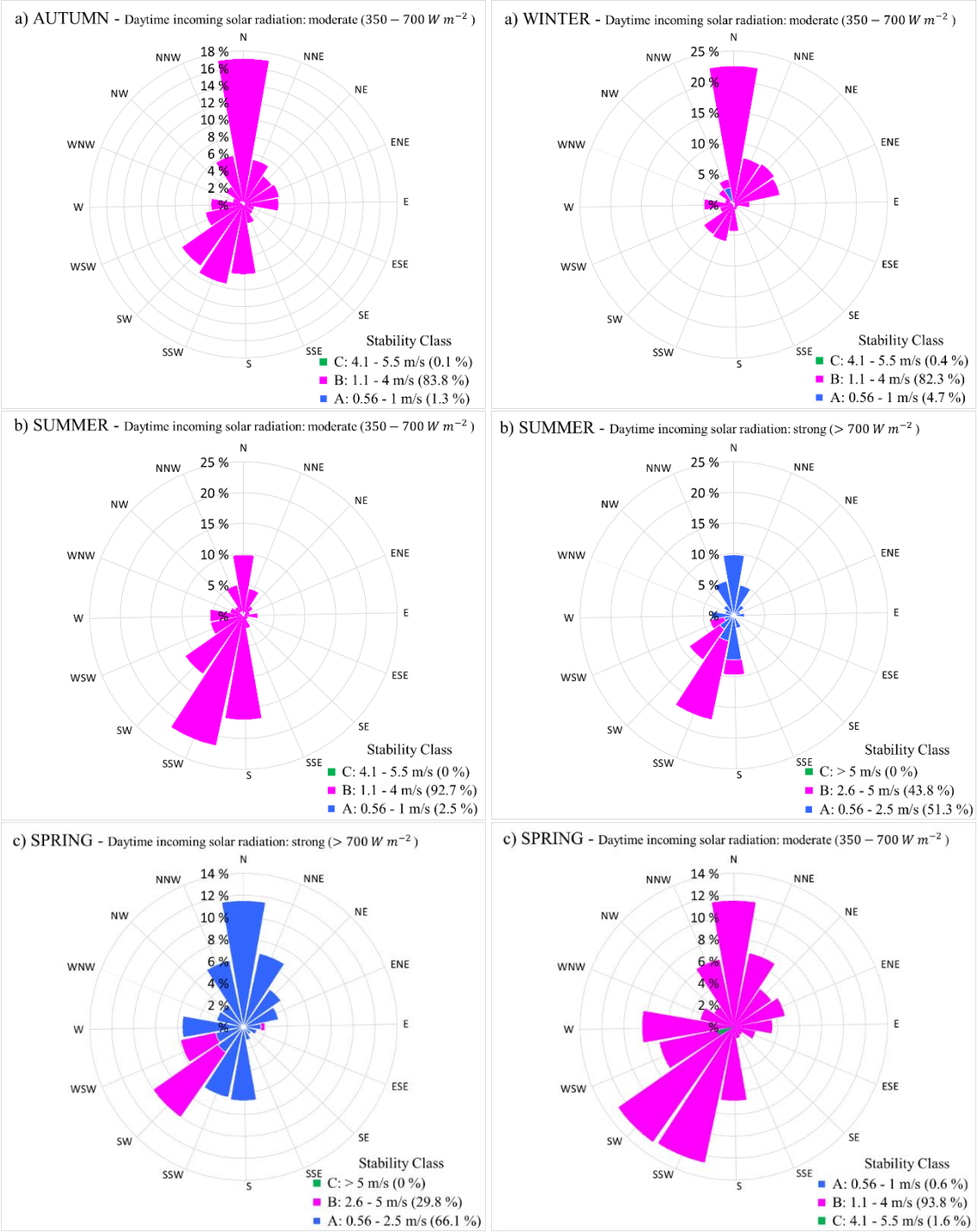

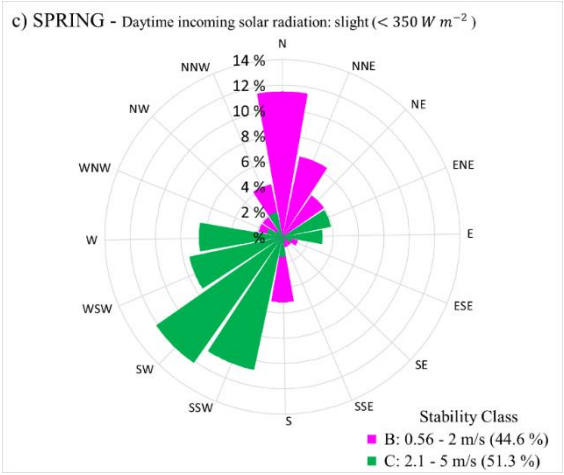

Fig. 3. Stability category in each season of the year according to the daytime incoming solar radiation: (a) autumn and winter in moderate incoming solar radiation, (b) summer in moderate and strong incoming solar radiation and (c) spring in slight, moderate and strong incoming solar radiation.

The calculation domain was 4.0 km in the north and south directions and 5.5 km in the east and west directions, around the emitting source. Non-uniform gridding with finer mesh near the sources, where the concentration gradients are large, was used. In this way, a higher resolution at locations where the numerical error is high is obtained. For surface sources, the uniform meshing of 10 m was used 550 m around the source and increased to 45 m after that. Point sources needed a finer meshing to obtain higher precision in the results since their OERs were very high with very small dimensions, generating high gradients of OIC. A mesh size of 1 metre was used 20 m around the point sources, increasing to 20 m and 40 m far away from the source. The 100 × 100 × 30 nodes in the X, Y and Z axes form the grid. These are also the dimensions of the matrix [A] and the total number of unknown OIC, which are the elements of the vector {c} in the matrix system Eq. (22). Although the number of unknowns is very high, the optimisation of the discretisation method and the MSI procedure allows each time step to be carried out very quickly. There are no restrictions to the time step, fixed to a small-time scale of 5 seconds. Approximately one hour of time evolution for point sources and 20 minutes for surface sources leads to reaching the steady state. It is approximately 1 hour of real time on a 7-core workstation, which is a very short time considering the high spatial resolution used in the model that gives rise to a 3D system matrix of the order of 10^5 elements.

3.3. Assessment of the estimated OIC at the ground level

The two-dimensional distribution of OIC at the ground level is shown in **Figs. 4** and **5**. **Figure 4** shows the distribution in autumn-winter and spring (S) grouping, whereas **Fig. 5** shows spring (NE) and summer. It can be observed that odour diffusion is different if it comes from point sources or surface sources. Around the point sources, a plume reminiscent of the form of the Gaussian column is obtained since we worked in a steady state. Around the surface sources, a more dispersed OC area is observed since it is a larger emitting area located at a lower height and with a lower OER. The overlap of all of them gives rise to the total OIC. The highest OICs were located around S1 and S2, along the wind direction, that is, along the S direction in autumn-winter and spring (S), the NE direction in spring and NNE in summer. These point sources presented the highest OERs at their outlets, compared with the others point sources (**Tables 4** and **5**). The OIC near S5.1 was also important, but lower than that due to S1 and S2. The contribution of S5.1 to the total OIC was three orders of magnitude lower than the contribution of S1 and S2, indicating that the contribution of the sludge line to the odour impact was very small in this study. In all cases, the OIC near the surface sources (S3 and S4) was much lower than that near the point sources (S1, S2 and S5.1), due to the large emission surface of the first mentioned sources. Therefore, it can be said that the contribution of the surface sources to the total OIC was practically negligible compared to that of the point sources under the study conditions. In the case of the surface sources mentioned above, a slightly higher contribution of S4 to the odour impact can be observed, especially in spring (NE) and summer (**Fig. 5**), which could be due to the stagnation of odour caused by the negative height of this source (**Table 3**).

The maximum OIC in all the seasons was predicted near the outlet of the point source S1 and had the value of 538 ou/m^3 in autumn-winter and spring (S) grouping (**Fig. 4**). In spring (NE) and summer, the maximum values were 210 and 306 ou/m^3, respectively (**Fig. 5**). Therefore, the highest odour impact occurred in the south direction in autumn, winter and sometimes in spring. In spring NE (the other main wind direction of spring), the maximum OIC fell by 60% compared to its values in autumn-winter and spring (S), and in summer the maximum OIC fell by 40%. In both cases, the wind speeds were much higher, thus facilitating odour dispersion. In all cases, the maximum OIC is located 3 m from source S1 in the wind direction. The S1 source is the deodorisation tower of the pre-treatment header and is the point source with the highest emission, which

allows us to conclude that controlling the emission of this source during the operation of the plant will be decisive in the odour immission.

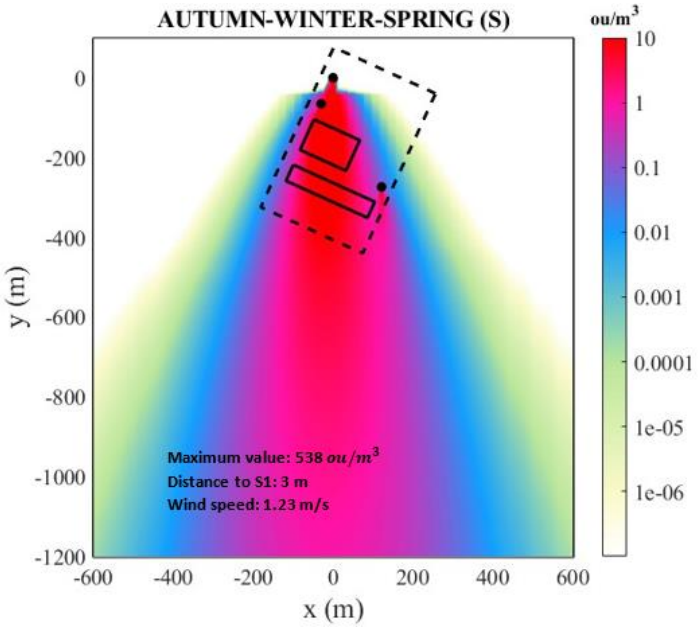

Fig. 4. Two-dimensional distribution of the odour immission concentration (ou/m^3) in autumn-winter and spring (S).

Sattler and Devanathan (2007) evaluated odour emissions derived from a large urban WWTP located in Dallas (United States), with a wastewater treatment capacity of 715,500 m^3/d. The odour impact modelling was carried out using the Gaussian dispersion models AERMOD and ISCST3 and supposing constant and variable sources emissions. Their study focused on the primary clarifier as the main source of odour emissions, only modelling H_2S as the most odour-causing pollutant associated with the WWTP, in a 5000 × 5000 m Cartesian grid receptor network with a uniform grid spacing of 250 × 250 m (in contrast to a non-uniform grid and a spatial resolution of 1 metre used in this article). They evaluated all PGT stability classes to determine those associated with the highest odour immissions and concluded that they are classes D, E and F. These stability classes do not occur in our case (**Fig. 3**) due to the situation of the WWTP. However, in concordance with these authors, when source emissions are constant, higher odour immission values were expected in winter (and also in autumn) because stable conditions occur more frequently during those seasons. This can be observed in **Fig. 1**, which shows that the wind was less variable in winter and autumn compared to spring and summer, both in direction and speed. The present study goes a step further since, in addition to estimating the maximum odour impact in the different seasons of the year, it also allows

calculating the evolution of the impact around each of the critical odour sources. This information might be very useful to increase or modify odour control strategies in unit operations that cause a higher odour impact, to guarantee the occupational safety of the employees, while reducing odour levels in the nearby areas. In this context, it is important to note that an increase in OIC corresponds to a higher health risk for workers of a WWTP, due to exposure to volatile odorous compounds (Byliński et al., 2019). Therefore, it would be advisable to strengthen safety measures in autumn and winter, given the higher OICs estimated for these seasons.

Figure 6 also shows the variation in the total odour immission derived from the WWTP, along the wind direction, with the distance to the most intense source, S1 (where the zero of the abscissa axis is located). The maximum OIC was located at around 3 m from S1 in all cases, within the perimeter of the WWTP. This fact was also observed when Dinçer et al. (2020) studied the odour impact of a large urban WWTP in Turkey (by using AERMOD) that treats 605,000 m^3/d mixed domestic and pre-treated industrial wastewater, with all treatment units open to the atmosphere. Moreover, this facility operates with extended aeration as a biological treatment method, without anaerobic digestion of sludge. Although they did not evaluate the odour impact in the different seasons of the year, they estimated a maximum annual OIC of 1551 ou/m^3, three times higher than our highest maximum obtained in autumn-winter-spring (S). The highest concentration of the maximum at ground level was due to the non-existence of emission control systems. Odour control systems are effective in reducing odorous emissions and therefore significantly improve the quality of the surrounding air (Senatore et al., 2021). There is a wide variety of works that study the odour emission of WWTP, using different models. Sówka et al. (2014) modelled the odour emission from a WWTP designed for 1,200,000 equivalent inhabitants by using CALPUFF. However, their study mainly focused on odours derived from primary clarifiers and thermal drying processes of partially dewatered and digested sludge, during only winter and summer seasons. An additional study using CALPUFF was carried out by Beghi et al. (2012) on the impact assessment of the odours derived from sewage sludge in the WWTP of Domingos Martins (Brazil). The authors focused on hydrogen sulphide as an important odorant in wastewater treatment. The studies carried out are also influenced by seasonality. Atmospheric conditions not only conditioned the emission, but the subsequent dispersion was also affected.

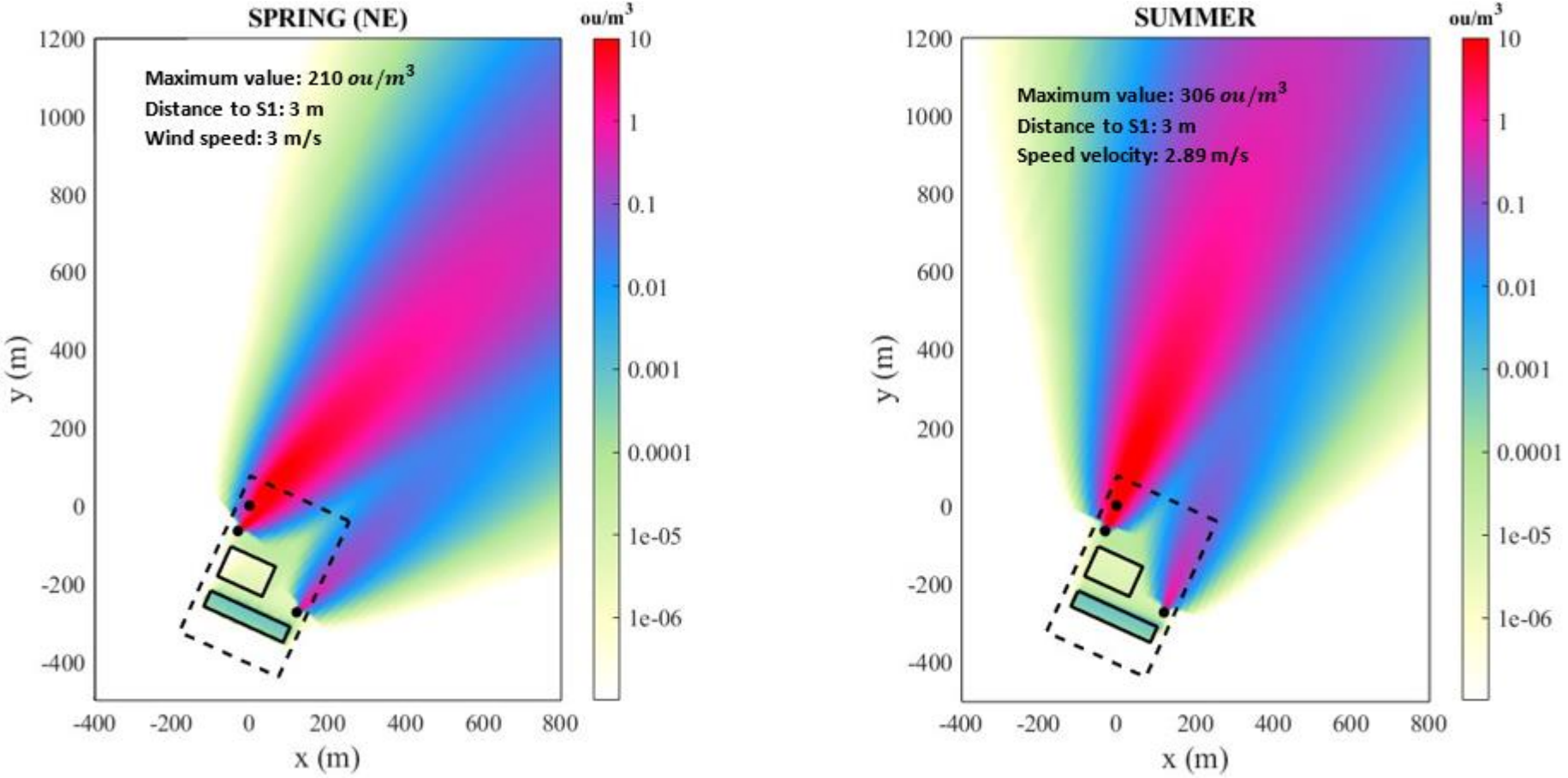

Fig. 5. Two-dimensional distribution of the odour immission concentration (ou/m^3) in spring (NE) (left) and summer (right).

According to Botta et al. (2020) and Conti et al. (2020), Gaussian models are the most widely used for air quality modelling because of their efficient compromise between manageable computational time and reasonable accuracy, followed by the Lagrangian and Eulerian models. Gaussian steady-state plume models assume a Gaussian distribution of the plume in the vertical and horizontal directions, considering continuous emissions of particles and gases, without chemical reactions between compounds, steady-state atmospheric conditions and uniform wind flow (Danuso et al., 2015). Nevertheless, low wind speeds (calm atmospheric conditions) and complex terrains limit the application of Gaussian models (Liu et al., 2019). The AERMOD Gaussian model is an advanced plume model that includes the module AERMAP to characterise complex terrains and the module AERMET to establish vertical profiles of meteorological variables (Dinçer et al., 2020; Liu et al., 2019). Some authors have shown that AERMOD under-predicts odour concentrations when configured as an area source (Baawain et al., 2017). Other authors claim that AERMOD overestimates the concentrations downwind significantly, especially under stable atmospheric conditions (Busini et al., 2012; Dresser and Huizer, 2011). For its part, Lagrangian models are stochastic and describe the motion of individual and non-interacting elementary contaminants by considering random particle movements (Ferrero and Oettl, 2019; Pisso et al., 2017). CALPUFF is a non-steady-state Lagrangian puff model. Puff models represent a continuous plume as several discrete packets of pollutants and evaluate the contribution of a puff to the concentration at a receptor by a "snapshot" approach. Each puff is "frozen" at particular time intervals (sampling steps). The puff is then allowed to move, evolving in size and strength until the next sampling step. The total concentration at a receptor is the sum of the contributions of all nearby puffs averaged for all sampling steps within the basic time step. The sampling step and time step may both be 1 h, indicating only one "snapshot" of the puff is taken each hour. The basic equation of the puff has the form of a Gaussian distribution (Busini et al., 2012; Nanni et al., 2022). CALPUFF constitutes an improvement on Gaussian models to be able to consider non-homogeneous and non-uniform flows. However, CALPUFF is limited to long-range transport (scale > 50 km) and requires a meteorological data field throughout the three-dimensional meshing provided by the CALMET module, which makes it dependent on external data and that must be re-evaluated along the time (Wang et al., 2006). As a drawback, it can be noted that CALPUFF tends to underestimate peak intensities close to the source (Ranzato et al., 2012; Vieira de Melo et al., 2012). Comparisons of odour immission in flat terrain

obtained with AERMOD and CALPUFF show important differences at some wind speeds and stability classes caused by the different algorithms used for the calculation of dispersion coefficients (Tartakovsky et al., 2016).

As can also be observed in **Fig. 6**, in autumn-winter-spring (S), the OIC dropped quickly along the wind direction, until 5 ou/m^3 at approximately 519 m away from S1 and until 1 ou/m^3 at 1113 m from the same location. In spring (NE) and summer, this parameter decreased at a similar rate but the position will be different as the maximum values are lower than in autumn-winter-spring (S). In spring (NE), a value of 5 ou/m^3 was reached at about 258 m from S1, and 1 ou/m^3 was achieved at approximately 651 m from S1, whereas in summer, the same OIC values were reached at around 333 and 780 m from S1, respectively. It is worth noting that the immission values of 1 and 5 ou/m^3 were evaluated because the first is considered the threshold for human odour perception (EN 13725, 2003), whereas the second one is the maximum permissible OIC for WWTPs according to the draft bill "Against Odour Pollution" (Government of Catalonia, 2005), this being the document that has been taken as a reference by many odour consultants in Spain (Bokowa et al., 2021).

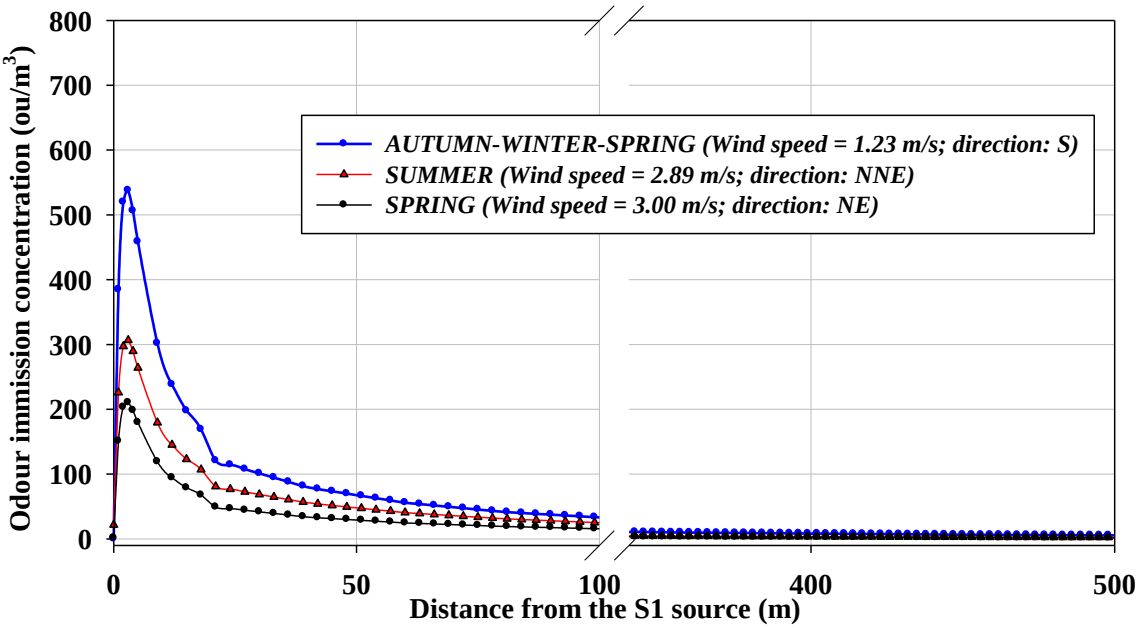

Fig. 6. Variation in the total odour immission (ou/m3) derived from the WWTP, along the wind direction, with the distance to the deodorisation tower of the pre-treatment header (it is the zero of the abscissa axis), for each season of the year.

An estimation of OIC was also carried out in the population centres closest to the urban WWTP under study (**Table 4**). The position of each population area relative to the plant is shown in **Table 4** and **Fig. S1** (Supplementary Material). In this table, source S1 is the reference point used to measure the distance of each area to the WWTP. The direction indicates the angle that forms the line joining the population centre with S1, in the north direction. The OIC was calculated using the present odour dispersion model in each population centre for the different seasons of the year. The solution of the model gave the OIC in all cells of the calculation domain and was interpolated in the position of each population centre. To this end, all populations were located within the computing domain. In this sense, the size of the calculation domain in the west direction was increased to 7 km in spring and summer. Thus, the population centres VIII and IX, which were the furthest in the direction of the wind in those seasons, were included in the domain. In autumn-winter-spring (S), the most affected population centre was "VII) Polígono industrial La Isla", which is the population centre closest to the south of the WWTP, which was the main wind direction in those seasons. However, the OIC was very small, on the order of 10^{-3} ou/m^3. In spring (NE) and summer, the most affected nucleus was "II) Barrio Bellavista". In spring (NE), the OIC was $7.4 \cdot 10^{-2}$ ou/m^3, whereas in summer it was $4.1 \cdot 10^{-5}$ ou/m^3. Although in both cases the OIC was very small, in spring (NE) it was higher than in summer because the nucleus II) in spring (NE) is aligned with the WWTP in the main wind direction. Given the above results, it can be said that neither the limit immission value set by the reference Spanish regulation (Government of Catalonia, 2005) nor the threshold for human odour perception (EN 13725, 2003) were exceeded in the nearby populations under the study conditions. Therefore, the GAC beds adequately fulfil their function of retaining odoriferous pollutants, making the odour impact of the large urban WWTP in the above-mentioned areas negligible, without forgetting the key role of the prevailing atmospheric conditions in the odour dispersion.

Finally, it is important to note that this study provides an important advance in terms of accurate dynamic odour-processes modelling, where a wide range of odour sources in an urban WWTP and weather conditions are considered. Such a promising tool might allow for improving the total feasibility of urban wastewater treatment by estimating the environmental odour impact derived from such an important process within the context of achieving sustainable development goals.

4. Conclusions

This study focused on the evaluation of both the odour emission and the odour impact of a large urban WWTP, which mainly treats domestic wastewater, also including contributions from industrial wastewater. Odour emissions were mainly due to the odour sources of the wastewater line, which contributed 98.86% of the total emission of the facility. Although the pre-treatment header and sand and fat removal had an odour treatment system based on adsorption by GAC, these constituted point sources with high OERs, and together they were responsible for more than 50% of the total odour emission of the urban WWTP.

The odour impact in the different seasons of the year was successfully estimated using an Eulerian dispersion model formulated by the authors. The maximum odour immission concentration was always predicted near the pre-treatment area, with a value of 538 ou/m^3 in autumn-winter-spring (S). In spring (NE) the maximum OIC fell by 60% and 40% in summer, compared to its values in autumn-winter-spring (S). In any case, the maximum OIC always remained within the WWTP site approximately 3 m from source S1. The estimation of odour immission levels was also carried out in the population centres closest to the WWTP, showing that odour impact was negligible, with values being less than 1 ou/m^3 (the threshold for human odour perception).

Finally, the development of a dispersion model that allows estimating the total odour impact generated by the different odour sources of a WWTP on surrounding areas at the same time as in the different seasons of the year might help wastewater managers to increase or modify the odour control strategies in unfavourable situations (in terms of odour impact). Analyses of this kind would be beneficial for improving occupational safety within WWTPs while reducing the odour impact in nearby populations.

Acknowledgements

This work was supported by the Spanish Ministry of Science and Innovation (MICINN), the Spanish State Research Agency (AEI) and the European Regional Development Fund (FEDER) through Project PID2020-117438RB-I00 and the Regional Government of Andalusia through project AT21_00189 (FEDER).

Appendix A. Supplementary data

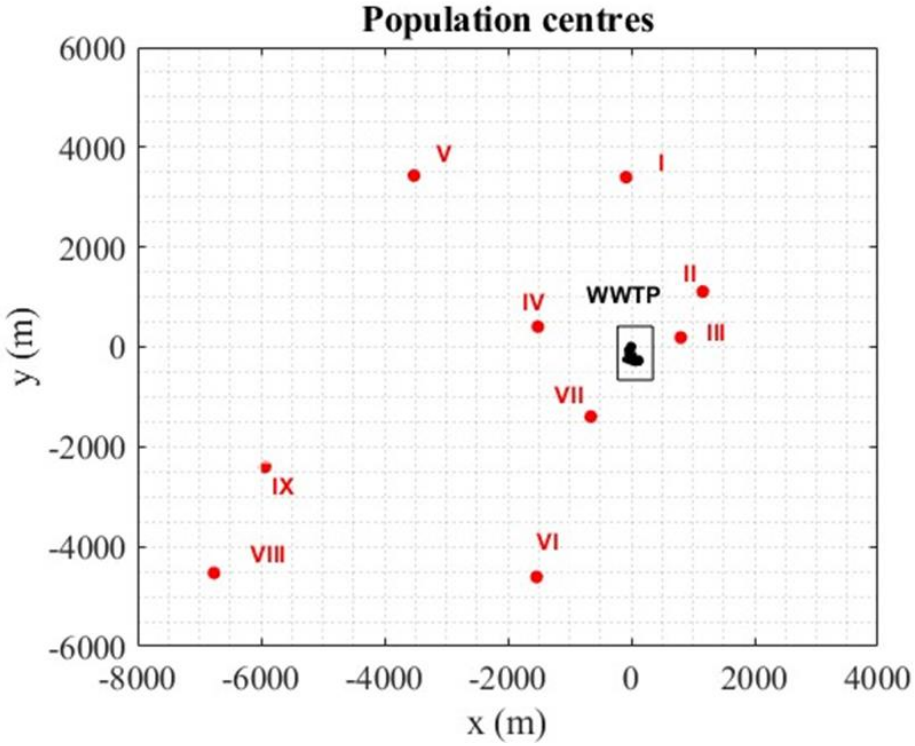

Fig. S1. Location of the population centres around the urban WWTP. I) Barrio Los Bermejales, II) Barrio Bellavista, III) Urbanización Fuente del Rey, IV) Base militar El Copero, V) Gelves, VI) Urbanización Tixe, VII) Polígono industrial La Isla, VIII) La Puebla del Río, IX) Coria del Río.

Table S1. Common odorous compounds present in gaseous emissions from WWTPs.

Chemical compound	Formula	Odour description [1]	Odour threshold (ppm, v/v) [2]
Acetaldehyde	CH_3CHO	Pungent, fruity	0.0015
Acetic acid	CH_3COOH	Pungent, vinegar-like	0.0060
Ammonia	NH_3	Pungent, irritating	1.5
n-Amyl mercaptan	$CH_3(CH_2)_4SH$	Unpleasant, putrid	0.00000078
Benzene	C_6H_6	Sweet, solventy	2.7
Butanone	$CH_3COCH_2CH_3$	Sweet, minty	0.44
n-Butylamine	$CH_3(CH_2)NH_2$	Sour, ammonia	0.17
n-Butyric acid	C_3H_7COOH	Rancid butter	0.00019
Dimethylamine	$(CH_3)_2NH$	Putrid, fishy	0.033
Dimethyl disulfide	$(CH_3)_2S_2$	Decayed vegetables	0.0022
Dimethyl sulfide	$(CH_3)_2S$	Decayed cabbage	0.0030
Ethylamine	$C_2H_5NH_2$	Ammonia-like	0.046
Ethyl mercaptan	C_2H_5SH	Decayed cabbage	0.0000087
Hydrogen sulfide	H_2S	Rotten eggs	0.00041
Indole	$C_6H_4(CH)_2NH$	Fecal, nauseating	0.00030
d-Limonene	$C_{10}H_{16}$	Citrusy	0.038
Methylamine	CH_3NH_2	Putrid, fishy	0.035
Methyl mercaptan	CH_3SH	Rotten cabbage	0.000070
n-Propyl mercaptan	C_3H_7SH	Unpleasant	0.000013
Pyridine	C_5H_5N	Pungent, irritating	0.063
Skatole	C_9H_9N	Fecal, nauseating	0.0000056
Thiocresol	$CH_3C_6H_4SH$	Rancid	0.000062
Toluene	$C_6H_5CH_3$	Tarry, mothballs	0.33
Trimethylamine	$(CH_3)_3N$	Pungent, fishy	0.000032

[1] Fisher et al., 2018; Gebicki et al., 2016; Talaiekhozani et al., 2016

[2] Nagata, 2003

References

Baawain, M., Al-Mamun, A., Omidvarborna, H., Al-Jabri, A., 2017. Assessment of hydrogen sulfide emission from a sewage treatment plant using AERMOD. Environ. Monit. Assess. 189, 263. https://doi.org/10.1007/S10661-017-5983-6

Bañuelos-Ruedas, F., Angeles-Camacho, C., Rios-Marcuello, S., 2010. Analysis and validation of the methodology used in the extrapolation of wind speed data at different heights. Renew. Sustain. Energy Rev. 14, 2383–2391. https://doi.org/10.1016/J.RSER.2010.05.001

Barbusinski, K., Kalemba, K., Kasperczyk, D., Urbaniec, K., Kozik, V., 2017. Biological methods for odor treatment – A review. J. Clean. Prod. 152, 223–241. https://doi.org/10.1016/j.jclepro.2017.03.093

Beghi, S.P., Santos, J.M., Reis, N.C., De Sá, L.M., Goulart, E.V., De Abreu Costa, E., 2012. Impact assessment of odours emitted by a wastewater treatment plant. Water Sci. Technol. 66, 2223–2228. https://doi.org/10.2166/WST.2012.409

Bokowa, A., Diaz, C., Koziel, J.A., McGinley, M., Barclay, J., Schauberger, G., Guillot, J.M., Sneath, R., Capelli, L., Zorich, V., Izquierdo, C., Bilsen, I., Romain, A.C., Del Carmen Cabeza, M., Liu, D., Both, R., Van Belois, H., Higuchi, T., Wahe, L., 2021. Summary and overview of the odour regulations worldwide. Atmosphere (Basel). 12, 1–53. https://doi.org/10.3390/atmos12020206

Botta, S., Onofrio, M., Spataro, R., 2020. A review on the use of air dispersion models for odour assessment. Int. J. Environ. Pollut. 67, 1–21. https://doi.org/10.1504/IJEP.2020.10030406

Busini, V., Capelli, L., Sironi, S., Nano, G., Rossi, A.N., Bonati, S., 2012. Comparison of calpuff and aermod models for odour dispersion simulation. Chem. Eng. Trans. 30, 205–210. https://doi.org/10.3303/CET1230035

Byliński, H., Gębicki, J., Namieśnik, J., 2019. Evaluation of health hazard due to emission of volatile organic compounds from various processing units of wastewater treatment plant. Int. J. Environ. Res. Public Health 16, 1712. https://doi.org/10.3390/ijerph16101712

Capelli, L., Sironi, S., Del Rosso, R., Céntola, P., 2009. Predicting odour emissions from wastewater treatment plants by means of odour emission factors. Water Res. 43, 1977–1985. https://doi.org/10.1016/j.watres.2009.01.022

Capodaglio, A.G., Conti, F., Fortina, L., Pelosi, G., Urbini, G., 2002. Assessing the environmental impact of WWTP expansion: odour nuisance and its minimization. Water Sci. Technol. 46, 339–346. https://doi.org/10.2166/wst.2002.0620

Conti, C., Guarino, M., Bacenetti, J., 2020. Measurements techniques and models to assess odor annoyance: A review. Environ. Int. 134, 105261. https://doi.org/10.1016/J.ENVINT.2019.105261

Danuso, F., Rocca, A., Ceccon, P., Ginaldi, F., 2015. A software application for mapping livestock waste odour dispersion. Environ. Model. Softw. 69, 175–186. https://doi.org/10.1016/J.ENVSOFT.2015.03.016

De Nevers, N., 1998. Ingeniería de control de la contaminación del aire. Mc Graw-Hill.

Díaz, C., Cartelle, D., Barclay, J., 2014. Revision of Regulatory Dispersion Models, an Important Key in Environmental Odour Management. Ist International Seminar of Odours in the Environment, Santiago, Chile.

Dinçer, F., Dinçer, F.K., Sarı, D., Ceylan, Ö., Ercan, Ö., 2020. Dispersion modeling and air quality measurements to evaluate the odor impact of a wastewater treatment plant in İzmir. Atmos. Pollut. Res. 11, 2119–2125. https://doi.org/10.1016/J.APR.2020.05.018

Dresser, A.L., Huizer, R.D., 2011. CALPUFF and AERMOD Model Validation Study in the Near Field: Martins Creek Revisited. J. Air Waste Manage. Assoc. 61, 647–659. https://doi.org/10.3155/1047-3289.61.6.647

EN 13725, 2003. Air Quality - Determination of Odour Concentration by Dynamic Olfactometry. European Committee for Standardization, Brussels.

EPA, 1987. Industrial Source Complex (ISC) Dispersion Model User's Guide. Second Edition. Research Triangle Park, NC., U.S. Environmental Protection Agency.

Estrada, J.M., Kraakman, N.J.R., Lebrero, R., Muñoz, R., 2015. Integral approaches to wastewater treatment plant upgrading for odor prevention: Activated Sludge and Oxidized Ammonium Recycling. Bioresour. Technol. 196, 685–693. https://doi.org/10.1016/j.biortech.2015.08.044

Estrada, J.M., Kraakman, N.J.R.B., Muñoz, R., Lebrero, R., 2011. A comparative analysis of odour treatment technologies in wastewater treatment plants. Environ. Sci. Technol. 45, 1100–1106. https://doi.org/10.1021/es103478j

Ferrero, E., Oettl, D., 2019. An evaluation of a Lagrangian stochastic model for the assessment of odours. Atmos. Environ. 206, 237–246. https://doi.org/10.1016/J.ATMOSENV.2019.03.004

Fisher, R.M., Barczak, R.J., Suffet, I.H.M., Hayes, J.E., Stuetz, R.M., 2018. Framework for the use of odour wheels to manage odours throughout wastewater biosolids processing. Sci. Total Environ. 634, 214–223. https://doi.org/10.1016/j.scitotenv.2018.03.352

Frechen, F.B., 2004. Odour emission inventory of German wastewater treatment plants - Odour flow rates and odour emission capacity. Water Sci. Technol. 50, 139–146. https://doi.org/10.2166/WST.2004.0244

Gadian, A., Dewsbury, J., Featherstone, F., Levermore, J., Morris, K., Sanders, C., 2004. Directional persistence of low wind speed observations. J. Wind Eng. Ind. Aerodyn. 92, 1061–1074. https://doi.org/10.1016/J.JWEIA.2004.05.007

Gavira, V., Sosa González, A.E.;, Casanova, P., Cervantes, Y., Aguilar Vega, M.A.;, Chacha Coto, M.;, Zavala Loría, J.;, Dzul López, J.D.C.;, García Villena, L.A.;, Area, S., Bajío, M., Enrriqueta, A., Sosa González, W.E., De Jesús, R., Alfredo, M., Vega, M.A., Coto, J.C., Del Carmen, J., Loría, Z., Dzul López, L.A., García Villena, E., 2022. Application of the Gaussian Model for Monitoring Scenarios and Estimation of SO2 Atmospheric Emissions in the Salamanca Area, Bajío, Mexico. Atmosphere (Basel). 13, 874. https://doi.org/10.3390/ATMOS13060874

Gebicki, J., Byliński, H., Namieśnik, J., 2016. Measurement techniques for assessing the olfactory impact of municipal sewage treatment plants. Environ. Monit. Assess. 188, 1–15. https://doi.org/10.1007/s10661-015-5024-2

Giungato, P., Di Gilio, A., Palmisani, J., Marzocca, A., Mazzone, A., Brattoli, M., Giua, R., de Gennaro, G., 2018. Synergistic approaches for odor active compounds monitoring and identification: State of the art, integration, limits and potentialities of analytical and sensorial techniques. TrAC Trends Anal. Chem. 107, 116–129. https://doi.org/10.1016/J.TRAC.2018.07.019

Gostelow, P., Parsons, S.A., Stuetz, R.M., 2001. Odour measurements for sewage treatment works. Water Res. 35, 579–97.

Government of Catalonia, 2005. Draft of the Law Against Odor Pollution. Departamento de Medio Ambiente y Vivienda. Generalitat de Cataluña. [WWW Document]. URL https://www.olores.org/images/pdfs/borrador_anteproyecto_ley_contaminacion_odorifera.pdf (accessed 12.12.21).

Gutiérrez, M.C., Martín, M.A., Serrano, A., Chica, A.F., 2015. Monitoring of pile composting process of OFMSW at full scale and evaluation of odour emission impact. J. Environ. Manage. 151, 531–539. https://doi.org/10.1016/j.jenvman.2014.12.034

Hayes, J.E., Stevenson, R.J., Stuetz, R.M., 2017. Survey of the effect of odour impact on communities. J. Environ. Manage. 204, 349–354. https://doi.org/10.1016/j.jenvman.2017.09.016

Hesthaven, J.S., Gottlieb, D., 2012. A Stable Penalty Method for the Compressible Navier–Stokes Equations: I. Open Boundary Conditions. SIAM J. Sci. Comput. 17, 579–612. https://doi.org/10.1137/S1064827594268488

Hoffman, J.D., Frankel, S., 2001. Numerical Methods for Engineers and Scientists, 2nd ed. CRC Press, Boca Raton, FL.

Jiang, G., Melder, D., Keller, J., Yuan, Z., 2017. Odor emissions from domestic wastewater: A review. Crit. Rev. Environ. Sci. Technol. 47, 1581–1611. https://doi.org/10.1080/10643389.2017.1386952

Karageorgos, P., Latos, M., Kotsifaki, C., Lazaridis, M., Kalogerakis, N., 2010. Treatment of unpleasant odors in municipal wastewater treatment plants. Water Sci. Technol. 61, 2635–2644. https://doi.org/10.2166/wst.2010.211

Lamprea Pineda, P.A., Demeestere, K., Toledo, M., Van Langenhove, H., Walgraeve, C., 2021. Enhanced removal of hydrophobic volatile organic compounds in biofilters and biotrickling filters: A review on the use of surfactants and the addition of hydrophilic compounds. Chemosphere 279, 130757. https://doi.org/10.1016/J.CHEMOSPHERE.2021.130757

Lebrero, R., Bouchy, L., Stuetz, R., Muñoz, R., 2011. Odor Assessment and Management in Wastewater Treatment Plants: A Review. Crit. Rev. Environ. Sci. Technol. 41, 915–950. https://doi.org/10.1080/10643380903300000

Li, Q., Lan, Y., Liu, Z., Wang, X., Wang, X., Hu, J., Geng, H., 2020. Cyclic volatile methylsiloxanes (cVMSs) in the air of the wastewater treatment plants in Dalian, China - Levels, emissions, and trends. Chemosphere 256, 127064. https://doi.org/10.1016/J.CHEMOSPHERE.2020.127064

Li, R., Han, Z., Shen, H., Qi, F., Ding, M., Song, C., Sun, D., 2021. Emission characteristics of odorous volatile sulfur compound from a full-scale sequencing batch reactor wastewater treatment plant. Sci. Total Environ. 776, 145991. https://doi.org/10.1016/j.scitotenv.2021.145991

Liu, Y., Zhao, Y., Lu, W., Wang, H., Huang, Q., 2019. ModOdor: 3D numerical model for dispersion simulation of gaseous contaminants from waste treatment facilities. Environ. Model. Softw. 113, 1–19. https://doi.org/10.1016/J.ENVSOFT.2018.12.001

Márquez, P., Benítez, A., Caballero, Á., Siles, J.A., Martín, M.A., 2021a. Integral evaluation of granular activated carbon at four stages of a full-scale WWTP deodorization system. Sci. Total Environ. 754, 142237. https://doi.org/10.1016/j.scitotenv.2020.142237

Márquez, P., Benítez, A., Hidalgo-Carrillo, J., Urbano, F.J., Caballero, Á., Siles, J.A., Martín, M.A., 2021b. Simple and eco-friendly thermal regeneration of granular activated carbon from the odour control system of a full-scale WWTP: Study of the process in oxidizing atmosphere. Sep. Purif. Technol. 255, 117782. https://doi.org/10.1016/j.seppur.2020.117782

Márquez, P., Siles, J.A., Gutiérrez, M.C., Alhama, J., Michán, C., Martín, M.A., 2022. A comparative study between the biofiltration for air contaminated with limonene or butyric acid using a combination of olfactometric, physico-chemical and genomic approaches. Process Saf. Environ. Prot. 160, 362–375. https://doi.org/10.1016/J.PSEP.2022.02.024

Martin, D.O., 1976. Comment On"The Change of Concentration Standard Deviations with Distance." J. Air Pollut. Control Assoc. 26, 145–147. https://doi.org/10.1080/00022470.1976.10470238

Martin, M.J., Anfruns, A., Lebrero, R., Estrada, J.M., Canals, C., Vega, E., 2010. Procesos de adsorción, in: Muñoz, R., Lebrero, R., Estrada, J.M. (Eds.), Caracterización Y Gestión de Olores En Estaciones Depuradoras de Aguas Residuales. Gráficas Germinal S.C.L., Valladolid, España, pp. 115–126.

Mudliar, S., Giri, B., Padoley, K., Satpute, D., Dixit, R., Bhatt, P., Pandey, R., Juwarkar, A., Vaidya, A., 2010. Bioreactors for treatment of VOCs and odours - A review. J. Environ. Manage. 91, 1039–1054. https://doi.org/10.1016/j.jenvman.2010.01.006

Naddeo, V., Belgiorno, V., Zarra, T., 2012. Odour characterization and exposure effects, in: Naddeo, V., Belgiorno, V., Zarra, T. (Eds.), Odour Impact Assessment Handbook. John Wiley & Sons Inc., Hoboken, pp. 8–29.

Nagata, Y., 2003. Odor Measurement Review, Measurement of Odor Threshold by Triangle Odor Bag Method. Minist. Environ. Gov. Japan 122–123.

Nanni, A., Tinarelli, G., Solisio, C., Pozzi, C., 2022. Comparison between Puff and Lagrangian Particle Dispersion Models at a Complex and Coastal Site. Atmosphere (Basel). 13, 508. https://doi.org/10.3390/ATMOS13040508

Orzi, V., Scaglia, B., Lonati, S., Riva, C., Boccasile, G., Alborali, G.L., Adani, F., 2015. The role of biological processes in reducing both odor impact and pathogen content during mesophilic anaerobic digestion. Sci. Total Environ. 526, 116–126. https://doi.org/10.1016/j.scitotenv.2015.04.038

Patankar, S.V., 1980. Numerical heat transfer and fluid flow. Mc Graw-Hill.

Pisso, I., Sollum, E., Grythe, H., Kristiansen, N., Cassiani, M., Eckhardt, S., Thompson, R., Groot Zwaaftnik, C., Evangeliou, N., Hamburger, T., 2017. The Lagrangian Particle Dispersion Model FLEXPART Version 10. EGU General Assembly Conference.

Ranzato, L., Barausse, A., Mantovani, A., Pittarello, A., Benzo, M., Palmeri, L., 2012. A comparison of methods for the assessment of odor impacts on air quality: Field inspection (VDI 3940) and the air dispersion model CALPUFF. Atmos. Environ. 61, 570–579. https://doi.org/10.1016/J.ATMOSENV.2012.08.009

Ren, B., Zhao, Y., Lyczko, N., Nzihou, A., 2019. Current Status and Outlook of Odor Removal Technologies in Wastewater Treatment Plant. Waste and Biomass Valorization 10, 1443–1458. https://doi.org/10.1007/s12649-018-0384-9

Sattler, M., Devanathan, S., 2007. Which Meteorological Conditions Produce Worst-Case Odors from Area Sources? J. Air Waste Manage. Assoc. 57, 1296–1306. https://doi.org/10.3155/1047-3289.57.11.1296

Schiffman, S.S., McLaughlin, B., Katul, G.G., Nagle, H.T., 2005. Eulerian-Lagrangian model for predicting odor dispersion using instrumental and human measurements. Sensors Actuators B Chem. 106, 122–127. https://doi.org/10.1016/J.SNB.2004.05.067

SCRAM, 2018. Support Center for Regulatory Atmospheric Modeling (SCRAM) [WWW Document]. URL https://www.epa.gov/scram/air-quality-dispersion-modeling-preferred-and-recommended-models (accessed 4.4.19).

Seinfeld, J.H., Pandis, S.N., 2016. Atmospheric Chemistry and Physics: From Air Pollution to Climate Change. John Wiley & Sons, Hoboken.

Senatore, V., Zarra, T., Galang, M.G., Oliva, G., Buonerba, A., Li, C.-W., Belgiorno, V., Naddeo, V., 2021. Full-Scale Odor Abatement Technologies in Wastewater Treatment Plants (WWTPs): A Review. Water 13, 3503. https://doi.org/10.3390/w13243503

Sironi, S., Capelli, L., Dentoni, L., 2012. Odour regulation and policies, in: Naddeo, V., Belgiorno, V., Zarra, T. (Eds.), Odour Impact Assessment Handbook. John Wiley & Sons Inc., Hoboken, pp. 176–186.

Sówka, I., Skrętowicz, M., Sobczyński, P., Zwoździak, J., 2014. Estimating odour impact range of a selected wastewater treatment plant for winter and summer seasons in Polish conditions using CALPUFF model. Int. J. Environ. Pollut. 54, 242–250. https://doi.org/10.1504/IJEP.2014.065125

Stuetz, R., Frechen, F.B., 2001. Odours in Wastewater Treatment - Measurement, Modelling and Control. IWA, London, England. https://doi.org/10.2166/9781780402932

Sucker, K., Both, R., Winneke, G., 2009. Review of adverse health effects of odours in field studies. Water Sci. Technol. 59, 1281–1289. https://doi.org/10.2166/WST.2009.113

Talaiekhozani, A., Bagheri, M., Goli, A., Talaei Khoozani, M.R., 2016. An overview of principles of odor production, emission, and control methods in wastewater collection and treatment systems. J. Environ. Manage. 170, 186–206. https://doi.org/10.1016/j.jenvman.2016.01.021

Tartakovsky, D., Stern, E., Broday, D.M., 2016. Comparison of dry deposition estimates of AERMOD and CALPUFF from area sources in flat terrain. Atmos. Environ. 142, 430–432. https://doi.org/10.1016/J.ATMOSENV.2016.08.035

Tian, Y., Desouza, P., Mora, S., Yao, X., Duarte, F., Norford, L.K., Lin, H., Ratti, C., 2021. Evaluating the Meteorological Effects on the Urban Form-Air Quality Relationship Using Mobile Monitoring. Environ. Sci. Technol. 56, 7328–7336. https://doi.org/10.1021/ACS.EST.1C04854/SUPPL_FILE/ES1C04854_SI_001.PDF

Toledo, M., Gutiérrez, M.C., Siles, J.A., Martín, M.A., 2018. Full-scale composting of sewage sludge and market waste: Stability monitoring and odor dispersion modeling. Environ. Res. 167, 739–750. https://doi.org/10.1016/J.ENVRES.2018.09.001

Turner, D.B., 1970. Workbook of Atmospheric Dispersion Estimates. U.S. Public Heatlh Service Publication 999-AP-26 (revised edition), U.S. Govt. Printing Office, Washington D.C.

VDI 3880, 2011. Olfactometry – Static Sampling. Beuth Verlag GmbH, Berlin, pp. 10772.

Vieira de Melo, A.M., Santos, J.M., Mavroidis, I., Reis Junior, N.C., 2012. Modelling of odour dispersion around a pig farm building complex using AERMOD and CALPUFF. Comparison with wind tunnel results. Build. Environ. 56, 8–20. https://doi.org/10.1016/J.BUILDENV.2012.02.017

Wang, L., Parker, D.B., Parnell, C.B., Lacey, R.E., Shaw, B.W., 2006. Comparison of CALPUFF and ISCST3 models for predicting downwind odor and source emission rates. Atmos. Environ. 40, 4663–4669. https://doi.org/10.1016/J.ATMOSENV.2006.04.043

Water Environment Federation, 2017. Liquid Stream Fundamentals: Odor Management and Control [Fact Sheet] [WWW Document]. URL https://www.wef.org/globalassets/assets-wef/direct-download-library/public/03---resources/wsec-2017-fs-028-liquid-stream-fundamentals--odor-control_final.pdf (accessed 3.11.20).

Wroniszewska, A., Zwoździak, J., 2020. Odor Annoyance Assessment by Using Logistic Regression on an Example of the Municipal Sector. Sustainability 12, 6102. https://doi.org/10.3390/SU12156102

Zedan, M., Schneider, G.E., 1983. A three-dimensional modified strongly implicit procedure for heat conduction. AIAA J. 21, 295–303. https://doi.org/10.2514/3.8068

BLOQUE II. CONTROL SOSTENIBLE DE EMISIONES ODORÍFERAS EN EDAR DE GRAN TAMAÑO

SECTION II. SUSTAINABLE CONTROL OF ODOR EMISSIONS IN LARGE WWTPs

II. Resumen del Bloque: "*Control sostenible de emisiones odoríferas en EDAR de gran tamaño*"

El CAG es el relleno adsorbente más utilizado y eficaz para la descontaminación odorífera en las EDAR, debido a su capacidad para adsorber fácilmente una amplia gama de compuestos olorosos, siendo sus variedades activadas con NaOH o KOH idóneas para la eliminación de sulfuro de hidrógeno y compuestos orgánicos sulfurados. Sin embargo, el CAG, activado o no, una vez concluida su vida útil, se convierte en un residuo industrial peligroso que es frecuentemente depositado en vertedero a través de gestores autorizados, lo que supone un coste económico y ambiental destacable. Es por ello por lo que, desde el punto de vista de la economía circular, la regeneración del CAG contaminado puede constituir una alternativa atractiva para las instalaciones que utilizan este adsorbente de forma rutinaria. En este sentido, la regeneración térmica del CAG en atmósfera inerte es la más utilizada a escala industrial, pero las condiciones requeridas (temperatura y atmósfera inerte, fundamentalmente) hacen actualmente más económico su depósito en vertedero, ya que requiere de una corriente continua de gas inerte y elevadas temperaturas de regeneración, costes de recursos materiales y energéticos que incrementan el coste de regeneración.

Ante el panorama mencionado anteriormente, el objetivo de este segundo bloque es caracterizar la emisión odorífera de la EDAR urbana de gran tamaño contemplada en el Bloque I, así como estudiar y optimizar el proceso de regeneración del CAG contaminado procedente de la desodorización de la citada instalación, de cara a su posible reutilización en el proceso original, es decir, como nuevo lecho adsorbente, o para otros usos, en función de sus propiedades texturales respuesta e incluso mejoradas, tales como su utilización como cátodo en baterías de litio-azufre (Li-S), tecnología que reúne perspectivas muy prometedoras tanto en términos de rendimiento energético como de sostenibilidad ambiental o coste económico, y que se podría postular como una gran alternativa a las baterías de litio-ion con las que funcionan actualmente los vehículos eléctricos.

En el primer trabajo del Bloque II, se ha realizado una caracterización textural y olfatométrica del CAG empleado como relleno adsorbente. Además, con el objetivo de profundizar en la naturaleza de la emisión gaseosa asociada a los diferentes focos de olor, se ha llevado a cabo la cuantificación cromatográfica de los compuestos odoríferos retenidos por el material adsorbente. Se ha comprobado que, tras un mismo tiempo de

operación, los rellenos relacionados con la desodorización de la línea de aguas de la EDAR en cuestión son los que han presentado mayor cantidad y variedad de compuestos odoríferos retenidos, lo que se ha relacionado también con la gran contribución relativa de la mencionada línea al olor global emitido en comparación con la línea de fangos.

Una vez caracterizado el CAG contaminado, en el segundo estudio del presente bloque se ha propuesto su regeneración térmica en atmósfera oxidante (aire), evaluándose las propiedades de este material antes y después de su regeneración, de tal manera que las propiedades del CAG regenerado han permitido plantear su valorización para constituir nuevos lechos adsorbentes de olor. Adicionalmente, en el tercer artículo, se ha comparado la regeneración térmica oxidativa del CAG con su homóloga en atmósfera inerte de nitrógeno, demostrándose que la primera constituye una opción más simple y económica que la segunda para la obtención de CAG susceptible de ser reutilizado como adsorbente de malos olores. Finalmente, el cuarto y último trabajo del Bloque II ha demostrado el buen comportamiento del CAG regenerado como matriz para alojar azufre en el electrodo positivo de las baterías de Li-S, obteniéndose unas excelentes propiedades electroquímicas con un notable rendimiento de ciclado y retención de capacidad, tanto a densidades de corriente fijas como variables.

Teniendo en cuenta todo lo anterior, se puede decir que se ha demostrado un avance sustancial en la circularidad y sostenibilidad del proceso de tratamiento de aguas residuales a través de la optimización de los recursos utilizados en la línea de olor de las instalaciones industriales.

II.1. Breve descripción del artículo: "*Integral evaluation of granular activated carbon at four stages of a full-scale WWTP deodorization system*"

II.1. Breve descripción del artículo: "*Integral evaluation of granular activated carbon at four stages of a full-scale WWTP deodorization system*"

En este artículo se ha llevado a cabo la caracterización fisicoquímica, olfatométrica y textural del GAC procedente de los lechos desodorizantes de una EDAR urbana, así como la cuantificación cromatográfica de los compuestos volátiles retenidos en el material adsorbente. Estas técnicas han permitido realizar una evaluación del GAC contaminado y caracterizar de forma indirecta la emisión gaseosa de cuatro etapas diferentes del tratamiento integral del agua residual (cabecera de pretratamiento: GAC-1; desarenado−desengrasado: GAC-2; espesamiento del fango: GAC-3; deshidratación del fango: GAC-4). Después del mismo tiempo de operación para todos los filtros adsorbentes (un año), se detectó una mayor cantidad y variedad de compuestos odoríferos retenidos en las muestras de GAC procedentes de la desodorización de la línea de aguas (GAC-1 y GAC-2), siendo GAC-1 el lecho adsorbente que retuvo la mayor masa de compuestos volátiles (aproximadamente 150 μg/g GAC). Además, variables como la concentración de olor específica eliminada ($ou_E/m^3 \cdot g$ GAC) y el volumen de microporo (cm^3/g GAC) fueron inversamente correlacionadas mediante un modelo de regresión lineal simple ($R^2 = 0,9945$). El análisis de la contribución al olor global de cada una de las familias de compuestos cuantificadas demostró que la familia de los compuestos sulfurados fue la principal contribuyente al olor global en todos los focos analizados (61−97%). Sin embargo, el sulfuro de hidrógeno no puede considerarse el compuesto odorífero más importante en esta EDAR en particular, ya que la eliminación de este compuesto no reduce la contribución significativa de otros compuestos (orgánicos) de azufre al olor global (especialmente el dimetil disulfuro). En consecuencia, el análisis multitécnica llevado a cabo podría constituir una alternativa adecuada para comprender en profundidad la eliminación de olores en EDAR mediante la adsorción con carbón activo.

Science of the Total Environment 754 (2021) 142237

Contents lists available at ScienceDirect

Science of the Total Environment

journal homepage: www.elsevier.com/locate/scitotenv

Integral evaluation of granular activated carbon at four stages of a full-scale WWTP deodorization system

Márquez, P. [a], Benítez, A. [b], Caballero, Á. [b], Siles, J.A. [a], Martín, M.A. [a,*]

[a] Department of Inorganic Chemistry and Chemical Engineering, Area of Chemical Engineering, University of Cordoba, Campus Universitario de Rabanales, Carretera N-IV, km 396, Edificio Marie Curie, 14071 Córdoba, Spain

[b] Dpto. Química Inorgánica e Ingeniería Química, Instituto Universitario de Nanoquímica, Universidad de Córdoba, 14071 Córdoba, Spain

* Corresponding author: iq2masam@uco.es

Received 6 May 2020; Received in revised form 2 September 2020; Accepted 4 September 2020;

Available online 07 September 2020

Abbreviations: D_{pore}, average pore width (nm); GAC, granular activated carbon; GC, gas chromatography; MS, mass spectrometry; OAV, odor activity value; OC, odor concentration (ou_E/m^3); ODT, odor detection threshold ($\mu g/m^3$); ou_E, European odor units; PC_i, chemical contribution (%); PO_i, odor contribution (%); S_{BET}, specific surface area (m^2/g); S_{micro}, micropore area (m^2/g); SOC, removed specific odor concentration ($ou_E/m^3 \cdot g$ GAC); TC, total concentration of desorbed gaseous compounds ($\mu g/g$ GAC); TD, thermal desorption; TN_s, soluble total nitrogen (mg/g GAC); TOC, soluble total organic carbon (mg/g GAC); V_{micro}, free micropore volume (cm^3/g); VOCs, volatile organic compounds; V_t, total pore volume (cm^3/g); WWTPs, wastewater treatment plants; XRF, X-ray fluorescence.

Graphical abstract

Abstract

Odor emissions from wastewater treatment plants (WWTPs) have always been a public concern. In this work, the physico-chemical, olfactometric and textural characterization of granular active carbon (GAC) used by an urban WWTP as a deodorization system, as well as the chromatographic quantification of the retained odoriferous compounds, have been carried out. These techniques have allowed an integral evaluation of the contaminated GAC and the characterization of the retained gaseous emission from four different stages of the wastewater treatment (pretreatment header: GAC-1; sand and fat removal: GAC-2; sludge thickening: GAC-3; sludge dehydration: GAC-4). A larger amount and variety of retained odoriferous compounds were found in GAC samples from the wastewater line deodorization (GAC-1 and GAC-2) after the same operation time (one year), GAC-1 being the adsorbent bed that retained the highest mass of volatile compounds (approximately 150 µg/g GAC). Furthermore, some variables such as the removed specific odor concentration and free micropore volume were inversely correlated (R^2 = 0.9945). The analysis of odor contribution showed that sulfur-containing compounds were the major odor contributors (61–97%). However, hydrogen sulfide cannot be considered a key odorant in this particular WWTP, since the elimination of this compound does not reduce the significant contribution of other (organic) sulfur compounds to the global odor (especially dimethyl disulfide). Consequently, multi-technical analysis might be a suitable alternative to better understand odor removal by GAC adsorption.

Keywords: emitted gaseous compounds; granular activated carbon; multi-technical analysis; odor contribution; WWTP.

1. Introduction

Odor emissions have traditionally had a secondary role in global environmental policies. Nevertheless, it is well known that long-term exposure to odorants can cause diverse negative effects on human health, such as headaches, nausea and vomiting, insomnia, respiratory tract alterations, irrational behavior and even cancer (Byliński et al., 2019b; Domingo and Nadal, 2009). For this reason, the odor impact caused by industrial activities and waste management has become increasingly important in international environmental regulations. The inclusion of odor impact in the second draft of the Biowaste Directive of 2001 is one such example (European Commission, 2001). The odoriferous impact of wastewater treatment plants (WWTPs) is the source of many complaints and protests in nearby residential areas (Easter et al., 2008; Hayes et al., 2017; Morales et al., 2008). This is due to the large number of volatile odorants present in the gaseous emissions from these facilities, some of which have very low odor threshold values in terms of ppb_v or ppt_v (Nagata, 2003). Hydrogen sulfide is commonly considered to be the main compound responsible for the odor impact of WWTPs (Talaiekhozani et al., 2016). Gaseous emissions from WWTPs also contain other sulfur compounds such as mercaptans, organic compounds (e.g., butyric acid, butanone, toluene, benzene and skatole), ammonia and nitrogen derivates such as amines (Fisher et al., 2018; Lebrero et al., 2011; Talaiekhozani et al., 2016).

In WWTPs, it is not only important to identify the compounds which cause malodor problems, but also the areas of these facilities that contribute most to odor impact. According to Lebrero et al. (2011), primary treatments (e.g. various kinds of grilles or initial settling tanks) and sludge handling activities constitute the main odor sources in WWTPs. By means of odor emission factors, Capelli et al. (2009) predicted odor emissions from WWTPs, highlighting primary sedimentation, pretreatments and sludge thickening as the main odor sources. Gebicki et al. (2016) also reported the average percentage distribution of odor emission sources from a sewage treatment plant: preliminary operations (53.5%), sludge dewatering, drying and thickening (36.6%), rinsing (6.2%), tank aeration (1.8%), fermentation tanks (1.4%) and clarifiers and sand traps (0.5%). Therefore, odor control strategies should focus especially on the first two sources, which may jointly account for up to 90% of emissions which can affect the occurrence of malodor in surrounding areas.

In general, odor control in sewage treatment plants includes (i) prevention of odorant formation and emission; and (ii) elimination of malodor compounds by means of end-of-the-pipe odor abatement systems (Talaiekhozani et al., 2016; Tchobanoglous et al., 2003). Prevention should be the priority strategy. However, this is a difficult task because compounds, such as sulfides, are already present in the wastewater reaching WWTPs (and subsequently transferred to the gaseous phase) or the result of existing design parameters. In the latter case, the solution would be a correct plant design, which requires a high capital investment. On the other hand, there are also simpler and less costly prevention operations such as the regular cleaning of screening units or grit chambers (Lebrero et al., 2011). When prevention is insufficient to mitigate nuisance emissions, odor treatment technologies must be applied. The nature and concentration of odorants, the required efficiency and the air flow rate to be deodorized are among the variables that influence the selection of a specific treatment system. Hence, different physico-chemical and biological methods might be of interest (Burgess et al., 2001).

Adsorption by granular activated carbon (GAC) is a reliable and well-established physico-chemical technique for treating odors in WWTPs due to its capability to easily adsorb a wide range of odorants, such as volatile organic compounds (VOCs), mercaptans, ammonia and hydrogen sulfide (Le-Minh et al., 2018; Lebrero et al., 2011). The replacement of GAC beds is based on empirical experience because GAC manufacturers do not often guarantee the adsorbent life of GAC beds in WWTP applications (Estrada et al., 2011). In this context, both odor removal efficiency and filter replacement are often based on H_2S removal. According to Jiang et al. (2017), H_2S is a key odorant in WWTPs, and the concentration of this compound is easily measurable in situ using online sensors (Lebrero et al., 2011; Martin et al., 2010). However, the deodorization of gaseous effluents from WWTPs requires the removal of a complex mixture of compounds with a wide range of molecular weights, volatilities and chemical functionalities. For instance, other malodorous volatile sulfur compounds beyond H_2S (dimethyl sulfide, dimethyl disulfide, dimethyl trisulfide, etc.) are widely reported in the literature (Watson and Jüttner, 2017). Therefore, analytical and sensory measurements should be combined to ensure the optimal design of deodorization operations (Martin et al., 2010).

In this context, this work proposes an integral evaluation of the GAC derived from the deodorization system of an urban WWTP, and the characterization of the retained

gaseous emission from four different stages of the integral wastewater treatment. For this purpose, physico-chemical, olfactometric and textural characterizations of the GAC used by the facility as an odor treatment system, as well as the chromatographic quantification of the retained odoriferous compounds, were carried out. To the best of our knowledge, a multi-technical analysis to better understand the odor removal process by GAC adsorption has not been previously reported in the literature. This information might aid in optimizing GAC operations in WWTPs that employ this deodorization system, with the consequent benefits for occupational health within the WWTP and the reduction of odor impact in the nearby population.

2. Material and methods

2.1. WWTP: Description of the activity

The urban WWTP of this study is located in the province of Seville, Spain, and has the capacity to treat wastewater from a population equivalent of 950,000. The facility has a current treatment capacity of 255,000 m^3/d and operates with a biological secondary treatment (active sludge) and the treatment of sludge stabilization by anaerobic digestion and dehydration. It carries out anaerobic co-digestion of sewage sludge with other agrifood waste. **Fig. 1** shows the schematic flow diagram of the facility.

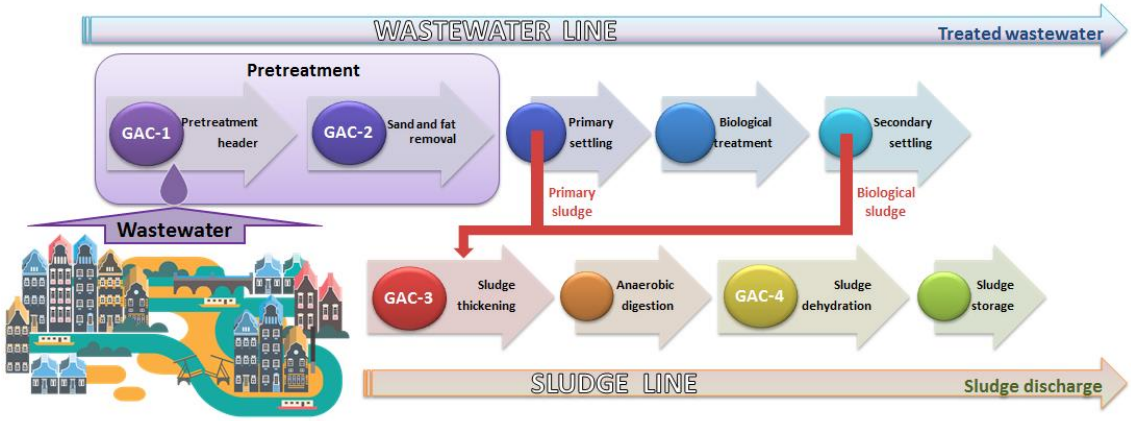

Fig. 1. Schematic diagram of the WWTP.

The WWTP under study uses GAC adsorption as a deodorization system. In addition, in order to avoid the presence of H_2S in the biogas produced in anaerobic digesters, ferric chloride ($FeCl_3$) is added to the wastewater line (before sludge

thickening), which reacts with H_2S to form an iron-sulfide precipitate (Fe_2S_3), which settles quickly in quiescent conditions (Water Environment Federation, 2017).

2.2. Granular activated carbon: description and operation

For purposes of the present study, four contaminated samples of the same GAC from different WWTP locations were evaluated. The four GAC samples had been subjected to the same operation time (one year). In the central part of each deodorization bed, 9 replicates per sample were taken, in accordance with an experimental design of a regular cube centered on the origin and avoiding the input and output surface of the GAC bed. The 9 replicates (approximately 200 g each) were homogenized and fractionated into 3 new replicates, with which the present study was carried out. The samples were kept cold during transportation and stored at 6 ± 2 ºC to prevent desorption of the retained gaseous compounds. The origin of the samples and a description of the deodorization towers are shown in **Table 1**. The pristine GAC (GAC-0) was made from coconut shell. The manufacturer´s technical specifications of GAC-0 were iodine number (minimum): 1000 mg/g; average particle diameter: 3.7 mm and ash content: 4%.

In the WWTP locations mentioned in **Table 1**, polluted air is sucked in by fans until it reaches the active carbon filters, where malodor compounds are adsorbed. Subsequently, clean air is expelled into the atmosphere through chimneys. The concentration of hydrogen sulfide at the system output is the most frequently used parameter in this WWTP to proceed with the replacement of the adsorbent material. To carry out this measurement, a portable analyzer (4000 series) manufactured by Interscan Corporation is used. Contaminated GAC is considered a hazardous waste (code: 06 13 02) by the European Commission (2018) and is deposited in landfill and replaced by fresh activated carbon (GAC-0).

2.3. Characterization of the GAC samples

For the different physico-chemical, textural, olfactometric and chromatographic experiments, three replicates per GAC sample were used.

2.3.1. Physico-chemical characterization

2.3.1.1. Acidic and basic surface groups

The Boehm method (Boehm, 1994) was used to determine the concentration of both basic and acidic remaining surface functional groups present in the GAC samples. To

quantify the concentration of basic groups (in mmol per gram of adsorbent), the samples (0.25 g each) were added to a 50 mL hydrochloric acid solution (0.1 M concentration) and stirred for 48 h at 170 rpm and 25 ºC. The suspension was then filtered and three aliquots (3 mL each) of the filtrates were back titrated using a 0.1 M NaOH solution (in order to neutralize the excess acid) and phenolphthalein as an indicator. To quantify the concentration of the acidic groups, the GAC samples were added to a 50 mL sodium hydroxide solution (0.1 M) and stirred under the same conditions described above. The suspension was then filtered and three aliquots of the filtrates were back titrated using a 0.1 M HCl solution in order to neutralize the excess base.

2.3.1.2. Elemental composition

The elemental composition (Na, K and S) of the GAC samples was determined by X-ray fluorescence (XRF). Spectra were obtained using a Rigaku Wavelength Dispersive X-ray Fluorescence (WDXRF) spectrometer (ZSX Primus IV model). The system is equipped with a 4 kW rhodium target X-ray tube (operating at a maximum voltage of 60 kV and a current of 150 mA), ten analyzer crystals, a flow proportional counter for detecting light elements and a scintillation counter for detecting heavy elements.

2.3.1.3. TOC, TN_s, pH and conductivity

The methodology proposed by the US Department of Agriculture and the US Composting Council (2002) was used to quantify, in triplicate and in the aqueous extract (1:25 ratio), the following variables: soluble total organic carbon (TOC, mg/g GAC), soluble total nitrogen (TN_s, mg/g GAC), pH and conductivity (mS/cm).

2.3.2. Determination of the textural properties

The nitrogen adsorption/desorption data were obtained at the liquid nitrogen temperature (77 K) using a Micromeritics ASAP 2020 M apparatus. The specific surface area (S_{BET}) was calculated using the Brunauer–Emmett–Teller (BET) equation in a relative pressure range of 0.04–0.20. Total pore volume (V_t) was calculated at relative pressure $p/p_0 = 0.98$. The t-plot method was used to estimate the micropore area (S_{micro}). Micropore volume (V_{micro}) was calculated according to the Dubinin-Radushkevich equation (Nguyen and Do, 2001). The average pore width (D_{pore}) was determined by the 4V/A following the BET method.

Table 1. Origin of GAC samples and description of deodorization towers.

GAC samples (acronym)	Origin	Operation description	Number of deodorization towers	Tower height (m)	Tower diameter (m)	Flow speed (m/s per tower)	Treated air flow (Nm^3/h per tower)	Amount of GAC (kg per tower)	Number of GAC beds (per tower)	Bed height (m)	Bed capacity (m^3)
Sample 1 (GAC-1)	Pretreatment header	Roughing operations, water elevation using worm screws and screening	1	3.60	3.00	2829	20,000	3900	2	0.50	3.53
Sample 2 (GAC-2)	Pretreatment	Sand and fat removal	2	3.80	3.50	2079	20,000	5300	2	0.50	4.81
Sample 3 (GAC-3)	Sludge thickening	Gravity thickening of sludge from primary treatment and flotation thickening of sludge from biological treatment	2	2.23	2.25	1006	4000	1325	1	0.60	2.39
Sample 4 (GAC-4)	Sludge dehydration	Dehydration of the sludge from anaerobic digestion	1	1.65	1.40	1299	2000	500	1	0.60	0.92

2.3.3. Olfactometric measurements

To desorb the odoriferous compounds adsorbed on the GAC samples and subsequently quantify their removed specific odor concentration (SOC, $ou_E/m^3 \cdot g$ GAC), 0.5 g of each sample was introduced into 20 mL glass bottles. After that, they were sealed and maintained under isothermal conditions for 24 h. Then, the above mentioned bottles were introduced into 4-L Nalophan® sampling bags. Once inside the bags, glass bottles were opened for 15 min (equilibrium time) and then closed again. The next step was to fill the bags with odorless compressed air at a filling time of 30 s. Finally, the sampling bags were also kept in isothermal conditions until the determination of their odor concentration. In order to evaluate the variation in SOC with the increase in temperature, five desorption experiments were carried out at different temperatures (25, 30, 35, 40 and 45 ºC, respectively). GAC-0 was also subjected to the same experiments. The SOC results presented in this study are the geometric mean of the SOC from three replicates of a GAC sample, at the same temperature. Depending on temperature, not all the retained gaseous compounds will migrate to the gas phase, but only those that are desorbed at the proposed temperatures (Martin et al., 2010).

Dynamic olfactometry was the method used to quantify the odor concentration (OC, ou_E/m^3), which is necessary to calculate the SOC at the above mentioned temperatures. All odor concentration data are expressed in accordance with the reference conditions described in standard EN 13725 (2003) (i.e. 20 ºC, 101.3 kPa on a wet basis). According to the European standard, all gaseous samples were analyzed within 30 h. However, in order to minimize the permeation and/or adsorption of odorants through/on the sampling bag walls, gaseous samples were analyzed within 6 h, as proposed by the guideline VDI 3880 (2011). Permeability and adsorption effects for odorants (such as volatile sulfur compounds) in Nalophan® sampling bags were studied by several authors, who demonstrated the influence of storage time on the above mentioned effects (Kasper et al., 2018; Le et al., 2015; Toledo et al., 2019a). A TO8 olfactometer based on the "Yes/No" method developed by Olfasense GmbH was used to determine the OC. The panelist group consisted of 4 people who were selected based on their sensitivity to the n-butanol reference gas as described in the above European standard. The individual sensitivities of the panelists are within the range 20-80 ppb_v as established by EN 13725 (2003), these being specifically 49, 52, 62 and 68 ppb_v of n-butanol. The odor concentration was

calculated as the geometric mean of the odor threshold values of each panelist multiplied by the square root of the dilution factor, which is 2 (Jiang et al., 2006).

2.3.4. Quantification of volatile organic compounds

A thermal desorption unit coupled with gas chromatography/mass spectrometry (TD-GC/MS) was used to quantify the VOCs retained by the GAC samples, which were grouped into families of odoriferous compounds. The methodology for this analysis is described in the following sections.

2.3.4.1. Preparation of blank samples and sampling

A total of 44.5 mg of each GAC sample (GAC-0, GAC-1, GAC-2, GAC-3 and GAC-4) was weighed and placed in individual microchambers at 40 ºC. Fifteen minutes after placing the samples in the microchambers (equilibrium time), individual, freshly cleaned adsorption tubes (TenaxTA/Carbograph5, Markes International, UK) were inserted in the lid of each microchamber with an adjusted dynamic flow of 50 mL/min (flow coming from the emitted headspace by the sample). After 30 min (sampling time), the tubes on the lid of each microchamber were removed and inserted in the TD-GC/MS system to perform the chromatographic analyses.

With respect to the preparation of the blank samples, the microchambers were set to 40 ºC and a blank, freshly cleaned adsorption tube was inserted in the lid of each microchamber under the same sampling conditions (30 min, 50 mL/min). These tubes constitute the blank subtracted from each sample according to the microchamber used.

2.3.4.2. Chromatographic analysis

After collecting the VOCs in the adsorption tubes, they were inserted in the TD-GC/MS system. As described above, the instrumentation system consisted of a thermal desorption unit (Unity2-xr Markes International, UK), a gas chromatograph (GC) (TRACE 1310, Thermo Fisher Scientific) and a mass spectrometer (MS) (ISQ 7000, Thermo Fisher Scientific).

The VOCs were then removed from the tubes by thermal desorption (280–330 ºC) and captured in a cold trap at low temperature (0–10 °C) by thermoelectric cooling. Subsequently, the cold trap was heated to 300–350 °C according to a programmed and optimized temperature profile to release all the VOCs into the GC column inlet through a transfer line for their subsequent chromatographic separation. At the end of the GC

column, the separated compounds reach the MS with different (retention) times (expressed in minutes), where they are fragmented and subsequently identified by the NIST 2017 spectra database based on the fragmentation patterns of each molecule.

The GC system was equipped with the mid polar TG-624 column (60 m; 0.25 mm; 1.5 µm; Thermo Fisher Scientific). Temperature program of GC/MS analysis: initial oven temperature 40 ºC, held for 5 min, ramped to 235 ºC at 5 ºC/min, held for 7 min. Carrier gas (He) was operated at 1.6 mL/min. Mass spectral detection was in electron impact mode at 70 eV ionization energy. The m/z range was 35-350 (in "SCAN" mode). The temperature of ion source was 230 ºC.

2.3.4.3. Quantification

Signals registered as (chromatographic) peaks were quantified by comparing their size (area under curve) with the obtained area of a known amount (ng) of a reference substance (Toluene-d_8), which was adsorbed (by direct injection using a syringe) in an additional clean tube. The peak produced by the Toluene-d_8 was used as a reference peak to quantify all peaks obtained in the sample analysis and served as an estimation of a more accurate quantification based on calibration curves for each compound detected in the samples. This method based on Toluene-d_8 is known as semiquantitative quantification.

2.3.4.4. Quality parameters of the method

Detection limits depend on the chemical nature of the compound and the sampling and instrumental method used. As a general approach, this TD-GC/MS system can detect substances from 0.01 to 1 ng. Depending on the sampling method used, these values can be equivalent to 0.1 and 0.5 µg/m^3, respectively. The relative standard deviation (RSD) of the values obtained by this method is below 10%.

Chemical identifications were obtained by GC-Analyzer software which compares all detected fragment ions to allow the detection of very small differences either free from interferences or buried under large peaks. Additionally, all identified peaks were confirmed by the retention index, according to an own database. In complex cases (low/saturated or overlapped signals), manual checking was performed and comparison with our own database was also used. The compounds reported in this study were identified with a certainty higher than 80%, most of them over 90%. Peaks identified with

a certainty below 80% were classified as an "unknown" group and their concentrations were added up. Additionally, values below 0.1 µg/m^3 were included in this group.

2.3.5. H_2S and SO_2 quantification

Other compounds of interest, such as hydrogen sulfide and sulfur dioxide, are too volatile to be retained by the adsorption tubes. For this reason, these volatile sulfur compounds were quantified using a fully automatic isothermal gas chromatograph (Chroma S) coupled to a flame photometric detector (GC/FPD) developed by Chromatotec. This equipment is adequate for the analysis of sulfur compounds and has been described by Toledo et al. (2019a). Its detection limit is 7 ppb_v for both H_2S and SO_2. To perform the analysis, 0.5 g of each GAC were placed in 4-L Nalophan® sampling bags at 40 ºC and maintained in isothermal conditions for 24 h. The bags had been previously filled with clean, filtered air. One bag was prepared for each replicate, each of which was analyzed in duplicate.

2.3.6. Chemical contribution determination

The chemical contribution (PC_i; Wu et al., 2017) of the chemical families detected by TD-GC/MS indicates their relative concentration with respect to the total chemical concentration. PC_i (%) was calculated as follows:

$$PC_i\ (\%) = \frac{\sum C_i}{C_t} * 100 \quad (1)$$

where $\sum C_i$ is the cumulative concentration of a specific chemical family (µg/m^3) and C_t is the total chemical concentration (µg/m^3).

2.3.7. Odor activity values and odor contribution calculation

It is well established in the literature (Rincón et al., 2019; Schiavon et al., 2017; Zhu et al., 2016) that the odor activity value (OAV) is the ratio of the chemical concentration of a single compound to its odor detection threshold (ODT). OAV is a dimensionless parameter that has been widely employed to determine the odorous potential of each compound contained in an odorous sample (Laor et al., 2014). In this work, OAV_i represents the odorous potential of each chemical family and was calculated as follows:

$$OAV_i = \frac{\sum C_i}{ODT_i} \quad (2)$$

where $\sum C_i$ is the cumulative concentration of a specific chemical family (μg/m^3) and ODT_i is the geometric mean of the odor detection thresholds (μg/m^3) of the compounds included in that specific chemical family. Of the ODTs used, 94% were reported by Nagata (2003), while the remaining 6% were documented in Van Gemert (2011).

To determine the odor contribution (PO_i; Wu et al., 2017) of a chemical family, it is useful to calculate OAV_i, as this value indicates the relative importance of each chemical family with respect to the global olfactory perception. In this context, PO_i (%) was calculated as follows:

$$PO_i\ (\%) = \frac{OAV_i}{SOAV} * 100 \quad (3)$$

where OAV_i is the odor activity value of a specific chemical family (calculated by Eq. 2) and $SOAV$ is the sum of all OAV_i (i.e. $SOAV = \sum OAV_i$).

In this context, it is important to mention that odor monitoring based on OAVs presents two limitations: 1) the significant variability among ODTs found in the literature and within the same chemical family, and 2) the omission of possible interactions among odorants which may produce synergistic, antagonistic or even neutralizing effect when perceiving odorous gases (Parker et al., 2012; Wu et al., 2015).

3. Results and discussion

3.1. GAC composition, surface functional groups and pH

Pristine coconut-based GACs adsorb VOCs, but they have a relatively low capacity to adsorb inorganic H_2S (Water Environment Federation, 2017). In order to neutralize this acid and malodorous gas, WWTPs typically use activated carbons impregnated with alkali substances, such as NaOH or KOH. The use of NaOH or KOH for the GAC impregnation does not affect its adsorbing properties (Martin et al., 2010). In this sense, the XRF results (**Table 2**) show the presence of Na or K in the GACs, which comes from the alkaline impregnating agents. It is clear from this analysis that GAC-1, GAC-3 and GAC-4 were impregnated with NaOH, since high values of Na (%) can be observed,

while GAC-2 was impregnated with KOH. The elemental sulfur content (%) was also analyzed. It is worth noting that GAC-1 presented the highest relative content of S, followed by GAC-2, GAC-4 and GAC-3, the latter two with very low sulfur values. The high presence of this element, mainly in GAC-1 and GAC-2, suggests a higher retention of H_2S (in terms of chemisorption) in the early stages of the wastewater treatment process (i.e. in the pretreatment). However, this does not occur with the activated carbons from the sludge line deodorization (GAC-3 and GAC-4), where H_2S is removed by the action of $FeCl_3$. Therefore, it could justify the low sulfur content in both GAC-3 and GAC-4.

Table 2. Characterization of GAC samples: acidic and basic surface groups and elemental composition of Na, K and S.

GAC samples	Boehm method		X-ray fluorescence (XRF)		
	Basic surface groups [OH^-] (mmol/g GAC)	Acidic surface groups [H^+] (mmol/g GAC)	Na	K	S
			(% by weight)		
GAC-1	-	2.73 ± 0.38	2.79 ± 0.05	0.05 ± 0.01	15.25 ± 1.02
GAC-2	-	1.89 ± 0.28	0.20 ± 0.01	2.35 ± 0.08	5.09 ± 0.14
GAC-3	2.31 ± 0.06	-	3.95 ± 0.07	0.07 ± 0.01	0.50 ± 0.02
GAC-4	1.88 ± 0.25	-	3.75 ± 0.11	0.07 ± 0.01	0.57 ± 0.02

With regard to surface functional groups, and considering that GAC-0 was impregnated with alkaline solution (NaOH or KOH), the presence of basic groups in the GAC samples would be logical. **Table 2** shows the presence of these groups in both GAC-3 and GAC-4. Nevertheless, both GAC-1 and GAC-2 have surface acidic groups. This indicates that a large amount of acid compounds were chemically adsorbed during deodorization at the wastewater pretreatment stage. In these carbons, the neutralization reaction was so effective that the retention of acid compounds exhausted the basic groups of GAC-0 and reversed their basic pH of 9.6 to acidic pH values (**Fig. 2**). In addition, a higher content of surface acidic groups can be observed in GAC-1, which is related to a greater adsorption of acid compounds with respect to GAC-2. This is also observed in **Fig. 2**, which shows a lower (more acidic) pH for GAC-1 (pH = 4.1). This is due to the fact that different circumstances coexist at the pretreatment header (GAC-1), such as the high organic matter and nutrients load and the high presence of microorganisms and

anaerobic conditions, both of which entail a higher emission of acid compounds (especially H_2S) compared to the rest of the WWTP operations (Jiang et al., 2017).

Finally, in the case of GAC-3 and GAC-4, the pH values are basic and very similar to the pH of GAC-0. Therefore, it could be said that the gaseous compounds, which are emitted in the operations related to GAC-3 and GAC-4 (sludge thickening and sludge dehydration, respectively), were mainly retained by means of physical adsorption (physisorption) and/or the adsorption capacity of the bed was not exhausted before replacement. Therefore, the neutralization process was minimal in both GAC-3 and GAC-4.

3.2. Conductivity, TOC and TN_s

Conductivity values provide an approximate idea of the amount of gaseous compounds retained in GAC samples, since the water extracts some of these compounds, which remain in solution as ions. As can be observed in **Fig. 2**, GAC-1 presents the highest conductivity value (≈ 6 mS/cm), meaning that a greater quantity of ionic compounds was retained in the adsorbent. This reaffirms that the emission of odoriferous sulfur compounds (which have an ionic character) is greater at the pretreatment header. Furthermore, this is related to the percentage of sulfur retained by GAC-1, which was far higher than any of the other GACs (**Table 2**). Considering these latter carbons, an increase in conductivity was detected in all cases with respect to GAC-0, thus indicating that all of them retained (ionic) compounds during use.

TOC and TN_s refer to the fraction of organic and nitrogen compounds, respectively, which have been solubilized in water during the aqueous extract. Regarding both physico-chemical variables (**Fig. 2**), GAC-0 presents the lowest concentrations since this carbon was not used in any adsorption process, and the values are due to the composition of the pristine carbon itself. Therefore, the differences in TOC and TN_s from these minimum values are a consequence of the adsorption of compounds by the different GAC WWTP operations.

On the one hand, as regards TN_s, higher values were observed in the wastewater line deodorization GACs than in the sludge line GACs, highlighting TN_s related to GAC-2 (1.09 mg/g GAC). According to Nguyen et al. (2019), the emission of nitrogen compounds (especially NH_3) is greater in aerobic conditions (such as those taking place in the sand and fat removal) due to the ammonification and nitrification reactions carried

out by ammonifying and nitrifying bacteria, respectively. In addition, wastewater has a long residence time at this step of the WWTP. In contrast, anaerobic conditions predominate in the pretreatment header due to the high content of organic matter and microorganisms, which cause the dissolved oxygen to be consumed quickly. Despite this, due to the high content of nutrients in the header, among them nitrogen, they can be transferred from the liquid phase to the gas phase, thus explaining the high value of TN_s in GAC-1 (0.97 mg/g GAC). Regarding GAC-3 and GAC-4, low TOC and TN_s values were observed, especially in GAC-4. This is because GAC-4 was used in the deodorization of the anaerobically treated sludge dewatering. As a consequence of this operation, the microbial activity is considerably reduced (Nguyen et al., 2019) and the emission of nitrogen compounds is therefore lower.

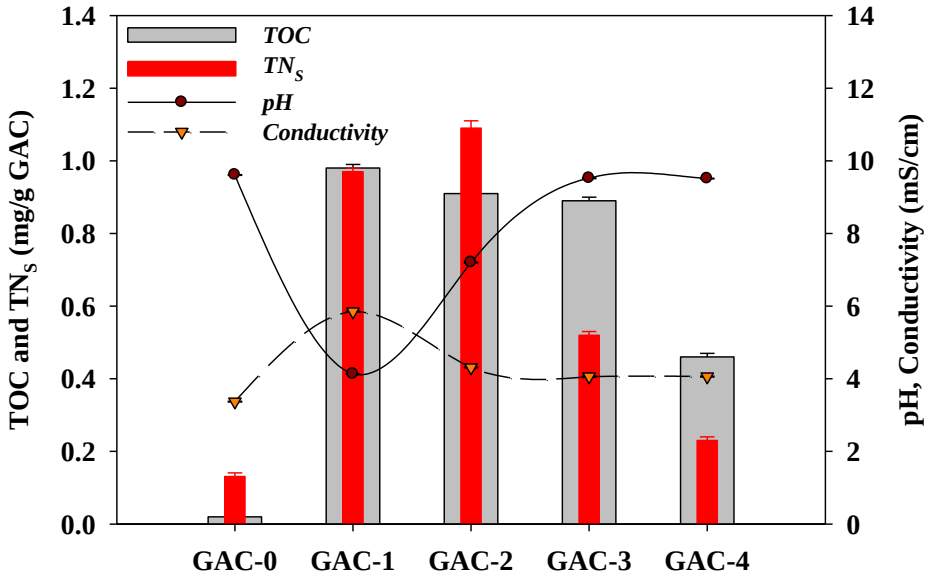

Fig. 2. Physico-chemical characterization of the GAC samples: soluble total organic carbon (TOC), soluble total nitrogen (TN_s), pH and conductivity.

Moreover, with respect to TOC, GAC-4 is also the adsorbent with the lowest value (0.46 mg/g GAC). This is due to two reasons: i) the reduction of microbial activity in the sludge dehydration step and ii) the reduction of biodegradable compounds in dehydrated sludge as a consequence of the previous anaerobic digestion carried out at the WWTP. Both processes reduce the typical odor emissions derived from sludge treatment (Orzi et al., 2015) and, consequently, the presence of TOC in GAC-4. In the case of GAC-1, GAC-2 and GAC-3, higher and similar values can be observed in **Fig. 2** (0.90–1.00 mg/g GAC) because of the higher organic load of the wastewater.

3.3. Specific odor concentration and quantified odorous families

In addition to the evaluation of the physico-chemical properties of the used GACs, their removed specific odor concentrations (SOCs) and the adsorbed gaseous families were studied.

It is well known that the odor concentration increases with increasing temperature (Toledo et al., 2019b; Wu et al., 2018). In the present study, SOC ($ou_E/m^3 \cdot g$ GAC) refers to the retained odor concentration per mass of adsorbent and the variation in SOC with temperature is shown in **Fig. 3**. As can be observed, SOC values increase with temperature up to 40 ºC (especially in GAC-1 and GAC-2), due to the higher desorption of retained compounds in comparison with lower temperatures. For this reason, 40 ºC was selected as the limiting temperature to study the desorbed compounds through TD-GC/MS and GC/FPD. In addition, that temperature is reached in summer in the province of Seville, where the WWTP is located, this being the most unfavorable situation in terms of odor nuisance. On this basis, controlling operational temperature in the different stages of wastewater treatment should be essential, especially in the sludge dehydration room when this waste comes from mesophilic anaerobic digestion (as occurs in the WWTP under study).

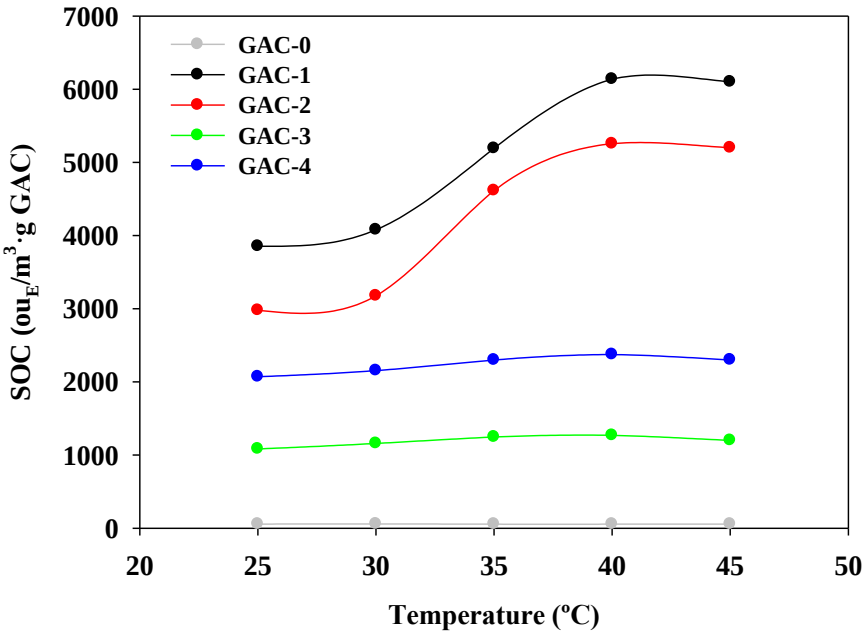

Fig. 3. Variation in the removed specific odor concentration (SOC) with temperature.

It is also important to note that the removed specific odor concentration followed a descending order of $SOC_{GAC-1} > SOC_{GAC-2} > SOC_{GAC-4} > SOC_{GAC-3} > SOC_{GAC-0}$. This

could suggest that the odor emissions were more significant in the first steps of the integral wastewater treatment (especially at the pretreatment header), which is line with the studies of Lebrero et al. (2011) and Gebicki et al. (2016). In order to clarify this issue, it is necessary to examine the results of the TD-GC/MS and GC/FPD analyses.

Semi-quantified volatile compounds (**Table S1**, Supplementary Material) are grouped into 14 gaseous families, which are shown in **Table 3**. Odor emissions from WWTPs often contain these families (Fisher et al., 2018; Lebrero et al., 2011). It is important to point out that ammonia was not quantified due to the limitations of the techniques used. Therefore, the amount of odorants retained was underestimated for the nitrogen-containing compounds family, since the emission of ammonia is common in WWTPs (Lebrero et al., 2011). Nevertheless, nitrogenous compounds are not major sources of WWTP odor due to the higher Henry's constants and higher ODTs with respect to other chemicals, such as sulfur compounds (Jiang et al., 2017). The major families retained in the GACs are analyzed in what follows.

- In GAC-1: terpenes, aliphatic hydrocarbons, aromatic compounds and sulfur-containing compounds were the predominant families. Terpenes are the family that most saturated this adsorbent and are possibly related to household discharges, because they are very common odoriferous compounds in cleaning agents and cosmetics (Lehtinen and Veijanen, 2011). Camphene (14.383 µg/g GAC) and d-limonene (8.751 µg/g GAC) together accounted for almost 60% of the total adsorbed terpenes. It is also important to highlight that GAC-1 was the carbon that retained a greater total amount of odorants.
- In GAC-2: sulfur-containing compounds and terpenes.
- In both GAC-3 and GAC-4, sulfur-containing compounds and, to a lesser extent, aromatic compounds predominated.

As can be seen in **Table 3**, there was a higher content of sulfur-containing compounds in all the carbons. According to Choi et al. (2012), the main chemical reactions which produce these compounds in wastewater are: (i) the reduction of sulfate to sulfide involving sulfate-reducing bacteria, (ii) the degradation of amino acids which contains sulfur, (iii) the methylation of methyl mercaptan by hydrogen sulfide and (iv) the generation of dimethyl sulfide by means of the oxidation of methyl mercaptan. In addition, it is important to note that H_2S, which is reported in the literature as the main

odoriferous compound in WWTPs (Talaiekhozani et al., 2016), was only present in GAC-1 (5.631 μg/g GAC) and GAC-2 (3.977 μg/g GAC) since this odorant was precipitated by the action of $FeCl_3$ in the sludge line operations. The presence of H_2S explains the lower pH values (**Fig. 2**) as well as the higher elemental sulfur values (**Table 2**) in both GAC-1 and GAC-2 with respect to the sludge line GACs due to the retention of the compound in terms of chemisorption. Therefore, it can be said that the combination of analytical techniques facilitates a better understanding of the physico-chemical processes that took place in each of the WWTP odor adsorption lines.

Table 3. Concentration of families of gaseous compounds identified in the GAC samples.

Families of compounds	**Concentration (μg/g GAC) (dry basis)**				
	GAC-0	**GAC-1**	**GAC-2**	**GAC-3**	**GAC-4**
Alcohols	0.230	1.513	0.735	0.150	0.512
Aldehydes	-	0.845	0.056	-	-
Aliphatic hydrocarbons	0.075	23.808	2.047	1.992	0.354
Aromatic compounds	-	23.001	9.384	6.177	9.143
Cyclic hydrocarbons	0.380	10.728	5.390	0.189	0.700
Esters	-	0.560	0.159	-	0.123
Ethers	0.108	0.562	0.160	0.032	0.070
Furans	0.588	-	0.010	0.133	0.135
Halogen-containing compounds	-	4.860	1.443	0.061	0.091
Ketones	-	5.213	1.483	-	0.091
Nitrogen-containing compounds	2.507	0.198	0.058	-	-
Organic acids	2.254	0.486	0.235	0.049	0.073
Sulfur-containing compounds	-	19.911	14.500	19.264	24.612
Terpenes	0.111	39.084	13.463	1.012	1.557
"Unknown"	3.061	18.210	1.351	0.309	0.135
Total concentration (TC)	9.314	148.978	50.475	29.368	37.596

Limit of detection (LOD): 0.0058 (μg/g GAC)

3.4. Chemical and odor contribution of the gaseous families

Taking into account the odor contribution of the gaseous families (PO_i), **Fig. 4** illustrates the results for this variable as well as the chemical contribution of each (PC_i) for purposes of comparison. As can be seen in the figure, the PO_i trend was different from the PC_i trend, especially in GAC-1 and GAC-2.

More specifically, in the case of the wastewater line GACs, **Fig. 4(a)** shows a very heterogeneous PC_i compared to the sludge line GACs, where sulfur compounds predominated (other than H_2S). It is also interesting that PC_i of aromatic compounds barely changed as the wastewater treatment process progressed. According to Maier (2019), this could be linked to the low water solubility of aromatic compounds, which results in slow biodegradation rates, thus hindering their bioelimination from wastewater and, consequently, from air (due to liquid-gas transfer).

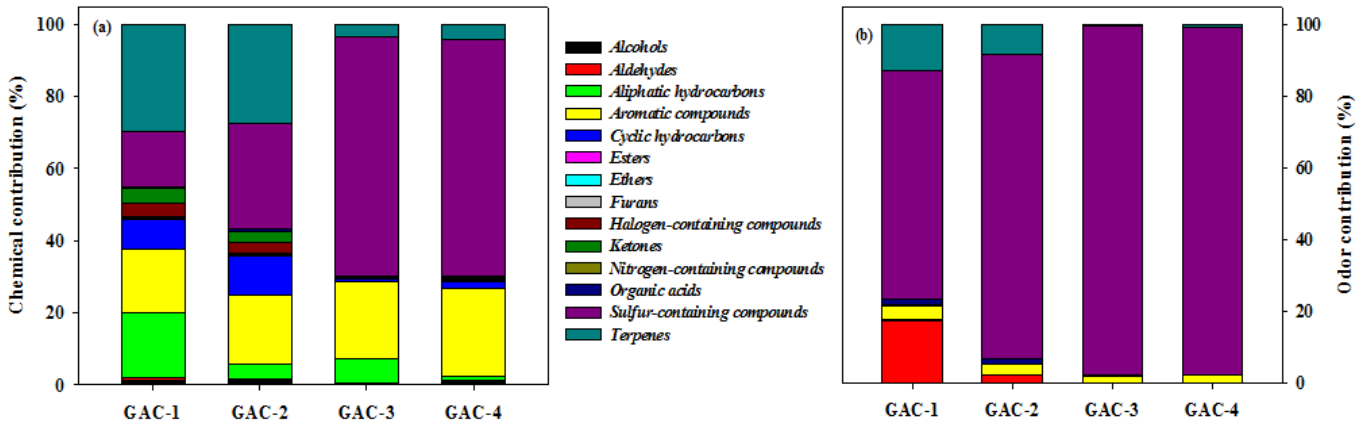

Fig. 4. Comparison between chemical contribution (a) and odor contribution (b) of the gaseous families.

Additionally, **Fig. 4(b)** shows that sulfur-containing compounds were the major odor contributors (PO_i = 61–97%) for all GACs, due to their very low ODTs (Byliński et al., 2019a). Taking into account the GACs derived from the wastewater line deodorization, hydrogen sulfide was by far the major odor contributor. However, in the case of the GACs from the sludge line deodorization, other volatile sulfur compounds continued to make a significant contribution to the total odor emitted from the sludge handling units, even when H_2S was eliminated by adding $FeCl_3$. These volatile sulfur compounds include the organic-reduced sulfur compounds, mainly dimethyl disulfide (DMDS), and to a lesser extent, dimethyl trisulfide (DMTS) and dimethyl sulfide (DMS), which are mainly produced by the anaerobic degradation of organic matter present in wastewater (Water Environment Federation, 2017). Therefore, the individual removal of

hydrogen sulfide from sewage results in a marginal reduction in the odor contribution if volatile organic sulfur compounds predominate. Finally, it is also important to note the odor contribution of aldehydes in GAC-1 ($PO_i \approx 17\%$). These compounds are most likely the result of the anaerobic degradation of organic matter (Lehtinen, 2013) and have also been reported as key odorants in WWTPs emissions (Jiang et al., 2017).

3.5. Textural properties

According to the previous analysis, a higher amount and variety of gaseous compounds were emitted in the first steps of the integral wastewater treatment, as can be seen in **Table 3** and **Fig. 4(a)**, respectively. This should cause a greater change in the textural properties of the GAC samples from the wastewater line deodorization (GAC-1 and GAC-2). In this context, **Table 4** shows very low values for both the free surface area (specific surface area, S_{BET}, and micropore area, S_{micro}) and the free pore volume (total pore volume, V_t, and micropore volume, V_{micro}) for the above mentioned carbons in comparison with pristine GAC-0 and the sludge line GACs (GAC-3 and GAC-4). It is also important to highlight the relevant role the micropores of the adsorbent beds had in deodorization, which were practically exhausted in GAC-1. Microporosity depletion caused an opposite effect in the value of the average pore width (D_{pore}), leading to an increase from 2.26 nm in GAC-0 to 4.54 and 2.48 nm in GAC-1 and GAC-2, respectively. These values confirm the textural change of GAC-0, which changed from a dual micro-mesoporous nature to a completely mesoporous character after the retention of the odoriferous compounds. With respect to the sludge line GACs, both the surface area and pore volume values decreased only slightly with respect to GAC-0 due to the lower intensity of the gaseous emissions in the sludge line operations, which was in turn related to the gradual decrease in the organic load as the treatment process progressed in the WWTP. Furthermore, the average pore width of both GAC-3 and GAC-4 was only slightly modified compared to GAC-0. As shown in **Table 4**, there was a slight increase in this variable due to the partial loss of microporosity and the consequent increase in mesoporosity.

Table 4. Textural properties of GAC samples.

GAC samples	S_{BET} (m^2/g)	S_{micro} (m^2/g)	V_t (cm^3/g)	V_{micro} (cm^3/g)	D_{pore} (nm)
GAC-0	406	236	0.229	0.180	2.26
GAC-1	36	-	0.041	0.012	4.54
GAC-2	156	63	0.097	0.049	2.48
GAC-3	336	229	0.191	0.170	2.28
GAC-4	328	169	0.191	0.145	2.33

S_{BET}, specific surface area; S_{micro}, micropore area; V_t, total pore volume; V_{micro}, micropore volume; D_{pore}, average pore width.

3.6. Relationships between variables: TC, SOC and V_{micro}

This last section provides an overview of the integral evaluation of the deodorization system of the urban WWTP in terms of total concentration of desorbed gaseous compounds (TC, µg/g GAC), free micropore volume (V_{micro}, cm^3/g) and removed specific odor concentration (SOC, $ou_E/m^3 \cdot g$ GAC). As shown in **Fig. 5**, GAC-1 is the adsorbent that retained the highest TC (≈ 150 µg/g GAC), while GAC-3 retained the lowest (≈ 30 µg/g GAC). Consequently, GAC-1 shows the lowest V_{micro} value, followed (in ascending order) by GAC-2, GAC-4 and finally GAC-3. As mentioned, NH_3 was not quantified, thus leading to an underestimation of TC. This is particularly noteworthy in GAC-2, where a high retention of NH_3 was detected (**Fig. 2** shows the highest TN_s for GAC-2). Given this, GAC-2 was excluded from a simple linear regression model (R^2 = 0.9925) used to inversely correlate TC with V_{micro}. GAC-0 was excluded from the model as it is the pristine sample.

Finally, the relationship between SOC and V_{micro} was also studied. Thus, without taking into account GAC-0, and by means of a simple linear regression model (R^2 = 0.9945), SOC was found to be inversely proportional to V_{micro} for the samples under study. This means that the lower V_{micro}, the higher SOC. For this reason, SOC might also be an indicator of the GAC adsorption capacity loss in the WWTP.

These results show that a multi-technical study of the most important characteristics of the adsorbent used in the urban WWTP contributes to a better understanding of the odor removal process (through adsorption by GAC) in the different steps of the integral wastewater treatment, as well as in possible operation strategies that optimize the efficiency and usage time of GAC systems.

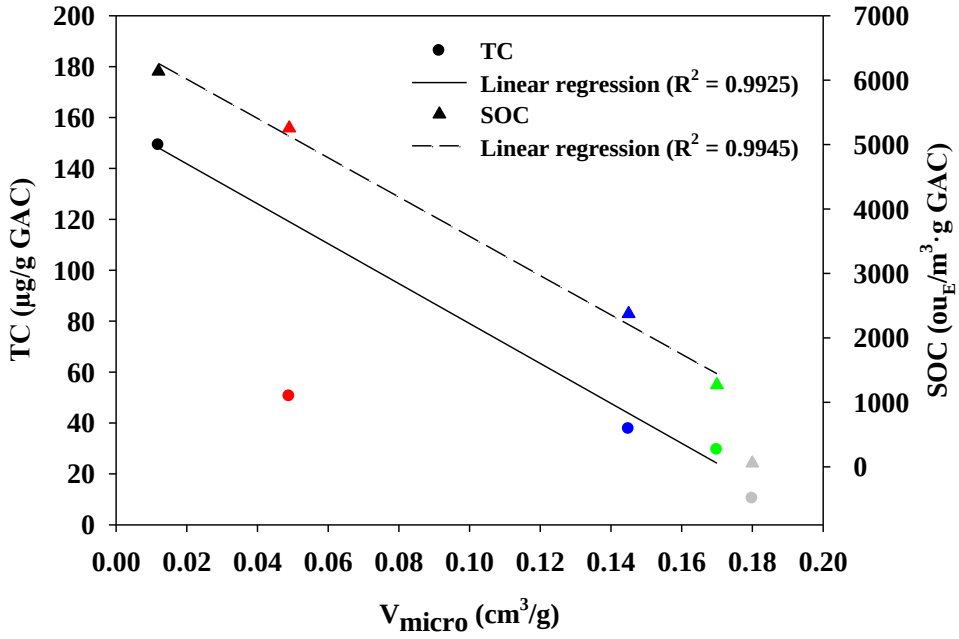

Fig. 5. Relationships between variables: total concentration of desorbed gaseous compounds (TC), removed specific odor concentration (SOC) and free micropore volume (V_{micro}). Legend: gray, GAC-0; black, GAC-1; red, GAC-2; green, GAC-3; blue, GAC-4 (For interpretation of the references to colour in this figure legend, the reader is referred to the web version of this article).

4. Limitations section

It is well known that the adsorption of compounds onto activated carbon follows different adsorption models (Le-Minh et al., 2018). However, GAC beds provide an averaged overview of all compounds removed after a long period of time of continuous operation (one year in the present study), including possible fluctuations both in the wastewater characteristics and the operation of the WWTP. The quantification of compound removal efficiencies has not been the objective of this work, but rather to determine those VOCs (and their concentrations) not emitted into the atmosphere. In this context, a semiquantitative quantification was carried out by TD-GC/MS, it being understood that for this type of determinations it constitutes the most robust method, although not the most sensitive. Recognizing that the quantification by TD-GC/MS has limitations, other volatile compounds of interest in WWTPs, such as H_2S and SO_2, were quantified using GC/FPD. Finally, it is assumed that chromatographic methods quantify

both odorous and non-odorous compounds, whereas dynamic olfactometry only quantifies odor concentration.

5. Conclusions

The main conclusions of this work are presented in what follows.

- In the urban WWTP under study, the wastewater line gaseous emissions were found to be more significant than the sludge line emissions. Thus, GAC-1 and GAC-2 showed a lower pH than GAC-3 and GAC-4, with the basic surface groups being exhausted in the first adsorbents.
- In line with the above, odor emissions mainly affect the textural properties of the wastewater line GACs, since these materials have a higher amount (and variety) of retained odoriferous compounds (especially GAC-1). The retention of odorants is also important in the sludge line GACs and is mainly related to the physisorption of sulfur VOCs (especially DMDS). In addition, TC and V_{micro} have been inversely correlated using a simple linear regression model (R^2 = 0.9925).
- SOC provides an estimated view of the odor concentration emitted at the different odor sources considered and might also be an indicator of the GAC adsorption capacity loss. Thus, SOC and V_{micro} have also been inversely correlated (R^2 = 0.9945).
- Sulfur-containing compounds were the major odor contributors in all the odor sources (PO_i = 61-97%). However, H_2S cannot be considered as the major odorant in the WWTP, since the removal of this compound alone led to a marginal reduction in odor contribution.

Given the above, the multi-technical analysis carried out in this study could be useful for the optimal design of deodorization operations based on GAC, as not all GAC beds have the same lifespan and the quantification of H_2S alone is insufficient to determine their odor removal efficiencies. In this sense, the dynamic olfactometric and/or the quantification of the GAC textural properties (S_{BET} and V_{micro}) provide better evidence of the saturation level of the GAC beds, which in turn may result in optimizing the use of the adsorbent material, operating costs and ambient air quality. With regard to the latter,

analyses of this kind would be beneficial for improving occupational health within WWTPs and reducing the odor impact in nearby populations.

Acknowledgements

This work was supported by the Spanish Ministry of Economy, Industry, and Competitiveness (MINECO), the Spanish State Research Agency (AEI) and the European Regional Development Fund (FEDER) through Projects CTM2017-88723-R and MAT2017-87541-R, and the Ministry of Education, Culture, and Sport of Spain (Grant FPU2016). The European Regional Development Fund (Project UCO-FEDER-1262384-R) and the Chelonia Association (Mares Circulares Project) also supported the work. A. Benítez is grateful to the Universidad de Córdoba (Plan Propio de Investigación 2019; sub. 2.4.) and the Andalusian Regional Government (FQM-175 group) for their financial support. The authors are very grateful to Olfasense GmbH for collaborating in this study. Finally, we wish to express our gratitude to Inmaculada Bellido and María Luisa López for their contribution to this research.

Appendix A. Supplementary data

Table S1. Concentration of chemical compounds identified in the GAC samples.

Chemical family	Compound	CAS number	ODT (µg/m^3)	Concentration (µg/g GAC) (dry basis)				
				GAC-0	GAC-1	GAC-2	GAC-3	GAC-4
Alcohols	Methyl Alcohol	67-56-1	43,221	-	0.187	0.126	-	0.415
	Ethanol	64-17-5	979	-	0.237	0.104	0.074	0.060
	Isopropyl Alcohol	67-63-0	63,872	-	0.601	0.285	0.034	0.037
	2-Propanol, 2-methyl-	75-65-0	13,634	-	0.057	-	-	-
	1-Propanol	71-23-8	231	-	0.185	0.142	-	-
	2-Butanol	78-92-2	667	-	0.138	0.015	0.042	-
	1-Propanol, 2-methyl-	78-83-1	33	-	0.036	0.016	-	-
	1-Butanol	71-36-3	115	-	0.073	0.047	-	-
	Propylene Glycol	57-55-6	NF	0.230	-	-	-	-
Aldehydes	Methacrolein	78-85-3	24	-	0.064	0.031	-	-
	Butanal	123-72-8	1.97	-	-	0.025	-	-
	Butanal, 3-methyl-	590-86-3	0.35	-	0.042	-	-	-
	Benzaldehyde	100-52-7	NF	-	0.739	-	-	-
Aliphatic Hydrocarbons	Isobutane	75-28-5	NF	0.075	0.616	0.098	-	-
	Pentane	109-66-0	4129	-	0.668	0.128	0.019	0.074
	1,4-Pentadiene	591-93-5	NF	-	0.047	-	0.012	0.045
	Pentane, 2-methyl-	107-83-5	24,658	-	1.154	0.183	0.055	-
	1-Pentene	109-67-1	287	-	-	-	1.723	-
	Pentane, 3-methyl-	96-14-0	31,352	-	0.845	0.122	-	-
	1-Hexene	592-41-6	482	-	0.097	-	-	0.026
	n-Hexane	110-54-3	5284	-	9.920	0.701	0.139	0.152
	3-Hexene, (Z)-	2097470	NF	-	0.040	-	-	-
	Pentane, 2,4-dimethyl-	108-08-7	3850	-	0.043	-	-	-
	1,5-Heptadiene	1541-23-7	NF	-	0.127	-	-	-
	Hexane, 3-methyl-	589-34-4	3440	-	0.083	-	-	-

	Heptane	142-82-5	2744	-	0.568	0.047	-	-
	Heptane, 2-methyl-	592-27-8	514	-	0.024	-	-	-
	Heptane, 3-methyl-	589-81-1	7004	-	0.025	-	-	-
	Octane	111-65-9	7938	-	0.813	0.074	0.043	0.058
	Octane, 3-methyl-	2216-33-3	NF	-	0.084	-	-	-
	Nonane	111-84-2	11,533	-	0.479	-	-	-
	4-Octene, 2,6-dimethyl-, [S-(E)]-	62960-76-3	NF	-	0.240	0.047	-	-
	Octane, 2,6-dimethyl-	2051-30-1	NF	-	0.294	0.027	-	-
	Heptane, 3-ethyl-2-methyl-	14676-29-0	NF	-	0.196	-	-	-
	Nonane, 4-methyl-	17301-94-9	NF	-	0.236	0.019	-	-
	Nonane, 2-methyl-	871-83-0	NF	-	0.247	-	-	-
	Decane	124-18-5	3606	-	2.134	0.260	-	-
	Decane, 4-methyl-	2847-72-5	NF	-	0.877	0.124	-	-
	Decane, 2-methyl-	6975-98-0	NF	-	0.547	0.028	-	-
	Decane, 3-methyl-	13151-34-3	NF	-	0.618	0.071	-	-
	Undecane	1120-21-4	5559	-	1.250	0.064	-	-
	Octane, 3,4,5,6-tetramethyl-	62185-21-1	NF	-	0.195	-	-	-
	Octane, 2,6,6-trimethyl-	54166-32-4	NF	-	0.044	-	-	-
	Undecane, 2-methyl-	7045-71-8	NF	-	0.164	-	-	-
	Undecane, 3-methyl-	1002-43-3	NF	-	0.238	-	-	-
	Dodecane	112-40-3	766	-	0.207	-	-	-
	Undecane, 2,6-dimethyl-	17301-23-4	NF	-	0.105	-	-	-
	C_9H_{20}	-	NF	-	0.135	0.011	-	-
	$C_{10}H_{22}$	-	NF	-	-	0.042	-	-
	$\sum C_{11}H_{24}$	-	NF	-	0.447	-	-	-
Aromatic compounds	Benzene	71-43-2	8620	-	0.104	0.028	-	0.101
	Toluene	108-88-3	1243	-	8.124	4.447	3.018	4.033
	Ethylbenzene	100-41-4	738	-	-	0.214	0.096	0.139
	m,p-Xylene	106-42-3	215	-	0.647	0.443	1.515	2.115
	o-Xylene	95-47-6	1649	-	0.054	0.083	0.046	0.087
	Styrene	100-42-5	149	-	-	0.069	-	-

	Benzene, propyl-	103-65-1	19	-	0.033	0.023	-	-
	Benzene, 1-ethyl-4-methyl-	622-96-8	NF	-	0.319	0.202	-	0.016
	Benzene, 1,2,4-trimethyl-	95-63-6	590	-	0.059	0.058	-	-
	Benzene, (1-methylethyl)-	98-82-8	41	-	0.026	0.030	-	-
	p-Cymene	99-87-6	313	-	12.927	3.575	1.501	2.639
	Phenol	108-95-2	22	-	-	0.019	-	0.013
	$\sum C_9H_{12}$	-	NF	-	0.708	0.195	-	-
Cyclic Hydrocarbons	Cyclopropane, ethyl-	1191-96-4	NF	-	0.049	-	-	-
	Cyclopropane, 1,1-dimethyl-	1630-94-0	NF	-	-	-	-	0.032
	Cyclopentene	142-29-0	NF	-	-	0.388	0.164	-
	Cyclopentane	287-92-3	NF	0.380	1.998	3.761	-	0.589
	Cyclopentane, methyl-	96-37-7	5848	-	0.581	0.085	0.025	0.022
	Cyclohexane, 1,2,4-trimethyl-, (1à,2á,4á)-	7667-60-9	NF	-	0.042	-	-	-
	1-Ethyl-4-methylcyclohexane	3728-56-1	NF	-	0.098	-	-	-
	Cyclopentene, 1,4-dimethyl-5-(1-methylethyl)-	61142-33-4	NF	-	0.047	-	-	-
	Cyclohexene, 4-methyl-1-(1-methylethyl)-, (R)-	619-52-3	NF	-	0.159	-	-	-
	Cyclopentene, 1,3-dimethyl-2-(1-methylethyl)-	61142-32-3	NF	-	0.185	0.017	-	-
	Cyclohexane, butyl-	1678-93-9	NF	-	0.576	0.081	-	-
	Cyclohexane, 1-ethyl-2-propyl-	62238-33-9	NF	-	0.292	0.048	-	-
	trans-Decalin	493-02-7	NF	-	3.597	0.497	-	0.040
	cis-Decalin	493-01-6	NF	-	1.403	0.223	-	0.016
	Cyclohexane, pentyl-	4292-92-6	NF	-	-	0.057	-	-
	Naphthalene, decahydro-2-methyl-	2958-76-1	NF	-	0.702	0.127	-	-
	$\sum C_{10}H_{20}$	-	NF	-	0.812	0.108	-	-
	$C_{11}H_{22}$	-	NF	-	0.186	-	-	-
Esters	Ethyl Acetate	141-78-6	3133	-	0.095	0.063	-	-
	Fenchyl acetate	13851-11-1	NF	-	0.465	0.096	-	-
	4-Penten-1-ol acetate	1576-85-8	NF	-	-	-	-	0.123
Ethers	Propane, 2-methoxy-	598-53-8	NF	-	0.227	0.067	-	-
	Ethyl ether	60-29-7	NF	-	0.246	0.093	0.032	0.070
	Propane, 2-ethoxy-2-methyl-	637-92-3	NF	-	0.081	-	-	-

	2-Propanol, 1-butoxy-	5131-66-8	865	0.108	-	-	-	-
	Diphenyl ether	101-84-8	696	-	0.009	-	-	-
Furans	Furan	110-00-9	27,546	0.588	-	0.010	-	-
	Furan, 2-methyl-	534-22-5	NF	-	-	-	0.121	0.114
	Furan, 2-pentyl-	3777-69-3	19	-	-	-	0.012	0.021
Halogen-containing compounds	Methylene chloride	75-09-2	NF	-	0.009	0.021	-	0.007
	Ethylene, 1,2-dichloro-, (E)-	156-60-5	NF	-	0.442	0.227	0.013	0.013
	Trichloromethane	67-66-3	18,541	-	0.900	0.283	-	-
	Carbon Tetrachloride	56-23-5	28,919	-	0.011	-	-	-
	Trichloroethylene	79-01-6	20,944	-	0.720	0.159	0.025	0.039
	Methane, bromodichloro-	75-27-4	NF	-	0.025	-	-	-
	Tetrachloroethylene	127-18-4	5218	-	2.752	0.753	0.022	0.032
Ketones	Acetone	67-64-1	99,710	-	4.089	1.330	-	0.058
	Methyl vinyl ketone	78-94-4	NF	-	-	0.018	-	-
	Cyclobutanone, 2,3-dimethyl-, cis-	28113-36-2	NF	-	0.057	-	-	-
	Cyclohexanone, 3,3,5-trimethyl-	873-94-9	NF	-	0.169	-	-	-
	Cyclobutanone, 2,3-dimethyl-, trans-	1942-42-3	NF	-	0.168	-	-	-
	Fenchone	1195-79-5	2261	-	0.690	0.135	-	0.033
	Ethanone, 1-(4-methylphenyl)-	122-00-9	NF	-	0.039	-	-	-
Nitrogen-containing compounds	6-Aminotetrazolo(b)pyridazine	19195-43-8	NF	-	0.019	-	-	-
	2-Pyrazoline, 4-ethyl-1-isopropyl-	33193-27-0	NF	-	0.049	-	-	-
	1-Butanamine, N-butyl-	111-92-2	423	0.189	-	-	-	-
	5-Amino-3-methylpyrazole	31230-17-8	NF	-	-	0.058	-	-
	Methenamine	100-97-0	NF	2.318	0.094	-	-	-
	$C_4H_7N_3$	-	NF	-	0.037	-	-	-
Organic Acids	Acetic acid	64-19-7	15	2.254	0.486	0.235	0.049	0.073
Sulfur-containing compounds	Dimethyl sulfide	75-18-3	7.62	-	0.016	-	0.095	-
	Methyl thiolacetate	1534-08-3	NF	-	0.025	-	-	-
	Disulfide, dimethyl	624-92-0	8.47	-	12.755	4.142	15.397	21.212
	Thiophene, 3-methyl-	616-44-4	NF	-	0.050	-	-	0.039

	Methyl ethyl disulfide	20333-39-5	NF	-	0.016	-	-	0.018
	Dimethyl trisulfide	3658-80-8	14	-	1.418	0.693	0.255	0.255
	Hydrogen sulfide	7783-06-4	0.57	-	5.631	3.977	-	-
	Sulfur dioxide	7446-09-5	2278	-	-	5.689	3.517	3.089
Terpenes	Cyclofenchene	488-97-1	NF	-	0.531	0.030	-	-
	Tricyclene	508-32-7	NF	-	1.486	0.425	0.045	0.090
	(-)-β-Citronellene	10281-56-8	NF	-	1.327	0.245	0.018	0.018
	à-Pinene	80-56-8	100	-	3.133	3.597	0.339	0.471
	à-Phellandrene	99-83-2	NF	-	-	0.021	-	-
	Bicyclo[2.2.1]heptane, 2,2-dimethyl-5-methylene-	497-32-5	NF	-	0.233	0.036	-	-
	(+)-Camphene	5794-03-6	NF	-	3.047	0.785	0.122	0.184
	Camphene	79-92-5	4900	-	14.383	3.184	0.373	0.587
	3-p-Menthene	500-00-5	NF	-	-	0.085	0.027	0.052
	(-)-β-Pinene	18172-67-3	184	-	-	0.073	0.027	0.035
	1,4-Cineol	470-67-7	NF	-	2.112	0.562	-	-
	D-Limonene	5989-27-5	212	0.111	8.751	3.537	0.054	0.089
	Eucalyptol	470-82-6	5.01	-	2.123	0.566	0.006	0.023
	m-Cymenene	1124-20-5	NF	-	0.111	0.016	-	0.008
	Fenchol	1632-73-1	NF	-	-	0.129	-	-
	(+)-2-Bornanone	464-49-3	NF	-	1.052	0.119	-	-
	endo-Borneol	507-70-0	NF	-	0.578	0.036	-	-
	(-)-Bornyl acetate	5655-61-8	NF	-	0.218	0.018	-	-
"Unknown"	∑ unknown	-	-	3.061	18.210	1.351	0.309	0.135

Odor detection threshold (ODT) column: Underlined ODTs were obtained from Van Gemert (2011). The rest of ODT were obtained from Nagata (2003). NF: not found.

References

Boehm, H.P., 1994. Some aspects of the surface chemistry of carbon blacks and other carbons. Carbon N. Y. https://doi.org/10.1016/0008-6223(94)90031-0

Burgess, J.E., Parsons, S.A., Stuetz, R.M., 2001. Developments in odour control and waste gas treatment biotechnology: a review. Biotechnol. Adv. 19, 35–63. https://doi.org/10.1016/S0734-9750(00)00058-6

Byliński, H., Aszyk, J., Kubica, P., Szopińska, M., Fudala-Książek, S., Namieśnik, J., 2019a. Differences between selected volatile aromatic compound concentrations in sludge samples in various steps of wastewater treatment plant operations. J. Environ. Manage. 249, 109426. https://doi.org/10.1016/j.jenvman.2019.109426

Byliński, H., Gębicki, J., Namieśnik, J., 2019b. Evaluation of health hazard due to emission of volatile organic compounds from various processing units of wastewater treatment plant. Int. J. Environ. Res. Public Health 16. https://doi.org/10.3390/ijerph16101712

Capelli, L., Sironi, S., Del Rosso, R., Céntola, P., 2009. Predicting odour emissions from wastewater treatment plants by means of odour emission factors. Water Res. 43, 1977–1985. https://doi.org/10.1016/j.watres.2009.01.022

Choi, I., Lee, H., Shin, J., Kim, H., 2012. Evaluation of the effectiveness of five odor reducing agents for sewer system odors using an on-line total reduced sulfur analyzer. Sensors (Switzerland) 12, 16892–16906. https://doi.org/10.3390/s121216892

Domingo, J.L., Nadal, M., 2009. Domestic waste composting facilities: A review of human health risks. Environ. Int. 35, 382–389. https://doi.org/10.1016/j.envint.2008.07.004

Easter, C., Witherspoon, J., Voigt, R., and Cesca, J., 2008. An odor control master planning approach to public outreach programs. Pap. Present. 3rd IWA Int. Conf. Odour VOCs, Barcelona, Spain.

EN 13725, 2003. Air Quality - Determination of Odour Concentration by Dynamic Olfactometry. European Committee for Standardization, Brussels.

Estrada, J.M., Kraakman, N.J.R.B., Muñoz, R., Lebrero, R., 2011. A comparative analysis of odour treatment technologies in wastewater treatment plants. Environ. Sci. Technol. 45, 1100–1106. https://doi.org/10.1021/es103478j

European Commission, 2018. Commission notice on technical guidance on the classification of waste (2018/C 124/01). Brussels.

European Commission, 2001. Working document: biological treatment of biowaste, 2nd draft. Brussels.

Fisher, R.M., Barczak, R.J., Suffet, I.H.M., Hayes, J.E., Stuetz, R.M., 2018. Framework for the use of odour wheels to manage odours throughout wastewater biosolids processing. Sci. Total Environ. 634, 214–223. https://doi.org/10.1016/j.scitotenv.2018.03.352

Gebicki, J., Byliński, H., Namieśnik, J., 2016. Measurement techniques for assessing the olfactory impact of municipal sewage treatment plants. Environ. Monit. Assess. 188, 1–15. https://doi.org/10.1007/s10661-015-5024-2

Hayes, J.E., Stevenson, R.J., Stuetz, R.M., 2017. Survey of the effect of odour impact on communities. J. Environ. Manage. 204, 349–354. https://doi.org/10.1016/j.jenvman.2017.09.016

Jiang, G., Melder, D., Keller, J., Yuan, Z., 2017. Odor emissions from domestic wastewater: A review. Crit. Rev. Environ. Sci. Technol. 47, 1581–1611. https://doi.org/10.1080/10643389.2017.1386952

Jiang, J., Coffey, P., Toohey, B., 2006. Improvement of odor intensity measurement using dynamic olfactometry. J. Air Waste Manag. Assoc. 56, 675–683. https://doi.org/10.1080/10473289.2006.10464474

Kasper, P.L., Oxbøl, A., Hansen, M.J., Feilberg, A., 2018. Mechanisms of Loss of Agricultural Odorous Compounds in Sample Bags of Nalophan, Tedlar, and PTFE. J. Environ. Qual. 47, 246–253. https://doi.org/10.2134/jeq2017.07.0289

Laor, Y., Parker, D., Pagé, T., 2014. Measurement, prediction, and monitoring of odors in the environment: A critical review. Rev. Chem. Eng. 30, 139–166. https://doi.org/10.1515/revce-2013-0026

Le-Minh, N., Sivret, E.C., Shammay, A., Stuetz, R.M., 2018. Factors affecting the adsorption of gaseous environmental odors by activated carbon: A critical review. Crit. Rev. Environ. Sci. Technol. 48, 341–375. https://doi.org/10.1080/10643389.2018.1460984

Le, H. V., Sivret, E.C., Parcsi, G., Stuetz, R.M., 2015. Impact of Storage Conditions on the Stability of Volatile Sulfur Compounds in Sampling Bags. J. Environ. Qual. 44, 1523–1529. https://doi.org/10.2134/jeq2014.12.0532

Lebrero, R., Bouchy, L., Stuetz, R., Muñoz, R., 2011. Odor Assessment and Management in Wastewater Treatment Plants: A Review. Crit. Rev. Environ. Sci. Technol. 41, 915–950. https://doi.org/10.1080/10643380903300000

Lehtinen, J., 2013. Case Studies for Assessment, Control and Prediction of Odour Impact: Urban Wastewater Treatment Plant, in: Belgiorno, V., Naddeo, V., Zarra, T. (Eds.), Odour Impact Assessment Handbook. John Wiley & Sons, Ltd., pp. 205–218. https://doi.org/10.1002/9781118481264

Lehtinen, J., Veijanen, A., 2011. Determination of odorous VOCs and the risk of occupational exposure to airborne compounds at the waste water treatment plants. Water Sci. Technol. 63, 2183–2192. https://doi.org/10.2166/wst.2011.372

Maier, R.M., 2019. Biological Processes Affecting Contaminants Transport and Fate, in: Brusseau, M.L., Gerba, C.P., Pepper, I.L. (Eds.), Environmental and Pollution Science. Elsevier, pp. 131–146. https://doi.org/10.1016/b978-0-12-814719-1.00009-4

Martin, M.J., Anfruns, A., Lebrero, R., Estrada, J.M., Canals, C., Vega, E., 2010. Procesos de adsorción, in: Muñoz, R., Lebrero, R., Estrada, J.M. (Eds.), Caracterización y Gestión de Olores En Estaciones Depuradoras de Aguas Residuales. Gráficas Germinal S.C.L., Valladolid (España), pp. 115–126.

Morales, J.J., Köning, H., Garcés, J., and Senante, E., 2008. Integrated odour control and management in WWTP of the Region Metropolitana of Santiago de Chile. Pap. Present. 3rd IWA Int. Conf. Odour VOCs, Barcelona, Spain.

Nagata, Y., 2003. Odor Measurement Review, Measurement of Odor Threshold by Triangle Odor Bag Method. Minist. Environ. Gov. Japan 122–123.

Nguyen, C., Do, D.D., 2001. The Dubinin-Radushkevich equation and the underlying microscopic adsorption description. Carbon N. Y. 39, 1327–1336. https://doi.org/10.1016/S0008-6223(00)00265-7

Nguyen, T.K.L., Ngo, H.H., Guo, W., Chang, S.W., Nguyen, D.D., Nghiem, L.D., Liu, Y., Ni, B., Hai, F.I., 2019. Insight into greenhouse gases emissions from the two popular treatment technologies in municipal wastewater treatment processes. Sci. Total Environ. 671, 1302–1313. https://doi.org/10.1016/j.scitotenv.2019.03.386

Orzi, V., Scaglia, B., Lonati, S., Riva, C., Boccasile, G., Alborali, G.L., Adani, F., 2015. The role of biological processes in reducing both odor impact and pathogen content during mesophilic anaerobic digestion. Sci. Total Environ. 526, 116–126. https://doi.org/10.1016/j.scitotenv.2015.04.038

Parker, D.B., Koziel, J.A., Cai, L., Jacobson, L.D., Akdeniz, N., Bereznicki, S.D., Lim, T.T., Caraway, E.A., Zhang, S., Hoff, S.J., Heber, A.J., Heathcote, K.Y., Hetchler, B.P., 2012. Odor and Odorous Chemical Emissions from Animal Buildings: Part 6. Odor Activity Value. Trans. ASABE 55, 2357–2368. https://doi.org/10.13031/2013.42498

Rincón, C.A., De Guardia, A., Couvert, A., Le Roux, S., Soutrel, I., Daumoin, M., Benoist, J.C., 2019. Chemical and odor characterization of gas emissions released during composting of solid wastes and digestates. J. Environ. Manage. 233, 39–53. https://doi.org/10.1016/j.jenvman.2018.12.009

Schiavon, M., Martini, L.M., Corrà, C., Scapinello, M., Coller, G., Tosi, P., Ragazzi, M., 2017. Characterisation of volatile organic compounds (VOCs) released by the composting of different waste matrices. Environ. Pollut. 231, 845–853. https://doi.org/10.1016/j.envpol.2017.08.096

Talaiekhozani, A., Bagheri, M., Goli, A., Talaei Khoozani, M.R., 2016. An overview of principles of odor production, emission, and control methods in wastewater collection and treatment systems. J. Environ. Manage. 170, 186–206. https://doi.org/10.1016/j.jenvman.2016.01.021

Tchobanoglous, G., Burton, F.L., Stensel, H.D., 2003. Wastewater engineering: Treatment and reuse. McGraw Hill, New York, NY.

Toledo, M., Guillot, J.M., Siles, J.A., Martín, M.A., 2019a. Permeability and adsorption effects for volatile sulphur compounds in Nalophan sampling bags: Stability influenced by storage time. Biosyst. Eng. 188, 217–228. https://doi.org/10.1016/j.biosystemseng.2019.10.023

Toledo, M., Márquez, P., Siles, J.A., Chica, A.F., Martín, M.A., 2019b. Co-composting of sewage sludge and eggplant waste at full scale: Feasibility study to valorize eggplant waste and minimize the odoriferous impact of sewage sludge. J. Environ. Manage. 247, 205–213. https://doi.org/10.1016/j.jenvman.2019.06.076

US Department of Agriculture and The US Composting Council, 2002. Test Methods for the Examination of Composting and Compost (TMECC). Edaphos International, Houston (TX).

Van Gemert, L.J., 2011. Odor Thresholds – Compilation of Odor Threshold Values in Air, Water and Other Media, second. ed. Oliemans, Punter & Partners BV, the Netherlands.

VDI guideline 3880, 2011. Olfactometry – Static Sampling. Beuth Verlag GmbH, Berlin, pp. 10772, n.d.

Water Environment Federation, 2017. Liquid Stream Fundamentals: Odor Management and Control [Fact Sheet] [WWW Document]. URL https://www.wef.org/globalassets/assets-wef/direct-download-library/public/03---resources/wsec-2017-fs-028-liquid-stream-fundamentals--odor-control_final.pdf (accessed 3.11.20).

Watson, S.B., Jüttner, F., 2017. Malodorous volatile organic sulfur compounds: Sources, sinks and significance in inland waters. Crit. Rev. Microbiol. https://doi.org/10.1080/1040841X.2016.1198306

Wu, C., Liu, J., Liu, S., Li, W., Yan, L., Shu, M., Zhao, P., Zhou, P., Cao, W., 2018. Assessment of the health risks and odor concentration of volatile compounds from a municipal solid waste landfill in China. Chemosphere 202, 1–8. https://doi.org/10.1016/j.chemosphere.2018.03.068

Wu, C., Liu, J., Yan, L., Chen, H., Shao, H., Meng, T., 2015. Assessment of odor activity value coefficient and odor contribution based on binary interaction effects in waste disposal plant. Atmos. Environ. 103, 231–237. https://doi.org/10.1016/j.atmosenv.2014.12.045

Wu, C., Liu, J., Zhao, P., Li, W., Yan, L., Piringer, M., Schauberger, G., 2017. Evaluation of the chemical composition and correlation between the calculated and measured odour concentration of odorous gases from a landfill in Beijing, China. Atmos. Environ. 164, 337–347. https://doi.org/10.1016/j.atmosenv.2017.06.010

Zhu, Y., Zheng, G., Gao, D., Chen, T., Wu, F., Niu, M., Zou, K., 2016. Odor composition analysis and odor indicator selection during sewage sludge composting. J. Air Waste Manage. Assoc. 66, 930–940. https://doi.org/10.1080/10962247.2016.1188865

II.2. Breve descripción del artículo: "*Simple and eco-friendly thermal regeneration of granular activated carbon from the odour control system of a full-scale WWTP: Study of the process in oxidizing atmosphere*"

II.2. Breve descripción del artículo: "*Simple and eco-friendly thermal regeneration of granular activated carbon from the odour control system of a full-scale WWTP: Study of the process in oxidizing atmosphere*"

La adsorción mediante GAC constituye un sistema eficiente y confiable para el tratamiento de los malos olores en EDAR. Sin embargo, una vez agotada la vida útil del mencionado adsorbente, éste se convierte en residuo industrial peligroso, siendo frecuentemente depositado en vertedero. En el marco de la economía circular, el presente artículo ha tenido por objeto la regeneración térmica en flujo simple de aire del GAC procedente del sistema de control de olores de una EDAR urbana, persiguiendo su reutilización como adsorbente de olores en este tipo de instalaciones y evitando, a su vez, el empleo de atmósferas inertes de elevado coste y postratamientos adicionales complejos. En este sentido, se caracterizó en profundidad el GAC derivado de dos puntos de desodorización de la EDAR mencionada anteriormente, tanto antes como después de su regeneración térmica oxidativa. Las muestras de adsorbente procedieron de la desodorización de la cabecera de pretratamiento (muestra P1) y la deshidratación del fango (muestra P2). La caracterización previa demostró que las condiciones de regeneración del GAC dependían de la naturaleza de los compuestos adsorbidos después de un mismo tiempo de operación (un año), mientras que la caracterización posterior a la regeneración demostró la recuperación e incluso mejora de las propiedades originales del material adsorbente. Así, se alcanzaron valores de área superficial específica (S_{BET}) superiores a 550 m^2/g, tanto para la muestra P1 como para la P2, superándose considerablemente el valor de 406 m^2/g de la muestra prístina (muestra P0). Además, en ambas muestras también se recuperó la estructura microporosa, destacando el caso de la muestra P1, que se encontraba prácticamente saturada y, tras la regeneración, su volumen de microporo fue 1,27 veces superior al valor de la muestra P0 (0,180 cm^3/g). En base a lo anterior y teniendo en cuenta las buenas eficacias de regeneración alcanzadas (72−98%), se puede decir que la regeneración térmica oxidativa a temperaturas no superiores a 350ºC puede constituir una alternativa sencilla y sostenible para revalorizar el carbón activado granular utilizado en los sistemas de desodorización de las EDAR.

Separation and Purification Technology 255 (2021) 117782

Contents lists available at ScienceDirect

Separation and Purification Technology

journal homepage: www.elsevier.com/locate/seppur

Simple and eco-friendly thermal regeneration of granular activated carbon from the odour control system of a full-scale WWTP: Study of the process in oxidizing atmosphere

Márquez, P. [a,ϕ], Benítez, A. [b,ϕ], Hidalgo-Carrillo, J. [c], Urbano, F.J. [c], Caballero, Á. [b], Siles, J.A. [a], Martín, M.A. [a,*]

[a] Department of Inorganic Chemistry and Chemical Engineering, Area of Chemical Engineering, University of Cordoba, Campus Universitario de Rabanales, Carretera N-IV, km 396, Edificio Marie Curie, 14071 Córdoba, Spain

[b] Dpto. Química Inorgánica e Ingeniería Química, Instituto Universitario de Nanoquímica (IUNAN), Universidad de Córdoba, 14071 Córdoba, Spain

[c] Departamento de Química Orgánica, Instituto Universitario de Nanoquímica (IUNAN), Universidad de Córdoba, 14071 Córdoba, Spain

[ϕ] Márquez, P. and Benítez, A. contributed equally to the work.

* Corresponding author: iq2masam@uco.es

Received 5 June 2020; Received in revised form 15 September 2020; Accepted 19 September 2020; Available online 25 September 2020

Abbreviations: AC, activated carbon; FS, fixed solids (%); GAC, granular activated carbon; GC, gas chromatography; MS, mass spectrometry; ou_E, European odour units; P0, pristine GAC sample; P1, GAC sample from pretreatment header deodorization; P1-R4, sample P1 regenerated at 4 hours (350 ºC); P2, GAC sample from sludge dewatering deodorization; P2-R3, sample P2 regenerated at 3 hours (250 ºC); S_{BET}, specific surface area (m^2/g); S_{micro}, micropore area (m^2/g); SOC, removed specific odour concentration ($ou_E/m^3 \cdot g$ GAC); TC, total concentration of desorbed gaseous compounds (µg/g GAC); TD, thermal desorption; TGA, thermogravimetric analysis; TN_s, soluble total nitrogen (mg/g GAC); TOC, soluble total organic carbon (mg/g GAC); V_{micro}, micropore volume (cm^3/g); VOCs, volatile organic compounds; VS, volatile solids (%); V_t, total pore volume (cm^3/g); WWTPs, wastewater treatment plants; XRD, X-ray diffraction; XRF, X-ray fluorescence.

Graphical abstract

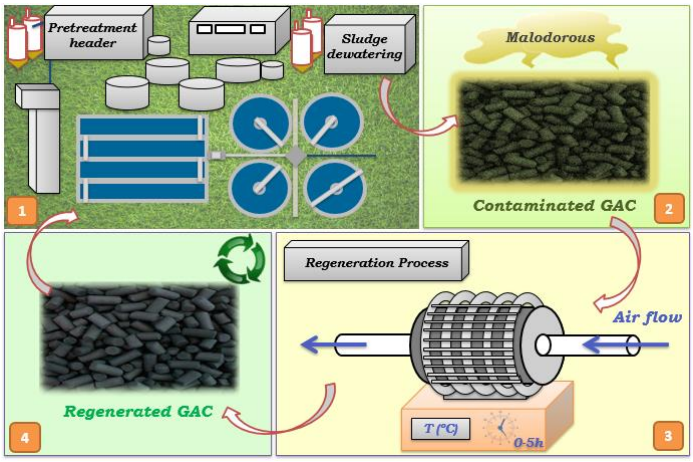

Abstract

Adsorption by granular activated carbon (GAC) is an efficient, reliable, and well-established technique for treating malodours in wastewater treatment plants (WWTPs). However, when the lifespan of GAC is over, it becomes a hazardous industrial waste, which is mostly discarded in landfills. In the framework of a sustainable economy, this work proposes an oxidative thermal regeneration of GAC from the odour control system of an urban WWTP for reuse, mainly as an odour adsorbent in WWTPs, avoiding the use of high-cost inert atmosphere and complex additional post-treatments. In this sense, GAC, from two deodorization points of the abovementioned facility, the pretreatment header (P1 sample) and sludge dewatering (P2 sample), has been characterized in depth, both before and after its regeneration. Previous characterization has shown that GAC regeneration conditions depend on the nature of adsorbed odorants after the same operating time, while post-regeneration characterization has proven the recovery of the GAC's original properties. Thus, specific surface area (S_{BET}) values above 550 m^2/g have been reached for both P1 and P2, considerably exceeding the pristine sample (P0) value of 406 m^2/g. Furthermore, the microporous structure was also recovered in both samples, highlighting the case of the almost non-porous P1 sample, whose micropore volume exceeded 1.27 times the value of the P0 sample (0.180 cm^3/g) after regeneration. On the basis of the above, and taking into account the good regeneration efficiencies reached (72 - 98 %), the oxidative thermal regeneration at temperatures no higher than 350 ºC can be a simple and sustainable alternative to revalue GAC used in WWTPs.

Keywords: deodorization; granular activated carbon; oxidative thermal regeneration; reuse; WWTP.

1. Introduction

Increasingly stringent environmental regulations, the recovery of high added value chemicals in industry, or the need to find new solutions for energy storage have increased the production and use of activated carbon (AC) in recent decades [1–3]. In this context, AC is an excellent material for removing pollutants from water environments [4], for gas purification [5], or as a component of advanced energy storage systems, such as rechargeable batteries [6,7] and supercapacitors [8,9].

Traditionally, the raw materials used for ACs' production come from non-renewable and high-cost sources, such as wood, peat, lignite, coal, petroleum fractions, and derivatives, such as polymers [10,11]. Therefore, much research has been devoted to the preparation of AC using more sustainable and economic precursors, including agricultural residues (rice husk, corn straw, bagasse, etc.) and industrial or household wastes (sludge, animal waste, garden waste, etc.) [10,12]. Moreover, coconut shells, woods, and bamboo have been used to develop an alternative method of low-cost AC production [1,13]. The mentioned biomass sources allow for low-cost and sustainable ACs. However, large quantities are required to be used in energy storage systems, and in certain cases, these products may be competitive with human or animal feed. The most common example of this problem could be for the bioethanol production process, where edible products, such as corn and sugar cane, are usually used [14].

At present, AC regeneration is a way to avoid using raw materials to manufacture fresh ACs. According to El Gamal et al. [15], several regeneration methods can be selected, depending on the nature of the pollutant, recovery cost, and process conditions. The regeneration methods include thermal, chemical, microwave, electrochemical, supercritical carbon dioxide, and bio-regeneration processes. Among them, thermal regeneration under inert atmosphere is the most widely used one at industrial scale, with three main indicators to evaluate its feasibility: mass loss, adsorption capacity, and granular strength of the regenerated AC. Nevertheless, because of the operational conditions required for thermal regeneration, deposition of AC in landfill is still considered the most economical option, due to both the high cost of the inert gasifying agent and energy requirement, since high operating temperatures (above 500 ºC) are necessary [16].

The properties of AC depend on the starting material used for its manufacture and the conditions of the regeneration process (if this is carried out). The most characteristic properties are surface area, pore size, particle size, surface chemistry, hardness, ash content, and pH (in aqueous suspensions). These properties can be modified depending on the activation and carbonization processes used to obtain AC. It is predominantly performed by a physical or chemical activation method. In addition, ACs can be subjected to various chemical treatments, such as acidic and alkaline treatments, that increase their pore volume, adsorption selectivity, and functional groups content [17,18]. Agricultural waste-based ACs have been treated with different chemical agents such as HCl, H_2SO_4, HNO_3, and H_3PO_4 [19–21], as well as $ZnCl_2$, KOH, and NaOH [22–24]. As a result of these activation processes, active carbons can be designed with the appropriate characteristics to retain different types of compounds on their surface, for example, acting as filters to remove gaseous pollutants [5,25].

In wastewater treatment plants (WWTPs), activated and impregnated carbons can be used independently or in combination to remove many different odour-causing compounds [26]. In this sense, granular activated carbon (GAC) packed-bed systems are widely used for deodorization in WWTPs, due to their ability to easily adsorb a wide range of odorants, such as VOCs, mercaptans, ammonia and H_2S [27]. Virgin GAC adsorbs volatile organic compounds (VOCs), but it has a relatively low capacity to adsorb inorganic H_2S, which has been reported in the literature as the main malodorous compound in WWTPs [28,29]. For this reason, in order to neutralize this odorant, WWTPs typically use GAC impregnated with alkali compounds, such as NaOH or KOH. The reaction of these compounds with atmospheric CO_2 leads to the formation of corresponding carbonates, facilitating the transfer of H_2S to the solid phase and promoting its oxidation to elemental sulphur or sulphur oxides [30,31]. According to Estrada et al. [25], a disadvantage of GAC filtration in WWTPs is that this system presents high annual packed-bed-material requirements (0.8 ± 0.6 kg/$(m^3/h)_{air\ treated}$) because of the short lifespan of GAC (approximately six months). Such type of carbon beds could use up to a maximum of 10,000 kg of GAC [31]. When the lifespan of GAC used in deodorization is over, it becomes a hazardous industrial waste, which is mostly discarded in landfills through authorized waste managers, resulting in a significant economic and environmental cost [27]. Thus, with the objective of promoting circular economy, different international organizations have established legislation to reduce landfill waste

deposition. For example, the European Parliament and Council [32] established, in its Directive 2018/850, that "Member States shall take the necessary measures to ensure that by 2035 the amount of municipal waste landfilled is reduced to 10% or less of the total amount of municipal waste generated (by weight)".

In this context, the regeneration of contaminated GAC is an attractive alternative for facilities that use such adsorbent routinely. Moreover, in a non-profit sector such as wastewater treatment (which includes the deodorization of its gaseous emissions), simple and low-cost alternatives are necessary in order to avoid the drawbacks of thermal regeneration under inert atmosphere. For this reason, a simple oxidative thermal regeneration of GAC from an urban WWTP is proposed in this work. The objective is to evaluate the above-mentioned regeneration process, based on the physico-chemical, textural and structural properties of GAC. To achieve this, two GAC samples from different deodorization points at the WWTP were characterized, both before and after regeneration. High regeneration efficiencies and recovery of original properties of the GAC might promote its valorisation, thereby avoiding the use of raw materials to manufacture new GACs and the accumulation of hazardous waste in landfill. In this sense, this study demonstrates, for the first time, that thermal regeneration in an air atmosphere at temperatures no higher than 350 ºC can be a sustainable alternative to revalue GAC used in WWTPs, mainly as an odour adsorbent in such facilities.

2. Materials and methods

2.1. Deodorization process and GAC samples

GAC samples were supplied by an urban WWTP located in the province of Seville, Spain. This treatment plant, based on conventional treatment with activated sludge, anaerobic digestion and mechanical dehydration of sludge, with an average daily flow of 255,000 m^3/d, serves a population equivalent of 950,000. It uses adsorption by GAC as an odour control system. In this deodorization system, the air stream is passed over a bed of adsorbent (GAC), and the odour-causing compounds are retained. In this work, the GAC samples, with the same operation time, came from two different odour sources (**Scheme 1**):

- P1 is a GAC sample which comes from pretreatment header deodorization. At this WWTP, pretreatment header includes roughing operations, water elevation using worm screws, and screening. It is the first step of integral wastewater treatment.
- P2 is a GAC sample which comes from sludge dewatering deodorization. Sludge from anaerobic digestion is dehydrated by centrifuges. This is one of the last steps of the abovementioned treatment, prior to sludge storage in silos.

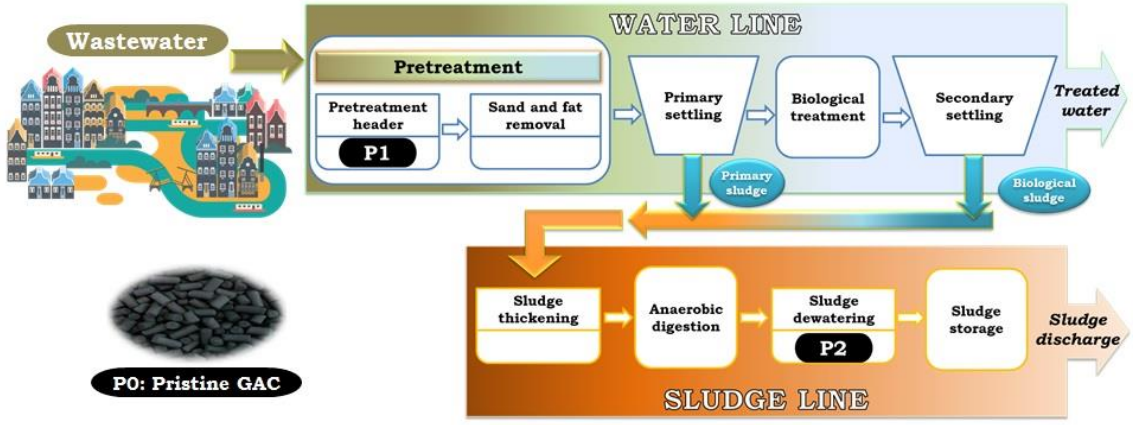

Scheme 1. Schematic flow diagram of the urban WWTP.

When the adsorbent needs to be replaced, the used GAC is discarded in a landfill as hazardous waste (code: 06 13 02) [33], and it is subsequently replaced by pristine GAC, impregnated with NaOH (P0 sample). This GAC is made from coconut shell and its technical characteristics, specified by the manufacturer, are as follows: average particle diameter of 3.7 mm, iodine number (minimum) of 1000 mg/g, and 4% ash content.

2.2. Characterization of the used and regenerated GAC samples

2.2.1. Physico-chemical characterization

2.2.1.1. Elemental analysis

X-ray fluorescence (XRF) was used to analyse the elemental composition of the adsorbent materials. Spectra were acquired with a Rigaku wavelength dispersive X-ray fluorescence (WDXRF) spectrometer ZSX Primus IV. The system was equipped with a 4 kW rhodium target X-ray tube (operating at maximum voltage of 60 kV and current of 150 mA), ten analyser crystals, a flow proportional counter for light elements detection, and a scintillation counter for heavy elements.

2.2.1.2. Surface functional groups

The Boehm method [34] was used to determine the concentration of remaining surface functional groups present in the GAC samples under study. To quantify the concentration of acidic groups (in mmol per gram of adsorbent), the abovementioned samples (0.25 g each) were added to a 50 mL NaOH solution (0.1 M) and stirred for 48 h at 170 rpm and 25 ºC. After that, the suspension was filtered and three aliquots (3 mL each) of the filtrates were back titrated using 0.1 M HCl solution (in order to neutralize the excess base) and phenolphthalein as an indicator. To quantify the concentration of basic groups, the GAC samples were added to a 50 mL HCl solution (0.1 M), being stirred under the same conditions described above. Then, the suspension was filtered, and three aliquots of the filtrates were back titrated using 0.1 M NaOH, in order to neutralize the excess acid.

2.2.1.3. Moisture, FS, VS, pH, conductivity, TOC, and TN_s

The methodology proposed by the U.S. Department of Agriculture and the U.S. Composting Council [35] was used to quantify the following variables (in triplicate): pH, conductivity (mS/cm), soluble total organic carbon (TOC, mg/g GAC), and soluble total nitrogen (TN_s, mg/g GAC), which were measured in the aqueous extract (1:25 ratio), while moisture (%), fixed solids (FS, %), and volatile solids (VS, %) were analysed in the solid fraction.

2.2.2. Textural properties

Nitrogen adsorption/desorption data were obtained at liquid nitrogen temperature (77 K) using a Micromeritics ASAP 2020 M apparatus. Pore size distribution was calculated by the density functional theory (DFT) method applied to the adsorption branch of the isotherms. The specific surface area (S_{BET}) was calculated using the Brunauer–Emmett–Teller (BET) equation in a relative pressure range of 0.04–0.20. The t-plot method was used to estimate the micropore area (S_{micro}). The total pore volume (V_t) was calculated at a relative pressure of $p/p_0 = 0.98$. The micropore volume (V_{micro}) was calculated according to the Dubinin-Radushkevich equation [36].

2.2.3. Structural characterization

X-ray diffraction (XRD) patterns for both pristine and regenerated samples were obtained in a Bruker D8 Discover X-ray diffractometer equipped with monochromatic

Cu Kα radiation (λ = 1.5406 Å). The patterns were recorded within the 5–80° (2θ) range, using a step size of 0.04° and 1.05 s per step. Pattern Diffraction File database was used for the identification of crystalline phases.

2.3. Olfactometric measurements

With the objective of quantifying the removed specific odour concentration (SOC, $ou_E/m^3 \cdot g$ GAC) by the GAC samples, 0.5 g of each sample was introduced into 4-L Nalophan® sampling bags and maintained in isothermal conditions for 24 h. The bags were previously filled with odourless compressed air. The filling time was 30 s, and experiments were carried out at 40 ºC.

Dynamic olfactometry was the method used to quantify the odour concentration (ou_E/m^3), which is necessary to subsequently calculate the SOC. All odour concentration data are expressed in accordance with the reference conditions described in standard EN 13725 [37] (i.e. 20 ºC, 101.3 kPa on a wet basis). A TO8 olfactometer developed by Olfasense GmbH, based on the 'Yes/No' method, was used to determine the odour concentration. This variable was calculated as the geometric mean of the odour threshold values of each panellist, multiplied by a factor which depends on the olfactometer dilution step factor. The panellist group consisted of four people, each selected based on their sensitivity to the n-butanol reference gas, as described in EN 13725 [37].

2.4. Quantification of desorbed compounds

A gas chromatography/mass spectrometry (GC/MS) instrument, coupled to a thermal desorption (TD) unit, was used to quantify the VOCs retained by the GAC samples. Both H_2S and SO_2 were quantified by gas chromatography/flame photometric detector (GC/FPD). Thus, the total concentration of desorbed gaseous compounds (TC, µg/g GAC) was calculated by taking into account the two abovementioned measurements.

2.4.1. TD-GC/MS

First, 44.5 mg of each GAC sample (P0, P1, and P2) was weighed and put in individual microchambers at 40 ºC. Fifteen minutes after putting the samples in the microchambers (equilibrium time), individual, freshly cleaned adsorption tubes were inserted in the lid of each microchamber with an adjusted dynamic flow at 50 mL/min (flow coming from the emitted headspace by the sample). After 30 min (sampling time),

the tubes on the lid of each microchamber were removed and inserted into the TD-GC/MS system for chromatographic analyses.

After collecting the VOCs in the adsorption tubes, they were inserted into the TD unit coupled to the GC/MS. The instrumentation system consisted of a gas chromatograph (GC; TRACE 1310, Thermo Fisher Scientific), mass spectrometer (MS; ISQ 7000, Thermo Fisher Scientific), and thermal desorption unit (Unity2-xr Markes International, UK). After being removed from the tube by thermal desorption (280–330 ºC), volatile compounds were captured in a cold trap at a low temperature (0 to 10°C) by thermoelectric cooling. Subsequently, the cold trap was heated to 300–350°C, according to a programmed and optimized temperature profile, to release all volatiles up to the inlet of the GC column through a transfer line for subsequent chromatographic separation. At the end of the GC column, once separated, the compounds reached the MS with different retention times, where they were fragmented and, subsequently, identified by the NIST 2017 spectra database.

Registered signals as (chromatographic) peaks were quantified by comparing their size (area under curve) with the obtained area of a known amount (ng) of a reference substance (Toluene-d_8), which was adsorbed (by direct injection using a syringe) in an additional clean tube. The peak produced by Toluene-d_8 is used as reference peak for quantification of all peaks obtained in the sample analysis. This type of quantification, based on Toluene-d_8, is known as semiquantitative. As general approach, this TD-GC/MS system can detect substances from 0.01 to 1 ng. Depending on the sampling method used, these values can be equivalent to 0.1 and 0.5 µg/m^3, respectively. The relative standard deviation (RSD) of the values obtained by this method was below 10%. VOCs were identified with a certainty higher than 80%, most of them over 90%.

2.4.2. GC/FPD

To carry out this analysis, 0.5 g of each sample (P0, P1, and P2) were introduced into 4-L Nalophan® sampling bags, which were placed at 40 ºC and maintained in isothermal conditions for 24 h. The bags were previously filled with clean and filtered air. Three bags were prepared for each GAC, analysing each bag in duplicate. H_2S and SO_2 were quantified by a fully automatic isothermal GC (Chroma S) coupled to a FPD, developed by Chromatotec. This equipment is adequate for the analysis of sulphur

compounds and is described by Toledo et al. [38]. Its detection limit is 7 ppb for both H_2S and SO_2.

2.5. Thermogravimetric analysis (TGA) and MS

To determine the limit temperature of the oxidative thermal regeneration process, P1 and P2 were subjected to TGA. These measurements were made using a Mettler Toledo-TGA/DSC under oxidizing atmosphere (21% O_2 and 79% N_2 flow) by heating the GAC samples from 35 to 350°C at 15 °C/min. In order to make comparisons, P0 was subjected to the same analysis, while P2 was also subjected to TGA from 35 to 250 ºC. During the thermogravimetric measurements, the TGA/DSC equipment was coupled to a VG PROLAB Benchtop QMS MS (Thermo Scientific) to detect some compounds resulting from TGA. Signals for CO_2, H_2O, and SO_2 were monitored through their MS peaks at m/z 44, 18, and 64, respectively.

2.6. Thermal regeneration process

The thermal regeneration of the used GAC was carried out in a tubular furnace (Carbolite Gero CTF, Parsons Lane, Hope Valley, UK) using an oxidizing atmosphere with an air flow of 50 mL/min. Before heating, a purge of the atmosphere was performed inside the furnace to ensure stable conditions of the oxidizing atmosphere, increasing the oxidant flow to 100 mL/min for at least 30 min. The thermal conditions used for the regeneration of the P1 sample were a temperature range from 35 to 350 ºC at 15 °C/min. However, for the P2 sample, heating was carried out from 35 to 250 ºC using the same temperature ramp. Therefore, the regeneration process was carried out for the GAC without physical or mechanical treatment (**Scheme 2**), in order to achieve two added advantages: (1) additional stages of pre-conditioning of the samples for their treatment are avoided, that is, less complexity of the process, and (2) the regenerated material is obtained, keeping the original format, and can be revalued for the same use without the need for post-treatments.

2.7. Regeneration efficiency calculation

The regeneration efficiency is an important indicator of the process feasibility. This parameter was calculated according to Eq. (1):

$$\textit{Regeneration efficiency (dry basis) (\%)} = \frac{m_{GAC}\ (A.R.)}{m_{GAC}\ (B.R.) \cdot \left(\frac{100 - moisture}{100}\right)} \cdot 100 \qquad (1)$$

where m_{GAC} *(A.R.)* is the GAC mass after regeneration, m_{GAC} *(B.R.)* is the GAC mass before regeneration, and *moisture* is the GAC moisture (%) before regeneration.

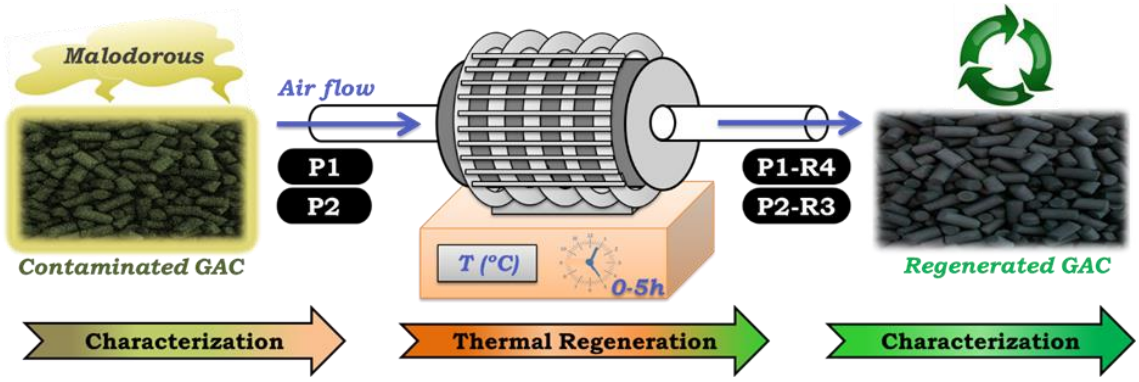

Scheme 2. Overview of the analysis and regeneration process.

3. Results and discussion

3.1. Assessment of pristine and contaminated GAC samples

3.1.1. Physico-chemical assessment

The results of the physico-chemical characterization of the GAC samples are shown in **Table 1**. Considering that pristine GAC (P0) was impregnated by the manufacturer with NaOH, the presence of basic surface groups in the GAC samples is logical. **Table 1** shows the presence of the abovementioned groups in P0 and P2. However, P1 presents acidic groups because a high amount of acid compounds were chemically adsorbed during pretreatment header deodorization in the WWTP. Thus, these compounds have exhausted the basic surface groups of P0, reversing its basic pH of 9.61 towards an acidic pH of 4.13. A greater emission of acid compounds (especially H_2S) takes place at the pretreatment header, with respect to the other integral steps of wastewater treatment, because different circumstances coexist at the abovementioned step, such as anaerobic conditions, a high load of organic matter, and a high presence of microorganisms [39]. For the P2 sample, its pH is basic and very close to that of pristine GAC (P0). This observation is confirmed by analysing the concentration of basic surface groups. In this sense, the gaseous compounds emitted at the sludge dewatering step have been mainly retained by means of physical adsorption, and/or the adsorption capacity of P2 has not been exhausted for the same operational time.

Table 1. Physico-chemical characterization of the GAC samples.

	P0	**P1**	**P1-R4**	**P2**	**P2-R3**
pH	9.61 ± 0.01	4.13 ± 0.01	4.87 ± 0.01	9.51 ± 0.01	12.43 ± 0.01
Acidic surface groups [H^+] (mmol/g GAC)	-	2.73 ± 0.38	1.05 ± 0.14	-	-
Basic surface groups [OH^-] (mmol/g GAC)	1.12 ± 0.39	-	-	1.88 ± 0.25	1.20 ± 0.25
Conductivity (mS/cm)	3.37 ± 0.01	5.85 ± 0.01	8.41 ± 0.01	4.06 ± 0.01	10.37 ± 0.01
Moisture (%)	7.20 ± 0.16	5.52 ± 0.11	3.12 ± 0.00	16.99 ± 0.00	6.17 ± 0.00
FS (%)	19.24 ± 0.18	22.35 ± 0.06	26.75 ± 0.03	21.29 ± 0.03	23.85 ± 0.15
VS (%)	80.76 ± 3.40	77.65 ± 0.17	73.25 ± 0.08	78.71 ± 0.17	76.15 ± 0.07
TOC (mg/g GAC)	0.02 ± 0.01	0.98 ± 0.01	0.61 ± 0.01	0.46 ± 0.01	3.44 ± 0.01
TN_S (mg/g GAC)	0.13 ± 0.01	0.97 ± 0.01	0.15 ± 0.01	0.23 ± 0.01	0.13 ± 0.01

FS, fixed solids; P0, pristine GAC sample; P1, GAC sample from pretreatment header deodorization; P1-R4, sample P1 regenerated at 4 hours (350 ºC); P2, GAC sample from sludge dewatering deodorization; P2-R3, sample P2 regenerated at 3 hours (250 ºC); TN_s, soluble total nitrogen; TOC, soluble total organic carbon; VS, volatile solids.

With regard to conductivity values, these show a view of the number of gaseous compounds retained in GAC samples. As observed in **Table 1**, P1 presents a higher conductivity value than P2 because a higher number of ionic compounds has been retained in the first adsorbent. This fact suggests that the emission of sulphur-containing compounds (which have ionic character) is greater at the pretreatment header. In addition, the high percentage of sulphur retained by P1 (15.25%, **Table 2**) in comparison with P2 (0.57%) reaffirms this observation. It is also important to note that ferric chloride ($FeCl_3$) is added to the wastewater line before sludge thickening, aiding phosphorus precipitation. Although, in parallel, $FeCl_3$ addition minimizes the presence of H_2S in the gas phase; $FeCl_3$ reacts with H_2S to form a precipitate of iron sulphide (Fe_2S_3), which settles in quiescent conditions [29]. Therefore, this also justifies the low sulphur content in P2.

Table 2. Elemental composition of the GAC samples determined by XRF.

Elemental composition (% by weight)	P0	P1	P1-R4	P2	P2-R3
C	90.87 ± 0.08	78.95 ± 1.08	87.66 ± 0.17	91.55 ± 0.12	91.10 ± 0.04
Na	3.63 ± 0.02	2.79 ± 0.05	4.25 ± 0.04	3.75 ± 0.11	4.57 ± 0.18
S	2.05 ± 0.01	15.25 ± 1.02	4.66 ± 0.10	0.57 ± 0.02	0.46 ± 0.01
Si	1.14 ± 0.00	0.92 ± 0.03	1.00 ± 0.02	1.20 ± 0.01	1.06 ± 0.01
Al	0.63 ± 0.01	0.67 ± 0.01	0.77 ± 0.01	0.95 ± 0.02	0.83 ± 0.03
Ca	0.54 ± 0.00	0.57 ± 0.02	0.65 ± 0.02	0.77 ± 0.00	0.73 ± 0.01
Fe	0.50 ± 0.00	0.56 ± 0.02	0.64 ± 0.01	0.81 ± 0.02	0.73 ± 0.03
K	0.21 ± 0.02	0.05 ± 0.01	0.07 ± 0.00	0.07 ± 0.01	0.07 ± 0.00
Cl	0.20 ± 0.00	0.02 ± 0.01	0.02 ± 0.00	0.02 ± 0.00	0.03 ± 0.00
Mg	0.11 ± 0.00	0.17 ± 0.01	0.16 ± 0.01	0.17 ± 0.00	0.17 ± 0.01
Sr	0.02 ± 0.00	0.02 ± 0.00	0.02 ± 0.00	0.02 ± 0.00	0.02 ± 0.00
P	0.01 ± 0.00	0.02 ± 0.00	0.02 ± 0.00	0.03 ± 0.00	0.03 ± 0.00

P0, pristine GAC sample; P1, GAC sample from pretreatment header deodorization; P1-R4, sample P1 regenerated at 4 hours (350 ºC); P2, GAC sample from sludge dewatering deodorization; P2-R3, sample P2 regenerated at 3 hours (250 ºC).

TOC and TN_s values are shown in **Table 1**. Taking into account both variables, pristine GAC presents the lowest values, since this material has not been used in any odour adsorption process, and the determined concentrations are due to the composition of the P0 sample itself. Therefore, the differences in TOC and TN_s from these minimum values are due to odorants' adsorption. P2 presents lower TOC and TN_s values than P1, since P2 was used in the deodorization related to mechanical dehydration of sludge from anaerobic digestion. In this context, the reduction of biodegradable compounds in dehydrated sludge, because of the previous biomethanization as well as the reduction of microbial activity at the sludge dewatering step, reduce the typical odour emission derived from sludge treatment [40,41]. Consequently, the values of TOC and TN_s are also reduced in P2. Another highlight is the high moisture content of P2 compared to P1 and P0 (**Table 1**), which is due to sludge dewatering. The abovementioned fact could have limited the adsorption efficiency of P2, since higher moisture content lowers adsorption capacity [28].

Finally, regarding FS and VS, it is important to note that FS (%) values increase slightly (approximately 2–3%) in the contaminated GAC samples. This might be

explained by the transformation of retained gases to solid compounds (such as elemental sulphur or sulphur oxides), remaining fixed in the GAC matrix [31]. For this reason, VS (%) values decrease by the same percentage as FS values increase. In addition, this retention of compounds in the form of FS is connected to the increase in conductivity values observed for P1 and P2 with respect to pristine GAC.

3.1.2. Textural assessment

In addition to evaluating the physical-chemical properties of both the pristine and used GAC samples, it is essential to know the textural properties of these samples, since the active surface and porosity of the material are key parameters in the gas retention process of ACs (**Table 3**). Textural measurements are crucial to achieving optimal thermal conditions in the design of the regeneration treatment.

Table 3. Textural properties of the GAC samples.

GAC samples	Regeneration time (h)	Regeneration efficiency (dry basis) (%)	S_{BET} (m^2/g)	S_{micro} (m^2/g)	V_t (cm^3/g)	V_{micro} (cm^3/g)
P0	-	-	406	236	0.229	0.180
P1	-	-	36	-	0.041	0.012
P1-R1	1	81.08	482	288	0.264	0.213
P1-R2	2	78.95	509	225	0.283	0.211
P1-R3	3	75.01	535	203	0.324	0.216
P1-R4	4	75.32	569	204	0.347	0.228
P1-R5	5	72.07	480	198	0.295	0.204
P2	-	-	328	169	0.191	0.145
P2-R1	1	98.44	467	280	0.265	0.214
P2-R2	2	94.45	497	246	0.277	0.218
P2-R3	3	94.53	606	227	0.346	0.252
P2-R4	4	91.96	519	181	0.293	0.214
P2-R5	5	91.53	517	172	0.294	0.212

P0, pristine GAC sample; P1, GAC sample from pretreatment header deodorization; P2, GAC sample from sludge dewatering deodorization; S_{BET}, specific surface area; S_{micro}, micropore area; V_{micro}, micropore volume; V_t, total pore volume.

The N_2 adsorption/desorption isotherms and pore size distributions (obtained by the DFT method) of samples P0, P1, and P2 are shown in **Fig. 1**, and the values of the textural properties were collected in **Table 3**. **Fig. 1(a)** shows that the shape of the isotherms is

similar for P0 and P2, where adsorption occurs at low relative pressures, corresponding to the typical curve of microporous solids that belong to type I of the BDDT classification. The presence of a small hysteresis loop on the desorption curve is due to the presence of mesopores in the carbonaceous texture, providing both samples with a dual pore system. The S_{BET} values for P0 and P2 samples were 406 and 328 m^2/g, respectively. Likewise, S_{micro} was calculated using the t-plot method, providing, in both cases, similar values. However, the adsorption/desorption curves for the P1 sample, shown in **Fig. 1(a)**, present a different profile than the previous ones, which can be associated with type IV of the BDDT classification, where an increase in the amount of absorbed gas occurs at intermediate relative pressures, characteristic of mesoporous solids. P1 showed a low S_{BET} of 36 m^2/g with the absence of S_{micro}. This drastic decrease in the S_{BET} is indicative of the high number of gaseous compounds retained in P1 (pretreatment header). Additionally, these data reveal that the microporosity of AC plays a crucial role in this gas retention process, according to a report by Dissanayake et al. [42].

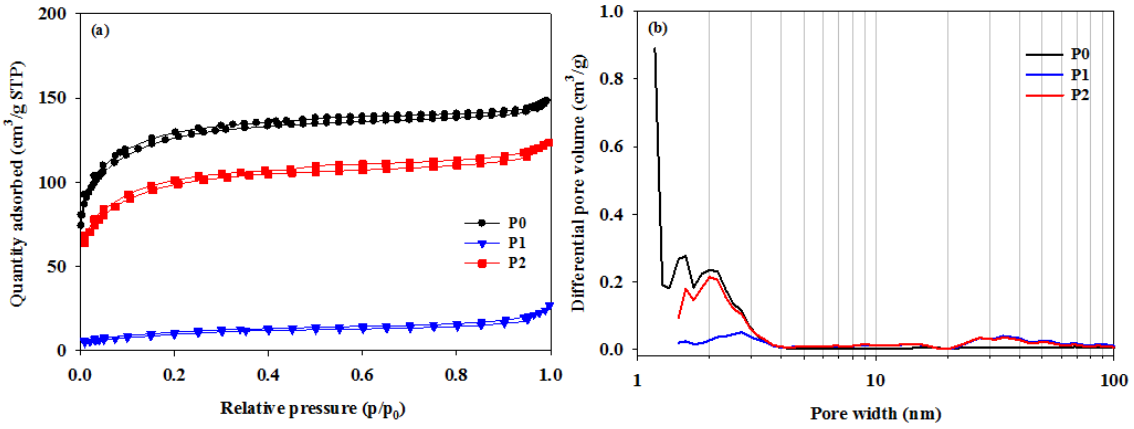

Fig. 1. N_2 adsorption/desorption isotherms (a) and pore size distribution (b) of the GAC samples.

Regarding the pore size distribution, **Fig. 1(b)** shows a range of values between 1.5–4.0 nm for samples P0 and P2, indicative of the expected dual pore system. V_t for P0 and P2 was 0.229 and 0.191 cm^3/g, respectively, covering, in both cases, a high percentage of microporosity, around 76–79%. In contrast, the P1 sample did not show micropore sizes (below 2 nm), and its mesopore size distribution had values between 2–4 nm. Furthermore, the V_t for P1 declined sharply compared to P0, and the V_{micro} value decreased practically in the same proportion, confirming the relevant role of microporosity in the gas retention process from the WWTP.

3.1.3. Relationships between olfactometric and textural variables

Once the textural properties of the GAC samples were studied, it was interesting to connect the TC (µg/g GAC) and SOC ($ou_E/m^3 \cdot g$ GAC) with variations in S_{BET} and V_{micro} (**Fig. 2**). On one hand, P1 presents the highest retention of odoriferous compounds (≈ 150 µg/g GAC), which is correlated with the greatest loss of S_{BET} (with respect to P0). Regarding P2, it retained a lower number of odorants (≈ 40 µg/g GAC), which is in connection with a lower S_{BET} loss. In this latter GAC, the quantified sulphur-containing compounds represent almost 66% of total adsorbed compounds (**Table 4**). In P1, the abovementioned odoriferous compounds (including H_2S) represent only 15%, while other chemical families such as terpenes (30%), aliphatic hydrocarbons (18%), and aromatic compounds (18%) are more predominant. On the other hand, SOC, which provides an estimated view of the odour concentration emitted at the two odour sources considered, is also directly proportional to the S_{BET} loss. P1 presents a SOC approximately 2.5 times higher than that of P2. Therefore, the SOC might also be indicative of the GAC adsorption capacity loss.

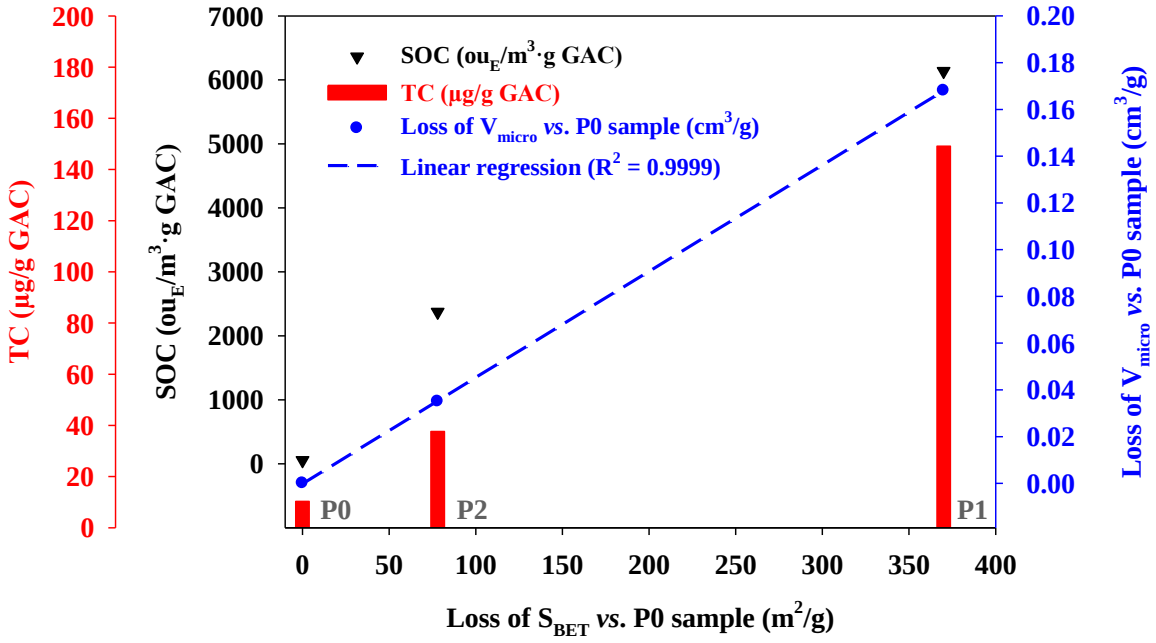

Fig. 2. Relationships between variables: SOC, TC, S_{BET}, and V_{micro}.

Changes in V_{micro} values are also important to consider. A simple linear regression model (R^2 = 0.9999) has been used to directly correlate the loss of V_{micro} with the loss of S_{BET}. On this basis, the influence of TC and SOC on the variation of S_{BET} is practically

the same as on the V_{micro} variation, thus, reinforcing the important role of micropores in WWTP deodorization.

Given all of the above, the systematic and correlative study of a large number of parameters related to pristine and used GAC samples provides a necessary basis for the subsequent analysis of the regeneration process when the GAC lifespan is over.

Table 4. Mass concentration (%) of the odorous families identified in the contaminated GAC samples.

Odorous families	Mass concentration (%)	
	P1	**P2**
Terpenes	29.89	4.16
Aliphatic hydrocarbons	18.21	0.95
Aromatic compounds	17.59	24.41
Sulfur-containing compounds	15.23	65.70
Cyclic hydrocarbons	8.20	1.87
Ketones	3.99	0.24
Halogen-containing compounds	3.72	0.24
Alcohols	1.16	1.37
Aldehydes	0.65	-
Esters	0.43	0.33
Ethers	0.43	0.19
Organic acids	0.37	0.20
Nitrogen-containing compounds	0.15	-
Furans	-	0.36

P1, GAC sample from pretreatment header deodorization; P2, GAC sample from sludge dewatering deodorization.

3.2. Oxidative thermal regeneration process

Both mass loss and adsorption capacity of the regenerated GAC are primary indicators to evaluate the feasibility of the thermal regeneration process [15]. In this sense, mass loss has been studied based on the regeneration limit temperature, while S_{BET} and V_{micro} have been used to determine the feasibility of using the regenerated GAC as an odour adsorbent material.

3.2.1. Assessment of the regeneration limit temperature

The limit temperature of the oxidative thermal regeneration, for the two used adsorbents, was determined based on the TGA results (**Fig. 3**). Initially, a limit temperature of 350 ºC was proposed for both GACs. The treatment of P1 at this temperature led to a mass loss of 25%. The abovementioned value is not too high, considering that mass losses range from 5 to 15% when GACs are thermally regenerated in an inert atmosphere [43]. Nevertheless, in the case of P2, the mass loss was above 80% at 350 ºC, making it necessary to reduce the regeneration limit temperature to 250 ºC for this GAC, leading to a mass loss value slightly lower than that of P1 (22%).

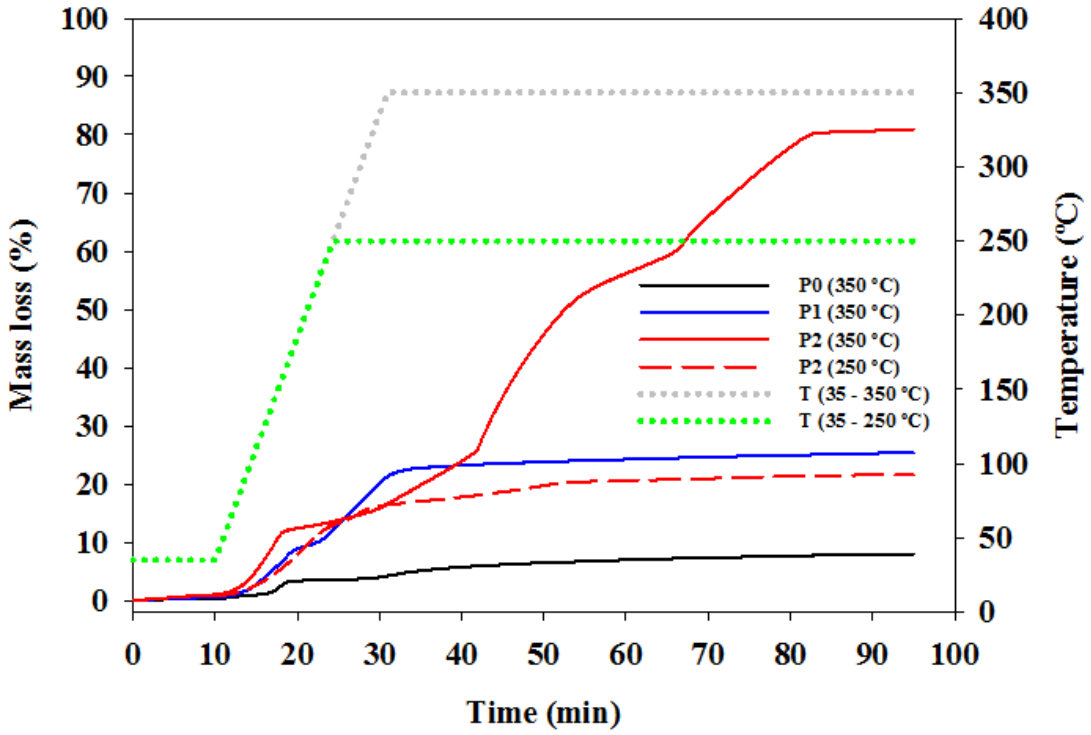

Fig. 3. Evolution of mass loss of the GAC samples with temperature during TGA under oxidizing atmosphere (21% O_2 and 79% N_2 flow).

Due to TGA-MS coupling, it has been proven that P1 and P2 show different behaviours, with respect to P0, under the same operating conditions, that is, when the abovementioned adsorbents were subjected to temperatures up to 350 ºC (**Fig. 4**). On one hand, **Fig. 4(a)** shows a peak, which begins around 250 ºC and extends up to 350 ºC. It represents SO_2, which first comes from the oxidation of elemental sulphur and later from the decomposition of sulfuric acid strongly adsorbed in small pores [30]. These facts are the main causes of the mass loss that takes place in the regeneration of P1. Therefore, it

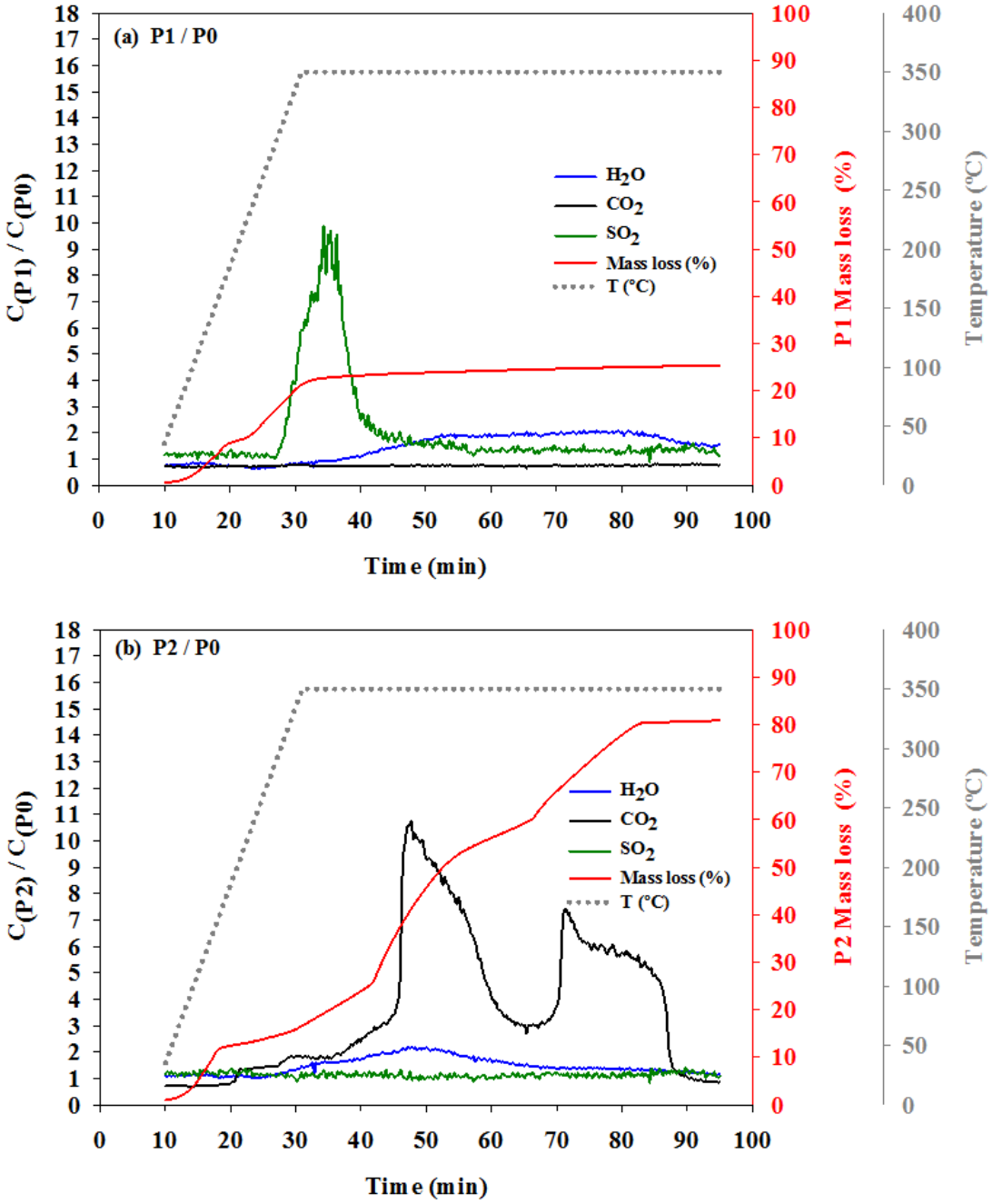

Fig. 4. Results from TGA-MS coupling for P1 (a) and P2 (b) compared to P0 under oxidizing atmosphere (21% O_2 and 79% N_2 flow). C = gas concentration (ppm_v).

can be said that P1 regeneration (up to a limit temperature of 350 ºC) is carried out in an appropriate manner, but treatment of the SO_2 emission will be necessary if this regeneration process is transferred to an industrial scale. For example, the exhausted gases from thermal regeneration can be collected in an absorber and converted into sulfuric acid [30]. In P1 regeneration, the combustion of adsorbed VOCs also takes place, but it is less significant than sulphur removal. On the other hand, **Fig. 4(b)** shows that the combustion of P2 itself prevailed over its regeneration, due to the high CO_2 concentration detected in

comparison with P0. Furthermore, an almost parallel trend of CO_2 and H_2O is observed with respect to the mass loss of P2, when this variable begins to increase significantly, because of the combustion of this adsorbent. This also justifies the need to carry out regeneration of this adsorbent at a temperature below 350 ºC (i.e. 250 ºC). It is also important to note that in P2 regeneration, the release of SO_2, with respect to P0, is insignificant. After all, this GAC has not (chemically) adsorbed H_2S because it had previously been removed by the action of $FeCl_3$. Additionally, the differences in SO_2 release between P1 and P2 during thermal regeneration are consistent with the sulphur content determined for both samples (**Table 2**).

3.2.2. Assessment of the adsorption capacity

Once the regeneration limit temperatures for P1 and P2 were determined (350 and 250 ºC, respectively), different regeneration times were proposed, in order to evaluate the main characteristics of the regenerated GACs, especially those that determine their adsorption capacity. As can be observed in **Table 3**, both regenerated carbons exceed the S_{BET} value of P0 (406 m^2/g) for all regeneration times studied (1–5 h). For these times, the regeneration efficiencies ranged between 72 – 81 % for P1, and between 91 – 98 % for P2. In addition, optimal regeneration times were established, defining themselves as those that maximize the S_{BET} of the regenerated material. The objective of establishing an optimum is because subsequent basic impregnation of the GACs (partially or totally) would result in reduction of the surface available for physical adsorption and, therefore, the retention capacity of compounds that are adsorbed in this way, such as VOCs [29]. In this context, the optimal regeneration time was reached first for P2 (3 h), which might be due to a rapid removal of the physically adsorbed VOCs, also resulting in a better adsorption capacity of the abovementioned GAC compared to P1. In the latter case, both a higher optimal regeneration time (4 h) and limit temperature (350 ºC) were required, which could be related to the chemical adsorption (chemisorption) of H_2S that was carried out during the deodorization process at the pretreatment header, since chemisorption leads to the formation of strong bonds between adsorbate molecules (H_2S) and GAC impregnated with NaOH [31].

Finally, all gaseous pollutants have molecular diameters of less than 2 nm, which means that they are preferably adsorbed on the GAC micropores. Therefore, in order to study the possible reuse of regenerated GACs (P1 and P2) in the original process (deodorization), the V_{micro} of these materials was analysed in parallel, considering the

same proposed regeneration times (1–5 h). Thus, it is observed in **Table 3** that, for both P1 and P2, the V_{micro} values exceed the V_{micro} of pristine GAC (0.180 cm^3/g) for all regeneration times studied. Furthermore, the V_{micro} values are maximized for the optimal times previously considered: 0.228 cm^3/g for P1-R4 and 0.252 cm^3/g for P2-R3. Given this, it is important to highlight the result obtained in the regeneration of the almost non-porous P1 sample, recovering its original porosity, and even increasing it, through this simple and fast thermal treatment process. These results show that the regenerated GACs maintain the porous structure of pristine GAC, with a dual system of micropores and mesopores. On this basis, the granular adsorbent carbons resulting from oxidative thermal regeneration could be reused for deodorization in WWTPs. Moreover, good regeneration efficiencies were achieved in the above-mentioned thermal process, especially in the case of P2, thus demonstrating the feasibility of the proposed methodology.

3.3. Assessment of the regenerated GAC samples

Once the optimal conditions for the regeneration process were established based on the GAC mass loss and adsorption capacity, the data from the physico-chemical, structural, and compositional characterization of the regenerated materials was evaluated. In this way, it is possible to make comparisons with P0 to further explore the possibility of reusing the regenerated GACs (without the need for post-treatments), these samples being P1-R4 (P1 regenerated at 350 ºC for 4 h) and P2-R3 (P2 regenerated at 250 ºC for 3 h).

3.3.1. Physico-chemical assessment

Table 1 shows that the pH of P1-R4 is slightly higher than that of P1, which is due to the removal of acidic species because of the high temperature (350 ºC) proposed for P1 regeneration [30]. Although the pH after regeneration is higher, it does not come back to the pH of pristine GAC (9.61). Therefore, P1-R4 should be impregnated with an alkaline agent for future reuse as an odour adsorbent at the pretreatment header. The same observation can be made by taking into account the concentrations of surface functional groups. In this sense, the regeneration of P1 reduced the concentration of acidic groups, but there continues to be no evidence of the presence of basic groups (mainly required to carry out H_2S chemisorption). In the case of P2, the oxidative thermal regeneration affects pH in a similar way, obtaining a more basic pH value for P2-R3. This suggests that P2-R3 would not need to be impregnated for reuse in sludge dewatering deodorization, which

represents a difference from the P1-R4 sample. This is further confirmed by the concentrations of basic surface groups in P2-R3, which are as high as the concentrations in pristine GAC (**Table 1**).

Conductivity values depend on the number of gaseous compounds that have been retained in the adsorbent material. For this reason, it would be expected that the conductivity of the GAC samples would decrease after regeneration, since a thermal desorption or combustion of retained compounds is carried out. However, as observed in **Table 1**, the conductivity values increase for both P1-R4 and P2-R3. This might be due to the regeneration method used. According to Sabio et al. [16], high temperatures would be capable of modifying the original carbon structure, causing the transfer of certain compounds from the adsorbent composition itself to the aqueous extract, which, in turn, leads to higher conductivity values compared to unregenerated GACs. Something similar happens with the TOC value (%) in P2-R3, where a reduction after regeneration would be expected, instead of an increase. In the case of P2-R3, as mentioned above, a loss of compounds, mainly carbonaceous, occurs, which are transferred to the aqueous solution, resulting in higher TOC values compared to P2. Nevertheless, this does not happen for P1-R4, since a large number of sulphur compounds are chemically adsorbed on P1 and are strongly bound to carbon, thus, limiting the transfer of carbonaceous compounds to the aqueous extract. In this way, a reduction of the TOC value after regeneration is obtained. In terms of TN_s (%), the oxidative thermal regeneration was similarly efficient for both GACs, since the concentration of soluble nitrogen compounds was reduced to values very close to that of P0.

Table 1 also shows a decrease in moisture content (%) after regeneration, as some of the water was evaporated during the thermal regeneration process itself. Similarly, a lower concentration of VS (%) and a slightly higher percentage of FS are also observed. Although, the variation in this respect was not very significant.

3.3.2. Structural assessment

The structural characteristics of GAC samples were analysed by XRD in **Fig. 5**, which shows a comparison between the XRD patterns of P0 (black line), P1-R4 (blue line), and P2-R3 (red line). P0 shows two wide and low intensity signals at ca. 26º and 43º (2θ), which are attributed to the (002) and overlapped (100) and (101) crystallographic planes of graphite (Pattern Diffraction File, PDF #41-1487). These bands demonstrate the

presence of highly disordered carbons with low crystallinity, characteristics of biomass-derived carbons obtained through activation and pyrolysis processes [7,44]. According to XRF, the coconut shell AC presents, in its composition, silicon, calcium, and sodium. For this reason, other peaks of low intensity appear in the diffractogram and could be associated with minority phases, such as SiO_2 (PDF #33-1161) at 28º (2θ), CaO (PDF #37-1497), and even the usual sodium salts remaining in ACs after the synthesis process with NaOH as the activating agent [45,46].

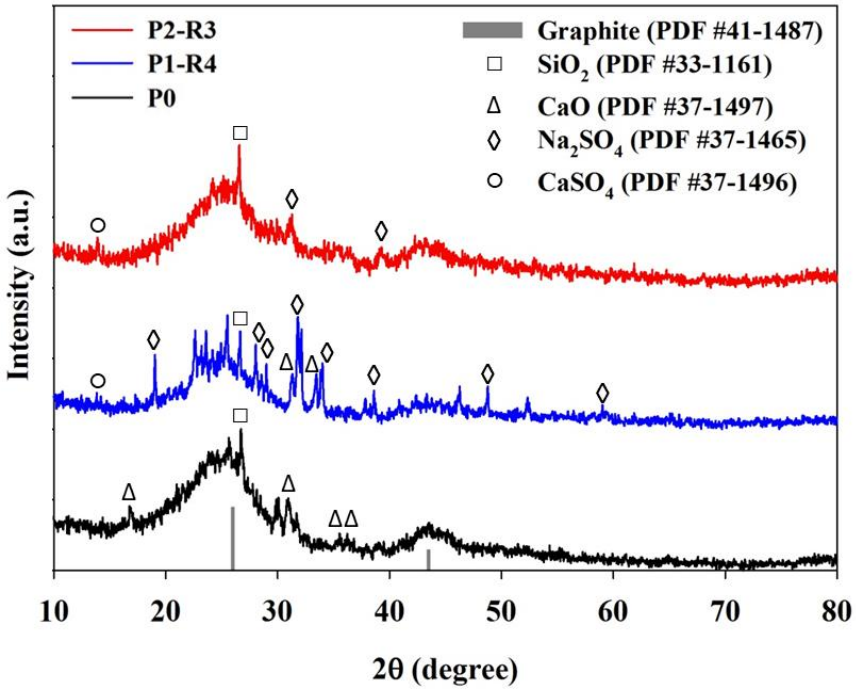

Fig. 5. XRD patterns of pristine (P0) and regenerated GAC samples (P1-R4 and P2-R3).

Once the regeneration process is carried out, the XRD patterns of P1-R4 and P2-R3 samples retain the main signals of P0, with slightly varying relative intensity. However, the P1-R4 regenerated sample shows several additional peaks of higher intensity, corresponding to the Na_2SO_4 phase (PDF #37-1465). The presence of this compound after regeneration must be explicated according to the oxidation of sulphides to sulphates produced during pyrolysis in an oxidizing atmosphere. AC has been confirmed as a catalyst itself for the selective oxidation of sulphide into elemental sulphur or sulphate [47,48]. This catalytic performance is dependent on its surface chemistry and volumes of the micropores. The presence of this soluble salt (sodium sulphate) in sample P1-R4 explains the increase in conductivity of this regenerated carbon with respect to pristine GAC.

Especially noteworthy is the similarity of the diffractograms for P0 and P2-R3, demonstrating that this regenerated carbon maintains a practically unchanged crystalline structure. Thus, only a new peak is detected around 15º (2θ) and is assigned to $CaSO_4$ as a minority phase (PDF #37-1496) [46]. In this context, XRD analysis confirms that the thermal regeneration in an air atmosphere, proposed for the GAC used in WWTP deodorization, does not alter the structural properties of these ACs.

Therefore, in order to avoid both the use of raw materials to manufacture fresh ACs and the accumulation of hazardous waste in landfills, this work proposed a simple methodology to efficiently remove odorous contamination and obtain adsorbents that might be reused. Future additional research is necessary to evaluate recovery of the VOCs emitted during the regeneration process, in order to achieve integral use of the contaminated GAC.

4. Conclusions

From the study to evaluate the GAC thermal regeneration under oxidizing atmosphere, the following conclusions can be drawn:

- The regeneration conditions for GAC depend on the nature of the adsorbed compounds after the same operational time. Thus, the sludge dewatering GAC sample (P2) is representative of the physical adsorption of VOCs, requiring a limit regeneration temperature of 250 ºC and optimal regeneration time of 3 h. In contrast, the pretreatment header GAC sample (P1), which is representative of the chemical adsorption of H_2S, requires both a higher temperature (350 ºC) and longer optimal time (4 h).
- At the optimal regeneration times, regeneration efficiencies reached values of 94% and 75% for P2 and P1, respectively, thus demonstrating the feasibility of the proposed regeneration methodology.
- Textural properties of the GAC are recovered and even improved after regeneration. Thus, in the optimal cases, specific surface area and micropore volume values exceeded, in average, 1.45 and 1.33 times the original values, respectively. Furthermore, the oxidative thermal regeneration did not alter the GACs structural properties.

- The P1 sample need to be impregnated with an alkaline agent after regeneration to be reused at the pretreatment header deodorization system in the WWTP, while the regenerated P2 sample might be reused in the same application without the need for post-treatments.

Given the above, thermal regeneration under oxidizing atmosphere might be considered a simple and sustainable alternative to revalorize GAC used in WWTPs, avoiding the use of high-cost inert gasifying agents, waste accumulation in landfills and the use of raw materials to manufacture fresh activated carbons.

Acknowledgements

This work was supported by the Spanish Ministry of Economy, Industry, and Competitiveness (MINECO), the Spanish State Research Agency (AEI) and the European Regional Development Fund (FEDER) through Projects CTM2017-88723-R and MAT2017-87541-R, and the Ministry of Education, Culture, and Sport of Spain (Grant FPU2016). The European Regional Development Fund (Project UCO-FEDER-1262384-R) and the Chelonia Association (Mares Circulares Project) also supported the work. A. Benítez thanks the financial support from the University of Cordoba (UCO Research Plan 2019; Sub. 2.4.). Finally, the authors wish to acknowledge the technical staff from the Instituto Universitario de Nanoquímica (IUNAN) of the University of Cordoba and express their gratitude to Inmaculada Bellido and María Luisa López for their contribution to this research.

References

[1] S. Wong, N. Ngadi, I.M. Inuwa, O. Hassan, Recent advances in applications of activated carbon from biowaste for wastewater treatment: A short review, J. Clean. Prod. 175 (2018) 361–375. https://doi.org/10.1016/J.JCLEPRO.2017.12.059.

[2] M. Sevilla, R. Mokaya, Energy storage applications of activated carbons: Supercapacitors and hydrogen storage, in: Energy Environ. Sci., Royal Society of Chemistry, 2014: pp. 1250–1280. https://doi.org/10.1039/c3ee43525c.

[3] S. Román, J.M. Valente Nabais, B. Ledesma, J.F. González, C. Laginhas, M.M. Titirici, Production of low-cost adsorbents with tunable surface chemistry by conjunction of hydrothermal carbonization and activation processes, Microporous Mesoporous Mater. 165 (2013) 127–133. https://doi.org/10.1016/j.micromeso.2012.08.006.

[4] I. Ali, V.K. Gupta, Advances in water treatment by adsorption technology, Nat. Protoc. 1 (2007) 2661–2667. https://doi.org/10.1038/nprot.2006.370.

[5] X. Zhang, B. Gao, A.E. Creamer, C. Cao, Y. Li, Adsorption of VOCs onto engineered carbon materials: A review, J. Hazard. Mater. 338 (2017) 102–123. https://doi.org/10.1016/j.jhazmat.2017.05.013.

[6] M.M. Alam, M.A. Hossain, M.D. Hossain, M.A.H. Johir, J. Hossen, M.S. Rahman, J.L. Zhou, A.T.M.K. Hasan, A.K. Karmakar, M.B. Ahmed, The Potentiality of Rice Husk-Derived Activated Carbon: From Synthesis to Application, Processes. 8 (2020) 203. https://doi.org/10.3390/pr8020203.

[7] A. Benítez, J. Morales, Á. Caballero, Pistachio Shell-Derived Carbon Activated with Phosphoric Acid: A More Efficient Procedure to Improve the Performance of Li–S Batteries, Nanomaterials. 10 (2020) 840. https://doi.org/10.3390/nano10050840.

[8] V. Subramanian, C. Luo, A.M. Stephan, K.S. Nahm, S. Thomas, B. Wei, Supercapacitors from activated carbon derived from banana fibers, J. Phys. Chem. C. 111 (2007) 7527–7531. https://doi.org/10.1021/jp067009t.

[9] H. Yang, X. Sun, H. Zhu, Y. Yu, Q. Zhu, Z. Fu, S. Ta, L. Wang, H. Zhu, Q. Zhang, Nano-porous carbon materials derived from different biomasses for high performance supercapacitors, Ceram. Int. 46 (2020) 5811–5820. https://doi.org/10.1016/j.ceramint.2019.11.031.

[10] Y. Chen, Y. Zhu, Z. Wang, Y. Li, L. Wang, L. Ding, X. Gao, Y. Ma, Y. Guo, Application studies of activated carbon derived from rice husks produced by chemical-thermal process—A review, Adv. Colloid Interface Sci. 163 (2011) 39–52. https://doi.org/10.1016/J.CIS.2011.01.006.

[11] V.K. Gupta, A. Nayak, B. Bhushan, S. Agarwal, A critical analysis on the efficiency of activated carbons from low-cost precursors for heavy metals remediation, Crit. Rev. Environ. Sci. Technol. 45 (2015) 613–668. https://doi.org/10.1080/10643389.2013.876526.

[12] M.A. Yahya, Z. Al-Qodah, C.W.Z. Ngah, Agricultural bio-waste materials as potential sustainable precursors used for activated carbon production: A review, Renew. Sustain. Energy Rev. 46 (2015) 218–235. https://doi.org/10.1016/J.RSER.2015.02.051.

[13] P. Rajapaksha P., A. Power, S. Chandra, J. Chapman, Graphene, electrospun membranes and granular activated carbon for eliminating heavy metals, pesticides and bacteria in water and wastewater treatment processes, Analyst. 143 (2018) 5629–5645. https://doi.org/10.1039/C8AN00922H.

[14] H.B. Aditiya, T.M.I. Mahlia, W.T. Chong, H. Nur, A.H. Sebayang, Second generation bioethanol production: A critical review, Renew. Sustain. Energy Rev. 66 (2016) 631–653. https://doi.org/10.1016/j.rser.2016.07.015.

[15] M. El Gamal, H.A. Mousa, M.H. El-Naas, R. Zacharia, S. Judd, Bio-regeneration of activated carbon: A comprehensive review, Sep. Purif. Technol. 197 (2018) 345–359. https://doi.org/10.1016/j.seppur.2018.01.015.

[16] E. Sabio, E. González, J.. González, C.. González-García, A. Ramiro, J. Gañan, Thermal regeneration of activated carbon saturated with p-nitrophenol, Carbon N. Y. 42 (2004) 2285–2293. https://doi.org/10.1016/J.CARBON.2004.05.007.

[17] C.Y. Yin, M.K. Aroua, W.M.A.W. Daud, Review of modifications of activated carbon for enhancing contaminant uptakes from aqueous solutions, Sep. Purif. Technol. 52 (2007) 403–415. https://doi.org/10.1016/j.seppur.2006.06.009.

[18] Z.M. Yunus, Y. G, A. Al-Gheethi, N. Othman, R. Hamdan, N.N. Ruslan, Advanced methods for activated carbon from agriculture wastes; a comprehensive review, Int. J. Environ. Anal. Chem. (2020) 1–25. https://doi.org/10.1080/03067319.2020.1717477.

[19] S.N. Nandeshwar, A.S. Mahakalakar, R.R. Gupta, G.Z. Kyzas, Green activated carbons from different waste materials for the removal of iron from real wastewater samples of Nag River, India, J. Mol. Liq. 216 (2016) 688–692. https://doi.org/10.1016/j.molliq.2015.12.065.

[20] Z.M. Yunus, A. Al-Gheethi, N. Othman, R. Hamdan, N.N. Ruslan, Removal of heavy metals from mining effluents in tile and electroplating industries using honeydew peel activated carbon: A microstructure and techno-economic analysis, J. Clean. Prod. 251 (2020) 119738. https://doi.org/10.1016/j.jclepro.2019.119738.

[21] J. Zhu, M. Wagner, P. Cornel, H. Chen, X. Dai, Feasibility of on-site grey-water reuse for toilet flushing in China, J. Water Reuse Desalin. 8 (2018) 1–13. https://doi.org/10.2166/wrd.2016.086.

[22] M.B. Hasan, Z.A. Hammood, Wastewater Remediation via Modified Activated Carbon: A Review, Pollution. 4 (2018) 707–723. https://doi.org/10.22059/POLL.2018.255031.430.

[23] U. Tezcan Un, F. Ates, N. Erginel, O. Ozcan, E. Oduncu, Adsorption of Disperse Orange 30 dye onto activated carbon derived from Holm Oak (Quercus Ilex) acorns: A 3k factorial design and analysis, J. Environ. Manage. 155 (2015) 89–96. https://doi.org/10.1016/j.jenvman.2015.03.004.

[24] J.F. Vivo-Vilches, E. Bailón-García, A.F. Pérez-Cadenas, F. Carrasco-Marín, F.J. Maldonado-Hódar, Tailoring the surface chemistry and porosity of activated carbons: Evidence of reorganization and mobility of oxygenated surface groups, Carbon N. Y. 68 (2014) 520–530. https://doi.org/10.1016/j.carbon.2013.11.030.

[25] J.M. Estrada, N.J.R.B. Kraakman, R. Muñoz, R. Lebrero, A comparative analysis of odour treatment technologies in wastewater treatment plants, Environ. Sci. Technol. 45 (2011) 1100–1106. https://doi.org/10.1021/es103478j.

[26] H. Cui, S.Q. Turn, M.A. Reese, Removal of sulfur compounds from utility pipelined synthetic natural gas using modified activated carbons, Catal. Today. 139 (2009) 274–279. https://doi.org/10.1016/j.cattod.2008.03.024.

[27] P. Márquez, A. Benítez, Á. Caballero, J.A. Siles, M.A. Martín, Integral evaluation of granular activated carbon at four stages of a full-scale WWTP deodorization system, Sci. Total Environ. 754 (2021) 142237. https://doi.org/10.1016/j.scitotenv.2020.142237.

[28] R. Lebrero, L. Bouchy, R. Stuetz, R. Muñoz, Odor Assessment and Management in Wastewater Treatment Plants: A Review, Crit. Rev. Environ. Sci. Technol. 41 (2011) 915–950. https://doi.org/10.1080/10643380903300000.

[29] Water Environment Federation, Liquid Stream Fundamentals: Odor Management and Control [Fact Sheet], (2017) 1–7. https://www.wef.org/globalassets/assets-wef/direct-download-library/public/03---resources/wsec-2017-fs-028-liquid-stream-fundamentals--odor-control_final.pdf (accessed March 11, 2020).

[30] A. Bagreev, H. Rahman, T.J. Bandosz, Thermal regeneration of a spent activated carbon previously used as hydrogen sulfide adsorbent, Carbon N. Y. 39 (2001) 1319–1326. https://doi.org/10.1016/S0008-6223(00)00266-9.

[31] M.J. Martin, A. Anfruns, R. Lebrero, J.M. Estrada, C. Canals, E. Vega, Procesos de adsorción, in: R. Muñoz, R. Lebrero, J.M. Estrada (Eds.), Caracter. y Gestión Olores En Estac. Depuradoras Aguas Residuales, Gráficas Germinal S.C.L., Valladolid (España), 2010: pp. 115–126.

[32] European Parliament and Council, Directive (EU) 2018/850 of the European Parliament and of the Council of 30 May 2018 amending Directive 1999/31/EC on the landfill of waste, Brussels, 2018.

[33] European Commission, Commission notice on technical guidance on the classification of waste (2018/C 124/01), Brussels, 2018. http://ec.europa.eu/environment/waste/hazardous_index.htm.

[34] H.P. Boehm, Some aspects of the surface chemistry of carbon blacks and other carbons, Carbon N. Y. 32 (1994) 759–769. https://doi.org/10.1016/0008-6223(94)90031-0.

[35] US Department of Agriculture and The US Composting Council, Test Methods for the Examination of Composting and Compost (TMECC), Edaphos International, Houston (TX), 2002. https://compostingcouncil.org/tmecc/ (accessed August 16, 2018).

[36] C. Nguyen, D.D. Do, The Dubinin-Radushkevich equation and the underlying microscopic adsorption description, Carbon N. Y. 39 (2001) 1327–1336. https://doi.org/10.1016/S0008-6223(00)00265-7.

[37] EN 13725, Air Quality - Determination of Odour Concentration by Dynamic Olfactometry, European Committee for Standardization, Brussels, 2003.

[38] M. Toledo, J.M. Guillot, J.A. Siles, M.A. Martín, Permeability and adsorption effects for volatile sulphur compounds in Nalophan sampling bags: Stability influenced by storage time, Biosyst. Eng. 188 (2019) 217–228. https://doi.org/10.1016/j.biosystemseng.2019.10.023.

[39] G. Jiang, D. Melder, J. Keller, Z. Yuan, Odor emissions from domestic wastewater: A review, Crit. Rev. Environ. Sci. Technol. 47 (2017) 1581–1611. https://doi.org/10.1080/10643389.2017.1386952.

[40] T.K.L. Nguyen, H.H. Ngo, W. Guo, S.W. Chang, D.D. Nguyen, L.D. Nghiem, Y. Liu, B. Ni, F.I. Hai, Insight into greenhouse gases emissions from the two popular treatment technologies in municipal wastewater treatment processes, Sci. Total Environ. 671 (2019) 1302–1313. https://doi.org/10.1016/j.scitotenv.2019.03.386.

[41] V. Orzi, B. Scaglia, S. Lonati, C. Riva, G. Boccasile, G.L. Alborali, F. Adani, The role of biological processes in reducing both odor impact and pathogen content during mesophilic anaerobic digestion, Sci. Total Environ. 526 (2015) 116–126. https://doi.org/10.1016/j.scitotenv.2015.04.038.

[42] P.D. Dissanayake, S.W. Choi, A.D. Igalavithana, X. Yang, D.C.W. Tsang, C.H. Wang, H.W. Kua, K.B. Lee, Y.S. Ok, Sustainable gasification biochar as a high efficiency adsorbent for CO2 capture: A facile method to designer biochar fabrication, Renew. Sustain. Energy Rev. 124 (2020) 109785. https://doi.org/10.1016/j.rser.2020.109785.

[43] C.A. Chiu, K. Hristovski, S. Huling, P. Westerhoff, In-situ regeneration of saturated granular activated carbon by an iron oxide nanocatalyst, Water Res. 47 (2013) 1596–1603. https://doi.org/10.1016/j.watres.2012.12.021.

[44] A. Benítez, M. González-Tejero, Á. Caballero, J. Morales, Almond shell as a microporous carbon source for sustainable cathodes in lithium-sulfur batteries, Materials (Basel). 11 (2018). https://doi.org/10.3390/ma11081428.

[45] T.B. Vidovix, E.F.D. Januário, R. Bergamasco, A.M.S. Vieira, Bisfenol A adsorption using a low-cost adsorbent prepared from residues of babassu coconut peels, Environ. Technol. (United Kingdom). (2019). https://doi.org/10.1080/09593330.2019.1701568.

[46] Y. Zhao, J. Dou, X. Duan, H. Chai, J. Oliveira, J. Yu, Adverse Effects of Inherent CaO in Coconut Shell-Derived Activated Carbon on Its Performance during Flue Gas Desulfurization, Environ. Sci. Technol. 54 (2020) 1973–1981. https://doi.org/10.1021/acs.est.9b06689.

[47] C. Yang, Y. Wang, H. Fan, G. de Falco, S. Yang, J. Shangguan, T.J. Bandosz, Bifunctional ZnO-MgO/activated carbon adsorbents boost H2S room temperature adsorption and catalytic oxidation, Appl. Catal. B Environ. 266 (2020) 118674. https://doi.org/10.1016/j.apcatb.2020.118674.

[48] Y. Pan, M. Chen, M. Hu, M. Tian, Y. Zhang, D. Long, Probing the room-temperature oxidative desulfurization activity of three-dimensional alkaline graphene aerogel, Appl. Catal. B Environ. 262 (2020) 118266. https://doi.org/10.1016/j.apcatb.2019.118266.

II.3. Breve descripción del artículo: "*Evaluating the thermal regeneration process of massively generated granular activated carbons for their reuse in wastewater treatments plants*"

II.3. Breve descripción del artículo: "*Evaluating the thermal regeneration process of massively generated granular activated carbons for their reuse in wastewater treatments plants*"

Las EDAR utilizan lechos de GAC para su desodorización debido a la porosidad (especialmente micro y mesoporosidad) y elevada superficie específica de este material. Los compuestos volátiles retenidos en estos lechos saturan sus poros, siendo el adsorbente reemplazado periódicamente por nuevo material, que suele derivar de materiales biomásicos como la cáscara de coco. En el presente trabajo, al objeto de reciclar el GAC contaminado y reutilizarlo como adsorbente de olores en una EDAR, se ha propuesto la regeneración térmica de tal residuo. Con el objetivo de conseguir una producción más sostenible y eficiente, se han evaluado, a escala de laboratorio, los pros y las contras de utilizar una atmósfera oxidante de regeneración en comparación con el uso de una atmósfera inerte. Un simple proceso de regeneración térmica oxidativa, durante una hora y a temperaturas no superiores a 350ºC, permitió lograr la regeneración de las condiciones estructurales del GAC contaminado, permitiendo su posible reutilización como adsorbente de olores en EDAR. El material contaminado procedió tanto de la desodorización de la cabecera de pretratamiento como de la deshidratación del fango en una EDAR urbana. A su vez, mediante la realización de un balance económico comparativo, se evidenció un menor coste para el proceso mencionado anteriormente en comparación con un proceso análogo, pero en atmósfera inerte de nitrógeno (alrededor de un 20% menos en atmósfera oxidante). Los valores de área superficial específica (S_{BET}) y volumen de microporo obtenidos con el proceso térmico oxidativo se encontraron en torno a 475 m^2/g y 0,264 cm^3/g, respectivamente, siendo superiores a los valores del GAC prístino (406 m^2/g y 0,229 cm^3/g). El mejor rendimiento de regeneración se obtuvo para la muestra derivada de la desodorización de la deshidratación del fango, con un valor del 96,8% cuando ésta se regeneró a 300ºC en atmósfera de nitrógeno.

Por otra parte, es importante destacar que la regeneración térmica en atmósfera inerte de nitrógeno a 900ºC fue la única que permitió la producción de GAC regenerado con mejores propiedades texturales ($S_{BET} \approx 675$ m^2/g) y un sistema dual de micro/mesoporos (volumen total de poro de aproximadamente 0,40 cm^3/g y volumen de microporo de 0,27 cm^3/g), obteniéndose una eficacia de regeneración de hasta el 90,5% en el caso de la muestra derivada de la desodorización de la deshidratación del fango. Por tanto, mediante esta última vía regenerativa, aunque más costosa, sería posible obtener

GAC susceptible de ser utilizado en aplicaciones de alto valor añadido que requieran de mejores propiedades texturales.

Journal of Cleaner Production 366 (2022) 132685

Contents lists available at ScienceDirect

Journal of Cleaner Production

journal homepage: www.elsevier.com/locate/jclepro

Evaluating the thermal regeneration process of massively generated granular activated carbons for their reuse in wastewater treatments plants

Márquez, P. [a], Benítez, A. [b,**], Chica, A.F. [a], Martín, M.A. [a,*], Caballero, A. [b]

[a] Department of Inorganic Chemistry and Chemical Engineering, Area of Chemical Engineering, Campus de Excelencia ceiA3, Institute of Nanochemistry (IUNAN). University of Cordoba, Campus Universitario de Rabanales, Carretera N-IV, km 396, Edificio Marie Curie, 14071, Córdoba, Spain.

[b] Dpto. Química Inorgánica e Ingeniería Química, Instituto Universitario de Nanoquímica (IUNAN), Universidad de Córdoba, Campus de Rabanales, 14071, Córdoba, Spain.

* Corresponding authors: M.A. Martín (iq2masam@uco.es);

** A. Benítez (q62betoa@uco.es)

Received 7 February 2022; Received in revised form 30 May 2022; Accepted 12 June 2022; Available online 14 June 2022

Abbreviations: AC, activated carbon; DFT, density functional theory; DSC, differential scanning calorimetry; EDAX, energy dispersive X-ray analysis; GAC, granular activated carbon; IUPAC, International Union of Pure and Applied Chemistry; S_{BET}, specific surface area (m^2/g); SEM, scanning electron microscope; S_{micro}, micropore area (m^2/g); STP, standard temperature and pressure; TGA, thermogravimetric analysis; V_{micro}, micropore volume (cm^3/g); VOC, volatile organic compound; V_t, total pore volume (cm^3/g); WWTP, wastewater treatment plant; XRD, X-ray diffraction.

Graphical abstract

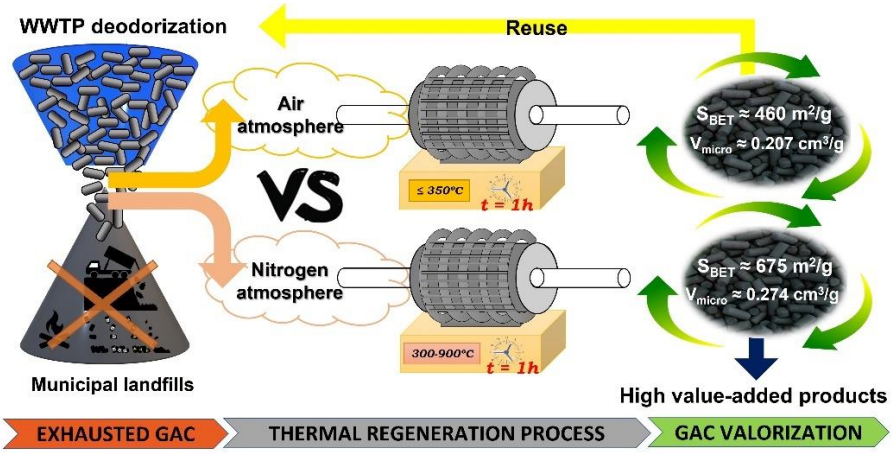

Abstract

Wastewater treatment plants (WWTPs) use granular activated carbons (GACs) as odor retainers because of their high surface area and porosity. The volatile compounds retained in these GAC beds saturate their pores and are periodically replaced by pristine GACs, which are frequently made from biomass materials such as coconut shell. Here, in order to recycle these exhausted GACs and reuse them again as adsorbents in a WWTP, a thermal regeneration of these wastes is proposed. Aiming to achieve more efficient and cleaner production, the pros and cons of using an oxidizing versus an inert atmosphere are evaluated. This work demonstrates that a simple thermal process at temperatures no higher than 350 °C for 1 h using an oxidizing atmosphere can achieve the regeneration of exhausted GAC with the appropriate characteristics for reuse as an adsorbent for gaseous emissions in a WWTP, evidencing a lower cost against a regenerative process in an inert atmosphere (about 20% lower in an oxidizing atmosphere). Their specific surface area and micropore volume values are around 475 m^2/g and 0.264 cm^3/g, respectively, which are in the range of characteristics of pristine GAC (406 m^2/g and 0.229 cm^3/g). The best regeneration yield was 96.8% for the SL-300-N_2 sample. Interestingly, a regeneration at 900 °C using an inert atmosphere allows for the production of GACs with optimized textural properties (S_{BET} ≈ 675 m^2/g), a dual system of micro/mesopores (V_t ≈ 0.4 cm^3/g and V_{micro} ≈ 0.27 cm^3/g), and also a regeneration efficiency of 90.5% for SL-900-N_2, which would make it a raw material of interest for applications with more stringent requirements.

Keywords: Granular activated carbon; Odor treatment; Porosity; Reuse; Thermal regeneration; WWTP.

1. Introduction

Nowadays, air pollution is one of the biggest environmental threats to human health and is responsible for about one in every nine deaths annually (World Health Organization, 2021). In this sense, odor pollution is a type of environmental stressor that has become increasingly important in the context of air pollution and in international environmental regulations. The regulation of odor through the Directive 2010/75/EU of the European Parliament and of the Council of 24 November 2010 on Industrial Emissions in the European Union countries is one such example (Bokowa et al., 2021). It is well known that wastewater treatment plants (WWTPs) are responsible for unpleasant odor emissions, which unavoidably harm the quality of life of local communities and lead to psychological stress and symptoms such as nausea, headache, insomnia, respiratory diseases, and even cancer (Byliński et al., 2019; Sucker et al., 2009). This fact is the cause of many complaints and protests in nearby residential areas, especially in countries with a high population density (Hayes et al., 2017; Morales et al., 2008).

To mitigate the risk of odors and depending on the mechanisms underlying odor removal, different biological and physico-chemical odor treatment technologies can be distinguished (Lebrero et al., 2011; Ren et al., 2019; Senatore et al., 2021). Biological technologies such as biofilters and biotrickling filters are preferable at full-scale WWTPs due to their low-cost, effective, catalyst-free, and environmentally friendly properties (Barbusinski et al., 2017; Estrada et al., 2012; Senatore et al., 2021). However, physico-chemical technologies such as adsorption systems and chemical scrubbing are also commonly used in practice for odor removal in WWTPs due to their widespread design and operation, as well as low empty bed residence times, rapid start-up, etc. (Ren et al., 2019).

Adsorption systems generally consist of static beds of granular materials in vertical cylindrical columns. In this context, it is important to note that the specific surface area, pore structure, and surface chemical functional groups are three crucial factors of adsorbent materials that directly determine their performance in odorant adsorption (Zhang et al., 2017). Nevertheless, it is difficult to find a material with all the features of an excellent adsorbent, and therefore, some of the adsorbent properties must be compromised, such as the removal capacity, cost impact, or regeneration (Aziz and Kim, 2017). Among the different existing adsorbents, activated carbon (AC) is widely used for

odor control in WWTPs due to its capability to easily adsorb a wide range of odorants, such as volatile organic compounds (VOCs), mercaptans, ammonia, and hydrogen sulfide. Moreover, this adsorbent material is often impregnated with caustics (NaOH or KOH) to achieve high H_2S removal efficiencies (Le-Minh et al., 2018; Lebrero et al., 2011; Ren et al., 2019). The main disadvantage of granular activated carbon (GAC)-based deodorization in WWTPs is its high annual packed-bed-material requirements because of the short lifespan of GAC, which generally ranges between six and nine months (Estrada et al., 2011; International Environmental Association of Odour Managers, 2019). Therefore, large amounts of exhausted GAC are generated after losing its adsorption capacity because adsorbent beds can use between 1 and 10 tons of GAC (Márquez et al., 2021a; Turk and Bandosz, 2001). Because of the periodic replacement of the adsorptive material, adsorption systems have the highest operating cost (10–200 EUR m^{-3} h^{-1}) compared to chemical scrubbers (5–6 EUR m^{-3} h^{-1}), biofilters (2–4 EUR m^{-3} h^{-1}), biotrickling filters (3–6 EUR m^{-3} h^{-1}), and bioscrubbers (3–5 EUR m^{-3} h^{-1}) (Senatore et al., 2021). Furthermore, when the lifespan of GAC used in deodorization is over, it is considered a hazardous waste (code: 06 13 02*) by the European Commission (2018) and is mostly discarded in landfills through authorized waste managers, also resulting in a significant economic and environmental cost. These facts make GAC-based deodorization one of the least sustainable alternatives for the treatment of odoriferous emissions (Estrada et al., 2011; Senatore et al., 2021). Therefore, in order to improve the sustainability of the adsorption systems (and hence also the sustainability of the WWTPs), a change in legislation is necessary together with the development of simple and low-cost technologies aimed at the regeneration of the GAC, especially considering that wastewater treatment (which includes the deodorization of its gaseous emissions) is a non-profit sector (Ferrer and Seco, 2021; Márquez et al., 2021b).

The regeneration of ACs is more environmentally effective than its replacement by fresh ACs, allowing for the reduction in the amount of hazardous waste and the preservation of natural resources (Nasruddin et al., 2018). In this context, some authors even maintain that AC regeneration is less expensive compared to the replacement by fresh adsorbent material (Hwang et al., 2020; Park et al., 2019). Moreover, there are numerous studies where commercial ACs commonly used in WWTPs have been replaced by ACs obtained from different biomass sources in order to reduce their price and revalue biomass waste, thus also contributing to the sustainability of WWTPs. Many recent

studies on biowaste-derived-ACs have focused on the adsorption of dyes and heavy metal ions from simulated effluents (Ani et al., 2020; Aragaw and Bogale, 2021; Sherugar et al., 2022), and only a few publications have information on other pollutants, particularly non-metallic pollutants, pesticides, and air pollutants (Reza et al., 2020; Wong et al., 2018). According to Reza et al. (2020), an appropriate selection of precursors, the carbonization process, and optimum activation conditions are the most significant parameters to improve and optimize the adsorption capacities of ACs for the removal of organic and inorganic pollutants from water and gas pollutants from the air. In this context, AC regeneration is gaining attention among researchers, as such an eco-friendly alternative is generally applied for ACs that are already known to be efficient for a certain use and do not require the search for precursors and the subsequent synthesis of new ACs (Fagbohun et al., 2022; Oladejo et al., 2020; Santos et al., 2022; Vega and Valdés, 2021).

Regeneration of ACs is based on the elimination of absorbates on ACs and the recovery of their original surface area by desorption and/or decomposition (Nasruddin et al., 2018). In this way, several methods of regenerating exhausted ACs have been developed, including steam regeneration, thermal regeneration, chemical regeneration, microwave regeneration, wet oxidation regeneration, electrochemical regeneration, and bio-regeneration processes (El Gamal et al., 2018). Among these regeneration methods, thermal regeneration under an inert atmosphere has been widely used due to its simplicity and versatility (Berenguer et al., 2010; Larasati et al., 2020; Ledesma et al., 2014). While various types of thermal devices can be used for the regeneration of exhausted GAC, rotary kilns and multiple hearth furnaces are the two most widely used approaches by far. During this process, exhausted ACs are exposed to high temperatures (~500–850 °C) in an inert gas, requiring a subsequent oxidation of released volatile compounds (two stages: pyrolysis plus oxidation) (Álvarez et al., 2004; Larasati et al., 2021; Raso et al., 2014; Sabio et al., 2004). Sun et al. (2020) consider that thermal treatment is the best method in the regeneration of exhausted adsorbents when considering the cost, the adsorption efficiency, and the number of regeneration cycles. Furthermore, the cost of thermal regeneration can be reduced by replacing the high-cost inert gasifying agents and lowering the high temperatures of thermal treatment, which are associated with a high energy cost (Larasati et al., 2021). In a previous study, our research consisted of the oxidative thermal regeneration of exhausted GACs during malodor treatment in WWTPs, proving that thermal regeneration in an air atmosphere at temperatures no higher than

350 °C can be an alternative to revalue this material, mainly as an odor adsorbent in such facilities (Márquez et al., 2021b). The results of this research also enhanced the sustainability of the regeneration process within the cycle of a WWTP because a greater variety of gaseous compounds would be emitted through pyrolysis. In addition, unlike pyrolysis, oxidative thermal regeneration does not require a subsequent stage of oxidative elimination of released gaseous compounds, which increases the simplicity of the regeneration process.

In the present work, a comparative study between oxidative regeneration (a process already shown to be efficient) and regeneration in a nitrogen atmosphere (as an alternative process) has been carried out through the combination of physico-chemical, textural, and structural analysis techniques, showing that both alternatives are suitable for the treatment of exhausted GACs and thus avoiding the use of raw materials to manufacture fresh ACs and the accumulation of hazardous waste in landfills. To the best of our knowledge, a comprehensive comparative analysis between oxidative and inert conditions for the regeneration of GAC from the odor control system of a full-scale WWTP has not been previously reported in the literature. On the one hand, oxidative regeneration allows the regenerated ACs to be reused for the same application (odor abatement). However, through a pyrolysis process, ACs with improved textural properties would be obtained, allowing for their use in other applications such as electrochemical energy storage (batteries, supercapacitors, or hydrogen storage) (Bora et al., 2021; Sevilla and Mokaya, 2014), adsorption of environmental pollutants (heavy metals, organic contaminants, or miscellaneous pollutants) (Benstoem et al., 2018; Pui et al., 2019), or CO_2 capture (Abuelnoor et al., 2021; Zhang et al., 2014). It is worth noting that the cost of ACs usually depends on their specific surface area (Park et al., 2019). Therefore, obtaining ACs with high surface areas through their regeneration creates high value-added products using the waste. Finally, it should be noted that while most of the researchers in this field analyze the quality of the regenerated waste, the novelty of this work is the evaluation of the cost of regeneration through a complete comparative study.

2. Materials and methods

2.1. Raw materials from WWTP

The raw materials (pelletized AC or GAC) were supplied by an urban WWTP located at Sevilla, Spain. The commercial pristine GAC (GAC-0) used as an odor control

system – adsorbent beds – was manufactured from coconut shell. The design of the biomass-derived AC with a high carbon content, large specific surface area and pore volume, and the desired pore network distribution is based on a widely used procedure, where the sequence of the following stages is required: resource pretreatment, activation, heat treatment, and washing (Jawad et al., 2017, 2021; Jawad and Abdulhameed, 2020; Rashid et al., 2016). According to the manufacturer's information, the adsorbent, once activated, was impregnated with NaOH in order to increase the rate of adsorption and, therefore, the efficiency in the removal of inorganic H_2S and had an appropriate surface area (406 m^2/g). The reaction of NaOH with atmospheric CO_2 leads to the formation of Na_2CO_3, facilitating the transfer of H_2S to the solid phase and promoting its oxidation to elemental sulfur or sulfur oxides (Martin et al., 2010; Water Environment Federation, 2017).

For the development of this study, contaminated GACs from two different locations of the WWTP were collected after their use for one year in the odor control system of this facility together with the non-contaminated GAC sample, that is, GAC-0. Sampling took place in the pretreatment header and sludge dewatering deodorization areas, and the samples were denoted by PR and SL, respectively. Scheme 1 simplifies the processes that take place in the WWTP through a flow diagram.

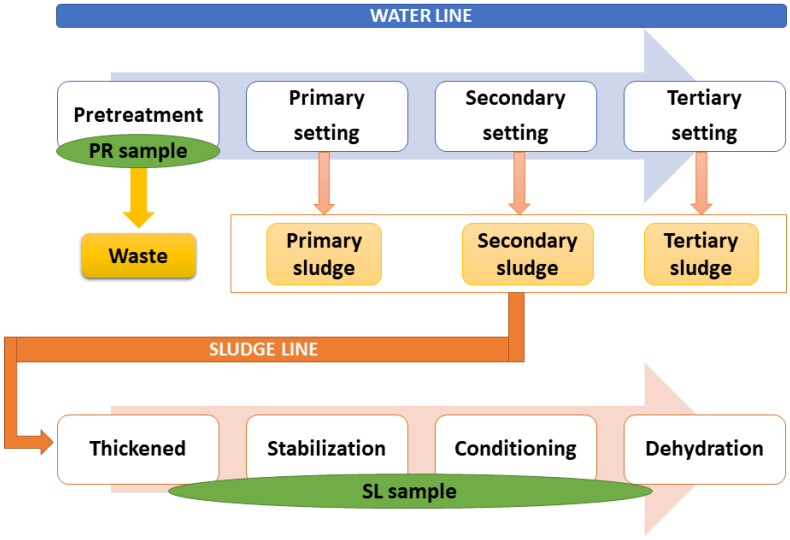

Scheme 1. Schematic representation of the stages of a WWTP.

2.2. Thermal regeneration process

The regeneration process of all the contaminated samples from the odor system of the WWTP was carried out in a tube furnace. Samples were heated at different

temperatures, but the temperature ramp was always maintained at 15 °C/min and the final temperature was held for 1 h. Prior to heating, the samples were purged for 30 min to ensure stable conditions in the atmosphere within the tube. During the thermal process, the carrier gases used were an oxidizing or inert atmosphere (with air or nitrogen flows of 50 mL/min, respectively). All the experiments were carried out in triplicate, and the results of the structural determinations were performed on the homogenized mass of the three experiments. All the acronyms of the samples and their regeneration conditions are listed in **Table 1**.

Once the thermal regeneration was completed, the efficiency calculations of the global regeneration process were carried out using Eq. (1):

$$Regeneration\ efficiency\ (dry\ basis, \%) = \frac{w_f \cdot \left(\frac{100 - m_f}{100}\right)}{w_0 \cdot \left(\frac{100 - m_0}{100}\right)} \cdot 100 \qquad (1)$$

where w_0 is the GAC mass before regeneration or the initial weight of the GAC, w_f is the mass after regeneration or the final weight, and m_o and m_f are the moisture of the initial and final samples (in percent, %), respectively.

Table 1. Sample name, origin, and regeneration conditions.

Samples	Origin	Regeneration temperature	Regeneration atmosphere
GAC-0	Pristine	-	-
PR		-	-
PR-350-O_2	Pretreatment	350 ºC	Air
PR-300-N_2	header	300 ºC	Nitrogen
PR-600-N_2	deodorization	600 ºC	Nitrogen
PR-900-N_2		900 ºC	Nitrogen
SL		-	-
SL-250-O_2	Sludge	250 ºC	Air
SL-300-N_2	dewatering	300 ºC	Nitrogen
SL-600-N_2	deodorization	600 ºC	Nitrogen
SL-900-N_2		900 ºC	Nitrogen

2.3. Characterization

Thermogravimetric analysis (TGA) was performed on GAC-0, PR-300-N_2, PR-600-N_2, PR-900-N_2, PR-350-O_2, SL-300-N_2, SL-600-N_2, SL-900-N_2, and SL-250-O_2 samples by increasing the temperature from 30 °C to 900 °C at a rate of 10 °C min^{-1} in air and nitrogen flows through a Mettler Toledo-TGA/DSC. The ashes obtained after the carbonization of the PR and SL samples were analyzed with a JEOL JSM-7800F scanning electron microscope/energy dispersive X-ray analysis (SEM/EDAX). The textural properties of all samples were determined from the N_2 adsorption–desorption isotherms measured at the liquid nitrogen temperature (77 K) with a Micromeritics ASAP 2020 M apparatus. The regenerated samples were previously outgassed under vacuum at 100 °C overnight. The t-plot method was applied to perform micropore analysis, and the density functional theory (DFT) method was used to calculate the pore size distribution. The crystalline phases were checked by powder X-ray diffraction (XRD) on a Bruker D8 Discover diffractometer using filtered Cu K radiation within a 5–80° (2θ) range and a scan rate of 0.04°/s in continuous mode. Finally, Raman spectroscopy was performed using a Renishaw Raman instrument (InVia Raman Microscope) furnished with a Leica microscope using a green laser light excitation source (532 nm).

3. Results and discussion

In our previous study on the regeneration of contaminated GAC using an oxidizing atmosphere, the sustainability of the regeneration process within the cycle of a WWTP was enhanced (Márquez et al., 2021b). Unlike the previous study, this work focuses on the comparative evaluation of the regeneration of the same waste – used GACs from a WWTP – under a nitrogen atmosphere. It was determined that under the set inert conditions, a higher concentration of gaseous compounds was emitted during the thermal process. In addition, pyrolysis allows ACs with optimal textural properties and high added value to be obtained.

3.1. Thermogravimetric assessment

To evaluate the behavior of the samples as a function of temperature in different atmospheres (N_2 or air flow), thermogravimetric analysis (TGA) measurements were performed. **Fig. 1** (**a** and **b**) shows the TGA curves performed in a nitrogen atmosphere

for GAC-0 and the regenerated PR and SL samples, respectively. Analyzing **Fig. 1(a)** in depth, it can be verified that the PR-300-N_2 sample presents two stages of weight loss: the first between 250 °C and 450 °C due to the elimination of adsorbed volatile compounds and the second above 700 °C due to the pyrolysis of unregenerated organic matter. By contrast, the PR-600-N_2 sample shows a single pronounced weight loss above 600 °C, indicating that the temperature set during the thermal regeneration process is not sufficient to achieve a successful regeneration of the GAC. Focusing on the PR-900-N_2 sample, a weight loss above 600 °C is also observed, although it is less pronounced than in the case of the PR-600-N_2 sample. This behavior, in principle unexpected because the sample has been regenerated at a higher temperature (900 °C), can be argued by the use of a short regeneration time, which is insufficient to fully regenerate the sample. Furthermore, the original GAC-0 sample also shows a weight loss above 700 °C, which minimizes the weight loss values of the PR-900-N_2 sample. The PR-350-O_2 sample regenerated in an oxidizing atmosphere presented a TGA curve with a progressive weight loss between 350 °C and 700 °C. From that point, a change in the value of the slope similar to the rest of the samples was observed.

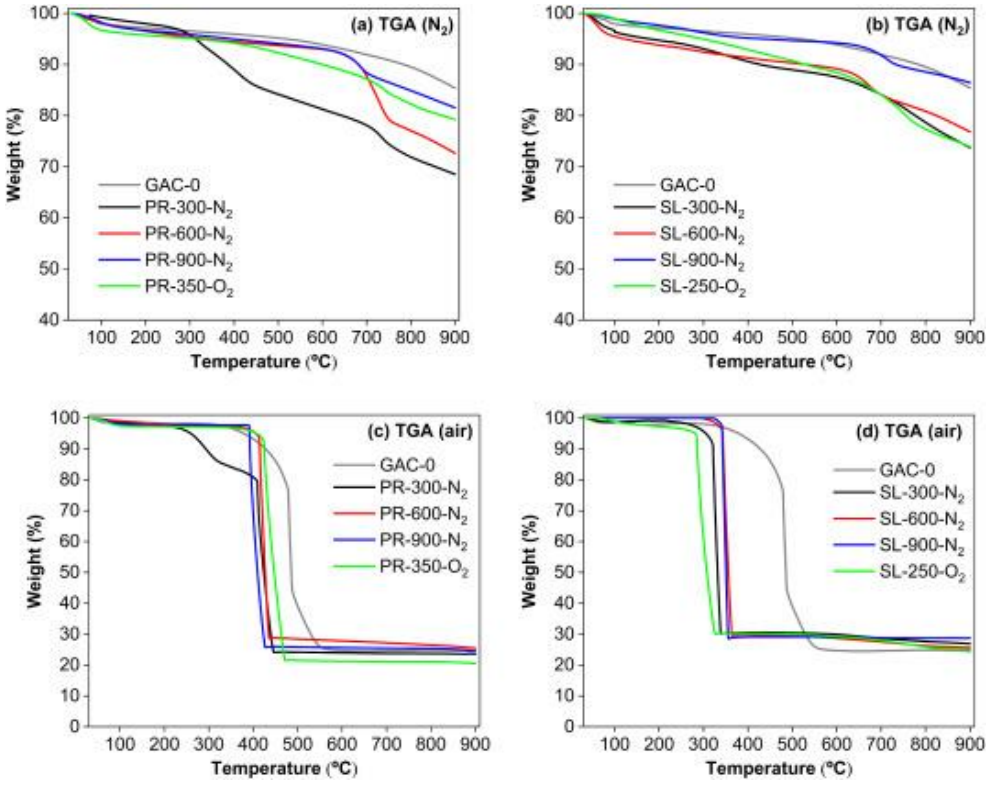

Fig. 1. Evolution of the mass loss with temperature during TGA under (a and b) N_2 or (c and d) air atmosphere for the regenerated PR (pretreatment header) and SL (sludge dewatering) samples, respectively.

TGA measurements carried out for the regenerated SL samples are shown in **Fig. 1(b)**. A behavior similar to that described for each one of the regenerated PR samples was observed. However, in this case, it should be noted that the SL-900-N_2 sample has a thermogravimetric profile very similar to that of the GAC-0 sample, differing only in the weight loss that the SL-900-N_2 sample presented between 600 and 800 °C. This last loss was caused by the presence of non-regenerated organic matter because the regeneration time of 1 h was insufficient to complete the process. Likewise, the difference in the first stage of the weight loss between the PR and SL samples regenerated at 300 °C also stands out. The highest loss observed in PR-300-N_2 is correlated with the higher amount of volatile compounds adsorbed at this point in the WWTP process.

3.2. Regeneration efficiency assessment

In order to evaluate the viability of the process, the regeneration efficiency was calculated in each regeneration considering the humidity of each sample before the process and their masses before and after heat treatment. **Table 2** shows the values obtained for each regenerated sample. The regeneration efficiency of both the PR and SL samples regenerated in an inert atmosphere decreases when the heating temperature is increased. This is due to the fact that the samples desorb the volatile compounds retained in the pores of the GAC above 300 °C; thus, when the regeneration temperature exceeds this value, these compounds are completely eliminated and, therefore, the overall yield of the process decreases. A lower efficiency was calculated for the PR samples compared to the SL samples due to a greater mass loss of the PR samples after regeneration. This behavior was expected for the PR samples from GACs used in a WWTP because in the first step of the integral wastewater treatment, specifically at the head pretreatment point of the wastewater line, the AC beds adsorb a greater quantity of gaseous compounds than in the rest of the stages of the deodorization process (Márquez et al., 2021a, 2021b). In this context, the odor filters at this point (the PR samples) become saturated with gaseous compounds earlier, and they become contaminated more quickly and must be replaced more frequently than the rest of the GAC filters present in the odor control system of a WWTP of municipalities with more than 100,000 equivalent inhabitants, as in the present study.

Table 2. Regeneration efficiencies of the GAC samples.

GAC samples	PR				SL			
	350-O_2	**300-N_2**	**600-N_2**	**900-N_2**	**250-O_2**	**300-N_2**	**600-N_2**	**900-N_2**
Regeneration efficiency (%)	78.6	91.9	77.6	70.8	95.7	96.8	96.6	90.5

PR, GAC sample from pretreatment header deodorization; SL, GAC sample from sludge dewatering deodorization.

On the other hand, the samples regenerated in an oxidizing atmosphere presented coherent and lower regeneration efficiency values than the sample regenerated with an inert atmosphere at a temperature of 300 °C (close to the temperature used for regeneration in air), specifically 78.6% and 95.7% for the PR-350-O_2 and SL-250-O_2 samples, respectively. Once again, the regeneration process in an oxidizing atmosphere for the SL sample was more efficient than for the PR sample because, as mentioned previously, the GAC beds of the sludge line adsorb a lower amount of volatile compounds than the GAC beds from the wastewater line. Furthermore, in both cases, the overall yield of the regeneration process decreases as the temperature increases from 300 °C to 900 °C.

3.3. GAC composition and surface functional groups

To confirm the composition of the regenerated GAC, TGA measurements were carried out in an air atmosphere (21% O_2 and 79% N_2 flow). The TGA curves are shown in **Fig. 1** (**c** and **d**). In **Fig. 1(c)**, it is observed again that the PR-300-N_2 sample shows a weight loss in two stages. In this case, the first stage over 250 °C is due to the desorption of volatile compounds that were retained on the surface of the GACs after regeneration at 300 °C, as previously detected by TGA in a N_2 atmosphere (**Fig. 1(a)**). The second weight loss begins above 400 °C and is attributed to the complete combustion of carbon. Thus, this stage is present in all regenerated PR samples. Finally, after performing the TGA curves up to 900 °C, it can be verified that the amount of mineral matter present in all the samples is approximately 25% by weight, and no significant variation in this content was detected with respect to the GAC-0. The TGA curves for the regenerated SL samples are shown in **Fig. 1(d)**. It can be verified that all the samples present a single weight loss over 300 °C due to the progressive combustion of these ACs. The mineral material content determined at 900 °C by this technique was below 30% by weight.

Furthermore, for both the regenerated PR and SL samples, a decrease in the combustion temperature of the regenerated ACs with respect to GAC-0 is observed (**Fig. 1(c)** and **d**). This effect has been reported by other authors and is due to the catalytic effect generated by the presence of the remaining metal oxide in the samples after the regeneration process (San Miguel, 2003; Wang et al., 2017).

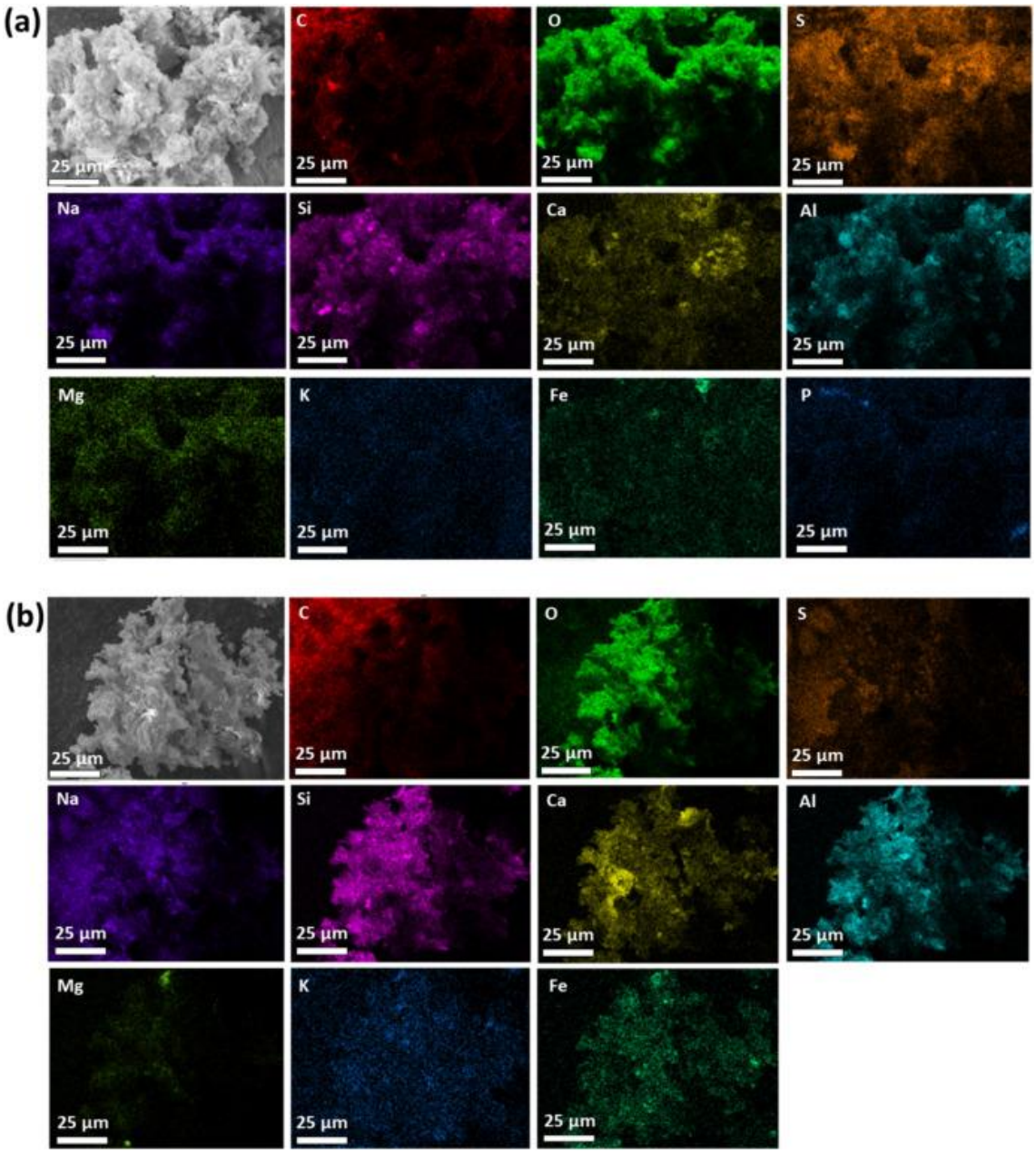

Fig. 2. SEM images and EDAX mapping of the (a) PR and (b) SL-derived ashes.

In order to evaluate the elemental composition of the mineral matter present in the contaminated GACs, PR and SL samples previously dried at 100 °C for 24 h to eliminate moisture were calcined at 550 °C in a muffle furnace for 3 h. The ashes obtained after

this treatment correspond to the mineral solids present in the contaminated GAC samples and were analyzed by SEM combined with EDAX. In **Fig. 2** (**a** and **b**), the SEM image and the mapping of each element detected by microanalysis for the PR and SL-derived ashes, respectively, are shown. In both ashes, in addition to C and O, a series of elements such as S, Na, Si, Ca, and Al are detected, among others.

As depicted in **Fig. 2(a)**, the elemental mapping of the PR ashes shows a higher concentration of S with respect to the S detected for the SL ashes (**Fig. 2(b)**). This result confirms that a greater amount of sulfur-containing compounds are adsorbed during the first stage of the deodorization process, corresponding to the pretreatment header point. The large presence of this element in the PR ashes is due to the retention of H_2S in terms of chemisorption. However, in the sludge line deodorization, the H_2S is reduced by the addition of $FeCl_3$ used to precipitate phosphorus; hence, the coloration in the S mapping for SL ashes decreases compared to PR ashes (Márquez et al., 2021a). Nevertheless, in the SL ashes shown in **Fig. 2(b)**, the presence of other elements such as Si, Na, Ca, and Al becomes more evident, a fact that agrees with the elemental composition reported previously for other ACs derived from coconut shell (Araga and Sharma, 2017; Liyanage and Pieris, 2015).

Delving into the composition of these regenerated carbons, their acid/base character must be determined to support their possible reuse in a WWTP. Boehm's method was performed on GAC samples to quantify the concentration of their acidic and basic groups, which was described in detail in our previous article (Márquez et al., 2021a). GAC-0 is an AC from coconut shell that has been chemically impregnated with an alkaline solution (NaOH) (Márquez et al., 2021a). Hence, only basic surface groups are detected for the pristine GAC sample, supplying a value of 2.11 mmol/g GAC (**Table 3**). A greater retention of H_2S during the first deodorization stage has been confirmed for the PR sample, implying a decrease in pH, even losing the alkaline character. This adsorption phenomenon causes a significant difference in the acidity/basicity of the PR samples compared to the GAC-0 and SL samples that have been analyzed in **Table 3**. For the regenerated PR samples, the concentration of acid surface groups decreases when the pyrolysis temperature increases, obtaining the lowest value for the PR-900-N_2 sample (0.20 mmol/g GAC). The acid/base behavior of the regenerated SL samples differs greatly from that shown by the regenerated PR samples because they maintain a basic character similar to GAC-0. The concentrations of basic surface groups for the SL

samples regenerated in nitrogen flow are slightly higher in all cases than the GAC-0 sample. In this context, the decrease in the regeneration yield due to the loss of carbonaceous organic matter might favor the relative increase in the concentration of the remaining basic groups. Thus, this material would be an ideal candidate as a reusable adsorbent in a WWTP without the need to carry out a chemical post-impregnation with basic agents such as NaOH or KOH.

Table 3. Concentration of surface functional groups in the GAC samples.

GAC samples	Acidic surface groups [H^+] (mmol/g GAC)	Basic surface groups [OH^-] (mmol/g GAC)
GAC-0	-	2.11 ± 0.21
PR	2.73 ± 0.38	-
PR-350-O_2	0.84 ± 0.18	-
PR-300-N_2	1.79 ± 0.18	-
PR-600-N_2	0.22 ± 0.19	-
PR-900-N_2	0.20 ± 0.17	-
SL	-	1.88 ± 0.25
SL-250-O_2	-	1.71 ± 0.21
SL-300-N_2	-	2.32 ± 0.24
SL-600-N_2	-	2.67 ± 0.22
SL-900-N_2	-	2.76 ± 0.23

GAC-0, pristine GAC sample; PR, GAC sample from pretreatment header deodorization; SL, GAC sample from sludge dewatering deodorization.

3.4. Textural assessment

The textural properties of the adsorbent materials are one of the critical features that must be evaluated to ensure the efficiency of these beds in the different stages of the odor control system within a WWTP. In our previous work, it was determined that regeneration in an oxidizing atmosphere at temperatures of 350 °C and 250 °C for the PR and SL samples, respectively, mainly involved the presence of micropores in the regenerated ACs (Márquez et al., 2021b). In addition, it is important to highlight that the increase in the calcination time during the regeneration process did not affect the microporosity because the volume of the micropores remained the same. **Table 4** shows the results of the specific surface area (S_{BET}), micropore area (S_{micro}), total pore volume (V_t), and micropore volume (V_{micro}) of the different samples that were analyzed.

Table 4. Textural properties of the GAC samples.

GAC samples	S_{BET} (m^2/g)	S_{micro} (m^2/g)	V_t (cm^3/g)	V_{micro} (cm^3/g)
GAC-0	406	236	0.229	0.180
PR	36	-	0.041	0.012
PR-350-O_2	482	288	0.264	0.213
PR-300-N_2	139	34	0.089	0.053
PR-600-N_2	430	246	0.245	0.190
PR-900-N_2	670	218	0.413	0.261
SL	328	169	0.191	0.145
SL-250-O_2	467	280	0.265	0.214
SL-300-N_2	233	135	0.127	0.106
SL-600-N_2	481	257	0.263	0.212
SL-900-N_2	677	343	0.387	0.287

GAC-0, pristine GAC sample; PR, GAC sample from pretreatment header deodorization; SL, GAC sample from sludge dewatering deodorization; S_{BET}, specific surface area; S_{micro}, micropore area; V_t, total pore volume; V_{micro}, micropore volume.

The AC from the PR wastewater line shows a drastic decrease in surface area with respect to GAC-0 due to the large concentration of volatile compounds physically and chemically adsorbed by the beds during deodorization. For the PR samples, if the regeneration is carried out at a low temperature and in an oxidizing atmosphere, it is possible to obtain an AC with textural properties similar to GAC-0, even slightly higher (GAC-0: S_{BET} = 406 m^2/g and V_t = 0.229 cm^3/g; PR-350-O_2: S_{BET} = 482 m^2/g and V_t = 0.264 cm^3/g). Analogously, this effect is also observed for the SL-250-O_2 sample (S_{BET} = 467 m^2/g and V_t = 0.265 cm^3/g), thus confirming that regeneration in an oxidizing atmosphere allows these exhausted GACs to recover their initial textural properties and, therefore, be reused as adsorbent beds. On the other hand, if the regeneration takes place in an inert atmosphere at a low temperature of 300 °C, the GAC-0 values are not reached. For this reason, it was necessary to increase the temperature to 600 °C so that the surface area and pore volume parameters of the PR-600-N_2 and SL-600-N_2 samples were comparable to GAC-0. In addition, it is worth noting that the surface area and porosity reached by the PR-900-N_2 sample are higher because the PR samples are more contaminated than the SL samples; specifically, the S_{BET} is 165% larger and the V_t is twice that of GAC-0. The high content of volatile compounds that are retained in the GACs during pretreatment header deodorization implies the saturation of the pores in the

PR samples and causes this residue to be generated in greater quantities; therefore, the beds must be replaced more frequently to maintain adequate adsorbent properties. Because the best results were obtained for the samples treated at 900 °C in an inert atmosphere, far exceeding the previous data, the GACs regenerated under these conditions open the way for their use in new areas, not only in the deodorization system of WWTPs but in higher added value applications.

Focusing on the analysis of the microporosity, this parameter does not increase in the same order as V_t when regeneration is carried out at 900 °C with a nitrogen flow (both in PR and SL samples). For this reason, as an example, the nitrogen adsorption/desorption isotherms and the pore size distribution of the GAC-0, PR-350-O_2, and PR-900-N_2 samples are shown in **Fig. 3**. The nitrogen gas adsorbed by the samples was evaluated using the adsorption isotherms as a function of the relative pressure (P/P_0), where P is the gas vapor pressure and P_0 is the saturation pressure of the adsorbent. According to the International Union of Pure and Applied Chemistry (IUPAC) classification, the three ACs show a combined type I-IV adsorption isotherm, which means that there are both micro- and mesopore structures in the samples (**Fig. 3(a)**). All samples at low relative pressures ($P/P_0 < 0.2$) adsorb a large amount of nitrogen as the adsorbent, indicating the presence of micropores in the structure. Meanwhile, at high relative pressures ($P/P_0 > 0.4$), the shape of the samples is also similar; however, for the PR-900-N_2 sample, the presence of a H4 hysteresis loop is more pronounced, which is attributed to capillary condensation inside the mesopores. The greater mesoporosity in this sample can also be observed by comparing the pore volume values (total and micro) of GAC-0 and PR-900-N_2 (**Table 4**). The total pore volume increases from 0.229 cm^3/g (GAC-0) to 0.413 cm^3/g (PR-900-N_2), whereas V_{micro} only increases from 0.180 cm^3/g to 0.261 cm^3/g, respectively. Therefore, the generation of new and numerous mesopores during the regeneration in a nitrogen atmosphere is confirmed.

In turn, the pore size distribution shown in **Fig. 3(b)** made it possible to analyze, with greater precision, the type of pores present in the different samples. GAC-0 and PR-350-O_2 samples have a higher differential pore volume in the micropore range (pore diameter <2 nm) than the PR-900-N_2 sample, which has a higher proportion of mesopores (pore diameter of 2–50 nm).

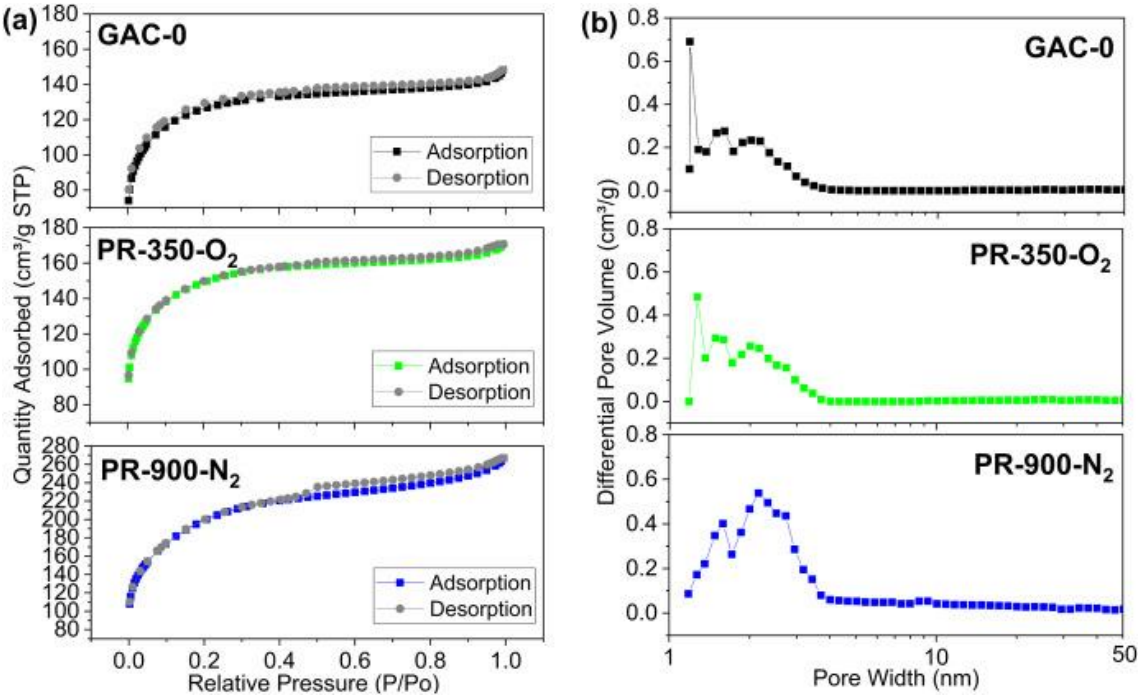

Fig. 3. (a) N_2 adsorption/desorption isotherm and (b) pore size distribution calculated by the DFT method for GAC-0, PR-350-O_2, and PR-900-N_2 samples.

These results confirm that it is possible to regenerate contaminated GACs both at low temperatures (air flow) and at high temperatures (nitrogen flow), obtaining carbons with interesting chemical and textural properties. In addition, it is worth noting the successful valorization of the PR samples because they are the beds that suffer the greatest adsorption of volatile compounds and most frequently must be replaced. For this reason, GAC samples from pretreatment header deodorization are analyzed by XRD and Raman spectroscopy in order to evaluate their crystalline structure and ordering.

3.5. Structural assessment

The X-ray diffractograms of the samples under study are shown in **Fig. 4**. First, it can be verified that the crystallinity of GAC-0 is slightly lost when the sample has adsorbed compounds, that is, for the PR sample. However, the original crystallinity is recovered after the regeneration processes in both oxidizing and inert atmospheres. GAC-0 shows two wide and low intensity signals at ca. 26° and 43° (2θ), which are attributed to the (002) and overlapped (100) and (101) crystallographic planes of graphite (Pattern Diffraction File, PDF #41–1487) (Keppetipola et al., 2021). The intensity of both bands decreases in the PR sample but is recovered in the regenerated PR samples, demonstrating that it is possible to prepare highly disordered ACs with low crystallinity, characteristic

of ACs derived from biomass. Secondly, additional peaks are observed in the regenerated samples, as in the GAC-0 sample, because they are compounds that are present in the pristine coconut shell. These minor phases, such as SiO_2 (PDF #33–1161), CaO (PDF #37–1497), and Al_2O_3 (PDF #04–0875), have previously been detected in coconut shell-derived carbons or their ashes by X-ray fluorescence (Bheel et al., 2020; Joshua et al., 2018; Promdee et al., 2017) and even the usual sodium salts, Na_2SO_4 (PDF #37–1465), that are retained after the impregnation process with NaOH (Márquez et al., 2021b).

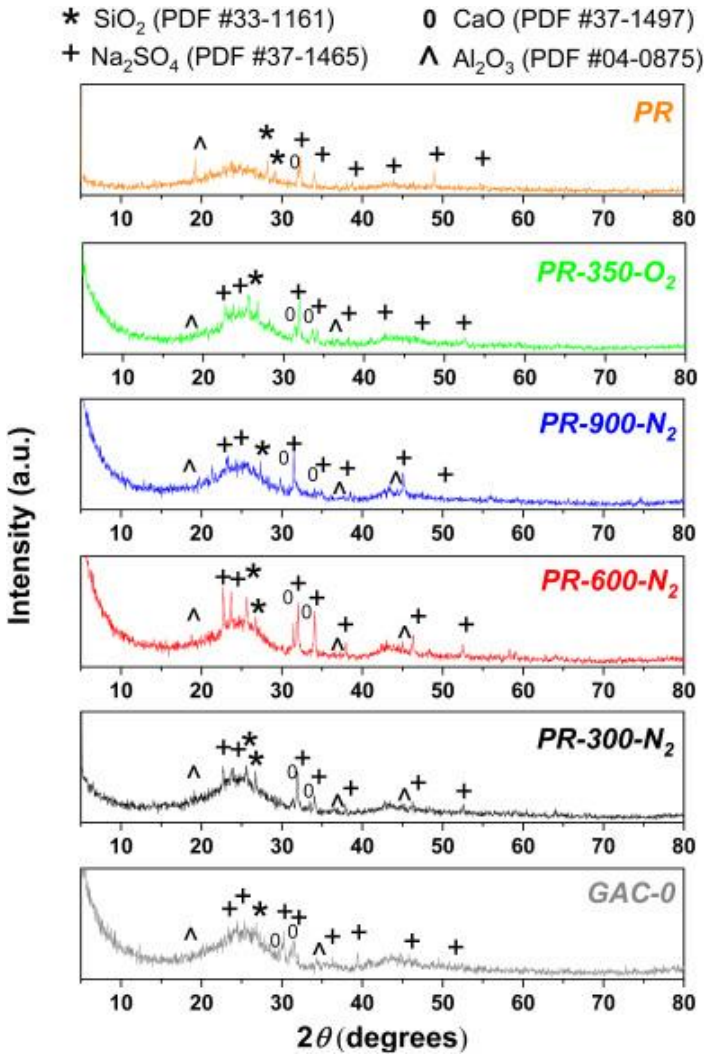

Fig. 4. XRD patterns of the pristine GAC sample (GAC-0) and PR samples from pretreatment header deodorization (not regenerated and regenerated in air or nitrogen).

Additionally, the degree of disorder of these samples was evaluated using Raman spectroscopy by analyzing the intensity ratio of the D and G bands of graphite located approximately at 1346 cm^{-1} and 1595 cm^{-1}, respectively. The D band corresponds to a disordered graphitic structural defect and the G band to a graphitic lattice vibrational

mode (Kumaresan et al., 2021; Nita et al., 2021). In **Fig. 5**, a significant variation in the ordering of the samples is not observed; however, a certain increase in the disorder – increasing I_D/I_G – takes place while the regeneration temperature increases, thus confirming the aggressiveness of the thermal treatment and the effectiveness of the process of regeneration.

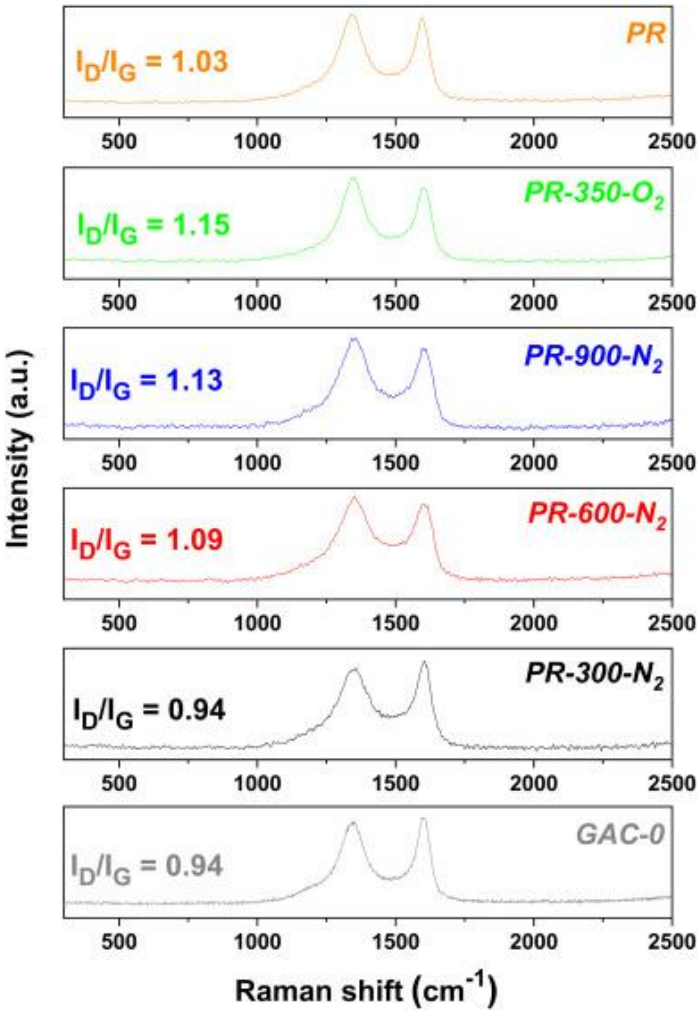

Fig. 5. Raman spectra of the pristine GAC sample (GAC-0) and PR samples from pretreatment header deodorization (not regenerated and regenerated in air or nitrogen).

The study of the structural properties by XRD and Raman spectroscopy confirms that the generated GACs, after their use in the WWTP deodorization system, have not been structurally degraded during the regeneration process and can, therefore, be recovered for similar applications.

3.6. Economic and energy balance

In the absence of a pilot plant to scale the results, a preliminary economic balance has been made based on the experimental laboratory conditions and the cost of energy supplied by the equipment used during the thermal regeneration of the exhausted samples. Although the most energy efficient equipment has not been used, this study allows the environmental, energy, and economic impact of the thermal process to be compared. The starting hypothesis includes the aspects shown in **Table 5**, considering the conditions of our laboratory.

Table 5. Actual laboratory conditions.

Average electricity unit price in 2021 (€/kWh)	0.18
N_2 gas unit price (€/m^3)	4.50
Air gas unit price (€/m^3)	5.00
Tube furnace power (kW)	2.50
Flowmeter power (W)	2.00

To estimate the energy and economic balance, for an average regenerated mass of 200 g, all the inputs invested in the regeneration process of the different samples were considered: temperatures, times, gases consumed, gas flows, electricity consumption, equipment power, etc (**Table 6**).

Table 6. Economic and energy balance for thermal processing of all exhausted GACs according to their regeneration conditions on a laboratory scale.

Regeneration conditions (Units)	**Consumed volume*** *(L STP)*	**Gas cost** *(€)*	**Consumed energy** *(kW·h)*	**Electric cost** *(€)*	**Total cost** *(€)*	**Cost/ raw material** *(€·kg^{-1})*
Air (250 ºC)	5.333	0.03	3.20	0.58	0.61	3.05
Air (350 ºC)	5.667	0.03	3.48	0.63	0.66	3.30
N_2 (300 ºC)	5.501	0.02	3.34	0.61	0.63	3.15
N_2 (600 ºC)	6.500	0.03	4.17	0.76	0.79	3.95
N_2 (900 ºC)	7.502	0.03	5.01	0.91	0.94	4.68

* The volume of gas consumed at standard temperature and pressure has been calculated based on the heating time, which varies according to the target temperature + 1 h of heating to the target temperature + 30 min of cooling. Heating ramp: 15 ºC/min.

Based on the above data, it is confirmed that the atmosphere used (air or nitrogen) during the regeneration process does not lead to significant cost differences. However, the target temperature is the key parameter to be evaluated because it determines the main economic differences between the different experiments. This can be verified by comparing the experiments in an air atmosphere at 250 °C and 350 °C and in nitrogen at 300 °C, whose total cost is less than €0.70, with the experiments in a nitrogen atmosphere at 600 °C and 900 °C, whose values increase to €0.79 and €0.94, respectively. Furthermore, in relation to the total costs, an air capture and filtration system would make the process cheaper because the purchase of an air cylinder would not be required.

3.7. Comparative study with other published works

Additionally, a brief comparative study of the experimental conditions used for the thermal regeneration of spent ACs in different applications has been carried out, as well as an evaluation of the textural properties acquired by the regenerated samples and their subsequent applications (**Table 7**).

For this study, different raw materials have been selected, all of them having in common that they are ACs initially from a biomass source that have been spent or contaminated after use in some industrial application. In addition, in order to make an adequate comparison, the type of regeneration has been by thermal treatment in all cases; however, some parameters such as temperature, time, or gas flow vary.

The data shown in **Table 7** allowed for some interesting comparisons. In the first two works, their regenerated samples were obtained by incorporating activating agents during pyrolysis at a high temperature. So, although they achieved excellent textural properties in their regenerated ACs, the regeneration efficiency was low (Fagbohun et al., 2022; Park et al., 2019).

Sun et al. (2020) regenerated ACs saturated with SO_2 through a thermal treatment at a moderate temperature for 1.5 h and obtained clean ACs with textural properties similar to those shown in our work (regeneration efficiency data were not reported by the authors).

Durán-Jiménez et al. (2019) focused their efforts on reducing heating times during regeneration. This research group applied a similar temperature range under an inert atmosphere, shortening the time by half, and finally obtaining similar regeneration

efficiencies and higher textural properties than those reported in the present work. This fact is not due to the regeneration conditions but to the starting raw material that was used, specifically, the fresh AC from coconut, which in their case had a surface area of 1131 m^2/g and a pore volume of 0.431 cm^3/g, whereas in our work, the values for GAC-0 were S_{BET} = 406 m^2/g and V_t = 0.229 cm^3/g; therefore, the thermal treatment developed in our work managed to prepare regenerated ACs that maintained and even improved their textural properties.

Table 7. Experimental conditions used and textural properties acquired by different ACs from biomass after thermal regeneration.

Raw materials	**Thermal regeneration conditions**					**Textural properties**		**Ref.**
	Temperature	Time	Activating agent	Gas flow	Reg. efficiency	S_{BET}	V_T	
	ºC	min			%	$m^2\ g^{-1}$	$cm^3\ g^{-1}$	
Spent ACs from pharmaceutical factory	850	60	K_2CO_3 + KCl	N_2	73.7	1686	0.80	(Fagbohun et al., 2022)
Spent ACs from food factory	950	60	K_2CO_3 + KCl	N_2	35.4	1703	1.23	
Spent ACs from a WWTP	850	180	- KOH	N_2	- -	709 1380	0.40 0.78	(Park et al., 2019)
AC saturated with SO_2	420	90	-	N_2 + O_2 + SO_2	-	498	0.27	(Sun et al., 2020)
AC from coconut saturated with textile dyes	250 500	30 30	- -	N_2	97.7 92.0	800 1087	0.30 0.42	(Durán-Jiménez et al., 2019)
AC saturated with tetracycline	200	120	-	Air	100	383	-	(de Carvalho Costa et al., 2020)
Exhausted GAC from WWTP (PR)	350 600	60	-	Air N_2	78.6 77.6	482 430	0.26 0.25	This work
Exhausted GAC from WWTP (SL)	250 600	60	-	Air N_2	95.7 96.6	467 481	0.27 0.26	

Finally, de Carvalho Costa et al. (2020) obtained remarkable regeneration efficiencies in their study, working at a low temperature and an oxidizing atmosphere; however, they doubled the residence time during the thermal treatment compared to ours. Furthermore, it is worth noting that the ACs regenerated by these authors decreased their surface area around 20% after the first regeneration cycle.

All of the above, together with the textural properties and the composition of the different samples regenerated in the present work, confirm that with oxidative regeneration at low temperatures, it is possible to recover AC for use in the same application, that is, as adsorbent beds of the odor control system of a WWTP. In addition, carrying out regeneration in an inert atmosphere, it has been shown that pyrolysis increases the dual presence of micro/mesopores of these carbons, which is useable in other applications where these properties are required.

4. Limitations and prospects for this study

Although the strategies described above have been successful in the regeneration of exhausted AC from the odor control system of an urban WWTP, certain aspects require improvement, especially in the regeneration carried out under an inert atmosphere. In these cases, the critical factor was the temperature, which had to be doubled to obtain similar values of surface area and total pore volume as the samples regenerated at a low temperature (350 °C maximum) under an oxidizing atmosphere. The TGA results for the samples regenerated at 300 °C under nitrogen flow indicated that this temperature was not sufficient to completely desorb the compounds retained on the surface of the exhausted GACs. However, another appropriate alternative to remove all the adsorbed compounds, without having to increase the temperature to 600 °C, could be to increase the heating time because the TGA data allow us to deduce that 1 h was not enough to achieve a complete regeneration.

Another aspect that can be improved for the GAC samples from the deodorization of the pretreatment head (or PR samples) is the regeneration efficiency of the pyrolyzed GAC at moderate and high temperatures, that is, at 600 °C and 900 °C, respectively, because in both cases, the values are below 80%. These values could be increased by decreasing the heating ramp during the thermal process.

Even though this study has made it possible to ensure the reduction of this type of hazardous waste, giving a second life to this adsorbent and also contributing to find a solution to this social and environmental problem, additional life cycle analyses should be carried out in future works for the full-scale application of these regenerated GACs in WWTPs.

5. Conclusions

Thermal regeneration is a simple and economical method to achieve a second life or reuse of exhausted GAC from the odor control system of a WWTP. The thermal treatment in an air atmosphere at temperatures no higher than 350 °C allowed the recovery of the specific surface area and micropore volume of the pristine GAC sample (482 m^2/g and 0.213 cm^3/g for the PR-350-O_2 sample, and 467 m^2/g and 0.214 cm^3/g for the SL-250-O_2 sample), reaching values very similar to those achieved with regeneration under a nitrogen atmosphere at 600 °C (430 m^2/g and 0.190 cm^3/g for PR, and 481 m^2/g and 0.212 cm^3/g for SL). This study has shown that oxidative thermal regeneration represents a cheaper alternative than pyrolysis under a nitrogen atmosphere to reuse GACs (≈3.18 *vs.* 3.95 €·kg^{-1}, respectively) because it allows for the reduction of the energy requirement, which is the main factor affecting the operating cost of thermal regeneration.

Finally, it is important to note that the pyrolysis at 900 °C provided the highest values of surface area (S_{BET} > 670 m^2/g, almost 50% higher than the best samples regenerated in air) together with the favourable presence of a dual system of micro/mesopores. Therefore, the GAC regenerated under these last conditions might be used for other applications with high added value that require these needs.

Acknowledgements

The work is funded by the Spanish Ministry of Economy, Industry, and Competitiveness (MINECO), the Spanish State Research Agency (AEI) and the European Regional Development Fund (FEDER) through Projects CTM2017-88723-R, MAT2017-87541-R PID2020-117438RB-I00 & PID2020-113931RB-I00, and the Ministry of Education, Culture, and Sport of Spain (Grant FPU2016). The European Regional

Development Fund (Project UCO-FEDER-1262384-R) and the Chelonia Association (Mares Circulares Project) also supported the work. A.B. thanks the financial support from the European Social Fund and Junta de Andalucía (Project PY20_00432, PAIDI 2020 – FSE & FQM-175 Group). Also, the authors wish to acknowledge the technical staff from the University Institute of Nanochemistry (IUNAN).

References

Abuelnoor, N., AlHajaj, A., Khaleel, M., Vega, L.F., Abu-Zahra, M.R.M., 2021. Activated carbons from biomass-based sources for CO2 capture applications. Chemosphere 282, 131111. https://doi.org/10.1016/J.CHEMOSPHERE.2021.131111

Álvarez, P.M., Beltrán, F.J., Gómez-Serrano, V., Jaramillo, J., Rodríguez, E.M., 2004. Comparison between thermal and ozone regenerations of spent activated carbon exhausted with phenol. Water Res. 38, 2155–2165. https://doi.org/10.1016/J.WATRES.2004.01.030

Ani, J.U., Akpomie, K.G., Okoro, U.C., Aneke, L.E., Onukwuli, O.D., Ujam, O.T., 2020. Potentials of activated carbon produced from biomass materials for sequestration of dyes, heavy metals, and crude oil components from aqueous environment. Appl. Water Sci. 10, 1–11. https://doi.org/10.1007/s13201-020-1149-8

Araga, R., Sharma, C.S., 2017. One step direct synthesis of multiwalled carbon nanotubes from coconut shell derived charcoal. Mater. Lett. 188, 205–207. https://doi.org/10.1016/j.matlet.2016.11.014

Aragaw, T.A., Bogale, F.M., 2021. Biomass-Based Adsorbents for Removal of Dyes From Wastewater: A Review. Front. Environ. Sci. 9, 764958. https://doi.org/10.3389/FENVS.2021.764958/BIBTEX

Aziz, A., Kim, K.S., 2017. Adsorptive Volatile Organic Removal from Air onto NaZSM-5 and HZSM-5: Kinetic and Equilibrium Studies. Water, Air, Soil Pollut. 2017 2289 228, 1–11. https://doi.org/10.1007/S11270-017-3497-Z

Barbusinski, K., Kalemba, K., Kasperczyk, D., Urbaniec, K., Kozik, V., 2017. Biological methods for odor treatment – A review. J. Clean. Prod. 152, 223–241. https://doi.org/10.1016/j.jclepro.2017.03.093

Benstoem, F., Becker, G., Firk, J., Kaless, M., Wuest, D., Pinnekamp, J., Kruse, A., 2018. Elimination of micropollutants by activated carbon produced from fibers taken from wastewater screenings using hydrothermal carbonization. J. Environ. Manage. 211, 278–286. https://doi.org/10.1016/J.JENVMAN.2018.01.065

Berenguer, R., Marco-Lozar, J.P., Quijada, C., Cazorla-Amorós, D., Morallón, E., 2010. Comparison among chemical, thermal, and electrochemical regeneration of phenol-saturated activated carbon. Energy and Fuels 24, 3366–3372. https://doi.org/10.1021/EF901510C/SUPPL_FILE/EF901510C_SI_001.PDF

Bheel, N., Mahro, S.K., Adesina, A., 2020. Influence of coconut shell ash on workability, mechanical properties, and embodied carbon of concrete. Environ. Sci. Pollut. Res. 28, 5682–5692. https://doi.org/10.1007/S11356-020-10882-1

Bokowa, A., Diaz, C., Koziel, J.A., McGinley, M., Barclay, J., Schauberger, G., Guillot, J.M., Sneath, R., Capelli, L., Zorich, V., Izquierdo, C., Bilsen, I., Romain, A.C., Del Carmen Cabeza, M., Liu, D., Both, R., Van Belois, H., Higuchi, T., Wahe, L., 2021. Summary and overview of the odour regulations worldwide. Atmosphere (Basel). 12, 1–53. https://doi.org/10.3390/atmos12020206

Bora, M., Bhattacharjya, D., Saikia, B.K., 2021. Coal-Derived Activated Carbon for Electrochemical Energy Storage: Status on Supercapacitor, Li-Ion Battery, and Li-S Battery Applications. Energy and Fuels 35, 18285–18307. https://doi.org/10.1021/acs.energyfuels.1c02518

Byliński, H., Gębicki, J., Namieśnik, J., 2019. Evaluation of health hazard due to emission of volatile organic compounds from various processing units of wastewater treatment plant. Int. J. Environ. Res. Public Health 16, 1712. https://doi.org/10.3390/ijerph16101712

de Carvalho Costa, L.R., de Moraes Ribeiro, L., Hidalgo, G.E.N., Féris, L.A., 2020. Evaluation of efficiency and capacity of thermal, chemical and ultrasonic regeneration of tetracycline exhausted activated carbon. Environ. Technol. 43, 907–917. https://doi.org/10.1080/09593330.2020.1811391

Durán-Jiménez, G., Stevens, L.A., Hodgins, G.R., Uguna, J., Ryan, J., Binner, E.R., Robinson, J.P., 2019. Fast regeneration of activated carbons saturated with textile dyes: Textural, thermal and dielectric characterization. Chem. Eng. J. 378, 121774. https://doi.org/10.1016/J.CEJ.2019.05.135

El Gamal, M., Mousa, H.A., El-Naas, M.H., Zacharia, R., Judd, S., 2018. Bio-regeneration of activated carbon: A comprehensive review. Sep. Purif. Technol. 197, 345–359. https://doi.org/10.1016/j.seppur.2018.01.015

Estrada, J.M., Kraakman, N.J.R. (Bart., Lebrero, R., Muñoz, R., 2012. A sensitivity analysis of process design parameters, commodity prices and robustness on the economics of odour abatement technologies. Biotechnol. Adv. 30, 1354–1363. https://doi.org/10.1016/J.BIOTECHADV.2012.02.010

Estrada, J.M., Kraakman, N.J.R.B., Muñoz, R., Lebrero, R., 2011. A comparative analysis of odour treatment technologies in wastewater treatment plants. Environ. Sci. Technol. 45, 1100–1106. https://doi.org/10.1021/es103478j

European Commission, 2018. Commission notice on technical guidance on the classification of waste (2018/C 124/01). Brussels.

Fagbohun, E.O., Wang, Q., Spessato, L., Zheng, Y., Li, W., Olatoye, A.G., Cui, Y., 2022. Physicochemical regeneration of industrial spent activated carbons using a green activating agent and their adsorption for methyl orange. Surfaces and Interfaces 29, 101696. https://doi.org/10.1016/J.SURFIN.2021.101696

Ferrer, J., Seco, A., 2021. Economía circular de las aguas residuales. RETEMA 231, 18–19.

Hayes, J.E., Stevenson, R.J., Stuetz, R.M., 2017. Survey of the effect of odour impact on communities. J. Environ. Manage. 204, 349–354. https://doi.org/10.1016/j.jenvman.2017.09.016

Hwang, S.Y., Lee, G.B., Kim, J.H., Hong, B.U., Park, J.E., 2020. Pre-Treatment Methods for Regeneration of Spent Activated Carbon. Molecules 25, 4561. https://doi.org/10.3390/MOLECULES25194561

International Environmental Association of Odour Managers (AMIGO), 2019. Basic Guideline on Odour Management.

Jawad, A.H., Abdulhameed, A.S., 2020. Statistical modeling of methylene blue dye adsorption by high surface area mesoporous activated carbon from bamboo chip using KOH-assisted thermal activation. Energy, Ecol. Environ. 5, 456–469. https://doi.org/10.1007/S40974-020-00177-Z/FIGURES/6

Jawad, A.H., Abdulhameed, A.S., Wilson, L.D., Syed-Hassan, S.S.A., ALOthman, Z.A., Khan, M.R., Jawad, A.H., Abdulhameed, A.S., Wilson, L.D., Syed-Hassan, S.S.A., ALOthman, Z.A., Khan, M.R., 2021. High surface area and mesoporous activated carbon from KOH-activated dragon fruit peels for methylene blue dye adsorption: Optimization and mechanism study. Chinese J. Chem. Eng. 32, 281–290. https://doi.org/10.1016/J.CJCHE.2020.09.070

Jawad, A.H., Ishak, M.A.M., Farhan, A.M., Ismail, K., 2017. Response surface methodology approach for optimization of color removal and COD reduction of methylene blue using microwave-induced NaOH activated carbon from biomass waste. Desalin. Water Treat. 62, 208–220. https://doi.org/10.5004/dwt.2017.20132

Joshua, O., Olusola, K.O., Busari, A.A., Omuh, I.O., Ogunde, A.O., Amusan, L.M., Ezenduka, C.J., 2018. Data on the pozzolanic activity in coconut shell ash (CSA) for use in sustainable construction. Data Br. 18, 1142–1145. https://doi.org/10.1016/j.dib.2018.03.125

Keppetipola, N.M., Dissanayake, M., Dissanayake, P., Karunarathne, B., Dourges, M.A., Talaga, D., Servant, L., Olivier, C., Toupance, T., Uchida, S., Tennakone, K., Kumara, G.R.A., Cojocaru, L., 2021. Graphite-type activated carbon from coconut shell: a natural source for eco-friendly non-volatile storage devices. RSC Adv. 11, 2854–2865. https://doi.org/10.1039/D0RA09182K

Kumaresan, T.K., Masilamani, S.A., Raman, K., Karazhanov, S.Z., Subashchandrabose, R., 2021. High performance sodium-ion battery anode using biomass derived hard carbon with engineered defective sites. Electrochim. Acta 368, 137574. https://doi.org/10.1016/j.electacta.2020.137574

Larasati, A., Fowler, G.D., Graham, N.J.D., 2021. Insights into chemical regeneration of activated carbon for water treatment. J. Environ. Chem. Eng. 9, 105555. https://doi.org/10.1016/J.JECE.2021.105555

Larasati, A., Fowler, G.D., Graham, N.J.D., 2020. Chemical regeneration of granular activated carbon: preliminary evaluation of alternative regenerant solutions. Environ. Sci. Water Res. Technol. 6, 2043–2056. https://doi.org/10.1039/D0EW00328J

Le-Minh, N., Sivret, E.C., Shammay, A., Stuetz, R.M., 2018. Factors affecting the adsorption of gaseous environmental odors by activated carbon: A critical review. Crit. Rev. Environ. Sci. Technol. 48, 341–375. https://doi.org/10.1080/10643389.2018.1460984

Lebrero, R., Bouchy, L., Stuetz, R., Muñoz, R., 2011. Odor Assessment and Management in Wastewater Treatment Plants: A Review. Crit. Rev. Environ. Sci. Technol. 41, 915–950. https://doi.org/10.1080/10643380903300000

Ledesma, B., Román, S., Álvarez-Murillo, A., Sabio, E., González-García, C.M., 2014. Fundamental study on the thermal regeneration stages of exhausted activated carbons: kinetics. J. Therm. Anal. Calorim. 115, 537–543. https://doi.org/10.1007/S10973-013-3293-Y

Liyanage, C.D., Pieris, M., 2015. A Physico-Chemical Analysis of Coconut Shell Powder. Procedia Chem. 16, 222–228. https://doi.org/10.1016/J.PROCHE.2015.12.045

Márquez, P., Benítez, A., Caballero, Á., Siles, J.A., Martín, M.A., 2021a. Integral evaluation of granular activated carbon at four stages of a full-scale WWTP deodorization system. Sci. Total Environ. 754, 142237. https://doi.org/10.1016/j.scitotenv.2020.142237

Márquez, P., Benítez, A., Hidalgo-Carrillo, J., Urbano, F.J., Caballero, Á., Siles, J.A., Martín, M.A., 2021b. Simple and eco-friendly thermal regeneration of granular activated carbon from the odour control system of a full-scale WWTP: Study of the process in oxidizing atmosphere. Sep. Purif. Technol. 255, 117782. https://doi.org/10.1016/j.seppur.2020.117782

Martin, M.J., Anfruns, A., Lebrero, R., Estrada, J.M., Canals, C., Vega, E., 2010. Procesos de adsorción, in: Muñoz, R., Lebrero, R., Estrada, J.M. (Eds.), Caracterización Y Gestión de Olores En Estaciones Depuradoras de Aguas Residuales. Gráficas Germinal S.C.L., Valladolid, España, pp. 115–126.

Morales, J.J., Köning, H., Garcés, J., and Senante, E., 2008. Integrated odour control and management in WWTP of the Region Metropolitana of Santiago de Chile. Pap. Present. 3rd IWA Int. Conf. Odour VOCs, Barcelona, Spain.

Nasruddin, M.N., Fahmi, M.R., Abidin, C.Z.A., Yen, T.S., 2018. Regeneration of Spent Activated Carbon from Wastewater Treatment Plant Application. J. Phys. Conf. Ser. 1116, 32022. https://doi.org/10.1088/1742-6596/1116/3/032022

Nita, C., Zhang, B., Dentzer, J., Matei Ghimbeu, C., 2021. Hard carbon derived from coconut shells, walnut shells, and corn silk biomass waste exhibiting high capacity for Na-ion batteries. J. Energy Chem. 58, 207–218. https://doi.org/10.1016/j.jechem.2020.08.065

Oladejo, J., Shi, K., Chen, Y., Luo, X., Gang, Y., Wu, T., 2020. Closing the active carbon cycle: Regeneration of spent activated carbon from a wastewater treatment facility for resource optimization. Chem. Eng. Process. - Process Intensif. 150, 107878. https://doi.org/10.1016/J.CEP.2020.107878

Park, J.E., Lee, G.B., Hong, B.U., Hwang, S.Y., 2019. Regeneration of activated carbons spent by waste water treatment using KOH chemical activation. Appl. Sci. 9, 5132. https://doi.org/10.3390/app9235132

Promdee, K., Chanvidhwatanakit, J., Satitkune, S., Boonmee, C., Kawichai, T., Jarernprasert, S., Vitidsant, T., 2017. Characterization of carbon materials and differences from activated carbon particle (ACP) and coal briquettes product (CBP) derived from coconut shell via rotary kiln. Renew. Sustain. Energy Rev. 75, 1175–1186. https://doi.org/10.1016/j.rser.2016.11.099

Pui, W.K., Yusoff, R., Aroua, M.K., 2019. A review on activated carbon adsorption for volatile organic compounds (VOCs). Rev. Chem. Eng. 35, 649–668. https://doi.org/10.1515/REVCE-2017-0057/MACHINEREADABLECITATION/RIS

Rashid, R.A., Jawad, A.H., Ishak, M.A.M., Kasim, N.N., 2016. KOH-activated carbon developed from biomass waste: adsorption equilibrium, kinetic and thermodynamic studies for Methylene blue uptake. Desalin. Water Treat. 57, 27226–27236. https://doi.org/10.1080/19443994.2016.1167630

Raso, R.A., Zeltner, M., Stark, W.J., 2014. Indoor air purification using activated carbon adsorbers: Regeneration using catalytic combustion of intermediately stored VOC. Ind. Eng. Chem. Res. 53, 19304–19312. https://doi.org/10.1021/IE503851Q

Ren, B., Zhao, Y., Lyczko, N., Nzihou, A., 2019. Current Status and Outlook of Odor Removal Technologies in Wastewater Treatment Plant. Waste and Biomass Valorization 10, 1443–1458. https://doi.org/10.1007/s12649-018-0384-9

Reza, M.S., Yun, C.S., Afroze, S., Radenahmad, N., Bakar, M.S.A., Saidur, R., Taweekun, J., Azad, A.K., 2020. Preparation of activated carbon from biomass and its' applications in water and gas purification, a review. Arab J. Basic Appl. Sci. 27, 208–238. https://doi.org/10.1080/25765299.2020.1766799

Sabio, E., González, E., González, J.F., González-García, C.M., Ramiro, A., Gañan, J., 2004. Thermal regeneration of activated carbon saturated with p-nitrophenol. Carbon N. Y. 42, 2285–2293. https://doi.org/10.1016/J.CARBON.2004.05.007

San Miguel, G., 2003. The effect of thermal treatment on the reactivity of field-spent activated carbons. Appl. Catal. B Environ. 40, 185–194. https://doi.org/10.1016/S0926-3373(02)00155-8

Santos, D.H.S., Santos, J.P.T.S., Duarte, J.L.S., Oliveira, L.M.T.M., Tonholo, J., Meili, L., Zanta, C.L.P.S., 2022. Regeneration of activated carbon adsorbent by anodic and cathodic electrochemical process. Process Saf. Environ. Prot. 159, 1150–1163. https://doi.org/10.1016/J.PSEP.2022.01.083

Senatore, V., Zarra, T., Galang, M.G., Oliva, G., Buonerba, A., Li, C.-W., Belgiorno, V., Naddeo, V., 2021. Full-Scale Odor Abatement Technologies in Wastewater Treatment Plants (WWTPs): A Review. Water 13, 3503. https://doi.org/10.3390/w13243503

Sevilla, M., Mokaya, R., 2014. Energy storage applications of activated carbons: Supercapacitors and hydrogen storage, in: Energy and Environmental Science. Royal Society of Chemistry, pp. 1250–1280. https://doi.org/10.1039/c3ee43525c

Sherugar, P., Padaki, M., Naik, N.S., George, S.D., Murthy, D.H.K., 2022. Biomass-derived versatile activated carbon removes both heavy metals and dye molecules from wastewater with near-unity efficiency: Mechanism and kinetics. Chemosphere 287, 132085. https://doi.org/10.1016/J.CHEMOSPHERE.2021.132085

Sucker, K., Both, R., Winneke, G., 2009. Review of adverse health effects of odours in field studies. Water Sci. Technol. 59, 1281–1289. https://doi.org/10.2166/WST.2009.113

Sun, Z., Wang, M., Fan, J., Zhou, Y., Zhang, L., 2020. Regeneration performance of activated carbon for desulfurization. Appl. Sci. 10, 6107. https://doi.org/10.3390/app10176107

Turk, A., Bandosz, T.J., 2001. Adsorption systems for odour treatment, in: Stuetz, R., Frechen, F.B. (Eds.), Odours in Wastewater Treatment: Measurement, Modelling and Control. IWA, London, England.

Vega, E., Valdés, H., 2021. Regeneration of odorous sulphur compound-exhausted activated carbons using wet peroxide oxidation: The impact of chemical surface characteristics. Process Saf. Environ. Prot. 156, 109–120. https://doi.org/10.1016/J.PSEP.2021.10.002

Wang, W., Wang, Z., Wang, J., Zhong, C.-J., Liu, C.-J., 2017. Highly Active and Stable Pt-Pd Alloy Catalysts Synthesized by Room-Temperature Electron Reduction for Oxygen Reduction Reaction. Adv. Sci. 4, 1600486. https://doi.org/10.1002/advs.201600486

Water Environment Federation, 2017. Liquid Stream Fundamentals: Odor Management and Control [Fact Sheet] [WWW Document]. URL https://www.wef.org/globalassets/assets-wef/direct-download-library/public/03---resources/wsec-2017-fs-028-liquid-stream-fundamentals--odor-control_final.pdf (accessed 3.11.20).

Wong, S., Ngadi, N., Inuwa, I.M., Hassan, O., 2018. Recent advances in applications of activated carbon from biowaste for wastewater treatment: A short review. J. Clean. Prod. 175, 361–375. https://doi.org/10.1016/J.JCLEPRO.2017.12.059

World Health Organization, 2021. New WHO Global Air Quality Guidelines aim to save millions of lives from air pollution [WWW Document]. URL https://www.who.int/news/item/22-09-2021-new-who-global-air-quality-guidelines-aim-to-save-millions-of-lives-from-air-pollution (accessed 1.7.22).

Zhang, X., Gao, B., Creamer, A.E., Cao, C., Li, Y., 2017. Adsorption of VOCs onto engineered carbon materials: A review. J. Hazard. Mater. 338, 102–123. https://doi.org/10.1016/j.jhazmat.2017.05.013

Zhang, X., Zhang, S., Yang, H., Feng, Y., Chen, Y., Wang, X., Chen, H., 2014. Nitrogen enriched biochar modified by high temperature CO2–ammonia treatment: Characterization and adsorption of CO2. Chem. Eng. J. 257, 20–27. https://doi.org/10.1016/J.CEJ.2014.07.024

II.4. Breve descripción del artículo: "*Simple and sustainable preparation of cathodes for Li–S batteries: Regeneration of granular activated carbon from the odour control system of a wastewater treatment plant*"

II.4. Breve descripción del artículo: "*Simple and sustainable preparation of cathodes for Li–S batteries: Regeneration of granular activated carbon from the odour control system of a wastewater treatment plant*"

El carbón activo granular contaminado procedente de los lechos de control de olores de las EDAR que utilizan esta tecnología, constituye un residuo peligroso abundante y susceptible de ser valorizado. El reciclaje de materiales residuales resulta un aspecto clave, especialmente para el desarrollo sostenible de los sistemas de almacenamiento de energía emergentes, como las baterías de litio-azufre (Li−S). En este artículo, el carbón activo (AC) procedente de dos puntos diferentes de la desodorización de una EDAR urbana (la cabecera de pretratamiento, WL-AC, y la deshidratación del fango, SL-AC) se ha regenerado en flujo simple de aire a baja temperatura (≤ 350ºC) y posteriormente se ha utilizado como huésped de azufre gracias a su estructura micro/mesoporosa. Los composites azufre−carbón (regenerado) se han empleado como cátodos para baterías de Li-S. El electrodo compuesto por SL-AC (regenerado en 3 horas) y azufre (60% en peso) mostró una notable capacidad específica inicial de 1100 mAh g^{-1} cuando se cicló a una velocidad de corriente C/10 (es decir, la batería se carga en 10 h y se descarga también en 10 h), y superior a 800 mAh g^{-1} cuando se cicló a una velocidad C/2. Incluso a una velocidad de corriente 1C se mantuvo una alta capacidad específica de casi 700 mAh g^{-1}, con una retención de capacidad del 85,4% después de 350 ciclos, lo que demostró una disminución de capacidad muy baja de solo 0,042% por ciclo. Es importante señalar que la eficiencia coulómbica siempre fue superior al 96% durante todos los ciclos, lo que indica que apenas existió pérdida de energía entre los procesos de carga y descarga de estas baterías sostenibles. Por tanto, los resultados obtenidos constituyen una primera etapa para la valorización del carbón activo regenerado (procedente de la desodorización de EDAR) como parte del cátodo carbonoso de las prometedoras baterías de Li-S.

ChemSusChem | Full Papers doi.org/10.1002/cssc.202101231 | Chemistry Europe European Chemical Societies Publishing

Simple and sustainable preparation of cathodes for Li–S batteries: Regeneration of granular activated carbon from the odour control system of a wastewater treatment plant

Almudena Benítez[+],[a] Pedro Márquez[+],[b] M. Ángeles Martín,[b] and Álvaro Caballero*[a]

[a] Dpto. Química Inorgánica e Ingeniería Química, Instituto de Química Fina y Nanoquímica, Universidad de Córdoba, Campus Universitario de Rabanales, Edificio Marie Curie, 14071 Córdoba (Spain)

[b] Department of Inorganic Chemistry and Chemical Engineering, Area of Chemical Engineering, University of Cordoba, Campus Universitario de Rabanales, Edificio Marie Curie, Carretera N-IV, km 396, 14071 Córdoba (Spain)

[+] These authors contributed equally to this work.

* Corresponding author: alvaro.caballero@uco.es

Manuscript received: June 14, 2021; Revised manuscript received: July 19, 2021; Accepted manuscript online: July 21, 2021; Version of record online: August 5, 2021

Graphical abstract

Abstract

To obtain a wide variety of green materials, numerous investigations have been undertaken on industrial waste that can act as sustainable resources. The use of hazardous wastes derived from wastewater treatment plants (WWTPs), especially the activated carbon used in odor control systems, is a highly abundant, scalable, and cost-effective strategy. The reuse of waste materials is a key aspect, especially for the sustainable development of emerging energy storage systems, such as lithium-sulfur (Li−S) batteries. Herein, granular active carbons from two WWTP treatment lines were regenerated in air at low temperature and utilized as the sulfur host with micro-/mesoporous framework. The resulting regenerated carbon and sulfur composites were employed as cathodes for Li−S cells. The SL-ACt3@S composite electrode with 60 wt% loaded sulfur exhibited a remarkable initial capacity of 1100 mAh g^{-1} at C/10 rate and higher than 800 mAh g^{-1} at C/2. Even at a rate of 1C, it maintained a high capacity of almost 700 mAh g^{-1} with a capacity retention of 85.4 % after 350 cycles, demonstrating a very low capacity fading of only 0.042 % per cycle. It is essential to note that the coulombic efficiency was always higher than 96 % during all the cycles. In this proposal, the only used source material was expired carbon from WWTP that was obtained with a simple and effective regeneration process. This "trash into treasure" strategy leads to a new way for using hazardous waste material as high-performance and environmentally safe electrodes for advanced Li−S batteries.

Keywords: activated carbon; biomass; lithium-sulfur batteries; thermal regeneration; wastewater treatment plant.

1. Introduction

Lithium-sulfur (Li−S) batteries have been postulated as the next-generation rechargeable battery system owing to a high theoretical energy density (2552 Wh kg^{-1}), a high theoretical capacity (1672 mAh g^{-1}), its low cost, and an abundance of sulfur in nature. Furthermore, it is considered an environmentally benign element compared to some transition metals used in lithium-ion batteries (LIBs).[1-4] However, certain barriers must be overcome in order to avoid capacity fading during cycling and to achieve its commercialization, such as the following: (a) sulfur and solid reduction products (Li_2S_2 and Li_2S) are poor electrical conductors, leading to poor electrochemical utilization of S and lithium polysulfides (LiPSs); (b) the formation of intermediate polysulfides causes a huge volume expansion of the cathode during lithiation; and (c) the dissolution of some formed polysulfides (Li_2S_x, $2 \leq x \leq 8$) in the electrolyte gives rise to unfavorable reactions of the LiPSs with the Li anode due to the formation of an insulating layer of Li_2S_2/Li_2S, which increases the resistance of the Li−S batteries and decreases the amount of active components in the cathode and, therefore, the life cycle of the cells.[5, 6] To address these challenges, the impregnation of sulfur into non-polar porous conductive carbons and other functionalized carbons was first attempted to improve its development because they possess good conductivity and large surface areas.[7-10]

Among various nanostructured carbon-based materials, carbon nanotubes,[11] microporous carbons,[12] porous hollow carbons,[13] hollow carbon spheres,[14] graphenes,[15] and graphenes doped with heteroatoms[16] can be highlighted as sulfur scavenging/trapping materials with good performance in this battery technology. Although this type of carbonaceous material has been highly efficient as a sulfur host and its study has contributed to the development of Li−S batteries, its design is usually not carried out using sustainable or low-cost methods. In most cases, the preparation of nanostructured carbons involves complex synthesis processes (such as soft templates, hard templates, and multiple templates) and expensive and non-renewable precursors, consequently limiting its commercial applications.[17, 18] Hence, considerable efforts have been devoted to design activated carbons (ACs) from biomass residues, wherein the raw material is normally cheap and abundant, and in addition, its usual manufacturing methods are fast and simple.[19-21]

Nevertheless, the processes used for the production of carbons derived from biomass as Li−S electrodes usually require three basic conditions: (1) high pyrolysis temperature, (2) use of physical or chemical activating agents, and (3) inert atmospheres to avoid combustion.[22] **Table 1** shows some of the most relevant studies reported on this type of carbons, its main synthesis conditions, textural properties, and electrochemical performance in Li−S batteries.

Table 1. Production process, textural properties, and electrochemical behavior of biomass-derived carbons from industrial treatments.

Biomass source [Ref]	**Production Process Conditions**			**Textural Properties**		**Electrochemical Performance**		
	Temperature *ºC* (time)	Activating agent	Gas flow	S_{BET} $m^2\ g^{-1}$	V_T $cm^3\ g^{-1}$	S loading *mg* cm^{-2}	Rate *C*	Capacity *mAh* g^{-1} (cycle)
Sawdust [23]	800 (1h)	K_2CO_3	N_2	2988	1.94	2.7	C/10	980 (50^{th})
Rice husk [24]	900 (-)	-	Ar	525	0.49	1.0	C/2	600 (500^{th})
Rice straw [25]	800 (3h)	KOH	Ar	1187	-	1.2	2 C	584 (500^{th})
Wheat straw [26]	800 (2h)	KOH	N_2	3102	1.92	1.0-1.2	1 C	455 (500^{th})
Soybean hull [27]	700 (2h)	KOH	N_2	1232	0.54	1.5	C/2	450 (200^{th})
Spent coffee [28]	800 (12h)	-	N_2	1037	0.54	-	C/5	474 (400^{th})
Paper [29]	700 (2h)	KOH	Ar	2970	1.4	2.0	1 C	540 (200^{th})
Tobacco stem [30]	700 (2h)	KOH	N_2	833	0.65	1.1	C/2	754 (400^{th})
Brewing waste [31]	900 (1h)	-	N_2	414	0.28	1.0	1 C	800 (450^{th})
WWTP (WL-ACt4) [This work]	350 (4h)	-	Air	569	0.35	2.0	1 C	410 (350^{th})
WWTP (SL-ACt3) [This work]	250 (3h)	-	Air	606	0.35	2.0	1 C	646 (350^{th})

In the few cases where activating agents are not used, such as rice husk, spent coffee, and brewing waste, temperatures above 800 °C are necessary to obtain carbons with appropriate textural properties to act as a sulfur matrix. Thus, high values of specific surface and pore volume are required of the carbons for this application, and the use of activating agents, such as potassium hydroxide or potassium carbonate, helps to fulfil this objective in the synthesis process. Likewise, the inert atmosphere with a stream of argon or nitrogen is an essential requirement to achieve the synthesis of activated carbon. These conditions and basic operations complicate the valorization process of biomass by-products or residues to obtain suitable porous carbons for low-cost and sustainable Li−S batteries.

This work presents an activated carbon obtained by a simple, low-cost, and sustainable process, which also does not involve high temperatures, inert flow, or the incorporation of chemical agents for its thermal regeneration, resulting in an effective material for use as an electrode matrix for Li−S batteries. Specifically, the selected material is a granular activated carbon (GAC) from the odor control system of an urban wastewater treatment plant (WWTP). After a certain time of use, the replacement of the GAC beds is necessary to ensure the correct functioning and effectiveness during the odor adsorption process. Regarding the fate of the contaminated GACs, it is worth noting that they are classified as hazardous industrial waste (code: 06 13 02) by the European Commission (2018), and therefore, they are transported and stored in landfills.[32] In this context, an environmental and ecological problem arises due to the accumulation of this waste from WWTP in garbage piles that, a priori, have not been used for other applications.

In the present study, for the first time, a second useful life was provided for carbon residue from WWTP through a simple thermal regeneration process. Herein, we report the electrochemical results obtained using regenerated activated carbons as a sulfur matrix. AC@S composites were prepared by an effective and easily scalable process, achieving electrodes with a high sulfur loading that demonstrated remarkable electrochemical performance. Within this framework, the results demonstrate an approach to not only reduce the accumulation of carbon residues from WWTP in landfills through a simple thermal regeneration process under oxidizing atmosphere, but also to revalue it in a new application as an effective component for Li−S cells. Therefore, the

insights from this study are important for further development of sustainable cathodes applied to high-performance Li−S batteries.

2. Experimental section

2.1. GACs from WWTP

Commercial GACs from coconut shells and impregnated in NaOH are used as pristine GAC (P-AC) in the odor adsorption process carried out in the urban wastewater plant of Seville (Spain).[32] During the deodorization process, GACs are used as adsorbent beds for odorants, such as volatile organic compounds (VOCs), mercaptans, ammonia, and hydrogen sulfide, among others. After a certain time of use, the porosity of the adsorbents is saturated with these compounds, and the GAC beds must be replaced. As previously mentioned, contaminated GACs are considered hazardous waste and destined for landfills. For this study, contaminated GACs were collected from two different points of the odor control system to regenerate them and turn them into a by-product. Specifically, the treated samples were: (a) WL is a contaminated GAC sample from the head pre-treatment point of the water line and (b) SL is a contaminated GAC sample from sludge dewatering point of the sludge line.

2.2. Thermal regeneration process

The contaminated WL and SL samples were subjected to a thermal regeneration process to transform them into WL-AC and SL-AC, respectively.[33] In general, the regeneration process was carried out in a tube furnace (Carbolite Gero CTF, Parsons Lane, Hope Valley, UK) using a constant flow of air. The heat treatment conditions were analyzed in this study, keeping the heating ramp at 15 °C min^{-1}, selecting the target temperature of 350 °C for WL-AC samples and 250 °C for SL-AC samples, and varying the rest time at the set temperature. After the regeneration treatment, the samples were identified as WL-ACt*x* or SL-ACt*x*, where *x* is the value of the resting time maintained during heating (*x*=1, 2, 3, 4, or 5 h). The samples were weighed before and after the heat treatment to calculate the efficiency of the regeneration process. A schematic illustration of the thermal regeneration process is shown in **Scheme 1**.

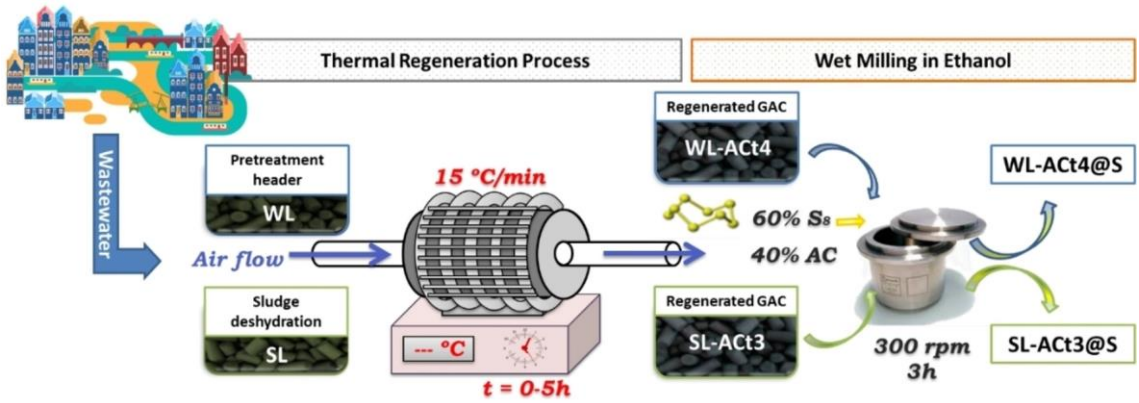

Scheme 1. Schematic diagram of the thermal regeneration and composites preparation processes.

2.3. Composites and cathodes preparation

The two composites studied (WL-ACt4@S and SL-ACt3@S) were prepared by grinding the corresponding AC and commercial sublimated sulfur in a 4:6 mass ratio using ethanol as a wetting agent in a Retsch PM100 planetary ball mill (**Scheme 1**). The wet milling conditions to achieve a homogeneous mixture were a rotation speed of 300 rpm for 3 h, including a rotation inversion every 15 min with a pause time of 5 min prior to each rotation inversion, as was demonstrated in our previous work.[49] After this process, the obtained product was dried at 50 °C overnight.

In the next stage, the positive electrodes were prepared by mixing the composites with polyvinylidene fluoride (PVDF 6020, binder, Solvay) and carbon Super P (conducting agent, Timcal) in a weight proportion of 80:10:10 in a manual agate mortar and adding 1-methyl-2-pyrrolidone (Sigma Aldrich, 0.5 mL per 100 mg). The slurry was ground to the proper consistency and cast on a carbon cloth (GDL, ELAT LT1400 W) as an effective current collector by doctor blading to an areal sulfur loading of 2.0 $mg_s\,cm^{-2}$.[50] The electrodes were allowed to dry at ambient conditions, cut into circular discs of the desired size (13 mm in diameter), and dried again in a vacuum oven (Buchi, Flawil, Switzerland) at 45 °C for 3 h before transferring them to the Ar-filled glovebox (M-Braun 150, M-Braun, Garching, Germany).

2.4. Materials characterization

XRD patterns were recorder on a BrukerD8 Discover A25 X-ray diffractometer by using filtered CuK_α radiation within a 2θ angle range between 10 and 80° at a rate of 1.05 s per step with a step size of 0.04° in continuous mode. Specific surface areas and total

pore volumes were examined from the N_2 adsorption–desorption isotherms using a Micromeritics ASAP 2020 M apparatus. The pore size distribution was calculated by the DFT method applied to the adsorption branch of the isotherms. The samples were previously outgassed under vacuum at 120 °C overnight. TGA was performed in a Mettler Toledo TGA/DSC (Mettler-Toledo, Columbus, OH, USA) under a nitrogen or oxygen atmosphere and heating the samples from 30 to 900 °C at 10 °C min^{-1}. Raman spectra were recorded in a Renishaw Raman instrument (InVia Raman Microscope) equipped with a Leica microscope and a Renishaw CCD Camera detector (578×400) using a spectral range of 100–2500 cm^{-1}. A total of 10 scans per spectrum were acquired to improve the signal-to-noise ratio. The exposure time was 10 s, and the laser power was set at 0.5 % over the maximum provided using a green laser (532 nm) excitation source. The morphology of the powder and electrode was determined with a JEOL JSM-7800F SEM equipped with EDX to analyze images of the surface topography. Finally, the absorption power of the samples was evaluated by UV/vis spectra recorded in a wavelength range of 190–600 nm with an UV/Vis double beam spectrophotometer (Zuzi model 4260/50) equipped with two detectors.

2.5. Cells assembly and electrochemical measurements

Li−S batteries were systematically assembled into CR2032 coin cells inside a glovebox with the previously prepared electrodes as the cathode and a lithium metal foil as the anode. The electrolyte was a mixture of DOL and DME (1:1, *v*/*v*) by dissolving 1 mol L^{-1} LiTFSI with 0.4 mol L^{-1} lithium nitrate ($LiNO_3$) as an additive. A polyethylene membrane (PE, 25 μm thick, Celgard 2400) was used as a separator, and it was soaked in 50 μL of the electrolyte solution (electrolyte/sulfur ratios around 19 μL mg_S^{-1}).

The galvanostatic tests were carried out using an Arbin BT2143 potentiostat–galvanostat system within a voltage range of 1.8–2.8 V vs. Li^+/Li. Specific capacity values are referred to the mass of elemental sulfur in the electrodes. CV curves and EIS spectra were recorded on an Autolab PGSTAT-204 equipment. CV measurements were recorded at variable rates of 0.1, 0.2, 0.4, 0.8, and 1.0 mV s^{-1} between 1.8 and 2.8 V vs. Li^+/Li. Impedance spectra were recorded at OCV condition and after the 5th CV cycle by applying an alternative voltage signal of 10 mV amplitude within the 500 kHz to 0.1 Hz frequency range.

3. Results and discussion

The structural properties of the samples were analyzed by X-ray diffraction (XRD). **Figure 1a**, **b** compares the diffractograms of the pristine GAC (P-AC) sample with the regenerated samples at different resting times, WL-ACt and SL-ACt, respectively. All samples present two dominant broad signals characteristic of activated carbons corresponding to reflection peaks (002) and (100) at 2θ values of 26 and 43°, respectively, which are attributed to the crystallographic planes of graphite (PDF #41-1487). Additional peaks due to the presence of minor phases are observed, such as SiO_2, Na_2SO_4, or CaO, which are formed after the regeneration process since silicon and sodium and calcium salts are present in the composition of the coconut shell itself, as confirmed by X-ray fluorescence (XRF analyses are not shown).[33] In addition, activated carbons derived from the water line (WL-ACt) contain more impurities than activated carbons derived from the sludge line (SL-ACt), which is verified by the greater number of peaks present in their diffractogram that are associated with the phase of Na_2SO_4.

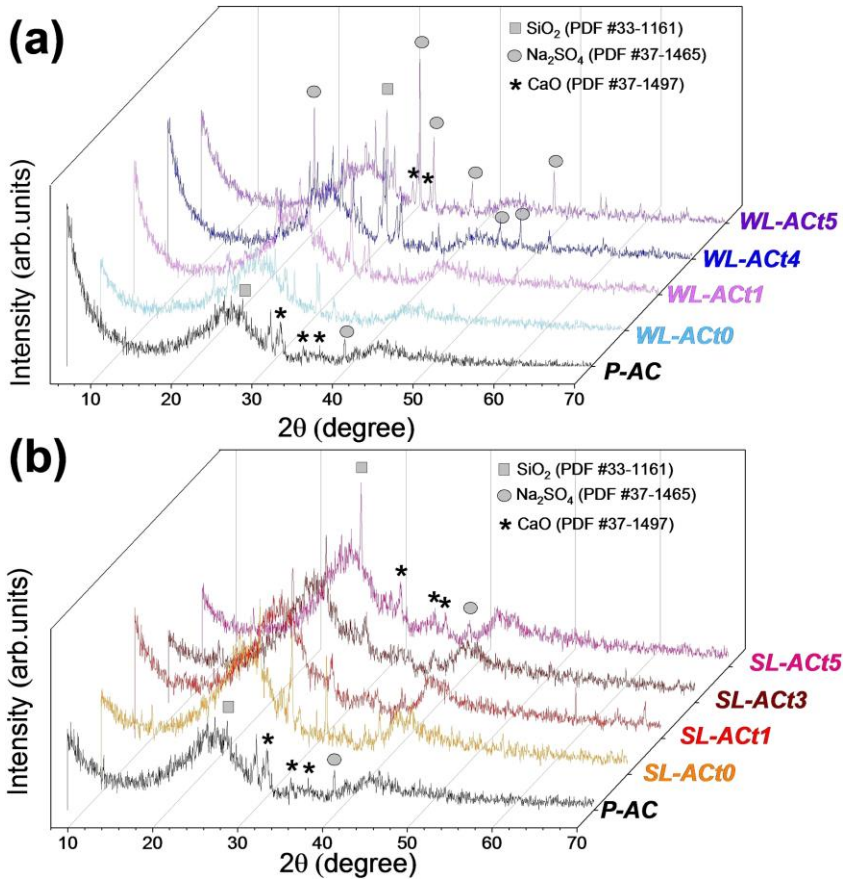

Figure 1. XRD pattern of pristine GAC (P-AC) compared to (**a**) WL-ACtx (x=0, 1, 4, 5), and (**b**) SL-ACtx (x=0, 1, 3, 5).

Figure 2 shows a summary of the textural properties of the different samples obtained by regeneration in an oxidizing atmosphere. After carrying out the nitrogen adsorption-desorption isotherms of all the regenerated samples, different textural parameters were analyzed. The values of Brunauer-Emmett-Teller surface area (S_{BET}) in blue, micropore area (S_{micro}) in green, total pore volume (V_T) in red, and micropore volume (V_{micro}) in pink are represented in **Figure 2**. In the case of the WL-ACtx sample, the best results were obtained after regeneration at 350 °C for 4 h, providing a surface area of 569 $m^2\,g^{-1}$ and a total pore volume of 0.35 $cm^3\,g^{-1}$. However, for the SL-ACtx sample, the best characteristics were obtained after regeneration at 250 °C for 3 h, with the activated carbon acquiring a surface area of 606 $m^2\,g^{-1}$ and a total pore volume of 0.35 $cm^3\,g^{-1}$, the latter being the same value as for the previous sample (WL-ACt4).

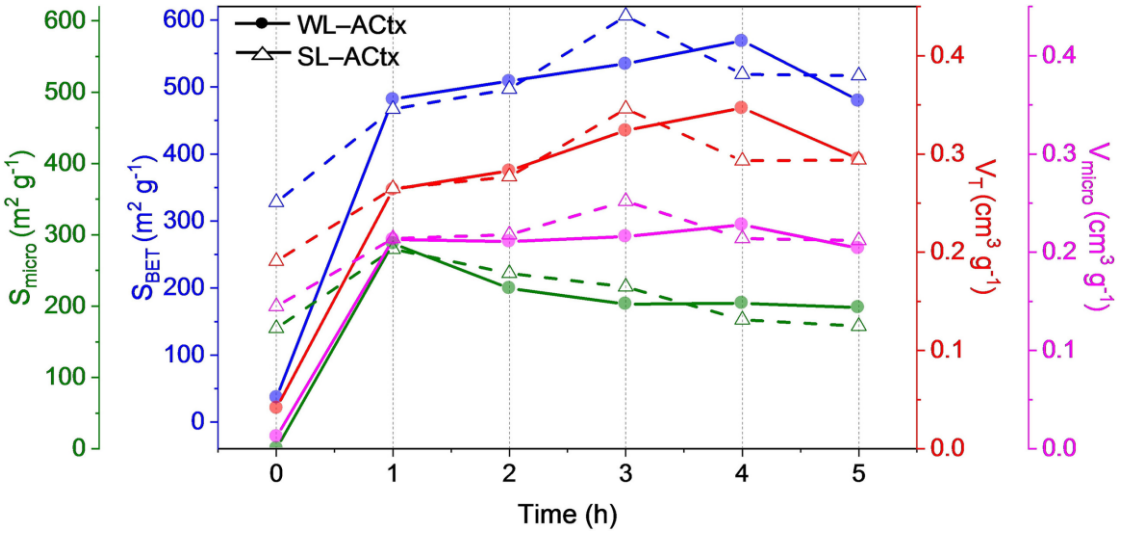

Figure 2. Graphical representation of the textural properties (S_{BET}, S_{micro}, V_T, V_{micro}) of the WL-ACtx (represented with a circle) and SL-ACtx (represented with a triangle) samples for different regeneration times (0–5 h).

The shape of the isotherm obtained for each material provides information about the porosity of the solid. The profiles of the nitrogen adsorption and desorption isotherms corresponding to the selected samples (WL-ACt4 and SL-ACt3) are illustrated in **Figure 3a**. Both samples are attributed to type IV isotherms according to the BDDT (Brunauer-Deming-Deming-Teller) classification, mainly mesoporous solid characteristics.[34] Furthermore, at intermediate relative pressure values, the samples show an increase in the amount adsorbed as observed by the hysteresis loop that appears in the isotherms, which is due to capillary condensation. However, the SL-ACt3 sample at low relative pressure values has a shape that can be associated with a type I isotherm, indicating the presence

of micropores. Thus, the slope of volume adsorbed at low relative pressures is higher for SL-ACt3 than WL-ACt4. After the incorporation of sulfur into the carbonaceous matrices, the samples were analyzed again using gas adsorption–desorption isotherms, confirming in both cases that the WL-ACt4@S and SL-ACt3@S samples belong to type II isotherms, that is, non-porous samples. This result affirms the correct preparation of the composite samples.

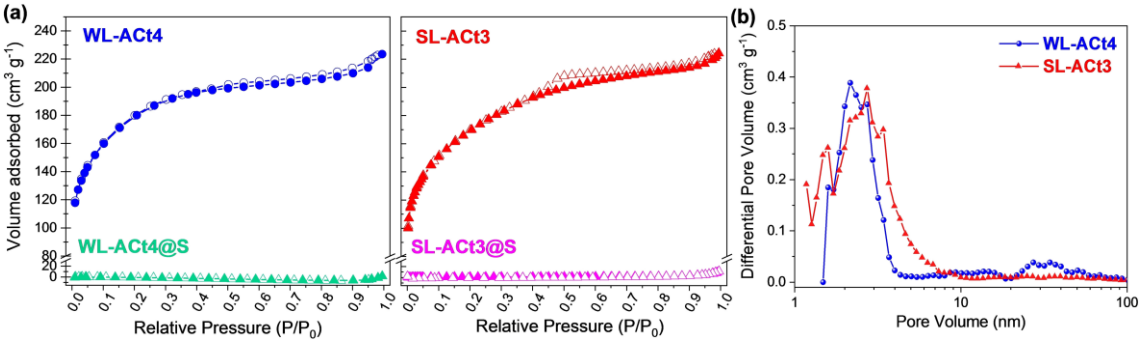

Figure 3. (**a**) Nitrogen (77 K) adsorption–desorption isotherms for WL-ACt4 and SL-ACt3 samples and their corresponding composites. (**b**) Pore size distribution by DFT of WL-ACt4 and SL-ACt3 activated carbons.

Figure 3b shows the pore size distribution by density functional theory (DFT) of the carbonaceous matrices. The WL-ACt4 sample presents a porosity composed mostly of mesopores (2–50 nm), while the SL-ACt3 sample contains a mixture of micro- (<2 nm) and mesopores.[35, 36] These results corroborate the presence of micropores in the SL-ACt3 sample, confirming the evidence deduced from **Figure 3a**.

Figure 4 shows thermogravimetric analysis (TGA) of the samples. Since the regeneration of the activated carbons was done in an oxidizing atmosphere, the TGA experiments for the WL-ACt4 and SL-ACt3 samples were carried out under a mixture of oxygen and nitrogen gases from room temperature to 900 °C at a heating rate of 10 °C min^{-1}, as represented in **Figure 4a,b**, respectively. Both samples consist of 75 % by weight of C, but their thermal behavior is different because the thermal decomposition of the activated carbon from the water line begins around 350 °C and ends at 500 °C, while the sample from the sludge line decomposes at a lower temperature, starting around 250 °C. This variation is justified by the temperature limit that was set during the regeneration of both samples, which was 350 °C for the WL-ACt4 sample and 250 °C for the SL-ACt3 sample. The temperature limit for the regeneration of each sample was already explained in our previous work,[33] and it was due to the fact that the adsorbent

from pretreatment header deodorization (WL) led to a mass loss of 25 % at 350 °C, while the adsorbent coming from sludge dewatering deodorization (SL) resulted in a higher mass loss at 350 °C, close to 80 % by weight.

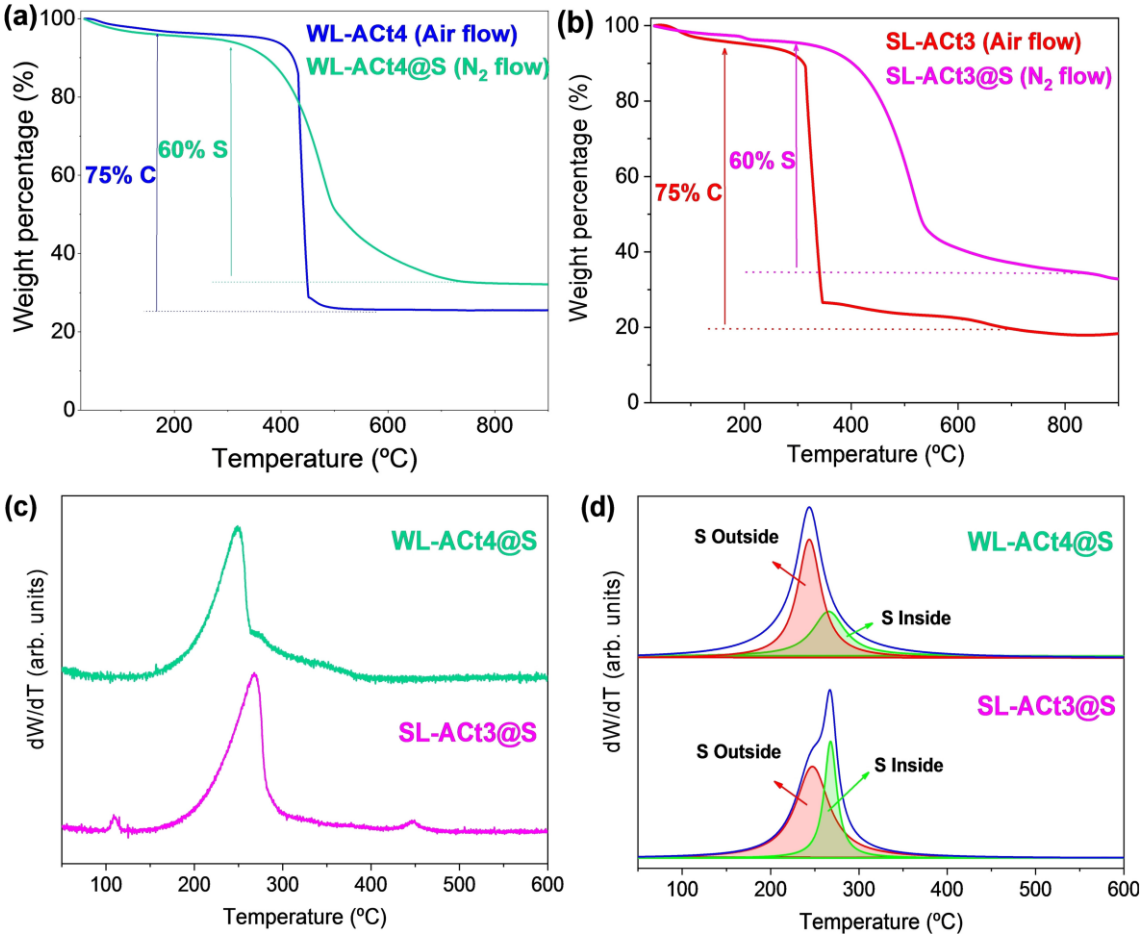

Figure 4. TGA curves for (**a**) WL-ACt4 and WL-ACt4@S samples and (**b**) SL-ACt3 and SL-ACt3@S samples. (**c**) DTG curves for WL-ACt4@S and SL-ACt3@S samples. (**d**) Deconvolution of DTG curves of the same composite samples.

The results obtained from the TGA measurements for the composite samples are also shown in **Figure 4**. These experiments were carried out under a nitrogen atmosphere, and for both the WL-ACt4@S and SL-ACt3@S samples, the presence of a 60 % by weight of sulfur was confirmed, corresponding to the mass ratio used in the preparation of composites by the wet ball milling route.

Additionally, the TG curves were processed by calculating their derivatives to analyze the loss of mass corresponding to sulfur. **Figure 4c**,**d** shows differential thermogravimetric curves (d*W*/d*T*, DTG) to obtain more information about the sulfur contained in the composites. In general, the sulfur environments can be classified into

three categories depending on the temperature range: S outside the pore (30–280 °C), S inside the pore (280–400 °C), and S interacting with carbon (400–600 °C).[37] Focusing on **Figure 4d**, the deconvolution of the S peak is shown for the WL-ACt4@S and SL-ACt3@S samples. Two sulfur environments can be observed. In the WL-ACt4@S sample, there is a greater amount of surface sulfur (red line around 245 °C, marked as "S Outside" in **Figure 4d** than pore sulfur (green line around 280 °C, marked as "S Inside"), while the opposite occurs in the SL-ACt3@S sample. Based on these results, the SL-ACt3@S composite has a priori better characteristics for use as an electrode for Li−S batteries since most of the sulfur has been incorporated into the porosity of the carbonaceous matrix, making the dissolution of lithium polysulfides in the electrolyte more difficult, thus mitigating the shuttle effect.

The structural properties of the composite samples were studied by XRD and Raman spectroscopy. XRD measurements were also performed for the composites containing sulfur (**Figure 5a**). Intense and narrow diffraction peaks ascribed to the orthorhombic phase of sulfur (PDF #08-0247) were observed. It should be noted that although most of the S is contained within the porosity of the carbonaceous matrix for the SL-ACt3 sample, there is a certain excess of S that remains lodged on the surface. This fact justifies the presence of signals attributed to S orthorhombic in the XRD measurements.[38] Furthermore, in both diffractograms, it is possible to observe the two broad bands at 26 and 43° (2θ) corresponding to (002) and (100) reflections of amorphous carbon and disordered graphitic structure, respectively. The Raman spectra of the composite samples confirmed the presence of amorphous carbon and sulfur in the structure. The first signals to appear in the spectrum are associated with the Raman vibrations of S_8 at room temperature and correspond to the bands at 471 (υ, a_1+e_2), 430 (υ, e_3), 245 (δ, e_3), 215 (δ, a_1), and 150 (δ, e_2) cm^{-1}.[39] Advancing in the spectrum, two broad and intense bands appear at 1350 and 1599 cm^{-1}, which correspond to the D and G bands of graphite, respectively. The degree of graphitization of the materials can be estimated by examining the relative intensity between the D band (for disordered carbons) and the G band (for graphitized carbons).[40] The intensity ratio (I_D/I_G) for the WL-ACt4@S and SL-ACt3@S composites is close to 1, which confirms the high degree of disorder in the samples.

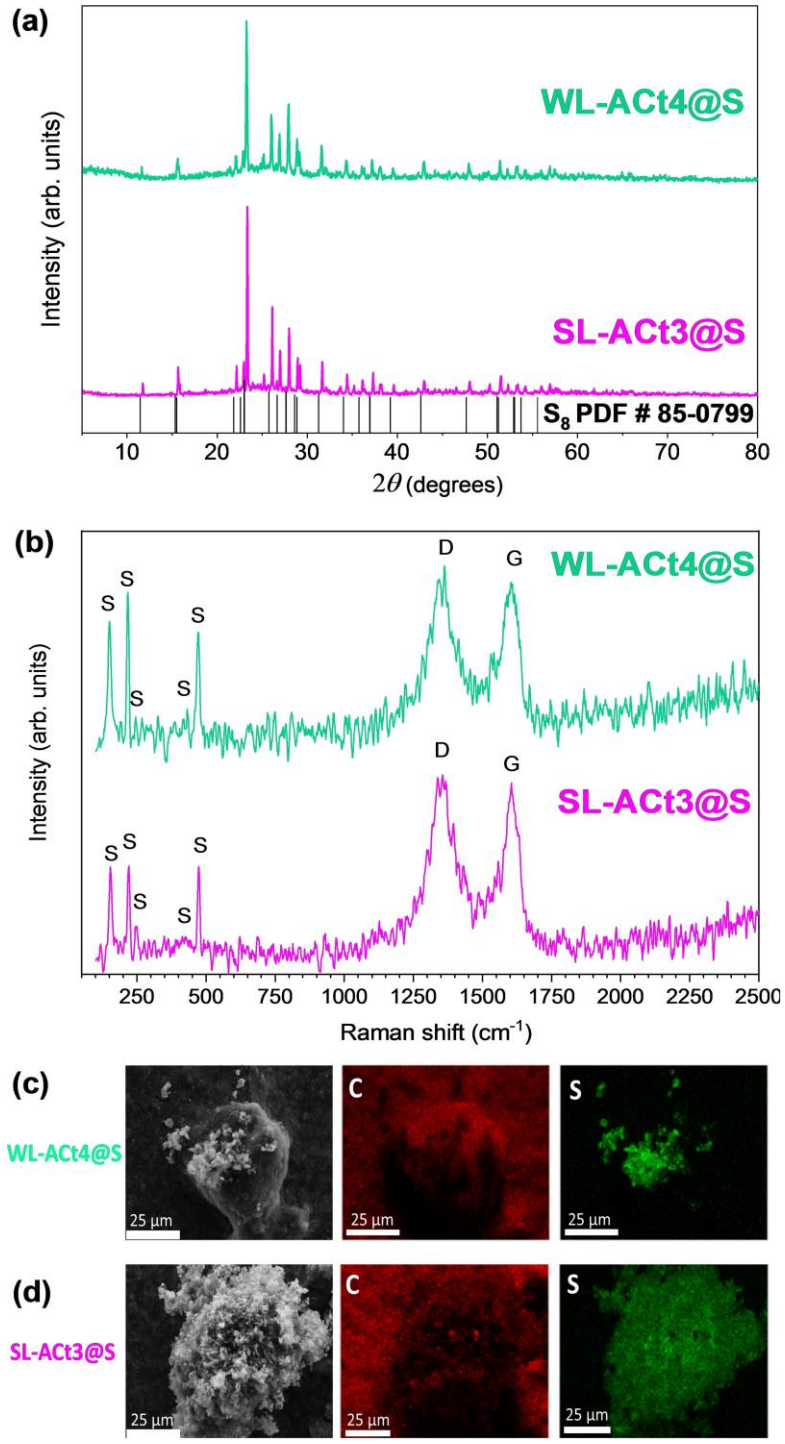

Figure 5. (**a**) XRD patterns and (**b**) Raman spectra of WL-ACt4@S and SL-ACt3@S composites; SEM images and elemental mapping of C and S for (**c**) WL-ACt4@S and (**d**) SL-ACt3@S composites.

Figure 5c,**d** shows scanning electron microscopy (SEM) images recorded at the same magnification for WL-ACt4@S and SL-ACt3@S samples, respectively. To the right of each SEM image, the results obtained from the elemental mapping of C (red) and S (green) for both images are collected. Comparing the analysis of both samples, clear

differences can be observed. For the WL-ACt4@S composite, a heterogeneous distribution of elements is observed on the surface of the particle chosen in the analysis. However, for the SL-ACt3@S composite, the placement of the elemental components on the particle is uniformly distributed along the porous surface, indicating an effective incorporation of sulfur into the porosity of the carbonaceous-based material. These results are in agreement with those obtained through the analysis and treatment of the TG data, where it was already possible to verify that the WL-ACt4 sample had a greater amount of surface sulfur, while the SL-ACt3 sample mainly presents sulfur located within the pores (**Figure 4d**).

After the characterization of the materials, the electrodes were prepared and the Li−S cells were assembled to study the electrochemical behavior of both composites. Sequentially, different electrochemical measurements in the potentiostatic and galvanostatic regime were performed.

In **Figure 6a**,**b**, cyclic voltammograms (CVs) at increasing scan rates from 0.1 to 1.0 mV s^{-1} of the WL-ACt4@S and SL-ACt3@S cathodes are shown, respectively. They were used to check the reversibility of the reaction of sulfur to short-chain polysulfides, and vice versa. The CV data of both samples exhibit two cathodic (C_1 and C_2) and anodic peaks (A_1 and A_2). C_1 between 2.1 and 2.4 V represents the cathodic reduction process of $S_8 \rightarrow Li_2S_x$ ($3 \leq x \leq 8$), and C_2 between 1.7 and 2.1 V represents the cathodic reduction: $Li_2S_x \rightarrow Li_2S_2/Li_2S$ ($3 \leq x \leq 8$). Similarly, during the charging process, the A_1 peak appearing between 2.1 and 2.4 V represents the anodic oxidation process and corresponds to $Li_2S_2/Li_2S \rightarrow Li_2S_x$ ($3 \leq x \leq 8$), while the corresponding A_2 peak between 2.4 and 2.8 V is related to Li_2S_x ($3 \leq x \leq 8$)$\rightarrow S_8$+Li. A displacement of the anodic and cathodic peaks takes place towards lower potentials with increasing current density, implying a decrease in cell polarization and an increase in the participation of active materials in the redox reaction.

Considering these four peaks (C_1, C_2, A_1, and A_2), the Randles–Sevcik equation was used to calculate the diffusion coefficient of Li^+ (D_{Li^+}) in the WL-ACt4@S-based and SL-ACt3@S-based electrodes. Slope values when plotting I_P versus $v^{0.5}$ are fitted and calculated in **Figure 6c**,**d**. The Randles–Sevcik equation is as follows [Eq. 1]:

$$I_P = 2.69 \cdot 10^5 \, n^{3/2} \, A \, D_{Li}^{0.5} \, v^{0.5} \, C_{Li} \quad (1)$$

where I_P is the peak current, n represents the electron number, A represents the electrode area, D_{Li} is the Li ion diffusion coefficient, C_{Li} is the Li ion concentration in the electrochemical reaction, and v is the scan rate.

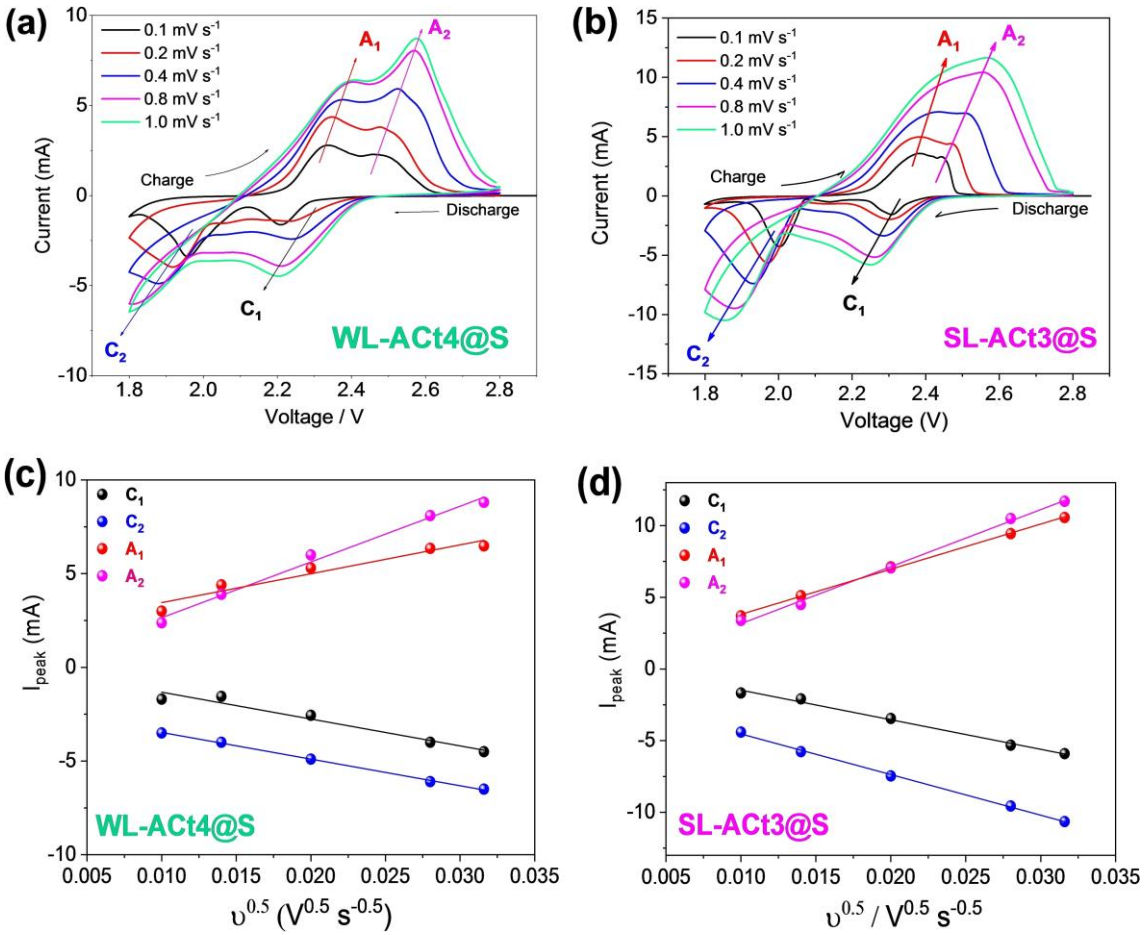

Figure 6. (**a**, **b**) CV measurements performed at various scan rates (0.1, 0.2, 0.4, 0.8, and 1.0 mV s^{-1}). (**c**, **d**) Linear fitting of the peak currents obtained from the voltammograms located above for Li/1 m LiTFSI(DOL/DME)/WL-ACt4@S and Li/1 m LiTFSI(DOL/DME)/SL-ACt3@S cells, respectively. LiTFSI: lithium bis(trifluoromethanesulfonyl)imide. DOL/DME: 1,3-dioxolane/1,2-dimethoxyethane.

For WL-ACt4@S, the values are: $D_{Li}(C_1)=1.92 \cdot 10^{-8}$ cm^2 s^{-1}, $D_{Li}(C_2)=5.15 \cdot 10^{-7}$ cm^2 s^{-1}, $D_{Li}(A_1)=4.46 \cdot 10^{-7}$ cm^2 s^{-1}, and $D_{Li}(A_2)=1.30 \cdot 10^{-8}$ cm^2 s^{-1}. For SL-ACt3@S, the values are: $D_{Li}(C_1)=4.13 \cdot 10^{-8}$ cm^2 s^{-1}, $D_{Li}(C_2)=3.52 \cdot 10^{-7}$ cm^2 s^{-1}, $D_{Li}(A_1)=5.30 \cdot 10^{-8}$ cm^2 s^{-1}, and $D_{Li}(A_2)=8.25 \cdot 10^{-8}$ cm^2 s^{-1}. These values are comparable to those calculated in our previous works[41, 42] and confirm that both cathodes can provide high capacity values during cycling.

Analyzing the electrochemical impedance spectroscopy (EIS) measurements recorded at open circuit voltage (OCV) and after 3 voltammetric cycles, more information was obtained on the electrochemical behavior of the cells. A two-electrode setup is exploited, where Li metal performs as both the counter and reference electrodes. As shown in **Figure 7a**,**b**, the charge transfer resistance at OCV of the WL-ACt4@S composite electrodes (R_{ct}=129 Ω) is higher than the SL-ACt3@S electrodes (R_{ct}=36.4 Ω), indicating a lower electron conductivity. After several cycles of CV, a change in the semi-circles can be observed, showing a pronounced decrease in the charge transfer resistance for the WL-ACt4@S and SL-ACt3@S electrodes, providing values of 12.56 and 4.18 Ω, respectively.

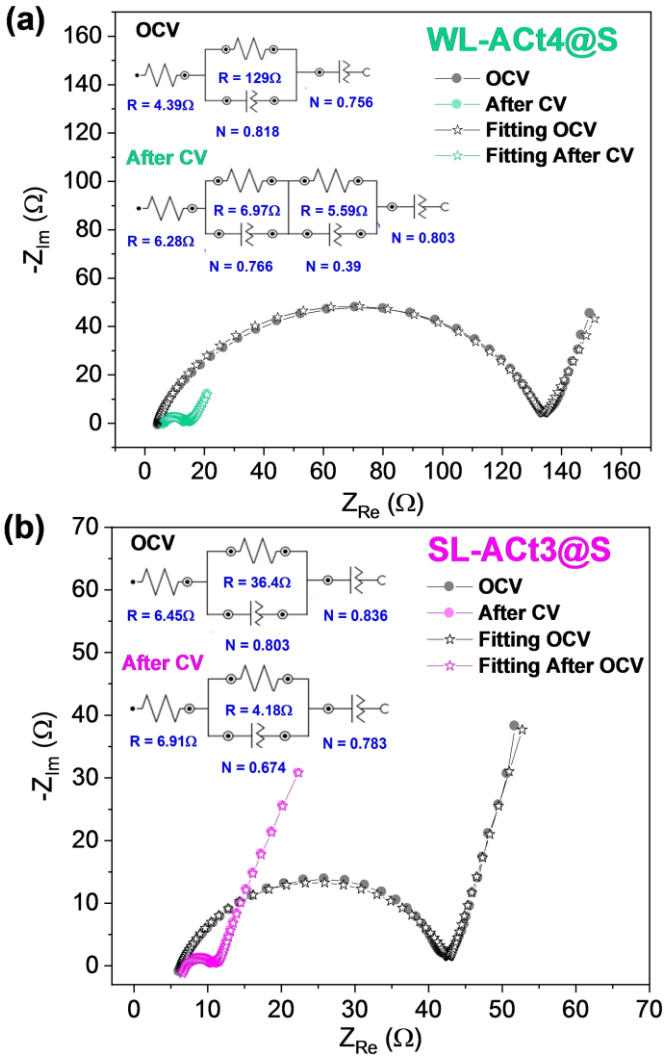

Figure 7. Nyquist plots recorded by EIS at OCV of the cell and after 3 cycles of CV at 0.1 mV s^{-1} for (**a**) Li/1 m LiTFSI(DOL/DME)/WL-ACt4@S and (**b**) Li/1 m LiTFSI(DOL/DME)/SL-ACt3@S cells. The fitting results are shown together with the equivalent circuits in the inset for OCV and after the third CV cycle.

Focusing on **Figure 7b**, the behavior of the Li/1 m LiTFSI(DOL/DME)/SL-ACt3@S cell is associated with an equivalent circuit of type $R_e(R_1Q_1)Q_2$, where R_e is the electrolyte resistance that appears at high frequency and whose values are very similar for OCV and after CV (6.45 and 6.91 Ω, respectively). At medium-high frequency and in series with R_e, the element R_1Q_1 appears where a semicircle is observed and is assigned to the resistance (R_1: 36.4 Ω for OCV and R_1: 4.18 Ω after CV) and capacitance of the electrode/electrolyte interface (Q_1), including the solid electrolyte interphase layer (SEI) formed on the surface electrodes. At the low-frequency region, the last capacitive element (Q_2) can explain the diffusion of lithium ions at the electrode/electrolyte interface.

Figure 8a,**b** shows the registered charge and discharge profiles for Li/1 m LiTFSI(DOL/DME)/WL-ACt4@S and Li/1 m LiTFSI(DOL/DME)/SL-ACt3@S cells, respectively. Both tests were carried out under the same conditions, that is, the cells were cycled during the first 5 cycles at a slow rate (C/10) as an activation step, and subsequently, the cycling was maintained at C/2 within a potential range of 1.8–2.6 V up to 150 cycles. In both cases, the profiles are very similar, showing two plateaus around 2.35 and 2.05 V at C/2 during the discharge process. Similarly, two plateaus are differentiated during the charging process at 2.25 and 2.45 V, confirming the reversibility of the electrochemical process.

Figure 8c,**d** shows the comparative electrochemical results between both cells when cycled at C/2 and 1C rates, respectively. At a moderate rate of C/2, an appropriate electrochemical behavior is shown for both materials, achieving a coulombic efficiency close to 100 % and good stability during 150 cycles (**Figure 8c**). The WL-ACt4@S electrode provided average capacity values of 676.5 mAh g^{-1}, while the SL-ACt3@S electrode provided better performance, reaching an average capacity value of 842 mAh g^{-1}. However, at a high rate of 1C, the behavior of both materials is different, as shown in **Figure 8d**. In this test, the WL-ACt4@S electrode loses stability during cycling, starting with values of 575 mAh g^{-1} and decreasing its capacity to 410 mAh g^{-1} after 350 cycles. While the average capacity for the WL-ACt4@S electrode is 506 mAh g^{-1}, the value for the SL-ACt3@S electrode is 698 mAh g^{-1}, which is 27.5 % higher, with a capacity retention of 85.4 % after 350 cycles, demonstrating a very low capacity fading of only 0.042 % per cycle.

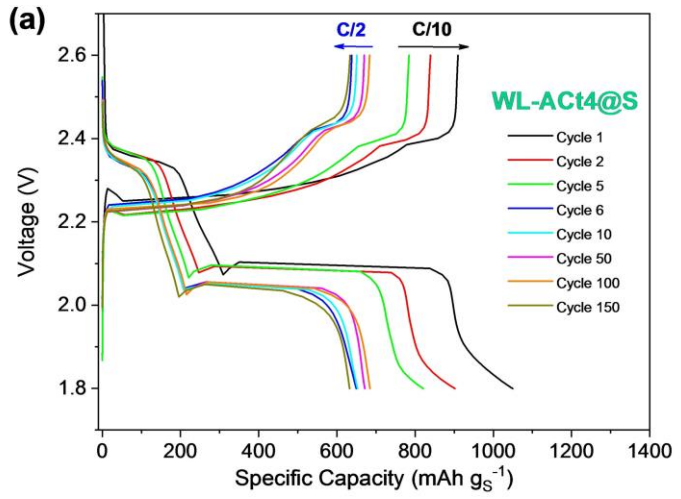
(a)
C/2
C/10
WL-ACt4@S
Cycle 1
Cycle 2
Cycle 5
Cycle 6
Cycle 10
Cycle 50
Cycle 100
Cycle 150
Voltage (V)
Specific Capacity (mAh g$_S^{-1}$)

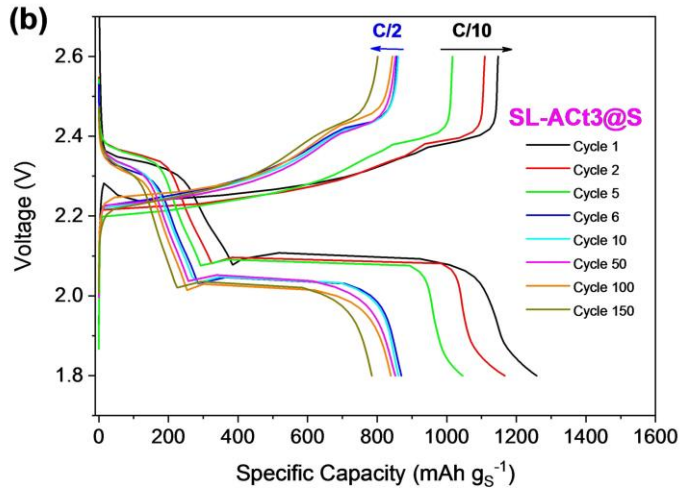
(b)
C/2
C/10
SL-ACt3@S
Cycle 1
Cycle 2
Cycle 5
Cycle 6
Cycle 10
Cycle 50
Cycle 100
Cycle 150
Voltage (V)
Specific Capacity (mAh g$_S^{-1}$)

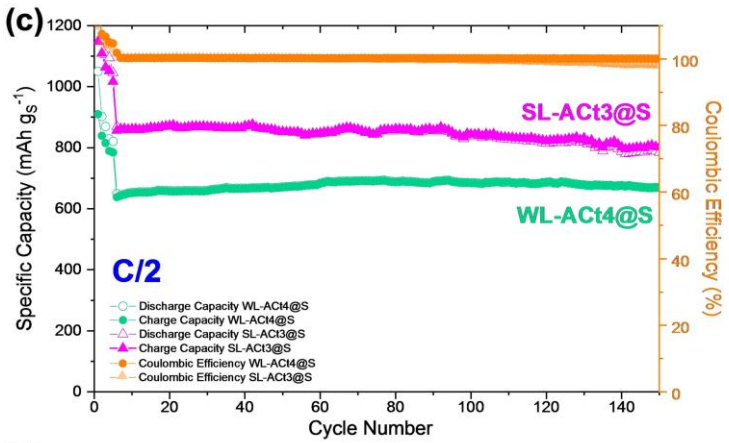
(c)
SL-ACt3@S
WL-ACt4@S
C/2
Discharge Capacity WL-ACt4@S
Charge Capacity WL-ACt4@S
Discharge Capacity SL-ACt3@S
Charge Capacity SL-ACt3@S
Coulombic Efficiency WL-ACt4@S
Coulombic Efficiency SL-ACt3@S
Specific Capacity (mAh g$_S^{-1}$)
Coulombic Efficiency (%)
Cycle Number

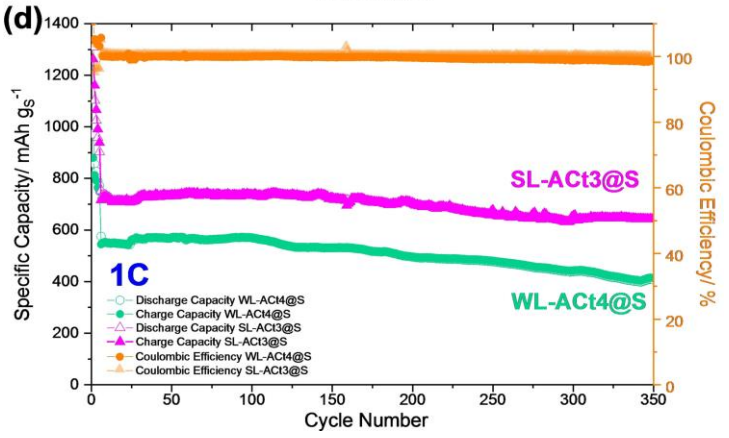
(d)
SL-ACt3@S
WL-ACt4@S
1C
Discharge Capacity WL-ACt4@S
Charge Capacity WL-ACt4@S
Discharge Capacity SL-ACt3@S
Charge Capacity SL-ACt3@S
Coulombic Efficiency WL-ACt4@S
Coulombic Efficiency SL-ACt3@S
Specific Capacity/ mAh g$_S^{-1}$
Coulombic Efficiency/ %
Cycle Number

Figure 8. Discharge and charge profiles for (**a**) Li/1 m LiTFSI(DOL/DME)/WL-ACt4@S and (**b**) Li/1 m LiTFSI(DOL/DME)/SL ACt3@S cells using a constant rate of C/2 for 150 cycles after activating the cells during the first 5 cycles at a rate of C/10 (1C=1672 mA g^{-1}) within a potential range of 1.8–2.6 V vs. Li^+/Li. Electrochemical performance of WL-ACt4@S and SL-ACt3@S cathodes (**c**) at C/2 for 150 cycles and (**d**) at a high rate of 1C during 350 cycles within a potential range of 1.8–2.6 V vs. Li^+/Li.

Figure 9 represents a graph in which the electrochemical results collected in **Table 1** for different wastes used as a conductive cathode matrix for Li−S cells are compared. Li−S cells prepared with spent coffee were cycled at a slower rate of C/5.[28] The retention capacity of the electrochemical measurements for the coffee residue was also low (32.5 %). However, the textural properties obtained after the activation process were excellent, accommodating 80 % sulfur in the matrix. At the C/2 rate, three residues (rice husk, soybean hull, and tobacco stem) were cycled. After activating the soybean hull with KOH,[27] textural properties very similar to those of activated carbon derived from spent coffee were obtained. In this case, the composite had a load of almost 64 % sulfur, and the retention capacity was close to the previous residue, with values around 36.5 %. Rice husk[24] and tobacco stems[43] obtained retention capacity values of 72 and 67 %, respectively, similar to 71 % in the WL-ACt4 sample, but the sulfur load per electrode in both cases was 1.0 mg cm^{-2}, that is, half of that used for our Li−S cells. Although the wheat straw and paper residues were cycled at the same rate of 1C as the ACs studied in this work, to obtain these activated carbons, the use of KOH and carbonizations at high temperatures of 700–800 °C under an inert atmosphere (nitrogen or argon flow) were required. On the one hand, the electrochemical measurements for wheat straw were carried out during 500 cycles, obtaining a fading capacity per cycle of 0.088 % and working with a sulfur loading of 1.0–1.2 mg cm^{-2}.[26] On the other hand, the results obtained for the paper working with a sulfur loading of 2.0 mg cm^{-2} had a fading capacity per cycle of 0.14 % after 200 cycles.[29] Although the results obtained were successful in the aforementioned works, the SL-ACt3 sample managed to improve the cyclical stability at 1C for 350 cycles working with a sulfur load of 2.0 mg cm^{-2}. The Li−S cells assembled with WL-ACt4 and SL-ACt3 achieved a retention capacity of 71 and 85.4 %, respectively. Furthermore, the fading capacity per cycle was 0.083 % for WL-ACt4 and only 0.042 % for SL-ACt3, confirming the excellent electrochemical performance

provided by these residues from activated carbon used in the odor control systems of WWTPs.

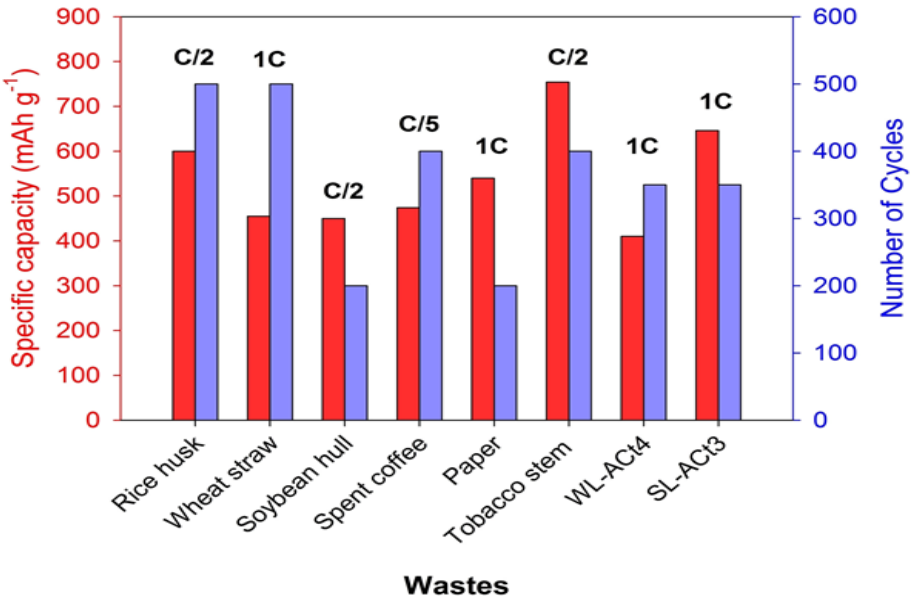

Figure 9. Electrochemical performance of WL-ACt4@S and SL-ACt3@S cathodes compared to other wastes used as a cathodic matrix.

The post-mortem analysis of Li/1 m LiTFSI(DOL/DME)/WL-ACt4@S and Li/1 m LiTFSI(DOL/DME)/SL-ACt3@S cells are carried out inside an argon-filled glovebox. **Figure 10a**, **b** makes it possible to compare the surface of both electrodes after cycling. Thus, it can be verified that for the WL-ACt4 cathode, the chemical and electrochemical reactions at the interface caused more cracks with a more pronounced thickness than for the SL-ACt3 cathode, which could explain why the Li/1 m LiTFSI(DOL/DME)/WL-ACt4@S cell will show lower capacity values to the Li/1 m LiTFSI(DOL/DME)/SL-ACt3@S cell in all electrochemical tests. The deterioration of the electrode surface and the appearance of cracks causes the sulfur to be less retained in the porosity of the carbonaceous matrix, putting the electrolyte in contact with more active material and favoring the shuttle effect. Furthermore, the dissolution of the polysulfides in the electrolyte entails an irreversible loss of active material and therefore, a decrease in the capacity that the cell is capable of supplying.

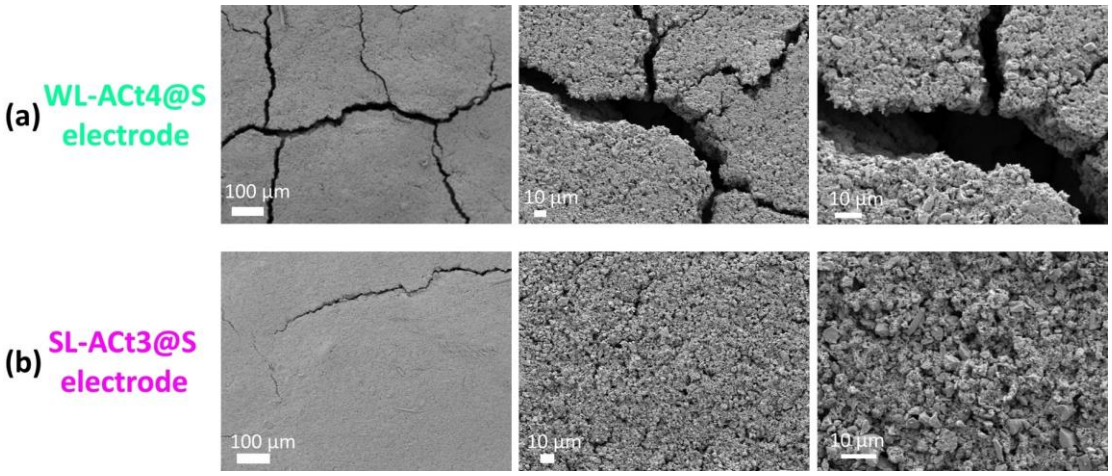

Figure 10. SEM images post-mortem for (**a**) WL-ACt4@S and (**b**) SL-ACt3@S electrodes at different magnifications. Scale bars: 100 µm (left) and 10 µm (middle and right).

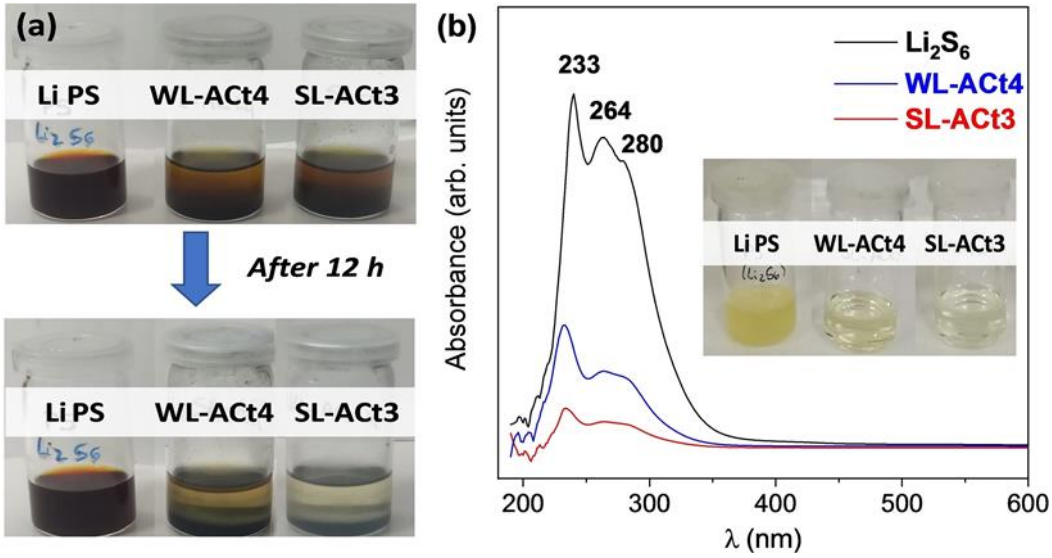

Figure 11. (**a**) Photographs showing the color changes of the Li_2S_6 solution (Li PS) after exposure to WL-ACt4 and SL-ACt3 for 12 h. (**b**) The UV/Vis spectra of the Li_2S_6 solution after absorption. The inserted photograph shows the dilutions that were analyzed by the absorbance measurements.

Finally, to evaluate the adsorption capability of activated carbons, the lithium polysulfide adsorption measurements were carried out. Specifically, 5 mm of Li_2S_6 solution was prepared by mixing Li_2S and S in anhydrous DME and DOL (1:1 *v*/*v*) in an Ar-filled glovebox.[44] In the adsorption tests shown in **Figure 11a**, a 2 mL Li_2S_6 solution was added to 5 mg of WL-ACt4 and SL-ACt3 materials, respectively. Initially, the

samples showed an orange coloration, but after 12 h of impregnation of Li_2S_6 with the different activated carbons, the solution gradually became discolored and had a light-yellow color. At first glance, it can be confirmed that the SL-ACt3 sample had a greater ability to adsorb polysulfides than the WL-ACt4. However, UV/Vis measurements were performed to get a more accurate result of the adsorption behavior. As shown in **Figure 11b**, a broad band is observed between 190 and 450 nm relative to the absorption of lithium polysulfides.[45-48] Three characteristic peaks at 233, 264, and 280 nm correspond to the S_6^{2-} species. After absorption for 12 h, color changes of the polysulfide solution with the WL-ACt4 and SL-ACt3 samples from light yellow to colorless were observed (inset of **Figure 11b**). To perform the absorbance measurements, all samples were diluted ten times.

4. Conclusions

Cathodes for Li−S batteries were developed through a facile and efficient method that allows the activated carbons used in the odor systems of a wastewater treatment plant (WWTP) to be regenerated. The regeneration process of the contaminated granular activated carbon (GAC) consisted of carbonization at moderate temperatures of 250 and 350 °C without the need to use an inert gas stream, which reduces the cost of manufacturing. The sample from the head pre-treatment point of the water line (WL) presented a lower electrochemical performance than the sample obtained from the sludge dewatering point of the sludge line (SL). The exhaustive analysis of both samples led us to the following conclusions:

The WL-ACt4 sample is representative of the chemical adsorption of H_2S; therefore, it has a higher proportion of impurities and requires a higher temperature and time for its regeneration than the SL-ACt3 sample, which is representative of the physical adsorption of volatile organic compounds.

The textural properties obtained for both samples were similar, indicating an effective regeneration process. Although both were mainly mesoporous activated carbons, the SL-ACt3 sample also contained micropores, which favor the adsorption of lithium polysulfides, as confirmed by absorption tests.

The WL-ACt4@S and SL-ACt3@S composites were successfully prepared by a simple wet milling method. The presence of sulfur was verified by various characterization techniques, such as X-ray diffraction, Raman spectroscopy, scanning electron microscopy energy-dispersive X-ray spectroscopy (EDX), and thermogravimetric analysis (TGA). Thus, TGA revealed the existence of two different sulfur environments in the composites (inside and outside the pore). The sulfur deposited within the pores contributed to the high electrochemical activity and cycling stability, as verified by the Li−S cells prepared with the SL-ACt3@S sample. In addition, by mapping the C and S elements by EDX, it was confirmed that the distribution of sulfur in the WL-ACt4@S composite was more heterogeneous, and sulfur agglomerations that would be harmful during cycling were observed.

SL-ACt3@S composite-based cells provided lower charge transfer resistance and higher specific capacity than WL-ACt4@S composite-based cells. Furthermore, the stability was maintained for an appropriate number of cycles at different cycling rates.

Additionally, the post-mortem study of the electrodes corroborated a higher quality in the materials from the sludge line because the surface of these electrodes suffered fewer alterations during the charge and discharge measurements in prolonged cycles.

Therefore, it can be concluded that the SL material after regeneration offered excellent characteristics for use as a cathodic matrix in Li−S batteries. Furthermore, this study contributes to reducing the amount of this type of waste in landfills by providing it with a new utility and promoting a sustainable and circular economy.

Acknowledgements

This work was supported by the Spanish Ministry of Economy, Industry, and Competitiveness (MINECO), the Spanish State Research Agency (AEI) and the European Regional Development Fund (FEDER) through Projects CTM2017-88723-R, MAT2017-87541-R, PID2020-113931RB−I00, and the Ministry of Education, Culture, and Sport of Spain (Grant FPU2016). The European Regional Development Fund (Project UCO-FEDER-1262384-R) and the Chelonia Association (Mares Circulares Project) also supported the work. A.B. thanks the financial support from the European Social Fund and Junta de Andalucía. Also, the authors wish to acknowledge the technical staff from the

University Institute of Nanochemistry (IUNAN) and the Central Service for Research Support (SCAI) of the University of Cordoba. Finally, we wish to express our gratitude to Juan Amaro-Gahete for his contribution to this research by performing Raman spectroscopy measurements, and to Inmaculada Bellido and María Luisa López for their contribution to this research. Funding for open access charge: Universidad de Córdoba/CBUA.

References

[1] K. H. Wujcik, D. R. Wang, A. A. Teran, E. Nasybulin, T. A. Pascal, D. Prendergast, N. P. Balsara, in *Electrochem. Eng.*, John Wiley & Sons, Ltd, **2018**, pp. 41–74.

[2] J. He, A. Manthiram, *Energy Storage Mater.* **2019**, *20*, 55–70.

[3] Y. Yan, J. Xiaobo, F. Hongjin, *Green Energy Environ.* **2018**, *3*, 1.

[4] J. Zhu, J. Zou, H. Cheng, Y. Gu, Z. Lu, *Green Energy Environ.* **2019**, *4*, 345–359.

[5] S. Li, W. Zhang, J. Zheng, M. Lv, H. Song, L. Du, *Adv. Energy Mater.* **2021**, DOI 10.1002/aenm.202000779.

[6] H. Shin, M. Baek, A. Gupta, K. Char, A. Manthiram, J. W. Choi, *Adv. Energy Mater.* **2020**, *10*, 2001456.

[7] A. Manthiram, Y. Fu, Y.-S. Su, *Acc. Chem. Res.* **2013**, *46*, 1125–1134.

[8] X. Fan, W. Sun, F. Meng, A. Xing, J. Liu, *Green Energy Environ.* **2018**, *3*, 2–19.

[9] L. Zhang, Y. Wang, Z. Niu, J. Chen, *Carbon N. Y.* **2019**, DOI 10.1016/j.carbon.2018.09.067.

[10] J. Zhao, M. Yang, N. Yang, J. Wang, D. Wang, *Chem. Res. Chinese Univ.* **2020**, *36*, 313–319.

[11] M. Li, R. Carter, A. Douglas, L. Oakes, C. L. Pint, *ACS Nano* **2017**, *11*, 4877–4884.

[12] Q. Wang, Z.-B. Wang, C. Li, D.-M. Gu, *J. Mater. Chem. A* **2017**, *5*, 6052–6059.

[13] Y. Yan, M. Shi, Y. Wei, C. Zhao, L. Chen, C. Fan, R. Yang, Y. Xu, *J. Nanoparticle Res.* **2018**, *20*, 260.

[14] J. Wang, H. Yang, Z. Chen, L. Zhang, J. Liu, P. Liang, H. Yang, X. Shen, Z. X. Shen, *Adv. Sci.* **2018**, *5*, 1800621.

[15] A. Benítez, D. Di Lecce, G. A. Elia, Á. Caballero, J. Morales, J. Hassoun, *ChemSusChem* **2018**, *11*, 1512–1520.

[16] A. Benítez, D. Di Lecce, Á. Caballero, J. Morales, E. Rodríguez-Castellón, J. Hassoun, *J. Power Sources* **2018**, *397*, DOI 10.1016/j.jpowsour.2018.07.002.

[17] S. Imtiaz, J. Zhang, Z. A. Zafar, S. Ji, T. Huang, J. A. Anderson, Z. Zhang, Y. Huang, *Sci. China Mater.* **2016**, *59*, 389–407.

[18] M. Wang, X. Xia, Y. Zhong, J. Wu, R. Xu, Z. Yao, D. Wang, W. Tang, X. Wang, J. Tu, *Chem. – A Eur. J.* **2019**, *25*, 3710–3725.

[19] L. Yan, J. Yu, J. Houston, N. Flores, H. Luo, *Green Energy Environ.* **2017**, *2*, 84–99.

[20] P. Liu, Y. Wang, J. Liu, *J. Energy Chem.* **2019**, *34*, 171–185.

[21] Q. Li, Y. Liu, Y. Wang, Y. Chen, X. Guo, Z. Wu, B. Zhong, *Ionics (Kiel).* **2020**, *26*, 4765–4781.

[22] H. Yuan, T. Liu, Y. Liu, J. Nai, Y. Wang, W. Zhang, X. Tao, *Chem. Sci.* **2019**, DOI 10.1039/c9sc02743b.

[23] C. Schneidermann, C. Kensy, P. Otto, S. Oswald, L. Giebeler, D. Leistenschneider, S. Grätz, S. Dörfler, S. Kaskel, L. Borchardt, *ChemSusChem* **2019**, *12*, 310–319.

[24] M. K. Rybarczyk, H.-J. Peng, C. Tang, M. Lieder, Q. Zhang, M.-M. Titirici, *Green Chem.* **2016**, *18*, 5169–5179.

[25] J. Zhang, C. You, J. Wang, S. Guo, W. Zhang, R. Yang, P. Fu, *ChemElectroChem* **2019**, *6*, 5051–5059.

[26] F. Chen, L. Ma, J. Ren, M. Zhang, X. Luo, B. Li, Z. Song, X. Zhou, *Materials (Basel).* **2018**, *11*, 989.

[27] Y. Zhu, G. Xu, X. Zhang, S. Wang, C. Li, G. Wang, *J. Alloys Compd.* **2017**, *695*, 2246–2252.

[28] B. Kim, J. Park, S. Baik, J. W. Lee, *J. Porous Mater.* **2020**, *27*, 451–463.

[29] L. Li, L. Huang, R. J. Linhardt, N. Koratkar, T. Simmons, *Sustain. Energy Fuels* **2018**, *2*, 422–429.

[30] M. Zhong, J. Guan, J. Sun, H. Guo, Z. Xiao, N. Zhou, Q. Gui, D. Gong, *Electrochim. Acta* **2019**, *299*, 600–609.

[31] A. Y. Tesio, J. L. Gómez-Cámer, J. Morales, A. Caballero, *ChemSusChem* **2020**, *13*, 3439–3446.

[32] P. Márquez, A. Benítez, Á. Caballero, J. A. Siles, M. A. Martín, *Sci. Total Environ.* **2021**, *754*, 142237.

[33] P. Márquez, A. Benítez, J. Hidalgo-Carrillo, F. J. Urbano, Á. Caballero, J. A. Siles, M. A. Martín, *Sep. Purif. Technol.* **2021**, *255*, 117782.

[34] M. Muttakin, S. Mitra, K. Thu, K. Ito, B. B. Saha, *Int. J. Heat Mass Transf.* **2018**, *122*, 795–805.

[35] Z. Ryu, J. Zheng, M. Wang, B. Zhang, *Characterization of Pore Size Distributions on Carbonaceous Adsorbents by DFT*, **1999**.

[36] R. L. Tseng, *J. Colloid Interface Sci.* **2006**, *303*, 494–502.

[37] K. Suzuki, M. Tateishi, M. Nagao, Y. Imade, T. Yokoi, M. Hirayama, T. Tatsumi, R. Kanno, *J. Electrochem. Soc.* **2017**, *164*, A6178–A6183.

[38] K. Zhang, Q. Zhao, Z. Tao, J. Chen, *Nano Res.* **2013**, *6*, 38–46.

[39] B. A. Trofimov, L. M. Sinegovskaya, N. K. Gusarova, *J. Sulfur Chem.* **2009**, *30*, 518–554.

[40] J. L. Gómez-Urbano, J. L. Gómez-Cámer, C. Botas, T. Rojo, D. Carriazo, *J. Power Sources* **2019**, *412*, 408–415.

[41] A. Benítez, A. Caballero, J. Morales, J. Hassoun, E. Rodríguez-Castellón, J. Canales-Vázquez, *Nano Res.* **2019**, *12*, 759–766.

[42] A. Benítez, V. Marangon, C. Hernández-Rentero, Á. Caballero, J. Morales, J. Hassoun, *Mater. Chem. Phys.* **2020**, *255*, 123484.

[43] M. e. Zhong, J. Guan, J. Sun, H. Guo, Z. Xiao, N. Zhou, Q. Gui, D. Gong, *Electrochim. Acta* **2019**, DOI 10.1016/j.electacta.2019.01.024.

[44] X. Guo, K. Li, W. Bao, Y. Zhao, J. Xu, H. Liu, G. Wang, *Energy Technol.* **2018**, *6*, 251–256.

[45] J. Hou, X. Tu, X. Wu, M. Shen, X. Wang, C. Wang, C. Cao, H. Pang, G. Wang, *Chem. Eng. J.* **2020**, *401*, 126141.

[46] X. Wang, Z. Sun, Y. Zhao, J. Li, Y. Zhang, Z. Zhang, *J. Solid State Electrochem.* **2020**, *24*, 111–119.

[47] Y. Xia, R. Fang, Z. Xiao, H. Huang, Y. Gan, R. Yan, X. Lu, C. Liang, J. Zhang, X. Tao, W. Zhang, *ACS Appl. Mater. Interfaces* **2017**, *9*, 23782–23791.

[48] J. He, W. Lv, Y. Chen, J. Xiong, K. Wen, C. Xu, W. Zhang, Y. Li, W. Qin, W. He, *J. Mater. Chem. A* **2018**, *6*, 10466–10473.

[49] A. Benítez, J. Morales, Á. Caballero, *Nanomaterials* **2020**, *10*, 840.

[50] A. Benítez, Á. Caballero, E. Rodríguez-Castellón, J. Morales, J. Hassoun, *ChemistrySelect* **2018**, *3*, 10371–10377.

BLOQUE III. SISTEMAS DE BIOFILTRACIÓN A ESCALA PILOTO: ELIMIMACIÓN DE COMPUESTOS ORGÁNICOS VOLÁTILES PRESENTES EN EMISIONES OLOROSAS DE EDAR

SECTION III. PILOT-SCALE BIOFILTRATION SYSTEMS: REMOVAL OF VOLATILE ORGANIC COMPOUNDS CONTAINED IN ODOR EMISSIONS FROM WWTPs

III. Resumen del Bloque: "*Sistemas de biofiltración a escala piloto: Eliminación de compuestos orgánicos volátiles presentes en emisiones olorosas de EDAR*"

En este tercer y último bloque de la presente Tesis Doctoral se han analizado diversos aspectos relacionados con la biofiltración, que, al igual que la adsorción de contaminantes odoríferos mediante CAG, constituye una tecnología de tratamiento de olor de final de línea. En concreto, se ha evaluado a escala piloto la eliminación de olor de corrientes gaseosas de ácido butírico (olor característico a rancio) y D-limoneno (compuesto que caracteriza el olor a cítrico). Su selección se debe a que son compuestos habitualmente presentes en las emisiones gaseosas derivadas del tratamiento biológico de residuos orgánicos, incluyéndose aquí operaciones como la depuración de las aguas residuales y el tratamiento de los residuos sólidos urbanos mediante compostaje, incluyendo el compostaje de los lodos de EDAR.

Como es bien sabido, la eficacia de los sistemas de biofiltración está condicionada por una serie de variables que deben ser tenidas en cuenta en el diseño y operación de los mismos: caudal de la corriente gaseosa y concentración de contaminantes, humedad y pH del relleno filtrante, temperatura de operación, tiempo de residencia en lecho vacío (EBRT), composición del relleno y las comunidades microbianas presentes en él, entre otras. Es por ello por lo que en los estudios que componen este bloque se ha llevado a cabo una evaluación integral de los siguientes aspectos relacionados con la biofiltración de compuestos gaseosos: eficacias de eliminación de olor, evolución de las variables fisicoquímicas y respirométricas del relleno a lo largo del proceso, recuentos de microorganismos aerobios mesófilos y estudio de las diferentes comunidades bacterianas implicadas en la biodegradación, cuantificadas mediante técnicas de genómica (ARN-16S). Como rellenos biológicos se han utilizado dos residuos orgánicos sin ninguna inoculación microbiológica: virutas de madera, bien como relleno único, o bien en mezcla con compost estabilizado de lodos procedentes de una EDAR urbana (1:1 en volumen).

En el primer estudio del presente bloque se ha evaluado la influencia del relleno filtrante en la biofiltración de una corriente gaseosa conteniendo ácido butírico. Para ello, se ha llevado a cabo el seguimiento de las eficacias de eliminación de olor (mediante olfatometría dinámica) y de la composición y evolución de las comunidades microbianas en dos biofiltros independientes, ambos con las mismas características de diseño y operando bajo las mismas condiciones de EBRT, pero con rellenos diferentes, concretamente los mencionados con anterioridad. En este sentido, el biofiltro operado con

la mezcla de virutas de madera y compost ha sido capaz de soportar mayores cargas de olor en comparación con el basado únicamente en virutas de madera, lo que se ha relacionado fundamentalmente con la mayor diversidad microbiana del primero, proporcionándole una mayor capacidad de adaptación frente a los cambios en las diferentes variables estudiadas (factor de carga odorífera, tasa de olor y rendimiento) a medida que avanzó el tiempo de biofiltración. Por tanto, se pone de manifiesto el papel crucial que juega la elección de un lecho empacado adecuado al objeto de reducir el impacto odorífero de una determinada instalación mediante la técnica de biofiltración.

Finalmente, en el segundo trabajo del Bloque III se ha dado un paso más allá, estudiándose las diferencias en la eficacia de eliminación de olores de biofiltros operados para compuestos gaseosos de naturaleza opuesta (como son el ácido butírico y el D-limoneno), y utilizando los mismos rellenos filtrantes mencionados hasta el momento. Los resultados de este último trabajo han demostrado que, con independencia de los lechos utilizados (virutas de madera exclusivamente o la mezcla compost-virutas), cuando los biofiltros son utilizados para eliminar de corrientes gaseosas compuestos olorosos de carácter ácido y solubles en agua como el ácido butírico, la eficacia siempre ha sido más elevada, aunque menos duradera que en la eliminación de compuestos menos miscibles en agua, como es el D-limoneno. Por tanto, no sólo resulta importante una adecuada selección del relleno biológico sino que también resulta indispensable evaluar previamente la naturaleza del compuesto a biofiltrar. Por lo tanto, la biofiltración de corrientes gaseosas contaminadas con variedad de compuestos de diversa naturaleza tendrá una eficacia global en la eliminación de olor aunque una específica para cada odorante.

III.1. Breve descripción del artículo: "*Influence of packing material on the biofiltration of butyric acid: A comparative study from a physico-chemical, olfactometric and microbiological perspective*"

III.1. Breve descripción del artículo: "*Influence of packing material on the biofiltration of butyric acid: A comparative study from a physico-chemical, olfactometric and microbiological perspective*"

En el presente artículo se ha estudiado la influencia del material de relleno en la eficacia de eliminación de olores de un biofiltro a escala piloto. En este sentido, un biofiltro operó con una mezcla de compost estabilizado de lodos de EDAR y virutas de madera (relación 1:1 en volumen), mientras que otro operó solamente con virutas de madera como relleno. Ambos trataron una corriente gaseosa contaminada con ácido butírico y fueron evaluados comparativamente desde una perspectiva olfatométrica, fisicoquímica y microbiológica. Las variables analizadas en ambos biofiltros se correlacionaron con las familias específicas de su composición microbiana. Además de un mayor contenido en nutrientes (nitrógeno y fósforo), el biofiltro relleno con la mezcla compost−madera registró los valores más altos en cuanto al recuento de microorganismos aerobios mesófilos ($3{,}6 \cdot 10^8$ UFC/g) y actividad microbiológica aeróbica (consumo acumulado de oxígeno a las 20 h de aproximadamente 40 mg O_2/g SV). Todo ello puede explicar el mayor rendimiento de este biofiltro en comparación con el biofiltro basado únicamente en virutas de madera, soportando cargas de olor de hasta 1450 $ou_E/m^2 \cdot s$ con eficacias de eliminación de olores cercanas al 100%. El análisis de las comunidades microbianas demostró que el filo Actinobacteria y en particular la familia Microbacteriaceae (en su mayoría aeróbica) podrían desempeñar un papel fundamental en la degradación del ácido butírico y, por tanto, en la reducción del impacto odorífero. De esta manera, el análisis multidisciplinar llevado a cabo en este trabajo podría constituir una estrategia muy útil para un diseño óptimo de las operaciones de biofiltración.

Journal of Environmental Management 294 (2021) 113044

Contents lists available at ScienceDirect

Journal of Environmental Management

journal homepage: www.elsevier.com/locate/jenvman

Influence of packing material on the biofiltration of butyric acid: A comparative study from a physico-chemical, olfactometric and microbiological perspective

Márquez, P. [a,ϕ], Herruzo-Ruiz, A.M. [b,ϕ], Siles, J.A. [a], Alhama, J. [b], Michán, C. [b], Martín, M.A. [a,*]

[a] Department of Inorganic Chemistry and Chemical Engineering, Area of Chemical Engineering, Universidad de Córdoba, Campus Universitario de Rabanales, Carretera N-IV, km 396, Edificio Marie Curie, 14071 Córdoba, Spain

[b] Department of Biochemistry and Molecular Biology, Universidad de Córdoba, Campus de Excelencia Internacional Agroalimentario CeiA3, Edificio Severo Ochoa, 14071 Córdoba, Spain

[ϕ] Márquez, P. and Herruzo-Ruiz, A.M. contributed equally to this work.

* Corresponding author: iq2masam@uco.es

Received 18 March 2021; Received in revised form 10 May 2021; Accepted 7 June 2021;

Available online 12 June 2021

Abbreviations: CON, conductivity (μS/cm); EBRT, empty bed residence time (s); FS, fixed solids (%); IC, soluble inorganic carbon (%); MAC, total mesophilic aerobic count (CFU/g); N-NH_4^+, ammoniacal nitrogen (%); N-TKN, total Kjeldahl nitrogen (%); N-TN_s, soluble total nitrogen (%); OC, odor concentration (ou_E/m^3); OD_{20}, cumulative oxygen demand at 20 h (mg O_2/g VS); OER, odor emission rate (ou_E/s); OIR, odor incoming rate (ou_E/s); ou_E, European odor units; P-P_2O_5, phosphorus content expressed as P_2O_5 (%); $SOUR_{max}$, maximum specific oxygen uptake rate (mg O_2/g VS·h); TC, soluble total carbon (%); TOC, soluble total organic carbon (%); VFAs, volatile fatty acids; VOCs, volatile organic compounds; VS, volatile solids (%).

Abstract

The influence of bed material on the odor removal performance of a biofilter was studied. A compost-wood biofilter and a wood biofilter were treated with a gaseous stream contaminated with butyric acid and comparatively evaluated at pilot scale using olfactometric, physico-chemical and microbiological approaches. The variables analyzed in both biofilters were correlated with specific families of their microbiota composition. In addition to a higher nutrients content (nitrogen and phosphorus), the compost-wood biofilter registered maximum values in number of aerobic microorganisms ($3.6 \cdot 10^8$ CFU/g) and in aerobic microbiological activity (≈ 40 mg O_2/g VS of cumulative oxygen demand at 20 h). This may explain the higher performance of this biofilter compared to the wood biofilter, withstanding odor loads of up to 1450 $ou_E/m^2 \cdot s$ with odor removal efficiencies close to 100%. The analysis of the microbial community showed that Actinobacteria, particularly the mostly aerobic Microbacteriaceae family, might play an important role in butyric acid degradation and hence reduce odor impact. The multidisciplinary analysis carried out in this work could be a very useful strategy for the optimal design of biofiltration operations.

Keywords: biofiltration; butyric acid; microbial taxonomy; multidisciplinary analysis; odor removal; packing material.

1. Introduction

Odor emission from waste management and industrial activities is currently a major public concern, as this is the source of many protests and complaints in nearby residential areas (De Feo et al., 2013; Hayes et al., 2017). Volatile organic compounds (VOCs) and some inorganic gases (i.e., hydrogen sulfide and ammonia) produced during the biodegradation of organic residues are responsible for unpleasant emissions (Cabeza et al., 2013; Márquez et al., 2021). Volatile fatty acids (VFAs) are one of the most representative groups of VOCs emitted in waste treatment facilities, where carbohydrates can be degraded into VFAs through an anaerobic bacterial process called acidogenesis (Reyes et al., 2020). Among these compounds, butyric acid is one of the major intermediates in the anaerobic degradation of organic compounds and is therefore found in gaseous emissions from wastewater and solid waste treatment facilities (González et al., 2019; Lebrero et al., 2011). Butyric acid has both a sweet rancid odor and a very low

odor detection threshold (0.00019 ppm_v), leading to a high olfactory perception (Nagata, 2003). However, the water solubility of that acid facilitates its removal through biological treatments, since the diffusion from the gas phase to the aqueous biofilm is not a limiting step (Cheng et al., 2016; Sheridan et al., 2003).

Biological treatments are based on the capability of certain microorganisms to break down odorous pollutants into simpler, odorless compounds, such as water, carbon dioxide and mineral salts. Biological technologies are more environment-friendly than chemical and physical odor abatement methods because they do not require the use of harmful chemicals and can be carried out at atmospheric pressure and environmental temperatures (10-40 ºC) (Barbusinski et al., 2017). Biofiltration, bioscrubbing and biotrickling filtration are efficient biological technologies for treating large volumes of residual gas streams with low concentrations of odorous compounds (Mudliar et al., 2010). Compared to physicochemical methods and other biological technologies, biofiltration requires little maintenance, is easy to operate and entails low investment and operating costs (Barbusinski et al., 2017).

Biofilters are bioreactors where contaminated air streams are carried through a packed bed that contains microorganisms for the biodegradation of gaseous compounds (Cabeza et al., 2013). According to Elias et al. (2002), the filter bed is the key component of a biofilter and should have the following main characteristics: (i) high porosity, (ii) adequate water retention capacity, (iii) high buffer capacity, (iv) a diverse and adaptable microbial population, (v) high available nutrient content, (vi) long life and (vii) low cost. Soil, compost, peat and wood chips are packing materials that satisfy most of those criteria (Mudliar et al., 2010). Compost from various organic materials (i.e., sewage sludge, municipal solid waste, etc.) is frequently used as packing material and often mixed with wood chips to prevent bed crushing and compaction (Barbusinski et al., 2017; López et al., 2011).

The packing material and the contaminated air stream to be treated influence the composition of the microbiological community and its survival in the biofilter equipment (Singh and Ward, 2005). Microorganisms are the catalysts for the biodegradation of gaseous pollutants and odors. Biofilms contain a complex mixture of bacteria and fungi, which are the two dominant groups in biofilters, but also ciliated protozoa, yeasts, nematodes, amoebae and algae. Among them, bacteria are the primary degraders and, as they grow, they can also sustain some of the other organisms (Kennes and Veiga, 2013).

After a period of acclimatization, the populations most resistant to the toxic compounds are naturally selected, and a microbial hierarchy is established in the filter bed (Mudliar et al., 2010). For easily soluble compounds (such as butyric acid), it is possible to reduce the acclimatization period to a few days by inoculating packing material with a specific culture that efficiently degrades the odorant to be treated (Datta and Allen, 2005). For example, Sheridan et al. (2003) used wood chips as bed material, which was inoculated with liquid collected under the base of a diesel storage tank that contained the microbial consortium used for the biofiltration of butyric acid. Nevertheless, some researchers prefer taking advantage of the ecosystems already prevailing in the packing materials. In this regard, Otten et al. (2004) and Reyes et al. (2020) reported high butyric acid removal efficiencies using compost or compost/perlite and wood chips without inoculation, respectively. Moreover, Reyes et al. (2020) carried out a taxonomic identification of the microbial communities responsible for the degradation of butyric acid and found that Proteobacteria was the most abundant phylum in the two biofilters studied, which operated with odor load factors (ranging between 400–1400 $ou_E/m^2 \cdot s$ and 180–800 $ou_E/m^2 \cdot s$). Chung et al. (2010) and Friedrich et al. (2002) reported the same findings in other biofiltration systems with different packing materials and gaseous compounds treated at both pilot and full scale, respectively. Chung et al. (2010) used two inter-connected PVC columns packed with a mixture of granular activated carbon and peat inoculated with wastewater sludge for dimethyl sulfide removal processes, while Friedrich et al. (2002) investigated an industrial biofilter packed with tree bark compost and crushed tree roots used for waste gas treatment in an animal-rendering plant.

In this research study, two pilot-scale biofilters to treat a gaseous stream containing butyric acid gas have been comparatively evaluated from an olfactometric, physico-chemical and microbiological approach. One biofilter was filled with sewage sludge compost and wood chips, while the other used wood chips only. To the best of our knowledge, a multidisciplinary analysis to better understand the influence of filter bed material on the odor removal performance of a biofiltration system has not been previously reported. Thus, this information might aid to optimize biofiltration operations in facilities using such efficient deodorization system. Our final goal is to reduce the odor impact of activities that emit waste streams containing butyric acid, with the consequent environmental and social benefits.

2. Material and methods

2.1 Pilot-scale biofiltration system: design and operation

Two pilot-scale biofilters, prepared by the authors and packed with different materials, were operated individually in this study. Both biofilters (PVC cylinders) had the same constructive characteristics: total height 0.86 m; inner diameter 0.16 m; height of packing material 0.49 m; height of headspace 0.20 m and height of bed space at the bottom of the biofilter 0.17 m. With these dimensions, the total biofilter volume was 0.0173 m^3, while the packing volume was 0.0099 m^3 (57.23% of the total volume). One biofilter (biofilter 1) was filled with a mixture of sewage sludge compost and wood chips at a volumetric ratio of 1:1, while the other one (biofilter 2) only consisted of wood chips. Sewage sludge derived from the urban wastewater treatment plant of Cordoba ("La Golondrina") (Spain) was used as packing material after composting in the urban waste management plant of the same city ("SADECO, S.A."). Both sewage sludge compost and wood chips were collected from the last mentioned facility. The granulometry of both materials ranged from 7 to 20 mm in order to favor the bed porosity and avoid operational problems such as clogging and control of air flux (Cabeza et al., 2013).

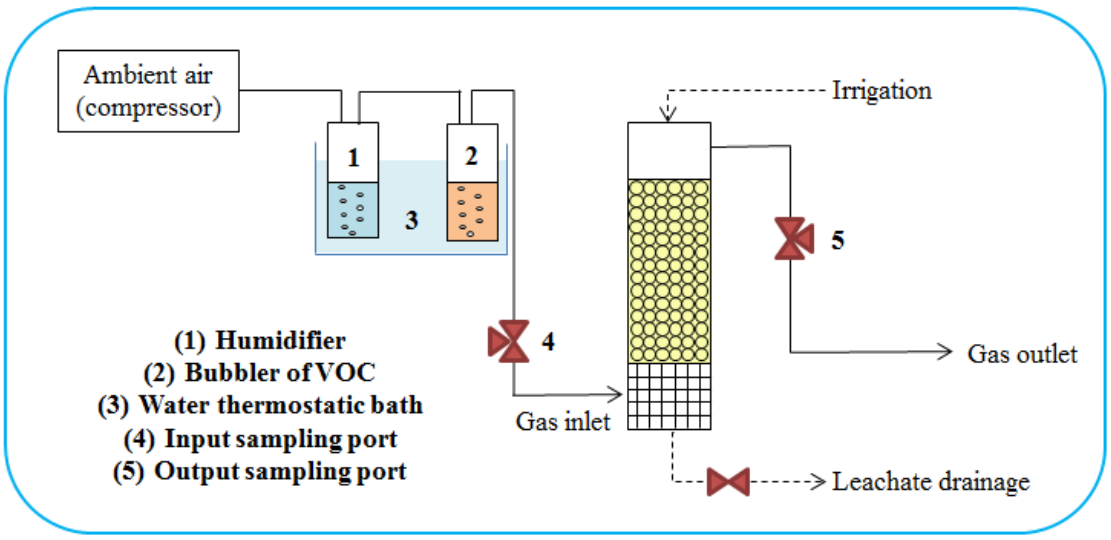

Fig. 1. Schematic diagram of the biofiltration system.

Ambient air was supplied to the biofiltration system by a compressor and the gas flow was controlled by a flow meter (Trotec TA400). As can be seen from the schematic flow diagram (**Fig. 1**), a water thermostatic bath was connected between the air compressor and the biofilter. This bath contained two bubblers and its temperature was

set at a value of 22 ºC in the case of biofilter 2, and measured continuously by a datalogger (Testo 175 T1). In contrast, room conditions conditioned the temperature of the water bath in biofilter 1, which ranged from 22 ºC (minimum value) to 31 ºC (maximum value), with an average temperature of 27.5 ºC. In both biofiltration systems, compressed air was humidified in the first bubbler with distilled water. In order to generate the contaminated gas flow, humidified air was then fed to a second bubbler placed in series, which contained liquid butyric acid (PanReac, >99% purity). Subsequently, the contaminated gas stream was introduced into the biofilter. The connections between the elements of the biofiltration system shown in **Fig. 1** were made with 8 mm Ø plastic pipes.

Both biofiltration experiments (with biofilters 1 and 2) were performed over a 62-day period. The experiments were separated into two stages by modifying the empty bed residence time (EBRT), which was calculated by equation (1):

$$EBRT\ (s) = \frac{V_p}{Q_i} \quad (1)$$

where V_p is the packing volume (m^3) and Q_i is the inlet gas flow to the biofilter (m^3/s).

As shown in **Table 1**, the two experimental stages mentioned above took place as follows: (i) Start-up period, with an EBRT ranging from 188 to 83 s. This stage corresponds to an acclimatization period of the microorganisms to the pollutant, which is an important factor to achieve efficient biofilter operation (Boswell, 2004); and (ii) operational period, with a constant EBRT of 59 s. It is important to note that EBRT values of about 60 s are frequent in biofiltration experiments in order to achieve high removal efficiencies (Dorado et al., 2008; Omri et al., 2011; Ramírez et al., 2011). Bed inoculation and supplementary micronutrients addition were not performed in either of the two stages.

Table 1. Operational conditions of the biofilters.

	Biofiltration time (d)	**Inlet gas flow (m^3/s)**	**EBRT (s)**
Start-up period	0-3	$5.2 \cdot 10^{-5}$	188
	4-7	$7.1 \cdot 10^{-5}$	138
	8-11	$9.5 \cdot 10^{-5}$	103
	12-14	$1.19 \cdot 10^{-4}$	83
Operational period	15-62	$1.67 \cdot 10^{-4}$	59

EBRT, empty bed residence time.

The moisture content of the packed bed is another important factor for biofilter performance because microorganisms require water to carry out their metabolic activity. For this reason, it is crucial to maintain sufficiently high moisture content in the packing material (Barbusinski et al., 2017; Mudliar et al., 2010). In the experiments, moisture level was maintained around 60% and controlled regularly by measuring the difference in weight between the complete biofilter bed and its initial weight. When moisture decreased below 60%, water was added to the biofilters. In this regard, it is important to note that both biofilters were operated in down-flow mode in order to allow the easy addition of water to the packed beds (Sheridan et al., 2003).

2.2 Solid and gaseous sampling

For the physico-chemical, respirometric and microbiological characterizations, a total of 80 g of the packing material were collected at different heights. This operation was repeated at the start (S, day 0), in the middle (M, day 28) and at the end (E, day 62) of each biofiltration experiment. A physico-chemical and respirometric characterization of the raw materials of the packed beds (sewage sludge compost and wood chips) was also carried out. In order to monitor the odor removal efficiency of the biofiltration process, gaseous samples were collected in 4-L Nalophan® sampling bags through the input and output sampling ports of the biofilter. Samples were taken at least twice a week during the entire experiment.

2.3 Olfactometric analysis

After gaseous sampling, the odor samples were immediately analyzed in order to prevent the permeation of odorants through the sampling bag walls (Kasper et al., 2018; Toledo et al., 2019). The odor concentration (OC, ou_E/m^3) of the gaseous samples was quantified by dynamic olfactometry (EN 13725, 2003) using a TO8 olfactometer (Olfasense GmbH) based on the 'Yes/No' method. In accordance with this European standard, the panelist group consisted of 4 assessors, which were selected based on their sensitivity to the reference gas (n-butanol). Each sample was analyzed in duplicate and the OC was calculated as the geometric mean of the odor threshold values of each assessor, which was multiplied by a factor that depends on the olfactometer dilution step factor. Once the inlet and outlet odor concentrations of the biofilter were determined, the odor incoming rate (OIR, ou_E/s) and the odor emission rate (OER, ou_E/s) were calculated by equations (2) and (3), respectively:

$$Odor\ incoming\ rate\ (OIR,\ ou_E/s) = OC_i \cdot Q_i \quad (2)$$

where OC_i is the inlet odor concentration (ou_E/m^3) and Q_i is the inlet gas flow (m^3/s).

$$Odor\ emission\ rate\ (OER,\ ou_E/s) = OC_o \cdot Q_o \quad (3)$$

where OC_o is the outlet odor concentration (ou_E/m^3) and Q_o is the outlet gas flow (m^3/s).

Considering both the OIR and the OER, it was possible to estimate the odor removal efficiency of the biofilters (%) by equation (4):

$$Odor\ removal\ efficiency\ (\%) = \frac{(OIR - OER)}{OIR} \cdot 100 \quad (4)$$

In line with Reyes et al. (2020), the odor load factor was calculated considering the biofilter transversal area, as shown in equation (5):

$$Odor\ load\ factor\ (ou_E/m^2 \cdot s) = \frac{OC_i \cdot Q_a}{A} \quad (5)$$

where OC_i is the inlet odor concentration (ou_E/m^3), Q_a is the average gas flow between inlet and outlet flow rate (m^3/s) and A is the transversal area of the biofilter (m^2).

It is important to highlight that at constant gas flow, the odor load factor can be modified by varying the temperature of the thermostatic bath (Reyes et al., 2020).

2.4 Physico-chemical, respirometric and textural characterization

The methodology proposed by the US Department of Agriculture and the US Composting Council (2002) was used to determine the following physico-chemical variables (in triplicate): pH, conductivity (CON, µS/cm), soluble total carbon (TC, %), soluble inorganic carbon (IC, %), soluble total organic carbon (TOC, %) and soluble total nitrogen ($N\text{-}TN_s$, %), which were analyzed through an aqueous extract (1:25 ratio); and moisture (%), fixed solids (FS, %), volatile solids (VS, %), phosphorus content ($P\text{-}P_2O_5$, %), total Kjeldahl nitrogen (N-TKN, %) and ammoniacal nitrogen ($N\text{-}NH_4^+$, %), which were measured in the solid fraction. In addition, the heavy metal content (Pb, Cd, Zn, Cu, Cr and Ni) in the raw materials of the packed beds (sewage sludge compost and wood chips) was analyzed by using an atomic absorption spectrophotometer (PerkinElmer AAnalyst 100/300).

A static respirometer in liquid phase at laboratory scale was used to determine the microbiological activity of the bed materials. The respirometer was patented by the Chemical Engineering Research Group (RNM-271) of the University of Cordoba (P2004-02908) (Chica et al., 2003). All solid samples were subjected to respirometric tests in order to quantify the maximum specific oxygen uptake rate ($SOUR_{max}$, mg O_2/g VS·h) and cumulative oxygen demand at 20 h (OD_{20}, mg O_2/g VS). Each sample was analyzed in duplicate under the same standardized conditions: neutral pH, temperature of 30 ºC, the addition of macronutrients (calcium chloride, magnesium sulfate and ferric chloride) and nitrification inhibition by adding thiourea.

Mercury intrusion porosimetry was used to evaluate the textural properties (total porosity and pore size distribution) of the raw materials of the packed beds. A Micromeritics AutoPore IV 9500 porosimeter was used for this purpose. The values of contact angle and surface tension in the porosimeter software were 141° and 0.484 N/m, respectively. The sewage sludge compost had a total porosity of 65.68% (99.71% macroporosity and 0.29% mesoporosity), while the wood chips presented a total porosity of 44.87% (98.42% macroporosity and 1.58% mesoporosity).

2.5 Analysis of mesophilic aerobic microorganisms

The total mesophilic aerobic count (MAC) of the bed materials was carried out by the Agri-food Laboratory of Cordoba (LABAGCO) in accordance with the ISO 4833-1 standard (2013).

2.6 Taxonomic identification of the microbial communities

2.6.1 DNA extraction

Three biological replicates from each biofilter sample were taken at the start (S, day 0), in the middle (M, day 28) and at the end (E, day 62) of the biofiltration processes and kept at -20 °C. The samples were ground twice with a Freezer/Mill® Grinder (SPEX Sample PreP) for 1 min at maximum rate (15 cycles per second). For DNA isolation with the ZymoBIOMICS DNA Miniprep kit, 250 mg of the grounded samples were used following the manufacturer's instructions. DNA concentration was determined spectrophotometrically and integrity was evaluated by visualization on a 1% agarose gel. The absence of inhibitors was checked by PCR using bacterial 16S standard primers.

2.6.2 Library construction, sequencing, gene prediction and taxonomy assignment

Amplification and sequencing of the 16S rRNA were carried out at the Genomic Unit of the Central Service for Research Support (SCAI) of the University of Cordoba (Spain) using the Ion Torrent system, their specific kit for 16S sequencing and the Ion Reporter™ 5.0 software Ion 16S™ Metagenomics for the analyses of the results. V3 regions primers always provided the largest identification numbers and were therefore used for further taxonomic studies.

2.7 Analysis of microbiota composition and relationship with the biofilter variables

Analysis of variance was used to identify significant differences in phylogenetic diversity and species richness indexes. As the detection limit of the sequencing technique is 10 contigs, for the statistical analysis the data gaps were filled with a 9 value. Data were normalized using a logarithmic scale with base 2. Statistical significance was evaluated using two-way ANOVA. This was followed by Tukey's post-hoc multiple comparison for parametric analysis using Graphpad InStat software. Statistically significant differences were expressed as: ****, $p < 0.0001$; ***, $p < 0.001$; **, $p < 0.01$; *, $p < 0.05$. Taxonomy at the family level was used for the evaluation of phylogenetic diversity, as it was the lowest level which provided full identification. Families that presented significant differences in their number of identifications were further analyzed and clustered using the Genesis Software (Sturn et al., 2002). Complete linkage hierarchical clustering and k-means clustering analyses were performed. Pearson's correlation was used as the distance measure.

The Shannon–Wiener (*H'*) index was calculated as follows: $H\acute{}(nats) = -\sum \frac{n_i}{N} ln \frac{n_i}{N} = -\sum Pi \ln Pi$, where n_i is the number of operational taxonomic units (OTUs) of the ith families, *N* is the total number of OTUs of all the families in the samples and $Pi = \frac{n_i}{N}$ (Thukral, 2017).

The Spearman correlation matrix was also calculated to study the relationship between the different biofilter parameters analyzed and the microbiota composition at the family level using the XLSTAT data analysis add-on for Excel.

3. **Results and discussion**

3.1 Monitoring of physico-chemical variables and microbial activity

The biofiltration process was monitored through the most relevant physico-chemical and respirometric variables. The characterization of the raw materials of the packed beds, as well as the characterization carried out at the start (S, day 0), in the middle (M, day 28) and at the end (E, day 62) of each biofiltration experiment, are shown in **Table S1** (Supplementary Material) and **Table 2**, respectively. As can be observed in **Table S1**, sewage sludge compost and wood chips have different pH and low water content. Moreover, both raw materials were microbiologically stabilized, since their $SOUR_{max}$ values were lower than the threshold of 1 mg O_2/g VS·h established by Lasaridi and Stentiford (1998). In terms of composition, the sewage sludge compost presented a higher mineral content than the wood chips, as shown by its higher FS (%) and CON values. Moreover, as can be observed in **Table S1**, sewage sludge compost contained a significantly higher metal concentration (Pb, Cd, Zn, Cu, Cr and Ni) than the wood chips, mainly due to the well-known high metal content of sewage sludge (Smith, 2009). The mineral content of the packing materials does not affect the biofilter odor removal, but it can be a source of nutrients for the microorganisms involved (Mudliar et al., 2010).

With regard to the moisture parameter in the biofilters, it is important to note that the removal efficiency of these systems depends strongly on the moisture content of the filter bed because microbial communities require water to carry out their normal metabolic activity (Cabeza et al., 2013; Mudliar et al., 2010). For this reason, the moisture levels of the experiments (shown in **Table 2**), were kept at average values of 61.52 ± 2.09% (biofilter 1) and 61.64 ± 1.21% (biofilter 2), which are within the adequate range (40–60%) for the operation of biofiltration systems (Chung, 2007; Mudliar et al., 2010). Regarding the concentration of VS (%) and FS (%), no significant variations were found throughout the process in any of the biofilters studied.

Another critical factor for biofiltration performance is the pH of the packed bed. Microorganisms activity is more effective at a specific pH range, but it can be severely affected above or below that range, thus affecting negatively gas pollutant removal, and hence, odor removal efficiency (Barbusinski et al., 2017; Mudliar et al., 2010). According to Delhoménie and Heitz (2005), most of the microbes involved in biofiltration systems are typically neutrophilic (optimal pH around 7). In this study, the bed material of biofilter

1 showed neutral pH at the beginning of the biofiltration process, while that of biofilter 2 reached a slightly acidic pH (**Table 2**). During the biofiltration process, the pH values showed a downward trend, which is typical of biofilters in which a buffered mineral salts medium is not used (Reyes et al., 2020). Nevertheless, the net decrease in pH was more pronounced in biofilter 2, both at 28 days and at the end of the experiment. This can be explained by the low pH-buffering capacity of the wood chips (packing material in biofilter 2) compared to compost (Mudliar et al., 2010), which was part of the filter bed in biofilter 1. In both systems, the decrease in pH (caused by the gas stream contaminated with butyric acid) might lead to a loss of aerobic microorganisms, particularly in the final days of the experiments, as indicated by the low concentration of mesophilic aerobic microorganisms compared to the beginning of biofiltration processes (**Table 2**). In this regard, it is important to note that the initial aerobic microorganisms were not an inoculum selected for the degradation of butyric acid, but were naturally present in the packing materials. Therefore, its reduction, among other factors, was influenced by the natural selection of microorganisms as the polluted gas stream was quite acidic and contained only one compound as a carbon source.

Regarding the aerobic microbial activity of the experiments, biofilter 1 showed higher activity throughout the entire biofiltration process in comparison to biofilter 2, as evidenced by the joint study of the respirometric variables ($SOUR_{max}$ and OD_{20}) and the mesophilic aerobic count. Specifically, $SOUR_{max}$ ranged from 1.16 (minimum) to 4.95 (maximum) mg O_2/g VS·h in biofilter 1 and from 0.11 to 0.17 mg O_2/g VS·h in biofilter 2; OD_{20} ranged from 8.61 to 39.89 mg O_2/g VS in biofilter 1 and from 1.02 to 2.69 mg O_2/g VS in biofilter 2; while the mesophilic aerobic microorganisms ranged from $2.4 \cdot 10^5$ to $3.6 \cdot 10^8$ CFU/g in biofilter 1 and from $3.2 \cdot 10^4$ to $3.6 \cdot 10^7$ CFU/g in biofilter 2. Since the only difference between biofilter 1 and biofilter 2 was the presence of sewage sludge compost, the marked increase in respirometric activity that took place at 28 days in biofilter 1 (see **Table 2**) might have been due to the biological activation of this type of compost. However, between the intermediate (day 28) and final stages (day 62) of the biofiltration process, a marked decrease in aerobic activity ($SOUR_{max}$ and OD_{20}) was observed for both biofilters. This fact coincided with the highest net decrease in pH values quantified in both experiments (1.30 pH units for biofilter 1, and 1.41 pH units for biofilter 2).

Table 2. Physico-chemical properties, respirometric variables and mesophilic aerobic count of the packing materials at the beginning, in the middle and at the end of the biofiltration experiments.

	Biofilter 1			Biofilter 2		
	Start (day 0)	**Middle (day 28)**	**End (day 62)**	**Start (day 0)**	**Middle (day 28)**	**End (day 62)**
pH	7.15 ± 0.01	6.33 ± 0.09	5.03 ± 0.01	5.98 ± 0.01	4.88 ± 0.06	3.47 ± 0.11
CON (μS/cm)	1109 ± 15	2220 ± 20	2100 ± 28	110 ± 1	199 ± 8	389 ± 24
Moisture (%)	59.22 ± 1.63	63.30 ± 2.52	62.05 ± 2.06	60.49 ± 1.08	62.91 ± 0.38	61.53 ± 2.96
FS (%)	14.67 ± 2.06	14.88 ± 0.93	13.74 ± 1.96	1.26 ± 0.40	2.07 ± 0.27	2.79 ± 0.19
VS (%)	85.33 ± 2.12	85.12 ± 0.95	86.26 ± 2.11	98.74 ± 0.40	97.93 ± 0.23	97.21 ± 0.22
N-TKN (%)	0.94 ± 0.01	0.90 ± 0.00	0.86 ± 0.01	0.21 ± 0.01	0.55 ± 0.06	0.51 ± 0.03
N-NH_4^+ (%)	0.09 ± 0.01	0.12 ± 0.03	0.15 ± 0.02	0.04 ± 0.01	0.03 ± 0.01	0.08 ± 0.00
N-TN_s (%)	0.14 ± 0.01	0.09 ± 0.00	0.11 ± 0.00	0.04 ± 0.00	0.02 ± 0.00	0.06 ± 0.01
P-P_2O_5 (%)	0.49 ± 0.03	0.46 ± 0.03	0.43 ± 0.07	0.22 ± 0.02	0.20 ± 0.02	0.19 ± 0.01
TC (%)	0.86 ± 0.05	3.71 ± 0.02	5.09 ± 0.03	0.40 ± 0.07	0.58 ± 0.01	2.18 ± 0.02
IC (%)	0.02 ± 0.00	0.01 ± 0.00	0.01 ± 0.00	0.01 ± 0.00	0.03 ± 0.00	0.01 ± 0.00
TOC (%)	0.83 ± 0.05	3.70 ± 0.02	5.09 ± 0.03	0.39 ± 0.08	0.55 ± 0.00	2.18 ± 0.02
$SOUR_{max}$ (mg O_2/g VS·h)	1.16 ± 0.03	4.95 ± 0.01	1.32 ± 0.01	0.17 ± 0.01	0.22 ± 0.01	0.11 ± 0.01
OD_{20} (mg O_2/g VS)	8.61 ± 0.41	39.89 ± 1.57	14.04 ± 0.73	2.69 ± 0.08	2.19 ± 0.07	1.02 ± 0.03
MAC (CFU/g)	$8.4 \cdot 10^7$	$3.6 \cdot 10^8$	$2.4 \cdot 10^5$	$3.6 \cdot 10^7$	$1.4 \cdot 10^7$	$3.2 \cdot 10^4$

CON, conductivity; FS, fixed solids; IC, soluble inorganic carbon; MAC, total mesophilic aerobic count; N-NH_4^+, ammoniacal nitrogen; N-TKN, total Kjeldahl nitrogen; N-TN_s, soluble total nitrogen; OD_{20}, cumulative oxygen demand at 20 h; P-P_2O_5, phosphorus content expressed as P_2O_5; $SOUR_{max}$, maximum specific oxygen uptake rate; TC, soluble total carbon; TOC, soluble total organic carbon; VS, volatile solids.
Note: All variables are expressed on a dry basis except pH, CON, moisture and MAC.

The above mentioned biological activation of sewage sludge compost could be related to its high amount of intrinsic nutrients compared to wood chips (Janni et al., 2011; Mudliar et al., 2010), which provided important support for the exponential growth of the microorganisms present in biofilter 1 (at 28 days of this experiment). Butyric acid was the main source of easily biodegradable carbon and energy for microbial activity in both biofilters. However, the availability of the other macronutrients (nitrogen, phosphorus, potassium, sulphur, etc.) and micronutrients (metals or vitamins, among others) was partially achieved in the packing materials used in biofilters, where materials such as composts are known to contain several of these nutrients (Mudliar et al., 2010). As can be observed in **Table 2**, biofilter 1 showed a higher concentration of nitrogen in its different forms (N-TKN, $N\text{-}NH_4^+$ and $N\text{-}TN_s$) and phosphorus ($P\text{-}P_2O_5$) throughout the entire biofiltration process compared to biofilter 2, which was due to the higher content of these nutrients in sewage sludge compost compared to wood chips (**Table S1**).

In addition, the concentration of soluble total organic carbon, which tends to be more readily assimilable and biodegradable by microbial communities, was higher in biofilter 1 (0.83%) than in biofilter 2 (0.39%) at the beginning of the experiment. The accumulation of non-degraded butyric acid over time is the cause of the increased TOC in both biofilters (**Table 2**). Thus, at the end of the experiments, the concentration of TOC increased up to 6.13 and 5.59 times with respect to the initial TOC values in biofilter 1 and biofilter 2, respectively. Moreover, the acid character of butyric acid and its accumulation in the packed beds produced an acid hydrolysis effect that led to an increase in all the variables that could be solubilized (thus increasing CON values in both biofiltration systems). In this sense, the increase in $N\text{-}NH_4^+$ (%) throughout the biofiltration process could be one such example.

The joint evaluation of both experiments showed similarities in the acidification of the filter beds, the accumulation of soluble carbon and the decrease in aerobic microbial activity. Nevertheless, the benefits that compost brings to biofilter 1, such as higher buffer capacity and nutrient content in comparison with the biofilter based only on wood chips (biofilter 2), could play a determining role in biofiltration performance.

3.2 Monitoring of olfactometric variables and odor removal efficiency

The biofiltration process was also monitored at odor level. **Fig. 2** shows the evolution of the odor load factor ($ou_E/m^2 \cdot s$) with biofiltration time. Given that both

biofiltration systems were operated under the same conditions shown in **Table 1**, the differences in the odor load factor between biofilters 1 and 2 were only due to the temperature of the water bath, which contained the butyric acid bubbler (**Fig. 1**). Bath temperature affected the vapor pressure of liquid butyric acid and, consequently, the concentration of this compound in gaseous phase and the odor concentration at the biofilter inlet. Therefore, the higher temperature of the water bath of biofilter 1 explains the higher odor load factors observed at all times in comparison to biofilter 2 (**Fig. 2**). Specifically, in the start-up period (acclimatization), the odor load factor increased from 281 to 903 $ou_E/m^2 \cdot s$ in biofilter 1 and from 137 to 479 $ou_E/m^2 \cdot s$ in biofilter 2, while in the operational period, the odor load factor ranges were 904–3279 $ou_E/m^2 \cdot s$ and 480–1462 $ou_E/m^2 \cdot s$ for biofilter 1 and 2, respectively. It is important to note that in the operational period, biofilter 1 operated with an odor load factor approximately 2.2 times higher (on average) than the odor load factor of biofilter 2, which eventually established differences in microbial activity and hence in odor removal efficiencies. **Fig. 3A** shows the cumulative average of odor removal efficiency (%) with regard to the cumulative average of odor load factor ($ou_E/m^2 \cdot s$) for both biofilters. As can be observed, at cumulative average of load factor values below 900 $ou_E/m^2 \cdot s$, biofilters 1 and 2 showed similar performances, with cumulative average of odor removal efficiency values above 99%. However, from 900 $ou_E/m^2 \cdot s$, the cumulative average of odor removal efficiency values began to drop below 99% in biofilter 2, while in biofilter 1 this variable remained above the mentioned value up to 1450 $ou_E/m^2 \cdot s$. From this value, as the cumulative average of odor load factor increased in biofilter 1, the cumulative average of odor removal efficiency decreased in a parallel way, because the biofiltration system operated with higher odor load factors compared to biofilter 2. This fact might explain why the biofilter 1 experiment finished with lower odor removal efficiencies (**Fig. 3A**), even though both biofilters operated for the same length of time. Despite this, biofilter 1 was able to withstand higher odor loads while maintaining high removal efficiencies (close to 100%). Furthermore, these results are in line with the fact that biofilter 1 accumulated up to 6.73 times more TOC than biofilter 2, while the odor removal efficiency was similar to that of biofilter 2 at 28 days of the biofiltration process (**Fig. S1**). Maintaining high odor removal efficiencies is highly desirable when gaseous compounds with very low odor detection thresholds are emitted, such as butyric acid and hydrogen sulfide (Iranpour et al., 2005; Nagata, 2003). Nevertheless, the increasingly worse process conditions like the decrease in pH (acidification) of the bed materials, with values far from neutral pH in

the final stages of the biofiltration process (**Table 2**), led to a decrease in odor removal efficiency in both biofilters (**Fig. 3A**), since no buffered mineral salts medium was added in any case.

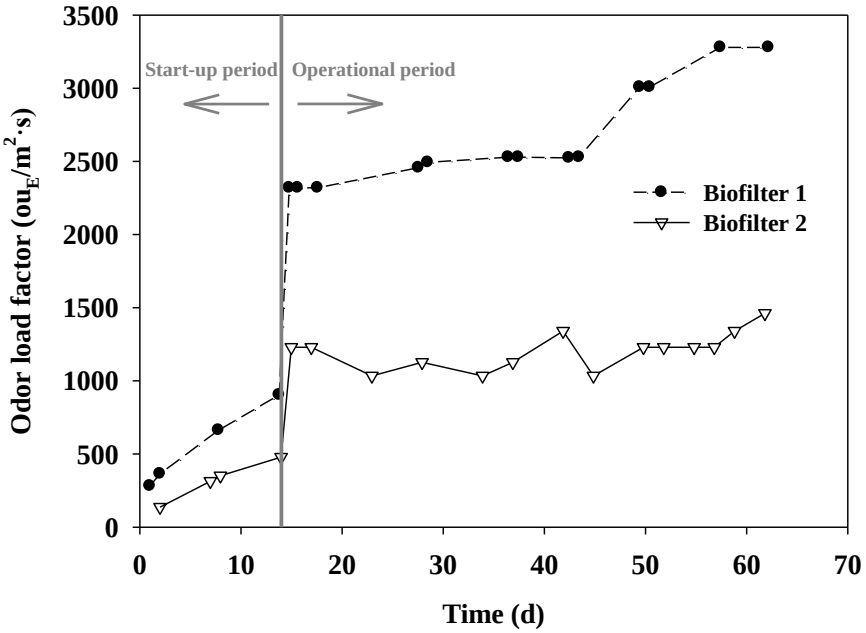

Fig. 2. Variation in odor load factor over biofiltration time in biofilters 1 and 2.

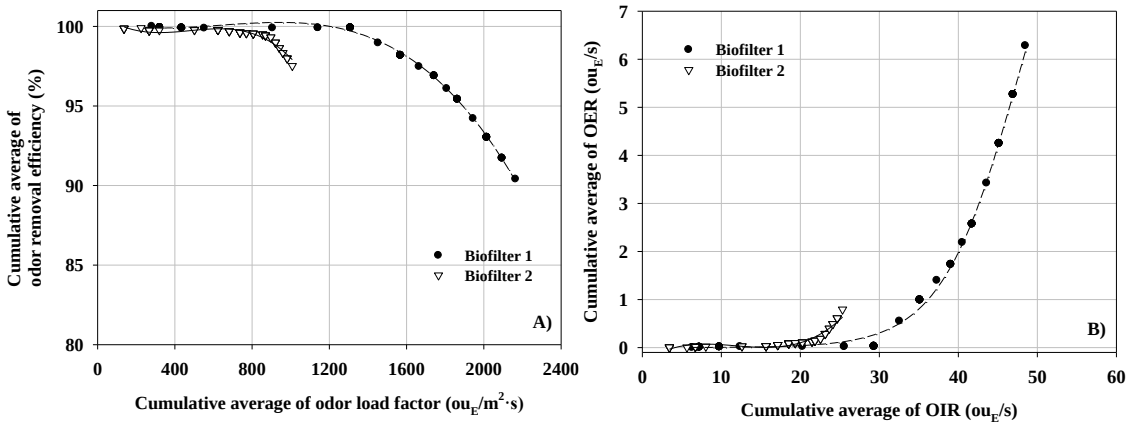

Fig. 3. (**A**) Influence of the cumulative average of odor load factor on the cumulative average of odor removal efficiency and (**B**) evolution of the cumulative average of odor emission rate (OER) depending on the cumulative average of odor incoming rate (OIR) in biofilters 1 and 2.

It is well known that biological systems show a slow response to sudden fluctuations in odor flow rates (Lebrero et al., 2011). Thus, the cumulative average of OER (ou_E/s) was also evaluated depending on the cumulative average of OIR (ou_E/s), as

shown in **Fig. 3B**. As can be seen, biofilter 2 began to increase its emission at a cumulative average OIR value of approximately 20 ou_E/s, while for biofilter 1 that fact did not occur until a value close to 30 ou_E/s was reached. Given the above results, this study shows that a biofiltration system based on sewage sludge compost with wood chips might be a better technological alternative than a biofilter based solely on wood chips for reducing the odor impact of activities that emit gas streams containing butyric acid.

3.3 Taxonomic analysis of the biofilter microbiota

The 16S rRNA sequencing analysis identified more than 560,000 bacteria in the two biofilters. The number of identifications was superior in biofilter 1 than in biofilter 2 in the initial and intermediate stages of the experiments (129,829 vs. 66,623 at the beginning, 89,823 vs. 55,215 in the middle) but inferior at the end (82,922 vs. 137,455). The differences between the trends of these sequencing identification amounts and MAC (**Table 2**) could have been due to an increase in anaerobic microorganisms during the biofiltration process. Thus, anaerobic microbes seem to be particularly relevant in biofilter 2 where the number of total counts calculated by sequencing increased about 2-fold at the end of the experiment, while aerobic microbes decreased approximately 1000-fold. As the nutrient content in biofilter 2 was very limited and wood chips have a lower soluble total carbon content (**Table 2**), butyric acid can constitute an extra carbon source that promotes microbial growth. Additionally, biofilter 1 decreased both the number of mesophilic aerobic counts (350-fold) and total sequenced counts (1.6-fold).

As can be observed in **Fig. 4**, the initial microbiota of the biofilters differed greatly depending on the filling. At the start point, Firmicutes were clearly predominant in the compost-wood matrix (46.7 ± 0.8%), while Proteobacteria was by far the most common in the wood biofilter (84.5 ± 5.1%). The predominance of Proteobacteria in the initial composition of biofilter 2 is in accordance with the findings of Reyes et al. (2020) for a wood-filled biofilter, while the initial phyla of biofilter 1 have also been reported by Chung (2007) in a biofilter based on mature compost with activated carbon and sludge sourced from a sewage treatment plant.

The evolution of the microbiota composition during the process was also different in both biofilters (**Fig. 4**, **Table S2**). In biofilter 1: (i) Firmicutes decreased throughout the procedure (47%, start → 27%, middle → 21%, end), (ii) Proteobacteria diminished in the middle of the procedure (17%) but returned to the initial levels at the end (38%),

(iii) Actinobacteria increased remarkably to become the most common phylum in both the intermediate and final stages (9% → 50% → 41%), (iv) Bacteroidetes were fairly abundant in the initial stage (7%) but practically disappeared during the procedure, and Cyanobacteria presented a clear peak in the middle stage (6%). In biofilter 2: (i) Proteobacteria diminished throughout the procedure (84% → 67% → 40%), while (ii) Firmicutes went from being almost non-existent to being predominant in the final stage (47%), (iii) Bacteroidetes increased for a time and finally decreased (14% →18% → 6%), while Actinobacteria were slightly promoted by butyric acid exposure (1% → 8% → 5%).

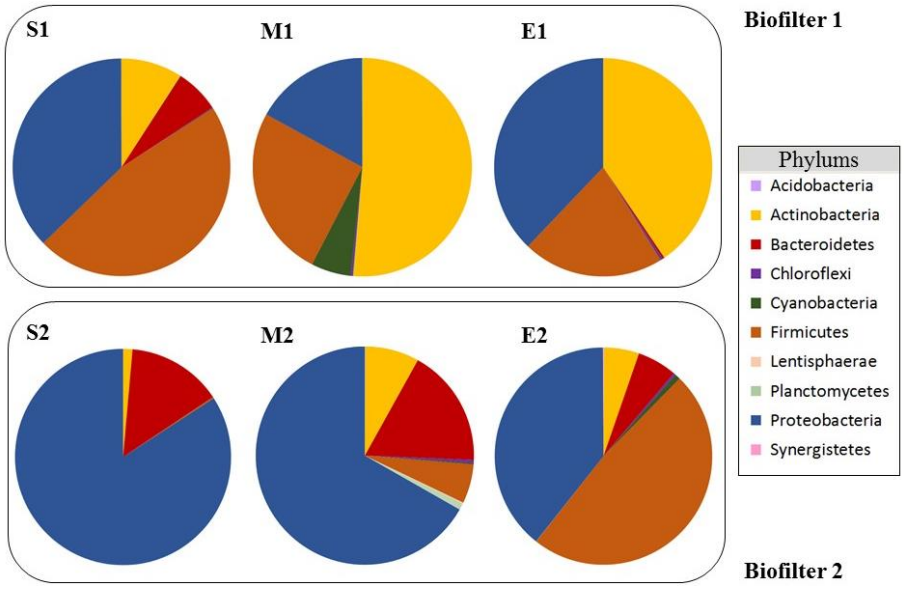

Fig. 4. Microbial composition at the phylum level determined by massive 16S rRNA sequencing at the start (S, day 0), in the middle (M, day 28) and at the end (E, day 62) of the biofiltration process. Biofilter 1 is shown at the top (S1, M1 and E1) and biofilter 2 at the bottom (S2, M2 and E2).

According to the above results, it can be said that Actinobacteria played an important role throughout the biofiltration process, especially in biofilter 1. Similarly, in a trickle biofilter treating air from a livestock facility, Kristiansen et al. (2011) found that Actinobacteria was the major bacterial phylum assimilating butyric acid. Therefore, the greater presence of Actinobacteria in biofilter 1 would explain why this system was able to withstand higher odor loads while maintaining high odor removal efficiencies compared to biofilter 2 (**Fig. 3A**). Nevertheless, at the end of the biofiltration period, where removal efficiencies are lowest, the set formed by Proteobacteria and Firmicutes predominated in both biofilters, since these phyla can survive under adverse conditions, such as acid pH (Reyes et al., 2020).

3.4 Evolution of the microbiota structure

Although the matrixes inside biofilters were not totally homogeneous, the biological replicates were very similar in both experimental sets during the process. This can be observed in **Fig. 5**, which shows the relative abundance of the sixty most abundant families. Overall, the microbial variety in biofilter 1 (122 families) was much higher than in biofilter 2 (77 families) coinciding with the higher complexity of the filling matrix of biofilter 1. Furthermore, more than half of the families identified in biofilter 1 (52%) were not present in biofilter 2. By contrast, only 18 families (23%) were found exclusively in biofilter 2, while most (77%) were also present in biofilter 1. Nevertheless, in general, the proportion of the different microbes varied greatly between the two filling conditions, as Microbacteriaceae and Bacillaceae were predominant in biofilter 1 (17% and 13%, respectively), while Pseudomonadaceae and Sphingomonadaceae were predominant in biofilter 2 (16% and 15%) (**Fig. 5**). Microbacteriaceae was the main family responsible for the marked growth of the phylum Actinobacteria in biofilter 1 (**Fig. 4**). Moreover, microbes of this family are mostly aerobic (von Graevenitz, 2004), which may account for the increase in mesophilic aerobic microorganisms in the middle stage of biofilter 1 (**Table 2**). Members of Microbacteriaceae, as well as Bacillaceae and Pseudomonadaceae, have been associated with the degradation of butyric acid in other studies (Kristiansen et al., 2011; Njalam'mano and Chirwa, 2019). It should also be highlighted that although the phylum patterns in the initial stage of biofilter 1 and in the final stage of biofilter 2 were very similar (**Fig. 4**), the composition at the family level was very different in both biofilter stages (**Fig. 5**).

To estimate changes in the microbial biodiversity throughout the biofiltration process, the Shannon–Wiener index (H') was calculated (**Fig. 5**). This index determines the abundance of species by their relative evenness. As expected, the initial biodiversity was significantly higher in the more complex biofilter 1 than in biofilter 2 (4.3 vs. 2.8; ****, $p < 0.0001$). The two biofilters increased their microbial diversity in the final stages of butyric acid exposure, although the compost-wood filling showed an intermediate decrease that was not observed in biofilter 2 (**Fig. 5**). The Pielou (J') and Gini-Simpson (SiD) indexes were also calculated, and the observed patterns were very similar (data not shown) (Thukral, 2017).

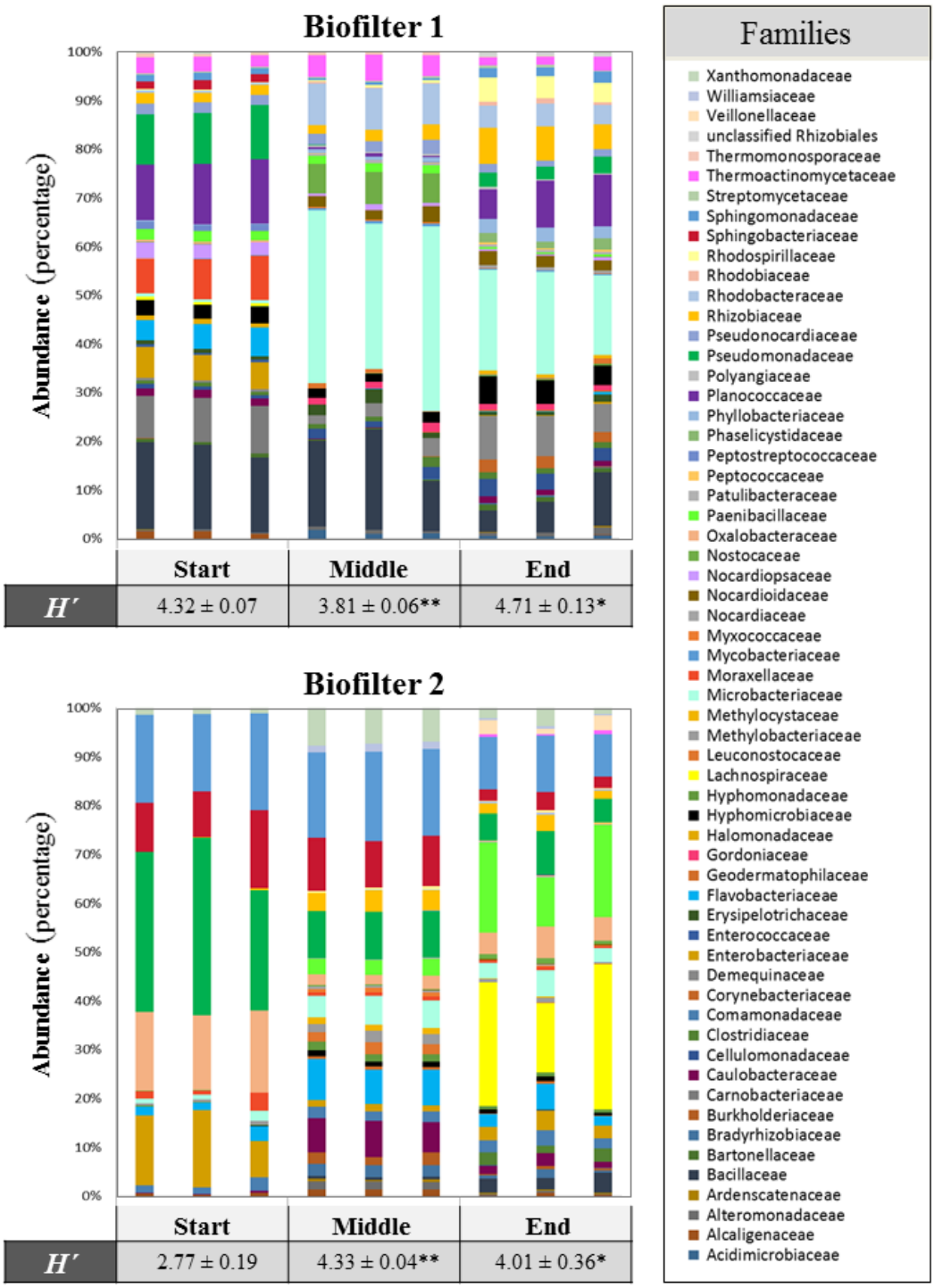

Fig. 5. Relative abundance of microbial families and microbial diversity during the biofiltration process. The abundance (percentage) for the 60 most abundant families was represented (top on each biofilter) and the Shannon–Wiener index was calculated (bottom on each biofilter) for the three biological replicates in biofilter 1 (above) and biofilter 2 (below) in the three stages of the process (start: day 0; middle: day 28; end: day 62). H'max = 7.23. Asterisks indicate significance relative to their initial stages (**, $p < 0.01$; *, $p < 0.05$).

Approximately half of the families in each biofilter (64 in biofilter 1 and 35 in biofilter 2) showed statistically significant changes during the procedure (**Fig. 6**). A clustering analysis was performed to identify microbial trends upon butyric acid exposure. The analysis showed three different trends, with families presenting the top levels at the start (cluster A), in the middle (cluster B) or at the end (cluster C) of the experiments. The number of families belonging to clusters B and C were similar in both biofilters, but the number of families in cluster A was much higher in biofilter 1 than in biofilter 2 (28 vs. 4). A correlation analysis was performed to associate the family trends with the biofilter variables included in **Table 2** (**Fig. 6**). Notably, families belonging to cluster C in both biofilters were negatively correlated with pH values and positively correlated with TC and TOC. This suggests that members of this cluster can survive in acidic environments (which are caused by the accumulation of non-degraded butyric acid). Otherwise, some differences between both biofilters were also found in the cluster C members: N-TKN was negatively correlated and $N\text{-}NH_4^+$ was positively correlated in biofilter 1, while CON and FS were positively correlated and VS was negatively correlated in biofilter 2. No common patterns were found in the two biofilters for clusters A and B. Thus, cluster A members in biofilter 1 showed remarkable positive correlations with N-TKN, N-TN and IC, but negative correlations with CON, TC and TOC. By contrast, biofilter 2 members only correlated negatively with N-TKN. Here, it is important to note that the addition of nitrogen to the biofilter bed can significantly increase the performance of a biofilter (Delhoménie et al., 2001; Detchanamurthy and Gostomski, 2012). Therefore, the higher nitrogen content of biofilter 1 (**Table 2**) promoted a greater diversity of microbial families at the beginning of the experiment and a better performance with respect to biofilter 2. With regard to cluster B, the members were positively correlated with CON and negatively correlated with $N\text{-}TN_s$ and IC in biofilter 1, while biofilter 2 did not show a defined pattern. Finally, none of the clusters showed a correlation with MAC as would be expected when anaerobic microorganisms are predominant during the biofiltration process, as discussed in Section 3.3. However, it is important to remember that aerobic microbial communities (such as Microbacteriaceae in biofilter 1) were primarily responsible for butyric acid removal, since the reduction of these communities led to a decrease in the odor removal efficiencies of the biofilters (**Table 2** and **Fig. 3A**).

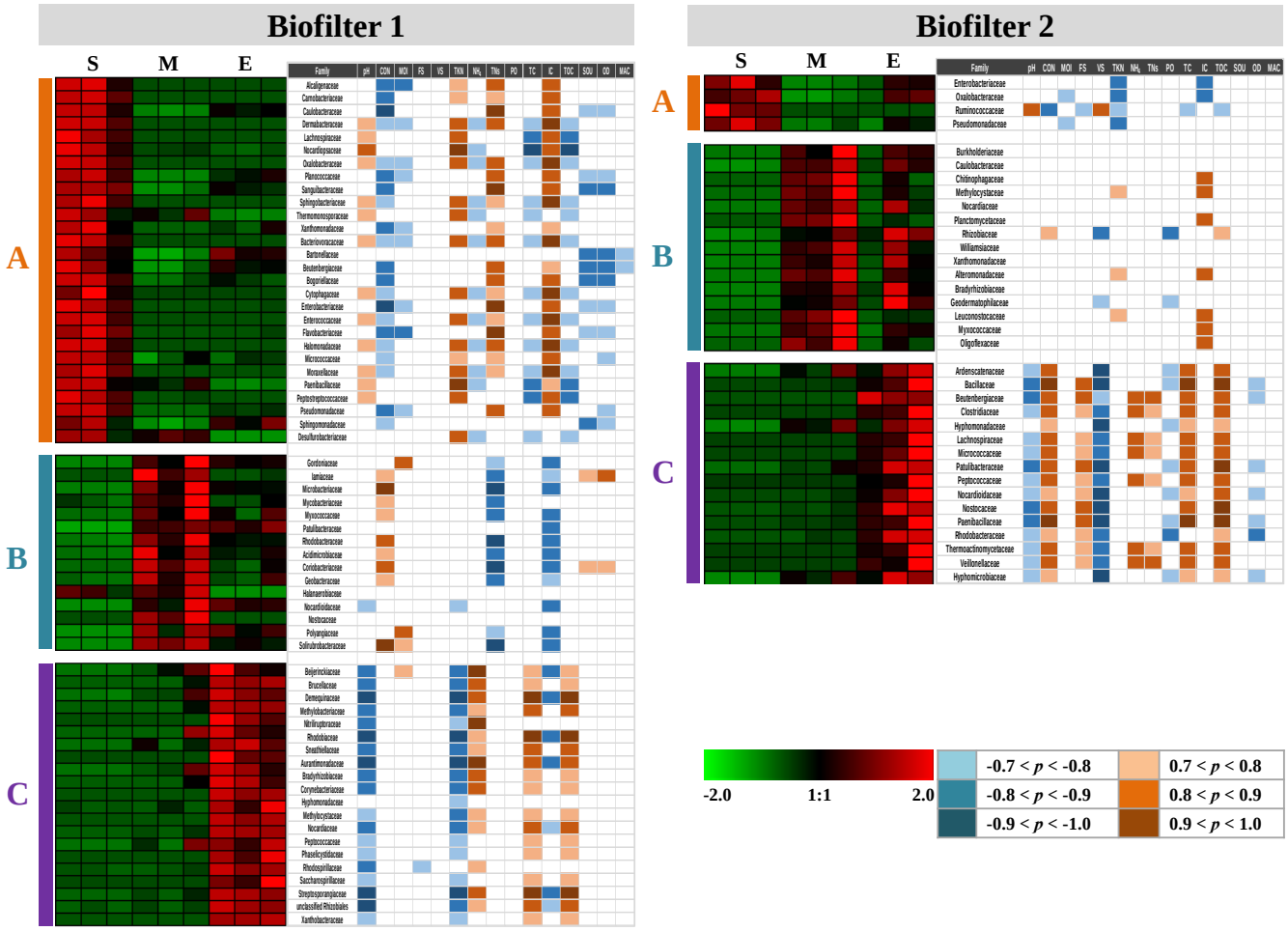

Fig. 6. Hierarchical clustering analysis of the microbial families showing statistically different abundances during the biofiltration process and Spearman correlation analysis compared to the biofilter variables for biofilter 1 (left) and biofilter 2 (right). Abundance percentages were compared along the biofiltration process for each biofilter (left side on each biofilter) using the Genesis package. Families are grouped into three clusters (A, B and C). Green rectangles indicate families with less abundance relative to other conditions, while red rectangles represent higher abundance. The color intensity is proportional to the fold-change as represented by the scale. Spearman correlation coefficients between the microbial families and the biofilter variables described in Table 2 are shown at the right side of each biofilter. Only correlations higher than 0.7 (blue) and lower than -0.7 (brown) are shown. A different color intensity is assigned to each correlation range (For interpretation of the references to color in this figure legend, the reader is referred to the Web version of this article).

4. Conclusions

From this pilot-scale study to evaluate the influence of bed material on the odor removal performance of a non-inoculated biofiltration system, the following conclusions can be drawn:

- The selection of a particular bed material for deodorization by biofiltration of the same gaseous stream (in this case butyric acid) determines the odor removal capacity of a biofiltration system largely. The compost-wood biofilter was able to withstand higher odor loads (≈1450 $ou_E/m^2 \cdot s$), achieving odor removal efficiencies close to 100%, while the wood biofilter began to decrease its efficiency at lower odor loads (≈ 900 $ou_E/m^2 \cdot s$).

- The higher buffer capacity and nutrient content (nitrogen and phosphorus) of the compost-wood biofilter might explain the marked growth of aerobic microorganisms after 28 days of biofiltration (4.29-fold with respect to the beginning). This fact explains the better performance of the compost-wood biofilter compared to the wood one, which exhibited less aerobic activity during the process.

- The microbiological analysis also showed that, overall, the microbial variety was much higher in the compost-wood biofilter (122 families) than in the wood biofilter (77 families). The phylum Actinobacteria increased markedly in the compost-wood biofilter and was the most common phylum in both the intermediate (50%) and final stages (41%). This marked growth was mainly due to the mostly aerobic Microbacteriaceae family. By contrast, the phylum Proteobacteria predominated in the initial and intermediate stages of the wood biofilter, while Firmicutes were the predominant phylum at the end of the process.

- A correlation analysis associated the microbial family trends with the analyzed biofilter variables. The analysis statistically demonstrated that the higher initial biodiversity of the compost-wood biofilter was due to its higher nitrogen content, while the families present in the final stages of both biofilters were able to survive in acidic environments caused by the accumulation of non-degraded butyric acid.

Given the above facts, the multidisciplinary analysis carried out in this work might be useful for the optimal design of biofiltration operations, since the choice of a suitable

packed bed to treat the gaseous stream can reduce the odor impact of a facility with the consequent environmental and social benefits. Furthermore, the utilization of compost in biofilters constitutes an effective way of recycling residual organic matter, such as abundant sewage sludge derived from urban wastewater treatment plants.

Acknowledgements

This work was supported by the Spanish Ministry of Economy, Industry and Competitiveness (MINECO), the Spanish State Research Agency (AEI) and the European Regional Development Fund (FEDER) through Project CTM2017-88723-R, and the Ministry of Education, Culture and Sport of Spain (Grant FPU2016). The European Regional Development Fund (Project UCO-FEDER-1262384-R) and the Chelonia Association (Mares Circulares Project) also supported the work. A.M. Herruzo-Ruiz received a predoctoral contract of the University of Cordoba ("Plan Propio"). The Genomic Unit staff of the Central Service for Research Support (SCAI) at the University of Cordoba is also acknowledged. Finally, we also wish to express our gratitude to Inmaculada Bellido and María Luisa López for their contribution to this research.

Appendix A. Supplementary data

Table S1. Physico-chemical and respirometric characterization of the raw materials of the packed beds.

	Sewage sludge compost	**Wood chips**
pH	8.46 ± 0.01	5.98 ± 0.01
CON (µS/cm)	2230 ± 30	110 ± 1
Moisture (%)	9.80 ± 0.13	9.32 ± 0.25
FS (%)	29.74 ± 3.93	1.26 ± 0.40
VS (%)	70.26 ± 4.05	98.74 ± 0.40
N-TKN (%)	1.77 ± 0.02	0.21 ± 0.01
N-NH_4^+ (%)	0.14 ± 0.00	0.04 ± 0.01
N-TN_s (%)	0.24 ± 0.01	0.04 ± 0.00
P-P_2O_5 (%)	0.79 ± 0.04	0.22 ± 0.02
TC (%)	1.37 ± 0.01	0.40 ± 0.07
IC (%)	0.03 ± 0.00	0.01 ± 0.00
TOC (%)	1.33 ± 0.01	0.39 ± 0.08
Pb (mg/kg)	38.36 ± 1.98	0.68 ± 0.05
Cd (mg/kg)	5.07 ± 0.16	1.65 ± 0.15
Zn (mg/kg)	485.48 ± 1.66	7.89 ± 0.15
Cu (mg/kg)	154.17 ± 0.40	0.68 ± 0.10
Cr (mg/kg)	16.33 ± 0.48	1.74 ± 0.53
Ni (mg/kg)	18.39 ± 0.40	0.68 ± 0.39
$SOUR_{max}$ (mg O_2/g VS·h)	0.81 ± 0.01	0.90 ± 0.04
OD_{20} (mg O_2/g VS)	7.66 ± 0.31	9.46 ± 0.49

CON, conductivity; FS, fixed solids; IC, soluble inorganic carbon; N-NH_4^+, ammoniacal nitrogen; N-TKN, total Kjeldahl nitrogen; N-TN_s, soluble total nitrogen; OD_{20}, cumulative oxygen demand at 20 h; P-P_2O_5, phosphorus content expressed as P_2O_5; $SOUR_{max}$, maximum specific oxygen uptake rate; TC, soluble total carbon; TOC, soluble total organic carbon; VS, volatile solids.
Note: All variables are expressed on a dry basis except pH, CON and moisture.

Table S2. Microbial composition (%) at the phylum level determined by massive 16S rRNA sequencing along the biofiltration process in biofilters 1 and 2.

	Biofilter 1			Biofilter 2		
	Start (day 0)	**Middle (day 28)**	**End (day 62)**	**Middle (day 28)**	**Start (day 0)**	**End (day 62)**
Acidobacteria	ND	ND	ND	ND	0.08 ± 0.02	0.08 ± 0.02
Actinobacteria	8.97 ± 0.71	**49.81 ± 6.17*** **	**40.79 ± 5.59*** **	1.35 ± 0.68	**7.98 ± 0.89*** **	**5.31 ± 1.97***
Bacteroidetes	6.73 ± 0.98	**0.04 ± 0.07*** **	**0.28 ± 0.26*** **	13.89 ± 4.54	17.58 ± 1.28	5.97 ± 2.65
Chloroflexi	0.09 ± 0.06	0.34 ± 0.38	0.30 ± 0.27	ND	0.44 ± 0.12	0.36 ± 0.05
Cyanobacteria	0.07 ± 0.02	**5.94 ± 0.31**** **	0.06 ± 0.03	0.04 ± 0.04	**0.20 ± 0.04****	**0.85 ± 0.22****
Firmicutes	46.71 ± 0.77	**26.84 ± 6.09****	**20.68 ± 6.84****	0.21 ± 0.10	**5.78 ± 0.34***** **	**47.38 ± 15.68****
Lentisphaerae	ND	ND	ND	ND	0.17 ± 0.06	ND
Planctomycetes	ND	ND	ND	ND	1.00 ± 0.10	0.03 ± 0.05
Proteobacteria	37.33 ± 0.73	**16.83 ± 0.68***** **	37.90 ± 2.03	84.49 ± 5.12	**66.80 ± 0.11****	**39.93 ± 10.84****
Synergistetes	ND	ND	ND	ND	ND	0.08 ± 0.04

ND, non-detected. Statistical significance was evaluated using a t test with Graphpad InStat software. Significant differences with respect to the start point (day 0) are highlighted in bold and are expressed as follows: ****, $p < 0.0001$; ***, $p < 0.001$; **, $p < 0.01$; *, $p < 0.05$.

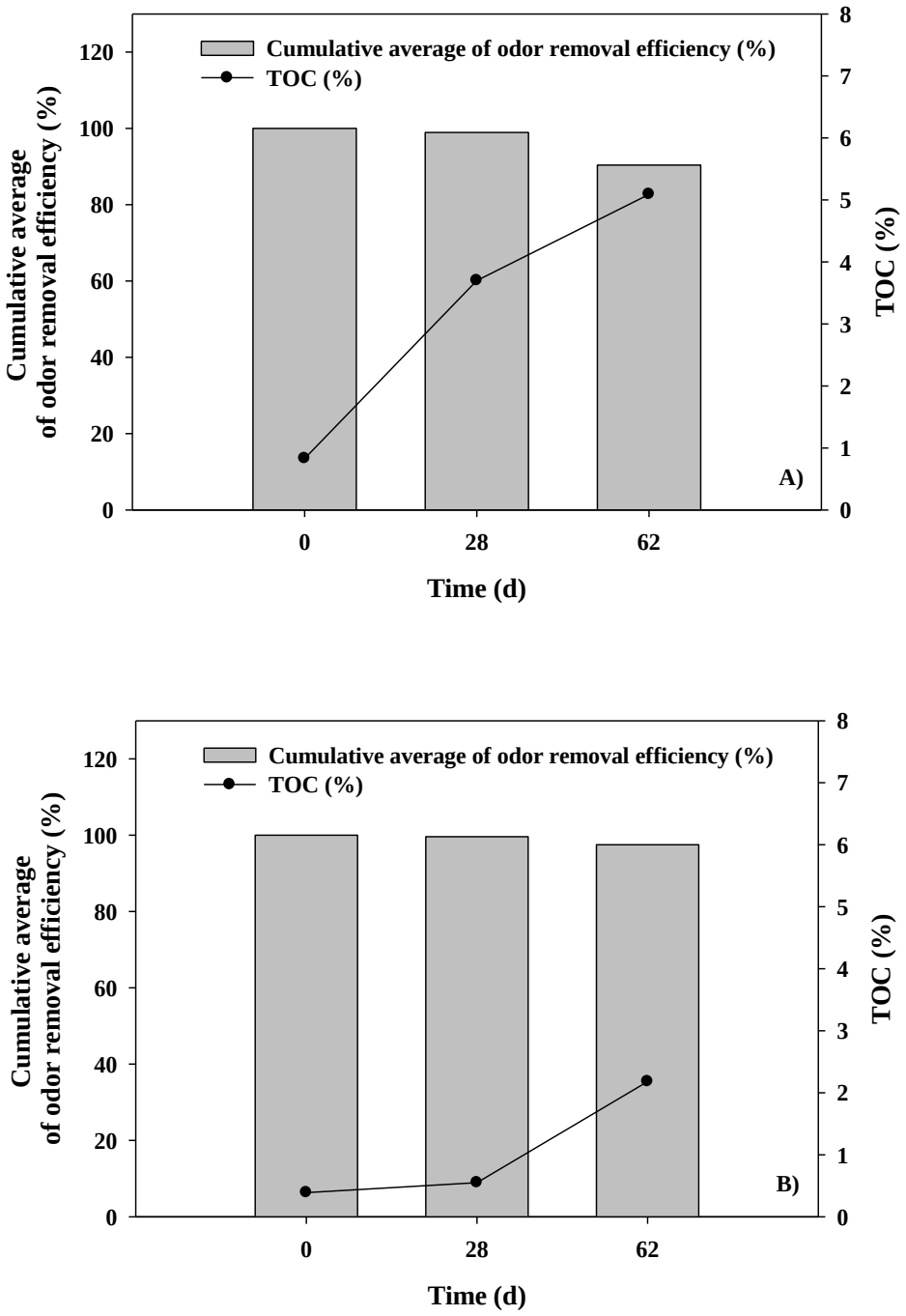

Fig. S1. Evolution of the cumulative average of odor removal efficiency (%) and TOC (%) with biofiltration time for biofilters 1 (**A**) and 2 (**B**).

References

Barbusinski, K., Kalemba, K., Kasperczyk, D., Urbaniec, K., Kozik, V., 2017. Biological methods for odor treatment – A review. J. Clean. Prod. https://doi.org/10.1016/j.jclepro.2017.03.093

Boswell, J., 2004. Compost-based biofilters control air pollution. Byocicle 45, 42–46.

Cabeza, I.O., López, R., Giraldez, I., Stuetz, R.M., Díaz, M.J., 2013. Biofiltration of α-pinene vapours using municipal solid waste (MSW) - Pruning residues (P) composts as packing materials. Chem. Eng. J. 233, 149–158. https://doi.org/10.1016/j.cej.2013.08.032

Cheng, Y., He, H., Yang, C., Zeng, G., Li, X., Chen, H., Yu, G., 2016. Challenges and solutions for biofiltration of hydrophobic volatile organic compounds. Biotechnol. Adv. https://doi.org/10.1016/j.biotechadv.2016.06.007

Chica, A., Mohedo, J.J., Martín, M.A., Martín, A., 2003. Determination of the stability of msw compost using a respirometric technique. Compost Sci. Util. 11, 169–175. https://doi.org/10.1080/1065657X.2003.10702122

Chung, Y.C., 2007. Evaluation of gas removal and bacterial community diversity in a biofilter developed to treat composting exhaust gases. J. Hazard. Mater. 144, 377–385. https://doi.org/10.1016/j.jhazmat.2006.10.045

Chung, Y.C., Cheng, C.Y., Chen, T.Y., Hsu, J.S., Kui, C.C., 2010. Structure of the bacterial community in a biofilter during dimethyl sulfide (DMS) removal processes. Bioresour. Technol. 101, 7165–7168. https://doi.org/10.1016/j.biortech.2010.03.131

Datta, I., Allen, D.G., 2005. Biofilter technology, in: Biotechnology for Odor and Air Pollution Control. Springer Berlin Heidelberg, pp. 125–145. https://doi.org/10.1007/3-540-27007-8_6

De Feo, G., De Gisi, S., Williams, I.D., 2013. Public perception of odour and environmental pollution attributed to MSW treatment and disposal facilities: A case study. Waste Manag. 33, 974–987. https://doi.org/10.1016/j.wasman.2012.12.016

Delhoménie, M.-C., Bibeau, L., Roy, S., Brzezinski, R., Heitz, M., 2001. Influence of nitrogen on the degradation of toluene in a compost-based biofilter. J. Chem. Technol. Biotechnol. 76, 997–1006. https://doi.org/10.1002/jctb.472

Delhoménie, M.C., Heitz, M., 2005. Biofiltration of air: A review. Crit. Rev. Biotechnol. https://doi.org/10.1080/07388550590935814

Detchanamurthy, S., Gostomski, P.A., 2012. Biofiltration for treating VOCs: An overview. Rev. Environ. Sci. Biotechnol. https://doi.org/10.1007/s11157-012-9288-5

Dorado, A.D., Baquerizo, G., Maestre, J.P., Gamisans, X., Gabriel, D., Lafuente, J., 2008. Modeling of a bacterial and fungal biofilter applied to toluene abatement: Kinetic parameters estimation and model validation. Chem. Eng. J. 140, 52–61. https://doi.org/10.1016/j.cej.2007.09.004

Elias, A., Barona, A., Arreguy, A., Rios, J., Aranguiz, I., Peñas, J., 2002. Evaluation of a packing material for the biodegradation of H2S and product analysis. Process Biochem. 37, 813–820. https://doi.org/10.1016/S0032-9592(01)00287-4

EN 13725, 2003. Air Quality - Determination of Odour Concentration by Dynamic Olfactometry. European Committee for Standardization, Brussels.

Friedrich, U., Prior, K., Altendorf, K., Lipski, A., 2002. High bacterial diversity of a waste gas-degrading community in an industrial biofilter as shown by a 16S rDNA clone library. Environ. Microbiol. 4, 721–734. https://doi.org/10.1046/j.1462-2920.2002.00349.x

González, D., Colón, J., Sánchez, A., Gabriel, D., 2019. A systematic study on the VOCs characterization and odour emissions in a full-scale sewage sludge composting plant. J. Hazard. Mater. 373, 733–740. https://doi.org/10.1016/j.jhazmat.2019.03.131

Hayes, J.E., Stevenson, R.J., Stuetz, R.M., 2017. Survey of the effect of odour impact on communities. J. Environ. Manage. 204, 349–354. https://doi.org/10.1016/j.jenvman.2017.09.016

Iranpour, R., Cox, H.H.J., Deshusses, M.A., Schroeder, E.D., 2005. Literature review of air pollution control biofilters and biotrickling filters for odor and volatile organic compound removal. Environ. Prog. 24, 254–267. https://doi.org/10.1002/ep.10077

ISO4833-1, 2013. Microbiology of the food chain-Horizontal method for the enumeration of microorganisms–Part 1: Colony count at 30 degrees C by the pour plate technique.

Janni, K., Nicolai, R., Hoff, S., Stenglein, R., 2011. Air Quality Education in Animal Agriculture: Biofilters for Odor and Air Pollution Mitigation in Animal Agriculture. Agric. Biosyst. Eng. Ext. Outreach Publ.

Kasper, P.L., Oxbøl, A., Hansen, M.J., Feilberg, A., 2018. Mechanisms of Loss of Agricultural Odorous Compounds in Sample Bags of Nalophan, Tedlar, and PTFE. J. Environ. Qual. 47, 246–253. https://doi.org/10.2134/jeq2017.07.0289

Kennes, C., Veiga, M.C., 2013. Bioreactors for waste gas treatment. Springer Science & Business Media.

Kristiansen, A., Lindholst, S., Feilberg, A., Nielsen, P.H., Neufeld, J.D., Nielsen, J.L., 2011. Butyric acid- and dimethyl disulfide-assimilating microorganisms in a biofilter treating air emissions from a livestock facility. Appl. Environ. Microbiol. 77, 8595–8604. https://doi.org/10.1128/AEM.06175-11

Lasaridi, K.E., Stentiford, E.D.I., 1998. a Simple Respirometric Technique for Assessing Compost Stability 32, 3717–3723.

Lebrero, R., Bouchy, L., Stuetz, R., Muñoz, R., 2011. Odor Assessment and Management in Wastewater Treatment Plants: A Review. Crit. Rev. Environ. Sci. Technol. 41, 915–950. https://doi.org/10.1080/10643380903300000

López, R., Cabeza, I.O., Giráldez, I., Díaz, M.J., 2011. Biofiltration of composting gases using different municipal solid waste-pruning residue composts: Monitoring by using an electronic nose. Bioresour. Technol. 102, 7984–7993. https://doi.org/10.1016/j.biortech.2011.05.085

Márquez, P., Benítez, A., Caballero, Á., Siles, J.A., Martín, M.A., 2021. Integral evaluation of granular activated carbon at four stages of a full-scale WWTP deodorization system. Sci. Total Environ. 754, 142237. https://doi.org/10.1016/j.scitotenv.2020.142237

Mudliar, S., Giri, B., Padoley, K., Satpute, D., Dixit, R., Bhatt, P., Pandey, R., Juwarkar, A., Vaidya, A., 2010. Bioreactors for treatment of VOCs and odours - A review. J. Environ. Manage. https://doi.org/10.1016/j.jenvman.2010.01.006

Nagata, Y., 2003. Odor Measurement Review, Measurement of Odor Threshold by Triangle Odor Bag Method. Minist. Environ. Gov. Japan 122–123.

Njalam'mano, J.B.J., Chirwa, E.M.N., 2019. Indigenous butyric acid-degrading bacteria as surrogate pit latrine odour control: isolation, biodegradability performance and growth kinetics. Ann. Microbiol. 69, 107–122. https://doi.org/10.1007/s13213-018-1408-1

Omri, I., Bouallagui, H., Aouidi, F., Godon, J.J., Hamdi, M., 2011. H2S gas biological removal efficiency and bacterial community diversity in biofilter treating wastewater odor. Bioresour. Technol. 102, 10202–10209. https://doi.org/10.1016/j.biortech.2011.05.094

Otten, L., Afzal, M.T., Mainville, D.M., 2004. Biofiltration of odours: Laboratory studies using butyric acid. Adv. Environ. Res. 8, 397–409. https://doi.org/10.1016/S1093-0191(02)00119-3

Ramírez, M., Fernández, M., Granada, C., Le Borgne, S., Gómez, J.M., Cantero, D., 2011. Biofiltration of reduced sulphur compounds and community analysis of sulphur-oxidizing bacteria. Bioresour. Technol. 102, 4047–4053. https://doi.org/10.1016/j.biortech.2010.12.018

Reyes, J., Toledo, M., Michán, C., Siles, J.A., Alhama, J., Martín, M.A., 2020. Biofiltration of butyric acid: Monitoring odor abatement and microbial communities. Environ. Res. 190. https://doi.org/10.1016/j.envres.2020.110057

Sheridan, B.A., Curran, T.P., Dodd, V.A., 2003. Biofiltration of n-butyric acid for the control of odour. Bioresour. Technol. 89, 199–205. https://doi.org/10.1016/S0960-8524(03)00045-2

Singh, A., Ward, O., 2005. Microbiology of bioreactors for waste gas treatment, in: Biotechnology for Odor and Air Pollution Control. Springer Berlin Heidelberg, pp. 101–121. https://doi.org/10.1007/3-540-27007-8_5

Smith, S., 2009. A critical review of the bioavailability and impacts of heavy metals in municipal solid waste composts compared to sewage sludge. Environ. Int. 35, 142–156. https://doi.org/10.1016/j.envint.2008.06.009

Sturn, A., Quackenbush, J., Trajanoski, Z., 2002. Genesis: Cluster analysis of microarray data. Bioinformatics 18, 207–208. https://doi.org/10.1093/bioinformatics/18.1.207

Thukral, A.K., 2017. A review on measurement of Alpha diversity in biology. Agric. Res. J. 54, 1–10. https://doi.org/10.5958/2395-146x.2017.00001.1

Toledo, M., Guillot, J.M., Siles, J.A., Martín, M.A., 2019. Permeability and adsorption effects for volatile sulphur compounds in Nalophan sampling bags: Stability influenced by storage time. Biosyst. Eng. 188, 217–228. https://doi.org/10.1016/j.biosystemseng.2019.10.023

US Department of Agriculture and The US Composting Council, 2002. Test Methods for the Examination of Composting and Compost (TMECC). Edaphos International, Houston (TX).

von Graevenitz, A., 2004. Rothia dentocariosa: Taxonomy and differential diagnosis. Clin. Microbiol. Infect. https://doi.org/10.1111/j.1469-0691.2004.00784.x

III.2. Breve descripción del artículo: "*A comparative study between the biofiltration for air contaminated with limonene or butyric acid using a combination of olfactometric, physico-chemical and genomic approaches*"

III.2. Breve descripción del artículo: "*A comparative study between the biofiltration for air contaminated with limonene or butyric acid using a combination of olfactometric, physico-chemical and genomic approaches*"

En este estudio se ha llevado a cabo un análisis multidisciplinar para comparar la biofiltración de ácido butírico con la de D-limoneno, que constituyen compuestos gaseosos de distinta naturaleza (el primero es hidrófilo y el segundo es hidrófobo), emitidos habitualmente en el tratamiento biológico de los residuos orgánicos. Para ello, se sometieron dos biofiltros, uno constituido por una mezcla de virutas de madera y compost estabilizado de lodos de EDAR (en la proporción 1:1 en volumen) y otro por virutas de madera solamente, a corrientes gaseosas conteniendo ácido butírico (BF B-1 y BF B-2, respectivamente). De manera análoga, otros dos biofiltros fueron sometidos a corrientes gaseosas contaminadas con D-limoneno (BF L-1 y BF L-2, respectivamente). Los cuatro biofiltros se evaluaron comparativamente desde perspectivas fisicoquímicas, olfatométricas y microbiológicas. Aunque los biofiltros alimentados con ácido butírico fueron sometidos a factores de carga de olor más elevados (280–3280 $ou_E/m^2 \cdot s$ para BF B-1 y 135–1460 $ou_E/m^2 \cdot s$ para BF B-2) que los biofiltros que trataron D-limoneno (30–170 $ou_E/m^2 \cdot s$ para BF L-1 y 15–130 $ou_E/m^2 \cdot s$ para BF L-2), los primeros sistemas lograron eficacias de eliminación de olores superiores al 90% durante la mayor parte del tiempo de biofiltración, mientras que en los biofiltros alimentados con gas contaminado con D-limoneno, las eficacias nunca fueron superiores al 70%. Con respecto a los lechos empacados, el análisis genómico de las comunidades bacterianas mostró una distribución más amplia de filos (Proteobacteria, Firmicutes, Bacteroidetes y Actinobacteria) en los biofiltros de compost−madera en comparación con los sistemas de virutas de madera, en los cuales el filo Proteobacteria fue claramente predominante. Por tanto, este estudio confirma la importancia de considerar tanto la naturaleza de los compuestos odorantes a biofiltrar como la composición del lecho empacado en las operaciones de biofiltración.

Process Safety and Environmental Protection 160 (2022) 362–375

Contents lists available at ScienceDirect

Process Safety and Environmental Protection

journal homepage: www.elsevier.com/locate/psep

A comparative study between the biofiltration for air contaminated with limonene or butyric acid using a combination of olfactometric, physico-chemical and genomic approaches

Márquez, P. [a], Siles, J.A. [a], Gutiérrez, M.C. [a], Alhama, J. [b], Michán, C. [b], Martín, M.A. [a,*]

[a] Department of Inorganic Chemistry and Chemical Engineering, Area of Chemical Engineering. Institute of Nanochemistry (IUNAN). Universidad de Córdoba, Campus Universitario de Rabanales, Carretera N-IV, km 396, Edificio Marie Curie, 14071 Córdoba, Spain

[b] Department of Biochemistry and Molecular Biology, Universidad de Córdoba, Campus de Excelencia Internacional Agroalimentario CeiA3, Edificio Severo Ochoa, 14071 Córdoba, Spain

* Corresponding author: iq2masam@uco.es

Received 26 November 2021; Received in revised form 25 January 2022; Accepted 11 February 2022; Available online 12 February 2022

Abbreviations: EBRT, empty bed residence time (s); FS, fixed solids (%); IC, soluble inorganic carbon (%); MAC, total mesophilic aerobic count (CFU/g); MTPs, municipal treatment plants; N-NH_4^+, ammoniacal nitrogen (%); N-TKN, total Kjeldahl nitrogen (%); N-TN_s, soluble total nitrogen (%); OC, odor concentration (ou_E/m^3); OD_{20}, cumulative oxygen demand at 20 h (mg O_2/g VS); ODT, odor detection threshold (ppm_v); OER, odor emission rate (ou_E/s); OIR, odor incoming rate (ou_E/s); ou_E, European odor units; P-P_2O_5, phosphorus content expressed as P_2O_5 (%); $SOUR_{max}$, maximum specific oxygen uptake rate (mg O_2/g VS·h); TC, soluble total carbon (%); TOC, soluble total organic carbon (%); VFAs, volatile fatty acids; VOCs, volatile organic compounds; VS, volatile solids (%).

Graphical abstract

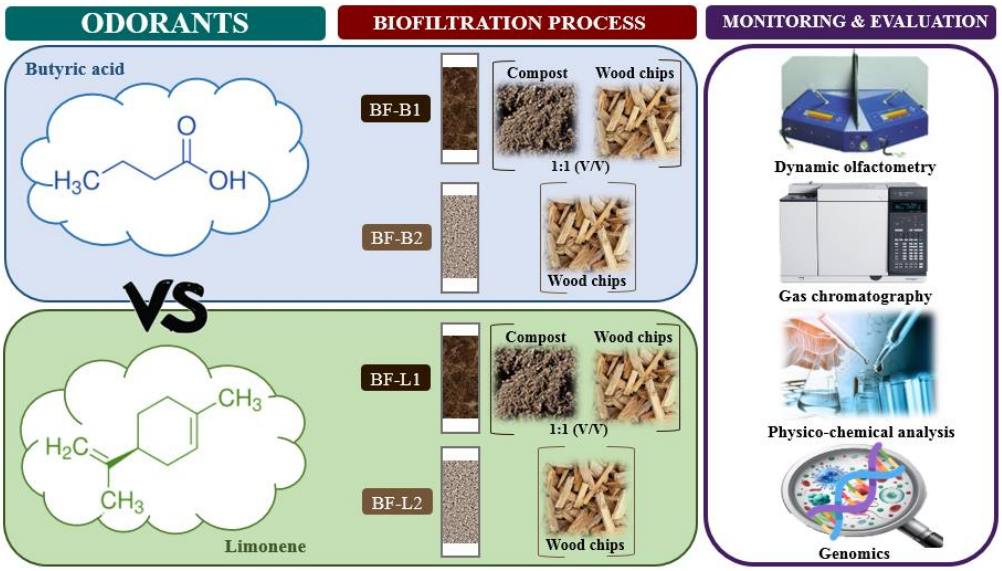

Abstract

A multidisciplinary analysis based on physico-chemical, olfactometric and microbiological perspectives was performed to compare the biofiltration of air contaminated with limonene or butyric acid. Two biofilters were subjected to butyric acid gaseous streams: one was filled with wood chips and sewage sludge compost (BF B-1) and the other with wood chips only (BF B-2). Similarly, two other biofilters were subjected to a gaseous stream containing limonene, with the same beds (BF L-1 and BF L-2, respectively). Although the biofilters fed with butyric acid received higher odor loads (280–3280 $ou_E/m^2 \cdot s$ for BF B-1 and 135–1460 $ou_E/m^2 \cdot s$ for BF B-2) than the biofilters treating limonene (30–170 $ou_E/m^2 \cdot s$ for BF L-1 and 15–130 $ou_E/m^2 \cdot s$ for BF L-2), the first systems achieved odor removal efficiencies greater than 90% during most of the biofiltration time, whereas in the limonene biofilters, these efficiencies never exceeded 70%. Regarding the packed beds, genomic analysis of the microbial communities showed a wider distribution of phyla (Proteobacteria, Firmicutes, Bacteroidetes, and Actinobacteria) in compost-wood biofilters than in wood chips systems where Proteobacteria was clearly predominant. This study reveals the importance of considering both the nature of the biofiltered compounds and the packed bed composition in biofiltration operations.

Keywords: biofiltration; butyric acid; packing material; genomic analysis; limonene; odor removal.

1. Introduction

Volatile organic compounds (VOCs) and odor emissions are associated to some activities that involve the management of organic waste in municipal treatment plants (MTPs). Due to accelerated industrialization and urbanization, these MTPs are usually located close to populations, and the emissions of many air pollutants generate an odoriferous impact that should be minimized (Ding et al., 2019). Furthermore, the evolution of public awareness promotes the implementation of international and national policies to consider odor emissions as an integral part of any activity involving the management of organic wastes, reinforcing the need for their efficient control (Charles and Ho, 2017; Otten et al., 2004; Ren et al., 2019). In the European Union, the corresponding basic legal requirements are specified in the Directive 2008/50/EC (European Parliament and Council, 2008) and Directive 2010/75/EU (European Parliament and Council, 2010). For these reasons, the development of efficient methods for treating unpleasant and harmful emissions has become increasingly necessary. Biological treatment technologies for VOCs and odoriferous compounds have been widely implemented in MTPs because of their advantages. Compared with physico-chemical treatments, biological technologies such as biotrickling and biofiltration are less costly and have a reliable performance and a high processing capacity (Lin et al., 2019; Meena et al., 2021; Senatore et al., 2021). Furthermore, biological treatments are ecologically clean because microbial degradation processes are generally oxidative in nature (Bindra et al., 2015; Cruz-García and Aizpuru, 2022; Revah and Morgan-Sagastume, 2005).

Since the 1980s, research on biofiltration has made considerable progress, mainly focusing on industrial applications based on different filter designs and microorganisms (Barbusinski et al., 2017; Lu et al., 2020; Natarajan, 2020; Natarajan et al., 2017). Biofilters consist of a packed bed where the microorganisms grow attached as a biofilm, and the odoriferous air to be treated is passed through the device (Lebrero et al., 2013a; Meena et al., 2021). The mass transfer of a target pollutant from gas to the biofilm phase as well as its solubility in the biofilm are important aspects that may affect the biofiltering performance (Cheng et al., 2016; Devinny and Ramesh, 2005; Lamprea Pineda et al., 2021; Staudinger and Roberts, 1996), and these two parameters are closely related to the used packing materials. Biofilters are usually filled with organic packing materials such as soil (Nelson et al., 2011), compost (Cabeza et al., 2013), peat, leaves, and/or wood

chips (Ferdowsi et al., 2017; Premkumar and Krishnamohan, 2012). Some authors also used inorganic packing materials such as commercial activated carbons (Bhadra et al., 2018) or derivatives from the activation of by-products such as lignin (Gonzalez-Serrano et al., 2004) or olive pits (García-Mateos et al., 2015). Additionally, the pH influence in the removal efficiencies of hydrophilic compounds, such as butyric acid and ammonia, was reported by Liu et al. (2008) and Reyes et al. (2020), determining the existence of different microbial communities. Therefore, the performance of the biofilter also depends on the characteristics of the compound being treated and the type of microorganisms.

Potential pollutants usually involved in MTPs include sulfur compounds, volatile fatty acids (VFAs), nitrogen compounds, and terpenes. In particular, the VFA butyric acid and the terpene limonene are frequent odorous and hazardous VOCs coming from MTPs (Charles and Ho, 2017; Gutierrez et al., 2015; Kissel et al., 1992; Pagans et al., 2006). In this context, it is important to note that inhalation of limonene may cause dizziness, rapid and shallow breathing, tachycardia, bronchial irritation, unconsciousness and convulsions (Kim et al., 2013; NTP, 1992), whereas irritation of mucous membrane and respiratory tract, nausea and vomiting may be caused by inhalation of butyric acid (New Jersey Department of Health, 2007; US Coast Guard, 1999). The American Industrial Hygiene Association sets an 8-hour time weighted average workplace environmental exposure level (WEEL) of 30 parts per million (ppm_v) for limonene (AIHA, 2021). However, to date, no occupational exposure limits have been established for butyric acid.

Regarding the treatment of these emissions by biofiltration, Lebrero et al. (2013a) evaluated a real odorous emission from wastewater treatment plant sludge and reported removal efficiencies of the biofilter as high as 99% for limonene, among others. The performance of two biofilters at laboratory scale was also studied by using butyric acid and other odorous compounds (Liu et al., 2008). This study reported that the removal efficiencies for hydrophilic compounds, such as butyric acid, were higher in a neutral pH biofilter, whereas the removal efficiencies for the compounds with poor water solubility were higher in a low-pH biofilter than those in a neutral-pH biofilter. Apart from the pH, the following variables condition the efficient operation of biofilters: adequate water retention capacity, high porosity and buffer capacity, and a diverse and adaptable microbial population coupled with high nutrient availability (Barbusinski et al., 2017; Elias et al., 2002; Mudliar et al., 2010). The empty bed residence time (EBRT) is another parameter with a significant impact on the biodegradation performance (Elmrini et al.,

2004; Moussavi et al., 2009). According to Delhoménie and Heitz (2005), to improve biofiltration performance, the EBRT should be higher than the time required for diffusion processes, which is the case for low operational flow rates. On the contrary, when the EBRTs are too short (usually because of high flow rates), the contact times between microorganisms and gases are not long enough to complete the biodegradation reaction. In this context, it is important to note that EBRT ranges from 15 s to several minutes in most biofiltration systems.

As mentioned above, the treatment of odorous compounds is intimately linked to the microorganisms present in the biofilters, which are the ultimately responsible for the process due to their metabolic activity. Thus, knowledge of the bacterial community structures in the biological treatment systems and their dynamics is vital to understand the processes taking place inside them (Allievi et al., 2018; Boada et al., 2021). As the vast majority of the microbes present in natural environments are unculturable, 16S rRNA gene sequencing has shown to be effective in revealing the composition/structure/diversity of bacterial communities (Delgado-Baquerizo et al., 2018). Furthermore, functional prediction can be inferred from the identified microbiota, increasing our understanding of their biodegradation potential (Lin et al., 2021). However, to date, the effects of the odorous compounds in the microbial community structure of biofilters are largely unknown.

In this research study, four semi-pilot scale biofilters treating two different gaseous streams containing butyric acid or limonene gases were comparatively evaluated from olfactometric, microbiological, and physico-chemical points of view. Two biofilters were filled with wood chips and sewage sludge compost, whereas the others used wood chips only, all of them without an initial external inoculum. In this sense, the aim of this work was to assess the influence of the biofiltered compound as well as the filter bed material on the odor removal performance by biofiltration. In parallel, the changes in the physico-chemical characteristics of the packed beds, the aerobic respirometric activity and total mesophilic aerobic microorganisms count, and the structure of the microbial communities present in the support media proposed were considered. To the best of our knowledge, this multidisciplinary and comparative approach to evaluate the differences in the biofiltration of two frequent VOCs present in the gaseous emissions from waste treatment facilities has not been reported before. Thus, the results from this study might aid in the

optimization of biofiltration operations in those facilities, with the consequent environmental and social benefits.

2. Material and methods

2.1. Description and operation of the biofiltration system

Four biofilters (PVC cylinders) were operated individually at semi-pilot scale, with the same design features: height of the packed bed 0.49 m; height of the bed space at the bottom of the biofilter 0.17 m; height of the headspace 0.20 m and inner diameter of 0.16 m. With these characteristics, the total volume of the biofilter was 17.3 L, and the packing volume represented 57% of the volume mentioned above (9.9 L). The packing materials, wood chips and municipal sewage sludge compost, used for the four biofilters of this work, were obtained from the urban waste management plant of Cordoba, Spain (**Table 1**). In accordance with Cabeza et al. (2013), the granulometry of the packing materials ranged from 7 to 20 mm in all biofilters to avoid operational problems such as clogging and to facilitate air flux control. In the case of BF B-1 and BF L-1, the volumetric ratio 1:1 of the packed bed composition was selected because this ratio has been widely reported in the literature when compost was mixed with other packing materials (such as wood chips, pruning residues and perlite, among others) for the efficient biofiltration of different VOCs (Cabeza et al., 2013; Iranpour et al., 2005; López et al., 2011; Premkumar and Krishnamohan, 2012).

Table 1. Overview of the biofilters under study.

Biofilters	VOC to be treated	Packed bed composition	Volumetric ratio
BF B-1	Butyric acid	Sewage sludge compost + wood chips	1:1
BF B-2	Butyric acid	Wood chips	—
BF L-1	Limonene	Sewage sludge compost + wood chips	1:1
BF L-2	Limonene	Wood chips	—

As shown in **Scheme 1**, a compressor (Silent DE-204) supplied ambient air to the biofiltration system, with the gas flow being controlled by a flow meter (Trotec TA400). A water thermostatic bath was placed between the biofilter and the air compressor. This bath contained two bubblers, and its temperature was measured continuously by a Testo

175 T1 datalogger. The water bath temperature was set at 22ºC in the case of BF B-2 and BF L-2. In contrast, room temperature conditioned the temperature of the water bath in BF B-1 and BF L-1, which ranged between 22 and 31ºC and from 16 to 29ºC, respectively. In all biofiltration experiments, compressed air was humidified in the first bubbler, which contained distilled water. Humidified air was then fed to a second bubbler placed in series, with the aim of generating the contaminated gas flow. Depending on the biofiltration experiment, this last bubbler contained liquid butyric acid, PanReac, > 99% purity (BF B-1 and BF B-2), or liquid limonene, Sigma-Aldrich, 97% purity (BF L-1 and BF L-2). Finally, the contaminated gas stream was introduced into the biofilter through an 8-mm Ø plastic pipe.

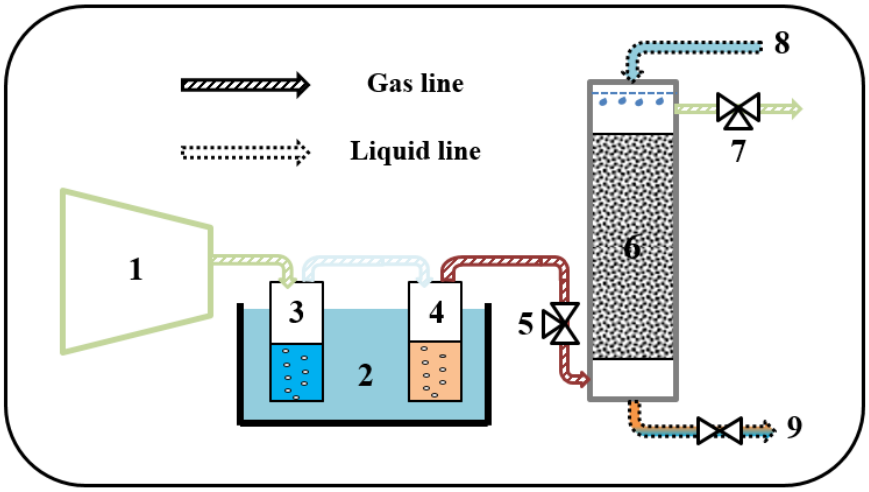

Scheme 1. Schematic diagram of the biofiltration system. (1) Air compressor; (2) water thermostatic bath; (3) humidifier; (4) bubbler of VOC (butyric acid or limonene); (5) inlet biofilter gas/input sampling port; (6) biofilter packed bed; (7) outlet biofilter gas/output sampling port; (8) irrigation; (9) leachate drainage.

The BF B-1 and BF B-2 experiments were carried out for 62 days, whereas BF L-1 and BF L-2 were performed over a 48-day period. By modifying the EBRT, calculated as the quotient between the packing volume (m^3) and the inlet gas flow to the biofilter (m^3/s), the four experiments were separated into two stages: start-up and operational periods. The start-up period represents an acclimatization period of the microbes. At this stage, the EBRTs were 188 s (days 0–3), 138 s (days 4–7), 103 s (days 8–11), and 83 s (days 12–14), which depended on the inlet gas flows of $5.2 \cdot 10^{-5}$, $7.1 \cdot 10^{-5}$, $9.5 \cdot 10^{-5}$, and $1.19 \cdot 10^{-4}$ m^3/s, respectively. The operational period lasted from day 15 to the end in all experiments, maintaining an EBRT of 59 s (inlet gas flow of $1.67 \cdot 10^{-4}$ m^3/s). In this

context, it is important to note that an EBRT of about 60 s is frequently used in biofiltration studies (Dorado et al., 2008; Ramírez et al., 2011).

With the aim of not increasing operational costs in view of a possible scaling of the evaluated biofilters in waste treatment plants, common operations in biofiltration studies such as bed inoculation, supplementary nutrient addition and/or buffer solutions addition were not carried out.

The moisture content of the packed beds was maintained around 60%. This important parameter was controlled by measuring the difference in weight between the complete biofilter bed and its initial weight, adding water and biofilter leachate at the top of the system when the moisture level decreased below 60%. Moreover, a stainless-steel water distribution plate (with pore diameters of 1 mm) was placed on the top of the headspace to ensure slow and uniform water/leachate distribution.

2.2. Sampling process: gaseous and solid samples

On one side, gaseous samples were taken through the biofilter sampling ports (input and output) at least twice a week during the four biofiltration experiments. Gaseous samples were collected in 4-L Nalophan® bags to perform the subsequent odor monitoring and quantify the concentration of the VOCs under study (butyric acid and limonene). On the other side, approximately 80 g of the bed material (solid samples) were collected at different heights (at approximately 0.10, 0.25 and 0.40 m from the bed surface) to determine the physico-chemical, respirometric, and microbiological characteristics. This operation was repeated at the beginning and at the end of each biofiltration experiment. Only for microbiological characterization, approximately 30 g of the bed material were also collected at 28 days of each of the experiments. Samples were kept at -20ºC until analyzed.

2.3. Physico-chemical, respirometric, and textural measurements

The solid samples were subjected to physico-chemical characterization, in accordance with the reference methodology proposed by the US Department of Agriculture and the US Composting Council (2002). It provides detailed protocols for the composting industry to verify the physical, chemical, and biological condition of composting feedstocks, material in process and compost products at the point of sale. In this context, the following variables were analyzed in triplicate: pH, conductivity

(µS/cm), soluble total nitrogen (N-TN_s, %), soluble total carbon (TC, %), soluble inorganic carbon (IC, %), and soluble total organic carbon (TOC, %), which were measured in an aqueous extract (1:25 ratio); moisture (%), fixed solids (FS, %), volatile solids (VS, %), total Kjeldahl nitrogen (N-TKN, %), ammoniacal nitrogen (N-NH_4^+, %), and phosphorus content (P-P_2O_5, %) were analyzed in the solid fraction.

Respirometric tests were carried out to determine the microbiological activity of the biofilter packed beds. Thus, the maximum specific oxygen uptake rate ($SOUR_{max}$, mg O_2/g VS·h) and the cumulative oxygen demand at 20 h (OD_{20}, mg O_2/g VS) were quantified by using a static respirometer in the liquid phase at laboratory scale, which was patented by the RNM-271 Research Group of the University of Cordoba (P2004–02908) (Chica et al., 2003). For this purpose, the following standardized conditions were applied: addition of macronutrients (magnesium sulfate, calcium chloride, and ferric chloride), temperature of 30ºC, neutral pH, and nitrification inhibition through thiourea addition. In respirometric tests, the solid samples were analyzed in duplicate.

The pore size distribution and the total porosity of the packing materials were determined by mercury intrusion porosimetry, using a Micromeritics AutoPore IV 9500 porosimeter. The values of surface tension and contact angle in the porosimeter software were 0.484 N/m and 141°, respectively. The wood chips had a total porosity of 44.87% (1.58% mesoporosity and 98.42% macroporosity), whereas the sewage sludge compost presented a total porosity of 65.68% (0.29% mesoporosity and 99.71% macroporosity). Moreover, the packed bed of BF B-1 and BF L-1 (mixture of sewage sludge compost and wood chips) had a total porosity of 54.67% (0.97% mesoporosity and 99.03% macroporosity). It is important to note that all values of total porosity are within the adequate range (40–80%) for the operation of biofiltration systems (Iranpour et al., 2005).

2.4. Olfactometric measurements

The inlet and outlet gaseous samples were immediately characterized in terms of odor concentration (OC, ou_E/m^3) after their collection, with the aim of preventing permeability through the Nalophan® bag walls (Le et al., 2015; Toledo et al., 2019). Dynamic olfactometry (EN 13725, 2003) was the reference method used for the quantification of the OC of the gaseous samples. It allows the measurement of OC in terms of dilutions required to reduce an odorous compound until its threshold concentration. This measurement is conducted inside a clean and odor-free laboratory

with trained panelists. The panelists have average sensing capability and are selected based on their sensitivity to the reference gas (n-butanol).

A TO8 olfactometer (Olfasense GmbH, Kiel, Germany), based on the 'Yes/No' method, was used to determine the OC of all gaseous samples. The lower detection limit of the olfactometer is 30 ou_E/m^3. Each odor sample was analyzed in duplicate by four panelists, with the OC being calculated as the geometric mean of the odor threshold values of each panel member. After that, some important parameters for odor monitoring, such as the odor load factor and the odor removal efficiency, were calculated (Reyes et al., 2020). The first one was determined by Eq. (1):

$$\textit{Odor load factor } (ou_E/m^2 \cdot s) = \frac{OC_i \cdot Q_a}{A} \quad (1)$$

where OC_i is the inlet odor concentration (ou_E/m^3), Q_a is the average gas flow between the inlet and outlet of the biofilter (m^3/s), and A is its transversal area (m^2). In this context and according to Reyes et al. (2020), at a constant gas flow, the odor load factor can be modified by varying the temperature of the thermostatic bath.

With regard to the odor removal efficiency, this important variable was estimated by Eq. (2):

$$\textit{Odor removal efficiency } (\%) = \frac{(OIR - OER)}{OIR} \cdot 100 \quad (2)$$

where OIR is the odor incoming rate (ou_E/s), calculated by multiplying the OC_i (ou_E/m^3) by the inlet gas flow (m^3/s), and OER is the odor emission rate (ou_E/s), determined by multiplying the outlet odor concentration (ou_E/m^3) by the outlet gas flow (m^3/s).

2.5. Quantification of VOCs

Gaseous samples were analyzed by gas chromatography with a flame ionization detector (GC-FID) on an Agilent Technologies 7890A gas chromatograph (Agilent, Santa Clara, CA, USA), using 1 mL of gas from the sampling bags. Its lower detection limit is 10 ppm_v for both limonene and butyric acid. The limonene gaseous samples were analyzed with an Agilent technologies HP-5 (19091J-413) column (Agilent, Santa Clara, CA, USA). Injector temperature was set at 175ºC and detector temperature at 275ºC. Nitrogen was used as carrier gas at 8 mL/min (5.4 psi, 0.8 mL/min through the column). The initial oven temperature was fixed at 100ºC and ramped up to 150ºC at 5ºC/min. For

butyric acid gaseous samples, a Supelco Nukol™ column (Sigma-Aldrich, Darmstadt, Germany) was used. Injector and detector temperatures were set at 250 and 275ºC, respectively. In this case, helium was used as carrier gas at 12 mL/min (5.4 psi, 4.3 mL/min through the column). An isotherm program at 180ºC was used for this analysis. The calibration curves used for the quantification of butyric acid and limonene are shown in **Fig. S1** (Supplementary Material).

2.6. Quantification of mesophilic aerobic microbes

The methodology proposed by the standard ISO4833-1 (2013) was used to carry out the total mesophilic aerobic microorganisms count (MAC, CFU/g) of the biofilter beds. This standard specifies a horizontal method for enumeration of microorganisms that are able to grow and form colonies in a solid medium after aerobic incubation at 30°C. The method is applicable to: (a) products intended for human consumption and for animal feed; (b) environmental samples in the area of food and feed production and handling. The said analysis was performed by the Agri-food Laboratory of Cordoba (LABAGCO), Spain.

2.7. DNA isolation from the biofilter packing material

Samples of the packing from the four biofilters were collected at the Start (0 days), Intermediate (28 days), and End (62 days for BF B-1 and B-2 and 48 days for L-1 and L-2) and kept at -20°C until processing. Three biological replicates were isolated from each condition. To optimize DNA extraction, samples underwent two 1-min rounds of grounding with a Freezer/Mill® Grinder (SPEX Sample PreP) at maximum rate (15 cycles per second). The DNA was isolated from 250 mg of the ground samples with the ZymoBIOMICS DNA Miniprep kit (Zymo Research), following the manufacturer´s instructions. The amount of the isolated DNA was determined spectrophotometrically, and its integrity was checked by visualization on a 1% agarose gel. To verify that PCR inhibitors have been efficiently removed prior to the 16S analysis, the DNA was amplified by PCR using bacterial 16S standard primers.

2.8. 16S rRNA analysis

The bacteria present in the four biofilters at the three stages tested were identified by 16S rRNA sequencing. The isolated DNAs from their bed materials were independently amplified and sequenced using the specific kit for 16S sequencing (Ion

Torrent System) at the Central Service for Research Support (SCAI) of the University of Cordoba (Spain), and the different taxa were assigned using the recommended software (Ion Reporter™ 5.0 for Ion 16S™ Metagenomics). Although all variable regions within the 16S were sequenced, only the identifications assigned from the V3 region sequencing were considered, as they always provided the largest variability in the microbiome composition.

For biodiversity estimation, the Shannon-Wiener (H′) index was calculated as $H'(nats) = -\sum \frac{n_i}{N} ln \frac{n_i}{N} = -\sum Pi \ln Pi,,$ where n_i is the number of operational taxonomic units (OTUs) of the ith families, N is the total number of OTUs of all the families in the samples, and $Pi = \frac{n_i}{N}$ (Márquez et al., 2021; Thukral, 2017).

Functional prediction to establish metabolic or other ecologically relevant functions was analyzed by FAPROTAX (Functional Annotation of Prokaryotic Taxa) (Louca et al., 2016).

2.9. Statistical analysis

The significance of the differences in phylogenetic diversity and species richness indices was evaluated using two-way Analysis of Variance (ANOVA), followed by a parametric analysis for post-hoc multiple comparison according to Tukey, using the GraphPad Prism v. 8.0.2 software. Statistically significant differences are expressed as follows: *, $p < 0.05$; **, $p < 0.01$; ***, $p < 0.001$; ****, $p < 0.0001$. To deal with missing data from the taxon assignments, as the detection limit of the technique is 10 contigs, gaps were filled with a value of 9.

3. Results and discussion

3.1. Assessment of the bed material: physico-chemical variables and microbial activity

The physico-chemical characteristics of the bed materials and their microbial activities were studied to find differences both in the behavior of each biofilter and among the different experiments carried out. In this context, **Table 2** shows the results of the monitored variables for both the butyric acid biofilters (BF B-1 and BF B-2) and the limonene biofilters (BF L-1 and BF L-2). It is important to highlight that BF B-1 and BF

L-1 contained the same packing material (a mixture of sewage sludge compost and wood chips). For this reason, the same initial characterization was considered for both biofilters, except for moisture content (%), $SOUR_{max}$ (mg O_2/g VS·h), OD_{20} (mg O_2/g VS), and MAC (CFU/g) due to initial differences in these variables because of the packing material storage. The above-mentioned consideration was also assumed for the biofilters with only wood chips as bed material (BF B-2 and BF L-2). Regarding the composition of the four filter beds, the main differences among them were the nature and concentration of the organic matter (expressed as VS, %). The addition of stabilized compost in BF B-1 and BF L-1 favors the presence of humic substances in these systems (Wu et al., 2017). Moreover, sewage sludge compost increased the concentration of FS (%) in those biofilters, thus decreasing the concentration of VS (%) compared to wood chips-based biofilters.

Butyric acid and limonene catabolic processes are very different. Short chain fatty acids as butyrate are usually metabolized to CO_2 or acetyl-CoA for lipid and glucose synthesis, using the well-known beta-oxidation pathway. Furthermore, in anaerobic conditions, microbes can convert butyric acid to methanogenic precursors: acetate, H_2, and formate, and, thus, participate in energy production from organic wastes (Wainaina et al., 2019). On the other hand, although limonene is the main component of citrus peel essential oils and the most widespread monoterpene in nature, its biodegradation is not so widespread. In general, monoterpenes can be degraded by chemical photolysis or by bacterial mineralization mainly using oxidative pathways (Marmulla and Harder, 2014).

Moisture and pH play a key role in the operation of biofilters since microbial activity is markedly dependent on the values of these parameters (Barbusinski et al., 2017; Detchanamurthy and Gostomski, 2012; Mudliar et al., 2010). Regarding the first variable, values around 60% were kept during all biofiltration experiments (**Table 2**), which is a moisture content widely reported in such assay types (Delhoménie and Heitz, 2005; Mudliar et al., 2010). With respect to pH, a clear difference could be established between the butyric acid and limonene biofilters. In this sense, pH showed a downward trend in BF B-1 and BF B-2, reaching values far from neutrality at the end of both experiments, especially in BF B-2. This fact could be related to the progressive accumulation of non-degraded butyric acid (Márquez et al., 2021; Reyes et al., 2020). However, the trend was completely different in the limonene biofilters, as the pH tended to be stable (BF L-2) or even increased (BF L-1). At this point, it is important to note that most of the

Table 2. Physico-chemical characterization and microbial activity of the bed materials at the beginning and at the end of the biofiltration assays.

	BF B-1		**BF B-2**		**BF L-1**		**BF L-2**	
	Start (0 d)	**End (62 d)**	**Start (0 d)**	**End (62 d)**	**Start (0 d)**	**End (48 d)**	**Start (0 d)**	**End (48 d)**
pH	7.15 ± 0.01	5.03 ± 0.01	5.98 ± 0.01	3.47 ± 0.11	7.15 ± 0.01	8.53 ± 0.01	5.98 ± 0.01	5.91 ± 0.04
Conductivity (µS/cm)	1109 ± 15	2100 ± 28	110 ± 1	389 ± 24	1109 ± 15	1023 ± 35	110 ± 1	120 ± 8
Moisture (%)	59.22 ± 1.63	62.05 ± 2.06	60.49 ± 1.08	61.53 ± 2.96	61.57 ± 1.02	62.83 ± 1.48	61.02 ± 0.25	60.50 ± 1.37
FS (%)	14.67 ± 2.06	13.74 ± 1.96	1.26 ± 0.40	2.79 ± 0.19	14.67 ± 2.06	21.00 ± 0.53	1.26 ± 0.40	8.18 ± 0.51
VS (%)	85.33 ± 2.12	86.26 ± 2.11	98.74 ± 0.40	97.21 ± 0.22	85.33 ± 2.12	79.01 ± 0.54	98.74 ± 0.40	91.82 ± 0.48
N-TKN (%)	0.94 ± 0.01	0.86 ± 0.01	0.21 ± 0.01	0.51 ± 0.03	0.94 ± 0.01	1.09 ± 0.07	0.21 ± 0.01	0.30 ± 0.01
N-NH_4^+ (%)	0.09 ± 0.01	0.15 ± 0.02	0.04 ± 0.01	0.08 ± 0.00	0.09 ± 0.01	0.12 ± 0.00	0.04 ± 0.01	0.08 ± 0.00
N-TN_s (%)	0.14 ± 0.01	0.11 ± 0.00	0.04 ± 0.00	0.06 ± 0.01	0.14 ± 0.01	0.12 ± 0.00	0.04 ± 0.00	0.02 ± 0.00
P-P_2O_5 (%)	0.49 ± 0.03	0.43 ± 0.07	0.22 ± 0.02	0.19 ± 0.01	0.49 ± 0.03	0.42 ± 0.04	0.22 ± 0.02	0.20 ± 0.01
TC (%)	0.86 ± 0.05	5.09 ± 0.03	0.40 ± 0.07	2.18 ± 0.02	0.86 ± 0.05	1.17 ± 0.00	0.40 ± 0.07	0.68 ± 0.01
IC (%)	0.02 ± 0.00	0.01 ± 0.00	0.01 ± 0.00	0.01 ± 0.00	0.02 ± 0.00	0.10 ± 0.00	0.01 ± 0.00	0.02 ± 0.01
TOC (%)	0.83 ± 0.05	5.09 ± 0.03	0.39 ± 0.08	2.18 ± 0.02	0.83 ± 0.05	1.07 ± 0.00	0.39 ± 0.08	0.66 ± 0.00
$SOUR_{max}$ (mg O_2/g VS·h)	1.16 ± 0.03	1.32 ± 0.01	0.17 ± 0.01	0.11 ± 0.01	0.56 ± 0.01	0.81 ± 0.01	0.45 ± 0.01	0.56 ± 0.01
OD_{20} (mg O_2/g VS)	8.61 ± 0.41	14.04 ± 0.73	2.69 ± 0.08	1.02 ± 0.03	3.26 ± 0.12	10.05 ± 0.36	2.94 ± 0.16	4.82 ± 0.13
MAC (CFU/g)	$8.4 \cdot 10^7$	$2.4 \cdot 10^5$	$3.6 \cdot 10^7$	$3.2 \cdot 10^4$	$2.9 \cdot 10^7$	$3.3 \cdot 10^8$	$2.9 \cdot 10^7$	$3.3 \cdot 10^7$

FS, fixed solids; IC, soluble inorganic carbon; MAC, total mesophilic aerobic count; N-NH_4^+, ammoniacal nitrogen; N-TKN, total Kjeldahl nitrogen; N-TN_s, soluble total nitrogen; OD_{20}, cumulative oxygen demand at 20 h; P-P_2O_5, phosphorus content expressed as P_2O_5; $SOUR_{max}$, maximum specific oxygen uptake rate; TC, soluble total carbon; TOC, soluble total organic carbon; VS, volatile solids.
Note: All variables, except pH, conductivity, moisture and MAC, are expressed on a dry basis.

microorganisms involved in biofiltration processes are typically neutrophilic. Thereby, changes in pH, with values too far from 7 pH units, might negatively affect microbial activity, consequently impairing gas pollutant removal and odor removal (Barbusinski et al., 2017; Delhoménie and Heitz, 2005; Mudliar et al., 2010). In this context, given that the moisture values remained practically constant throughout all experiments, the changes in the variables related to MAC and their activity ($SOUR_{max}$ and OD_{20}) might be related to the variations in the pH of the bed materials. In general terms, the decrease in pH led to a decrease of MAC in the butyric acid biofilters (**Table 2**). Nevertheless, in the limonene biofilters, MAC increased throughout the biofiltration process, which could be related to the progressive multiplication of aerobic microorganisms because of the non-significant pH variations in such types of biofilters. Furthermore, in these biofiltration systems, the respirometric variables followed a trend similar to that of the MAC, that is, an upward trend. In contrast, a different behavior was observed in BF B-2, where $SOUR_{max}$, OD_{20}, and MAC registered their minimum values at the end of the experiment (**Table 2**). It is worth noting that BF B-1 represented a particular case since in global terms, $SOUR_{max}$ and OD_{20} increased and MAC decreased. However, it is important to highlight that this biofilter registered the maximal values of $SOUR_{max}$, OD_{20}, and MAC at approximately 28 days of the biofiltration process (4.95 ± 0.01 mg O_2/g VS·h, 39.89 ± 1.57 mg O_2/g VS and $3.6 \cdot 10^8$ CFU/g, respectively; data not shown). This might be explained by the biological activation of sewage sludge compost (Márquez et al., 2021), which was part of the bed material in BF B-1. The biological activation of such organic material also took place in BF L-1, since at the end of this experiment, MAC was 11.38 times higher than at the beginning. Nevertheless, in the limonene biofilter without compost (BF L-2), the increase in MAC was only 1.14 times between the beginning and the end of the biofiltration process. Moreover, as seen in **Table 2**, a higher increase in the values of the respirometric variables was detected in BF L-1 compared to BF L-2 for the same period considered (48 days).

Table 2 also shows the concentrations of nitrogen (N-TKN and $N\text{-}NH_4^+$) and phosphorus ($P\text{-}P_2O_5$) at the beginning and at the end of the four biofiltration assays under study. As can be seen, no significant variations in their concentrations were found in any of the experiments for the biofiltration periods considered. Therefore, although no nutrients were added to any of the experiments, the existing microbial communities did not demand large amounts of them to degrade the odoriferous organic compounds

evaluated under the studied operating conditions. Nonetheless, it is important to highlight the higher concentrations of nitrogen and phosphorus in BF B-1 and BF L-1 compared to BF B-2 and BF L-2, most likely because of the higher concentrations of such nutrients in sewage sludge compost than in wood chips (Mudliar et al., 2010). Regarding the fractions determined in aqueous extract, N-TN_s (%) did not change significantly in any of the experiments, whereas TOC (%) increased in all of them (**Table 2**), especially in the butyric acid biofilters (6.13-fold in BF B-1 and 5.59-fold in BF B-2). This could be mainly due to the higher water solubility of non-degraded butyric acid compared to limonene.

Given the above, the joint study of the four biofiltration experiments showed similar evolutions in terms of nutrient contents (soluble carbon, nitrogen in its different forms, and phosphorus). However, the variations in pH, $SOUR_{max}$, OD_{20}, and MAC differed throughout the experiments and basically depended on the biofiltered compound (butyric acid or limonene).

3.2. Odor assessment

Once the characterization of the filter beds has been evaluated, it is equally important to assess the performance of the biofilters at odor level. In this context, **Fig. 1** shows the inlet and outlet OCs both in the butyric acid and limonene biofilters, considering that all biofiltration assays were carried out under the same stages and EBRTs. The difference in the order of magnitude between the OCs in the butyric acid and limonene biofilters was mainly due to the difference in the odor detection thresholds (ODTs) of such compounds ($1.9 \cdot 10^{-4}$ ppm_v for butyric acid and $3.8 \cdot 10^{-2}$ ppm_v for limonene) (Nagata, 2003). Thus, in the start-up period, the inlet OC was within the following ranges: 120,200–170,000 ou_E/m^3 (BF B-1, **Fig. 1A**), 65,500–101,000 ou_E/m^3 (BF B-2, **Fig. 1B**), 12,600–21,200 ou_E/m^3 (BF L-1, **Fig. 1C**), and 8200–12,800 ou_E/m^3 (BF L-2, **Fig. 1D**). In the operational period, the inlet OC ranges were as follows: 170,000–441,000 ou_E/m^3 (BF B-1), 101,000–220,500 ou_E/m^3 (BF B-2), 21,200–7500 ou_E/m^3 (BF L-1), and 12,800–16,400 ou_E/m^3 (BF L-2). As seen in **Fig. 1B** and **D**, considering that olfactometric values have a deviation between half and double, the inlet OC values remained roughly constant in BF B-2 and BF L-2 at the operational period since in both systems, the water bath temperature was kept at 22ºC (see Section 2.1.); therefore, the vapor pressure of the compounds to be biofiltered was not altered.

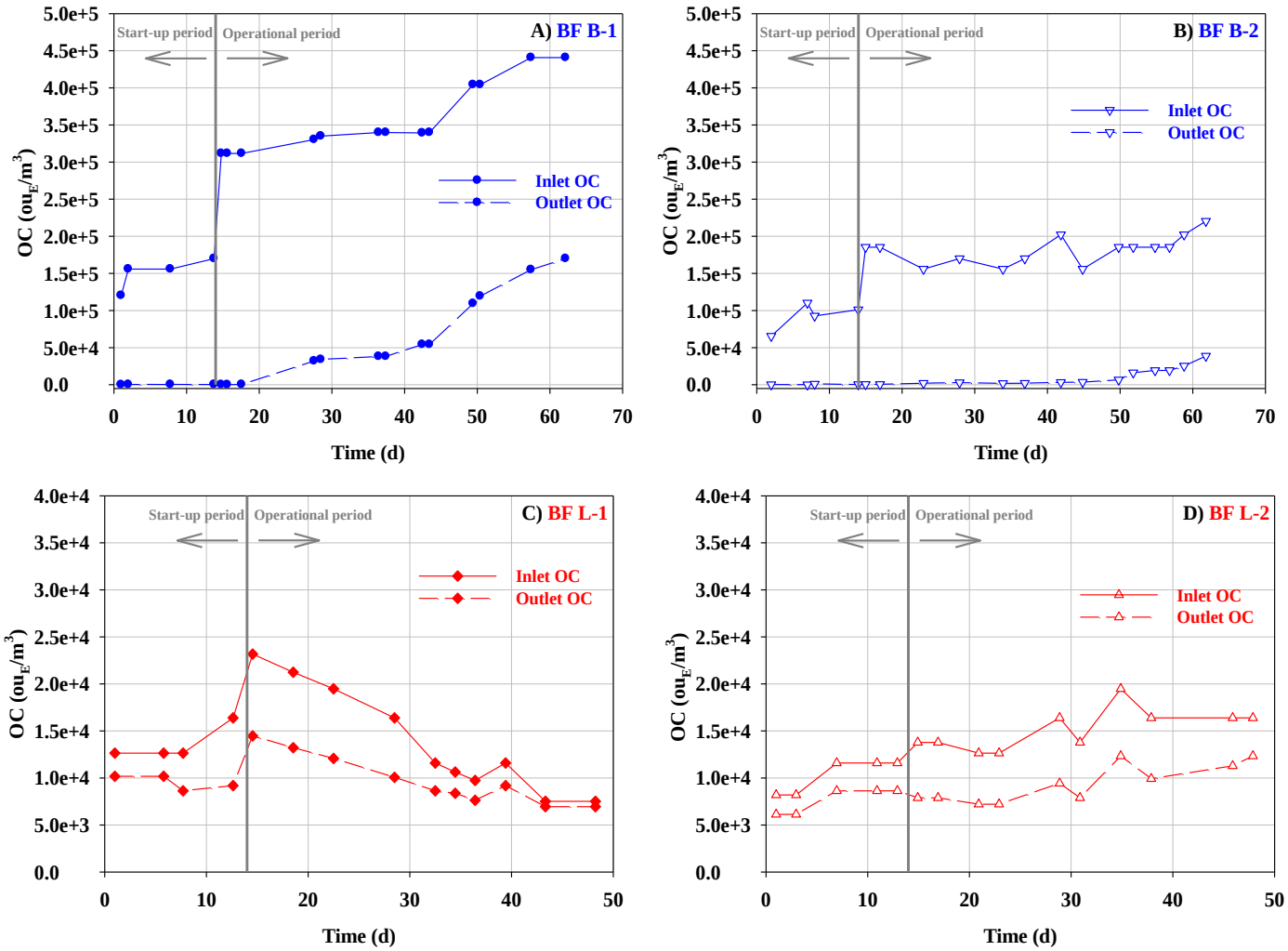

Fig. 1. Variations in inlet and outlet odor concentrations (OC) over biofiltration time for the butyric acid biofilters, BF B-1 (**A**) and BF B-2 (**B**), and limonene biofiltration systems, BF L-1 (**C**) and BF L-2 (**D**).

Nevertheless, this was not the case for BF B-1 and BF L-1, where room temperature conditioned the temperature of the water bath and, hence, the vapor pressure of the odorants and the inlet OCs (especially in the last days of such experiments).

The inlet and outlet OCs shown in **Fig. 1** were the basis for estimating the odor load factors and the odor removal efficiencies of the biofilters under study. As shown in **Fig. 2**, the compost-wood-based biofilters were subjected to higher accumulated odor loads than biofilters based only on wood chips, for both butyric acid (**Fig. 2A**) and limonene (**Fig. 2C**). These differences increased in the operational period, where BF B-1 was subjected to an odor load factor 2.2 times higher (on average) than BF B-2, whereas BF L-1 operated with an odor load factor about 1.5 times higher (on average) than that of BF L-2. Moreover, given that the inlet OCs were much higher for the butyric acid biofilters, the cumulative average of odor load factor values for BF B-1 and BF B-2 was one order of magnitude higher than those for BF L-1 and BF L-2. However, although the butyric acid biofilters operated with higher odor load factors, these systems reached higher odor removal efficiencies compared to the limonene biofilters. Thus, as seen in **Fig. 2B**, these efficiencies varied between 70 and 100% for BF B-1 and between 90 and 100% for BF B-2, whereas in limonene biofilters, the odor removal efficiencies were always lower than 70%, regardless of the filter bed used (**Fig. 2D**). This marked difference between the efficiency values could be mainly due to the hydrophobic nature of limonene, limiting its diffusion from the gas phase to the aqueous biofilm. For this reason, and according to Cheng et al. (2016) and Yang et al. (2018), the removal efficiencies of hydrophobic compounds are generally lower than those for hydrophilic compounds (such as butyric acid), where biofilter performance would be limited only by the reaction rate (Rybarczyk et al., 2020). Furthermore, it is important to highlight that the increase in the values of respirometric variables and MAC (**Table 2**) over the biofiltration time in the limonene biofilters (especially in BF L-1) did not result in a considerable increase in the odor removal efficiencies of these systems, which even decreased in the last days of the BF L-1 experiment (**Fig. 2D**) despite the fact that it was receiving lower odor loads compared to previous days (**Fig. 2C**). In this sense, it should be mentioned that the degrading species only represent between 1 and 15% of the total microbial population (Delhoménie et al., 2002; Pedersen et al., 1997). By contrast, the important aerobic microbiological activity

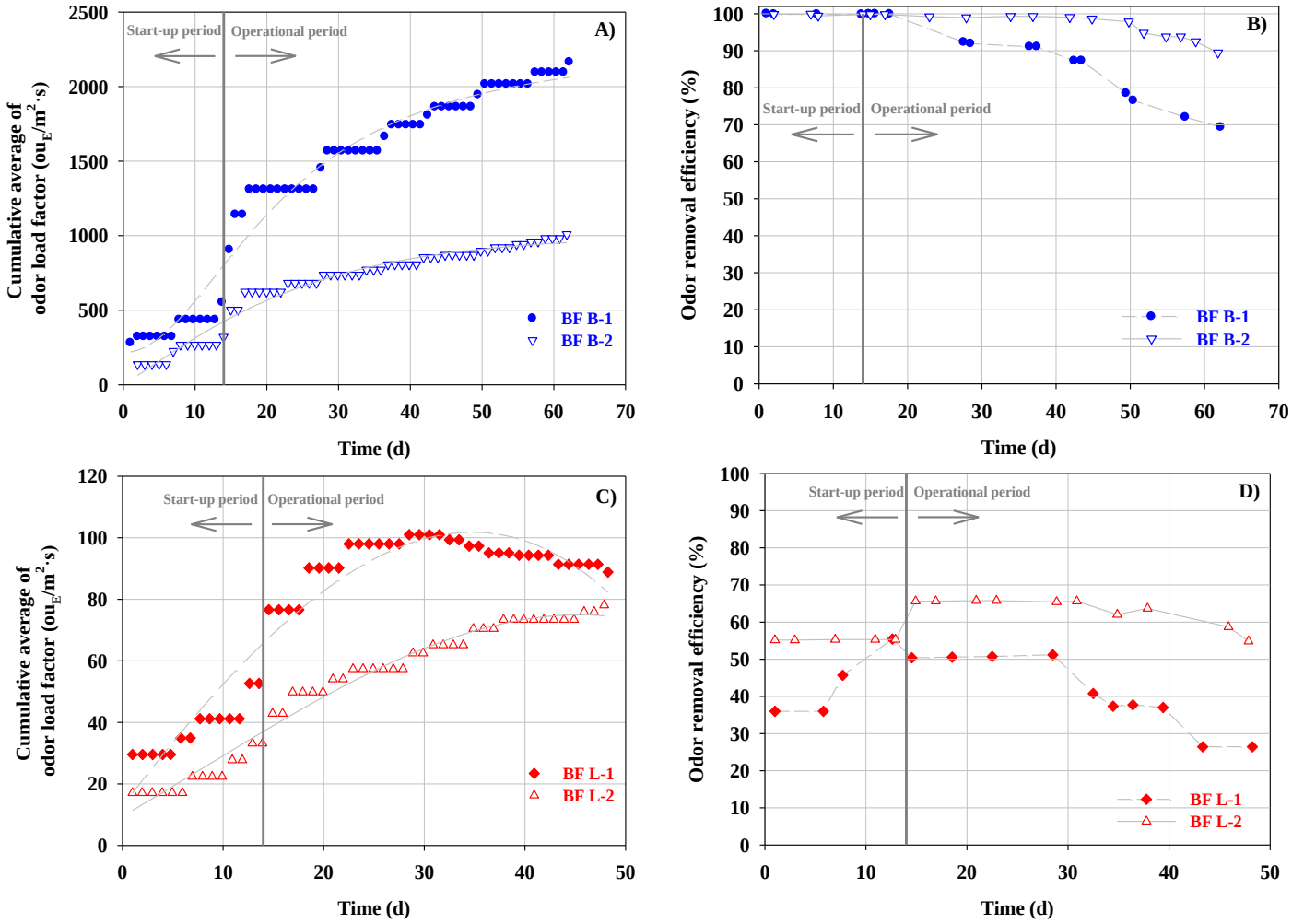

Fig. 2. Evolution of the cumulative average of odor load factor with biofiltration time for the butyric acid (**A**) and limonene (**C**) biofilters and variation in the odor removal efficiency for the same biofiltration systems (**B** and **D**, respectively).

of BF B-1, which reached maximum values at approximately 28 days of the biofiltration process, allowed this biofilter to withstand odor loads of approximately twice that of BF B-2 (**Fig. 2A**) while also maintaining high odor removal efficiencies (around 90%) (**Fig. 2B**). Regarding the biofilters based only on wood chips (BF B-2 and BF L-2), these reached more constant odor removal efficiencies with biofiltration time compared to the compost-wood-based biofilters, although BF B-2 and BF L-2 operated with lower odor load factors.

Finally, **Fig. 3** shows the joint evaluation of all biofilters under study based on two different ratios: odor removal efficiency (%)/odor load factor ($ou_E/m^2 \cdot s$) and VOC removal efficiency (%)/VOC load factor ($ppm_v \cdot m/s$). Thus, in comparison with the butyric acid biofiltration systems, the limonene biofilters always allowed better odor removal efficiency with respect to the odor load factor (**Fig. 3A**). Nevertheless, it should be kept in mind that the ODT of butyric acid is 200 times lower than that of limonene, and therefore, the emissions containing butyric acid led to higher inlet OCs, thus reducing the odor removal efficiency/odor load factor ratios for BF B-1 and BF B-2 (**Fig. 3A**). On the other hand, and according to **Fig. 3B**, the biofilters with compost and wood chips as bed material (BF B-1 and BF L-1) showed a lower VOC removal efficiency/VOC load factor ratio than wood chips-based biofilters in the start-up period, which suggests that the first type of biofilters was able to withstand a higher concentration of odorants (butyric acid or limonene) during such periods, possibly due to its greater adsorbent capacity, containing a higher total porosity. However, in the operational period, the biofilters tended to group according to the biofiltered compound, with BF B-1 and BF B-2 having the lowest VOC removal efficiency/VOC load factor ratios (**Fig. 3B**). Therefore, considering that these biofilters achieved odor removal efficiencies between 90 and 100% during most of the biofiltration process (**Fig. 2B**), it can be said that BF B-1 and BF B-2 were able to maintain high odor removal efficiencies for a long time while also receiving higher concentrations of compounds (BF B-1 range: 585–2,380 ppm_v and BF B-2 range: 280–1,145 ppm_v) compared to limonene biofilters (BF L-1 range: 160–585 ppm_v and BF L-2 range: 180–485 ppm_v).

Comparing with other biofiltration studies without bed inoculation, Otten et al. (2004) found that butyric acid (25–50 ppm_v) was effectively removed at efficiencies up to 100% using different packing materials such as compost or compost/perlite, over an 80-day run period. Moreover, Reyes et al. (2020) reported high odor removal efficiencies

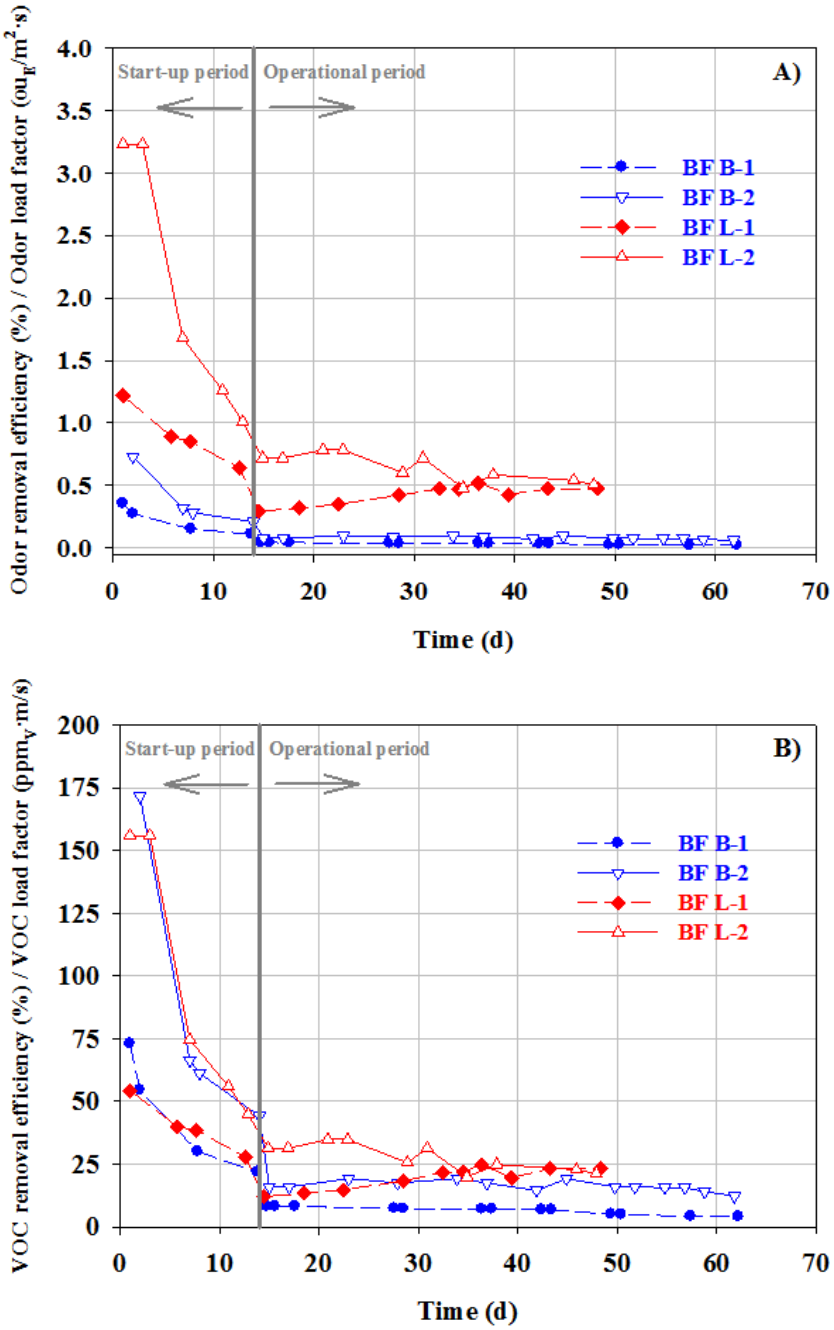

Fig. 3. Evolution of the odor removal efficiency/odor load factor ratio (**A**) and the VOC removal efficiency/VOC load factor ratio (**B**) with biofiltration time considering the butyric acid (BF B-1 and BF B-2) and limonene (BF L-1 and BF L-2) biofilters.

of butyric acid (98–100%) during the first 20 days of operation, using two biofilters based only on wood chips, which operated with odor load factors ranging between 400 and 1400 $ou_E/m^2 \cdot s$ and 180–800 $ou_E/m^2 \cdot s$. Regarding the biofiltration of gaseous limonene, Viswanathan et al. (2013) used a compost biofilter for beta-pinene and limonene removal, reporting that for a loading rate of 55 $g/m^3 \cdot h$, maximum removal efficiencies around 85%

for limonene and 45% for beta-pinene were attained. Therefore, given that in biofiltration studies of hydrophobic gaseous compounds (such as limonene) it is difficult to achieve high removal efficiencies (90-100%), many authors opt for their removal by using different strategies to improve their bioavailability and removal such as the use of membrane bioreactors, the addition of surfactants and the use of hydrophilic compounds (Cheng et al., 2016; Hosoglu and Fitch, 2012; Lamprea Pineda et al., 2021; Lebrero et al., 2013b).

3.3. Global microbiome analysis

More than 1,000,000 identifications were obtained from the four biofilters, the three stages, and the three biological replicates. Independently of the compound treated, the number of identifications decreased during the biofiltration process in the biofilters filled with the mixture of wood chips and sewage sludge compost, BF B-1 (129,829 at the Start *vs.* 82,922 at the End) and BF L-1 (55,794 *vs.* 45,673). Meanwhile, identifications increased in both biofilters filled with wood chips only, BF B-2 (66,623 *vs.* 137,455) and BF L-2 (102,127 *vs.* 128,726). The number of reads did not correlate with the microorganisms estimated through MAC values (**Table 2**) as this parameter only counts aerobic bacteria populations.

For BF B-1 and BF L-1, at the Start of the processes, Proteobacteria and Firmicutes percentages were similar, and these taxa together represented approximately 80% of the counts (**Fig. 4**). However, in these systems, at the End, Proteobacteria remained roughly at the same percentages, whereas Firmicutes decreased to finally represent 20.7 and 26.9% in BF B-1 and BF L-1, respectively. On the other hand, Actinobacter and Bacteriodetes were moderately abundant at the Start of BF B-1 and BF L-1 (ranging from 6.7 to 14.9%), but their evolution was highly different depending on the odorant as, at the End of the processes, in limonene-degrading BF L-1, their percentages remained similar, but in butyric BF B-1, Bacteriodetes became scarce (0.3%) and Actinobacter increased to be the most abundant phylum (40.8%).

Proteobacteria was by far the most abundant phylum at the Start point of both biofilters filled with wood chips, BF B-2 and BF L-2, accounting for 84.5 and 98.5%, respectively (**Fig. 4**). Nevertheless, this phylum responded differently to the odorant exposed. In the presence of butyric acid, at the End of the process, Proteobacteria diminished its proportion in BF B-2 to 39.9% and was mainly substituted with Firmicutes,

which reached 47.4%. On the other hand, limonene did not affect the phylum map of BF L-2, and Proteobacteria remained dominant during the entire process.

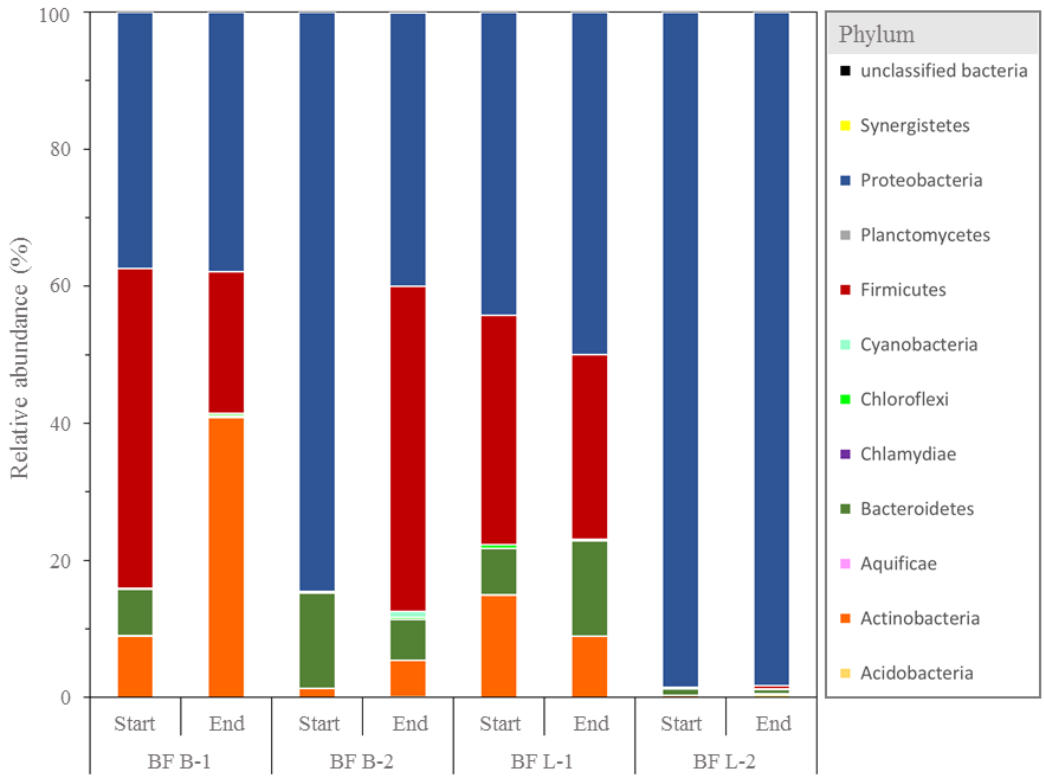

Fig. 4. Structure of the bacterial microbiota at the phylum level, determined by massive 16S rRNA sequencing of the four biofilters analyzed: BF B-1 (mixture of wood chips and sewage sludge compost as bed material, used for the removal of butyric acid), BF B-2 (wood chips, used for the removal of butyric acid), BF L-1 (mixture of wood chips and sewage sludge compost, used for the removal of limonene), and BF L-2 (wood chips, used for the removal of limonene), at the Start and at the End of the biofiltration processes. Percentages shown are the averages of three biological replicates.

3.4 Changes in the microbiome at the family level related to the biofilter bed, the biofiltered compound, and along the biofiltration processes

In total, 150 families were identified in the biofilters (**Table S1**, Supplementary Material). Of these, 32 were identified in the four biofilters, including abundant/common families such as Alcaligenaceae, Bacillaceae, Caulobacteraceae, Clostridiaceae, Enterobacteriaceae, Rhodobacteriaceae, or Sphingomonadaceae (**Table S1**, **Fig. 5A**). As expected, a high proportion of taxa, 64 families, were only present in the biofilters filled with the complex mixture of wood chips and sewage sludge compost (BF B-1 and/or BF L-1), including members of Acidimicrobiaceae, Nocardiopsaceae, or Gordoniaceae, but

only 18 were found exclusively in BF B-2 and/or BF L-2 wood chips biofilters, such as Veillonellaceae or Rickettsiaceae.

The biofiltered compound also influenced the microbiota as 44 families were found exclusively in the presence of butyric acid, *e.g.*, Geodermatophilaceae or Solirubrobacteraceae, and 10 in the presence of limonene, *e.g.*, Porphyromonadaceae (**Table S1**, **Fig. 5A**).

The evolution of the microbiota complexity varied along the biofiltration processes as estimated by the Shannon-Wiener index (**Fig. 5B**). According to the data above, at the starting point, the biodiversity indices of the biofilters filled with sewage sludge compost + wood chips, BF B-1 and BF L-1, were superior to those with only wood chips as bed material, BF B-2 and BF L-2. Nevertheless, BF B-1 and BF L-1 showed a mix evolution tendency along the biofiltration process, as butyric acid provoked an increase in microbiome diversity at the end of the biofiltration experiment, whereas limonene did the opposite. On the other hand, the evolution of the microbiota biodiversity in BF B-2 and BF L-2 was highly similar, independently of the biofiltered compound, with a low index at the starting point, which increased ≈ 50% at the intermediate and final stages (**Fig. 5B**).

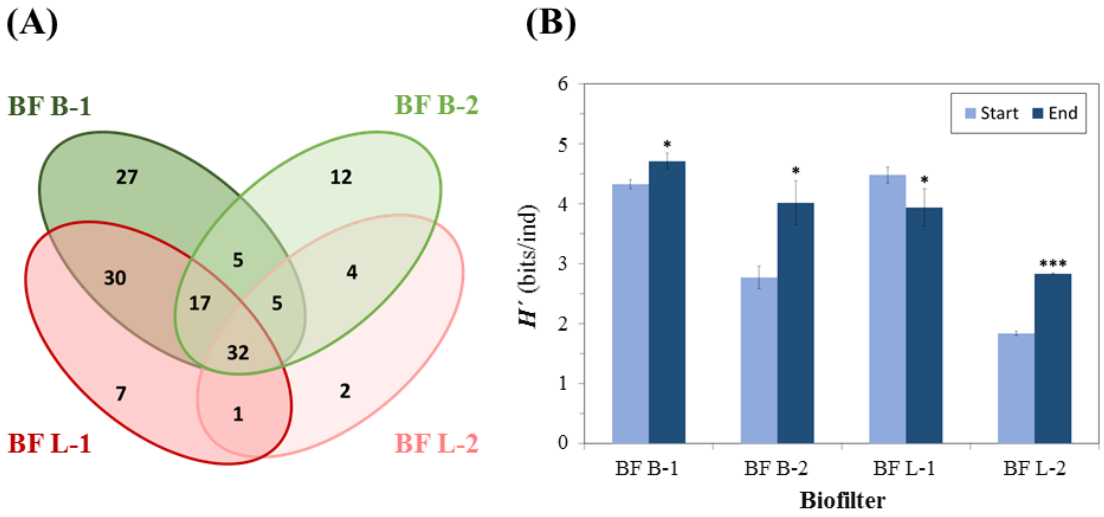

Fig. 5. Distribution of the bacterial families identified in the biofilters and estimation of the bacterial biodiversity. (**A**) Venn diagram showing the numbers of the identified families in the four biofilters analyzed, named as in Fig. 4, and their overlapping related to the biofilter beds or to the added odorous compounds. (**B**) Shannon-Wiener diversity index for the four biofilters at the Start and End stages. Mean values ± standard deviations of three biological replicates are plotted. $H'_{max} = 7.23$. Asterisks indicate the significance relative to their corresponding Start stages (***, $p < 0.001$; *, $p < 0.05$).

To further investigate the evolution of the bacterial microbiota along the biofiltering processes, the statistical significance of the changes in the abundance of families was determined comparing the Start *vs.* End stages for each biofilter (**Table 3**). In total, 102 significative alterations were found during the processes in 76 families, with the increments in abundance being more common than the decreases, 69 *vs.* 33. In agreement with their biodiversity evolution, changes in biofilters filled with wood chips mostly corresponded to increments in the proportion of families, 20 increments *vs.* 1 decrease for BF B-2 and 18 *vs.* 2 in BF L-2. The biofilters filled with compost + wood did not present a global common pattern as families in BF B-1 had more increment changes than decreases over time, 29 *vs.* 22, and BF L-1 had more decrements (2 *vs.* 18). Half of the significant changes corresponded to BF B-1, whereas only 10 families showed significant differences in BF L-1. Furthermore, the largest significant decrease corresponded to Moraxellaceae in BF B-1, which decreased 374-fold between the Start and the Ending stages, whereas the largest increase was observed for Lachnospiraceae with a 1,190-fold in BF B-2. In general, the changes observed were specific for each biofilter, but there were similar trends that could be related either to the bed material or to the biofiltered compound. The families Hyphomonadaceae, Nocardioidaceae, Patulibacteraceae, and Peptococcaceae increased their proportions in both butyric acid biofilters, BF B-1 and BF B-2, whereas no common pattern was identified in limonene biofilters. Caulobacteraceae and Rhizobiaceae increased in wood chips biofilters, BF B-2 and BF L-2, whereas Halomonadaceae always decreased in compost-wood biofilters, BF B-1 and BF L-1 (**Table 3**). A detailed microbial pathway for butyric acid fermentation was described in sulfate-reducing bacteria *Desulfobacterium cetonicum* (family Desulfobacteraceae), starting with the immediate incorporation of CoA to form butyril-CoA that is subsequently transformed in different acids, involving transferases, dehydrogenases and hydratases, to finally yield two molecules of acetyl-CoA (Janssen and Schink, 1995). A representative pathway for limonene biodegradation has been described in the bacteria *Rhodococcus erythropolis* DCL14 (family Nocardiaceae). This pathway starts the transformation with a limonene 1,2-monooxygenase followed by a hydrolase, a dehydrogenase and an oxidoreductase (Van Der Werf et al., 1999). Similar pathways have been described for bacteria as *Pseudomonas gladioli*, *Geobacillus stearothermophilys*, *Enterobacter agglomerans*, *Kosakonia cowanii*, *Pseudomonas putida* or *Castellaniella defragrans* (families Pseudomonadacea, Bacillaceae, Enterobacteriaceae or Alcaligenacea) and even a second pathway has been described in *R. erythropolis*

(Marmulla and Harder, 2014; Puentes-Cala et al., 2018). A general scheme of some of these pathways was reported by Tian and Fitzgerald (2000) (Supplementary Material).

Table 3. Bacterial families showing significant changes throughout the biofiltration process.

Bacterial families	Biofilters			
	BF B-1	BF B-2	BF L-1	BF L-2
Acetobacteraceae	-	-	-	18.3*
Acidimicrobiaceae	9.1*	-	0.16***	18.3*
Alcaligenaceae	0.015*	-	-	135.7*
Ardenscatenaceae	-	15.5*	-	-
Aurantimonadaceae	13.4*	-	-	-
Bacillaceae	-	165.7*	-	-
Bacteriovoracaceae	0.13***	-	-	-
Beijerinckiaceae	5.1*	-	-	232.1**
Beutenbergiaceae	-	1.4***	-	-
Bogoriellaceae	0.34*	-	-	-
Bradyrhizobiaceae	7.9*	36.6*	-	25.7**
Brucellaceae	7.6****	-	-	-
Burkholderiaceae	-	-	-	119.3*
Carnobacteriaceae	0.0046**	-	-	-
Caulobacteraceae	-	17.7*	-	7.6*
Clostridiaceae	-	118.1***	-	-
Comamonadaceae	-	-	-	50.9*
Corynebacteriaceae	69.6****	-	-	-
Cyclobacteriaceae	-	-	0.75***	-
Cytophagaceae	0.16***	-	-	-
Demequinaceae	9.6**	-	-	-
Dermabacteraceae	0.12***	-	-	-
Enterobacteriaceae	0.031**	-	-	0.16**
Enterococcaceae	0.043***	-	-	8.0*
Flavobacteriaceae	0.040*	-	-	-
Geodermatophilaceae	7.3****	-	-	-
Gordoniaceae	34.6****	-	-	-
Halanaerobiaceae	0.19*	-	-	-
Halomonadaceae	0.021***	-	0.036***	-
Hyphomicrobiaceae	-	26.2**	-	-
Hyphomonadaceae	6.5**	7.8*	-	-
Idiomarinaceae	-	-	0.025***	-
Lachnospiraceae	0.037**	1190.2***	-	-
Methylobacteriaceae	3.7***	-	-	3.6*
Methylocystaceae	19.2***	-	-	25.9**

Microbacteriaceae	**17.4****	-	-	-
Micrococcaceae	**0.40***	**4.7*****	-	-
Moraxellaceae	**0.0027*****	-	-	-
Nitriliruptoraceae	**3.9***	-	-	-
Nocardiaceae	**15.5******	-	-	-
Nocardioidaceae	**64.9******	**11.6***	-	-
Nocardiopsaceae	**0.10****	-	-	-
Nostocaceae	-	**34.4****	-	-
Oxalobacteraceae	**0.046*****	-	-	**0.19***
Paenibacillaceae	**0.13****	**794.8****	-	-
Patulibacteraceae	**14.1****	**10.1***	-	-
Peptococcaceae	**10.6****	**14.4*****	-	-
Peptostreptococcaceae	**0.016****	-	-	-
Phaselicystidaceae	**56.0*****	-	-	-
Piscirickettsiaceae	-	-	**0.77*****	-
Planococcaceae	-	-	**0.025***	-
Polyangiaceae	**11.2****	-	-	-
Porphyromonadaceae	-	-	**164.4***	-
Prolixibacteraceae	-	-	**31.3***	-
Pseudomonadaceae	**0.18****	-	-	-
Rhizobiaceae	-	**21.7***	-	**35.5****
Rhodobacteraceae	**5.0***	**15.6***	-	**17.1***
Rhodobiaceae	**23.8****	-	-	-
Rhodospirillaceae	**13.2***	-	-	**14.4***
Rickettsiaceae	-	-	-	**9.4***
Ruminococcaceae	-	**0.20*****	-	-
Saccharospirillaceae	**10.6*****	-	-	-
Sanguibacteraceae	**0.45***	-	-	-
Sneathiellaceae	**5.9*****	-	-	-
Solirubrobacteraceae	**6.5****	-	-	-
Sphaerobacteraceae	-	-	**0.12***	-
Sphingobacteriaceae	**0.012*****	-	-	-
Sphingomonadaceae	-	-	-	**4.9***
Streptosporangiaceae	**15.5******	-	-	-
Thermoactinomycetaceae	-	**30.1*****	-	-
Thermomonosporaceae	**0.11***	-	-	-
unclassifiedRhizobiales	**14.3***	-	**0.22******	-
Veillonellaceae	-	**117.2*****	-	-
Williamsiaceae	-	**18.9***	-	-
Xanthobacteraceae	**5.0*****	-	-	**3.8***
Xanthomonadaceae	-	-	-	**6.7***

The numbers indicate the ratio of abundance of each bacterial family at the end with respect to the beginning of the biofiltration process for each biofilter. Increments are highlighted in red while decreases in green. Statistically significant differences are expressed as: *, $p < 0.05$; **, $p < 0.01$; ***, $p < 0.001$; ****, $p < 0.0001$.

In aerobic conditions, the four-carbon butyric acid can be fully metabolized by the fatty acids β-oxidation pathway. Thus, butyric acid is converted to acetyl-CoA that can be further mineralized by the Citric Acid cycle to odorless CO_2, thus explaining the high odor removal efficiencies of the butyric acid biofilters (**Fig. 2B**). Acetyl-CoA could also be converted to acetic acid that has a characteristic vinegar odor, but with an ODT very superior to butyric acid ($6.0 \cdot 10^{-3}$ *vs.* $1.9 \cdot 10^{-4}$ ppm_v) (Nagata, 2003). On the other hand, limonene degrading pathways include substitution, derivatization or even ring-cleave reactions, usually generating less-odorous equimolar hydrophobic intermediates as carvone, α-terpineol or perillyl alcohol (Marmulla and Harder, 2014), since the limonene biofilters achieved odor removal efficiencies between 25–65% (**Fig. 2D**).

The FAPROTAX algorithm was used to investigate the functional changes in the microbiota among the different biofilters and their evolution between the Start and End stages (Louca et al., 2016). In total, 432 taxa were assigned to 45 functional groups (**Fig. 6** and data not shown). Furthermore, the biofilters were clustered according to the similarities in their predicted bacterial functions using the Genesis Software (Sturn et al., 2002). The results show that the bed material of the biofilters seemed to be more important than the treated compounds, as BF L-1 at the Start and End points (BF L-1.S and BF L-1.E) and BF B-1 at the final stage (BF B-1.E) were grouped together. The only exception was the initial stage of BF B-1 (BF B-1.S), which was grouped with BF B-2 and BF L-2. Thus, BF B-2 shows a clear increase in photoautotrophy and dark oxidation of sulfur compounds and the end of its filtration period, together with an increase in photosynthetic cyanobacteria and "Knallgas" bacteria. Those functions correlate with the significant increases in the abundances of the families Bradyrhizobiaceae, Hyphomicrobiaceae, Nostocaceae, and Rhodobacteraceae (**Table S1**). Furthermore, in BF L-2 at the final point (BF L-2.E), the functional pattern showed a clear increment in methanotrophy as well as nitrogen and nitrate respiration activities, together with the presence of parasites or human-associated bacteria. These functions correlate with the significant increases in Acetobacteraceae, Alcaligenaceae, Beijerinckiaceae, Methylocystaceae, Rhodobacteraceae, or Xanthomonadaceae families. Similar associations could be made for BF B-1 and BF L-1 (**Fig. 6**, **Table 3**).

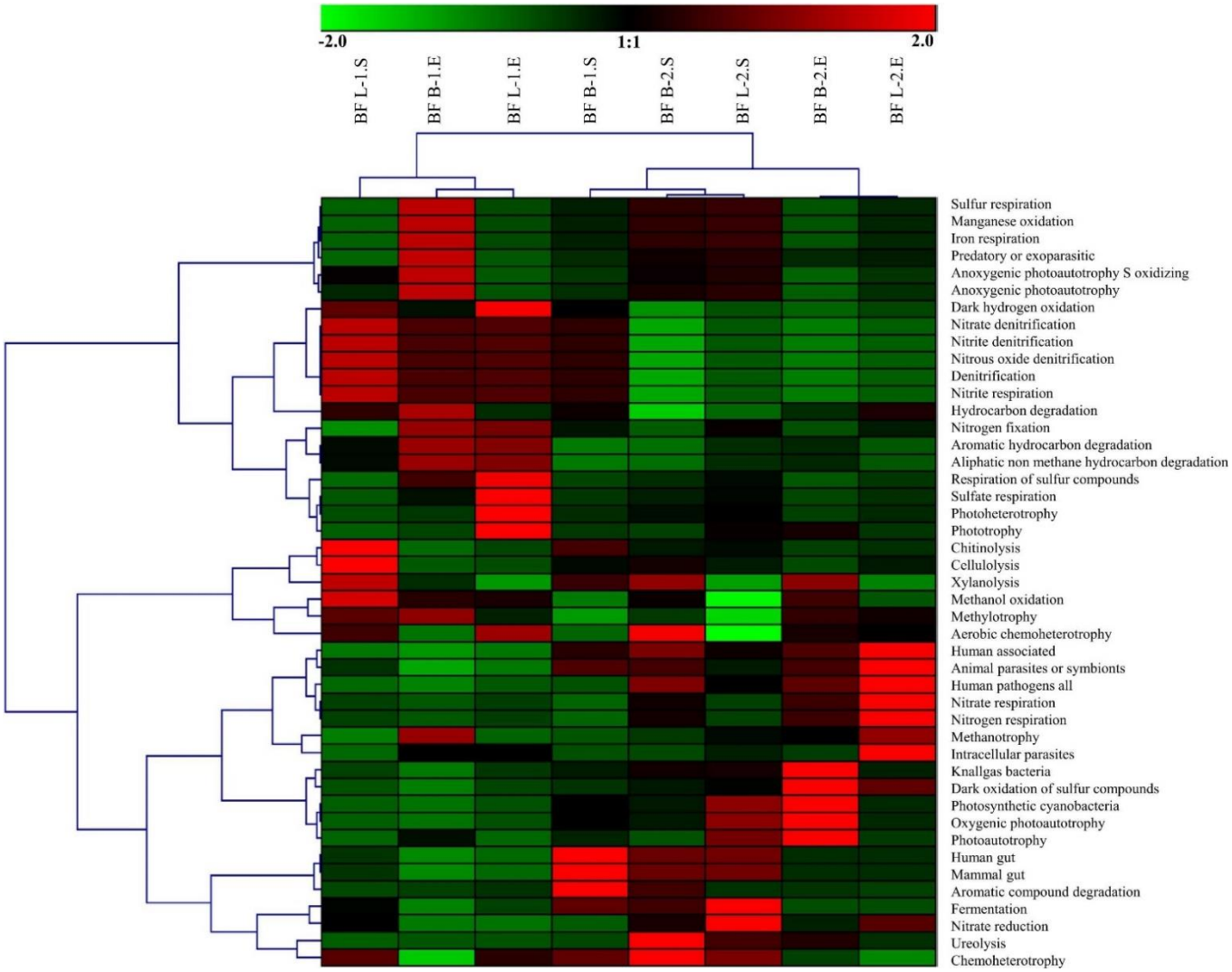

Fig. 6. Functional profiles of bacterial communities in the different biofilters at the Start and Ending stages predicted though the FAPROTAX algorithm. Data were clustered by the Genesis program. Each row in the heatmap represents a different function. Each column represents the different biofilters as named in Fig. 4 at the Start (B-1.S, B-2.S, L-1.S, and L-2.S) or End (B-1.E, B-2.E, L-1.E, and L-2.E) of the biofiltration processes. Green rectangles indicate samples with a lower intensity relative to other conditions; red rectangles represent higher levels. The color intensity is proportional to the fold-change as represented by the scale (For interpretation of the references to color in this figure legend, the reader is referred to the web version of this article).

In this work, a cross-disciplinary study of the operation of a biofiltration system to remove odors was carried out, varying both the nature of the odorants and the bed material. The process was analyzed both from olfactometric, microbiological, and physico-chemical points of view, highlighting the influence of the biofiltered gaseous compound on removal odor efficiencies and the importance of the bed material in

conditioning the microbiota of the biofilters, that is the ultimate responsible for the biodegradation of the odorous compounds. Research studies like this are necessary because real odorous gaseous streams derived from full-scale waste treatment plants are composed of different compounds which can, synergistically or antagonistically, affect the microbiota present in the biofiltration packing materials. Additionally, the packing material is one of the factors that most significantly conditions the right operation of the biofilter due to its porosity and nutrient content, all operating under adequate humidity and pH conditions. Thus, always depending on the characteristics of the gaseous stream to be treated, this study might help waste treatment plant managers to select potentially inexpensive and recyclable materials (such as sewage sludge compost and wood chips) as packing materials in deodorization operations by biofiltration.

4. Conclusions

Odor removal efficiencies of the biofilters which treated butyric acid varied between 70 and 100%. By contrast, in biofilters treating limonene, under the same EBRTs, the efficiencies were always lower than 70%, regardless of the filter bed used (compost-wood or wood chips only), which could be mainly due to the hydrophobic nature of limonene. The global microbiome analysis showed a higher biodiversity of the biofilters filled with the mixture of sewage sludge compost and wood chips (represented by the phyla Proteobacteria, Firmicutes, Bacteroidetes, and Actinobacteria) compared to biofilters with only wood chips (in which Proteobacteria was the most abundant phylum). Thus, it might be said that the differences in odor removal efficiencies of well-operated biofilters for the same gaseous compound depend on the composition of the packed beds, as long as the biofiltered compound has a hydrophilic nature (such as butyric acid).

Acknowledgments

This work was supported by the Spanish Ministry of Economy, Industry, and Competitiveness (MINECO), the Spanish State Research Agency (AEI) and the European Regional Development Fund (FEDER) through Project CTM2017-88723-R, and the Ministry of Education, Culture, and Sport of Spain (Grant FPU2016). The European Regional Development Fund (Project UCO-FEDER-1262384-R) and the Chelonia

Association (Mares Circulares Project) also supported this work. Finally, we also wish to express our gratitude to Inmaculada Bellido, María Luisa López, and Ana María Herruzo-Ruiz for their contribution to this research. Funding for open access charge: Universidad de Córdoba / CBUA.

Appendix A. Supplementary data

Table S1. Bacterial families identified in the different biofilters at the different stages along the biofiltration process.

Bacterial phyla Bacterial families	**Biofilters[a]**											
	BF B-1			**BF B-2**			**BF L-1**			**BF L-2**		
	S	**M**	**E**	**S**	**M**	**E**	**S**	**M**	**E**	**S**	**M**	**E**
Acidobacteria					0.23	0.23					0.55	1.08
Acidobacteriaceae					0.23	0.23					0.55	1.08
Actinobacteria	26.91	149.42	122.37	4.05	23.95	15.94	44.81	54.09	26.80	0.89	4.28	0.57
Acidimicrobiaceae	0.09	3.68	1.72				0.86					
Actinomycetaceae									0.04			
Beutenbergiaceae	0.33	0.04	0.34			0.11	1.45	1.75	0.79			
Bogoriellaceae	0.65	0.17	0.34				3.86	5.17	1.95			
Catenulisporaceae		0.17										
Cellulomonadaceae	2.38	5.46	9.00		0.16	0.20	4.22	4.94	2.55		0.61	0.23
Conexibacteraceae		0.32					0.08					
Coriobacteriaceae		1.11	0.31								0.08	
Corynebacteriaceae		0.03	6.82									
Demequinaceae	1.44	8.07	21.77			0.04	5.65	5.67	4.06		0.64	
Dermabacteraceae	0.54											
Dietziaceae	0.10											
Euzebyaceae	0.09	0.60	0.83				0.12					

Frankiaceae						0.02						
Gaiellaceae	0.11											
Geodermatophilaceae		0.07	0.74		1.71	0.81						
Gordoniaceae		4.60	3.39					6.36	1.91			
Lamiaceae		1.32	0.11									
Intrasporangiaceae		0.03	0.20				0.19				0.19	
Jiangellaceae	0.02	0.30	0.04									
Jonesiaceae		0.02					0.40	1.31				
Microbacteriaceae	2.06	99.36	55.47	4.01	15.60	11.33	4.25	10.15	5.63	0.89	2.18	0.34
Micrococcaceae	0.51	0.27	0.32			0.29	1.54	2.46	0.99			
Mycobacteriaceae	0.32	1.46	0.63			0.02	0.37	1.50	0.23			
Nitriliruptoraceae		0.10	0.39									
Nocardiaceae		0.14	1.53		1.46	0.35	0.18	3.46	1.01			
Nocardioidaceae	0.04	6.96	7.06		0.08	0.65	2.04	0.57	0.03			
Nocardiopsaceae	8.56	2.55	1.28				4.96	1.97	3.63			
Patulibacteraceae		1.36	1.37		0.49	0.65	0.21					
Promicromonosporaceae	0.02	0.04	0.10				0.13					
Propionibacteriaceae						0.05						
Pseudonocardiaceae	6.54	6.98	4.24		0.04	0.08	12.68	7.55	2.75			
Rubrobacteraceae											0.03	
Sanguibacteraceae	0.71	0.05	0.49	0.04	0.04	0.13	0.59	0.46	0.89		0.53	
Solirubrobacteraceae		1.29	0.64			0.02						

Streptomycetaceae	0.61	0.89	1.33				0.25	0.40	0.30		0.02	
Streptosporangiaceae	0.02	0.25	1.59				0.28					
Thermomonosporaceae	1.77	1.73	0.32				0.50		0.04			
Thermomonosporaceae								0.11				
unclassified Pseudonocardineae					4.37	1.19		0.26				
Williamsiaceae												
Aquificae	0.25	0.35					0.04					
Desulfurobacteriaceae	0.25	0.35					0.04					
Bacteroidetes	20.18	0.12	0.83	41.67	52.73	17.91	20.35	3.31	41.60	2.79	6.12	1.80
Chitinophagaceae					0.96	0.07			0.08			
Cyclobacteriaceae	0.05						0.22					
Cytophagaceae	0.39			0.11			0.08				0.93	0.18
Flammeovirgaceae							0.37					
Flavobacteriaceae	14.61	0.12	0.83	6.28	22.02	9.55	14.08	1.73	4.54	0.40	0.50	0.17
Marinilabiliaceae									0.13			
Porphyromonadaceae								1.26	30.38		0.08	
Prolixibacteraceae								0.32	5.69			
Sphingobacteriaceae	5.13			35.28	29.75	8.29	5.60		0.78	2.39	4.61	1.45
Chlamydiae									0.04			
Parachlamydiaceae									0.04			
Chloroflexi	0.27	1.01	0.91		1.32	1.08	1.56	1.05	0.78			
Ardenscatenaceae	0.02		0.25		1.32	0.91	0.25	0.85	0.64			

Ardenticatenaceae	0.08											
Dehalococcoidaceae		0.03	0.30						0.04			
Sphaerobacteraceae	0.17	0.91	0.22				1.26	0.13				
Thermogemmatisporaceae		0.04	0.14			0.17	0.05	0.07	0.10			
unclassified Dehalococcoidia		0.03										
Cyanobacteria	0.22	17.81	0.19	0.11	0.60	2.56				0.74	0.03	0.20
Nostocaceae	0.22	17.81	0.19	0.11	0.60	2.56				0.74	0.03	0.20
Firmicutes	140.14	80.51	62.03	0.63	17.35	142.15	100.55	61.15	80.83	0.03	5.82	1.43
Bacillaceae	49.52	46.70	20.73		1.59	9.22	62.80	50.72	38.81		1.29	0.15
Bacillales incertae sedis	0.07	0.12	0.04				0.14		0.03			
Carnobacteriaceae	26.94	0.05	0.15			0.13	6.03	2.65	15.28	0.03	0.05	
Christensenellaceae		0.22	0.14									
Clostridiaceae	2.11	3.85	3.55			6.93	1.68	0.14	15.06		0.96	0.54
Clostridiales Family XI. Incertae Sedis		0.02							0.69			
Clostridiales Family XIII. Incertae Sedis	0.02		0.17				0.63	0.06				
Clostridiales Family XIX. Incertae Sedis	0.09											
Defluviitaleaceae		0.21										
Enterococcaceae	1.45					0.05	0.92	0.07	0.32		0.74	0.67
Erysipelotrichaceae	2.39	5.97	2.73			0.32	1.76	1.45	1.88			
Gracilibacteraceae		0.04										
Halanaerobiaceae	0.33	0.66							0.04			

Lachnospiraceae	1.68	0.03				68.32			0.41		0.26	
Lactobacillaceae						0.18						
Leuconostocaceae		1.80	1.31		6.26	0.34						
Natranaerobiaceae	0.09											
Paenibacillaceae	6.24	5.04	1.24		9.50	46.88	3.99	2.42	2.44		2.45	0.01
Peptococcaceae	0.02	0.36	1.06			0.76			0.09		0.07	
Peptostreptococcaceae	3.96	0.10							0.09			
Planococcaceae	36.29	1.19	25.00			0.06	18.38	2.15	0.22			
Ruminococcaceae		0.18	0.16	0.63					0.03			
Staphylococcaceae	0.08						0.05					
Streptococcaceae						0.09						
Thermoactinomycetaceae	8.66	13.36	5.69			1.68	4.10	1.49	5.44			
Thermoanaerobacteraceae	0.03											
Thermoanaerobacterales Family III. Incertae Sedis	0.17	0.61	0.06				0.07					
unclassified Clostridiales						0.26						
Veillonellaceae						6.93						0.06
Lentisphaerae					0.50							
Victivallaceae					0.50							
Planctomycetes					3.01	0.09						
Planctomycetaceae					3.01	0.09						
Proteobacteria	111.99	50.50	113.69	253.48	200.39	119.80	132.63	180.42	149.91	295.53	283.17	294.89
Acetobacteraceae			0.10	0.10	0.47	0.46			0.13		1.02	1.11

Alcaligenaceae	4.03		0.03	1.51	4.01	1.09	2.67	0.43	0.99	0.02	4.57	8.33
Alteromonadaceae	0.89	2.03	3.04		4.66	0.80	2.90	1.25	0.31			
Aurantimonadaceae		0.48	1.34			0.03						
Bacteriovoracaceae	0.49				0.96	0.15	0.08					
Bartonellaceae	2.11	0.68	2.90				10.09	3.69	0.87			0.24
Bdellovibrionaceae	0.02				0.71	0.11	0.05	0.07				
Beijerinckiaceae		0.28	0.50		0.37	0.37					3.45	14.62
Bradyrhizobiaceae		0.08	0.80	0.06	7.27	2.85					1.09	1.72
Brucellaceae		0.06	0.74									
Burkholderiaceae	0.14		0.07		6.25	1.38	0.11				4.14	6.99
Caulobacteraceae	4.54	0.30	3.53	0.57	19.94	5.35	15.49	6.64	1.80	0.42	5.36	2.59
Cohaesibacteraceae			0.49									
Comamonadaceae				5.76	6.13	7.47				0.27	10.80	9.87
Coxiellaceae					0.04							
Cystobacteraceae	0.05	0.23	0.50				0.39					
Desulfovibrionaceae	0.51	0.23	0.16						0.04			
Desulfuromonadaceae		0.11	0.14									
Ectothiorhodospiraceae		0.19	0.08				0.06					
Enterobacteriaceae	16.79		0.78	37.53	4.19	9.24	15.99		1.25	142.13	15.29	19.48
Erythrobacteraceae			0.15					0.19			0.04	0.04
Geminicoccus			0.40					0.15				
Geobacteraceae	0.02	0.35	0.19						0.04			

Halomonadaceae	2.97						3.70					
Helicobacteraceae						0.05						
Hydrogenophilaceae						0.03						
Hyphomicrobiaceae	9.34	5.53	13.81	0.08	3.26	2.27	20.81	15.03	4.20		0.03	
Hyphomonadaceae	0.07	0.13	0.83	0.63	4.56	2.37		0.86	0.10		0.07	
Idiomarinaceae	0.27						5.87					
Kiloniellaceae			0.04									
Legionellaceae		0.22	0.22									0.01
Methylobacteriaceae			0.36	1.61	5.78	1.87				0.50	1.79	1.61
Methylocystaceae			1.88		3.80	0.47					0.74	1.72
Methylophilaceae											0.02	
Moraxellaceae	23.80			6.20	1.94	1.63	0.06		0.05		0.11	
Myxococcaceae	0.04	0.66	0.40		2.44	0.34						
Nannocystaceae		0.23					0.04					
Oligoflexaceae					2.02	0.16						
Oxalobacteraceae	1.36			48.14	6.71	15.74	0.15			16.23	5.26	2.48
Phaselicystidaceae			5.38									
Phyllobacteriaceae	0.55	2.33	7.96			0.02	1.06	0.28	0.04			0.10
Piscirickettsiaceae							0.21					
Polyangiaceae		1.16	1.09									
Pseudomonadaceae	31.14	0.09	8.56	93.39	27.94	18.90	18.74	9.59	58.42	103.99	102.25	86.08
Rhizobiaceae	5.78	7.04	18.69	0.59	11.95	6.93	19.67	10.27	13.39	0.18	5.84	5.83

Rhodobacteraceae	1.58	24.52	12.66	0.08	0.28	1.09	1.49	3.58	10.09		0.87	1.07
Rhodobiaceae		0.59	2.38		0.06	0.29		0.23	0.04	0.03		
Rhodospirillaceae	0.60	1.23	12.86		1.45	0.65	1.46	21.27	4.94		0.62	0.90
Rickettsiaceae						0.02					0.63	0.63
Saccharospirillaceae			1.00				0.05					
Sneathiellaceae			0.59									
Sphingomonadaceae	3.96	1.50	5.60	53.52	51.83	30.56	6.48	106.35	49.00	27.04	88.79	104.55
unclassified Myxococcales			0.04									
unclassified Rhizobiales	0.08	0.25	2.40		0.04	0.06	0.75	0.54				
Vibrionaceae			0.18									
Xanthobacteraceae			0.49			0.05			2.93		0.83	0.28
Xanthomonadaceae	0.86		0.33	3.71	21.33	7.00	4.26		1.28	4.72	29.56	24.64
Synergistetes						0.25						
Synergistaceae						0.25						
Thermodesulfobacteria		0.19										
Thermodesulfobacteriaceae		0.19										
unclassified bacteria	0.22											
Haloplasmataceae	0.22											
Total	300.18	299.91	300.02	299.94	300.08	300.01	299.94	300.02	299.96	299.98	299.97	299.97

[a] Biofilters are filled with a mixture of wood chips and sewage sludge compost (1) or wood chips only (2) for the removal of butyric acid (B) or limonene (L). The numbers indicate the abundance of each baterial family at the start (S), middle (M) and end (E) of the biofiltration process.

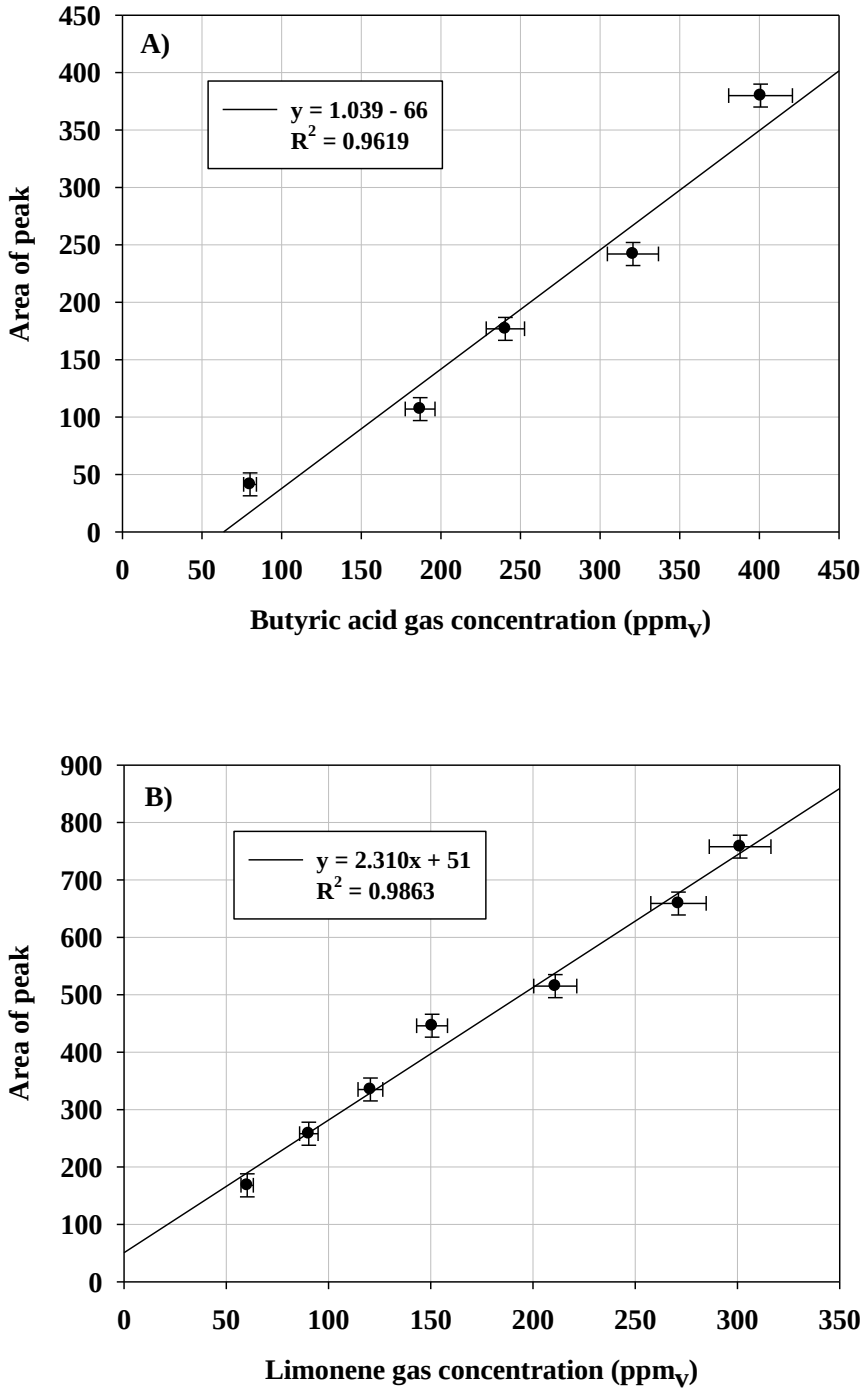

Fig. S1. Calibration curves used for the quantification of butyric acid (**A**) and limonene (**B**).

Limonene Pathway Map (source: http://eawag-bbd.ethz.ch/lim/lim_map.html).

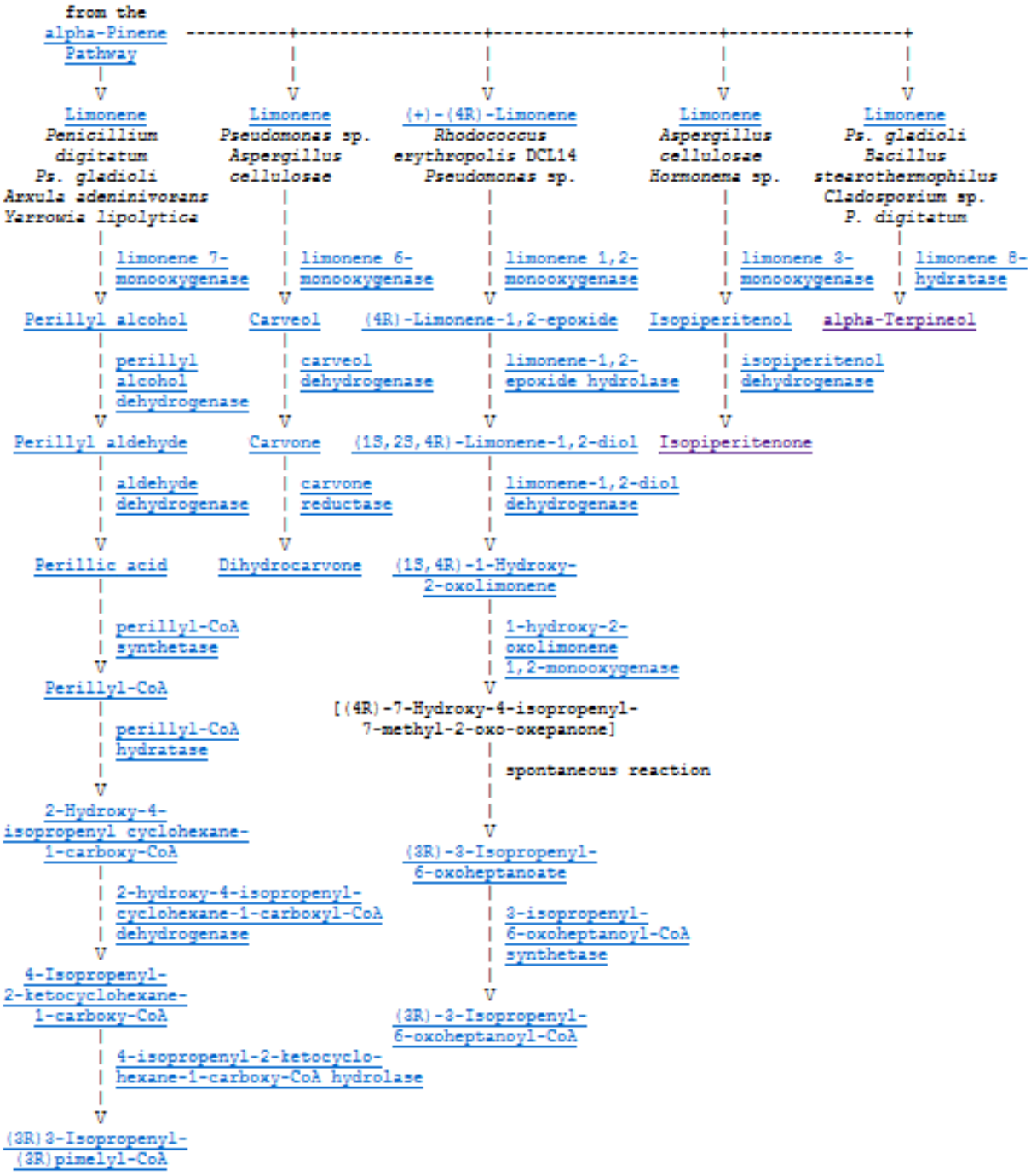

References

AIHA, 2021. Workplace Environmental Exposure Levels Guide of the American Industrial Hygiene Association.

Allievi, M.J., Silveira, D.D., Cantão, M.E., Filho, P.B., 2018. Bacterial community diversity in a full scale biofilter treating wastewater odor. Water Sci. Technol. 77, 2014–2022. https://doi.org/10.2166/WST.2018.114

Barbusinski, K., Kalemba, K., Kasperczyk, D., Urbaniec, K., Kozik, V., 2017. Biological methods for odor treatment – A review. J. Clean. Prod. https://doi.org/10.1016/j.jclepro.2017.03.093

Bhadra, B.N., Lee, J.K., Cho, C.W., Jhung, S.H., 2018. Remarkably efficient adsorbent for the removal of bisphenol A from water: Bio-MOF-1-derived porous carbon. Chem. Eng. J. 343, 225–234. https://doi.org/10.1016/j.cej.2018.03.004

Bindra, N., Dubey, B., Dutta, A., 2015. Technological and life cycle assessment of organics processing odour control technologies. Sci. Total Environ. 527–528, 401–412. https://doi.org/10.1016/j.scitotenv.2015.05.023

Boada, E., Santos-Clotas, E., Cabrera-Codony, A., Martín, M.J., Bañeras, L., Gich, F., 2021. The core microbiome is responsible for volatile silicon and organic compounds degradation during anoxic lab scale biotrickling filter performance. Sci. Total Environ. 798, 149162. https://doi.org/10.1016/J.SCITOTENV.2021.149162

Cabeza, I.O., López, R., Giraldez, I., Stuetz, R.M., Díaz, M.J., 2013. Biofiltration of α-pinene vapours using municipal solid waste (MSW) - Pruning residues (P) composts as packing materials. Chem. Eng. J. 233, 149–158. https://doi.org/10.1016/j.cej.2013.08.032

Charles, W., Ho, G., 2017. Biological Methods of Odor Removal in Solid Waste Treatment Facilities, in: Current Developments in Biotechnology and Bioengineering: Solid Waste Management. Elsevier, pp. 341–365. https://doi.org/10.1016/B978-0-444-63664-5.00015-0

Cheng, Y., He, H., Yang, C., Zeng, G., Li, X., Chen, H., Yu, G., 2016. Challenges and solutions for biofiltration of hydrophobic volatile organic compounds. Biotechnol. Adv. https://doi.org/10.1016/j.biotechadv.2016.06.007

Chica, A., Mohedo, J.J., Martín, M.A., Martín, A., 2003. Determination of the stability of msw compost using a respirometric technique. Compost Sci. Util. 11, 169–175. https://doi.org/10.1080/1065657X.2003.10702122

Cruz-García, B., Aizpuru, A., 2022. Proof of concept of a novel in tandem biofilter photobioreactor system for valorization of volatile organic compounds: mineralization of methanol vapors coupled with use of CO2 as a carbon source for Arthrospira maxima growth. J. Chem. Technol. Biotechnol. https://doi.org/10.1002/JCTB.6888

Delgado-Baquerizo, M., Oliverio, A.M., Brewer, T.E., Benavent-González, A., Eldridge, D.J., Bardgett, R.D., Maestre, F.T., Singh, B.K., Fierer, N., 2018. A global atlas of the dominant bacteria found in soil. Science (80-.). 359, 320–325. https://doi.org/10.1126/SCIENCE.AAP9516

Delhoménie, M.C., Bibeau, L., Bredin, N., Roy, S., Broussau, S., Brzezinski, R., Kugelmass, J.L., Heitz, M., 2002. Biofiltration of air contaminated with toluene on a compost-based bed. Adv. Environ. Res. 6, 239–254. https://doi.org/10.1016/S1093-0191(01)00055-7

Delhoménie, M.C., Heitz, M., 2005. Biofiltration of air: A review. Crit. Rev. Biotechnol. https://doi.org/10.1080/07388550590935814

Detchanamurthy, S., Gostomski, P.A., 2012. Biofiltration for treating VOCs: An overview. Rev. Environ. Sci. Biotechnol. https://doi.org/10.1007/s11157-012-9288-5

Devinny, J.S., Ramesh, J., 2005. A phenomenological review of biofilter models. Chem. Eng. J. https://doi.org/10.1016/j.cej.2005.03.005

Ding, Y., Xiong, J., Zhou, B., Wei, J., Qian, A., Zhang, H., Zhu, W., Zhu, J., 2019. Odor removal by and microbial community in the enhanced landfill cover materials containing biochar-added sludge compost under different operating parameters. Waste Manag. 87, 679–690. https://doi.org/10.1016/j.wasman.2019.03.009

Dorado, A.D., Baquerizo, G., Maestre, J.P., Gamisans, X., Gabriel, D., Lafuente, J., 2008. Modeling of a bacterial and fungal biofilter applied to toluene abatement: Kinetic parameters estimation and model validation. Chem. Eng. J. 140, 52–61. https://doi.org/10.1016/j.cej.2007.09.004

Elias, A., Barona, A., Arreguy, A., Rios, J., Aranguiz, I., Peñas, J., 2002. Evaluation of a packing material for the biodegradation of H2S and product analysis. Process Biochem. 37, 813–820. https://doi.org/10.1016/S0032-9592(01)00287-4

Elmrini, H., Bredin, N., Shareefdeen, Z., Heitz, M., 2004. Biofiltration of xylene emissions: bioreactor response to variations in the pollutant inlet concentration and gas flow rate. Chem. Eng. J. 100, 149–158. https://doi.org/10.1016/J.CEJ.2004.01.030

EN 13725, 2003. Air Quality - Determination of Odour Concentration by Dynamic Olfactometry. European Committee for Standardization, Brussels.

European Parliament and Council, 2010. Directive 2010/75/EU of the European Parliament and of the Council of 24 November 2010 on industrial emissions (integrated pollution prevention and control). Brussels.

European Parliament and Council, 2008. Directive 2008/50/EC of the European Parliament and of the Council of 21 May 2008 on ambient air quality and cleaner air for Europe. Brussels.

Ferdowsi, M., Avalos Ramirez, A., Jones, J.P., Heitz, M., 2017. Elimination of mass transfer and kinetic limited organic pollutants in biofilters: A review. Int. Biodeterior. Biodegrad. 119, 336–348. https://doi.org/10.1016/j.ibiod.2016.10.015

García-Mateos, F.J., Ruiz-Rosas, R., Marqués, M.D., Cotoruelo, L.M., Rodríguez-Mirasol, J., Cordero, T., 2015. Removal of paracetamol on biomass-derived activated carbon: Modeling the fixed bed breakthrough curves using batch adsorption experiments. Chem. Eng. J. 279, 18–30. https://doi.org/10.1016/j.cej.2015.04.144

Gonzalez-Serrano, E., Cordero, T., Rodriguez-Mirasol, J., Cotoruelo, L., Rodriguez, J.J., 2004. Removal of water pollutants with activated carbons prepared from H3PO4activation of lignin from kraft black liquors. Water Res. 38, 3043–3050. https://doi.org/10.1016/j.watres.2004.04.048

Gutierrez, M.C., Martin, M.A., Pagans, E., Vera, L., Garcia-Olmo, J., Chica, A.F., 2015. Dynamic olfactometry and GC-TOFMS to monitor the efficiency of an industrial biofilter. Sci. Total Environ. 512–513, 572–581. https://doi.org/10.1016/j.scitotenv.2015.01.074

Hosoglu, F., Fitch, M.W., 2012. Abatement of synthetic landfill gas including limonene by biotrickling filter and membrane biofiltration. J. Environ. Sci. Heal. Part A 47, 1065–1072. https://doi.org/10.1080/10934529.2012.667338

Iranpour, R., Cox, H.H.J., Deshusses, M.A., Schroeder, E.D., 2005. Literature review of air pollution control biofilters and biotrickling filters for odor and volatile organic compound removal. Environ. Prog. 24, 254–267. https://doi.org/10.1002/ep.10077

ISO4833-1, 2013. Microbiology of the food chain–Horizontal method for the enumeration of microorganisms–Part 1: Colony count at 30 degrees C by the pour plate technique.

Janssen, P.H., Schink, B., 1995. Pathway of butyrate catabolism by Desulfobacterium cetonicum. J. Bacteriol. 177, 3870–3872. https://doi.org/10.1128/JB.177.13.3870-3872.1995

Kim, Y.W., Kim, M.J., Chung, B.Y., Bang, D.Y., Lim, S.K., Choi, S.M., Lim, D.S., Cho, M.C., Yoon, K., Kim, H.S., Kim, K.B., Kim, Y.S., Kwack, S.J., Lee, B.M., 2013. Safety Evaluation And Risk Assessment Of d-Limonene. J. Toxicol. Environ. Heal. Part B 16, 17–38. https://doi.org/10.1080/10937404.2013.769418

Kissel, J.C., Henry, C.L., Harrison, R.B., 1992. Potential emissions of volatile and odorous organic compounds from municipal solid waste composting facilities. Biomass and Bioenergy 3, 181–194. https://doi.org/10.1016/0961-9534(92)90025-L

Lamprea Pineda, P.A., Demeestere, K., Toledo, M., Van Langenhove, H., Walgraeve, C., 2021. Enhanced removal of hydrophobic volatile organic compounds in biofilters and biotrickling filters: A review on the use of surfactants and the addition of hydrophilic compounds. Chemosphere 279, 130757. https://doi.org/10.1016/J.CHEMOSPHERE.2021.130757

Le, H. V., Sivret, E.C., Parcsi, G., Stuetz, R.M., 2015. Impact of Storage Conditions on the Stability of Volatile Sulfur Compounds in Sampling Bags. J. Environ. Qual. 44, 1523–1529. https://doi.org/10.2134/jeq2014.12.0532

Lebrero, R., Rangel, M.G.L., Muñoz, R., 2013a. Characterization and biofiltration of a real odorous emission from wastewater treatment plant sludge. J. Environ. Manage. 116, 50–57. https://doi.org/10.1016/j.jenvman.2012.11.038

Lebrero, R., Volckaert, D., Pérez, R., Muñoz, R., Van Langenhove, H., 2013b. A membrane bioreactor for the simultaneous treatment of acetone, toluene, limonene and hexane at trace level concentrations. Water Res. 47, 2199–2212. https://doi.org/10.1016/J.WATRES.2013.01.041

Lin, C.W., Tsai, S.L., Lai, C.Y., Liu, S.H., Wu, C.H., 2019. Biodegradation kinetics and microbial dynamics of toluene removal in a two-stage cell-biochar-filled biotrickling filter. J. Clean. Prod. 238, 117940. https://doi.org/10.1016/j.jclepro.2019.117940

Lin, G., Lu, J., Sun, Z., Xie, J., Huang, J., Su, M., Wu, N., 2021. Characterization of tissue-associated bacterial community of two Bathymodiolus species from the adjacent cold seep and hydrothermal vent environments. Sci. Total Environ. 796, 149046. https://doi.org/10.1016/J.SCITOTENV.2021.149046

Liu, J., Liu, J., LI, L., 2008. Performance of two biofilters with neutral and low pH treating off-gases. J. Environ. Sci. 20, 1409–1414. https://doi.org/10.1016/S1001-0742(08)62541-3

López, R., Cabeza, I.O., Giráldez, I., Díaz, M.J., 2011. Biofiltration of composting gases using different municipal solid waste-pruning residue composts: Monitoring by using an electronic nose. Bioresour. Technol. 102, 7984–7993. https://doi.org/10.1016/j.biortech.2011.05.085

Louca, S., Parfrey, L.W., Doebeli, M., 2016. Decoupling function and taxonomy in the global ocean microbiome. Science (80-.). 353, 1272–1277. https://doi.org/10.1126/SCIENCE.AAF4507

Lu, L., Wang, G., Yeung, M., Xi, J., Hu, H.Y., 2020. Shift of microbial community in gas-phase biofilters with different inocula, inlet loads and nitrogen sources. Process Biochem. 91, 57–64. https://doi.org/10.1016/J.PROCBIO.2019.11.032

Marmulla, R., Harder, J., 2014. Microbial monoterpene transformations-a review. Front. Microbiol. 5, 346. https://doi.org/10.3389/FMICB.2014.00346

Márquez, P., Herruzo-Ruiz, A.M., Siles, J.A., Alhama, J., Michán, C., Martín, M.A., 2021. Influence of packing material on the biofiltration of butyric acid: A comparative study from a physico-chemical, olfactometric and microbiological perspective. J. Environ. Manage. 294, 113044. https://doi.org/10.1016/j.jenvman.2021.113044

Meena, M., Sonigra, P., Yadav, G., 2021. Biological-based methods for the removal of volatile organic compounds (VOCs) and heavy metals. Environ. Sci. Pollut. Res. 28, 2485–2508. https://doi.org/10.1007/S11356-020-11112-4

Moussavi, G., Bahadori, M.B., Farzadkia, M., Yazdanbakhsh, A., Mohseni, M., 2009. Performance evaluation of a thermophilic biofilter for the removal of MTBE from waste air stream: Effects of inlet concentration and EBRT. Biochem. Eng. J. 45, 152–156. https://doi.org/10.1016/J.BEJ.2009.03.008

Mudliar, S., Giri, B., Padoley, K., Satpute, D., Dixit, R., Bhatt, P., Pandey, R., Juwarkar, A., Vaidya, A., 2010. Bioreactors for treatment of VOCs and odours - A review. J. Environ. Manage. https://doi.org/10.1016/j.jenvman.2010.01.006

Nagata, Y., 2003. Odor Measurement Review, Measurement of Odor Threshold by Triangle Odor Bag Method. Minist. Environ. Gov. Japan 122–123.

Natarajan, R., 2020. Performance Evaluation of Biodegradation of Isoprene–Acetone Mixture in Integrated Biofilter. J. Environ. Eng. 146, 4020030. https://doi.org/10.1061/(ASCE)EE.1943-7870.0001711

Natarajan, R., Al-Sinani, J., Viswanathan, S., Manivasagan, R., 2017. Biodegradation of ethyl benzene and xylene contaminated air in an up flow mixed culture biofilter. Int. Biodeterior. Biodegradation 119, 309–315. https://doi.org/10.1016/J.IBIOD.2016.10.041

Nelson, M., Bohn, H.L., Nelson, M., Bohn, H.L., 2011. Soil-Based Biofiltration for Air Purification:Potentials for Environmental and Space LifeSupport Application. J. Environ. Prot. (Irvine,. Calif). 2, 1084–1094. https://doi.org/10.4236/JEP.2011.28125

New Jersey Department of Health, 2007. Right to Know Hazardous Substance Fact Sheets [WWW Document]. URL https://www.nj.gov/health/eoh/rtkweb/documents/fs/0300.pdf

NTP, 1992. National Toxicology Program, Institute of Environmental Health Sciences, National Institutes of Health (NTP). National Toxicology Program Chemical Repository Database. Research Triangle Park, North Carolina.

Otten, L., Afzal, M.T., Mainville, D.M., 2004. Biofiltration of odours: Laboratory studies using butyric acid. Adv. Environ. Res. 8, 397–409. https://doi.org/10.1016/S1093-0191(02)00119-3

Pagans, E., Font, X., Sánchez, A., 2006. Emission of volatile organic compounds from composting of different solid wastes: Abatement by biofiltration. J. Hazard. Mater. 131, 179–186. https://doi.org/10.1016/J.JHAZMAT.2005.09.017

Pedersen, A.R., Møller, S., Molin, S., Arvin, E., 1997. Activity of toluene-degrading Pseudomonas putida in the early growth phase of a biofilm for waste gas treatment. Biotechnol. Bioeng. 54, 131–141. https://doi.org/10.1002/(SICI)1097-0290(19970420)54:2<131::AID-BIT5>3.0.CO;2-M

Premkumar, R., Krishnamohan, N., 2012. Effect of secondary parameters on biofilter treating industrial effluent. Int. J. PharmTech Res. 4, 1279–1287.

Puentes-Cala, E., Liebeke, M., Markert, S., Harder, J., 2018. Limonene dehydrogenase hydroxylates the allylic methyl group of cyclic monoterpenes in the anaerobic terpene degradation by Castellaniella defragrans. J. Biol. Chem. 293, 9520–9529. https://doi.org/10.1074/JBC.RA117.001557

Ramírez, M., Fernández, M., Granada, C., Le Borgne, S., Gómez, J.M., Cantero, D., 2011. Biofiltration of reduced sulphur compounds and community analysis of sulphur-oxidizing bacteria. Bioresour. Technol. 102, 4047–4053. https://doi.org/10.1016/j.biortech.2010.12.018

Ren, B., Zhao, Y., Lyczko, N., Nzihou, A., 2019. Current Status and Outlook of Odor Removal Technologies in Wastewater Treatment Plant. Waste and Biomass Valorization 10, 1443–1458. https://doi.org/10.1007/s12649-018-0384-9

Revah, S., Morgan-Sagastume, J.M., 2005. Methods of odor and VOC control, in: Biotechnology for Odor and Air Pollution Control. Springer Berlin Heidelberg, pp. 29–63. https://doi.org/10.1007/3-540-27007-8_3

Reyes, J., Toledo, M., Michán, C., Siles, J.A., Alhama, J., Martín, M.A., 2020. Biofiltration of butyric acid: Monitoring odor abatement and microbial communities. Environ. Res. 190. https://doi.org/10.1016/j.envres.2020.110057

Rybarczyk, P., Szulczyński, B., Gospodarek, M., Gębicki, J., 2020. Effects of n-butanol presence, inlet loading, empty bed residence time and starvation periods on the performance of a biotrickling filter removing cyclohexane vapors from air. Chem. Pap. 74, 1039–1047. https://doi.org/10.1007/s11696-019-00943-2

Senatore, V., Zarra, T., Galang, M.G., Oliva, G., Buonerba, A., Li, C.-W., Belgiorno, V., Naddeo, V., 2021. Full-Scale Odor Abatement Technologies in Wastewater Treatment Plants (WWTPs): A Review. Water 13. https://doi.org/10.3390/w13243503

Staudinger, J., Roberts, P. V., 1996. A critical review of Henry's law constants for environmental applications. Crit. Rev. Environ. Sci. Technol. https://doi.org/10.1080/10643389609388492

Sturn, A., Quackenbush, J., Trajanoski, Z., 2002. Genesis: Cluster analysis of microarray data. Bioinformatics 18, 207–208. https://doi.org/10.1093/bioinformatics/18.1.207

Thukral, A.K., 2017. A review on measurement of Alpha diversity in biology. Agric. Res. J. 54, 1–10. https://doi.org/10.5958/2395-146x.2017.00001.1

Tian, S., Fitzgerald, M., 2000. Limonene Degradation Pathway [WWW Document]. URL http://eawag-bbd.ethz.ch/lim/lim_map.html (accessed 1.24.22).

Toledo, M., Guillot, J.M., Siles, J.A., Martín, M.A., 2019. Permeability and adsorption effects for volatile sulphur compounds in Nalophan sampling bags: Stability influenced by storage time. Biosyst. Eng. 188, 217–228. https://doi.org/10.1016/j.biosystemseng.2019.10.023

US Coast Guard, 1999. Chemical Hazard Response Information System (CHRIS) - Hazardous Chemical Data. Commandant Instruction 16465.12C. Washington, D.C.: U.S. Government Printing Office.

US Department of Agriculture and the US Composting Council, 2002. Test Methods for the Examination of Composting and Compost (TMECC). Edaphos International, Houston (TX).

Van Der Werf, M.J., Swarts, H.J., De Bont, J.A.M., 1999. Rhodococcus erythropolis DCL14 Contains a Novel Degradation Pathway for Limonene. Appl. Environ. Microbiol. 65, 2092. https://doi.org/10.1128/aem.65.5.2092-2102.1999

Viswanathan, S., Neerackal, G., Buyuksonmez, F., 2013. Removal of beta-pinene and limonene using compost biofilter. J. Air Waste Manage. Assoc. 63, 237–245. https://doi.org/10.1080/10962247.2012.748522

Wainaina, S., Lukitawesa, Kumar Awasthi, M., Taherzadeh, M.J., 2019. Bioengineering of anaerobic digestion for volatile fatty acids, hydrogen or methane production: A critical review. Bioengineered 10, 437–458. https://doi.org/10.1080/21655979.2019.1673937

Wu, J., Zhao, Y., Zhao, W., Yang, T., Zhang, X., Xie, X., Cui, H., Wei, Z., 2017. Effect of precursors combined with bacteria communities on the formation of humic substances during different materials composting. Bioresour. Technol. 226, 191–199. https://doi.org/10.1016/j.biortech.2016.12.031

Yang, C., Qian, H., Li, X., Cheng, Y., He, H., Zeng, G., Xi, J., 2018. Simultaneous Removal of Multicomponent VOCs in Biofilters. Trends Biotechnol. https://doi.org/10.1016/j.tibtech.2018.02.004

CONCLUSIONES

CONCLUSIONS

Los resultados derivados de la presente Tesis Doctoral revelan la necesidad de evaluar y cuantificar el olor generado durante la depuración de las aguas residuales, tanto en términos de emisión como de inmisión, para identificar los principales motivos por los que se generan las emisiones odoríferas, así como la importancia de profundizar en los sistemas de tratamiento de dichas emisiones, bien para alargar su vida útil, o bien para buscar alternativas sostenibles que permitan la valorización de los materiales empleados una vez acabada su función original de desodorización en las EDAR.

En este contexto, se pueden extraer las siguientes conclusiones globales de los diferentes estudios llevados a cabo:

- En las EDAR de pequeño-mediano tamaño, las operaciones unitarias correspondientes a la línea de fangos constituyen las principales fuentes de emisión de olores. Además, la tecnología biológica de tratamiento de las aguas residuales condiciona las características de los lodos en lo que a biodiversidad microbiana y actividad respirométrica se refiere, lo que repercute finalmente en el mayor o menor impacto odorífero de este tipo de instalaciones (*Márquez y col. 2022. Activated sludge process versus rotating biological contactors in WWTPs: Evaluating the influence of operation and sludge bacterial content on their odor impact. Process Saf. Environ. Prot. 160, 775–785*).
- Los mapas de inmisión de olor de una EDAR urbana de gran tamaño, obtenidos a través del desarrollo de un modelo de dispersión Euleriano, han permitido simular el impacto odorífero generado por los focos con mayores emisiones de olor de la citada instalación, tanto en sus alrededores más inmediatos como en las poblaciones colindantes. Además, se ha comprobado cuantitativamente que los cambios estacionales juegan un importante papel en la dispersión de la contaminación odorífera, lo que resulta de especial interés al objeto de aumentar o modificar las estrategias de control de olor por parte de los gestores de aguas residuales (*Márquez y col. Odor impact simulation of a large urban wastewater treatment plant through the numerical solution of an Eulerian model. J. Environ. Manage. Under review*).
- El análisis integral del CAG contaminado, desde perspectivas como la olfatométrica, cromatográfica, fisicoquímica y textural, ha permitido profundizar en la comprensión del proceso de eliminación de olores en EDAR mediante la tecnología de adsorción. En este sentido, se ha demostrado que la olfatometría

dinámica y/o la cuantificación de las propiedades texturales de los carbones activados brindan una mejor evidencia del nivel de saturación de los lechos que la simple determinación de su eficacia de eliminación de sulfuro de hidrógeno, lo que a su vez puede redundar en la optimización del uso del material adsorbente, costes operativos y la calidad del aire ambiente (*Márquez y col. 2021. Integral evaluation of granular activated carbon at four stages of a full-scale WWTP deodorization system. Sci. Total Environ. 754, 142237*).

- La regeneración térmica del carbón activado granular en atmósfera oxidante (aire), a bajas temperaturas (< 350 ºC), constituye una alternativa sencilla y con menor coste operacional que su homóloga en atmósfera inerte, permitiendo obtener un carbón susceptible de ser empleado nuevamente como lecho desodorizante o como material que forme parte del cátodo de las prometedoras baterías de Li-S, cuyo rendimiento electroquímico ha demostrado ser bastante satisfactorio. A través de alternativas de valorización como las citadas, se contribuye a la sostenibilidad del tratamiento integral de las aguas residuales, dado que se evita la acumulación de residuos en vertederos y el uso de materias primas para la fabricación de nuevos carbones activados (*Márquez y col. 2021. Simple and eco-friendly thermal regeneration of granular activated carbon from the odour control system of a full-scale WWTP: Study of the process in oxidizing atmosphere. Sep. Purif. Technol. 255, 117782 | Márquez y col. 2022. Evaluating the thermal regeneration process of massively generated granular activated carbons for their reuse in wastewater treatments plants. J. Clean. Prod. 366, 132685 | Benítez y col. 2021. Simple and Sustainable Preparation of Cathodes for Li−S Batteries: Regeneration of Granular Activated Carbon from the Odor Control System of a Wastewater Treatment Plant. ChemSusChem. 14, 3915–3925*).
- Del análisis multidisciplinar de los experimentos de biofiltración estudiados, se ha comprobado que la elección del lecho empacado resulta una cuestión fundamental cuando se desean eliminar compuestos de carácter hidrofílico, como el ácido butírico, de corrientes gaseosas, lo que redunda en eficacias de eliminación de olor más elevadas (> 90%) y prolongadas durante el proceso de biofiltración, con los consiguientes beneficios sociales y ambientales. No obstante, cuando la corriente se compone mayoritariamente de compuestos de naturaleza hidrofóbica como el D-limoneno, el rendimiento de eliminación de

olores ya no resulta tan dependiente de la elección de un relleno u otro, pues habría que centrar los esfuerzos en mejorar primero la transferencia del contaminante gaseoso hidrofóbico a la biopelícula líquida de carácter hidrofílico o inocular los biofiltros con microorganismos más específicos, incrementando el coste de operación (*Márquez y col. 2021. Influence of packing material on the biofiltration of butyric acid: A comparative study from a physico-chemical, olfactometric and microbiological perspective. J. Environ. Manage. 294, 113044 | Márquez y col. 2022. A comparative study between the biofiltration for air contaminated with limonene or butyric acid using a combination of olfactometric, physico-chemical and genomic approaches. Process Saf. Environ. Prot. 160, 362–375*).

Para finalizar, dada la novedad del campo estudiado y la escasez de estudios que aborden aspectos relacionados con la contaminación odorífera de una forma integral mediante el empleo combinado de diferentes enfoques, esta Tesis Doctoral contribuye al avance científico en la aplicación de nuevas tecnologías, no sólo para facilitar el seguimiento del impacto oloroso derivado de las EDAR, sino también para conocer sus causas y tomar medidas correctivas que minimicen las molestias que dichas emisiones y los residuos generados al tratarlas generan en la sociedad y el medioambiente.

The results obtained in this Doctoral Thesis highlight the need to evaluate and quantify the odour derived from wastewater treatment in terms of emission and immission, in order to identify the main reasons why odour emissions are generated. Furthermore, it is essential to evaluate the feasibility of the treatment systems for such emissions, either to extend their useful life, or to find sustainable alternatives that allow the valorisation of the materials used once their original deodorisation function in the WWTP finishes.

In this context, the following global conclusions can be drawn from the different research studies carried out:

- The unit operations of the sludge line have been found to be the main sources of odour emission in the small-medium sized WWTPs under study. Moreover, the biological wastewater treatment technology conditions the characteristics of the sludge in terms of microbial biodiversity and respirometric activity, which ultimately affects the odour impact derived from such facilities (*Márquez et al. (2022). Activated sludge process versus rotating biological contactors in WWTPs: Evaluating the influence of operation and sludge bacterial content on their odor impact. Process Saf. Environ. Prot. 160, 775–785*).
- The odour immission maps of a large urban WWTP, obtained through the development of an Eulerian dispersion model, have simulated the odour impact generated by the sources with the highest odour emissions, both in its surroundings and in nearby populations. In addition, it has been quantitatively proven that seasonal changes play an important role in the dispersion of odour pollution. This information might help wastewater managers to increase or modify the odour control strategies in unfavourable situations (*Márquez et al. Odor impact simulation of a large urban wastewater treatment plant through the numerical solution of an Eulerian model. J. Environ. Manage. Under review*).
- The integral evaluation of the contaminated GAC, through physico-chemical, olfactometric, textural and chromatographic characterizations, has allowed for a deeper understanding of the odour removal process by GAC adsorption in WWTPs. In this sense, the dynamic olfactometric and/or the quantification of the GAC textural properties provide better evidence of the saturation level of the GAC beds than the determination of the hydrogen sulphide removal efficiency, which in turn may result in optimising the use of the adsorbent material, operating costs

and ambient air quality (*Márquez et al. (2021). Integral evaluation of granular activated carbon at four stages of a full-scale WWTP deodorization system. Sci. Total Environ. 754, 142237*).

- The thermal regeneration of GAC in oxidizing atmosphere (air) at temperatures no higher than 350 ºC constitutes a simple alternative with lower operational costs than its counterpart in an inert atmosphere, making it possible to obtain a regenerated carbon for reuse as odour adsorbent in WWTPs, or as a material forming part of the cathode of the promising Li-S batteries, whose electrochemical performance has proven to be highly satisfactory. Through such alternatives, the sustainability of integral wastewater treatment is enhanced, reducing the use of raw materials to manufacture new GACs and the accumulation of hazardous waste in landfill (*Márquez et al. (2021). Simple and eco-friendly thermal regeneration of granular activated carbon from the odour control system of a full-scale WWTP: Study of the process in oxidizing atmosphere. Sep. Purif. Technol. 255, 117782 | Márquez et al. (2022). Evaluating the thermal regeneration process of massively generated granular activated carbons for their reuse in wastewater treatments plants. J. Clean. Prod. 366, 132685 | Benítez et al. (2021). Simple and Sustainable Preparation of Cathodes for Li−S Batteries: Regeneration of Granular Activated Carbon from the Odor Control System of a Wastewater Treatment Plant. ChemSusChem. 14, 3915–3925*).
- From the multidisciplinary analysis of the biofiltration experiments carried out, it has been proven that the selection of a particular bed material plays a key role in removing gaseous compounds of hydrophilic nature, such as butyric acid, which results in high (> 90%) and prolonged odour removal efficiencies during the biofiltration process, with the consequent social and environmental benefits. Nevertheless, when the gaseous stream is constituted mainly of compounds of hydrophobic nature such as D-limonene, the odour removal performance becomes less dependent on the bed selection. In this context, efforts would have to be made in first improving the transfer of the hydrophobic gaseous contaminant to the hydrophilic liquid biofilm or inoculating the biofilters with more specific microorganisms, with the drawback of increasing operational costs (*Márquez et al. (2021). Influence of packing material on the biofiltration of butyric acid: A comparative study from a physico-chemical, olfactometric and microbiological perspective. J. Environ. Manage. 294, 113044 | Márquez et al. (2022). A*

comparative study between the biofiltration for air contaminated with limonene or butyric acid using a combination of olfactometric, physico-chemical and genomic approaches. Process Saf. Environ. Prot. 160, 362–375).

To sum up, given the novelty of this field of study and the scarce previous studies that address the integral evaluation of the odour pollution through the combined use of different approaches, this Doctoral Thesis contributes to scientific progress in the application of new technologies. Not only to facilitate monitoring of the odour impact derived from WWTPs, but also to find out its causes and take corrective measures that minimize the inconvenience that such emissions and the waste produced by treating them generate in society and the environment.

NOMENCLATURA

NOMENCLATURE

AC	Activated carbon
AMIGO	Asociación Medioambiental Internacional de Gestores del Olor
AOV	Ácidos orgánicos volátiles
ASP	Activated sludge process
BET	Brunauer-Emmet-Teller
BOD_5	Biochemical oxygen demand at 5 days
BREF	Documentos de referencia para las mejores técnicas disponibles
CAG	Carbón activado granular
CAO	Consumo acumulado de oxígeno
CBR	Contactor biológico rotativo
CFD	Computational fluid dynamics
CFU	Colony forming unit
CHD	Confederación Hidrográfica del Duero
C/N	Carbon/nitrogen ratio
COD	Chemical oxygen demand
CON	Conductivity
COV	Compuesto orgánico volátil
DBO_5	Demanda bioquímica de oxígeno a los 5 días
DFT	Density functional theory
D_{pore}	Average pore width
DQO	Demanda química de oxígeno
DSEAR	Depuración, Saneamiento, Eficiencia, Ahorro y Reutilización
DSC	Differential scanning calorimetry
EBRT	Empty bed residence time
EDAR	Estación depuradora de aguas residuales

EDAX	Energy dispersive X-ray analysis
EI	Equivalent inhabitant
EMPROACSA	Empresa Provincial de Aguas de Córdoba, S.A.
FID	Flame ionization detector
FIDOL	Frecuencia, Intensidad, Duración, Ofensividad y Localización
F/M	Food-to-microorganism ratio
FPD	Flame photometric detector
FS	Fixed solids
DO	Dissolved oxygen
GAC	Granular activated carbon
GC	Gas chromatography
hab-eq	Habitante equivalente
HRT	Hydraulic retention time
IC	Soluble inorganic carbon
INE	Instituto Nacional de Estadística
INSST	Instituto Nacional de Seguridad y Salud en el Trabajo
IOMS	Instrumental odor monitoring systems
ITE	Individual threshold estimate
IUPAC	International Union of Pure and Applied Chemistry
MAC	Total mesophilic aerobic count
MARM	Ministerio de Medio Ambiente y Medio Rural y Marino
MBBR	Moving bed biofilm reactor
MITECO	Ministerio para la Transición Ecológica y el Reto Demográfico
MLTSS	Mixed liquor total suspended solids
MLVSS	Mixed liquor volatile suspended solids

MS	Mass spectrometry
MTD	Mejor técnica disponible
MTPs	Municipal treatment plants
NEA-MTD	Niveles de emisión asociados a la mejor técnica disponible
N-NH_4^+	Ammoniacal nitrogen / Nitrógeno amoniacal
NTK	Nitrógeno total Kjeldahl
N-TKN	Total Kjeldahl nitrogen
$N\text{-}TN_s$	Soluble total nitrogen
N_{total}	Nitrógeno total
OAV	Odor activity value
OC	Odor concentration
OD_{20}	Cumulative oxygen demand at 20 h
ODS	Objetivos de desarrollo sostenible
ODT	Odor detection threshold
OER	Odor emission rate
OIC	Odor immission concentration
OIR	Odor incoming rate
ou_E	European odor units
P98	Percentil 98
PC_i	Chemical contribution
PID	Photoionization detector
PNCA	Plan Nacional de Calidad de las Aguas: Saneamiento y Depuración
PNSD	Plan Nacional de Saneamiento y Depuración
PO_i	Odor contribution
$P\text{-}P_2O_5$	Phosphorus content expressed as P_2O_5

P_{total}	Fósforo total
Q_e	Effluent waterflow
Q_i	Influent waterflow
RBC	Rotating biological contactors
S_{BET}	Specific surface area
SBR	Sequencing batch reactor
SCAI	Servicio Central de Apoyo a la Investigación
SEA	Servicio de Evaluación Ambiental
SEM	Scanning electron microscope
SL	Sludge
S_{micro}	Micropore area
SOC	Removed specific odor concentration
SOER	Specific odor emission rate
$SOUR_{max}$	Maximum specific oxygen uptake rate
SRT	Solids retention time
SS	Sólidos en suspensión
STP	Standard temperature and pressure
TC	Soluble total carbon
TD	Thermal desorption
TGA	Thermogravimetric analysis
TOC	Soluble total organic carbon
TRH	Tiempo de retención hidráulico
TSS	Total suspended solids
UFC	Unidad formadora de colonias

UNESCO	Organización de las Naciones Unidas para la Educación, la Ciencia y la Cultura
US EPA	U.S. Environmental Protection Agency
VECO	Velocidad específica de consumo de oxígeno
VFAs	Volatile fatty acids
VLA-EC	Valor límite ambiental - Exposición de corta duración
VLA-ED	Valor límite ambiental - Exposición diaria
$\mathbf{V_{micro}}$	Micropore volume
VOCs	Volatile organic compounds
VOEF	Volumetric odor emission factor
VS	Volatile solids
VSCs	Volatile sulfur compounds
$\mathbf{V_t}$	Total pore volume
WWTP	Wastewater treatment plant
XRD	X-ray diffraction
XRF	X-ray fluorescence

PRODUCCIÓN CIENTÍFICA DE LA TESIS DOCTORAL

SCIENTIFIC PRODUCTION OF THE PhD THESIS

ARTÍCULOS DE INVESTIGACIÓN / RESEARCH ARTICLES

- Ruiz-Muñoz, A., Siles J.A., Márquez P., Toledo M., Gutiérrez M.C., Martín M.A., 2023. **Odor emission assessment of different WWTPs with Extended Aeration Activated Sludge and Rotating Biological Contactor technologies in the province of Cordoba (Spain)**. J. Environ. Manage 326, 116741. https://doi.org/10.1016/j.jenvman.2022.116741 (JCR Impact factor 2021: 8.910; Rank (Environmental Sciences): 34/279; Quartile: Q1).
- Márquez, P., Muñoz-Serrano, E., Gutiérrez, M.C., Siles, J.A., Martín, M.A. **Odor impact simulation of a large urban wastewater treatment plant through the numerical solution of an Eulerian model**. J. Environ. Manage. (JCR Impact factor 2021: 8.910; Rank (Environmental Sciences): 34/279; Quartile: Q1) *(Under Review*).
- Márquez, P., Benítez, A., Chica, A.F., Martín, M.A., Caballero, A., 2022. **Evaluating the thermal regeneration process of massively generated granular activated carbons for their reuse in wastewater treatments plants**. J. Clean. Prod. 366, 132685. https://doi.org/10.1016/J.JCLEPRO.2022.132685 (JCR Impact factor 2021: 11.072; Rank (Environmental Sciences): 24/279; Quartile: Q1).
- Márquez, P., Gutiérrez, M.C., Toledo, M., Alhama, J., Michán, C., Martín, M.A., 2022. **Activated sludge process *versus* rotating biological contactors in WWTPs: Evaluating the influence of operation and sludge bacterial content on their odor impact**. Process Saf. Environ. Prot. 160, 775–785. https://doi.org/10.1016/J.PSEP.2022.02.071 (JCR Impact factor 2021: 7.926; Rank (Engineering, Chemical): 21/142; Quartile: Q1).
- Márquez, P., Siles, J.A., Gutiérrez, M.C., Alhama, J., Michán, C., Martín, M.A., 2022. **A comparative study between the biofiltration for air contaminated with limonene or butyric acid using a combination of olfactometric, physico-chemical and genomic approaches**. Process Saf. Environ. Prot. 160, 362–375. https://doi.org/10.1016/J.PSEP.2022.02.024 (JCR Impact factor 2021: 7.926; Rank (Engineering, Chemical): 21/142; Quartile: Q1).

- Márquez, P., Herruzo-Ruiz, A.M., Siles, J.A., Alhama, J., Michán, C., Martín, M.A., 2021. **Influence of packing material on the biofiltration of butyric acid: A comparative study from a physico-chemical, olfactometric and microbiological perspective**. J. Environ. Manage. 294, 113044. https://doi.org/10.1016/j.jenvman.2021.113044 (JCR Impact factor 2021: 8.910; Rank (Environmental Sciences): 34/279; Quartile: Q1).
- Benítez, A., Márquez, P., Martín, M.Á., Caballero, A., 2021. **Simple and sustainable preparation of cathodes for Li−S batteries: Regeneration of granular activated carbon from the odor control system of a wastewater treatment plant**. ChemSusChem. 14, 3915–3925. https://doi.org/10.1002/cssc.202101231 (JCR Impact factor 2021: 9.140; Rank (Chemistry, Multidisciplinary): 30/180; Quartile: Q1).
- Márquez, P., Benítez, A., Hidalgo-Carrillo, J., Urbano, F.J., Caballero, A., Siles, J.A., Martín, M.A., 2021. **Simple and eco-friendly thermal regeneration of granular activated carbon from the odour control system of a full-scale WWTP: Study of the process in oxidizing atmosphere**. Sep. Purif. Technol. 255, 117782. https://doi.org/10.1016/j.seppur.2020.117782 (JCR Impact factor 2021: 9.136; Rank (Engineering, Chemical): 14/142; Quartile: Q1).
- Márquez, P., Benítez, A., Caballero, A., Siles, J.A., Martín, M.A., 2021. **Integral evaluation of granular activated carbon at four stages of a full-scale WWTP deodorization system**. Sci. Total Environ. 754, 142237. https://doi.org/10.1016/j.scitotenv.2020.142237 (JCR Impact factor 2021: 10.753; Rank (Environmental Sciences): 26/279; Quartile: Q1).
- Márquez, P., Benítez, A., Caballero, A., Siles, J.A., Toro-Baptista, E., Martín, M.A., 2020. **Olores en EDAR: Evaluación de la emisión y regeneración del carbón adsorbente con reutilización en desodorización**. TecnoAqua. 46, 54-63. https://www.tecnoaqua.es/articulos/20210818/articulo-tecnico-olores-depuradora-evaluacion-emision-regeneracion-carbon-adsorbente-reutilizacion-desodorizacion#.YcIP7iaCHIU (No indexada).

- Ruiz, A., Márquez, P., Siles, J.A., Ranchal, M., Dios, M., Chica, A.F., Martín, M.A., 2020. **Estudio de las emisiones odoríferas en pequeñas y medianas EDARs.** Prevenidos (Aguas de Córdoba). 5, 18–21. https://issuu.com/aguasdecordoba/docs/prevenidos_5 (No indexada).
- Toledo, M., Márquez, P., Siles, J.A., Chica, A.F., Martín, M.A., 2019. **Co-composting of sewage sludge and eggplant waste at full scale: Feasibility study to valorize eggplant waste and minimize the odoriferous impact of sewage sludge**. J. Environ. Manage. 247, 205–213. https://doi.org/10.1016/j.jenvman.2019.06.076 (JCR Impact factor 2019: 5.647; Rank (Environmental Sciences): 33/265; Quartile: Q1).
- Gil, A., Siles, J.A., Márquez, P., Gutiérrez, M.C., Martín, M.A., 2019. **Optimizing the selection of organic waste for biomethanization**. Environ. Technol. (United Kingdom) 40, 564–575. https://doi.org/10.1080/09593330.2017.1397769 (JCR Impact factor 2019: 2.213; Rank (Environmental Sciences): 143/265; Quartile: Q3).

PARTICIPACIÓN EN CONGRESOS / CONGRESS CONTRIBUTION

Comunicaciones orales / Oral communications

- Gutiérrez, M.C., Hernández-Ceballos, M.A., Márquez, P., Martín, M.A. **Identification and simulation of atmospheric dispersion patterns of odour and VOCs generated by a waste treatment plant**. XXXVIII Reunión Bienal de la Sociedad Española de Química, 27-30 de junio de 2022. Granada (España).
- Gómez-Camer, J.L., Gutiérrez, M.C., Márquez, P., Martín, M.A., Benítez, A., Caballero, A. **Activated carbons derived from sewage sludge as sustainable cathodes for Li-S batteries**. XXXVIII Reunión Bienal de la Sociedad Española de Química, 27-30 de junio de 2022. Granada (España).
- Márquez, P., Benítez, A., Hidalgo-Carrillo, J., Chica, A.F., Siles, J.A., Caballero, A., Martín, M.A. **Regeneración del carbón activo granular procedente del sistema de tratamiento de olor en EDAR para su posterior valorización ambiental y energética**. XV Reunión del Grupo Español del Carbón (GEC2020), 24-27 de abril de 2022. Granada (España).
- Márquez, P., Benítez, A., Caballero, A., Siles, J.A., Martín, M.A. **Comprehensive evaluation of granular activated carbon from the deodorisation system of a WWTP and regeneration for subsequent reuse**. 9th IWA Odour and VOC/Air Emissions Conference, 26-27 de octubre de 2021. Bilbao (España).
- Márquez, P., Benítez, A., Caballero, A., Siles, J.A., Martín, M.A. **Estudio integral del carbón activo granular procedente del sistema de control de olores de una EDAR urbana**. II International Conference on Water and Sustainability, 24-26 de marzo de 2021. Terrassa, Barcelona (España).
- Márquez, P., Benítez, A., Hidalgo-Carrillo, J., Urbano, F.J., Caballero, A., Siles, J.A., Martín, M.A. **Regeneración del carbón activo granular procedente del sistema de desodorización de una EDAR urbana para su posterior reutilización**. II International Conference on Water and Sustainability, 24-26 de marzo de 2021. Terrassa, Barcelona (España).
- Chica, A.F., Gutiérrez, M.C., Toledo, M., Márquez, P., Martín, M.A. **Estudio de viabilidad para co-compostar gallinaza, alperujo, poda/hoja de olivo y paja de cereal: calidad del compost y emisión de olores**. Compostaje Webinars 2020 (Red Española de Compostaje), 6-27 de noviembre de 2020.

- Márquez, P., Benítez, A., Caballero, A., Siles, J.A., Martín, M.A. **Evaluación de la emisión odorífera de una EDAR y regeneración del carbón activo granular procedente del sistema de tratamiento de olor para su posterior valorización**. VIII Congreso Científico de Investigadores en Formación de la Universidad de Córdoba, 18-19 de febrero de 2020. Córdoba (España).

Póster / Poster

- Benítez, A., Gómez-Camer, J.L., Martínez, H., Gutiérrez, M.C., Márquez, P., Martín, M.A., Caballero, A. **Developing activated carbons from exhausted olive pomace as cathode material for Lithium-Sulfur batteries**. XXXVIII Reunión Bienal de la Sociedad Española de Química, 27-30 de junio de 2022. Granada (España).
- Benítez, A., Márquez, P., Gómez-Camer, J.L., Chica, A.F., Martín, M.A., Caballero, A. **Revalorización de filtros de olores usados en EDAR para la fabricación de baterías sostenibles Litio-Azufre**. XIV Congreso Español de Tratamiento de Aguas (META 2022), 1-3 de junio de 2022. Sevilla (España).
- Ruiz-Muñoz, A., Gutiérrez, M.C., Márquez, P., Siles, J.A., Martín, M.A. **Evaluación odorífera de 5 EDARs con diferentes tecnologías intensivas en la provincia de Córdoba (España)**. XIV Congreso Español de Tratamiento de Aguas (META 2022), 1-3 de junio de 2022. Sevilla (España).
- Márquez, P., Benítez, A., Siles, J.A., Caballero, A., Martín, M.A. **Simple thermal regeneration of granular activated carbon from the deodorization system of a WWTP for its reuse**. RSEQ Symposium 2021, 27-30 de septiembre de 2021.
- Benítez, A., Márquez, P., Martín, M.A., Caballero, A. **Simple regeneration of activated carbon from the odour control system of a WWTP for sustainable cathodes in Li–S batteries**. RSEQ Symposium 2021, 27-30 de septiembre de 2021.
- Márquez, P., Benítez, A., Torrecillas, A., Martín, M.A., Siles, J.A., Caballero, A., Hidalgo-Carrillo, J., Urbano, F.J. **Regeneración del carbón activo granular procedente del sistema de tratamiento de olor en una EDAR**. Reunión Bienal de la Sociedad Española de Catálisis (SECAT'19), 24-26 de junio de 2019. Córdoba (España).

- Benítez, A., Torrecillas, A., Márquez, P., Caballero, A., Morales, J., Martín, M.A., Siles, J.A., Chica, A.F. **Valorización de carbones activos residuales de EDAR: aplicación en baterías de Litio-Azufre**. Reunión Bienal de la Sociedad Española de Catálisis (SECAT'19), 24-26 de junio de 2019. Córdoba (España).
- González, I., Márquez, P., Martín, M.A., Siles, J.A., Chica, A.F., Herrero, N., García, C., Gómez, J.M. **Prototipo de fotobiorreactor Twin Layer para el cultivo de microalgas valorizando en forma de biomasa de N y P contaminantes terciarios en aguas residuales**. Reunión Bienal de la Sociedad Española de Catálisis (SECAT'19), 24-26 de junio de 2019. Córdoba (España).

Miembro de comités científicos organizadores

- VIII Congreso Científico de Investigadores en Formación de la Universidad de Córdoba, 18-19 de febrero de 2020. Córdoba (España).
- VII Congreso Científico de Investigadores en Formación de la Universidad de Córdoba, 6-7 de febrero de 2019. Córdoba (España).